European Commission

JRC SCIENCE AND POLICY REPORT

Eurocodes: Background & Applications Design of Steel Buildings

Worked Examples

Authors:
M. Veljkovic, L. Simões da Silva,
R. Simões, F. Wald, J.-P. Jaspart,
K. Weynand, D. Dubină, R. Landolfo,
P. Vila Real, H. Gervásio

Editors:
M. Veljkovic, M. L. Sousa, S. Dimova,
B. Nikolova, M. Poljanšek, A. Pinto

2015

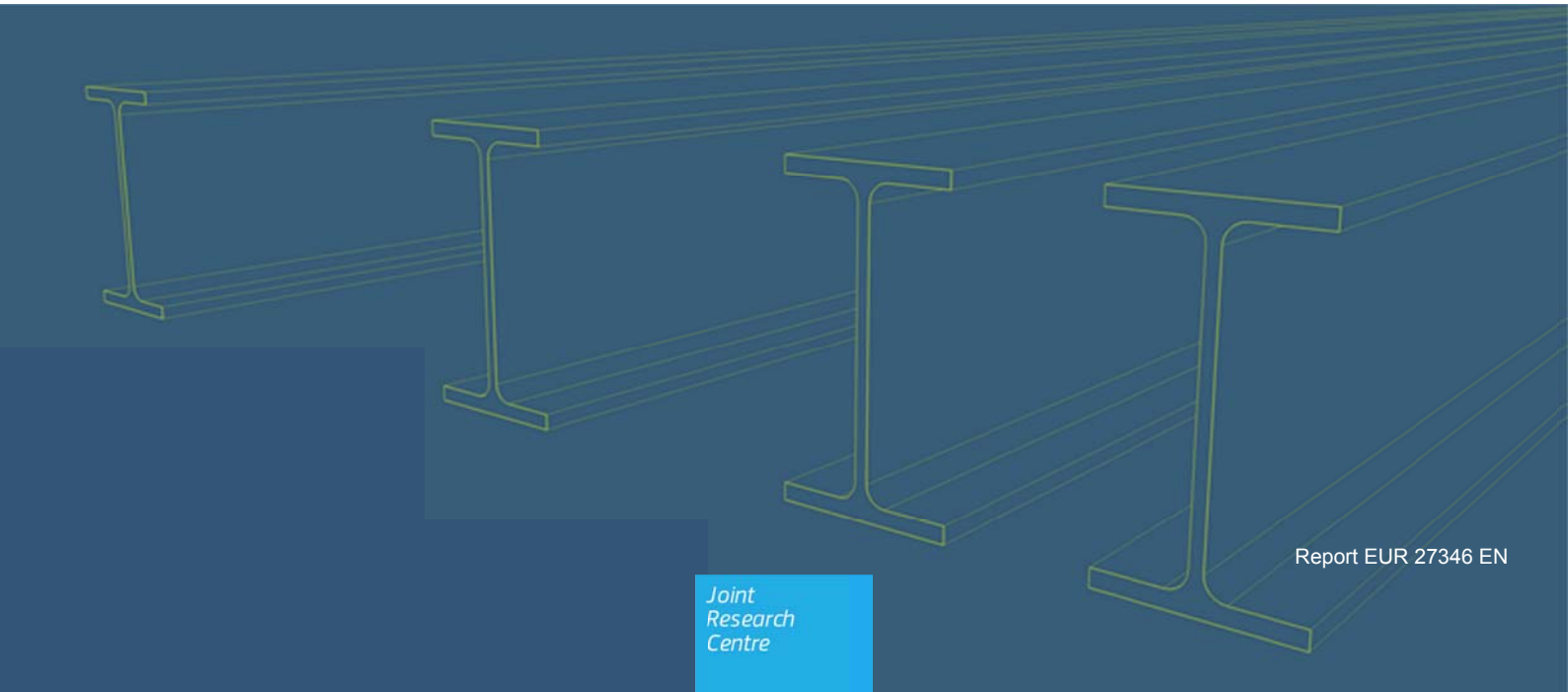

Report EUR 27346 EN

Joint Research Centre

European Commission
Joint Research Centre
Institute for the Protection and Security of the Citizen

Contact information
Maria Luísa Sousa
Address: TP480, Joint Research Centre, Via Enrico Fermi, 2749, 21027 Ispra, VA, Italy
E-mail: luisa.sousa@jrc.ec.europa.eu
Tel.: +39 0332 78 6381

JRC Science Hub
https://ec.europa.eu/jrc

JRC96658

EUR 27346 EN

ISBN 978-92-79-49573-1 (PDF)

ISSN 1831-9424 (online)

doi:10.2788/605700

Luxembourg: Publications Office of the European Union, 2015

Abstract

The present JRC report contains state-of-the-art training material on the structural design of steel buildings, with emphasis on worked examples. The technical papers here presented focus on specific parts of the structural design, namely basis of design, modelling of structure, design of members, connections, cold-formed steel, seismic and fire design and on sustainability aspects. The report intends to contribute towards the transfer of background knowledge and expertise on the Eurocodes, mainly the EN 1993, from specialists of the European Convention for Constructional Steelwork (ECCS) and of CEN/TC250/Sub Committee 3, to trainers at a national level and to Eurocodes users. The report includes a comprehensive description of Eurocodes rules and worked examples presented by the aforementioned specialists at the workshop "Design of steel buildings with the Eurocodes, with worked examples'' that was held on 16-17 October 2014, in Brussels, Belgium.

CONTENTS

List of authors and editors

Scientific Coordinator

Milan VELJKOVIC, University of Lulea, Sweden

Authors

CHAPTER 1 - **DESIGN OF STEEL STRUCTURES**

Luís SIMÕES DA SILVA and Rui SIMÕES — University of Coimbra, Portugal

CHAPTER 2 - **BOLTS, WELDS, COLUMN BASE**

František WALD — Czech Technical University in Prague, Czech Republic

CHAPTER 3 - **DESIGN OF MOMENT RESISTING JOINTS IN STEEL STRUCTURES**

Jean-Pierre JASPART[1] and Klaus WEYNAND[2] — [1]Université de Liège, Belgium; [2]Feldmann & Weynand Ingenieure, Germany

CHAPTER 4 - **COLD-FORMED STEEL DESIGN ESSENTIALS**

Dan DUBINĂ — Politehnica University Timisoara, Romania

CHAPTER 5 - **SEISMIC DESIGN OF STEEL STRUCTURES ACCORDING TO EN1998-1**

Raffaele LANDOLFO — University of Naples Federico II, Italy

CHAPTER 6 - **RESISTANCE OF MEMBERS AND CONNECTIONS TO FIRE.**

Paulo VILA REAL — University of Aveiro, Portugal

CHAPTER 7 - **SUSTAINABILITY ASPECTS OF STEEL BUILDINGS AND COMPONENTS**

Milan VELJKOVIC[1] and Helena GERVÁSIO[2] — [1]University of Lulea, Sweden; [2]University of Coimbra, Portugal

Editors

Milan VELJKOVIC	Chairman of the Technical Management Board European Convention for Constructional Steelwork
Maria Luísa SOUSA	European Commission, Joint Research Centre (JRC), Institute for the Protection and Security of the Citizen (IPSC), European Laboratory for Structural Assessment Unit (ELSA), Via Enrico Fermi, 2749, 21027 Ispra, VA, Italy
Silvia DIMOVA	European Commission, Joint Research Centre (JRC), Institute for the Protection and Security of the Citizen (IPSC), European Laboratory For Structural Assessment Unit (ELSA), Via Enrico Fermi, 2749, 21027 Ispra, VA, Italy
Borislava NIKOLOVA	European Commission, Joint Research Centre (JRC), Institute for the Protection and Security of the Citizen (IPSC), European Laboratory For Structural Assessment Unit (ELSA), Via Enrico Fermi, 2749, 21027 Ispra, VA, Italy
Martin POLJANŠEK	European Commission, Joint Research Centre (JRC), Institute for the Protection and Security of the Citizen (IPSC), European Laboratory For Structural Assessment Unit (ELSA), Via Enrico Fermi, 2749, 21027 Ispra, VA, Italy
Artur PINTO	European Commission, Joint Research Centre (JRC), Institute for the Protection and Security of the Citizen (IPSC), European Laboratory For Structural Assessment Unit (ELSA), Via Enrico Fermi, 2749, 21027 Ispra, VA, Italy

Foreword

The **construction sector** is of strategic importance to the EU as it delivers the buildings and transport infrastructure needed by the rest of the economy and society. It represents more than **10% of EU GDP and more than 50% of fixed capital formation**. It is the largest single economic activity and it is the biggest industrial employer in Europe. The sector employs directly almost 20 million people. Construction is a key element not only for the implementation of the **Single Market**, but also for other construction relevant EU Policies, e.g. **Sustainability, Environment and Energy**, since 40-45% of Europe's energy consumption stems from buildings with a further 5-10% being used in processing and transport of construction products and components.

The **EN Eurocodes** are a set of European standards (Européenne Normes) which provide common rules for the design of construction works, to check their strength and stability. In line with the EU's strategy for smart, sustainable and inclusive growth (EU2020), **Standardization** plays an important part in supporting the industrial policy for the globalization era. The improvement of the competition in EU markets through the adoption of the Eurocodes is recognized in the "Strategy for the sustainable competitiveness of the construction sector and its enterprises" – COM (2012)433, and they are distinguished as a tool for accelerating the process of convergence of different national and regional regulatory approaches.

With the publication of all the 58 Eurocodes Parts in 2007, the implementation of the Eurocodes is extending to all European countries and there are firm steps toward their adoption internationally. The Commission Recommendation of 11th December 2003 stresses the importance of training in the use of the Eurocodes, especially in engineering schools and as part of continuous professional development courses for engineers and technicians, which should be promoted both at national and international level. It is recommended to undertake research to facilitate the integration into the Eurocodes of the latest developments in scientific and technological knowledge. In light of this Recommendation, DG JRC is collaborating with DG GROW, CEN/TC250 "Structural Eurocodes" and other relevant stakeholders, and is publishing the Report Series 'Support to the implementation, harmonization and further development of the Eurocodes' as JRC Science and Policy Reports.

This report contains a comprehensive description of the practical examples presented at the workshop "Design of steel buildings with the Eurocodes" with emphasis on worked examples. The workshop was held on 16-17 October 2014, in Brussels, Belgium and was organized by the Joint Research Centre of the European Commission together with the European Convention for Constructional Steelwork (ECCS) and CEN/TC250/Sub-Committee 3, with the support of DG GROW, CEN and the Member States. The workshop addressed representatives of public authorities, national standardisation bodies, research institutions, academia, industry and technical associations involved in training on the Eurocodes. The main objective was to facilitate training on design of steel buildings through the transfer of knowledge and expertise from specialists of ECCS and CEN/TC250 to key trainers at national level and Eurocodes users.

The workshop was a unique occasion to compile a state-of-the-art training kit comprising the slide presentations and technical papers with the worked examples, focused on a specific part of structural design (e.g. basis of design, modelling of structure, design of members, connections, cold-formed steel, seismic and fire design, etc.). The present JRC Report compiles all the technical papers and the worked examples prepared by the workshop lecturers. The editors and authors have sought to present useful and consistent information in this report. However, it must be noted that the report does not present complete design examples. The chapters presented in the report have been prepared by different authors therefore are partly reflecting the different practices in the EU Member

States. Users of information contained in this report must satisfy themselves of its suitability for the purpose for which they intend to use it.

We would like to gratefully acknowledge the workshop lecturers for their contribution in the organization of the workshop and development of the training material comprising the slide presentations and technical papers with the worked examples.

All the material prepared for the workshop (slides presentations and JRC Report) is available to download from the "Eurocodes: Building the future" website (http://eurocodes.jrc.ec.europa.eu).

M. Veljkovic

European Convention for Constructional Steelwork

M.L. Sousa, S. Dimova, B. Nikolova, M. Poljanšek, A. Pinto

European Laboratory for Structural Assessment (ELSA)

Institute for the Protection and Security of the Citizen (IPSC)

Joint Research Centre (JRC)

Via Enrico Fermi 2749, 21027 Ispra VA, Italy

CHAPTER 1

DESIGN OF STEEL STRUCTURES

Luís SIMÕES DA SILVA and Rui SIMÕES

ISISE, University of Coimbra, Portugal

1 Design of steel structures

1.1 Definitions and basis of design

1.1.1 Introduction

Steel construction combines a number of unique features that make it an ideal solution for many applications in the construction industry. Steel provides unbeatable speed of construction and off-site fabrication, thereby reducing the financial risks associated with site-dependent delays. The inherent properties of steel allow much greater freedom at the conceptual design phase, thereby helping to achieve greater flexibility and quality. In particular, steel construction, with its high strength to weight ratio, maximizes the useable area of a structure and minimizes self-weight, again resulting in cost savings. Recycling and reuse of steel also mean that steel construction is well-placed to contribute towards reduction of the environmental impacts of the construction sector (Simões da Silva et al., 2013).

The construction industry is currently facing its biggest transformation as a direct result of the accelerated changes that society is experiencing. Globalisation and increasing competition are forcing the construction industry to abandon its traditional practices and intensive labour characteristics and to adopt industrial practices typical of manufacturing. This further enhances the attractiveness of steel construction.

The objective of the present chapter is to provide design guidance on the use of the Part 1-1 of Eurocode 3 through a brief explanation of the code's provisions, supported by detailed, practical design examples based on real structures.

1.1.2 Codes of practice and standardization

The European Union has spent several decades (since 1975) developing and unifying the rules for the design of structures. This work has culminated in a set of European standards called the Eurocodes which have recently been approved by member states.

The Construction Products Regulation established the basic requirements that all construction works must fulfil, namely: i) mechanical resistance and stability; ii) fire resistance; iii) hygiene, health and environment; iv) safety in use; v) protection against noise; vi) energy economy and heat retention and vii) sustainability. The first two requirements are addressed by the following nine Structural Eurocodes, produced by CEN (European Committee for Standardization) under the responsibility of its Technical Committee CEN/TC 250:

- EN 1990 Eurocode: Basis of Structural Design
- EN 1991 Eurocode 1: Actions on Structures
- EN 1992 Eurocode 2: Design of Concrete Structures
- EN 1993 Eurocode 3: Design of Steel Structures
- EN 1994 Eurocode 4: Design of Composite Steel and Concrete Structures
- EN 1995 Eurocode 5: Design of Timber Structures
- EN 1996 Eurocode 6: Design of Masonry Structures
- EN 1997 Eurocode 7: Geotechnical Design

- EN 1998 Eurocode 8: Design of Structures for Earthquake Resistance
- EN 1999 Eurocode 9: Design of Aluminium Structures

Each Eurocode contains provisions that are open for national determination. Such provisions include weather aspects, seismic zones, safety issues, etc. These are collectively called Nationally Determined Parameters (NDP). It is the responsibility of each member state to specify each NDP in a National Annex that accompanies each Eurocode.

The Structural Eurocodes are not, by themselves, sufficient for the construction of structures. Complementary information is required on:

- the products used in construction ("Product Standards", of which there are currently about 500);
- the tests used to establish behaviour ("Testing Standards", of which there are currently around 900);
- the execution standards used to fabricate and erect structures ("Execution Standards").

EN 1993, Eurocode 3: Design of Steel Structures (abbreviated in this document to EC3) is divided in the following parts:

- EN 1993-1 General rules and rules for buildings
- EN 1993-2 Steel bridges
- EN 1993-3 Towers, masts and chimneys
- EN 1993-4 Silos, tanks and pipelines
- EN 1993-5 Piling
- EN 1993-6 Crane supporting structures

EN 1993-1, Eurocode 3: Design of Steel Structures - General rules and rules for buildings is further sub-divided in the following 12 sub-parts:

- EN 1993-1-1 General rules and rules for buildings
- EN 1993-1-2 Structural fire design
- EN 1993-1-3 Cold-formed thin gauge members and sheeting
- EN 1993-1-4 Stainless steels
- EN 1993-1-5 Plated structural elements
- EN 1993-1-6 Strength and stability of shell structures
- EN 1993-1-7 Strength and stability of planar plated structures transversely loaded
- EN 1993-1-8 Design of joints
- EN 1993-1-9 Fatigue strength of steel structures
- EN 1993-1-10 Selection of steel for fracture toughness and through-thickness properties
- EN 1993-1-11 Design of structures with tension components made of steel
- EN 1993-1-12 Supplementary rules for high strength steel

EC3 is used together with a series of complementary standards. The execution standard for steel structures EN 1090-2 (2011) guarantees an execution quality that is compatible with the design assumption in EC3. The product standards provide the characteristic properties of the materials used, that in turn must conform to the quality control procedures specified in the test standards. Finally, the EC3 National Annexes specify the national parameters relating to actions and safety levels, as well as some options concerning design methodologies.

1.1.3 Basis of design

1.1.3.1 Basic concepts

Eurocode 3 must be used in a consistent way with EN 1990 Eurocode: Basis of structural design, EN 1991 Eurocode 1: Actions on Structures, EN 1998 Eurocode 8: Design of structures for earthquake resistance, and EN 1997 Eurocode 7: Geotechnical design.

Chapter 2 of EC3-1-1 introduces and complements the normative rules included in these standards. According to the basic requirements specified in EN 1990, a structure must be designed and executed so as to perform the functions for which it was conceived, for a pre-determined service life. This includes ensuring that the conditions that prevent failure (ultimate limit states) are verified, as well as conditions that guarantee proper performance in service (serviceability limit states) and those related to durability (among others, protection against corrosion). These basic requirements should be met by: i) the choice of suitable materials; ii) appropriate design and detailing of the structure and its components and iii) the specification of control procedures for design, execution and use.

The limit states shall be related to design situations, taking into account the circumstances under which the structure is required to fulfil its function. According to EN 1990 (2002) these situations may be: i) persistent design situations (conditions of normal use of the structure); ii) transient design situations (temporary conditions); iii) accidental design situations (exceptional conditions, e.g. fire or explosion) and iv) seismic design situations. Time dependent effects, such as fatigue, should be related to the design working life of the structure.

The Ultimate Limit States (ULS) correspond to states associated with failure of the structure, endangering people's safety; in general, the following ultimate limit states are considered: loss of equilibrium considering the structure as a rigid body, failure by excessive deformation, transformation of the structure or any part of it into a mechanism, rupture, loss of stability and failure caused by fatigue or other time-dependent effects.

The Serviceability Limit States (SLS) correspond to a state beyond which the specific service conditions, such as the functionality of the structure, the comfort of people and acceptable appearance are no longer met; in steel structures, limit states of deformation and of vibration are normally considered.

The requirements for limit state design are, in general, achieved by the partial factor method as described in section 6 of EN 1990; as an alternative, a design directly based on probabilistic methods, as described in Annex C of EN 1990, may be used.

In a design process, the loading on the structure must be quantified and the mechanical and geometrical properties of the material must be accurately defined; these topics are described in the subsequent sub-sections.

The effects of the loads for the design situations considered must be obtained by suitable analysis of the structure, according to the general requirements specified in section 5 of EN 1990.

For the design of a structure in circumstances where: i) adequate calculation models are not available; ii) a large number of similar components are to be used or iii) to confirm a design of a structure or a component, EN 1990 (Annex D) allows the use of design assisted by testing. However, design assisted by test results shall achieve the level of reliability required for the relevant design situation.

1.1.3.2 Basic variables

Introduction

The basic variables involved in the limit state design of a structure are the actions, the material properties and the geometric data of the structure and its members and joints.

When using the partial factor method, it shall be verified that, for all relevant design situations, no relevant limit state is exceeded when design values for actions or effects of actions and resistances are used in the design models.

Actions and environmental influences

The actions on a structure may be classified according to their variation in time: i) permanent actions (self-weight, fixed equipment, among others); ii) variable actions (imposed loads on building floors, wind, seismic and snow loads); and iii) accidental loads (explosions or impact loads). Certain actions, such as seismic actions and snow loads may be classified as either variable or accidental depending on the site location. Actions may also be classified according to: i) origin (direct or indirect actions); ii) spatial variation (fixed or free) and iii) nature (static or dynamic).

For the selected design situations, the individual actions for the critical load cases should be combined according to EN 1990. Load combinations are based on the design values of actions. The design values of actions F_d are obtained from the representative values F_{rep}. In general, their characteristic values F_k are adopted, considering adequate partial safety factors γ_f, through the expression:

$$F_d = \gamma_f F_{rep} . \tag{1.1}$$

The characteristic values of actions (permanent, variable or accidental actions) shall be specified as a mean value, an upper or a lower value, or even a nominal value, depending on the statistical distribution; for variable actions, other representative values shall be defined: combination values, frequent values and quasi-permanent values, obtained from the characteristic values, through the factors ψ_0, ψ_1 and ψ_2, respectively. These factors are defined according to the type of action and structure.

The design effects of an action, such as internal forces (axial forces, bending moments, shear forces, among others), are obtained by suitable methods of analysis, using the adequate design values and combinations of actions as specified in the relevant parts of EN 1990.

The environmental influences that could affect the durability of a steel structure shall be considered in the choice of materials, surface protection and detailing.

The classification and the quantification of all actions for the design of steel structures, including more specific examples such as the seismic action or the fire action, shall be obtained according to the relevant parts of EN 1990 and EN 1991.

Material properties

The material properties should also be represented by upper or lower characteristic values; when insufficient statistical data are available, nominal values may be taken as the characteristic values. The design values of the material properties are obtained from the characteristic values divided by appropriate partial safety factors γ_M, given in the design standards of each material, Eurocode 3 in the case of steel structures. The values of the partial safety factors γ_M, may vary depending on the failure mode and are specified in the National Annexes.

The recommended values in EC3-1-1 for the partial safety factors γ_{Mi} are the following: γ_{M0} = 1,00; γ_{M1} = 1,00 and γ_{M2} = 1,25.

The values of the material properties shall be determined from standard tests performed under specified conditions.

All steel is produced in several grades and according to different production processes and chemical compositions, as specified in EN 10020 (2000). In Europe, hot-rolled steel plating or profiles for use in welded, bolted or riveted structures must be produced in conformity with EN 10025-1 (2004). The first part of this European standard specifies the general technical delivery conditions for hot-rolled products. The specific requirements, such as classification of the main quality classes of steel grades in accordance with EN 10020 (2000), is given in parts 2 to 6 of EN 10025; these parts refer to the technical delivery conditions of the following steel products: non-alloy structural steels; normalized/normalized rolled weldable fine grain structural steels; thermo-mechanical rolled weldable fine grain structural steels; structural steels with improved atmospheric corrosion resistance; flat products of high yield strength structural steels in the quenched and tempered condition. Structural hollow sections and tubes must be specified in accordance with EN 10210 (2006) and EN 10219 (2006). According to EN 10025, the steel products are divided into grades, based on the minimum specified yield strength at ambient temperature, and qualities based on specified impact energy requirements. EN 10025 also specifies the test methods, including the preparation of samples and test pieces, to verify the conformity relating to the previous specifications.

The main material specifications imposed by EN 10025 for hot rolled products are: i) the chemical composition determined by a suitable physical or chemical analytical method; ii) mechanical properties: tensile strength, yield strength (or 0,2% proof strength), elongation after failure and impact strength; iii) technological properties, such as weldability, formability, suitability for hot-dip zinc-coating and machinability; iv) surface properties; v) internal soundness; vi) dimensions, tolerances on dimensions and shape, mass.

Connecting devices, such as bolts, nuts, are in general manufactured from high strength steels, in accordance with EN 15048-1 (2007) for non-preloaded connections or EN 14399-1 (2005) for preloaded connections.

Geometrical data

The geometry of a structure and its components must be evaluated with sufficient accuracy. Geometrical data shall be represented by their characteristic values or directly by their design values. The design values of geometrical data, such as dimensions of members that are used to assess action effects and resistances, may be, in general, represented by nominal values. However, geometrical data, referring to dimensions and form, must comply with tolerances established in applicable standards.

The main hot-rolled products are: I and H sections, box sections, channels, tees, angles, plates, among others. Alternatively it is possible to obtain welded sections with various cross section configurations. By the cold-form process it is possible to make a wide variety of sections.

All the steel products to be used in steel structures should fulfil geometrical tolerances (on dimensions and shape) dependent on the forming process. EN 1090-2 (2011) establishes two types of tolerances: i) essential tolerances – applicable for a range of criteria that are essential for the mechanical resistance and stability of the structure and ii) functional tolerances – required to fulfil other criteria such as fit-up and appearance of the structure. In specific cases special tolerances may be specified.

1.1.3.3 Ultimate limit states

For a structure, in general, the ultimate limit states to be considered are: loss of static equilibrium, internal failure of the structure or its members and joints, failure or excessive deformation of the ground and fatigue failure. In a steel structure, the ultimate limit state referring to internal failure involves the resistance of cross sections, the resistance of the structure and its members to instability phenomena and the resistance of the joints.

In general, the verification of the ultimate limit states consists of the verification of the condition:

$$E_d \leq R_d \,, \tag{1.2}$$

where E_d is the design value of the effect of actions, such as internal forces and R_d represents the design value of the corresponding resistance.

The design values of the effects of actions E_d shall be determined by combining the values of actions that are considered to occur simultaneously. EN 1990 specifies the following three types of combinations, and each one includes one leading or one accidental action:

i) combinations of actions for persistent or transient design situations (fundamental combinations);
ii) combinations of actions for accidental design situations;
iii) combinations of actions for seismic design situations.

The criteria for the establishment of these combinations and the values of all the relevant factors are defined in EN 1990 and its Annex A.

The verification of the ultimate limit state of loss of static equilibrium of the structure, considered as a rigid body, shall be verified comparing the design effect of destabilising actions with the design effect of stabilising actions. Other specific ultimate limit states, such as failure of the ground or fatigue failure, have to be verified according to the relevant rules specified in EN 1990 (EN 1997 and EN 1993-1-9).

1.1.3.4 Serviceability limit states

As defined before, the serviceability limit states correspond to a state beyond which the specific service conditions are no longer valid; in steel structures limit states of deformation and of vibration are normally considered.

The verification of the serviceability limit states consists of the verification of the condition:

$$E_d \leq C_d \,, \tag{1.3}$$

where E_d is the design value of the effect of actions specified in the serviceability criterion, determined by the relevant combinations, and C_d is the limiting design value of the relevant serviceability criterion (e.g. design value of a displacement).

The design values of the effects of actions E_d in the serviceability criterion shall be determined by one of the following three types of combinations specified in EN 1990 and its Annex A:

- characteristic combinations;
- frequent combinations;
- quasi-permanent combinations.

The limit values of the parameters for the verification of the serviceability limit states, according to EC3-1-1, section 7 and to EN 1990 – Basis of Structural Design, must be agreed between the client and the designer, and can also be specified in the National Annexes.

1.1.3.5 Durability

Clause 2.4 of EN 1990 defines the requirements for the durability of structures. For steel structures (chapter 4 of EC3-1-1), the durability depends on the effects of corrosion, mechanical wear and fatigue; consequently, the parts most susceptible should be easy to access, inspect, operate and maintain.

When building structures are not subjected to relevant cyclic loads it is not necessary to consider the resistance to fatigue, as it would be in the case of loads resulting from lifts, rolling bridges or vibrations of machines.

The durability of a steel structure depends essentially on its protection against corrosion. Corrosion is a chemical process of degradation of the steel, which grows in the presence of humidity, oxygen and existing pollutant particles in the environment.

1.1.3.6 Sustainability

Steel is one of the most sustainable materials on earth due to its natural properties. Steel is the most recyclable material in the world. It can be recycled over and over again without losing its properties, saving natural resources and reducing construction waste in landfills, thus minimizing two major problems faced by the construction sector.

However, it is not only the environmentally-friendly properties of steel that contribute to its sustainability credentials. Steel structures also have an important role to play. Steel structures are durable. With proper design, a steel structure can last for many years beyond its initial service life. The durability of steel, associated with the adaptability of steel structures, avoids the need for demolition and new construction.

In terms of impact on the environment, steel structures have major advantages: i) the prefabrication of steel frames provides a safer and cleaner working environment and minimizes the pollution and noise on the construction site; ii) frame elements are delivered in time for installation minimizing the area needed for storage and contributing to an efficient construction site; iii) prefabrication ensures accurate dimensions and ease of erection; iv) waste during construction is reduced to a minimum and most waste is recyclable.

1.2 Global analysis

1.2.1 Structural modelling

Steel structures are very often composed by linear members. The Figure 1.1 illustrates the structural framework of a steel industrial building.

In many applications two-dimensional elements, such as slabs in buildings, coexist with linear members. The slabs may be reinforced concrete, composite steel-concrete or prestressed concrete. Other common two-dimensional elements are concrete walls in buildings and slabs in decks of composite steel-concrete bridges (in reinforced concrete or steel orthotropic solutions).

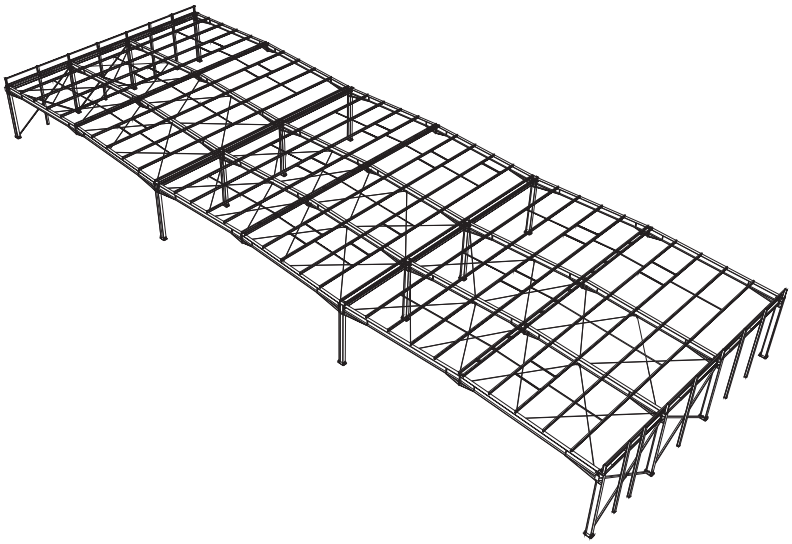

Figure 1.1 Industrial building

The modelling of steel structures using linear elements involves the consideration of several specific aspects such as the choice of the structural axis of a member, the influence of eccentricities, non-prismatic and curved members and the modelling of joints. This option is obviously adequate for linear members (beams, columns, bracing and cables). With a degree of approximation it may also be possible to model two-dimensional elements in this way, provided that the analysis results are sufficiently accurate for the intended purpose. Whenever deemed necessary, it is possible to analyse and design steel structures using the finite element method (FEM), combining in the modelling of the structure linear elements with two and three-dimensional elements.

1.2.2 Structural analysis

1.2.2.1 Introduction

In accordance with EC3-1-1 (EN 1993-1-1, 2005), the global analysis of a steel structure should provide with sufficient accuracy the internal forces and moments and the corresponding displacements. Analysis is to be based on appropriate calculations models (clause 5.1.1(1)) and the model and the basic assumptions should reflect the structural behaviour (clause 5.1.1(2)). In particular, it should ensure that the relevant non-linearities for a given limit state are adequately taken into account.

The internal forces and displacements may be determined using either a global elastic analysis or a global plastic analysis (clause 5.4.1(1)). Finite element analysis is also possible but it is not specifically covered in EC3-1-1, reference being made to EC3-1-5 (EN 1993-1-5, 2006).

Global elastic analysis is based on the assumption of a linear stress-strain relation for steel, whatever the stress level in the structure is (clause 5.4.2(1)). In practical terms, global elastic analysis assumes that the reference stress caused by the applied forces is lower than the yield stress of steel anywhere in the structure. Elastic global analysis may be used in all cases (clause 5.4.1(2)), provided that the provisions in clause 5.1 are met. It is noted that even though the internal forces and displacements are obtained using elastic analysis, the design resistance of the members may be evaluated on the basis of the plastic cross section resistance (clause 5.4.2(2)). A detailed practical example of a multi-storey building designed using global elastic analysis is presented in section 2.3.

Global plastic analysis assumes progressive yielding of some cross sections of the structure, normally leading to plastic hinges and a redistribution of forces within the structure. In this type of analysis it is mandatory that the cross sections where plastic hinges occur possess sufficient rotation capacity. Usually, the adopted stress-strain relation for steel is a bi-linear elastic-plastic relationship, although more precise relationships may be adopted (clause 5.4.3(4)). The use of plastic global analysis is subjected to several conditions and is detailed elsewhere (Simões da Silva et al., 2013).

Global analysis may also be of 1st or 2nd order. In a first order analysis, the internal forces and displacements are obtained with reference to the undeformed structure (clause 5.2.1(1)). In a 2nd order analysis, the influence of the deformation of the structure is taken into account. This should be considered whenever it increases the action effects significantly or modifies significantly the structural behaviour (clause 5.2.1(2)). The presence of compressive forces or stresses may induce 2nd order effects, amplifying internal forces and displacements. In terms of global analysis, it is then required to assess the structural stability of the frame, an aspect that will be detailed in the next section. A second situation where the deformed geometry of the structure must be taken into account occurs whenever the structure or parts of it present low stiffness, such as is the case of structures containing cables. In this case, a large-displacement analysis (or third-order analysis in german terminology) should be carried out (Simões da Silva et al., 2013).

Global analysis must also explicitly model imperfections, both at global level and member level, although some simplified procedures exist to avoid direct modelling of some imperfections. Also, the effects of shear lag and of local buckling on the stiffness should be taken into account if this significantly influences the global analysis (clause 5.2.1(5)). EC3-1-5 presents detailed procedures for such situations.

The choice of the analysis procedure (elastic or plastic, clause 5.4.1(1)), should take into account all the aspects discussed above (non-linear material behaviour, 2nd order effects and imperfections), aiming to achieve a good compromise between safety and simplicity of the calculation procedures. Some of these aspects are discussed in the following sections. Elastic 1st order analysis is the usual choice for most practitioners. However, in many cases, it does not ensure results on the safe side. A number of simplified procedures based on 1st order analysis were therefore developed to incorporate non-linearities and imperfections (Simões da Silva et al., 2013).

1.2.2.2 Structural stability of frames

Introduction

Steel structures are usually slender structures when compared to alternatives using other materials. Instability phenomena are potentially present, so that it is normally necessary to verify the global stability of the structure or of part of it. This verification leads to the need to carry out a 2nd order analysis, with the consideration of imperfections (clause 5.2.2(2)). There is a multiplicity of ways to assess 2nd order effects including imperfections. In general terms and according to clause 5.2.2(3), the different procedures can be categorized according to the following three methods (clause 5.2.2(3)):

- global analysis directly accounts for all imperfections (geometrical and material) and all 2nd order effects (method 1);
- global analysis partially accounts for imperfections (global structural imperfections) and 2nd order effects (global effects), while individual stability checks on members (clause 6.3) intrinsically account for member imperfections and local 2nd order effects (method 2);

- in basic cases, individual stability checks of equivalent members (clause 6.3), using appropriate buckling lengths corresponding to the global buckling mode of the structure (method 3).

Normally, it is usual to sub-divide the 2nd order effects into *P*-δ effects for members and *P*-Δ effects for the structure. *P*-δ effects correspond to the effects of the displacements along the length of a member (see Figure 1.2), while *P*-Δ effects correspond to the effects of the displacements at the ends of the members, also illustrated in Figure 1.2.

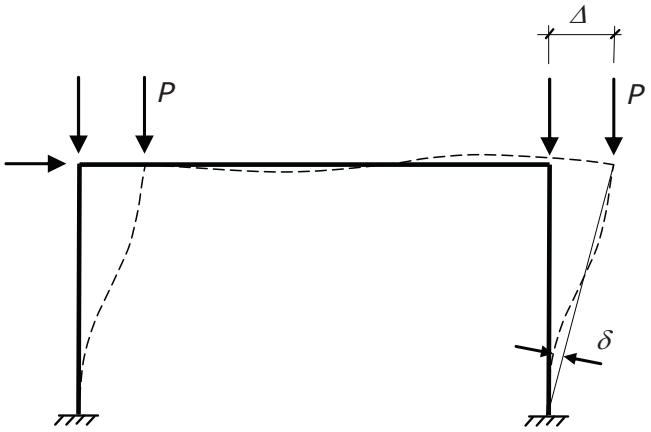

Figure 1.2 Typical displacements Δ and δ

This subdivision helps to understand the three methods described above. In fact, both the *P*-δ and the *P*-Δ effects can be approximately accounted for, through individual verifications of the stability of equivalent members (method 3). However, especially with respect to *P*-Δ effects, this method requires an accurate determination of the buckling modes and the corresponding equivalent lengths, as well as a structural behaviour in which the first buckling mode is dominant. It is therefore understandable that EC3 limits the application of this method to simple cases. It must also be pointed out that, in this method, imperfections are exclusively considered in the context of clause 6.3 in the verification of the stability of members.

Method 1 is the most sophisticated method because the global analysis, commonly called GMNIA (Geometrical and Material Non-linear Analysis with Imperfections), accounts for the 2nd order effects, as well as the global imperfections of the structure and local imperfections of the members. According to clause 5.2.2(7), if 2nd order effects in individual members and relevant member imperfections are totally accounted for in the global analysis of the structure, no individual stability check for the members according to clause 6.3 is necessary. However, either because of its complexity, or for the volume of work that it requires, this method still does not constitute the preferential option in design.

Method 2 constitutes the usual design procedure. The *P*-δ effects and the local member imperfections are incorporated in the normative expressions for the stability of members, whereas the *P*-Δ effects are directly evaluated by global analysis and the global imperfections are explicitly considered in the analysis of the structure. The individual stability of members should be checked according to the relevant criteria in clause 6.3 for the effects not included in the global analysis (clause 5.2.2(7)). This verification may be based on a buckling length equal to the system length as a safe estimate, although the non-sway buckling length may also be used.

2nd order effects increase not only the displacements but also the internal forces, in comparison to 1st order behaviour. It is thus necessary to assess if this increase is

relevant and, if so, to calculate (exactly or approximately) the real forces and displacements in the structure.

Usually, the sensitivity of a structure to 2nd order effects is assessed indirectly using the elastic critical load of the structure, F_{cr}. This assessment must be done for each load combination, through the ratio between the critical load and the corresponding applied loading (F_{cr}/F_{Ed}). EC3-1-1 requires the consideration of 2nd order effects whenever (clause 5.2.1(3)):

$$\alpha_{cr} = F_{cr}/F_{Ed} \leq 10 \quad \text{(in elastic analysis);} \tag{1.4}$$

$$\alpha_{cr} = F_{cr}/F_{Ed} \leq 15 \quad \text{(in plastic analysis).} \tag{1.5}$$

It is noted that a greater limit for α_{cr} for plastic analysis is given because structural behaviour may be significantly influenced by non-linear material properties in the ultimate limit state (e.g. where a frame forms plastic hinges with moment redistribution or where significant non-linear deformations arise from semi-rigid joints). EC3 allows National Annexes to give a lower limit for α_{cr} for certain types of frames where substantiated by more accurate approaches.

The elastic critical load of the structure, F_{cr}, may be determined analytically, or numerically, using commercial software. Alternatively, the critical loads can be calculated using approximate methods (Simões da Silva et al., 2013).

Second order analysis

The 2nd order analysis of structures invariably requires the use of computational methods, including step-by-step or other iterative procedures (clause 5.2.2(4)). Convergence of the results should be explicitly checked by imposing adequate error limits on the geometrical non-linear calculations. Finally, the results should be compared with a reference first order elastic analysis to ensure that the amplified internal forces and displacements are within expected limits.

In order to allow quicker approaches, approximate methods have been developed which, in many cases, estimate the exact results with acceptable error. Generically, the approach is through a linear combination of buckling modes of the structure to provide amplification methods of 1st order results (Simões da Silva et al., 2013), typically illustrated in the following equations for frames that are susceptible of instability in a sway mode:

$$d_{ap}^{II} = \left(d^{I} - d_{AS}^{I}\right) + \left(1 - \frac{1}{\alpha_{cr.AS}}\right)^{-1} d_{AS}^{I}; \tag{1.6}$$

$$M_{ap}^{II} = \left(M^{I} - M_{AS}^{I}\right) + \left(1 - \frac{1}{\alpha_{cr.AS}}\right)^{-1} M_{AS}^{I}; \tag{1.7}$$

$$V_{ap}^{II} = \left(V^{I} - V_{AS}^{I}\right) + \left(1 - \frac{1}{\alpha_{cr.AS}}\right)^{-1} V_{AS}^{I}; \tag{1.8}$$

$$N_{ap}^{II} = \left(N^{I} - N_{AS}^{I}\right) + \left(1 - \frac{1}{\alpha_{cr.AS}}\right)^{-1} N_{AS}^{I}, \tag{1.9}$$

where index *ap* means approximate, index *AS* denotes the anti-symmetric "sway" mode, *d*, *M*, *V* and *N* denote, respectively, displacement, bending moment, shear force and axial force.

This procedure provides the general framework for several simplified methods to assess 2nd order effects, allowing if necessary for the development of plasticity.

1.2.2.3 Imperfections

In steel structures, irrespective of the care taken in their execution, there are always imperfections, such as: residual stresses, eccentricities in joints, eccentricities of load, lack of verticality and lack of linearity in members (clause 5.3.1(1)). These imperfections are responsible for the introduction of additional secondary forces that must be taken into account in the global analysis and in the design of the structural elements. The type and amplitude of all imperfections are bounded by the tolerances specified in the execution standards (EN 1090-2, 2011).

According to EC3-1-1, the imperfections should be incorporated in the analysis preferably in the form of equivalent geometric imperfections, with values which reflect the possible effects of all types of imperfections (clause 5.3.1(2)). Unless these effects are already included in the resistance formulae for member design, the following imperfections should be taken into account: i) global imperfections of the frame and ii) local imperfections of the members (clause 5.3.1(3)).

Imperfections for global analysis should be considered with the shape and direction that lead to the most adverse effects. So, the assumed shape of global and local imperfections may be derived from the elastic buckling mode of a structure in the plane of buckling considered (clauses 5.3.2(1)). Account should be taken of both in-plane and out-of-plane buckling including torsional buckling with symmetric and asymmetric buckling shapes (clause 5.3.2(2)).

1.2.2.4 Classification of cross sections

The local buckling of cross sections affects their resistance and rotation capacity and must be considered in design. The evaluation of the influence of local buckling of a cross section on the resistance or ductility of a steel member is complex. Consequently, a deemed-to-satisfy approach was developed in the form of cross section classes that greatly simplify the problem.

According to clause 5.5.2(1), four classes of cross sections are defined, depending on their rotation capacity and ability to form rotational plastic hinges:

- Class 1 cross sections are those which can form a plastic hinge with the rotation capacity required from plastic analysis without reduction of the resistance;
- Class 2 cross sections are those which can develop their plastic resistance moment, but have limited rotation capacity because of local buckling;
- Class 3 cross sections are those in which the stress in the extreme compression fibre of the steel member, assuming an elastic distribution of stresses, can reach the yield strength. However, local buckling is liable to prevent development of the plastic resistance moment;
- Class 4 cross sections are those in which local buckling will occur before the attainment of yield stress in one or more parts of the cross section.

The bending behaviour of members with cross sections of classes 1 to 4 is illustrated in Figure 1.3, where M_{el} and M_{pl} are, respectively, the elastic moment and the plastic moment of the cross section.

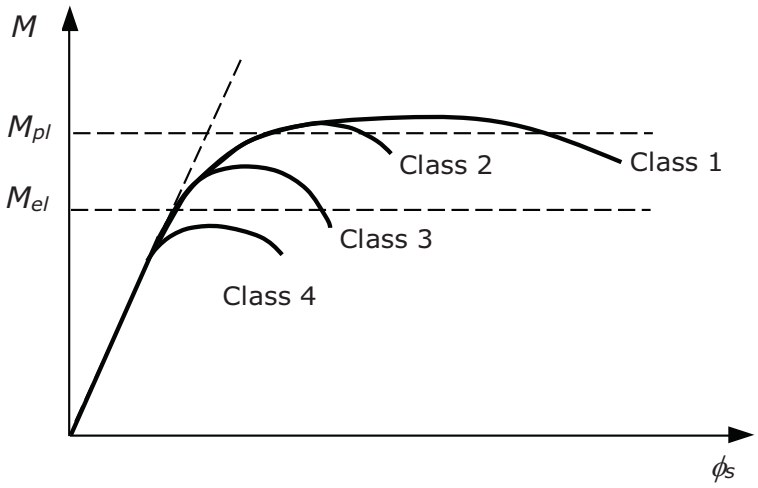

Figure 1.3 Cross section behaviour in bending

The classification of a cross section depends on the width to thickness ratio c/t of the parts subjected to compression (clause 5.5.2(3)), the applied internal forces and the steel grade. Parts subject to compression include every part of a cross section which is either totally or partially in compression under the load combination considered (clause 5.5.2(4)). The limiting values of the ratios c/t of the compressed parts are indicated in Table 1.1, Table 1.2 and Table 1.3 that reproduce Table 5.2 of EC3-1-1. In these tables, the various columns refer to the different types of stress distributions in each part of the cross section (webs or flanges); the steel grade is taken into account through the parameter $\varepsilon = (235/f_y)^{0,5}$, where f_y is the nominal yield strength.

The various compressed parts in a cross section (such as a web or flange) can, in general, be in different classes (clause 5.5.2(5)). In general, a cross section is classified according to the highest (least favourable) class of its compressed parts (clause 5.5.2(6)). For I or H cross sections and rectangular hollow sections, two types of compressed parts are defined: internal compressed parts (classified according to Table 1.1) and outstand flanges (classified according to Table 1.2); angles and tubular sections are classified according to Table 1.3. A cross section which fails to satisfy the limits for class 3 should be taken as class 4 (clause 5.5.2(8)).

EC3-1-1 envisages some exceptions to the general procedure for the classification of cross sections described in the previous paragraph: i) cross sections with a class 3 web and class 1 or 2 flanges may be classified as class 2 cross sections with an effective web in accordance with 6.2.2.4 (clause 5.5.2(11)); ii) whenever the web is considered to resist shear forces only and is assumed not to contribute to the bending and normal force resistance of the cross section, the section may be designed as class 2, 3 or 4, depending only on the flange class (clause 5.5.2(12)).

Table 1.1 Maximum width-to-thickness ratios for internal compression parts

Internal compression parts			
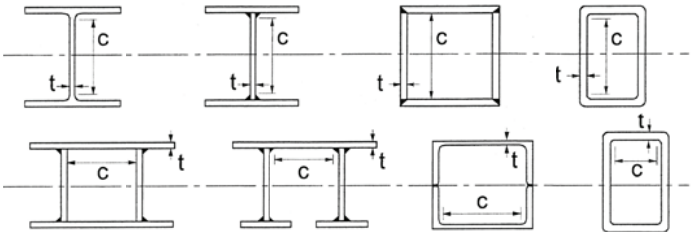			
Class	Part subjected to bending	Part subjected to compression	Part subjected to bending and compression
Stress distribution (compression +ve)	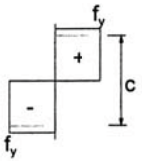	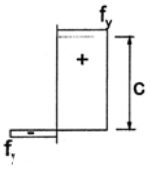	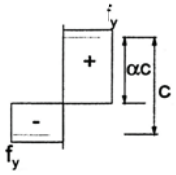
1	$c/t \le 72\varepsilon$	$c/t \le 33\varepsilon$	if $\alpha > 0{,}5$, $c/t \le \dfrac{396\varepsilon}{13\alpha - 1}$ if $\alpha \le 0{,}5$, $c/t \le \dfrac{36\varepsilon}{\alpha}$
2	$c/t \le 83\varepsilon$	$c/t \le 38\varepsilon$	if $\alpha > 0{,}5$, $c/t \le \dfrac{456\varepsilon}{13\alpha - 1}$ if $\alpha \le 0{,}5$, $c/t \le \dfrac{41{,}5\varepsilon}{\alpha}$
Stress distribution (compression +ve)	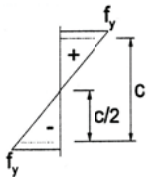	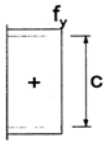	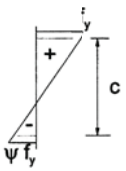
3	$c/t \le 124\varepsilon$	$c/t \le 42\varepsilon$	if $\Psi > -1$, $c/t \le \dfrac{42\varepsilon}{0{,}67 + 0{,}33\Psi}$ if $\Psi \le -1$ *), $c/t \le 62\varepsilon(1-\Psi)\sqrt{(-\Psi)}$

$\varepsilon = \sqrt{235/f_y}$	f_y (N/mm^2)	235	275	355	420	460
	ε	1,00	0,92	0,81	0,75	0,71

*) $\Psi \le -1$ applies where either the compression stress $\sigma < f_y$ or the tensile strain $\varepsilon_y > f_y/E$.

Table 1.2 Maximum width-to-thickness ratios of outstand flanges

<table>
<tr><td colspan="7">Outstand flanges
 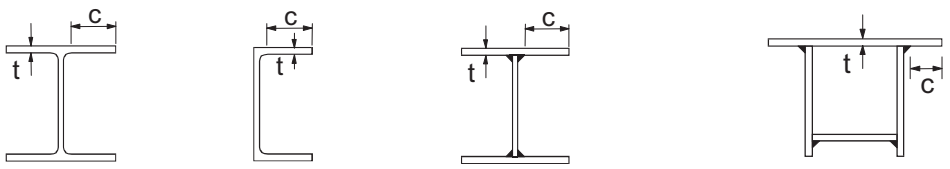
Rolled sections Welded sections</td></tr>
<tr><td rowspan="2">Class</td><td rowspan="2">Part subjected to compression</td><td colspan="5">Part subjected to bending and compression</td></tr>
<tr><td colspan="2">Tip in compression</td><td colspan="3">Tip in tension</td></tr>
<tr><td>Stress distribution
(compression +ve)</td><td> 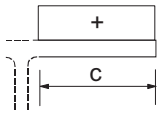 </td><td colspan="2"> 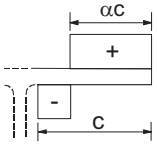 </td><td colspan="3"> 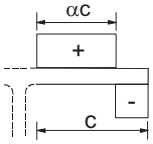 </td></tr>
<tr><td>1</td><td>$c/t \le 9\varepsilon$</td><td colspan="2">$c/t \le \frac{9\varepsilon}{\alpha}$</td><td colspan="3">$c/t \le \frac{9\varepsilon}{\alpha\sqrt{\alpha}}$</td></tr>
<tr><td>2</td><td>$c/t \le 10\varepsilon$</td><td colspan="2">$c/t \le \frac{10\varepsilon}{\alpha}$</td><td colspan="3">$c/t \le \frac{10\varepsilon}{\alpha\sqrt{\alpha}}$</td></tr>
<tr><td>Stress distribution
(compression +ve)</td><td> 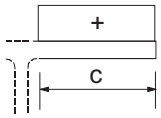 </td><td colspan="2"> 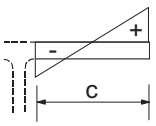 </td><td colspan="3"> 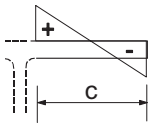 </td></tr>
<tr><td>3</td><td>$c/t \le 14\varepsilon$</td><td colspan="5">$c/t \le 21\varepsilon\sqrt{k_\sigma}$
For k_σ see EN 1993-1-5</td></tr>
<tr><td rowspan="2">$\varepsilon = \sqrt{235/f_y}$</td><td>$f_y$ (N/mm^2)</td><td>235</td><td>275</td><td>355</td><td>420</td><td>460</td></tr>
<tr><td>ε</td><td>1,00</td><td>0,92</td><td>0,81</td><td>0,75</td><td>0,71</td></tr>
</table>

According to EC3-1-1, the classification of a cross section is based on its maximum resistance to the type of applied internal forces, independent from their values. This procedure is straightforward to apply for cross sections subject to compression forces or bending moment, acting separately. However, in the case of bending and axial force, there is a range of *M-N* values that correspond to the ultimate resistance of the cross section. Consequently, there are several values of the parameter α (limit for classes 1 and 2) or the parameter ψ (limit for class 3), both being dependent on the position of the neutral axis. Bearing in mind this additional complexity, simplified procedures are often adopted, such as: i) to consider the cross section subjected to compression only, being

the most unfavourable situation (too conservative in some cases); or ii) to classify the cross section based on an estimate of the position of the neutral axis based on the applied internal forces. Example 6 (section 1.3.5) uses an alternative approach for the classification of cross sections submitted to a combination of axial force and bending moment (Greiner et al., 2011).

Rolled sections of usual dimensions (HEA, HEB, IPE, etc.) belong, in general, to classes 1, 2 or 3. Class 4 cross sections are typical of plate girders and cold-formed sections. Class 4 cross sections are characterized by local buckling phenomena, preventing the cross section from reaching its elastic resistance.

Table 1.3 Maximum width-to-thickness ratios of angles and tubular sections

<table>
<tr><td colspan="7">See also Table 1.2
Angles
 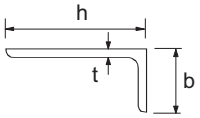

Does not apply to angles in continuous contact with other components</td></tr>
<tr><td>Class</td><td colspan="6">Section in compression</td></tr>
<tr><td>Stress distribution (compression +ve)</td><td colspan="6"> 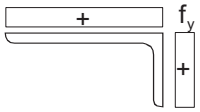
</td></tr>
<tr><td>3</td><td colspan="6">$h / t \le 15\varepsilon$: $\dfrac{b+h}{2t} \le 11{,}5\varepsilon$</td></tr>
<tr><td colspan="7">Tubular sections
 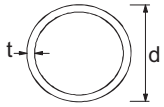
</td></tr>
<tr><td>Class</td><td colspan="6">Section in bending and/or compression</td></tr>
<tr><td>1</td><td colspan="6">$d / t \le 50\varepsilon^2$</td></tr>
<tr><td>2</td><td colspan="6">$d / t \le 70\varepsilon^2$</td></tr>
<tr><td>3</td><td colspan="6">$d / t \le 90\varepsilon^2$
NOTE: For $d / t > 90\varepsilon^2$ see EN 1993-1-6</td></tr>
<tr><td rowspan="3">$\varepsilon = \sqrt{235 / f_y}$</td><td>$f_y$ (N/mm^2)</td><td>235</td><td>275</td><td>355</td><td>420</td><td>460</td></tr>
<tr><td>ε</td><td>1,00</td><td>0,92</td><td>0,81</td><td>0,75</td><td>0,71</td></tr>
<tr><td>ε^2</td><td>1,00</td><td>0,85</td><td>0,66</td><td>0,56</td><td>0,51</td></tr>
</table>

1.2.3 Case-study building – elastic design of a braced steel framed building

1.2.3.1 Introduction

The building analysed in this case-study (**Example 1**) is based in the steel-framed structure shown in Figure 1.4, a building used as a test facility and erected at Cardington (UK), in 1993. The structure was designed as a typical modern multi-storey office building.

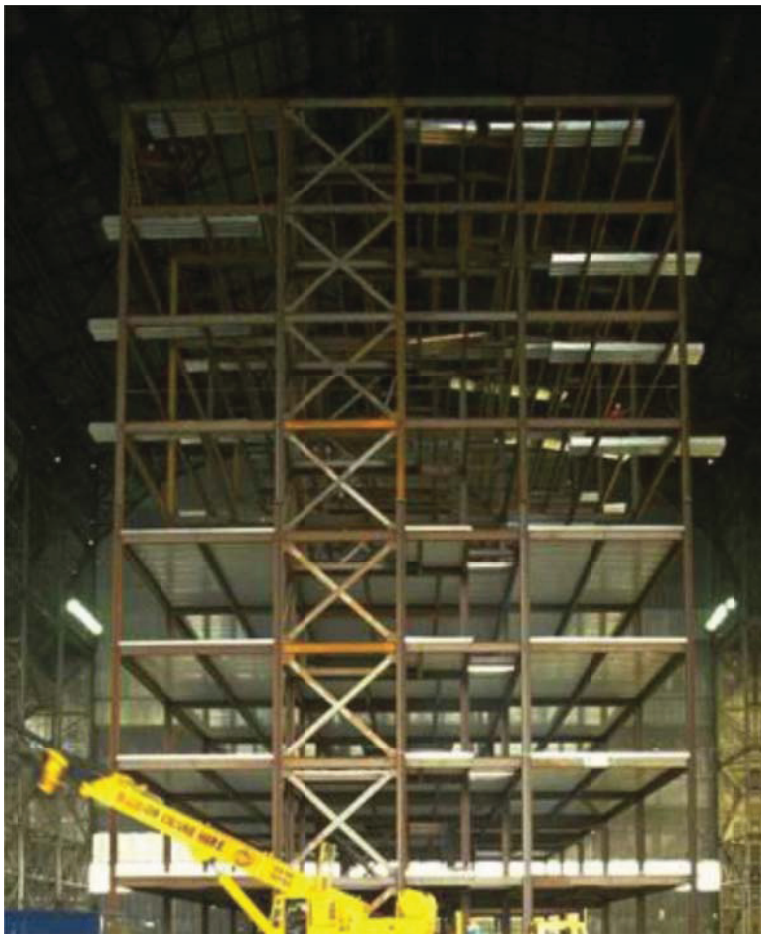

Figure 1.4 Side elevation view

The building has an area of 21 m by 45 m and a total height of 33 m. Along the length, there are 5 bays, each 9 m long. Across the width there are 3 bays of 6 m, 9 m and 6 m. The building has 8 storeys. The height of the first storey is 4,335 m from the ground floor to the top-of-steel height. All the other storeys have a height of 4,135 m from top-of-steel to top-of-steel.

On the south elevation there is a two storey ground floor atrium, 9 m x 8 m. At each side of the building there is a 4 m x 4,5 m void, to provide fireman's access and an escape stairwell. Additionally, on the west side, there is another 4 m x 2 m void, for a goods lift. In the middle of the building there's a central lift core, 9 m x 2,5 m. Figure 1.5 represents the typical floor plan of the building. All slabs are lightweight composite slabs with a thickness of 130 mm.

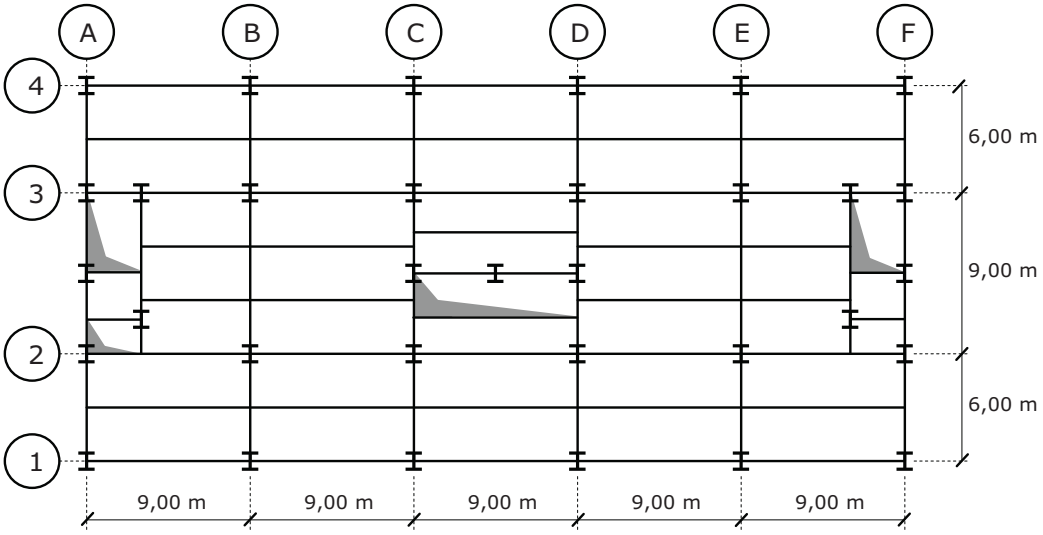

Figure 1.5 Plan of the 3rd to 7th floor

1.2.3.2 Description of the structure

The structure is designed as a braced frame with lateral restraint provided by cross bracing of flat steel plates, around the three vertical access shafts. Figure 1.6, Figure 1.7 and Figure 1.8 and Table 1.4, Table 1.5 and Table 1.6 represent the various structural floor plans and the geometry of the beams.

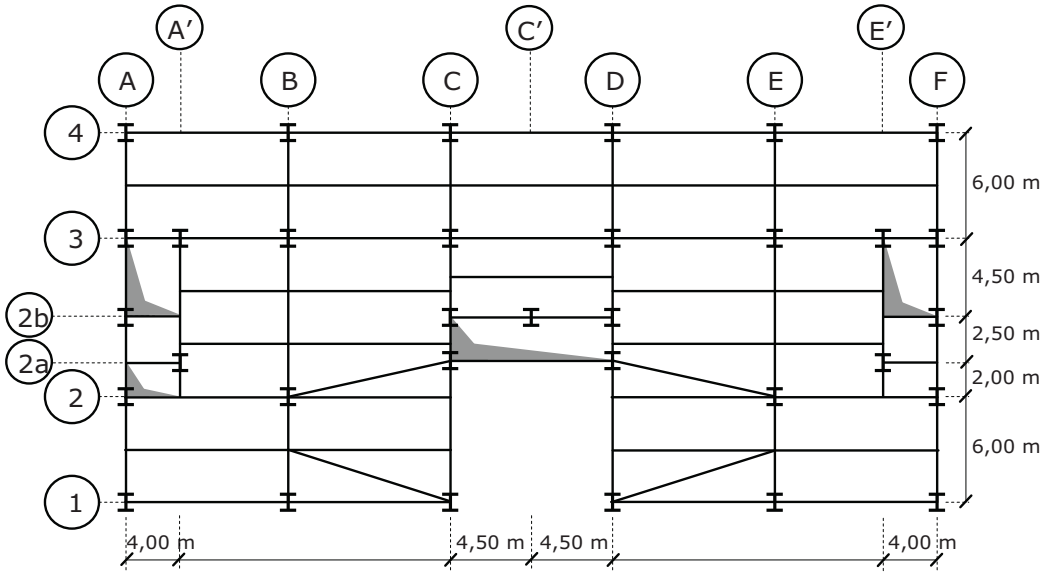

Figure 1.6 Plan of the 1st floor

Table 1.4 Geometric characteristics of the beams (1st floor)

Beams	Cross-section	Steel grade
A1 – F1, A4 – F4	IPE 400	S 355
A1 – A4, B1 – B2, B3 – B4, C2a – C4, D2a – D4, E1 – E2, E3 – E4, F1 – F4	IPE 400	S 355
C1 – C2a, D1 – D2a	IPE 600	S 355
B2 – B3, E2 – E3	IPE 600	S 355
A2 – B2, A2a – A'2a, A2b – A'2b, A3 – A'3, A'2 - A'3	IPE 400	S 355
E'2a – E'3, E'2b – F2b, E'3 – F3	IPE 400	S 355
C2a – D2a, C2b – D2b, C3 – D3	IPE 400	S 355
All others secondary beams	IPE 360	S 355

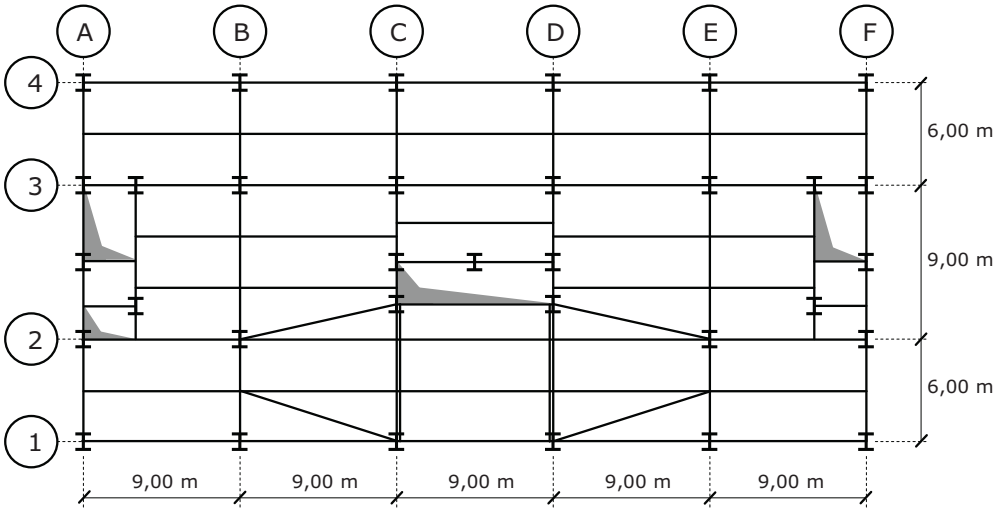

Figure 1.7 Plan of the 2nd floor

Table 1.5 Geometric characteristics of the beams (2nd floor)

Beams	Cross-section	Steel grade
A1 – F1, A4 – F4	IPE 400	S 355
A1 – A4, B1 – B2, B3 – B4, C2a – C4, D2a – D4, E1 – E2, E3 – E4, F1 – F4	IPE 400	S 355
C1 – C2a, D1 – D2a	2 x HEA 700	S 355
B2 – B3, E2 – E3	IPE 600	S 355
A2 – B2, A2a – A'2a, A2b – A'2b, A3 – A'3, A'2 - A'3	IPE 400	S 355
E'2a – E'3, E'2b – F2b, E'3 – F3	IPE 400	S 355
C2a – D2a, C2b – D2b, C3 – D3	IPE 400	S 355
All others secondary beams	IPE 360	S 355

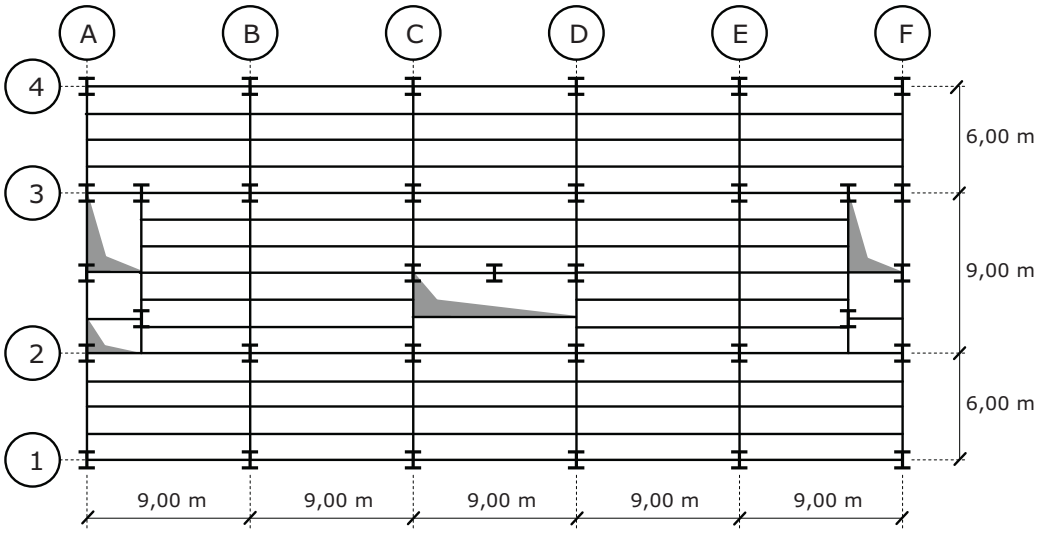

Figure 1.8 Plan of the 8th floor

Table 1.6 Geometric characteristics of the beams (3rd to 8th floor)

Beams	Cross-section	Steel grade
A1 – F1, A4 – F4	IPE 400	S 355
A1 – A4, B1 – B2, B3 – B4, C1 – C4, D1 – D4, E1 – E2, E3 – E4, F1 – F4	IPE 400	S 355
B2 – B3, E2 – E3	IPE 600	S 355
A2 – B2, A2a – A'2a, A2b – A'2b, A3 – A'3, A'2 - A'3	IPE 400	S 355
E'2a – E'3, E'2b – F2b, E'3 – F3	IPE 400	S 355
C2a – D2a, C2b – D2b, C3 – D3	IPE 400	S 355
All others secondary beams	IPE 360	S 355

Table 1.7 details the geometrical characteristics of the columns (S 355).

Table 1.7 Geometric characteristics of the columns

Columns	Ground floor – 2nd floor	2nd floor – 5th floor	5th floor – 8th floor
B2, C2, D2, E2, C2b, C'2b, D2b, B3, C3, D3, E3	HEB 340	HEB 320	HEB 260
	Ground floor – 4th floor	4th floor – 8th floor	
B1, C1, D1, E1, A2, F2, A3, F3, B4, C4, D4, E4, A'2a, A2b, A'3, E'2a, F2b, E'3	HEB 320	HEB 260	
	Ground floor – 8th floor		
A1, A4, F1, F4	HEB 260		

1.2.3.3 General safety criteria, actions and combinations of actions

General safety criteria

Actions are classified, according to EN 1990, by their variation in time as: i) permanent actions (G) (e.g. self-weight), ii) variable actions (Q) (e.g. imposed loads on buildings floors, wind loads, snow loads) and iii) accidental actions (A) (e.g. explosions).

The actions considered in this design example are described in the following paragraphs. All actions are quantified according to the relevant parts of EN 1991-1. In addition, the recommended values are always adopted whenever the specific choice is left to the National Annexes.

Permanent actions

The permanent actions include the self-weight of the structural elements and also the non-structural elements, such as coverings, partitions, thermal insulation, etc.

The self-weight of the structural elements includes the weight of the steel structure (78,5 kN/m^3) and the self-weight of a lightweight concrete slab (12,5 kN/m^3) with a constant thickness of 130 mm.

Imposed loads

The characteristic value of the imposed load depends of the category of the loaded area of the building. For an office building and according to Table 6.1 of EN 1991-1-1 (2002), the category of the loaded area is B, the corresponding characteristic values being given by: q_k = 2,0 to 3,0 kN/m^2 and Q_k = 1,5 to 4,5 kN. q_k is intended for the determination of global effects and Q_k for local effects. According to EN 1991-1-1, the characteristic value of the imposed load is given by the National Annexes; however, the recommended values are underlined.

Accessible roofs with occupancy according to category B are categorized according to clause 6.3.4.1 (Table 6.9 of EN 1991-1-1) as category I. In this case, the imposed load for the roof is given in Table 6.2 for the category of loaded area B: q_k = 2,0 to 3,0 kN/m^2 and Q_k = 1,5 to 4,5 kN.

In buildings with fixed partitions, their self-weight should be taken into account as a permanent load. In the case of movable partitions, and provided that the floor allows for lateral distribution of loads, their self-weight may be taken into account as a uniformly distributed load, q_k, that must be added to the imposed load on the floor (clause 6.3.1.2 (8) of EN 1991-1-1). In this design example, the partition walls were considered to be movable with a self-weight less than 1 kN/m per wall length, so that the value of the corresponding uniformly distributed load is 0,5 kN/m^2 (clause 6.3.1.2(8) of EN 1991-1-1).

Wind actions

i) Wind forces

The quantification of the wind actions on the building follows EN 1991-1-4 (2005). Two main directions are assumed for the wind: θ = 0° and θ = 90°. According to clause 5.3(3), the wind forces are calculated by the vectorial summation of the external forces, $F_{w,e}$, and the internal forces, $F_{w,i}$, given by Eqns. (1.10) and (1.11), respectively:

$$F_{w,e} = c_s c_d \sum_{surfaces} w_e \, A_{ref} \; ; \tag{1.10}$$

$$F_{w,i} = \sum_{surfaces} w_i \, A_{ref} \, , \tag{1.11}$$

where $c_s c_d$ is the structural factor, A_{ref} is the reference area of the individual surfaces, and w_e and w_i are the external and internal pressures on the individual surfaces at reference heights z_e and z_i, respectively for external and internal pressures, given by Eqns. (1.12) and (1.13),

$$w_e = q_p(z_e) c_{pe} \, ; \tag{1.12}$$

$$w_i = q_p(z_i) c_{pi} \, , \tag{1.13}$$

$q_p(z)$ is the peak velocity pressure, and c_{pe} and c_{pi} are the pressure coefficients for the external and internal pressures, respectively.

The structural factor $c_s c_d$ is defined in clause 6.1(1). For multi-storey steel buildings with rectangular plan layout and vertical external walls, with regular distribution of stiffness and mass, the structural factor, $c_s c_d$, may be taken from Annex D of EN 1991-1-4. For h = 33 m and b = 21 m (θ = 0º), $c_s c_d$ = 0,95, and for b = 45 m (θ = 90º), $c_s c_d$ = 0,89.

ii) Calculation of reference height

The reference heights, z_e, for vertical windward walls of rectangular plan buildings (see Figure 1.9 and Figure 1.10) depend on the aspect ratio h/b and are always the upper heights of the different parts of the walls (clause 7.2.2(1)). For θ = 0º (see Figure 1.11), b = 21 m < h = 33 m < 2b = 42 m, therefore the height of the building may be considered in two parts, comprising a lower part extending upwards from the ground to a height equal to b and an upper part consisting of the remainder. The resulting shape of the velocity pressure profile is shown in see Figure 1.9.

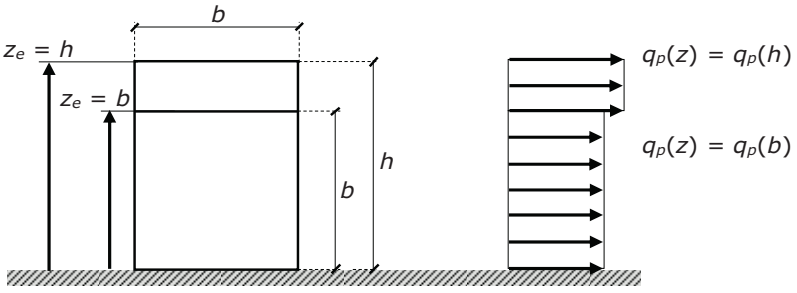

Figure 1.9 Velocity pressure distribution on face D (θ = 0º)

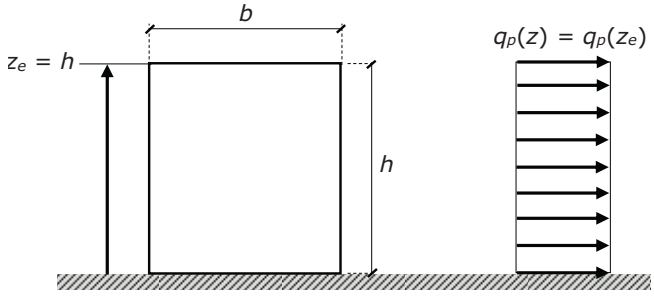

Figure 1.10 Velocity pressure distribution on face D (θ = 90º)

For θ = 90º (see Figure 1.12), h = 33 m < b = 45 m, and the shape of the velocity pressure profile is shown in Figure 1.10 and should be considered to be one part.

For the determination of the velocity pressure distribution for the leeward wall and sidewalls (faces A, B, C and E) the reference height may be taken as the height of the building.

iii) Calculation of external and internal pressure coefficients

External and internal pressure coefficients are determined according to clause 7.2 of EN 1991-1-4. Internal and external pressures shall be considered to act at the same time (clause 7.2.9). The worst combination of external and internal pressures shall be considered.

According to clause 7.2.2(2), the façades are divided in different pressure zones, defined as a function of e, where e is the lesser of b or 2h. For wind direction θ = 0º (see Figure 1.11):

e = min (21; 66) = 21 m < d = 45 m

and for wind direction θ = 90º (see Figure 1.12):

e = min (45; 66) = 45 m > d = 21 m.

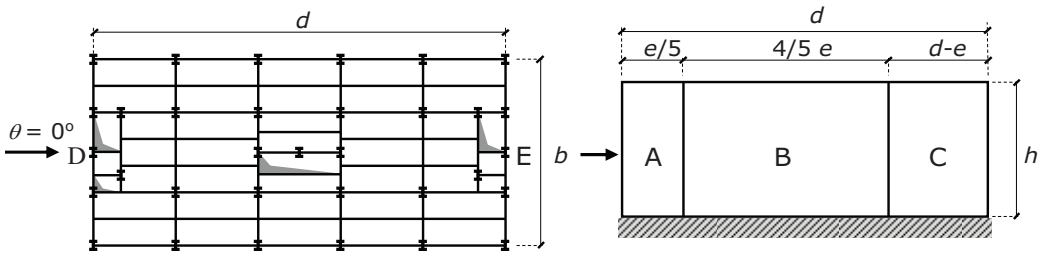

Figure 1.11 Pressure zones for wind direction θ = 0º

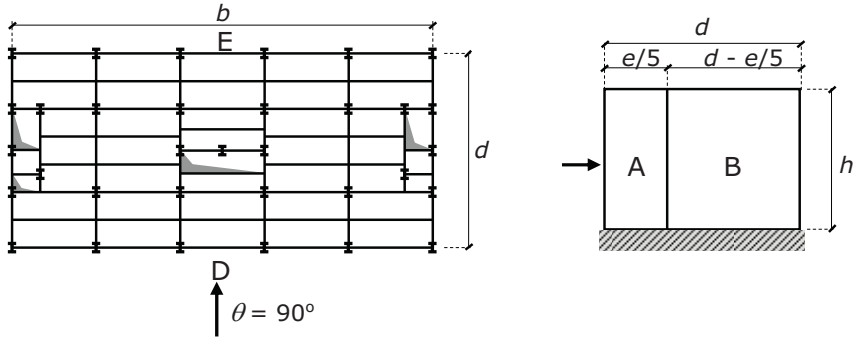

Figure 1.12 Pressure zones for wind direction θ = 90º

The resulting external pressure coefficients, c_{pe}, for zones A, B, C, D and E are obtained from Table 7.1 of EN 1991-1-4 and are represented in Table 1.8.

Table 1.8 External pressure coefficients c_{pe}

	zone	A	B	C	D	E
$\theta = 0^O$	h/d = 0,73	-1,20	-0,80	-0,50	+0,76	-0,43
$\theta = 90^O$	h/d = 1,57	-1,20	-0,80	-	+0,80	-0,53

According to clause 7.2.2(3), the lack of correlation of wind pressures between the windward and leeward sides may be taken into account by multiplying the resulting force by a factor, f, that depends on the relation h/d for each case. Therefore, by linear interpolation between f = 1,0 for $h/d \geq 5$ and f = 0,85 for $h/d \leq 1$, the following factors are obtained: for θ = 0º, f = 0,84, and for θ = 90º, f = 0,87.

The internal pressure coefficients, c_{pi}, depend on the size and distribution of the openings in the building envelope. For buildings without a dominant face and where it is not possible to determine the number of openings, then c_{pi} should be taken as the more onerous of +0,2 and -0,3.

Considering the values for external pressure coefficients from Table 1.8, the external and internal pressure coefficients are represented in Figure 1.13a and b, respectively, for θ = 0º and θ = 90º, according to the worst case for each face of the building.

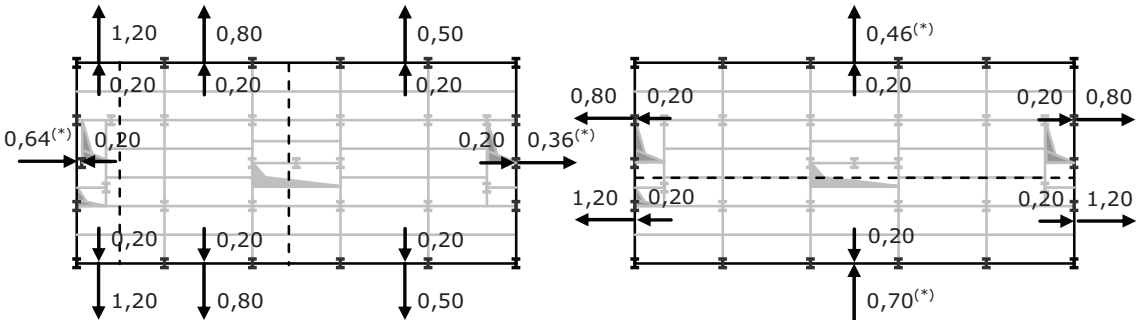

a) θ = 0º b) θ = 90º

Figure 1.13 External and internal coefficients

(*) the values for faces D and E are obtained by multiplying the external coefficient by f = 0,84 for θ = 0º and f = 0,87 for θ = 90º.

iv) Calculation of the peak velocity pressure $q_p(z)$

The peak velocity pressure $q_p(z)$, at height z, is given by the following equation (clause 4.5 of EN 1991-1-4):

$$q_p(z) = \left[1 + 7I_v(z)\right]\frac{1}{2}\rho v_m^2(z) = c_e(z)\, q_b \,, \tag{1.14}$$

where $I_v(z)$ is the turbulence intensity, ρ is the air density, $v_m(z)$ is the mean wind velocity, $c_e(z)$ is the exposure factor and q_b is the basic velocity pressure. Both options in Eqn. (1.14) may be used to calculate the peak velocity pressure. In this design example only the first will be applied, because EN 1991-1-4 only provides one graph for a limited range of cases for the direct determination of the exposure factor.

The air density ρ depends on the altitude, temperature and barometric pressure to be expected in the region during wind storms. EN 1991-1-4 recommends the value 1,25 kg/m^3.

v) Calculation of mean wind velocity (v_m)

The mean wind velocity is given by (clause 4.3.1 of EN 1991-1-4),

$$v_m(z) = c_r(z)\, c_o(z)\, v_b \,, \tag{1.15}$$

where $c_r(z)$ is the roughness factor and $c_o(z)$ is the orography factor, taken as 1,0 unless otherwise specified in clause 4.3.3, and v_b is the basic wind velocity. The roughness factor is specified in clause 4.3.2 and is given by:

$$\begin{cases} c_r(z) = k_r \ln\left(\dfrac{z}{z_0}\right) \Leftarrow z_{\min} \le z \le z_{\max} \\ c_r(z) = c_r(z_{\min}) \Leftarrow z < z_{\min}\,, \end{cases} \tag{1.16}$$

z_{max} may be taken as 200, z_{min} is the minimum height, z_0 is the roughness length, both defined in Table 4.1 of EN 1991-1-4 as a function of the terrain category, and k_r is the terrain factor, depending on the roughness length z_0 and given by:

$$k_r = 0{,}19\left(\frac{z_0}{z_{0,II}}\right), \tag{1.17}$$

where $z_{0,II}$ = 0,05 m. The basic wind velocity v_b is calculated from (clause 4.2):

$$v_b = c_{dir}\, c_{season}\, v_{b,0}\,, \tag{1.18}$$

where c_{dir} and c_{season} are directional and seasonal factors, respectively, which may be given by the National Annexes. The recommended value, for each case, is 1. The fundamental value of the basic wind velocity, $v_{b,0}$, is also given in the National Annexes as a function of the regional wind maps. Assuming $v_{b,0}$ = 30 m/s, then $v_b = v_{b,0}$ = 30 m/s.

Assuming a terrain of category II (i.e., area with low vegetation and isolated obstacles), from Table 4.1 of EN 1991-1-4, $z_0 = z_{0,II}$ = 0,05 and z_{min} = 2 m, thus k_r = 0,19. From Eqn. (1.16), with $z_{min} < z = 33 < z_{max}$,

$$c_r(z = 33) = 0{,}19 \cdot \ln\left(\frac{33}{0{,}05}\right) = 1{,}23$$

and from Eqn. (1.15),

$$v_m(z = 33) = 1{,}23 \cdot 1{,}00 \cdot 30 = 36{,}9\,\text{m/s}\,.$$

For $z_{min} < z = 21 < z_{max}$,

$$c_r(z = 21) = 0{,}19 \cdot \ln\left(\frac{21}{0{,}05}\right) = 1{,}15$$

and from Eqn. (1.15),

$$v_m(z = 21) = 1{,}15 \cdot 1{,}00 \cdot 30 = 34{,}5\,\text{m/s}\,.$$

vi) Calculation of turbulence intensity (I_v)

The turbulence intensity is given by (clause 4.4(1) of EN 1991-1-4):

$$\begin{cases} I_v = \dfrac{k_I}{c_o(z)\ln\left(\dfrac{z}{z_0}\right)} \Leftarrow z_{\min} \le z \le z_{\max} \\ I_v = I_v(z_{\min}) \Leftarrow z < z_{\min}\,, \end{cases} \tag{1.19}$$

where k_I is the turbulence factor.

The recommended value for k_I is 1,0, thus for $z_{min} < z = 33 < z_{max}$,

$$I_v = \frac{1,0}{1,0 \cdot \ln\left(\frac{33}{0,05}\right)} = 0,15 ,$$

and for $z_{min} < z = 21 < z_{max}$,

$$I_v = \frac{1,0}{1,0 \cdot \ln\left(\frac{21}{0,05}\right)} = 0,17 .$$

Finally, from Eqn. (1.14), for z = 33 m and z = 21 m:

$$q_p(z=33) = \left[1+7 \cdot 0,15\right] \cdot \frac{1}{2} \cdot 1,25 \cdot 36,9^2 = 1744,56 \text{N/m}^2 = 1,74 \text{kN/m}^2 .$$

$$q_p(z=21) = \left[1+7 \cdot 0,17\right] \cdot \frac{1}{2} \cdot 1,25 \cdot 34,5^2 = 1629,16 \text{N/m}^2 = 1,63 \text{kN/m}^2 .$$

vii) Calculation of external and internal pressures

The external and internal pressures are obtained from Eqns. (1.12) and (1.13) are indicated in Table 1.9. Note that external pressures are already multiplied by the structural factor, $c_s c_d$, from Eqn. (1.10). In Figure 1.14 and Figure 1.15 the resulting values are represented for θ = 0º and θ = 90º.

Table 1.9 External and internal pressures

		A	B	C	D		E
					z < 21	z > 21	
θ = 0º	$c_s c_d\, w_e$	-1,98	-1,32	-0,83	+0,99	+1,06	-0,60
	w_i	+0,35	+0,35	+0,35	+0,33	+0,35	+0,35
θ = 90º	$c_s c_d\, w_e$	-1,85	-1,24	-	+1,08		-0,71
	w_i	+0,35	+0,35	-	+0,35		+0,35

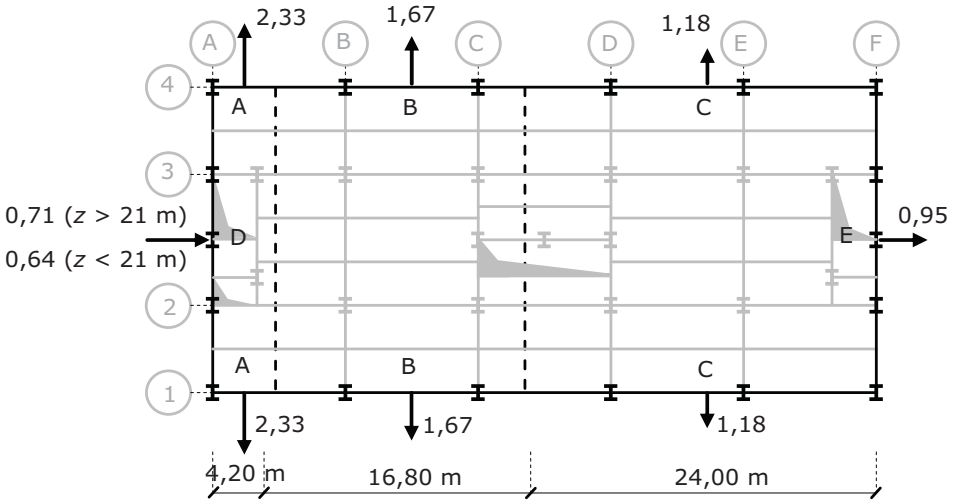

Figure 1.14 Wind pressures (kN/m²) on walls, θ = 0º

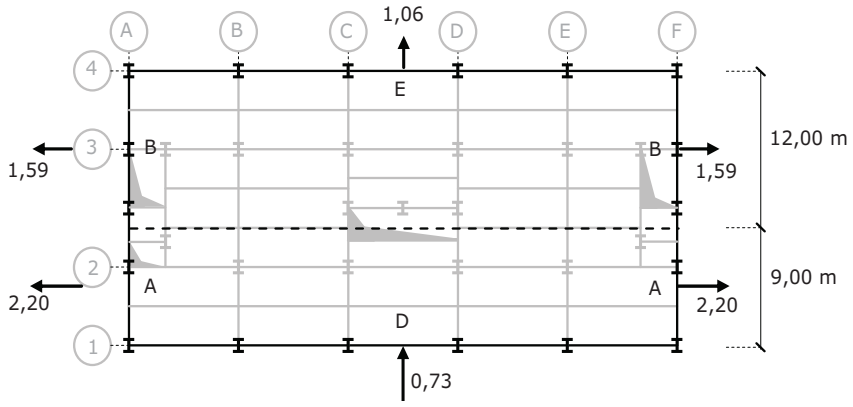

Figure 1.15 Wind pressures (kN/m^2) on walls, θ = 90º

Summary of basis actions

The resulting actions for this design example are summarized in Table 1.10.

Table 1.10 Summary of actions

Action no.	Description	Type	Value
LC1	Self-weight of structural elements	Permanent action	varies
LC2	Imposed load on office buildings (Cat. B)	Variable action	q_k^1 = 3,0 kN/m^2
LC3	Movable partitions	Variable action	q_k^2 = 0,5 kN/m^2
LC4	Wind direction θ = 0°	Variable action	varies (see Figure 1.14)
LC5	Wind direction θ = 90°	Variable action	varies (see Figure 1.15)

Frame imperfections

Frame imperfections are considered as equivalent horizontal loads, according to clause 5.3.2 of EC3-1-1. Thus, global initial sway imperfections are given by:

$$\phi = \phi_0 \, \alpha_h \, \alpha_m \,, \tag{1.20}$$

where: ϕ_0 = 1/200 ;

α_h is the reduction factor for height *h*, given by $\alpha_h = 2/\sqrt{h}$ but $2/3 \le \alpha_h \le 1{,}0$;

h is the height of the structure (in meters);

α_m is the reduction factor for the number of columns in a row, given by:

$$\alpha_m = \sqrt{0{,}5\left(1 + \frac{1}{m}\right)} ;$$

and *m* is the number of columns in a row.

Hence, for this structure, *h* = 33 m and α_h = 0,67. The number of columns changes according to the frame considered. In Table 1.11, the initial imperfection (ϕ) for each frame is presented.

Table 1.11 Initial imperfections

Frame	m	ϕ
A	7	0,00253
B	4	0,00265
C	5.5	0,00258
D	5.5	0,00258
E	4	0,00265
F	7	0,00253
1	6	0,00256
2	8	0,00251
2b	5	0,00259
3	8	0,00251
4	6	0,00256

The equivalent horizontal load at each floor is given by:

$$H_{Ed} = V_{Ed}\,\phi\ , \tag{1.21}$$

where V_{Ed} is the total design vertical load in each floor. The design vertical load in each floor is given by LC1 and LC2 + LC3. The relevant values, in each direction, are listed in Table 1.12 and Table 1.13. These values are added to the relevant combinations.

Table 1.12 Equivalent horizontal forces in transversal frames

Frame		kN	1st floor	2nd floor	3rd - 7th floor	8th floor
A	L1	V_{Ed}	165,1	218,1	206,8	214,8
		H_{Ed}	0,42	0,55	0,52	0,54
	LC2+LC3	V_{Ed}	208,7	269,2	264,9	241,2
		H_{Ed}	0,53	0,68	0,67	0,61
B	L1	V_{Ed}	406,9	387,8	373,4	390,6
		H_{Ed}	1,08	1,03	0,99	1,04
	LC2+LC3	V_{Ed}	682,6	648,4	636,3	511,5
		H_{Ed}	1,81	1,72	1,69	1,36
C	L1	V_{Ed}	254,4	412,3	373,2	401,4
		H_{Ed}	0,66	1,06	0,96	1,04
	LC2+LC3	V_{Ed}	355,4	582,5	540,9	477,4
		H_{Ed}	0,92	1,50	1,40	1,23
D	L1	V_{Ed}	254,4	412,3	362,3	401,3
		H_{Ed}	0,66	1,06	0,93	1,05
	LC2+LC3	V_{Ed}	355,2	582,2	563,6	476,9
		H_{Ed}	0,92	1,50	1,45	1,23
E	L1	V_{Ed}	406,6	388,1	374,0	391,6
		H_{Ed}	1,08	1,03	0,99	1,04
	LC2+LC3	V_{Ed}	682,9	649,8	638,4	514,5
		H_{Ed}	1,81	1,72	1,69	1,36
F	L1	V_{Ed}	179,5	228,9	217,0	224,6
		H_{Ed}	0,45	0,58	0,55	0,57
	LC2+LC3	V_{Ed}	238,2	299,7	294,1	265,1
		H_{Ed}	0,60	0,76	0,74	0,67

According to clause 5.3.2(8), the initial sway imperfections should be applied in all relevant horizontal directions, but they need only be considered in one direction at a time.

Table 1.13 Equivalent horizontal forces in longitudinal frames

Frame		kN	1st floor	2nd floor	3rd - 7th floor	8th floor
1	L1	V_{Ed}	265,1	560,6	301,7	314,6
		H_{Ed}	0,68	1,44	0,77	0,81
	LC2+LC3	V_{Ed}	383,2	832,1	474,9	400,9
		H_{Ed}	0,98	2,13	1,22	1,03
2	L1	V_{Ed}	554,4	506,4	553,9	629,9
		H_{Ed}	1,39	1,27	1,39	1,58
	LC2+LC3	V_{Ed}	833,7	757,1	914,2	810,5
		H_{Ed}	2,09	1,90	2,29	2,03
2b	L1	V_{Ed}	98,1	121,0	227,3	200,6
		H_{Ed}	0,25	0,31	0,59	0,52
	LC2+LC3	V_{Ed}	117,7	120,8	295,9	212,8
		H_{Ed}	0,30	0,31	0,77	0,55
3	L1	V_{Ed}	454,7	558,2	514,1	567,3
		H_{Ed}	1,14	1,40	1,29	1,42
	LC2+LC3	V_{Ed}	726,0	852,3	806,2	667,5
		H_{Ed}	1,82	2,14	2,02	1,68
4	L1	V_{Ed}	294,6	301,5	298,6	311,8
		H_{Ed}	0,75	0,77	0,76	0,80
	LC2+LC3	V_{Ed}	462,2	469,7	470,0	394,8
		H_{Ed}	1,18	1,20	1,20	1,01

Load combinations

The rules and methods for the definition of the load combination are given in Annex A1 of EN 1990.

The recommended values of the reduction factors ψ for the actions considered are indicated in Table 1.14 according to clause A1.2.2.

Table 1.14 Reduction factors ψ

Type of action	ψ_0	ψ_1	ψ_2
Imposed load in buildings: category B	0,7	0,5	0,3
Wind loads on buildings	0,6	0,2	0,0

Thus, the following load combinations are considered for the Ultimate Limit State (ULS) of resistance:

i) Combination 1

E_d1 = 1,35 LC1 + 1,5 [(LC2 + LC3) + 0,6 LC4].

ii) Combination 2

E_d2 = 1,35 LC1 + 1,5 [(LC2 + LC3) + 0,6 LC5].

iii) Combination 3

E_d3 = 1,00 LC1 + 1,5 LC4.

iv) Combination 4

E_d4 = 1,00 LC1 + 1,5 LC5.

v) Combination 5

E_d5 = 1,35 LC1 + 1,5 [LC4 + 0,7 (LC2 + LC3)].

vi) Combination 6

E_d6 = 1,35 LC1 + 1,5 [LC5 + 0,7 (LC2 + LC3)].

Other combinations for ULS may have been considered, however, they were not critical for the structure.

Regarding the serviceability limit states, limits for vertical deflections and sway are considered under the frequent values of the load combinations, considering a reversible limit state (Annex A1 of EN 1990):

i) Combination 7

E_d7 = 1,00 LC1 + 0,5 (LC2 + LC3).

ii) Combination 8

E_d8 = 1,00 LC1 + 0,2 LC4.

iii) Combination 9

E_d9 = 1,00 LC1 + 0,2 LC5.

iv) Combination 10

E_d10 = 1,00 LC1 + 0,2 LC4 + 0,3 (LC2 + LC3).

v) Combination 11

E_d11 = 1,00 LC1 + 0,2 LC5 + 0,3 (LC2 + LC3).

Additional load combinations should be considered for accidental design situations such as fire. Load combinations 12 to 14 are required for the fire design of the structure (Franssen and Vila Real, 2010), using the frequent value for the dominant variable action:

i) Combination 12

E_d12 = LC1 + 0,5 (LC2 + LC3).

ii) Combination 13

E_d13 = LC1 + 0,2 x LC4 + 0,3 (LC2 + LC3).

iii) Combination 14

E_d14 = LC1 + 0,2 LC5 + 0,3 (LC2 + LC3).

Load arrangements

According to clause 6.2.1(1) of EN 1991-1-1, for the design of a floor structure within one storey or a roof, the imposed load shall be taken into account as a free action applied at the most unfavourable part of the influence area of the action effects considered. Figure 1.16 represents the most unfavourable load arrangement for the imposed loads.

The distribution of the load to the secondary beams is represented in Figure 1.17.

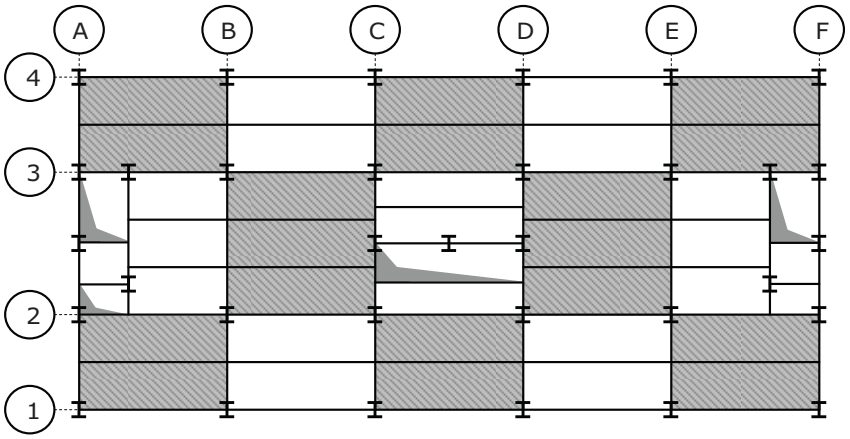

Figure 1.16 Load arrangement for the analysis of the shadow areas

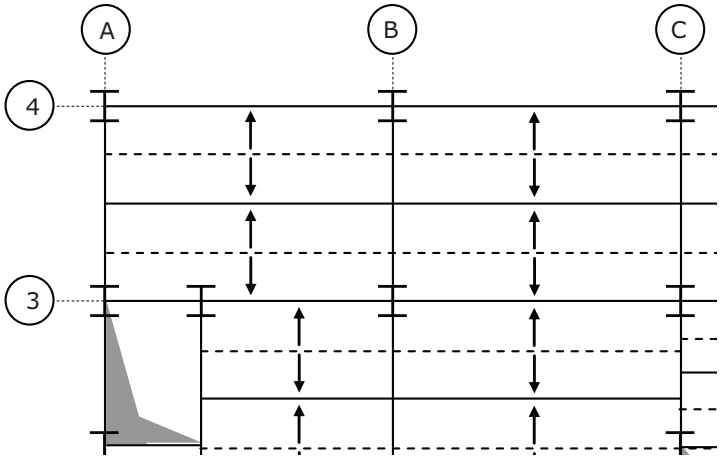

Figure 1.17 Load distribution in the secondary beams

For the design of the columns or the walls, loaded by several storeys, the total imposed loads on the floor of each storey should be assumed to be distributed uniformly over the whole floor area, but the total value may be reduced by a factor α_n according to the following expression (clause 6.3.1.2(11) of EN 1991-1-1)

$$\alpha_n = \frac{2 + (n-2)\,\psi_0}{n} = \frac{2 + (8-2)\cdot 0{,}70}{8} = 0{,}775S\,, \tag{1.22}$$

where n is the number of storeys (>2) and ψ_0 is given according to Annex A1 (Table A1.1) of EN 1990.

1.2.3.4 Structural analysis

Structural modelling

The structural model for the analysis is a 3D model, represented in Figure 1.18. All steel elements (columns, bracing elements and beams) are defined by beam elements. The main direction of the structure is in plane *zy*. Beams in plane *zy* are rigidly connected to the steel columns. Beams in plane *zx* are hinged at both ends. Elements defining the bracing system are also hinged at both ends.

Although the steelwork is the main supporting structure, the concrete slab has a strong influence on the global stiffness of the structure.

There are several ways of modelling the concrete slab. If the software allows the use of shell elements together with beam elements, then the slab can be modelled by those elements. However, proper attention needs to be given to the real behaviour of the composite structure; whether or not composite action arises through connection of the slab to the steel beams. If there is no composite action then the slab can be modelled by a horizontal bracing system, using beam elements connecting the main columns. The cross section of these elements needs to be equivalent to the stiffness provided by the real concrete slab. This simplified procedure was adopted in the example.

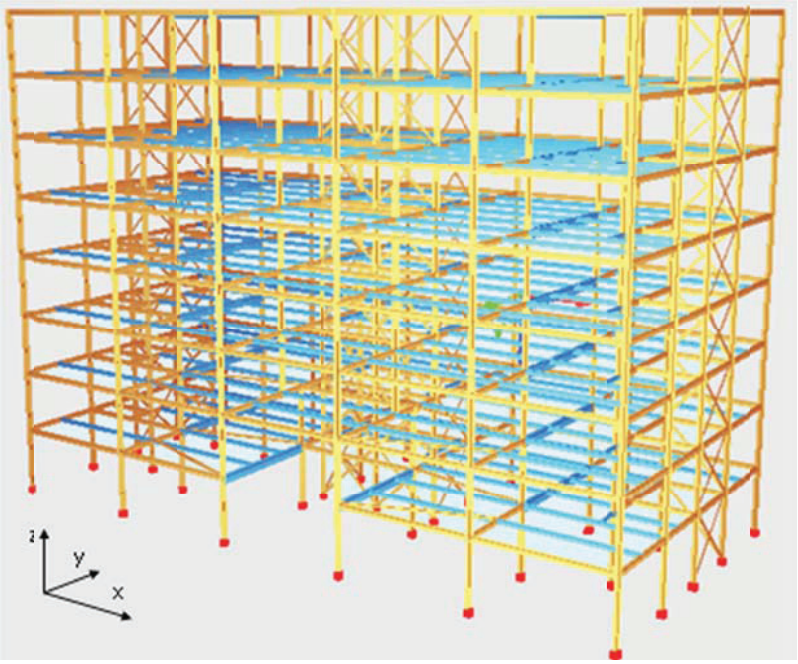

Figure 1.18 3D structural model

Linear elastic analysis

The linear elastic analysis was performed with a commercial structural analysis program and the internal forces and moments were determined.

Susceptibility to 2nd order effects: elastic critical loads

For design purposes, the internal forces and moments should be determined using a 2nd order analysis if relevant. Thus, the classification of the structure must be checked first. This is done by computing the elastic critical load factor (α_{cr}). Second-order effects must be considered whenever $\alpha_{cr} \leq 10$.

Numerical calculation of α_{cr}

In Table 1.15, the values of the first 5 elastic critical loads factors α_{cr} are indicated for each combination.

For combinations 1, 2, 5 and 6 the values of α_{cr} are smaller than 10. According to clause 5.2.1 of EC3-1-1, the frame requires a second-order analysis for load combinations 1, 2, 5 and 6. As a result, the 2nd order sway effects must be taken into consideration in the design and analysis. Moreover, combinations 1, 2 and 6 exhibit more than one buckling mode with a critical load factor lower than 10.

Figure 1.19 represents the 1st buckling mode for combination 1. The first buckling mode is clearly a local bucking mode. The same happens to the other critical load factors indicated in Table 1.15, although not represented graphically. This indicates that the structure is not very susceptible to 2nd order effects. Nevertheless, a 2nd order elastic analysis is performed to prove this statement.

Table 1.15 Elastic critical load factors

	α_{cr} 1	α_{cr} 2	α_{cr} 3	α_{cr} 4	α_{cr} 5
Combination 1	7,96	8,22	8,28	8,40	8,67
Combination 2	8,01	8,08	8,48	8,57	8,66
Combination 3	21,11	25,15	28,28	28,62	29,38
Combination 4	13,14	14,21	18,56	18,84	19,98
Combination 5	9,87	10,16	10,23	10,39	10,62
Combination 6	8,58	9,37	10,07	10,14	10,17

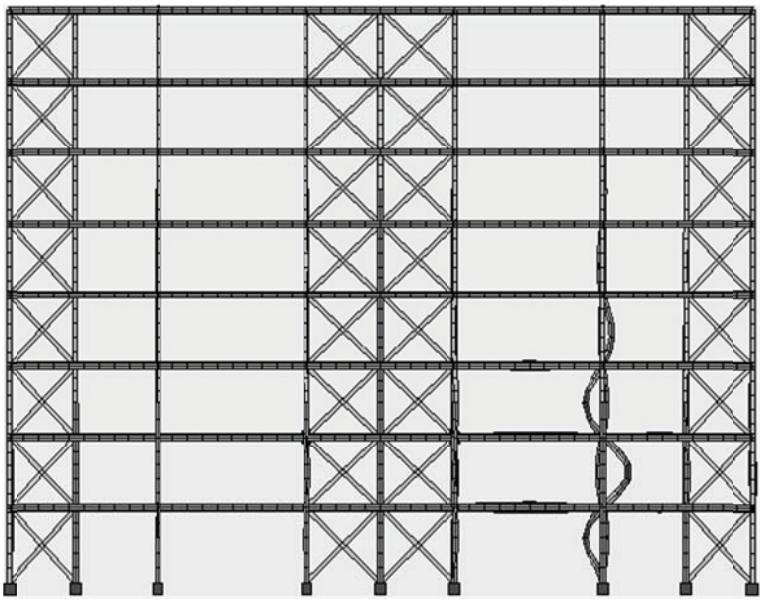

Figure 1.19 1st buckling mode for combination 1 – frontal view

Second order elastic analysis

Second order effects are calculated by a numerical analysis. In Table 1.16, the results obtained for load combination 1, using a 1st order and a 2nd order numerical analysis, are compared for column E1. For the bending moments, the moments at both ends of the elements are indicated.

The same comparison in made for beam E1 to E4 in 4th floor, and the results are indicated in Table 1.17.

Table 1.16 and Table 1.17 show that 2nd order effects are indeed negligible.

Table 1.16 Comparative results for column E1 (combination 1)

	1st Order		2nd Order			
	M_{Ed} (kNm)	N_{Ed} (kN)	M_{Ed} (kNm)	Δ (%)	N_{Ed} (kN)	Δ (%)
1st floor	25/14	1699	25/11	0/-21,4	1704	+0,3
2nd floor	62/47	1492	74/55	19,4/17,0	1496	+0,3
3rd floor	69/28	1261	69/29	0/3,6	1262	+0,1
4th floor	51/25	1052	54/28	5,9/12,0	1053	+0,1
5th floor	53/27	841	56/29	5,7/7,4	841	0
6th floor	54/29	630	57/32	5,6/10,3	630	0
7th floor	55/26	417	59/30	7,3/15,4	417	0
8th floor	69/63	201	72/66	4,3/4,8	201	0

Table 1.17 Comparative results for beam E1 to E4 (combination 1)

	1st Order		2nd Order			
	M_{Ed} (kNm)	N_{Ed} (kN)	M_{Ed} (kNm)	Δ (%)	N_{Ed} (kN)	Δ (%)
E1-E2	+114/-106	61	+114/-111	0/4,7	39	-36,1
E2-E3	+168/-269	155	+163/-256	-3,0/-4,8	139	-10,3
E3-E4	+113/-105	61	+114/-110	0,9/4,8	50	-18,0

1.3 Design of members

1.3.1 Introduction

This chapter contains the normative design rules and worked examples, in accordance with EC3-1-1, concerning the design of steel members. In general, the design of a steel member, for the various combinations of internal forces, is performed in two steps (Simões da Silva et al., 2013): i) cross section resistance and ii) member resistance.

1.3.1.1 Cross section resistance

The resistance of cross sections depends on their classes – class 1, 2, 3 or 4 in accordance with clause 6.2.1(3) of EC3-1-1. Cross section classes 1 and 2 reach their full plastic resistance, while class 3 cross sections only reach their elastic resistance. Class 4 cross sections are not able to reach their elastic resistance because of local buckling and they are outside the scope of the present chapter.

An elastic verification according to the elastic resistance may be carried out for all cross sectional classes provided that the effective cross sectional properties are used for the verification of class 4 cross sections (clause 6.2.1(4)). In the most general case and as a conservative approach, where local longitudinal, transverse and shear stresses coexist at the critical point of the cross section, the following yield criterion may be used in the context of an elastic verification (clause 6.2.1(5)).

$$\left(\frac{\sigma_{x,Ed}}{f_y/\gamma_{M0}}\right)^2+\left(\frac{\sigma_{z,Ed}}{f_y/\gamma_{M0}}\right)^2-\left(\frac{\sigma_{x,Ed}}{f_y/\gamma_{M0}}\right)\left(\frac{\sigma_{z,Ed}}{f_y/\gamma_{M0}}\right)+3\left(\frac{\tau_{Ed}}{f_y/\gamma_{M0}}\right)^2\le 1,0\,, \tag{1.23}$$

where $\sigma_{x,Ed}$ is the design value of the local longitudinal stress, $\sigma_{z,Ed}$ is the design value of the local transverse stress and τ_{Ed} is the design value of the local shear stress, all values at the point of consideration.

Another conservative approach (although less conservative than the previous), applicable to all cross section classes, consists in a linear summation of the utilization ratios for each stress resultant. For class 1, class 2 or class 3 cross sections subjected to a combination of N_{Ed}, $M_{y,Ed}$ and $M_{z,Ed}$ this method may be applied by using the following criterion (clause 6.2.1(7)):

$$\frac{N_{Ed}}{N_{Rd}}+\frac{M_{y,Ed}}{M_{y,Rd}}+\frac{M_{z,Ed}}{M_{z,Rd}}\le 1,0\,, \tag{1.24}$$

where N_{Rd}, $M_{y,Rd}$ and $M_{z,Rd}$ are the corresponding resistances.

Both previous approaches are in general conservative. Therefore it should only be performed where the interaction of on the basis of resistances N_{Rd}, M_{Rd}, V_{Rd} cannot be performed.

The properties of the gross cross section should be determined using the nominal dimensions. Holes for fasteners need not be deducted, but allowance should be made for larger openings.

Because of the existence of holes and other openings in tension zones (e.g. in bolted joints of tension members), it is necessary to define the net area of a cross section. Generally, it is defined as its gross area less appropriate deductions for all holes and other openings (clause 6.2.2.2(1)). For calculating net section properties, the deduction for a single fastener hole should be the gross cross sectional area of the hole in the plane of its axis (see Figure 1.20). For countersunk holes, appropriate allowance should be made for the countersunk portion (clause 6.2.2.2(2)).

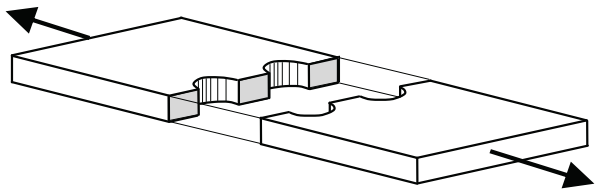

Figure 1.20 Net section

Cross sections with a class 3 web and flanges with class 1 or 2 may be classified and designed as class 2, considering a reduced effective area for the web. The effective area is obtained according to Figure 1.21 and the following iterative procedure: by replacing the portion of the web in compression by a part of $20\varepsilon t_w$ adjacent to the compression flange and another equal part adjacent to the plastic neutral axis of the effective cross section. Iteration results from the definition of the neutral axis as being that of the effective section (Figure 1.21).

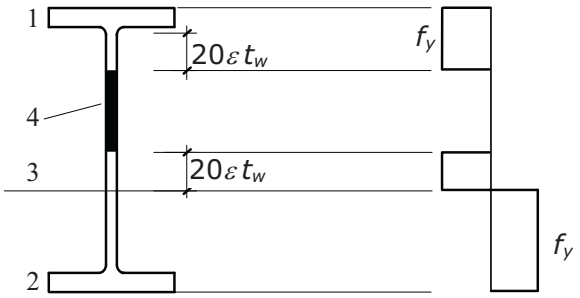

1 - compression; 2 - tension; 3 - plastic neutral axis; 4 - neglected part

Figure 1.21 Effective class 2 web

1.3.1.2 Member resistance

In addition to verification of the cross section resistance, the assessment of the resistance of members – columns, beams and beam-columns, subject to instability phenomena must also be checked, according to clauses 6.3 and 6.4. The buckling phenomenon depends on the presence of compressive stresses and therefore it must be checked for all members subjected to axial compression, bending moment or a combination of both. Shear buckling effects, particularly in cross sections with slender webs, should also be considered according to EC3-1-5.

For a member under pure compression the buckling modes to take into account are: i) flexural buckling; ii) torsional buckling and iii) torsional-flexural buckling. A member under bending moment must be checked against lateral-torsional buckling. A member under a combination of compression force and bending moment must be checked against all the buckling modes mentioned above.

1.3.2 Design of tension members

1.3.2.1 Code prescriptions

Tension members are commonly used in truss structures or bracing elements (see Figure 1.22). Simple or built-up rolled sections are commonly used in trusses, lattice girders and as bracing members. Cables, flats or bars are sometimes used in bridges or long-span roofs.

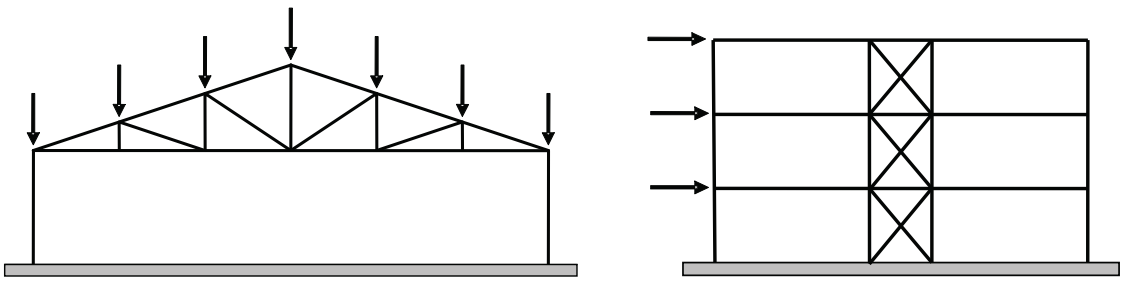

Figure 1.22 Structures with tension members

The design of a tension member may be governed by one of the following collapse modes: i) resistance of a gross cross section far from the joints or ii) resistance of the cross section close to the joints or other discontinuities, due to the reduction of cross

section, the second-order moments induced by small eccentricities or both effects (Figure 1.23). Typically, the second mode is the governing design mode.

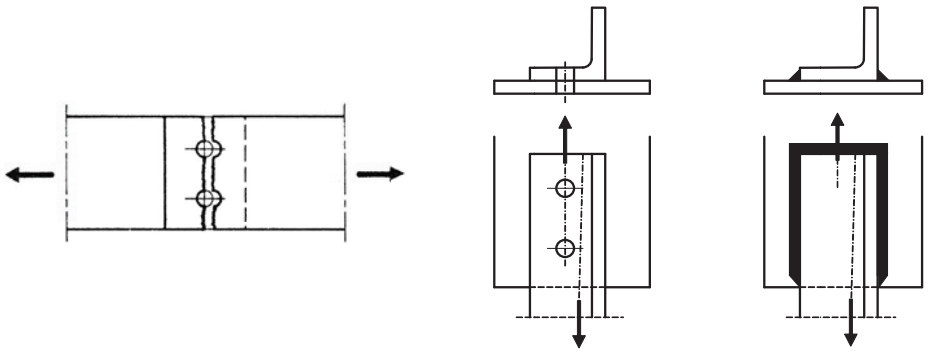

a) Collapse in the net cross section b) Eccentric joints

Figure 1.23 Collapse of tension members

A member exclusively subject to a tension force is under a uniaxial stress state. According to clause 6.2.3(1), the design value of the tension force N_{Ed} at each cross section, including cross sections in the vicinity of the joints, should satisfy:

$$\frac{N_{Ed}}{N_{t,Rd}} \leq 1,0\,, \tag{1.25}$$

where $N_{t,Rd}$ is the design tension resistance. For sections with holes the design tension resistance $N_{t,Rd}$ should be taken as the smallest of:

- design plastic resistance of the gross cross section,

$$N_{pl,Rd} = A f_y / \gamma_{M0}\,, \tag{1.26}$$

where A is the gross cross section area, f_y is the yield strength of steel and γ_{M0} is the partial safety factor.

- design ultimate resistance of the net cross section at holes for fasteners,

$$N_{pl,Rd} = A f_y / \gamma_{M0}\,, \tag{1.27}$$

where A_{net} is the net cross section area, f_u is the ultimate strength of steel and γ_{M2} is the partial safety factor.

Whenever dissipative behaviour is required under cyclic loading, such as in the case of capacity design, the design plastic resistance $N_{pl,Rd}$ should be less than the design ultimate resistance of the net section at fasteners holes $N_{u,Rd}$ (clause 6.2.3(3)), that is,

$$N_{u,Rd} > N_{pl,Rd} \;\Leftrightarrow\; \frac{A_{net}}{A} > \frac{f_y}{0,9 f_u}\frac{\gamma_{M2}}{\gamma_{M0}}\,. \tag{1.28}$$

In the case of members with Category C preloaded bolted connections loaded in shear, the design tension resistance $N_{t,Rd}$ at the cross section with holes for fasteners should be taken as $N_{net,Rd}$ (clause 6.2.3(4) of EC3-1-8 (EN 1993-1-8, 2005)):

$$N_{net,Rd} = A_{net} f_y / \gamma_{M0} \,. \tag{1.29}$$

For angles connected by one leg and other unsymmetrically connected members in tension (such as T sections or channel sections), the eccentricity in joints and the effects of the spacing and edge distances of the bolts should be taken into account in determining the design resistance (clause 3.10.3(1) of EC3-1-8).

Members that comprise angles connected by welding only in one leg can be treated as being concentrically loaded. The resistance is determined using Eqn. (1.26), but based on an effective cross section area. The area of the effective cross section, according to clause 4.13 of EC3-1-8, must be evaluated as follows: i) for angles of equal legs or unequal legs that are connected by the larger leg, the area of the effective section may be considered as equal to the gross area; ii) for angles of unequal legs, connected by the smaller leg, the area of the effective section should be taken as equal to the gross area of an equivalent angle, with legs that are equal to the smaller of the legs.

1.3.2.2 Worked examples

Example 2 – Consider the member AB of the steel truss, indicated in Figure 1.24, assuming it is submitted to a design tensile axial force of N_{Ed} = 220 kN. The cross section consists of two angles of equal legs, in steel grade S 235. Design member AB assuming two distinct possibilities for the joints:

a) welded joints;

b) bolted joints.

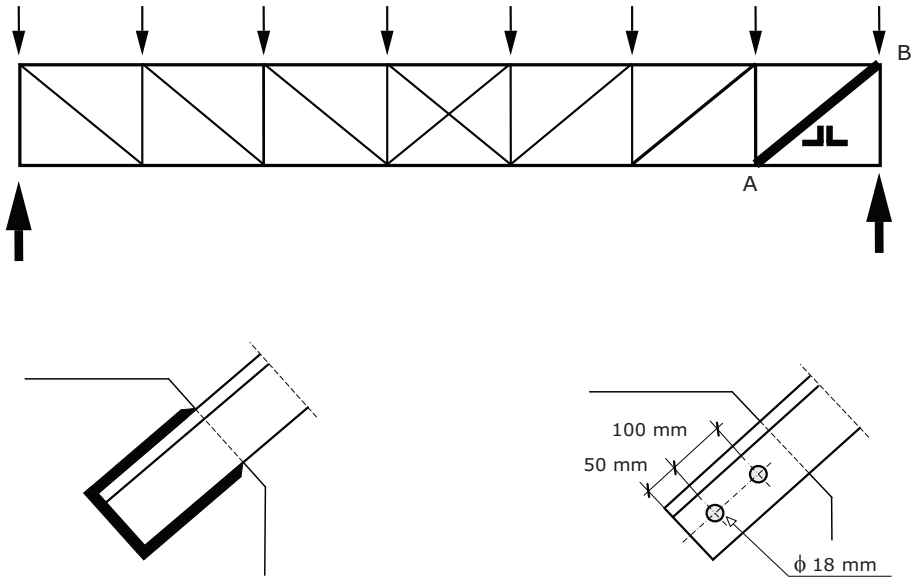

a) *Welded joints* b) *Bolted joints*

Figure 1.24 Steel truss

a) Welded joints

The member is made up by two angles of equal legs, but the joint is made only in one leg of the angle. Thus, according to clause 4.13 of EC3-1-8, the effective area can be considered equal to the gross area. Therefore, the following conditions must be satisfied:

$$N_{Ed} \le N_{t,Rd} = \frac{A f_y}{\gamma_{M0}} \ ,$$

where γ_{M0} = 1,00, f_y = 235 MPa and A is the gross area of the section. Considering the design axial force, N_{Ed} = 220 kN, then:

$$220\,\text{kN} \le \frac{A \cdot 235 \cdot 10^3}{1,0} \ \Rightarrow \ A \ge 9,36 \cdot 10^{-4}\,\text{m}^2 = 9,36\ \text{cm}^2 .$$

From a table of commercial profiles, a solution with two angles 50x50x5 mm, with a total area of 2 · 4,8 = 9,6 cm^2, satisfies the above safety requirement.

b) Bolted connections

In this case, the member, made up by angles of equal legs, is connected by 2 bolts only in one leg. According to clause 3.10.3 of EC3-1-8, the following design conditions must be ensured:

$$N_{Ed} \le N_{t,Rd} \text{ , with } \ N_{t,Rd} = \min\left[N_{pl,Rd} = \frac{A f_y}{\gamma_{M0}} ; N_{u,Rd} = \frac{\beta_2 \, A_{net} \, f_u}{\gamma_{M2}} \right],$$

where, γ_{M0} = 1,00, γ_{M2} = 1,25, f_y = 235 MPa, f_u = 360 MPa, A is the gross area of the cross section, A_{net} is the net area of the bolted section, and β_2 is a factor obtained from Table 1.18 (Table 3.8 of EC3-1-8). A first check based on the plastic design of the gross cross section leads to:

$$220\,\text{kN} \le \frac{A \cdot 235 \cdot 10^3}{1,00} \ \Rightarrow \ A \ge 9,36 \cdot 10^{-4}\,\text{m}^2 = 9,36\,\text{cm}^2 .$$

Hence, the section obtained in the previous design, two angles 50x50x5 mm (A = 9,6 cm^2), also satisfies this safety requirement.

The second condition, reproduced above, requires the evaluation of the net area A_{net}, (see Figure 1.25) and the factor β_2, both evaluated according to clause 3.10.3 of EC3-1-8.

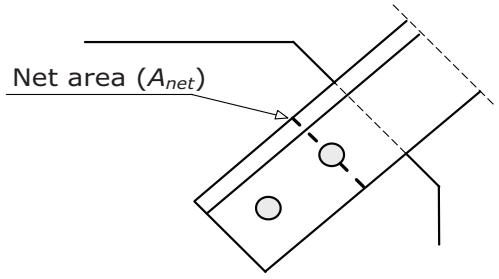

Figure 1.25 A_{net} in the bolted connection

For d_0 = 18 mm, 2,5 d_0 = 45 mm and 5 d_0 = 90 mm.

As p_1 = 100 mm > 90 mm, in accordance with the following table (Table 3.8 of EC3-1-8), β_2 =0,70 is obtained.

Table 1.18 Reduction factors β_2 and β_3

Distance p_1	$\leq 2,5\,d_0$	$\geq 5,0\,d_0$
2 bolts β_2	0,4	0,7
3 bolts or more β_3	0,5	0,7

The net area of the bolted section made up of two angles is given by:

$$A_{net} = A - 2\,t\,d_0 = 9,6 - 2 \cdot 0,5 \cdot 1,8 = 7,8 \text{ cm}^2 .$$

Thus, the design ultimate resistance in accordance with clause 3.10.3(1) of EC3-1-8 is given by:

$$N_{u,Rd} = \frac{0,7 \cdot 7,8 \cdot 10^{-4} \cdot 360 \cdot 10^3}{1,25} = 157,2\,\text{kNs} .$$

However, N_{Ed} = 220 kN > $N_{u,Rd}$ = 157,2 kN; therefore, the chosen cross section is not appropriate. By adopting a cross section with enhanced resistance, for example, two angles 60x60x6 mm (A = 13,82 cm^2 and A_{net} =11,66 cm^2), then:

$$N_{pl,Rd} = \frac{13,82 \cdot 10^{-4} \cdot 235 \cdot 10^3}{1,00} = 324,8\,\text{kN} > N_{Ed} = 220\,\text{kN} ,$$

$$N_{u,Rd} = \frac{0,7 \cdot 11,66 \cdot 10^{-4} \cdot 360 \cdot 10^3}{1,25} = 235,1\,\text{kN} > N_{Ed} = 220\,\text{kN} .$$

As $N_{pl,Rd}$ = 324,8 kN > $N_{u,Rd}$ = 235,1 kN, failure is non-ductile; however, since this is not a design condition, the section defined by two angles 60x60x6 mm can be accepted.

1.3.3 Design of columns

1.3.3.1 Code prescriptions

The resistance of a steel member subject to axial compression depends on the cross section resistance or the occurrence of instability phenomena. In general, the design for compression is governed by the second condition (instability phenomena) as steel members are usually of medium to high slenderness.

The cross section resistance to axial compression should be based on the plastic capacity (plastic axial force) in compact sections (class 1, 2 or 3), but taking into account the local buckling resistance through an effective elastic capacity in class 4 sections. According to

clause 6.2.4(1), the cross section resistance of axially compressed members is verified by the following condition:

$$\frac{N_{Ed}}{N_{c,Rd}} \leq 1,0\ , \tag{1.30}$$

where N_{Ed} is the design value of the axial compression force and $N_{c,Rd}$ is the design resistance of the cross section for uniform compression, given by (clause 6.2.4(2)):

$$N_{c,Rd} = A f_y / \gamma_{M0} \qquad \text{(cross sections class 1, 2 and 3);} \tag{1.31}$$

$$N_{c,Rd} = A_{eff} f_y / \gamma_{M0} \qquad \text{(cross sections class 4),} \tag{1.32}$$

where A is the gross area of the cross section, A_{eff} is the effective area of a class 4 cross section, f_y is the yield strength of steel and γ_{M0} is a partial safety factor. In evaluating $N_{c,Rd}$, holes for fasteners can be neglected, provided they are filled by fasteners and are not oversize or slotted (clause 6.2.4(3)).

The buckling resistance should be evaluated according to the relevant buckling mode and relevant imperfections of real members. The critical load of a column in flexural buckling (the most current mode for members composed by I, H and tubular sections) is given by:

$$N_{cr} = \frac{\pi^2 E I}{L_E^{\ 2}}\ , \tag{1.33}$$

where $E I$ is the flexural stiffness about the relevant axis and L_E is the buckling length. The buckling length of a pinned member (Euler's column) is equal to the real length; in other conditions, the buckling length may be defined accordingly.

The resistance of compressed members is based on the "European design buckling curves" (Simões da Silva et al., 2013). These (five) curves were the result of an extensive experimental and numerical research programme that accounted for all imperfections in real compressed members (initial out-of-straightness, eccentricity of the loads, residual stresses). The buckling resistance of a member submitted to a design axial compression N_{Ed} is verified by the following condition:

$$N_{Ed} \leq N_{b,Rd}\ , \tag{1.34}$$

where $N_{b,Rd}$ is the design buckling resistance of the compression member (clause 6.3.1.1(1)). The design flexural buckling resistance of prismatic members is given by:

$$N_{b,Rd} = \chi A f_y / \gamma_{M1} \qquad \text{(cross sections class 1, 2 and 3);} \tag{1.35}$$

$$N_{b,Rd} = \chi A_{eff} f_y / \gamma_{M1} \qquad \text{(cross sections class 4),} \tag{1.36}$$

where χ is the reduction factor for the relevant buckling mode and γ_{M1} is a partial safety factor (clause 6.3.1.1(3)). The reduction factor χ is obtained from the following equation:

$$\chi = \frac{1}{\Phi + \sqrt{\Phi^2 - \bar{\lambda}^2}} \qquad \text{but} \qquad \chi \leq 1{,}00, \tag{1.37}$$

where $\Phi = 0{,}5\left[1 + \alpha\left(\bar{\lambda} - 0{,}2\right) + \bar{\lambda}^2\right]$ and $\bar{\lambda}$ is the non-dimensional slenderness coefficient, given by:

$$\bar{\lambda} = \sqrt{A f_y / N_{cr}} = \frac{L_{cr}}{i}\frac{1}{\lambda_1} \qquad \text{(cross sections class 1, 2 and 3);} \tag{1.38}$$

$$\bar{\lambda} = \sqrt{A_{eff} f_y / N_{cr}} = \frac{L_{cr}}{i}\frac{\sqrt{A_{eff}/A}}{\lambda_1} \qquad \text{(cross sections class 4),} \tag{1.39}$$

where N_{cr} is the elastic critical load for the relevant buckling mode; L_{cr} is the critical length of the corresponding buckling mode; i is the radius of gyration of the cross section; $\lambda_1 = \pi\,(E/f_y)^{0,5} = 93{,}9\varepsilon$; $\varepsilon = (235/f_y)^{0,5}$ with f_y in N/mm^2; α is the imperfection factor.

The effect of imperfections is included by the imperfection factor α, which assumes values of 0,13, 0,21, 0,34, 0,49 and 0,76 for curves a_0, a, b, c and d (European design buckling curves), respectively. These curves, mathematically represented by Eqn. (1.37), are illustrated in Figure 1.26. The buckling curve to be adopted in design of a given member depends on the geometry of the cross sections, on the steel grade, on the fabrication process and on the relevant buckling plane, as described in Table 1.19.

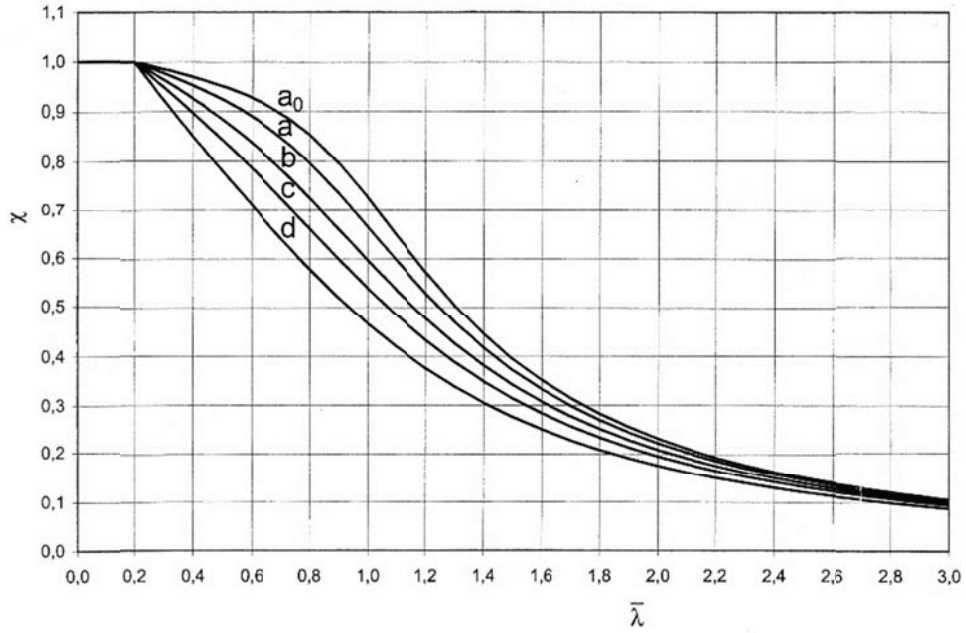

Figure 1.26 Buckling curves according to EC3-1-1

According to clause 6.3.1.2(4), for values of the non-dimensional slenderness $\bar{\lambda} \leq 0{,}2$ or if $N_{Ed}/N_{cr} \leq 0{,}04$, the effect of buckling can be neglected, and members are designed based only on the cross section resistance.

Table 1.19 Selection of the buckling curve

Cross section		Geometry limits		Buckling about axis	Buckling curve	
					S 235 S 275 S 355 S 420	S 460
Rolled I or H sections	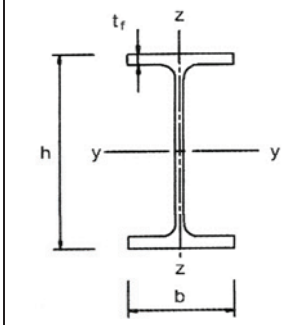	$h/b > 1,2$	$t_f \le 40\,\text{mm}$	y-y z-z	*a* *b*	a_0 a_0
			$40\ \text{mm} < t_f \le 100\ \text{mm}$	y-y z-z	*b* *c*	*a* *a*
		$h/b \le 1,2$	$t_f \le 100\,\text{mm}$	y-y z-z	*b* *c*	*a* *a*
			$t_f > 100\ \text{mm}$	y-y z-z	*d* *d*	*c* *c*
Welded I or H sections	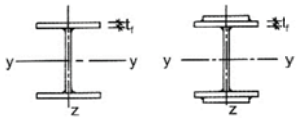	$t_f \le 40\ \text{mm}$		y-y z-z	*b* *c*	*b* *c*
		$t_f > 40\ \text{mm}$		y-y z-z	*c* *d*	*c* *d*
Hollow sections		hot finished		any	*a*	a_0
		cold formed		any	*c*	*c*
Welded box sections	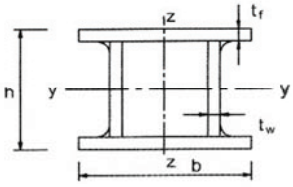	Generally (except as below)		any	*b*	*b*
		thick welds: $a > 0,5t_f$ $b/t_f < 30$ $h/t_w < 30$ (a – throat thickness)		any	*c*	*c*
U, T and solid sections	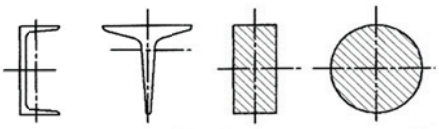			any	*c*	*c*
L Sections				any	*b*	*b*

In compression members with open cross sections, then according to clause 6.3.1.4(1), account should be taken of the possibility that resistance to torsional or flexural-torsional buckling could be less than the resistance to flexural buckling. The design process for these members is very similar to that for flexural buckling, the non-dimensional slenderness coefficient $\bar{\lambda}$ being replaced by the non-dimensional slenderness coefficient $\bar{\lambda}_T$, evaluated by the following equations (clause 6.3.1.4(2)):

$$\bar{\lambda}_T = \sqrt{A f_y / N_{cr}} \qquad \text{(cross sections class 1, 2 and 3);} \qquad (1.40)$$

$$\bar{\lambda}_T = \sqrt{A_{eff} f_y / N_{cr}} \qquad \text{(cross sections class 4),} \qquad (1.41)$$

where N_{cr} is the lower of the values $N_{cr,T}$ and $N_{cr,TF}$, corresponding to the elastic critical load for torsional buckling and for flexural-torsional buckling, respectively, which evaluation may be find elsewhere (Simões da Silva et al., 2013). For both phenomena, the imperfection coefficient α can be taken as corresponding to flexural buckling about the *z* axis, obtained from Table 1.19.

1.3.3.2 Worked examples

Example 3 – Safety verification of a column member of the building represented in Figure 1.27.

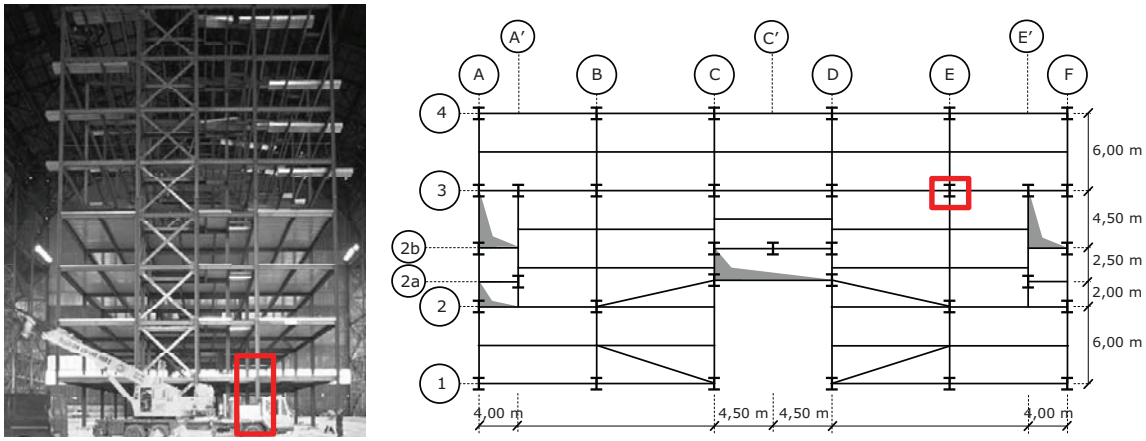

Figure 1.27 Case-study building

i) Internal forces

As the building under analysis (case-study building) is braced on both orthogonal directions, the bending moments on the columns are low, in particular in the inner columns. The inner column E-3 represented in the Figure 1.27, at base level, is selected in this example. The member has a length of 4,335 m and is composed by a section HEB 340 in steel S 355. For this column the bending moments (and consequently the shear force) may be neglected; the design axial force (of compression) obtained from the previous analysis (sub-section 1.2.3.4) is given by N_{Ed} = 3326,0 kN.

ii) Cross section classification – section HEB 340 in pure compression

The geometric characteristics of the section HEB 340 are: A = 170,9 cm^2, b = 300 mm, h = 340 mm, t_f = 21,5 mm, t_w = 12 mm, r = 27 mm, I_y = 36660 cm^4, i_y = 14,65 cm, I_z = 9690 cm^4, i_z = 7,53 cm. The mechanical properties of the steel are: f_y = 355 MPa and E = 210 GPa.

Web in compression (Table 5.2 of EC3-1-1),

$$\frac{c}{t} = \frac{(340 - 2 \cdot 21,5 - 2 \cdot 27)}{12} = 20,25 < 33\,\varepsilon = 33 \cdot 0,81 = 26,73 . \qquad \text{(class 1)}$$

Flange in compression (Table 5.2 of EC3-1-1),

$$\frac{c}{t} = \frac{300/2 - 12/2 - 27}{21,5} = 5,44 < 9\,\varepsilon = 9 \cdot 0,81 = 7,29 . \qquad \text{(class 1)}$$

Hence, the HEB 340 cross section, steel S 355, in pure compression is class 1.

iii) Cross section verification – class 1 in pure compression.

$$N_{Ed} = 3326,0\,\text{kN} < N_{c,Rd} = \frac{A f_y}{\gamma_{M0}} = \frac{170,9 \cdot 10^{-4} \cdot 355 \cdot 10^3}{1,00} = 6067,0\,\text{kN} .$$

iv) Buckling resistance

Buckling lengths – According to the structural analysis used (second order analysis), the buckling lengths are considered (conservatively) equal to the mid-distance between floors, given by:

Buckling in the plane x-z (around y) - $L_{Ey} = 4,335$ m.

Buckling in the plane x-y (around z) - $L_{Ez} = 4,335$ m.

v) Determination of the slenderness coefficients

$$\lambda_1 = \pi \cdot \sqrt{\frac{210 \cdot 10^6}{355 \cdot 10^3}} = 76,41 .$$

$$\lambda_y = \frac{L_{Ey}}{i_y} = \frac{4,335}{14,65 \cdot 10^{-2}} = 29,59 ; \qquad \bar{\lambda}_y = \frac{\lambda_y}{\lambda_1} = 0,39 .$$

$$\lambda_z = \frac{L_{Ez}}{i_z} = \frac{4,335}{7,53 \cdot 10^{-2}} = 57,57 ; \qquad \bar{\lambda}_z = \frac{\lambda_z}{\lambda_1} = 0,75 .$$

vi) Calculation of the reduction factor χ_{min}

$$\frac{h}{b} = \frac{340}{300} = 1,13 < 1,2 \text{ and } t_f = 21,5\,\text{mm} < 100\,\text{mm} \Rightarrow \begin{matrix} \textit{buckling around } y - \textit{curve } b\,(\alpha = 0,34) \\ \textit{buckling around } z - \textit{curve } c\,(\alpha = 0,49). \end{matrix}$$

As $\bar{\lambda}_z = 0,75 > \bar{\lambda}_y = 0,39$ and $\alpha_{curve\ c} > \alpha_{curve\ b} \Rightarrow \chi_{min} \Rightarrow \chi_z$.

$$\Phi_z = 0,5 \cdot \left[1 + 0,49 \cdot (0,75 - 0,2) + 0,75^2\right] = 0,92 ;$$

$$\chi_z = \frac{1}{0,92 + \sqrt{0,92^2 - 0,75^2}} = 0,69 ; \quad \chi_{min} = \chi_z = 0,69 .$$

vii) Safety verification

$$N_{b,Rd} = \chi A f_y / \gamma_{M1} = 0,69 \cdot 170,9 \cdot 10^{-4} \cdot 355 \cdot 10^3 / 1,00 = 4186,2\ \text{kN} > N_{Ed} = 3326,0\,\text{kN} .$$

1.3.4 Design of beams

1.3.4.1 Code prescriptions

Theoretical concepts

A beam is a member submitted to bending moment and shear force along its length. The resistance of a steel beam in bending depends on the cross section resistance or the occurrence of lateral instability – lateral-torsional buckling. In general, the lateral-torsional buckling is the governing mode of steel members composed of I or H sections bent about the major axis. Whenever one of the following situations occurs in a beam, lateral-torsional buckling cannot develop and assessment of the beam can be based just on the cross section resistance: i) the cross section of the beam is bent about its minor z axis; ii) the beam is laterally restrained by means of secondary steel members or any other method; iii) the cross section of the beam has high torsional stiffness and similar flexural stiffness about both principal axes of bending as, for example, closed hollow sections. I or H sections and rectangular hollow sections are usually chosen for beams because they possess high major axis bending resistance and bending stiffness.

The bending resistance of a cross section can be obtained from its plastic resistance, if the section is compact (class 1 or 2 section). On the other hand, in a slender cross section (class 3 or 4 section) the bending resistance must be based on its elastic resistance.

The elastic bending resistance of a cross section is attained when the normal stress in the point furthest away from the elastic neutral axis (e. n. a.) reaches the yield strength f_y; the corresponding bending moment is denoted the elastic bending moment M_{el}. The bending moment that is able to totally plastify a section is denoted as the plastic bending moment M_{pl}. In the calculation of the plastic bending moment of a steel cross section, the plastic neutral axis (p.n.a.) is located at the centroid only if the section is symmetrical, as for the case of rectangular sections, I sections or H sections with equal flanges. In case of non-symmetric cross sections, such as a T-section, the neutral axis moves in order to divide the section in two equal areas. The elastic bending moment and the plastic bending moment around the horizontal axis are given by:

$$M_{el} = \frac{I}{v} f_y = W_{el} f_y ; \tag{1.42}$$

$$M_{pl} = A_c f_y d_c + A_t f_y d_t = \left(S_c + S_t\right) f_y = W_{pl} f_y , \tag{1.43}$$

where, I is the second moment of area about the elastic neutral axis (coincident with the centroid of the cross section); v is the maximum distance from an extreme fibre to the same axis; $W_{el} = I/v$ is the elastic bending modulus; A_c and A_t are the areas of the section in compression and in tension, respectively (of equal value); f_y is the yield strength of the material; d_c and d_t are the distances from the centroid of the areas of the section in compression and in tension, respectively, to the plastic neutral axis; W_{pl} is the plastic bending modulus, given by the sum of first moment of areas A_c and A_t, in relation to the plastic neutral axis ($W_{pl} = S_c + S_t$). For symmetric sections the previous calculations are simpler because the plastic neutral axis coincides with the elastic neutral axis and, consequently, $d_c = d_t$.

In standard cross sectional shapes, such as I or H bent about the major axis (y axis), the typical instability phenomenon is lateral-torsional buckling. Lateral-torsional buckling is characterised by lateral deformation of the compressed part of the cross section (the compressed flange in the case of I or H sections). This part behaves like a compressed

member, but one continuously restrained by the part of the section in tension, which initially does not have any tendency to move laterally.

The design procedure to account this phenomenon is based on the elastic critical moment M_{cr} – the theoretical value of the maximum bending moment along a beam, without any type of imperfections, which induce the called lateral-torsional buckling. The elastic critical moment of the simply supported beam, with the supports preventing lateral displacements and twisting but allowing warping and bending rotations about the cross sectional axes (*y* and *z*), submitted to a constant bending moment M_y ("standard case") is given by:

$$M_{cr}^{E} = \frac{\pi}{L}\sqrt{G\,I_T\,E\,I_z\left(1+\frac{\pi^2\,E\,I_W}{L^2 G\,I_T}\right)}, \tag{1.44}$$

where I_z is the second moment of area in relation to *z* axis (weak axis), I_T is the torsion constant, I_W the warping constant, *L* is the length between laterally braced cross sections of the beam and *E* and *G* are the longitudinal modulus and the shear modulus of elasticity, respectively. Eqn. (1.44), in spite of being derived for a member with an I or H cross section, is valid for members with other doubly symmetric cross sections. The constant of uniform torsion I_T and the warping constant I_W for standard cross sections are usually supplied in tables of steel profiles.

Eqn. (1.44) is valid for the calculation of the elastic critical moment of a simply supported beam, with a doubly symmetric cross section and subjected to a constant bending moment ("standard case"). However, in reality, other situations often occur, such as beams with non-symmetrical cross sections, with other support conditions, subject to different loading patterns and, consequently, subject to different bending moment diagrams. In practical applications approximate formulae are used, which are applicable to a wide set of situations; the most used is formula reproduced by Eqn. (1.45), applicable to members subject to bending moment about the strong *y* axis, with cross sections mono-symmetric about the weak *z* axis (Boissonnade et al., 2006). For the estimation of the elastic critical moment in situations not covered by presented Eqns. (1.44) and (1.45), the user is advised to look at specific bibliography (Simões da Silva et al., 2013) or to use other types of computational processes such as the finite element method.

$$M_{cr} = C_1\frac{\pi^2\,E\,I_z}{\left(k_z\,L\right)^2}\left\{\sqrt{\left(\frac{k_z}{k_w}\right)^2\frac{I_W}{I_z}+\frac{\left(k_z\,L\right)^2 G\,I_T}{\pi^2\,E\,I_z}+\left(C_2\,z_g-C_3\,z_j\right)^2}-\left(C_2\,z_g-C_3\,z_j\right)\right\}^{0,5} \tag{1.45}$$

where:

C_1, C_2 and C_3 are coefficients depending on the shape of the bending moment diagram and on support conditions, given in Table 1.20 and Table 1.21 for some usual situations (Boissonnade et al., 2006); in the Table 1.20 and Table 1.21 the support conditions are those of the "standard case", however, lateral bending restraints and warping restraints may be taken into account through the parameters k_z and k_w described below;

k_z and k_w are effective length factors that depend on the support conditions at the end sections. Factor k_z is related to rotations at the end sections about the weak axis *z*, and k_w refers to warping restriction in the same cross sections. These factors vary between 0,5 (restrained deformations) and 1.0 (free deformations), and are equal to 0,7 in the case of free deformations at one end and restrained at the other. Since in most practical situations restraint is only partial, conservatively $k_z = k_w = 1{,}0$ may be adopted;

$z_g = (z_a - z_s)$, where z_a and z_s are the coordinates of the point of application of the load and of the shear centre, relative to the centroid of the cross section; these quantities are positive if located in the compressed part and negative if located in the tension part;

$z_j = z_s - \left(0,5 \int_A \left(y^2 + z^2 \right) \left(z / I_y \right) dA \right)$ is a parameter that reflects the degree of asymmetry of the cross section in relation to the *y* axis. It is zero for beams with doubly symmetric cross section (such as I or H cross sections with equal flanges) and takes positive values when the flange with the largest second moment of area about *z* is the compressed flange, at the cross section with maximum bending moment.

In case of mono-symmetric I or H cross sections, Table 1.20 and Table 1.21 must only be used if the following condition is verified: $-0,9 \leq \psi_f \leq 0,9$.

Table 1.20 Coefficients C_1 and C_3 for beams with end moments

Loading and support conditions	Diagram of moments	k_z	C_1	C_3	
				$\psi_f \leq 0$	$\psi_f > 0$
	$\Psi = +1$	1,0 0,5	1,00 1,05	1,000 1,019	
	$\Psi = +3/4$	1,0 0,5	1,14 1,19	1,000 1,017	
	$\Psi = +1/2$	1,0 0,5	1,31 1,37	1,000 1,000	
	$\Psi = +1/4$	1,0 0,5	1,52 1,60	1,000 1,000	
	$\Psi = 0$	1,0 0,5	1,77 1,86	1,000 1,000	
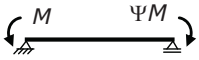	$\Psi = -1/4$	1,0 0,5	2,06 2,15	1,000 1,000	0,850 0,650
	$\Psi = -1/2$	1,0 0,5	2,35 2,42	1,000 0,950	$1,3\text{-}1,2\psi_f$ $0,77 - \psi_f$
	$\Psi = -3/4$	1,0 0,5	2,60 2,45	1,000 0,850	$0,55 - \psi_f$ $0,35 - \psi_f$
	$\Psi = -1$	1,0 0,5	2,60 2,45	$-\psi_f$ $-0,125-0,7\psi_f$	$-\psi_f$ $-0,125-0,7\psi_f$

- In beams subject to end moments, by definition $C_2 z_g = 0$.
- $\psi_f = \dfrac{I_{fc} - I_{ft}}{I_{fc} + I_{ft}}$, where I_{fc} and I_{ft} are the second moments of area of the compression and tension flanges respectively, relative to the weak axis of the section (z axis).
- C_1 must be divided by 1,05 when $\dfrac{\pi}{k_w L} \sqrt{\dfrac{E I_W}{G I_T}} \leq 1,0$, but $C_1 \geq 1,0$.

Table 1.21 Coefficients C_1, C_2 and C_3 for beams with transverse loads

Loading and support conditions	Diagram of moments	k_z	C_1	C_2	C_3
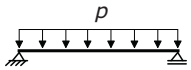		1,0 0,5	1,12 0,97	0,45 0,36	0,525 0,478
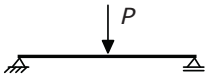		1,0 0,5	1,35 1,05	0,59 0,48	0,411 0,338
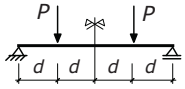		1,0 0,5	1,04 0,95	0,42 0,31	0,562 0,539

Cross section resistance

In the absence of shear forces, the design value of the bending moment M_{Ed} at each cross section should satisfy (clause 6.2.5(1)):

$$\frac{M_{Ed}}{M_{c,Rd}} \le 1,00\,, \tag{1.46}$$

where $M_{c,Rd}$ is the design resistance for bending. The design resistance for bending about one principal axis of a cross section is determined as follows (clause 6.2.5(2)):

$$M_{c,Rd} = W_{pl} f_y / \gamma_{M0} \qquad \text{(cross sections class 1 and 2);} \tag{1.47}$$

$$M_{c,Rd} = W_{el,\min} f_y / \gamma_{M0} \qquad \text{(cross sections class 3);} \tag{1.48}$$

$$M_{c,Rd} = W_{eff,\min} f_y / \gamma_{M0} \qquad \text{(cross sections class 4),} \tag{1.49}$$

where W_{pl} is the plastic section bending modulus; $W_{el,min}$ is the minimum elastic section bending modulus; $W_{eff,min}$ is the minimum elastic bending modulus of the reduced effective section; f_y is the yield strength of the material; γ_{M0} is the partial safety factor.

Design for bi-axial bending can be verified by plastic (class 1 or 2 cross sections) or elastic (class 3 and 4 cross sections) interaction formulae, according to clause 6.2.9, as described next:

$$\left[\frac{M_{y,Ed}}{M_{pl,y,Rd}}\right]^{\alpha} + \left[\frac{M_{z,Ed}}{M_{pl,z,Rd}}\right]^{\beta} \le 1,00 \qquad \text{(class 1 or 2 sections),} \tag{1.50}$$

where α and β are parameters that depend on the cross section's shape and $M_{pl,y,Rd}$ and $M_{pl,z,Rd}$ are the plastic moments of resistance about y and z, respectively. Parameters α and β can conservatively take the value 1.0; in alternative, they can take the values

defined in clause 6.2.9(6), that is, $\alpha = 2$ and $\beta = 1$ for I or H sections, $\alpha = \beta = 2$ for circular hollow sections and $\alpha = \beta = 1{,}66$ for rectangular hollow sections.

$$\sigma_{x,Ed} \leq \frac{f_y}{\gamma_{M0}} \qquad \text{(class 3 or 4 sections),} \tag{1.51}$$

where $\sigma_{x,Ed}$ is the design value of the longitudinal stress evaluated by elastic theory, based on the gross cross section, for class 3 sections, and on a reduced effective cross section, for class 4 sections.

Holes in the tension flange for bolts or other connection members may be ignored if the condition $0{,}9\ A_{f,net}\ f_u\ /\gamma_{M2} \geq A_f\ f_y\ /\gamma_{M0}$ is satisfied, where $A_{f,net}$ and A_f are the net section and the gross area of the tension flange, respectively, and γ_{M2} is a partial safety factor (defined according to EC3-1-8). A similar procedure must be considered for holes in the tensioned part of a web, as described in clause 6.2.5(5). The holes in the compressed parts of a section may be ignored, except if they are slotted or oversized, provided that they are filled by fasteners (bolts, rivets, etc.).

The web provides most of the shear resistance, as one can see from Figure 1.28. A common and conservative treatment assumes that the shear stress is uniformly distributed over the depth of the web, and any shear resistance of the flanges can be ignored, unless dealing with very thick flanges. EC3-1-1 recommends that whenever possible, the shear resistance of a steel section should be evaluated based on a plastic distribution of shear stress.

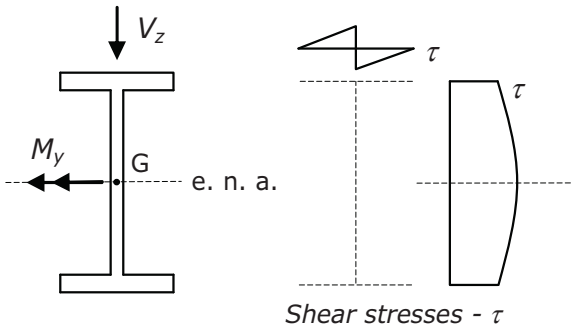

Figure 1.28 Elastic distributions of shear stresses

According to clause 6.2.6, the design value of the shear force V_{Ed}, must satisfy the following condition:

$$\frac{V_{Ed}}{V_{c,Rd}} \leq 1{,}00\,, \tag{1.52}$$

where $V_{c,Rd}$ is the design shear resistance. Considering plastic design, in the absence of torsion, the design shear resistance $V_{c,Rd}$, is given by the design plastic shear resistance $V_{pl,Rd}$, given by the following equation:

$$V_{pl,Rd} = A_v \left(f_y \big/ \sqrt{3}\right) \big/ \gamma_{M0}\,, \tag{1.53}$$

where A_v is the shear area, defined in a qualitative manner for an I section subjected to shear in Figure 1.29. The shear area corresponds approximately to the area of the parts of the cross section that are parallel to the direction of the shear force. Clause 6.2.6(3)

provides equations for the calculation of the shear area for standard steel sections; additionally, the shear area is specified in the tables of commercial profiles.

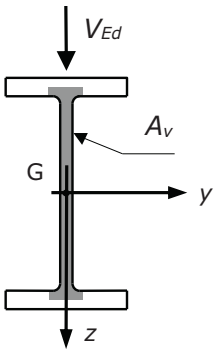

Figure 1.29 Shear area for an I cross section

As an alternative, an elastic design to shear force can be used.

The shear buckling resistance of webs should be verified, for unstiffened webs when $(h_w/t_w)>72\varepsilon/\eta$, where h_w and t_w represent the depth and the thickness of the web, respectively, η is a factor defined in EC3-1-5, which may be conservatively taken as 1,0, and ε is given by the relation $(235/f_y)^{0,5}$.

In an elastic stress analysis, the interaction between bending and shear force may be verified by applying a yield criterion. This procedure, valid for any type of cross section, requires calculation of elastic normal stresses (σ) and elastic shear stresses (τ), based on formulas from the theory of the elasticity, at the critical points of the cross section.

For plastic analysis, there are several models for combining shear and bending. The model used by EC3-1-1 evaluates a reduced bending moment obtained from a reduced yield strength (f_{yr}) along the shear area (Simões da Silva et al., 2013).

In general, when a section is subjected to bending moment and shear force, the design plastic bending resistance should be reduced to allow for the presence of the shear force. However, for low values of shear force, this reduction is not very significant. Also, as this reduction is counterbalanced by strain-hardening of the steel, it may be assumed that for low values of shear it is not necessary to reduce the design plastic bending resistance. Thus, clause 6.2.8 establishes the following interaction criterion between bending moment and shear force:

- when V_{Ed} < 50% of the plastic shear resistance $V_{pl,Rd}$, it is not necessary to reduce the design moment resistance $M_{c,Rd}$, except where shear buckling reduces the cross section resistance;
- when $V_{Ed} \geq$ 50% of the plastic shear resistance $V_{pl,Rd}$, the value of the design moment resistance should be evaluated using a reduced yield strength $(1-\rho)f_y$ for the shear area, where $\rho=(2V_{Ed}/V_{pl,Rd}-1)^2$.

In I or H sections with equal flanges, under major axis bending, the reduced design plastic moment resistance $M_{y,V,Rd}$ may be obtained from:

$$M_{y,V,Rd} = \left(W_{pl,y} - \frac{\rho A_w^{\ 2}}{4 t_w} \right) \frac{f_y}{\gamma_{M0}} \qquad \text{but} \qquad M_{y,V,Rd} \leq M_{y,c,Rd}\,, \tag{1.54}$$

where $A_w = h_w t_w$ is the area of the web (h_w is the depth of the web and t_w is the thickness) and $M_{y,c,Rd}$ is the design resistance for bending moment about the y axis.

Member resistance

The verification of resistance to lateral-torsional buckling of a prismatic member consists of the verification of the following condition (clause 6.3.2.1(1)):

$$\frac{M_{Ed}}{M_{b,Rd}} \leq 1,00\,, \tag{1.55}$$

where M_{Ed} is the design value of the bending moment and $M_{b,Rd}$ is the design buckling resistance, given by (clause 6.3.2.1(3)):

$$M_{b,Rd} = \frac{W_y f_y}{\gamma_{M1}}\,, \tag{1.56}$$

where:

$W_y = W_{pl,y}$ for class 1 and 2 cross sections;

$W_y = W_{el,y}$ for class 3 cross sections;

$W_y = W_{eff,y}$ for class 4 cross sections;

χ_{LT} is the reduction factor for lateral-torsional buckling.

In EC3-1-1 two methods for the calculation of the reduction coefficient χ_{LT} in prismatic members are proposed: a general method that can be applied to any type of cross section (more conservative) and an alternative method that can be applied to rolled cross sections or equivalent welded sections.

i) General method

According to the general method (clause 6.3.2.2), the reduction factor χ_{LT} is determined by the following equation:

$$\chi_{LT} = \frac{1}{\Phi_{LT} + \left(\Phi_{LT}^{\,2} - \overline{\lambda}_{LT}^{2}\right)^{0,5}} \quad \text{but} \quad \chi_{LT} \leq 1,00\,, \tag{1.57}$$

with:

$\Phi_{LT} = 0,5\left[1 + \alpha_{LT}\left(\overline{\lambda}_{LT} - 0,2\right) + \overline{\lambda}_{LT}^{2}\right]$;

α_{LT} is the imperfection factor, which depends on the buckling curve;

$\overline{\lambda}_{LT} = \left[W_y f_y / M_{cr}\right]^{0,5}$;

M_{cr} the elastic critical moment.

The buckling curves to be adopted depend on the geometry of the cross section of the member and are indicated in Table 1.22. For the imperfection factors α_{LT} associated to the various curves, the values given in section 3.3.1 for members in compression (reproduced in Table 6.3 of EC3-1-1) shall be adopted.

Table 1.22 Buckling curves for lateral-torsional buckling (General method)

Section	Limits	Buckling curve
I or H sections rolled	$h/b \le 2$	*a*
	$h/b > 2$	*b*
I or H sections welded	$h/b \le 2$	*c*
	$h/b > 2$	*d*
Other sections	---	*d*

ii) Alternative method – Rolled or equivalent welded sections

According to this second method, defined in clause 6.3.2.3, the reduction factor χ_{LT} is determined by the following equation:

$$\chi_{LT} = \frac{1}{\Phi_{LT} + \left(\Phi_{LT}^{\ 2} - \beta\,\overline{\lambda}_{LT}^{2}\right)^{0,5}} \quad \text{but} \quad \begin{matrix}\chi_{LT} \le 1,00 \\ \chi_{LT} \le 1/\overline{\lambda}_{LT}^{2}\end{matrix}, \tag{1.58}$$

with: $\Phi_{LT} = 0,5\left[1 + \alpha_{LT}\left(\overline{\lambda}_{LT} - \overline{\lambda}_{LT,0}\right) + \beta\,\overline{\lambda}_{LT}^{2}\right]$;

$\overline{\lambda}_{LT,0}$ and β are parameters to be defined in the National Annexes; the recommended values are: $\overline{\lambda}_{LT,0} \le 0,4$ (maximum value) and $\beta \ge 0,75$ (minimum value);

α_{LT} is the imperfection factor that depends on the appropriate buckling curve (defined as in the general method);

$\overline{\lambda}_{LT}$ the coefficient of non-dimensional slenderness (defined as in the general method);

M_{cr} the elastic critical moment.

The relevant buckling curves are indicated in Table 1.23.

Table 1.23 Buckling curves for lateral-torsional buckling (Alternative method)

Section	Limits	Buckling curve (EC3-1-1)
I or H sections rolled	$h/b \le 2$	*b*
	$h/b > 2$	*c*
I or H sections welded	$h/b \le 2$	*c*
	$h/b > 2$	*d*

According to this second method, the shape of the bending moment diagram, between braced sections, can be taken into account by considering a modified reduction factor $\chi_{LT,mod}$:

$$\chi_{LT,\text{mod}} = \frac{\chi_{LT}}{f} \quad \text{but} \quad \chi_{LT,\text{mod}} \le 1,00\,. \tag{1.59}$$

The parameter f can be obtained from the following equation, or from an alternative process provided in the National Annexes:

$$f = 1 - 0,5\left(1 - k_c\right)\left[1 - 2,0\left(\overline{\lambda}_{LT} - 0,8\right)^2\right] \qquad \text{but} \qquad f \le 1,00, \tag{1.60}$$

where k_c is a correction factor, defined according to Table 1.24.

Table 1.24 k_c correction factors

Diagram of bending moments	k_c
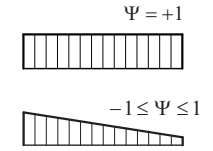	1,0 $\frac{1}{1,33 - 0,33\Psi}$
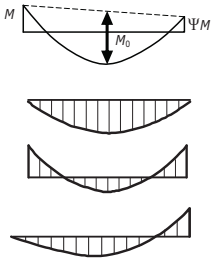	0,94 0,90 0,91
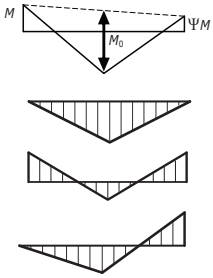	0,86 0,77 0,82
Ψ - ratio between end moments, with -1≤Ψ≤1.	

In Table 1.24, three sets of bending moment diagrams are presented. The first refers to beam spans subject to concentrated bending moments applied in the extreme sections. The second set of diagrams may be induced by uniformly distributed load and moments in the extreme sections. For the third set, the diagrams correspond to central point loads and moments in the extreme sections. The support conditions are not relevant as they are reproduced in the bending moment diagrams. The values of k_c presented in Table 1.24 correspond to some typical situations; some are exact values and other are approximate. More detailed information on k_c values may be obtained from Boissonnade et al. (2006).

iii) Conditions for ignoring lateral-torsional buckling verification

The verification of lateral-torsional buckling for a member in bending may be ignored if at least one of the following conditions is verified: $\overline{\lambda}_{LT} \le \overline{\lambda}_{LT,0}$ or $M_{Ed}/M_{cr} \le \overline{\lambda}_{LT,0}^{\,2}$ (clause 6.3.2.2(4) of EC3-1-1).

1.3.4.2 Worked examples

Example 4 – Safety check of a beam of the building illustrated in the Figure 1.30 (along line E). The beam is composed by an IPE 600 at the central span with 9 m length. The lateral spans with 6 m length (the governing spans) are composed by a section IPE 400 in steel S 355. For the lateral buckling check two cases are considered:

a) a beam with 6 m length, laterally braced only at the end support sections;

b) a beam with 6 m length, laterally braced at the end support sections and at mid-span section.

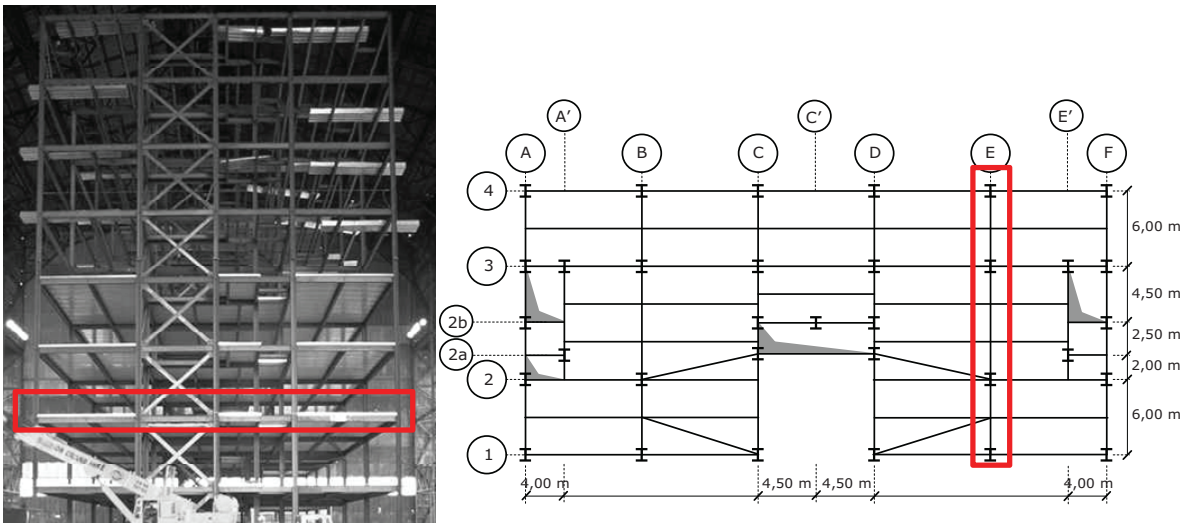

Figure 1.30 Case-study building

a) Beam laterally braced only at the end support sections

i) Diagrams of internal forces

The internal forces diagrams (neglecting the axial force) are represented in the Figure 1.31. From Figure 1.31, the critical cross section is the mid-span cross section (left span). Hence, the design values are M_{Ed} = 114,3 kNm and V_{Ed} = 75,9 kN.

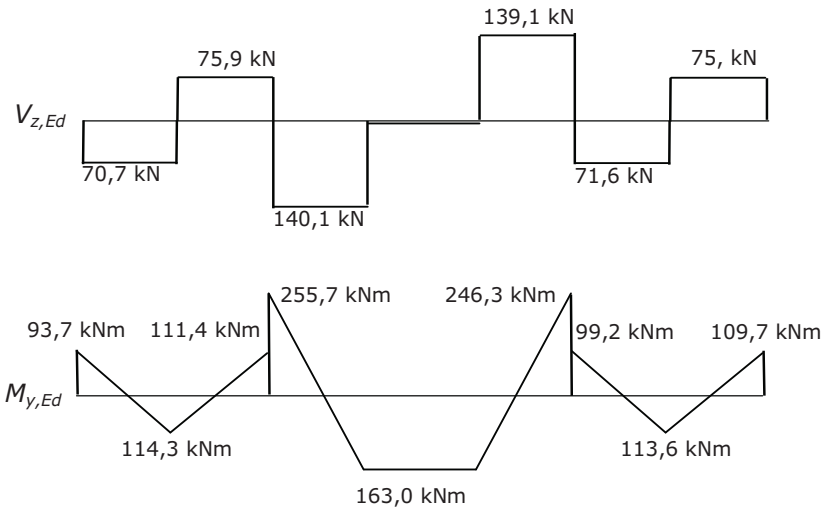

Figure 1.31 Diagrams

ii) Cross section classification – section IPE 400 in pure bending

The geometric characteristics of the section IPE 400 are: A = 84,46 cm^2, b = 180 mm, h = 400 mm, t_f = 13,5 mm, t_w = 8,6 mm, r = 21 mm, I_y = 23130 cm^4, i_y = 16,55 cm, I_z = 1318 cm^4, i_z = 3,95 cm; I_T = 51,08 cm^4; I_W = 490·10^3 cm^6. The mechanical properties of the steel S 355 are: f_y = 355 MPa and E = 210 GPa.

Web (internal part) in bending (Table 5.2 of EC3-1-1),

$$\frac{c}{t} = \frac{331}{8,6} = 38,49 < 72\,\varepsilon = 72 \cdot 0,81 = 58,32\,. \qquad \text{(class 1)}$$

Flange (outstand part) in compression (Table 5.2 of EC3-1-1),

$$\frac{c}{t} = \frac{(180/2 - 8,6/2 - 21)}{13,5} = 4,79 < 9\,\varepsilon = 9 \cdot 0,81 = 7,29\,. \qquad \text{(class 1)}$$

Hence, the IPE 400 cross section, steel S 355, in bending is class 1.

iii) Cross section verification

Bending resistance - For a class 1 cross section, the bending resistance is verified by the following condition:

$$M_{Ed} = 114,3\,\text{kNm} < W_{pl,y}\, f_y / \gamma_{M0} = 1307 \cdot 10^{-6} \cdot 355 \cdot 10^3 / 1,00 = 464,0\,\text{kNm}\,.$$

Verification of shear force - The shear area of the IPE 400 cross section is given by A_v = 42,69 cm^2. Hence:

$$V_{Ed} = 75,9\,\text{kN} < V_{c,Rd} = V_{pl,Rd} = \frac{42,69 \cdot 10^{-4} \cdot 355 \cdot 10^3 / \sqrt{3}}{1,00} = 875,0\,\text{kN}\,.$$

As $h_w/t_w = 43,4 < 72\,\varepsilon/\eta = 72 \cdot 0,81/1,00 = 58,3$ (conservatively taking η = 1,0), it is not necessary to verify the shear buckling resistance of the web. Therefore the IPE 400 cross section meets the requirements concerning shear force.

Bending-shear force interaction - As $V_{Ed} = 75,9\,\text{kN} < 0,50 \cdot V_{pl,Rd} = 437,5\,\text{kN}$, it is not necessary to reduce the bending resistance to account for the shear force.

iv) Lateral-torsional buckling resistance

Assuming the support conditions of the "standard case" and the loading applied at the upper flange level, the critical moment is obtained from Eqn. (1.45), with L = 6,00 m, $k_z = k_w$ = 1,0, $C_1 \approx 1,80$, $C_2 \approx 1,60$ (Boissonnade et al., 2006) and z_g = 200 mm, by:

$$M_{cr} = 164,7\ \text{kNm} \quad \Rightarrow \quad \bar{\lambda}_{LT} = \left[W_y\, f_y / M_{cr} \right]^{0,5} = \left[1307 \cdot 10^{-6} \cdot 355 \cdot 10^3 / 164,7 \right]^{0,5} = 1,68\,.$$

Since α_{LT} = 0,34 for a I rolled section, with h/b>2 (in accordance with general method),

$$\Phi_{LT} = 0,5 \cdot \left[1 + \alpha_{LT} \left(\bar{\lambda}_{LT} - 0,2 \right) + \bar{\lambda}_{LT}^2 \right] = 2,16\,;$$

$$\chi_{LT} = \frac{1}{\Phi_{LT} + \left(\Phi_{LT}^{\,2} - \bar{\lambda}_{LT}^2 \right)^{0,5}} = \frac{1}{2,16 + \left(2,16^2 - 1,68^2 \right)^{0,5}} = 0,28\,.$$

The design buckling resistance is given by:

$$M_{b,Rd} = 0,28 \cdot 1307 \cdot 10^{-6} \cdot \frac{355 \cdot 10^3}{1,00} = 129,9\,\text{kNm} > M_{Ed} = 114,3\,\text{kNm}\,.$$

So, the safety with a IPE 400 (S 355) is verified (utilization ratio = 114,3/129,9 = 0,88).

b) Beam laterally braced at the end support sections and at mid-span section

i) Cross section resistance – previous verifications are not changed.

ii) Lateral-torsional buckling resistance

If in addition the beam is laterally braced at the mid-span section by secondary beams (which prevent the lateral displacement of the compressed flange and consequently, the twist rotations), the lateral-torsional buckling behaviour is improved. The resistance to lateral-torsional buckling is performed for a beam segment with 3,00 m long, submitted to a linear bending moment diagram ($M_{Ed,left}$ =-93,7 kNm and $M_{Ed,right}$ =114,3 kNm), as shown in Figure 1.31. The critical moment of the beam is not aggravated by the loads applied at the upper flange, because these are applied at sections laterally restrained.

The elastic critical moment is given by Eqn. (1.45) (neglecting the continuity at mid-span cross section) with L = 3,00 m, $k_z = k_w$ = 1,0 and C_1 = 2,60 (from Table 1.20):

$$M_{cr} = 1778,8 \text{ kNm} \quad \Rightarrow \bar{\lambda}_{LT} = \left[W_y f_y / M_{cr}\right]^{0,5} = \left[1307 \cdot 10^{-6} \cdot 355 \cdot 10^3 / 1778,8\right]^{0,5} = 0,51 .$$

Since α_{LT} = 0,34 for a I rolled section, with h/b>2 (in accordance with general method),

$$\Phi_{LT} = 0,5 \cdot \left[1 + \alpha_{LT}\left(\bar{\lambda}_{LT} - 0,2\right) + \bar{\lambda}_{LT}^2\right] = 0,68 ;$$

$$\chi_{LT} = \frac{1}{\Phi_{LT} + \left(\Phi_{LT}{}^2 - \bar{\lambda}_{LT}^2\right)^{0,5}} = \frac{1}{0,68 + \left(0,68^2 - 0,51^2\right)^{0,5}} = 0,89 .$$

The design buckling resistance is given by:

$$M_{b,Rd} = 0,89 \cdot 1307 \cdot 10^{-6} \cdot \frac{355 \cdot 10^3}{1,00} = 412,9 \text{kNm} > M_{Ed} = 114,3 \text{kNm} .$$

So, the safety with a IPE 400 (S 355) is verified (utilization ratio = 114,3/412,9 = 0,28).

Example 5 – The frame illustrated in the Figure 1.32 is composed by a beam and a column, both with the same cross section. The beam is simple supported at the left end and connected to the column through a rigid joint. The column base is double supported. A vertical distributed load of 12 kN/m applied at top flange level and a horizontal point load of 20 kN at section B constitute the design loading. Design the beam A-B using an IPE section in steel S 275 for the ultimate limit states. The end sections A and B may be assumed as laterally braced by the secondary beams.

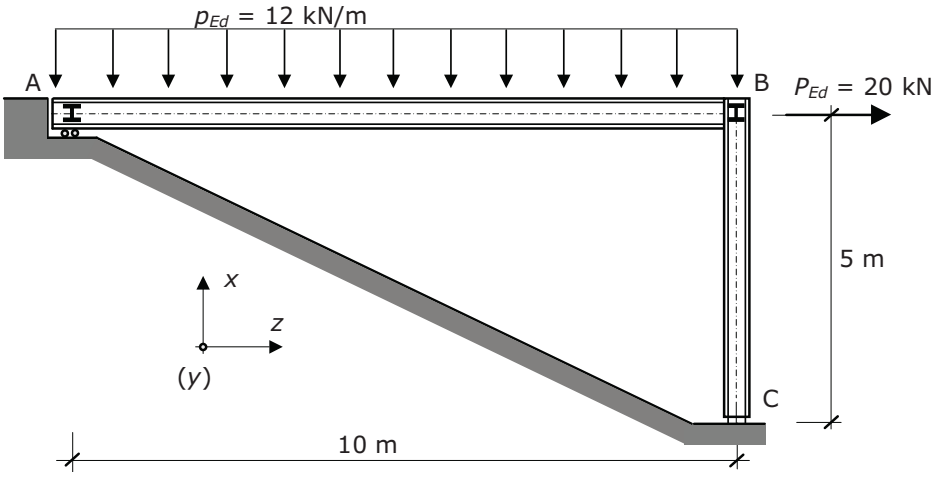

Figure 1.32 Steel frame

i) Internal forces

The internal forces obtained through an elastic analysis of the frame are represented in Figure 1.33. The beam is submitted to bending moment and shear force with the following design values: V_{Ed} = 70,0 kN (at cross section B) e M_{Ed} = 104,2 kNm (maximum value along the beam).

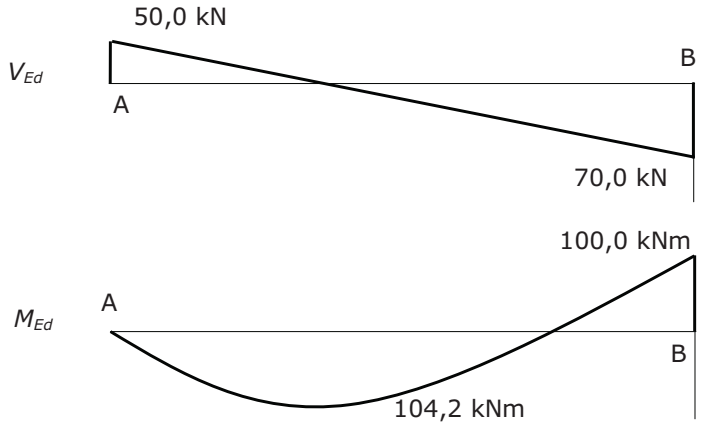

Figure 1.33 Diagrams of internal forces

ii) Cross section resistance to bending + shear force

A preliminary design for bending, assuming a cross section of class 1 or 2, leads to the following solution:

$$M_{Ed} = 104,2 \text{ kNm} \le W_{pl,y} f_y / \gamma_{M0} = W_{pl,y} \cdot 275 \cdot 10^3 / 1,00$$

$$\Rightarrow \quad W_{pl,y} \ge 378,9 \cdot 10^{-6} \text{m}^3 = 378,9 \text{ cm}^3 .$$

Based on a table of commercial sections, an IPE 270 with $W_{pl,y}$ = 484,0 cm^3 is required. As the beam is composed by an open cross section, laterally braced only at end sections, the lateral torsional buckling tends to be the governing mode; therefore, an IPE 450 is adopted.

The relevant geometrical properties of the cross section IPE 450 are: A = 98,82 cm^2, b = 190 mm, h = 450 mm, t_f = 14,6 mm, t_w = 9,4 mm, r = 21 mm I_z = 1676 cm^4, I_T = 66,87 cm^4, I_W = 791·10^3 cm^6 and $W_{pl,y}$ = 1702 cm^3. The main mechanical properties of the steel S 275 are: f_y = 275 MPa, E = 210 GPa and G = 81 GPa.

Cross section classification (Table 5.2 of EC3-1-1):

Web in bending,

$$\frac{c}{t} = \frac{378,8}{9,4} = 40,3 < 72\,\varepsilon = 72 \cdot 0,92 = 66,2 . \qquad \text{(class 1)}$$

Flange in compression,

$$\frac{c}{t} = \frac{190/2 - 9,4/2 - 21}{14,6} = 4,7 < 9\,\varepsilon = 9 \cdot 0,92 = 8,3 . \qquad \text{(class 1)}$$

The section is class 1, so the bending resistance based on the plastic capacity is verified.

For an IPE 450 the shear area is given by A_v = 50,85 cm^2; the shear resistance and the shear buckling (conservatively taking η = 1,0) are achieved by the verification of the following conditions:

$$V_{Ed} = 70,0 \text{ kN} < V_{pl,Rd} = \frac{A_v f_y}{\gamma_{M0}\sqrt{3}} = \frac{50,85 \cdot 10^{-4} \cdot 275 \cdot 10^3}{1,00 \cdot \sqrt{3}} = 807,4 \text{ kN}.$$

$$\frac{h_w}{t_w} = \frac{420,8}{9,4} = 44,8 < 72\frac{\varepsilon}{\eta} = 72 \cdot \frac{0,92}{1,00} = 66,2.$$

As $V_{Ed} = 70,0\text{kN} < 50\% V_{pl,Rd} = 0,50 \cdot 807,4 = 403,7\text{kN}$, it is not necessary to reduce the bending resistance to account for the shear force.

iii) Lateral-torsional buckling resistance

In the present example, the general method prescribed in clause 6.3.2.2 of EC3-1-1 for the verification of the lateral torsional buckling is used. On the prediction of the critical moment, the lateral bending and warping restraints at end sections A and B are neglected. The critical moment is evaluated through the Eqn. (1.45), with the coefficients $C_1 \approx 1,20$ and $C_2 \approx 0,70$ obtained from Boissonnade et al. (2006), based on the bending moment diagram shown in Figure 1.33.

For L = 10 m, considering $k_z = k_w = 1,0$ and z_g = 225 mm (loads applied at upper flange level), the elastic critical moment is given by:

$M_{cr} = 133.4 \text{ kNm}$.

The non-dimensional slenderness is given by:

$$\bar{\lambda}_{LT} = \left[W_y f_y / M_{cr}\right]^{0,5} = \left[1702 \cdot 10^{-6} \cdot 355 \cdot 10^3 / 133,4\right]^{0,5} = 1,87.$$

Since α_{LT} = 0,34 for a I rolled section, with h/b>2 (in accordance with general method), comes:

$$\Phi_{LT} = 0,5 \cdot \left[1 + \alpha_{LT}\left(\bar{\lambda}_{LT} - 0,2\right) + \bar{\lambda}_{LT}^2\right] = 2,53;$$

$$\chi_{LT} = \frac{1}{\Phi_{LT} + \left(\Phi_{LT}{}^2 - \bar{\lambda}_{LT}^2\right)^{0,5}} = 0,24.$$

The design buckling resistance is given by:

$$M_{b,Rd} = 0,24 \cdot 1702 \cdot 10^{-6} \cdot \frac{275 \cdot 10^3}{1,00} = 112,3 \text{ kNm}.$$

As $M_{b,Rd} = 112,3 \text{ kNm} > M_{Ed} = 104,2 \text{ kNm}$ (utilization ratio of 0,93), the cross section IPE 400 in steel S 355 is satisfactory.

In the present example the lateral-torsional buckling was clearly the governing mode of the beam design for the ultimate limit states. The cross section sufficient to achieve the cross section resistance (an IPE 270) is quite lower than the required cross section for the lateral-torsional buckling verification (an IPE 450). This is a consequence of the use an open I section with high slenderness (and consequently low lateral and torsional stiffness), submitted to a downward loading applied at the top flange level. In this case, the designed solution would be improved if it was possible to introduce intermediate lateral bracings.

1.3.5 Design of beam-columns

1.3.5.1 Code prescriptions

Theoretical concepts

A beam-column is a member subject to bending and axial force (in general the vertical members of framed structures as shown in Figure 1.34). The behaviour of such members results from the combination of both effects and varies with slenderness. At low slenderness, the cross sectional resistance dominates. With increasing slenderness, pronounced second-order effects appear, significantly influenced by both geometrical imperfections and residual stresses. Finally, in the high slenderness range, buckling is dominated by elastic behaviour, failure tending to occur by flexural buckling (typical of members in pure compression) or by lateral-torsional buckling (typical of members in bending) (Simões da Silva et al., 2013).

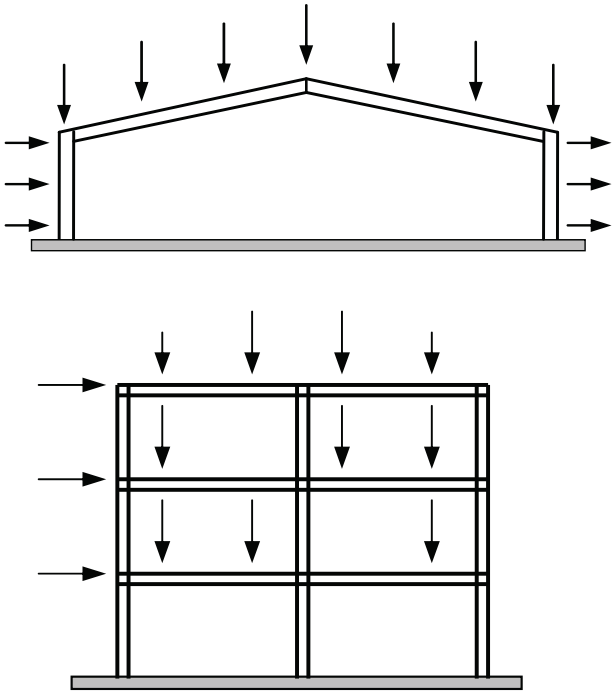

Figure 1.34 Steel members subjected to bending and axial force

The behaviour of a member under bending and axial force results from the interaction between instability and plasticity and is influenced by geometrical and material imperfections. The verification of the safety of members subject to bending and axial force is made in two steps:

- verification of the resistance of cross sections;
- verification of the member buckling resistance (in general governed by flexural or lateral-torsional buckling).

As referred before (section 1.2.2.4), the classification of a cross section is based on its maximum resistance with respect to the type of the applied internal forces, independent from their values. In the case of bending and axial force, there is a range of *M*-*N* values that correspond to the ultimate resistance of the cross section. Another additional

difficulty consists in the definition of the cross section class to be considered in the verification of the stability of a member, as in general it varies along the member as a consequence of varying internal forces. As EC3-1-1 does not provide clear procedures to deal with these two issues, example 6 follows the guidance from the SEMI-COMP+ project (Greiner et al., 2011). In accordance with this procedure, the classification for member buckling design is established as an equivalent class based on the cross section with maximum first-order utilization factor; the position of the neutral axis for the case of complete yielding of the cross section (limits between classes 1 and 2 and classes 2 and 3), is determined based on the proportionality of the acting forces.

Cross section resistance

The cross section resistance is based on its plastic capacity (class 1 or 2 sections) or on its elastic capacity (class 3 or 4 cross sections). When a cross section is subjected to bending moment and axial force ($N + M_y$, $N + M_z$ or even $N + M_y + M_z$), the bending moment resistance should be reduced, using interaction formulae. The interaction formulae to evaluate the elastic cross section capacity are the well-known formulae of simple beam theory, valid for any type of cross section. However, the formulae to evaluate the plastic cross section capacity are specific for each cross section shape.

Clause 6.2.9 provides several interaction formulae between bending moment and axial force, in the plastic range and in the elastic range. These are applicable to most cross sections.

a) Class 1 or 2 sections

In class 1 or 2 cross sections, the following condition should be satisfied (clause 6.2.9.1(2)):

$$M_{Ed} \leq M_{N,Rd}\,, \tag{1.61}$$

where M_{Ed} is the design bending moment and $M_{N,Rd}$ represents the design plastic moment resistance reduced due to the axial force N_{Ed}.

For I or H sections, rolled or welded, with equal flanges and where fastener holes are not to be accounted for, the reduced plastic moment resistances, $M_{N,y,Rd}$ and $M_{N,z,Rd}$ about the y and z axis respectively can be obtained from clause 6.2.9.1(5):

$$M_{N,y,Rd} = M_{pl,y,Rd}\,\frac{1-n}{1-0,5a} \qquad \text{but} \qquad M_{N,y,Rd} \leq M_{pl,y,Rd}\,; \tag{1.62}$$

$$M_{N,z,Rd} = M_{pl,z,Rd} \qquad \text{if} \qquad n \leq a\,; \tag{1.63}$$

$$M_{N,z,Rd} = M_{pl,z,Rd}\left[1-\left(\frac{n-a}{1-a}\right)^2\right] \qquad \text{if} \qquad n > a\,, \tag{1.64}$$

where $a = (A\text{-}2bt_f)/A$, but $a \leq 0{,}5$. For low values of axial force, the reduction of the plastic moment resistance is not significant, as can be seen in Figure 1.35. For doubly symmetric I or H sections, if the conditions prescribed in clause 6.2.9.1(4) are fulfilled the interaction bending moment-axial force can be neglected.

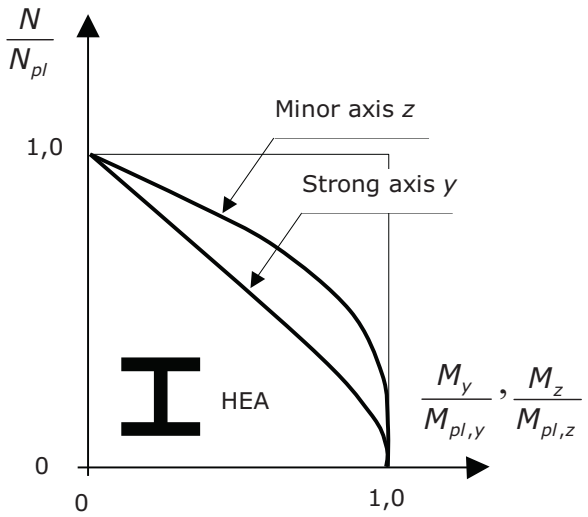

Figure 1.35 Interaction bending-axial force in an HEA section

For circular hollow sections, the reduced plastic moment resistance is given by:

$$M_{N,Rd} = M_{pl,Rd}\left(1 - n^{1,7}\right). \tag{1.65}$$

For rectangular hollow sections of uniform thickness and for welded box sections with equal flanges and equal webs and where fastener holes are not to be accounted for, the reduced plastic moment resistances, can also be obtained from clause 6.2.9.1(5):

$$M_{N,y,Rd} = M_{pl,y,Rd}\frac{1-n}{1-0,5a_w} \quad \text{but} \quad M_{N,y,Rd} \le M_{pl,y,Rd}; \tag{1.66}$$

$$M_{N,z,Rd} = M_{pl,z,Rd}\frac{1-n}{1-0,5a_f} \quad \text{but} \quad M_{N,z,Rd} \le M_{pl,z,Rd}, \tag{1.67}$$

where $a_w \le 0,5$ and $a_f \le 0,5$ are the ratios between the area of the webs and of the flanges, respectively, and the gross area of the cross section.

In a cross section under bi-axial bending and axial force, the $N + M_y + M_z$ interaction can be checked by the following condition (clause 6.2.9.1(6) of EC3-1-1):

$$\left[\frac{M_{y,Ed}}{M_{N,y,Rd}}\right]^{\alpha} + \left[\frac{M_{z,Ed}}{M_{N,z,Rd}}\right]^{\beta} \le 1,00, \tag{1.68}$$

where α and β are parameters that depend on the shape of the cross section and $M_{N,y,Rd}$ and $M_{N,z,Rd}$ are the reduced plastic moments resistances around y and z, respectively, evaluated as previously described. The values of α and β are given as follows:

- I or H sections $\alpha = 2$; $\beta = 5n$, but $\beta \ge 1$;
- circular hollow sections $\alpha = \beta = 2$;
- rectangular hollow sections $\alpha = \beta = 1,66/(1\text{-}1,13n^2)$, but $\alpha = \beta \le 6$.

b) Class 3 or 4 cross sections

In class 3 or 4 cross sections, the interaction between bending and axial force requires that the following condition be checked:

$$\sigma_{x,Ed} \leq \frac{f_y}{\gamma_{M0}}, \tag{1.69}$$

where $\sigma_{x,Ed}$ is the design value of the local longitudinal stress due to bending moment and axial force, taking into account the fastener holes where relevant. This stress is evaluated by an elastic stress analysis, based on the gross cross section for class 3 cross sections, and on a reduced effective cross section for class 4 sections. Additionally, in class 4 cross sections the bending moments due to the shift of the centroidal axis on the reduced effective cross section should be taken into account, see clause 6.2.9.3(2).

c) Interaction of bending, axial and shear force

The interaction between bending, axial and shear force should be checked as follows (clause 6.2.10 of EC3-1-1):

- when $V_{Ed} < 50\%$ of the design plastic shear resistance $V_{pl,Rd}$, no reduction need be made in the bending and axial force resistances obtained from clause 6.2.9;
- when $V_{Ed} \geq 50\%$ of $V_{pl,Rd}$, then the design resistance to the combination of bending moment and axial force should be calculated using a reduced yield strength for the shear area. This reduced strength is given by $(1-\rho)f_y$, where $\rho = (2V_{Ed}/V_{pl,Rd}-1)^2$.

Member resistance

For a member under bending and compression, besides the first-order moments and displacements (obtained based on the undeformed configuration), additional second-order moments and displacements exist ("*P*-δ" effects). In the past, various interaction formulae have been proposed to represent this situation over the full slenderness range. The present approach of EC3-1-1 is based on a linear-additive interaction formula, illustrated by Eqn. (1.70). According this approach, the effects of the axial compression and the bending moments are added linearly and the non-linear effects of the axial compression are taken into account by specific interaction factors.

$$f\left(\frac{N}{N_u}, \frac{M_y}{M_{uy}}, \frac{M_z}{M_{uz}}\right) \leq 1{,}00, \tag{1.70}$$

where N, M_y and M_z are the applied forces and N_u, M_{uy} and M_{uz} are the design resistances, that take in due account the associated instability phenomena.

EC3-1-1 provided various procedures for the verification of the global stability of a steel structure, including the different ways of considering the second order effects (local *P*-δ effects and global *P*-Δ effects). Local *P*-δ effects are generally taken into account according to the procedures given in clause 6.3 of EC3-1-1; global *P*-Δ effects are either directly considered in the global analysis of the structure, or they are indirectly considered, by an appropriate increase of the buckling lengths of the members.

The instability of a member of doubly symmetric cross section, not susceptible to distortional deformations, and subject to bending and axial compression, can be due to flexural buckling or to lateral torsional buckling. Therefore, clause 6.3.3(1) considers two distinct situations:

- members not susceptible to torsional deformation, such as members of circular hollow section or other sections restrained from torsion. Here, flexural buckling is the relevant instability mode;
- members that are susceptible to torsional deformations, such as members of open section (I or H sections) that are not restrained from torsion. Here, lateral torsional buckling tends to be the relevant instability mode.

Consider a single span member of doubly symmetric section, with the "standard case" end conditions. The member is subject to bending moment and axial compression. The following conditions should be satisfied:

$$\frac{N_{Ed}}{\chi_y N_{Rk}/\gamma_{M1}} + k_{yy}\frac{M_{y,Ed}+\Delta M_{y,Ed}}{\chi_{LT} M_{y,Rk}/\gamma_{M1}} + k_{yz}\frac{M_{z,Ed}+\Delta M_{z,Ed}}{M_{z,Rk}/\gamma_{M1}} \le 1,00\ ; \tag{1.71}$$

$$\frac{N_{Ed}}{\chi_z N_{Rk}/\gamma_{M1}} + k_{zy}\frac{M_{y,Ed}+\Delta M_{y,Ed}}{\chi_{LT} M_{y,Rk}/\gamma_{M1}} + k_{zz}\frac{M_{z,Ed}+\Delta M_{z,Ed}}{M_{z,Rk}/\gamma_{M1}} \le 1,00\ , \tag{1.72}$$

where:

N_{Ed}, $M_{y,Ed}$ and $M_{z,Ed}$ are the design values of the axial compression force and the maximum bending moments along the member about y and z, respectively;

$\Delta M_{y,Ed}$ and $\Delta M_{z,Ed}$ are the moments due to the shift of the centroidal axis on a reduced effective class 4 cross section;

χ_y and χ_z are the reduction factors due to flexural buckling about y and z, respectively, evaluated according to clause 6.3.1 of EC3-1-1;

χ_{LT} is the reduction factor due to lateral-torsional buckling, evaluated according to clause 6.3.2 of EC3-1-1 (χ_{LT} = 1.0 for members that are not susceptible to torsional deformation);

k_{yy}, k_{yz}, k_{zy} and k_{zz} are interaction factors that depend on the relevant instability and plasticity phenomena, obtained through Annex A (Method 1) or Annex B (Method 2);

$N_{Rk} = f_y A_i$, $M_{i,Rk} = f_y W_i$ and $\Delta M_{i,Ed}$ are evaluated according to Table 1.25, depending on the cross sectional class of the member.

Table 1.25 Values for the calculation of N_{Rk}, $M_{i,Rk}$ and $\Delta M_{i,Ed}$

Class	**1**	**2**	**3**	**4**
A_i	A	A	A	A_{eff}
W_y	$W_{pl,y}$	$W_{pl,y}$	$W_{el,y}$	$W_{eff,y}$
W_z	$W_{pl,z}$	$W_{pl,z}$	$W_{el,z}$	$W_{eff,z}$
$\Delta M_{y,Ed}$	0	0	0	$e_{N,y} N_{Ed}$
$\Delta M_{z,Ed}$	0	0	0	$e_{N,z} N_{Ed}$

In EC3-1-1 two methods are given for the calculation of the interaction factors k_{yy}, k_{yz}, k_{zy} and k_{zz}; Method 1, developed by a group of French and Belgian researchers, and Method 2, developed by a group of Austrian and German researchers (Boissonnade et al., 2006).

In members that are not susceptible to torsional deformation, it is assumed that there is no risk of lateral torsional buckling. The stability of the member is then verified by checking against flexural buckling about *y* and about *z*. This procedure requires application of Eqns. (1.71) (flexural buckling about *y*) and (1.72) (flexural buckling about *z*), considering χ_{LT} = 1,0 and calculating the interaction factors k_{yy}, k_{yz}, k_{zy} and k_{zz} for a member not susceptible to torsional deformation.

In members that are susceptible to torsional deformation, it is assumed that lateral torsional buckling is more critical. In this case, Eqns. (1.71) and (1.72) should be applied, with χ_{LT} evaluated according to clause 6.3.2 of EC3-1-1, and calculating the interaction factors for a member susceptible to torsional deformation.

According to Method 1, a member is not susceptible to torsional deformations if $I_T \geq I_y$, where I_T and I_y are the torsion constant and the second moment of area about *y*, respectively. If the section is such that $I_T < I_y$, but there are lateral restraints along the member, this situation could still be considered as not susceptible to torsional deformations, if the following condition is verified:

$$\bar{\lambda}_0 \leq 0,2\sqrt{C_1}\sqrt[4]{\left(1-\frac{N_{Ed}}{N_{cr,z}}\right)\left(1-\frac{N_{Ed}}{N_{cr,T}}\right)}, \tag{1.73}$$

where C_1 is a coefficient that depends on the shape of the bending moment diagram between laterally braced sections (obtained according to sub-section 3.4.1.1), $N_{cr,z}$ and $N_{cr,T}$ represent the elastic critical loads for flexural buckling about *z* and for torsional buckling, respectively, and $\bar{\lambda}_0$ is the non-dimensional slenderness coefficient for lateral torsional buckling, assessed for a situation with constant bending moment. If the condition (1.73) is not satisfied, the member must be considered as a member susceptible to torsional deformations.

According to Method 2, the following members may be considered as not susceptible to torsional deformation:

- members with circular hollow sections;
- members with rectangular hollow sections but, according to some authors (Kaim, 2004), only if $h/b \leq 10/\bar{\lambda}_z$, where *h* and *b* are the depth and width of the cross section respectively, and $\bar{\lambda}_z$ is the non-dimensional slenderness relative to the *z* axis;
- members with open cross section, provided that they are torsionally and laterally restrained. According to Boissonnade et al. (2006) a member with open I or H section, restrained by continuous restraints, may be classified as not susceptible to torsional deformation if the conditions predicted in the Annex BB.2 of EC3-1-1 are fulfilled; other situations must be demonstrated.

Members of open section, such as I or H sections, are considered as members susceptible to torsional deformations if they are not adequately torsionally and laterally restrained. Laterally restrained means that the cross section is laterally restrained at the compression level.

1.3.5.2 Worked examples

Example 6 – Verify the safety of column A-B of a typical industrial building, illustrated in Figure 1.36. The column' section is an IPE 360 (E = 210 GPa and G = 81GPa) in S 355 steel. The design loading is described in Figure 1.36. It can be assumed that shear is small enough to be neglected in the verification of the member. The structure is assumed to be a sway frame. So, in accordance with the second method described in 5.2.2(7)b of EC3-1-1, the design internal forces (given in Figure 1.36) were obtained from a second order analysis and the buckling length in the plane of the framework (plane x-z) to be used in the design checks is given by $L_{E,y}$ = 6,0 m, equal to the real length. For the buckling length in the x-y plane, consider that the column is braced at the bottom, at mid-height and at the top.

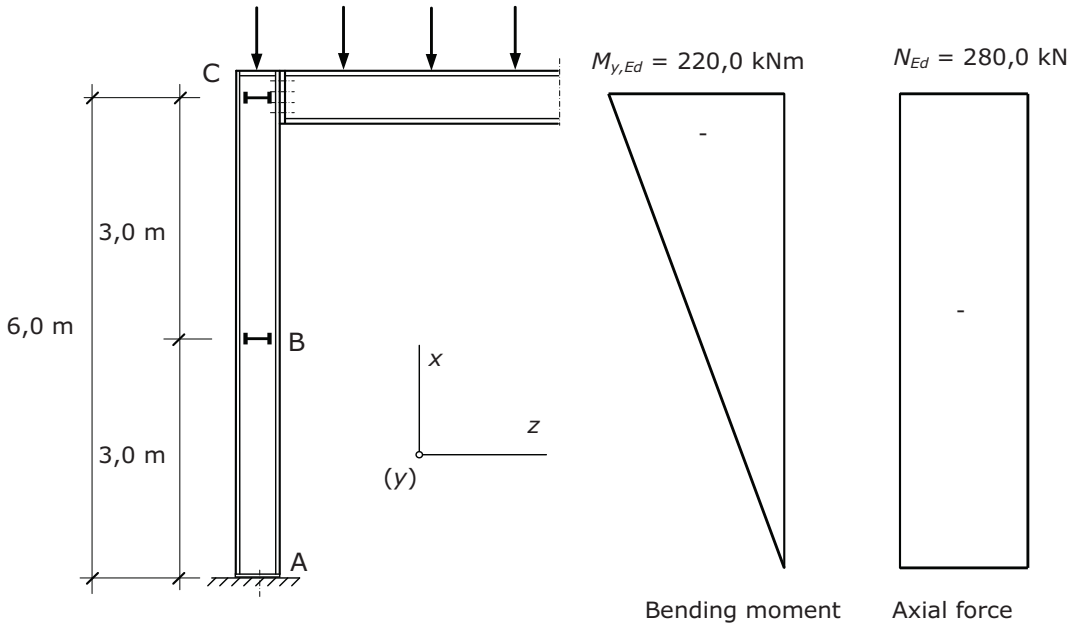

Figure 1.36 Column subjected to major-axis bending and compression

Geometrical characteristics of the IPE 360: A = 72,73 cm^2, h = 360 mm, b = 170 mm, $W_{el,y}$ = 903,6 cm^3, $W_{pl,y}$ = 1019 cm^3, I_y = 16270 cm^4, i_y = 14,95 cm, $W_{el,z}$ = 122,8 cm^3, $W_{pl,z}$ = 191,1 cm^3, I_z = 1043 cm^4, i_z = 3,79 cm, I_T = 37,32 cm^4 and I_W = 313,6·10^3 cm^6.

i) Cross section classification

EC3-1-1 does not provide criteria for the definition of the cross sectional class to be considered in the verification of the stability of a member, for the common case in which the class varies along the member as a consequence of varying internal forces. Following the guidance from the SEMI-COMP+ project (Greiner et al., 2011), the classification for member buckling design may be established as an equivalent class based on the cross section with maximum first-order utilization factor. In this case (see Figure 1.37), since the utilization factor is maximum at cross section C (UF = 0.61), the classification of the beam-column for member buckling design corresponds to the cross sectional class of section C. As this section is subjected to bending and compression, the position of the neutral axis for the situation of complete plastification of the section, which is necessary for the classification of the web, depends on the relation between the bending moment and the axial force. Following again the guidance from the SEMI-COMP+ project, the position of the neutral axis, for fully plastic stress distributions, may be obtained by the following equation:

$$\alpha = \frac{1}{2} + \frac{\left|-220\right|}{-280}\left(\frac{1}{298,6\cdot 10^{-3}} - \frac{1}{2\cdot 298,6\cdot 10^{-3}}\right)$$

$$\left(\sqrt{\left(298,6\cdot 10^{-3}\frac{(-280)}{(-220)}\right)^2 + \frac{-280^2\left(4\cdot 1019\cdot 10^{-6} - \left(298,6\cdot 10^{-3}\right)^2\cdot 8\cdot 10^{-3}\right)}{(-220)^2\cdot 8\cdot 10^{-3}}} + 4\right) = 0,759.$$

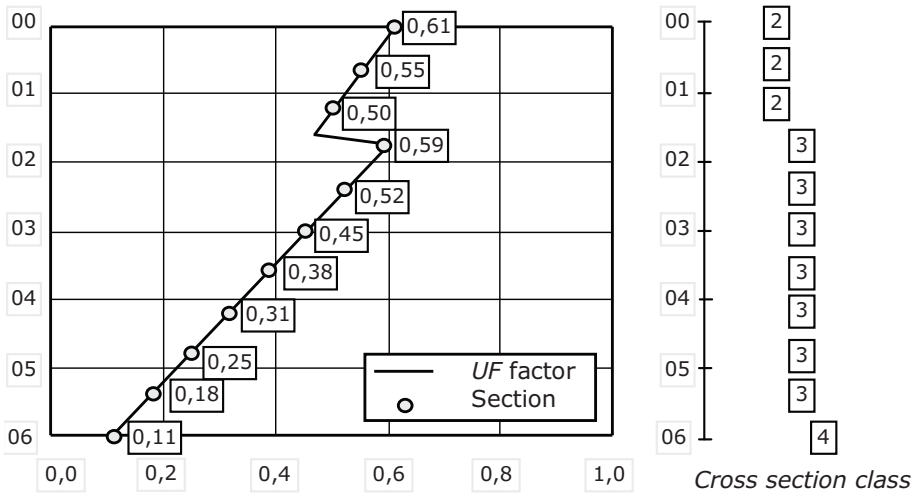

Figure 1.37 Utilization factor *UF* and cross section class along the member

For the web in bending and compression,

$$c/t = 298,6/8 = 37,3 > \frac{396\,\varepsilon}{13\,\alpha - 1} = \frac{396\cdot 0,81}{13\cdot 0,759 - 1} = 36,2\,;$$ (not of class 1)

$$c/t = 298,6/8 = 37,3 < \frac{456\,\varepsilon}{13\,\alpha - 1} = \frac{456\cdot 0,81}{13\cdot 0,759 - 1} = 41,7\,.$$ (class 2)

Compressed flange,

$$c/t = \left(170/2 - 8/2 - 18\right)/12,7 = 5,0 < 9\,\varepsilon = 9\cdot 0,81 = 7,3\,.$$ (class 1)

Therefore, the section is class 2. Note that if the cross section class were established based on the internal forces at section A (compression only), the class of the member for the stability check would be 4.

ii) Verification of the cross section resistance

Based on the internal force diagrams, section C is the critical cross section, with $M_{y,Ed}$ = 220,0 kNm and N_{Ed} = 280,0 kN. Since

$$N_{pl,Rd} = f_y\,A/\gamma_{M0} = 2581,9\,\text{kN}\,,$$

$$N_{Ed} = 280,0\,\text{kN} < 0,25\,N_{pl,Rd} = 645,5\,\text{kN} \quad \text{and} \quad N_{Ed} = 280,0\,\text{kN} < 0,5\,h_w\,t_w\,f_y/\gamma_{M0} = 475,1\,\text{kN}\,,$$

according to clause 6.2.9.1(4) of EC3-1-1 it is not necessary to reduce the plastic bending resistance, which is therefore given by:

$$M_{pl,y,Rd} = W_{pl,y}\frac{f_y}{\gamma_{M0}} = 361,7\,\text{kNm} > M_{y,Ed} = 220,0\,\text{kNm}\,.$$

It is further noted that strictly speaking the resistance of the cross section A and the section 1,20 m apart from the top (class 4 and 3, respectively) should also be checked; although those calculations are not here presented, the safety of those sections are also verified.

iii) Verification of the stability of the member

In this example only Method 2 is applied. As the member is susceptible to torsional deformations (thin-walled open cross section), it is assumed that lateral-torsional buckling constitutes the relevant instability mode. Since $M_{z,Ed}$ = 0, the following conditions must be verified:

$$\frac{N_{Ed}}{\chi_y N_{Rk}/\gamma_{M1}} + k_{yy}\frac{M_{y,Ed}}{\chi_{LT} M_{y,Rk}/\gamma_{M1}} \le 1,00 ;$$

$$\frac{N_{Ed}}{\chi_z N_{Rk}/\gamma_{M1}} + k_{zy}\frac{M_{y,Ed}}{\chi_{LT} M_{y,Rk}/\gamma_{M1}} \le 1,00 .$$

The following steps are required to calculate the buckling reduction factors χ_y, χ_z, χ_{LT} and the interaction factors k_{yy} and k_{zy}.

Step 1: characteristic resistance of the section

$$N_{Rk} = A f_y = 72,73\cdot 10^{-4}\cdot 355\cdot 10^{3} = 2581,9\,\text{kN};$$

$$M_{y,Rk} = W_{pl,y} f_y = 1019\cdot 10^{-6}\cdot 355\cdot 10^{3} = 361,7\,\text{kNm}.$$

Step 2: reduction coefficients due to flexural buckling, χ_y *and* χ_z

Plane *x-z* - $L_{E,y}$ = 6,0 m.

$$\bar{\lambda}_y = \frac{L_{E,y}}{i_y}\frac{1}{\lambda_1} = \frac{6,0}{14,95\cdot 10^{-2}}\cdot\frac{1}{93,9\cdot 0,81} = 0,53 .$$

Since α_{LT} = 0,21 (Table 6.2 of EC3-1-1, H rolled section, with h/b>1,2, t_f <40 mm and buckling about *y* axis), comes:

$$\Phi_y = 0,68 \qquad \Rightarrow \chi_y = 0,90 .$$

Plane *x-y* - $L_{E,z}$ = 3,0 m, assuming that secondary beams prevent displacements of the braced cross sections in the y direction.

$$\bar{\lambda}_z = \frac{L_{E,z}}{i_z}\frac{1}{\lambda_1} = \frac{3,0}{3,79\cdot 10^{-2}}\cdot\frac{1}{93,9\cdot 0,81} = 1,04 .$$

Since α_{LT} = 0,34 (Table 6.2 of EC3-1-1, H rolled section, with h/b>1,2, t_f<40 mm and buckling about *z* axis), comes:

$$\Phi_z = 1,18 \qquad \Rightarrow \chi_z = 0,58 .$$

Step 3: calculation of the χ_{LT} using the alternative method applicable to rolled or equivalent welded sections (clause 6.3.2.3 of EC3-1-1).

The length between braced sections is L = 3,00 m. Using Eqn. (1.45) and Table 1.20 for a member subjected to unequal end moments, gives:

$$\Psi = 0,50 \;\Rightarrow\; C_1 = 1,31 \;\Rightarrow\; M_{cr} = 649,9\,\text{kNm} \;\Rightarrow \bar{\lambda}_{LT} = 0,75 .$$

As $\alpha_{LT} = 0,49$ (rolled H sections with $h/b > 2 \Rightarrow$ curve c), from clause 6.3.2.3 of EC3-1-1, taking $\bar{\lambda}_{LT,0} = 0,4$ and $\beta = 0,75$, gives:

$\Phi_{LT} = 0,80 \quad \Rightarrow \quad \chi_{LT} = 0,79$.

The correction factor k_c, according to Table 1.24 (Table 6.6 of EC3-1-1), with Ψ = 0,50, is given by:

$$k_c = \frac{1}{1,33 - 0,33\,\Psi} = 0,86 .$$

From Eqn. (1.60),

$$f = 1 - 0,5 \cdot (1 - 0,86) \cdot \left[1 - 2,0 \cdot (0,75 - 0,8)^2\right] = 0,93 .$$

The modified lateral-torsional buckling reduction factor is obtained:

$$\chi_{LT,\mathrm{mod}} = 0,79/0,93 = 0,85 .$$

Step 4: interaction factors k_{yy} and k_{zy}.

Because the member is susceptible to torsional deformations, the interaction factors are obtained from Table B.2 of EC3-1-1.

First, the equivalent factors of uniform moment C_{my} and C_{mLT} are obtained based on the bending moment diagram, between braced sections according to the *z* direction in case of C_{my} and laterally in case of C_{mLT}. The factor C_{my} is taken for a non-sway structure, in accordance with the second method described in clause 5.2.2(7)b of EC3-1-1, that was adopted in this example. Assuming a member braced in z direction and laterally at the base and top, the factors C_{my} and C_{mLT} must be calculated based on the bending moment diagram along the total length of the member; since the bending moment diagram is linear, defined by $M_{y,Ed,base}$ = 0 kNm, $M_{y,Ed,1/2height}$ = -110 kNm and $M_{y,Ed,top}$ = -220 kNm, based on Table B.2 of EC3-1-1,

$$\Psi = M_{y,Ed,base}/M_{y,Ed,top} = (0)/(-220) = 0,0 ;$$

$$C_{my} = 0,60 + 0,4 \cdot (0,0) = 0,60 \quad (> 0,40) .$$

and

$$\Psi = M_{y,Ed,1/2height}/M_{y,Ed,top} = (-110)/(-220) = 0,5 ;$$

$$C_{mLT} = 0,60 + 0,4 \cdot (0,5) = 0,80 \quad (> 0,40) .$$

The interaction factors k_{yy} and k_{zy} are given by:

$$k_{yy} = C_{my}\left[1 + (\bar{\lambda}_y - 0,2)\frac{N_{Ed}}{\chi_y\, N_{Rk}/\gamma_{M1}}\right] = 0,60 \cdot \left[1 + (0,53 - 0,2) \cdot \frac{280,0}{0,90 \cdot 2581,9/1,00}\right] = 0,624;$$

$$\text{as } k_{yy} = 0,624 \le C_{my}\left(1 + 0,8\frac{N_{Ed}}{\chi_y\, N_{Rk}/\gamma_{M1}}\right) = 0,658 ,$$

$$\text{then } k_{yy} = 0,624 .$$

$$k_{zy} = \left[1 - \frac{0,1\bar{\lambda}_z}{(C_{mLT} - 0,25)}\frac{N_{Ed}}{\chi_z\, N_{Rk}/\gamma_{M1}}\right] = \left[1 - \frac{0,1 \cdot 1,04}{(0,80 - 0,25)} \cdot \frac{280,0}{0,58 \cdot 2581,9/1,00}\right] = 0,966 ;$$

$$\text{as } k_{zy} = 0,966 \ge \left[1 - \frac{0,1}{(C_{mLT} - 0,25)}\frac{N_{Ed}}{\chi_z\, N_{Rk}/\gamma_{M1}}\right] = 0,947 ,$$

$$\text{then } k_{zy} = 0,966 .$$

Step 5: Finally, the verification of Eqns. (1.71) and (1.72) yields:

$$\frac{280,0}{0,90 \cdot 2581,9/1,00} + 0,624 \cdot \frac{220,0}{0,85 \cdot 361,7/1,00} = 0,56 < 1,00 ;$$

$$\frac{280,0}{0,58 \cdot 2581,9/1,00} + 0,966 \cdot \frac{220,0}{0,85 \cdot 361,7/1,00} = 0,88 < 1,00 .$$

It is concluded that the section HEB 320 in steel S 355 is adequate.

Example 7 – Safety check of a beam-column of the first storey of the building illustrated in Figure 1.38. The member has a 4.335 m length and is composed by a HEB 320 cross section in steel S 355. The design internal forces obtained through the structure analysis for the various load combinations are illustrated in Figure 1.38. In accordance with these diagrams two simplifications are assumed for the subsequent design verifications: i) the shear force is sufficient small so can be neglected; ii) the shape for the bending moment diagram is linear. So, in accordance with the previous assumptions, the design values of the internal forces are: N_{Ed} = 1704,0 kN and $M_{y,Ed}$ = 24,8 kNm, at base level.

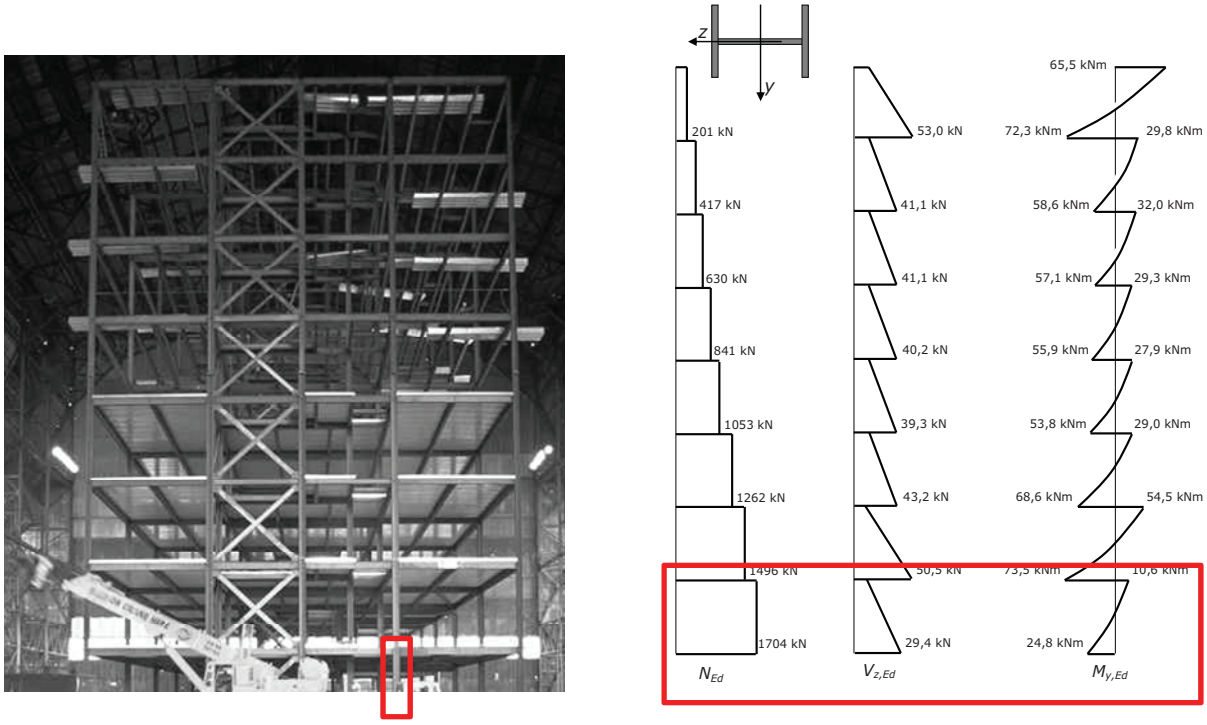

a) *Building* b) *Diagrams of internal forces*

Figure 1.38 Case-study building

The relevant geometric characteristics of HEB 320 cross section are: A = 161,3 cm^2; $W_{pl,y}$ = 2149 cm^3, I_y = 30820 cm^4, i_y = 13,82 cm; I_z = 9239 cm^4, i_z = 7,57 cm; I_T = 225,1 cm^4 and I_W = 2069 · 10^3 cm^6. The mechanical characteristics of the material are: f_y = 355 MPa, E = 210 GPa and G = 81 GPa.

i) Cross section classification

As the value of the compression force is high, the cross section is classified under compression only (conservative approach). As the section HEB 320 is a stocky section, even under this load condition, is class 1.

ii) Verification of the cross section resistance

Based on the internal force diagrams, the bottom cross section is the critical cross section, with $M_{y,Ed}$ = 24.8 kNm and N_{Ed} = 1704,0 kN.

$$N_{pl,Rd} = A f_y / \gamma_{M0} = 161,3 \cdot 10^{-4} \cdot 355 \cdot 10^3 / 1,00 = 5726,2\,\text{kN}.$$

As $N_{Ed} = 1704,0\,\text{kN} < N_{pl,Rd} = 5726,2\,\text{kN}$, the axial force resistance is verified.

Since $N_{Ed} = 1704,0\,\text{kN} > 0,25\,N_{pl,Rd} = 1431,5\,\text{kN}$,

according to clause 6.2.9.1(4) it is necessary to reduce the plastic bending resistance, which is evaluated in accordance with the following:

$$M_{pl,y,Rd} = \frac{W_{pl,y} f_y}{\gamma_{Mo}} = \frac{2149 \cdot 10^{-6} \cdot 355 \cdot 10^3}{1,00} = 762,9\,\text{kNm};$$

$$n = \frac{N_{Ed}}{N_{pl,Rd}} = \frac{1704,0}{5726,2} = 0,30;\ a = \frac{A - 2\,b\,t_f}{A} = \frac{161,3 - 2 \cdot 30 \cdot 2,05}{161,3} = 0,24;$$

$$M_{N,y,Rd} = M_{pl,y,Rd} \frac{1-n}{1-0,5\,a} = 762,9 \cdot \frac{1-0,30}{1-0,5 \cdot 0,24} = 606,9\,\text{kNm}.$$

As $M_{y,Ed} = 24,8\,\text{kNm} < M_{N,y,Rd} = 606,9\,\text{kNm}$,

the bending resistance, accounting the axial force, is verified.

iii) Verification of the stability of the member

In this example only Method 2 is applied. As the member is susceptible to torsional deformations (thin-walled open cross section), it is assumed that lateral-torsional buckling constitutes the relevant instability mode. Since $M_{z,Ed}$ = 0, the following conditions must be verified:

$$\frac{N_{Ed}}{\chi_y N_{Rk}/\gamma_{M1}} + k_{yy} \frac{M_{y,Ed}}{\chi_{LT} M_{y,Rk}/\gamma_{M1}} \le 1,00;$$

$$\frac{N_{Ed}}{\chi_z N_{Rk}/\gamma_{M1}} + k_{zy} \frac{M_{y,Ed}}{\chi_{LT} M_{y,Rk}/\gamma_{M1}} \le 1,00.$$

The following steps are required to calculate the buckling reduction factors χ_y, χ_z, χ_{LT} and the interaction factors k_{yy} and k_{zy}.

Step 1: characteristic resistance of the section

$$N_{Rk} = A f_y = 161,3 \cdot 10^{-4} \cdot 355 \cdot 10^3 = 5726,2\,\text{kN};$$

$$M_{y,Rk} = W_{pl,y} f_y = 2149 \cdot 10^{-6} \cdot 355 \cdot 10^3 = 762,9\,\text{kNm}.$$

Step 2: reduction coefficients due to flexural buckling, χ_y *and* χ_z

Plane *x-z* - $L_{E,y}$ = 4,335 m.

$$\bar{\lambda}_y = \frac{L_{E,y}}{i_y}\frac{1}{\lambda_1} = \frac{4,335}{13,58\cdot 10^{-2}}\cdot\frac{1}{93,9\cdot 0,81} = 0,42\,.$$

Since α_{LT} = 0,34 (Table 6.2 of EC3-1-1, H rolled section, with h/b=320/300=1,07<1,2, t_f=20,5 mm<40 mm and buckling about *y* axis), comes:

$$\Phi_y = 0,62 \qquad \Rightarrow \chi_y = 0,92\,.$$

Plane *x-y* - $L_{E,z}$ = 4,335 m.

$$\bar{\lambda}_z = \frac{L_{E,z}}{i_z}\frac{1}{\lambda_1} = \frac{4,335}{7,57\cdot 10^{-2}}\cdot\frac{1}{93,9\cdot 0,81} = 0,75\,.$$

Since α_{LT} = 0,49 (Table 6.2 of EC3-1-1, H rolled section, with h/b=320/300=1,07<1,2, t_f=20,5 mm<40 mm and buckling about *z* axis), comes:

$$\Phi_z = 0,92 \qquad \Rightarrow \chi_z = 0,69\,.$$

Step 3: calculation of the χ_{LT} using the alternative method applicable to rolled or equivalent welded sections (clause 6.3.2.3 of EC3-1-1).

The length between braced sections is *L* = 4,335 m. Using in the present example the software LTbeam (2002) for a member subjected to unequal end moments, gives:

$$M_{cr} = 5045,1\text{kNm} \quad \Rightarrow \bar{\lambda}_{LT} = 0,39\,.$$

As $\alpha_{LT} = 0,34$ (rolled H sections with $h/b = 320/300 = 1,07 < 2 \;\Rightarrow$ curve b), from clause 6.3.2.3 of EC3-1-1, taking $\bar{\lambda}_{LT,0} = 0,4$ and $\beta = 0,75$, gives:

$$\Phi_{LT} = 0,56 \quad \Rightarrow \quad \chi_{LT} = 0,99\,.$$

The correction factor k_c, according to Table 1.24 (Table 6.6 of EC3-1-1), being Ψ=10,6/(-24,8)=-0,43, is given by:

$$k_c = \frac{1}{1,33-0,33\,\Psi} == \frac{1}{1,33-0,33\cdot(-0,43)} = 0,68\,.$$

From Eqn. (1.60),

$$f = 1-0,5\cdot(1-0,68)\cdot\left[1-2,0\cdot(0,39-0,8)^2\right] = 0,89\,.$$

The modified lateral-torsional buckling reduction factor is obtained:

$\chi_{LT,\text{mod}} = 0,99/0,89 = 1,11 > 1,00$, so $\chi_{LT,\text{mod}} = 1,00$ must be adopted.

Step 4: interaction factors k_{yy} and k_{zy}.

Because the member is susceptible to torsional deformations, the interaction factors are obtained from Table B.2 of EC3-1-1.

First, the equivalent factors of uniform moment C_{my} and C_{mLT} are obtained based on the bending moment diagram, between braced sections according to the *z* direction in case of C_{my} and laterally in case of C_{mLT}. The factor C_{my} is taken for a non-sway structure, in accordance with the second method described in clause 5.2.2(7)b of EC3-1-1, that was adopted in this example. Assuming a member braced in *z* direction and laterally at the

base and top, the factors C_{my} and C_{mLT} must be calculated based on the bending moment diagram along the total length of the member; since the bending moment diagram is linear, defined by $M_{y,Ed,base}$ = 24,8 kNm and $M_{y,Ed,top}$ = -10,4 kNm, based on Table B.2 of EC3-1-1,

$$\Psi = M_{y,Ed,top}/M_{y,Ed,base} = (-10,6)/(24,8) = -0.43;$$

$$C_{my} = C_{mLT} = 0,60 + 0,4 \cdot (-0,43) = 0,43 \quad (> 0,40).$$

The interaction factors k_{yy} and k_{zy} are given by:

$$k_{yy} = C_{my}\left[1 + (\bar{\lambda}_y - 0,2)\frac{N_{Ed}}{\chi_y N_{Rk}/\gamma_{M1}}\right] = 0,43 \cdot \left[1 + (0,42 - 0,2) \cdot \frac{1704,0}{0,92 \cdot 5726,2/1,00}\right] = 0,46;$$

as $k_{yy} = 0,46 \le C_{my}\left(1 + 0,8\frac{N_{Ed}}{\chi_y N_{Rk}/\gamma_{M1}}\right) = 0,54$,

then $k_{yy} = 0,46$.

$$k_{zy} = \left[1 - \frac{0,1\bar{\lambda}_z}{(C_{mLT} - 0,25)}\frac{N_{Ed}}{\chi_z N_{Rk}/\gamma_{M1}}\right] = \left[1 - \frac{0,1 \cdot 0,75}{(0,43 - 0,25)} \cdot \frac{1704,0}{0,69 \cdot 5726,2/1,00}\right] = 0,82;$$

as $k_{zy} = 0,82 \ge \left[1 - \frac{0,1}{(C_{mLT} - 0,25)}\frac{N_{Ed}}{\chi_z N_{Rk}/\gamma_{M1}}\right] = 0,76$,

then $k_{zy} = 0,82$.

Step 5: Finally, the verification Eqns. (1.71) and (1.72) yields:

$$\frac{1704,0}{0,92 \cdot 5726,2/1,00} + 0,43 \cdot \frac{24,8}{1,00 \cdot 762,9/1,0} = 0,34 < 1,00;$$

$$\frac{1704,0}{0,69 \cdot 5726,2/1,00} + 0,82 \cdot \frac{24,8}{1,00 \cdot 762,1/1,00} = 0,46 < 1,00.$$

It is concluded that the section HEB 320 in steel S 355 is adequate.

Example 8 – Consider the column A-B that supports a steel cantilever B-C, represented in Figure 1.39. The column is fixed at section A, while the top section (B) is free to rotate, but restrained from horizontal displacements in both directions. The column is composed by a rectangular hollow section SHS 200x150x8 mm (hot finished) in S 355 steel (E = 210 GPa and G = 81 GPa). Assuming that the indicated loading is already factored for ULS, verify the column safety according to EC3-1-1.

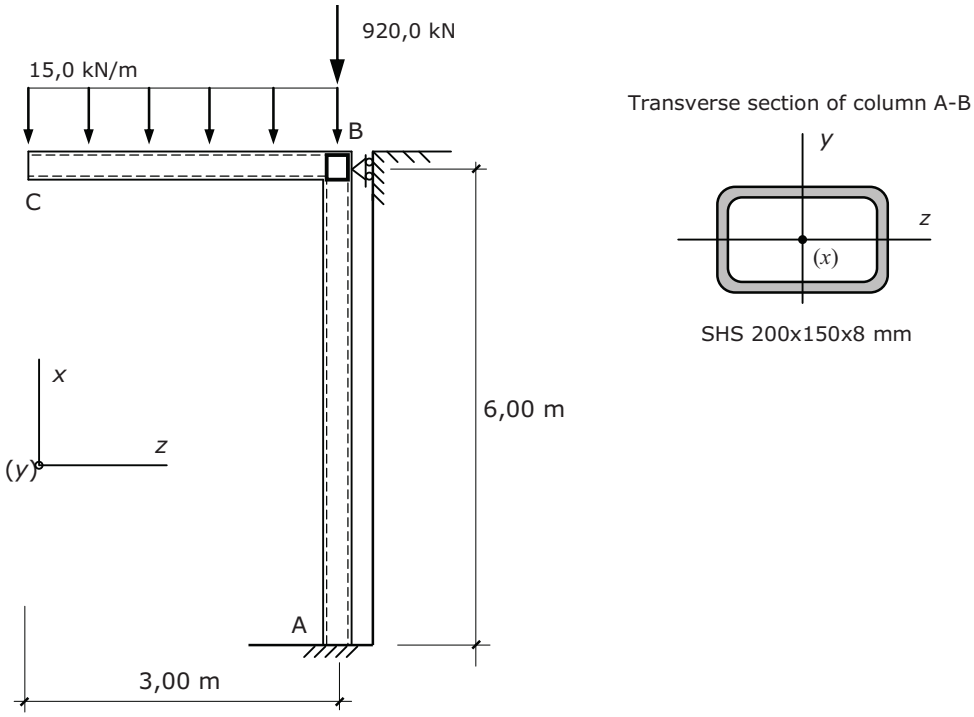

Figure 1.39 Structure with members of rectangular hollow section

i) Internal force diagrams

For the given design loading, the internal force diagrams are represented in Figure 1.40.

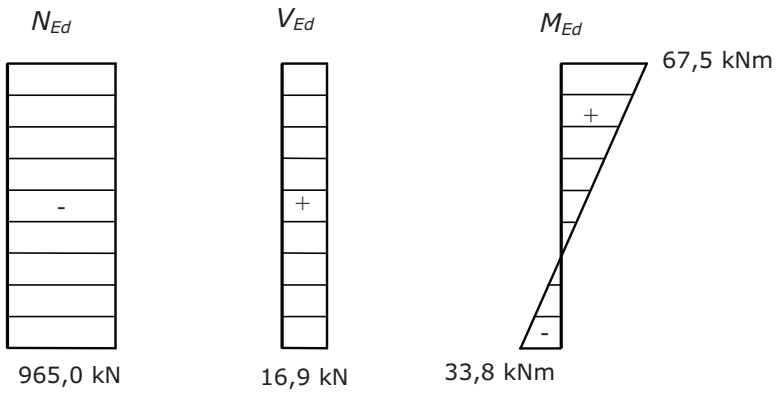

Figure 1.40 Internal force diagrams

ii) Verification of the cross section resistance

The relevant geometrical characteristics of a SHS 200x150x8 mm are the following: A = 52,75 cm^2, $W_{pl,y}$ = 358,8 cm^3, $W_{el,y}$ = 297,1 cm^3, I_y = 2971 cm^4, iy = 7,505 cm, $W_{pl,z}$ = 293,7 cm^3, $W_{el,z}$ = 252,6 cm^3, I_z = 1894 cm^4, i_z = 5,992 cm and I_T = 3643 cm^4.

As the cross section of the member is already known, the verification of its class is carried out according to clause 5.5 of EC3-1-1. For a member subjected to varying bending and compression, the class of the cross section may vary along the member. While this does not introduce any type of difficulty in the verification of the cross section resistance (each section is designed according to its own class), it is more difficult to

define the class of the cross section for the verification of the member's stability, as this is a global verification. In this example, a simplified approach is adopted, whereby the class of the cross section is verified for the most unfavourable situation (compressed section only). Thus, for the longer side, according to Table 1.1 (Table 5.2 in EC3-1-1),

$$c/t \approx (b-3t)/t = (200-3\cdot 8)/8 = 22,0 < 33\,\varepsilon = 33\cdot 0,81 = 26,7\,. \qquad \text{(class 1)}$$

The cross section is class 1 in compression and can be treated as a class 1 cross section for any other combination of stresses.

The resistance to bending about the y axis, combined with the axial force, is obtained from Eqn. (1.62), according to clause 6.2.9.1(5):

$$M_{N,y,Rd} = M_{pl,y,Rd}\,\frac{1-n}{1-0,5\,a_w} \le M_{pl,y,Rd}\,.$$

For the critical cross section (top of the column), subjected to N_{Ed} = 965,0 kN and $M_{y,Ed}$ = 67,5 kNm,

$$n = \frac{N_{Ed}}{N_{pl,Rd}} = \frac{965,0}{52,75\cdot 10^{-4}\cdot 355\cdot 10^{3}/1,00} = 0,52\,;$$

$$a_w = \frac{A-2\,b\,t}{A} = \frac{52,75-2\cdot 15\cdot 0,8}{52,75} = 0,55 > 0,5 \Rightarrow a_w = 0,5\,;$$

$$M_{pl,y,Rd} = 358,8\cdot 10^{-6}\cdot \frac{355\cdot 10^{3}}{1,00} = 127,4\,\text{kNm}\,.$$

The reduced design plastic moment resistance is given by:

$$M_{N,y,Rd} = 127,4\cdot \frac{1-0,52}{1-0,5\cdot 0,5} = 81,5\,\text{kNm} < M_{pl,y,Rd} \quad \Rightarrow \quad M_{N,y,Rd} = 81,5\,\text{kNm}\,.$$

so that, $M_{Ed} = 67,5\,\text{kNm} < M_{N,y,Rd} = 81,5\,\text{kNm}$.

Shear must be verified in any cross section, since the member is under constant shear. From clause 6.2.6(3):

$A_v = \dfrac{A\,h}{b+h} = \dfrac{52,75\cdot 20}{15+20} = 30,14\,\text{cm}^2$, leading to:

$$V_{pl,Rd} = \frac{A_v\,f_y}{\gamma_{M0}\,\sqrt{3}} = \frac{30,14\cdot 10^{-4}\cdot 355\cdot 10^{3}}{1,00\cdot\sqrt{3}} = 617,7\,\text{kN}\,.$$

As $V_{Ed} = 16,9\,\text{kN} < V_{pl,Rd} = 617,7\,\text{kN}$, the resistance to shear is satisfactory.

For the verification of the shear buckling of the web, according to clause 6.2.6(6), with $\eta = 1,0$, $h_w/t_w \approx (h-3t)/t = (200-3\cdot 8)/8 = 22,0 < 72\,\varepsilon/\eta = 58,3$, and so verification is not required.

The verification of the interaction of bending and compression with shear, according to clause 6.2.8 of EC3-1-1, must be done for cross section B. As

$$V_{Ed} = 16,9\,\text{kN} < 0,50\cdot V_{pl,Rd} = 0,50\cdot 617,7 = 308,9\,\text{kN}\,,$$

it is not necessary to reduce the resistance of the section due to this interaction.

iii) Verification of the stability of the member

For the beam-column subject to uniaxial bending (about y) and compression, using a class 1 section, the following conditions must be verified:

$$\frac{N_{Ed}}{\chi_y N_{Rk}/\gamma_{M1}} + k_{yy}\frac{M_{y,Ed}}{\chi_{LT} M_{y,Rk}/\gamma_{M1}} \le 1,00 ;$$

$$\frac{N_{Ed}}{\chi_z N_{Rk}/\gamma_{M1}} + k_{zy}\frac{M_{y,Ed}}{\chi_{LT} M_{y,Rk}/\gamma_{M1}} \le 1,00 .$$

The interaction factors k_{yy} and k_{zy} can be obtained using one of the methods given in clause 6.3.3, Method 1 or Method 2; for the sake of comparison, both are used in this example.

iii-1) Method 1

Since the member has a rectangular hollow section with I_T = 3643 cm^4 > I_y = 2971 cm^4, the member is not susceptible to torsional deformation, so flexural buckling constitutes the relevant instability mode. Therefore it is not necessary to verify lateral-torsional buckling and χ_{LT} = 1,00 in Eqns. (1.71) and (1.72). The following steps are required to calculate the interaction factors k_{yy} and k_{zy}.

Step 1: characteristic resistance of the section

$$N_{Rk} = A f_y = 52,75\cdot 10^{-4}\cdot 355\cdot 10^3 = 1872,6\,\text{kN};$$

$$M_{y,Rk} = W_{pl,y} f_y = 358,8\cdot 10^{-6}\cdot 355\cdot 10^3 = 127,4\,\text{kNm}.$$

Step 2: reduction coefficients due to flexural buckling, χ_y *and* χ_z

Plane *x-z* (buckling about *y*): $L_{E,y} = 0,7\cdot 6,0 = 4,2\,\text{m}$.

$$\bar{\lambda}_y = \frac{L_{E,y}}{i_y}\frac{1}{\lambda_1} = \frac{4,2}{7,505\cdot 10^{-2}}\cdot\frac{1}{93,9\cdot 0,81} = 0,74 ;$$

$\alpha = 0,21$ Curve a (Table 6.2 of EC3-1-1, hot finished hollow section);

$\Phi = 0,83$ $\Rightarrow \chi_y = 0,83$.

Plane *x-y* (buckling about *z*): $L_{E,z} = 0,7\cdot 6,0 = 4,2\,\text{m}$.

$$\bar{\lambda}_z = \frac{L_{E,z}}{i_z}\frac{1}{\lambda_1} = \frac{4,2}{5,992\cdot 10^{-2}}\cdot\frac{1}{93,9\cdot 0,81} = 0,92 ;$$

$\alpha = 0,21$ Curve a (Table 6.2 of EC3-1-1, hot finished hollow section);

$\varphi = 1,00$ $\Rightarrow \chi_z = 0,72$.

Step 3: calculation of the auxiliary terms, including factors C_{yy} and C_{zy} (factors that depend on the degree of plasticity of the section in the collapse situation), defined in Table A.1 of EC3-1-1.

$$N_{cr,y} = \frac{\pi^2 E I_y}{L_{E,y}^2} = \frac{\pi^2\cdot 210\cdot 10^6\cdot 2971\cdot 10^{-8}}{4,2^2} = 3490,8\,\text{kN};$$

$$N_{cr,z} = \frac{\pi^2 E I_z}{L_{E,z}^2} = \frac{\pi^2 \cdot 210 \cdot 10^6 \cdot 1894 \cdot 10^{-8}}{4,2^2} = 2225,4\,\text{kN};$$

$$\mu_y = \frac{1 - \frac{N_{Ed}}{N_{cr,y}}}{1 - \chi_y \frac{N_{Ed}}{N_{cr,y}}} = \frac{1 - \frac{965,0}{3490,8}}{1 - 0,83 \cdot \frac{965}{3490,8}} = 0,94;$$

$$\mu_z = \frac{1 - \frac{N_{Ed}}{N_{cr,z}}}{1 - \chi_z \frac{N_{Ed}}{N_{cr,z}}} = \frac{1 - \frac{965,0}{2225,4}}{1 - 0,72 \cdot \frac{965}{2225,4}} = 0,82;$$

$$w_y = \frac{W_{pl,y}}{W_{el,y}} = \frac{358,8}{297,1} = 1,21 \quad (< 1,5);$$

$$w_z = \frac{W_{pl,z}}{W_{el,z}} = \frac{293,7}{252,6} = 1,16 \quad (< 1,5);$$

$$n_{pl} = \frac{N_{Ed}}{N_{Rk}/\gamma_{M1}} = \frac{965,0}{1872,6/1,00} = 0,52;$$

$$\bar{\lambda}_{\max} = \max\left(\bar{\lambda}_y, \bar{\lambda}_z\right) = \max\left(0,74; 0,92\right) = 0,92.$$

As the member is not susceptible to torsional deformations, in accordance with Table A.1 of EC3-1-1, the equivalent factors of uniform moment are defined by $C_{my} = C_{my,0}$ and $C_{mLT} = 1,0$, where $C_{my,0}$ is the factor obtained based on Table A.2 of EC3-1-1. For a linear bending moment diagram, with $M_{y,Ed,base} = -33,8$ kNm and $M_{y,Ed,top} = 67,5$ kNm,

$$\Psi_y = M_{y,Ed,base}/M_{y,Ed,top} = -33,8/67,5 = -0,50;$$

$$C_{my,0} = 0,79 + 0,21\Psi_y + 0,36\left(\Psi_y - 0,33\right)\frac{N_{Ed}}{N_{cr,y}} =$$

$$= 0,79 + 0,21 \cdot \left(-0,5\right) + 0,36 \cdot \left(-0,50 - 0,33\right) \cdot \frac{965,0}{3490,8} = 0,60;$$

$$C_{my} = C_{my,0} = 0,60.$$

As $I_T > I_y \;\Rightarrow\; a_{LT} = 0 \;\Rightarrow\; b_{LT} = d_{LT} = 0$, factors C_{yy} and C_{zy} are given by:

$$C_{yy} = 1 + \left(w_y - 1\right)\left[\left(2 - \frac{1,6}{w_y} C_{my}^2\, \bar{\lambda}_{\max} - \frac{1,6}{w_y} C_{my}^2\, \bar{\lambda}_{\max}^2\right) n_{pl}\right] \geq \frac{W_{el,y}}{W_{pl,y}} \;\Leftrightarrow$$

$$C_{yy} = 1 + \left(1,21 - 1\right) \cdot \left[\left(2 - \frac{1,6}{1,21} \cdot 0,60^2 \cdot 0,92 - \frac{1,6}{1,21} \cdot 0,60^2 \cdot 0,92^2\right) \cdot 0,52\right] = 1,13$$

$$\left(> W_{el,y}/W_{pl,y} = 297,1/358,8 = 0,83\right);$$

$$C_{zy} = 1 + \left(w_y - 1\right)\left[\left(2 - 14 \frac{C_{my}^2\, \bar{\lambda}_{\max}^2}{w_y^5}\right) n_{pl}\right] \geq 0,6 \sqrt{\frac{w_y}{w_z}} \frac{W_{el,y}}{W_{pl,y}} \;\Leftrightarrow$$

$$C_{zy} = 1 + (1,21 - 1) \cdot \left[\left(2 - 14 \cdot \frac{0,60^2 \cdot 0,92^2}{1,21^5} \right) \cdot 0,52 \right] = 1,04$$

$$\left(> 0,6 \sqrt{\frac{w_y}{w_z}} \frac{W_{el,y}}{W_{pl,y}} = 0,6 \cdot \sqrt{\frac{1,21}{1,16}} \cdot \frac{297,1}{358,8} = 0,51 \right).$$

Step 4: interaction factors k_{yy} and k_{zy}

Based on all the calculated auxiliary terms, considering that the cross section is class 1, expressions in Table A.1 of EC3-1-1, give the following interaction factors k_{yy} and k_{zy}:

$$k_{yy} = C_{my} C_{mLT} \frac{\mu_y}{1 - \frac{N_{Ed}}{N_{cr,y}}} \frac{1}{C_{yy}} = 0,60 \cdot 1,0 \cdot \frac{0,94}{1 - \frac{965,0}{3490,8}} \cdot \frac{1}{1,13} = 0,69 ;$$

$$k_{zy} = C_{my} C_{mLT} \frac{\mu_z}{1 - \frac{N_{Ed}}{N_{cr,y}}} \frac{1}{C_{zy}} 0,6 \sqrt{\frac{w_y}{w_z}} = 0,60 \cdot 1,0 \cdot \frac{0,82}{1 - \frac{965,0}{3490,8}} \cdot \frac{1}{1,04} \cdot 0,6 \cdot \sqrt{\frac{1,21}{1,16}} = 0,40.$$

Finally, Eqns. (1.71) and (1.72) yield:

$$\frac{N_{Ed}}{\chi_y N_{Rk}/\gamma_{M1}} + k_{yy} \frac{M_{y,Ed}}{\chi_{LT} M_{y,Rk}/\gamma_{M1}} = \frac{965,0}{0,83 \cdot 1872,6/1,0} + 0,69 \cdot \frac{67,5}{1,0 \cdot 127,4/1,00} = 0,99 < 1,00 ;$$

$$\frac{N_{Ed}}{\chi_z N_{Rk}/\gamma_{M1}} + k_{zy} \frac{M_{y,Ed}}{\chi_{LT} M_{y,Rk}/\gamma_{M1}} = \frac{965,0}{0,72 \cdot 1872,6/1,00} + 0,40 \cdot \frac{67,5}{1,00 \cdot 127,4/1,00} = 0,93 < 1,00.$$

The rectangular hollow section 200x150x8 mm in S 355 steel is verified according to Method 1.

iii-2) Method 2

As the member has a rectangular hollow section, due to its high lateral bending and torsional stiffness the verification of lateral torsional buckling is not required, and χ_{LT} = 1,0. Because Method 2 only differs from Method 1 with respect to the interaction factors, the calculation of these factors is done directly.

As the member is not susceptible to torsional deformations, the interaction factors must be obtained from Table B.1 of EC3-1-1.

For a linear bending moment diagram, with $M_{y,Ed,base}$ =-33,8 kNm and $M_{y,Ed,top}$ =67,5 kNm,

$\Psi_y = M_{y,Ed,base}/M_{y,Ed,top} = -33,8/67,5 = -0,50$.

Table B.3 of EC3-1-1 gives:

$C_{my} = 0,6 + 0,4 \cdot (-0,50) = 0,40 \quad (\geq 0,40)$.

Based on the previous calculations for Method 1 and for a class 1 section, interaction factors k_{yy} and k_{zy} are given by:

$$k_{yy} = C_{my} \left[1 + (\bar{\lambda}_y - 0,2) \frac{N_{Ed}}{\chi_y N_{Rk}/\gamma_{M1}} \right] = 0,40 \cdot \left[1 + (0,74 - 0,2) \cdot \frac{965,0}{0,83 \cdot 1872,6/1,00} \right] = 0,53 ;$$

as $k_{yy} = 0,53 < C_{my} \left[1 + 0,8 \frac{N_{Ed}}{\chi_y N_{Rk}/\gamma_{M1}} \right] = 0,60$,

$k_{yy} = 0,53$.

According to Method 2, for a rectangular hollow section subject to compression and uniaxial bending about y, may be assumed k_{zy} = 0. Eqns. (1.71) and (1.72) become:

$$\frac{965,0}{0,83 \cdot 1872,6/1,00} + 0,53 \cdot \frac{67,5}{1,00 \cdot 127,4/1,00} = 0,90 < 1,00 ;$$

$$\frac{965,0}{0,72 \cdot 1872,6/1,00} = 0,72 < 1,00 ,$$

so that the rectangular hollow section RHS 200x150x8 mm in S 355 steel is also verified by Method 2. It is noted that, for this case, Method 2 yields less conservative results than Method 1.

References

Boissonnasde N., Greiner, R., Jaspart J. P., Lindner, J. 2006. New design rules in EN 1993-1-1 for member stability, ECCS Technical Committee 8 – Structural Stability, P119, European Convention for Constructional Steelwork, Brussels.

EN 10020:2000. Definition and classification of grades of steel, European Committee for Standardization, Brussels. CEN.

EN 10025-1:2004. Hot rolled products of structural steels – Part 1: General technical delivery conditions, European Committee for Standardization, Brussels. CEN.

EN 10210-1:2006. Hot finished structural hollow sections of non-alloy and fine grain steels – Part 1: Technical delivery conditions, European Committee for Standardization, Brussels. CEN.

EN 10219-1:2006. Cold formed welded structural hollow sections of non-alloy and fine grain steels – Part 1: Technical delivery conditions, European Committee for Standardization, Brussels. CEN.

EN 1090-2:2008+A1:2011. Execution of steel and aluminium structures – Part 2: Technical requirements for steel structures, European Committee for Standardization, Brussels. CEN.

EN 14399-1:2005. High-strength structural bolting assembling for preloaded – Part 1: General requirements, European Committee for Standardization, Brussels. CEN.

EN 15048-1:2007. Non-preloaded structural bolting assemblies – Part 1: General requirements, European Committee for Standardization, Brussels. CEN.

EN 1990:2002. Eurocode, Basis of Structural Design, European Committee for Standardization, Brussels. CEN.

EN 1991-1-1:2002. Eurocode 1: Actions on structures - Part 1-1: General actions - Densities, self-weight, imposed loads for buildings, European Committee for Standardization, Brussels. CEN.

EN 1991-1-4:2005. Eurocode 1: Actions on Structures – Part 1-4: General Actions – Wind actions, European Committee for Standardization, Brussels. CEN.

EN 1993-1-1:2005. Eurocode 3: Design of Steel Structures. Part 1.1: General rules and rules for buildings. CEN.

EN 1993-1-5:2006. Eurocode 3: Design of Steel Structures. Part 1.5: Plated structural elements. CEN.

EN 1993-1-8:2005. Eurocode 3: Design of Steel Structures, Part 1.8: Design of joints, European Committee for Standardization, Brussels.CEN.

Franssen, J. M., Vila Real, P. 2010. Fire design of steel structures, ECCS Eurocode Design Manuals, ECCS Press / Ernst&Sohn.

Greiner, R., Lechner, A., Kettler, M., Jaspart, J. P., Weynand, K., Ziller, C., Oerder, R., Herbrand, M., Simões da Silva, L., Dehan, V. 2011. Design guidelines for cross-section and member design according to Eurocode 3 with particular focus on semi-compact sections, Valorisation Project SEMICOMP+: "Valorisation action of plastic member capacity of semi-compactsteel sections – a more economic approach", RFS2-CT-2010-00023, Brussels.

Kaim, P. 2004. Spatial buckling behaviour of steel members under bending and compression, PhD Thesis, Graz University of Technology, Austria.

LTBeam. 2002. Lateral Torsional Buckling of Beams, LTBeam version 1.0.11, CTICM, France.

Simões da Silva, L., Simões, R., Gervásio, H. 2013. Design of Steel Structures, ECCS Eurocode Design Manuals. Brussels: Ernt & Sohn A Wiley Company, 1st Edition.

CHAPTER 2

BOLTS, WELDS, COLUMN BASE

František WALD

Czech Technical University in Prague, Czech Republic

2 Bolts, Welds, Column Base

2.1 Connections made with bolts, rivets or pins

2.1.1 Bolts

For bolted connections are used bolt classes 4.6, 4.8, 5.6, 5.8, 6.8, 8.8 and 10.9, which characteristic yield strength f_{yb} and characteristic ultimate tensile strength f_{ub} are given in Table 2.1.

Table 2.1 Nominal values of the yield strength f_{yb} and the ultimate tensile strength f_{ub} for bolts (Table 3.1 in EN 1993-1-8)

Bolt class	4.6	4.8	5.6	5.8	6.8	8.8	10.9
f_{yb} **(N/mm^2)**	240	320	300	400	480	640	900
f_{ub} **(N/mm^2)**	400	400	500	500	600	800	1000

Only bolt assemblies of classes 8.8 and 10.9 conform to the requirements. The material properties, dimensions and tolerances of steel rivets should comply with the national requirements. The materials specified in EN 1993-1-8 may be used for anchor bolts provided that the nominal yield strength does not exceed 640 N/mm^2 when the anchor bolts are required to act in shear and not more than 900 N/mm^2 otherwise. Bolted connections loaded in shear should be designed as one of the following:

Category A: Bearing type

In this category bolts from class 4.6 up to and including class 10.9 should be used. No preloading and special provisions for contact surfaces are required. The design ultimate shear load should not exceed the design shear resistance nor the design bearing resistance.

Category B: Slip-resistant at serviceability limit state

In this category bolts from class 8.8 and 10.9 should be used. Slip should not occur at the serviceability limit state. The design serviceability shear load should not exceed the design slip resistance. The design ultimate shear load should not exceed the design shear resistance or the design bearing resistance.

Category C: Slip-resistant at ultimate limit state

In this category bolts from class 8.8 and 10.9 should be used. Slip should not occur at the ultimate limit state. The design ultimate shear load should not exceed the design slip resistance nor the design bearing resistance. In addition for a connection in tension, the design plastic resistance of the net cross-section at bolt holes $N_{net,Rd}$, (see cl. 6.2 in EN 1993-1-1), should be checked at the ultimate limit state.

The design checks for these connections are summarized in Table 2.2.

Table 2.2 Categories of bolted connections (Table 3.2 in EN 1993-1-8)

Category	Criteria	Remarks
Shear connections		
A bearing type	$F_v,E_d \le F_v,R_d$ $F_v,E_d \le F_b,R_d$	No preloading required. Bolt classes from 4.6 to 10.9 may be used.
B slip-resistant at serviceability	$F_v,E_{d,ser} \le F_s,R_{d,ser}$ $F_v,E_d \le F_v,R_d$ $F_v,E_d \le F_b,R_d$	Preloaded 8.8 or 10.9 bolts should be used.
C slip-resistant at ultimate	$F_v,E_d \le F_s,R_d$ $F_v,E_d \le F_b,R_d$ $F_v,E_d \le N_{net},R_d$	Preloaded 8.8 or 10.9 bolts should be used.
Tension connections		
D non-preloaded	$F_t,E_d \le F_t,R_d$ $F_t,E_d \le B_p,R_d$	No preloading required. Bolt classes from 4.6 to 10.9 may be used.
E preloaded	$F_t,E_d \le F_t,R_d$ $F_t,E_d \le B_p,R_d$	Preloaded 8.8 or 10.9 bolts should be used.

Bolted connection loaded in tension should be designed as one of the following:

Category D: Non-preloaded

In this category bolts from class 4.6 up to and including class 10.9 should be used. No preloading is required. This category should not be used where the connections are frequently subjected to variations of tensile loading. However, they may be used in connections designed to resist normal wind loads.

Category E: Preloaded

In this category preloaded 8.8 and 10.9 bolts with controlled tightening should be used.

2.1.2 Positioning of holes for bolts and rivets

Minimum and maximum spacing and end and edge distances for bolts and rivets are given in Table 2.3 and Figure 2.1. Minimum and maximum spacing, end and edge distances for structures subjected to fatigue are given in EN1993-1-9.

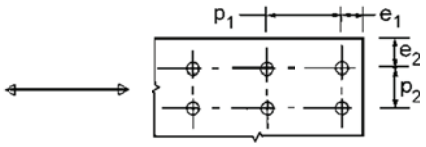

a) Symbols for spacing of fasteners

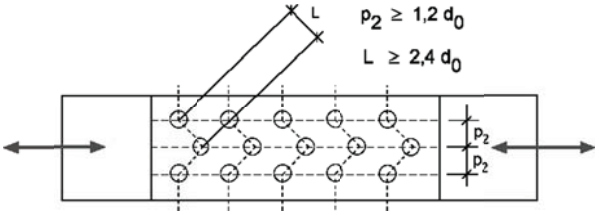

Staggered Rows of fasteners

b) Symbols for staggered spacing

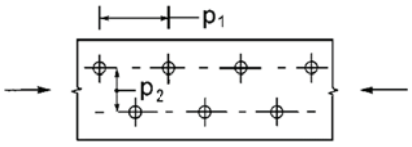

$p_1 \leq 14t$ a ≤ 200 mm $p_2 \leq 14t$ a ≤ 200 mm

c) Staggered spacing in compression members

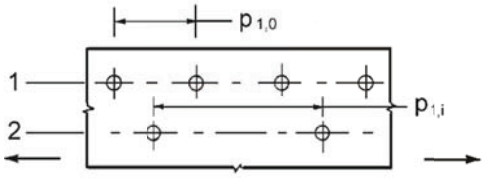

$p_{1,0} \leq 14t$ a ≤ 200 mm $p_{1,i} \leq 28t$ a ≤ 400 mm

1 outer row *2 inner row*

d) Staggered spacing in tension members

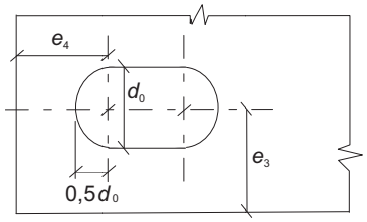

e) End and edge distances for slotted holes

Figure 2.1 Symbols for end and edge distances and spacing of fasteners (Figure 3.1 in EN 1993-1-8)

Table 2.3 Minimum and maximum spacing, end and edge distances (Table 3.3 in EN 1993-1-8)

Distances and spacing's, see Figure 3.1	**Minimum**	**Maximum[1) 2) 3)]**		
		Structures made from steels conforming to EN 10025-2 except steels conforming to EN 10025-5		Structures made from steels conforming to EN 10025-5
		Steel exposed to the weather or other corrosive influences	Steel not exposed to the weather or other corrosive influences	Steel used unprotected
End distance e_1	$1{,}2d_0$	$4t$ + 40 mm		The larger of $8t$ or 125 mm
Edge distance e_2	$1{,}2d_0$	$4t$ + 40 mm		The larger of $8t$ or 125 mm
Distance e_3 in slotted holes	$1{,}5d_0$ [4)]			
Distance e_4 in slotted holes	$1{,}5d_0$ [4)]			
Spacing p_1	$2{,}2d_0$	The smaller of $14t$ or 200 mm	The smaller of $14t$ or 200 mm	The smaller of $14t_{min}$ or 175 mm
Spacing $p_{1,0}$		The smaller of $14t$ or 200 mm		
Spacing $p_{1,i}$		The smaller of $28t$ or 400 mm		
Spacing p_2 [5)]	$2{,}4d_0$	The smaller of $14t$ or 200 mm	The smaller of $14t$ or 200 mm	The smaller of $14t_{min}$ or 175 mm

[1)] Maximum values for spacings, edge and end distances are unlimited, except in the following cases:

– for compression members in order to avoid local buckling and to prevent corrosion in exposed members and;

– for exposed tension members to prevent corrosion.

[2)] The local buckling resistance of the plate in compression between the fasteners should be calculated according to EN 1993-1-1 using 0.6 p_1 as buckling length. Local buckling between the fasteners need not to be checked if p_1/t is smaller than 9 ε. The edge distance should not exceed the local buckling requirements for an outstand element in the compression members, see EN 1993-1-1. The end distance is not affected by this requirement.

[3)] t is the thickness of the thinner outer connected part.

[4)] The dimensional limits for slotted holes are given in EN 1090-2.

[5)] For staggered rows of fasteners a minimum line spacing of $p_2 = 1{,}2d_0$ may be used, provided that the minimum distance, L, between any two fasteners is greater or equal than $2{,}4d_0$, see Figure 2.1b).

2.1.3 Design resistance of individual fasteners

The design resistance for an individual fastener subjected to shear and/or tension is given in Table 2.4. For preloaded bolts the design preload, $F_{p,Cd}$ should be taken as:

$$F_{p,Cd} = \frac{0{,}7\, A_S\, f_{ub}}{\gamma_{M7}} \tag{2.1}$$

The design resistances for tension and for shear through the threaded portion of a bolt are given in Table 2.4. For bolts with cut threads, such as anchor bolts or tie rods fabricated from round steel bars where the threads comply with EN 1090, the relevant values from Table 2.5 should be used. For bolts with cut threads where the threads do not comply with EN 1090 the relevant values from Table 2.4 should be multiplied by a factor of 0,85. The design shear resistance $F_{v,Rd}$ given in Table 2.4 should only be used where the bolts are used in holes with nominal clearances not exceeding those for normal holes as specified in EN 1090-2. M12 and M14 bolts may also be used in 2 mm clearance holes provided that the design resistance of the bolt group based on bearing is greater or equal to the design resistance of the bolt group based on bolt shear. In addition for class 4.8, 5.8, 6.8, 8.8 and 10.9 bolts the design shear resistance $F_{v,Rd}$ should be taken as 0,85 times the value given in Table 2.4.

Fit bolts should be designed using the method for bolts in normal holes. The thread of a fit bolt should not be included in the shear plane. The length of the threaded portion of a fit bolt included in the bearing length should not exceed 1/3 of the thickness of the plate, see Figure 2.2.

In single lap joints with only one bolt row, see Figure 2.3, the bolts should be provided with washers under both the head and the nut. Single rivets should not be used in single lap joints. In the case of class 8.8 or 10.9 bolts, hardened washers should be used for single lap joints with only one bolt or one row of bolts. The design bearing resistance $F_{b,Rd}$ for each bolt should be limited to:

$$F_{b,Rd} \le \frac{1,5\, d\, t\, f_u}{\gamma_{M2}} \tag{2.2}$$

Where bolts or rivets transmitting load in shear and bearing pass through packing of total thickness t_p greater than one-third of the nominal diameter d, see Figure 2.4, the design shear resistance $F_{v,Rd}$ should be multiplying by a reduction factor β_p given by:

$$\beta_p = \frac{9d}{8d + 3t_p}, \text{ but } \beta_p \le 1 \tag{2.3}$$

For double shear connections with packing on both sides of the splice, t_p should be taken as the thickness of the thicker packing.

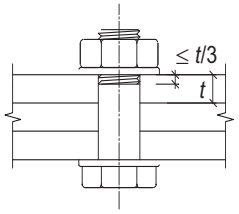

Figure 2.2 Threaded portion of the shank in the bearing length for fit bolts (Figure 3.2 in EN 1993-1-8)

Table 2.4 Design resistance for individual bolts subjected to shear and/or tension (in EN 1993-1-8 part of Table 3.4)

Failure mode	
Shear resistance per shear plane	$F_{v,Rd} = \frac{\alpha_V A f_{ub}}{\gamma_{M2}}$ - where the shear plane passes through the threaded portion of the bolt (A is the tensile stress area of the bolt A_s): - for classes 4.6, 5.6 and 8.8: α_v = 0,6 - for classes 4.8, 5.8, 6.8 and 10.9: α_v = 0,5 - where the shear plane passes through the unthreaded portion of the bolt (A is the gross cross section of the bolt): α_v = 0,6
Bearing resistance 1), 2), 3)	$F_{b,Rd} = k_1 \alpha_b f_u d t / \gamma_{M2}$ where α_b is the smallest of $\frac{f_{ub}}{f_u}$ or 1,0 and (in the direction of load transfer): - for end bolts: $e_1/3d_0$; for inner bolts: $(p_1/3d_0) - 0,25$ Parameter k_1 for perpendicular direction of load transfer: - for edge bolts: k_1 is the smallest of $2,8\frac{e_2}{d_0} - 1,7$ or 2,5 - for inner bolts: k_1 is the smallest of $1,4\frac{e_2}{d_0} - 1,7$ or 2,5
Tension resistance 2)	$F_{t,Rd} = \frac{k_2 A_S f_{ub}}{\gamma_{M2}}$ where k_2 = 0,63 for countersunk bolt, otherwise k_2 = 0,9
Punching shear resistance	$B_{p,Rd} = \frac{0,6 \pi d_m t_p f_u}{\gamma_{M2}}$
Combined shear and tension	$\frac{F_{V,Ed}}{F_{V,Rd}} + \frac{F_{t,Ed}}{1,4F_{t,Rd}} \le 1$

The bearing resistance $F_{b,Rd}$ for bolts

in oversized holes is 0,8 times the bearing resistance for bolts in normal holes.

in slotted holes, where the longitudinal axis of the slotted hole is perpendicular to the direction of the force transfer, is 0,6 times the bearing resistance for bolts in round, normal holes.

For countersunk bolt:

the bearing resistance $F_{b,Rd}$ should be based on a plate thickness t equal to the thickness of the connected plate minus half the depth of the countersinking.

for the determination of the tension resistance $F_{t,Rd}$ the angle and depth of countersinking should conform with EN 1090-2, otherwise the tension resistance $F_{t,Rd}$ should be adjusted accordingly.

When the load on a bolt is not parallel to the edge, the bearing resistance may be verified separately for the bolt load components parallel and normal to the end.

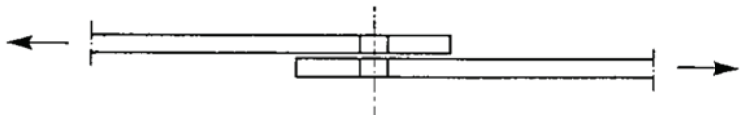

Figure 2.3 Single lap joint with one row of bolts (Figure 3.3 in EN 1993-1-8)

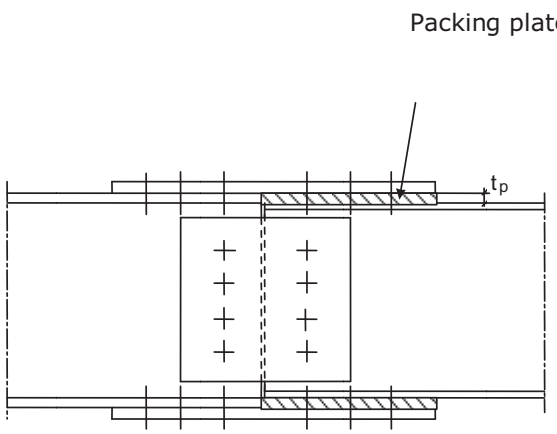

Figure 2.4 Fasteners through packings (Figure 3.4 in EN 1993-1-8)

The design resistance of a group of fasteners may be taken as the sum of the design bearing resistances $F_{b,Rd}$ of the individual fasteners provided that the design shear resistance $F_{v,Rd}$ of each individual fastener is greater than or equal to the design bearing resistance $F_{b,Rd}$. Otherwise the design resistance of a group of fasteners should be taken as the number of fasteners multiplied by the smallest design resistance of any of the individual fasteners.

2.1.4 Long joints

Where the distance L_j between the centres of the end fasteners in a joint, measured in the direction of force transfer, see Figure 2.5, the design shear resistance $F_{v,Rd}$ of all the fasteners calculated according to Table 2.5 should be reduced by multiplying it by a reduction factor β_{Lf}, given by:

$$\beta_{Lf} = 1 - \frac{L_j - 15d}{200d}, \text{ but } \beta_{Lf} \le 1 \text{ and } \beta_{Lf} \ge 0,75 \tag{2.4}$$

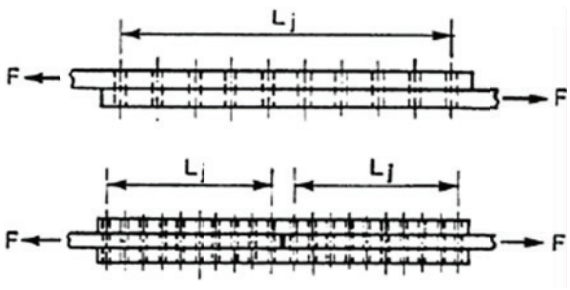

Figure 2.5 Long joints (Figure 3.7 in EN 1993-1-8)

2.1.5 Slip-resistant connections

The design slip resistance of a preloaded class 8.8 or 10.9 bolt should be taken as:

$$F_{s,Rd} = \frac{k_s n \mu}{\gamma_{M3}} F_{p,C} \tag{2.5}$$

where:

k_s is given in Table 2.5

n is the number of the friction surfaces

μ is the slip factor obtained either by specific tests for the friction surface or relevant as given in Table 2.6

For class 8.8 and 10.9 bolts with controlled tightening, the preloading force $F_{p,C}$ to be used in Eqn. (2.5) should be taken as:

$$F_{p,C} = 0,7 A_s f_{ub} \tag{2.6}$$

Table 2.5 Values of k_s (Table 3.6 in EN 1993-1-8)

Description	k_s
Bolts in normal holes.	1,00
Bolts in either oversized holes or short slotted holes with the axis of the slot perpendicular to the direction of load transfer.	0,85
Bolts in long slotted holes with the axis of the slot perpendicular to the direction of load transfer.	0,70
Bolts in short slotted holes with the axis of the slot parallel to the direction of load transfer.	0,76
Bolts in long slotted holes with the axis of the slot parallel to the direction of load transfer.	0,63

Table 2.6 Slip factor μ for pre-loaded bolts (Table 3.7 in EN 1993-1-8)

Class of friction surfaces	Slip factor μ
A	0,5
B	0,4
C	0,3
D	0,2

If a slip-resistant connection is subjected to an applied tensile force, $F_{t,Ed}$ or $F_{t,Ed,ser}$, in addition to the shear force, $F_{V,Ed}$ or $F_{V,Ed,ser}$, tending to produce slip, the design slip resistance per bolt should be taken as follows:

for a category B connection:

$$F_{s,Rd,serv} = \frac{k_s n \mu \left(F_{p,C} - 0,8 F_{t,Ed,serv}\right)}{\gamma_{M3}} \tag{2.7}$$

for a category C connection:

$$F_{s,Rd} = \frac{k_s n \mu \left(F_{p,C} - 0,8 F_{t,Ed}\right)}{\gamma_{M3}} \tag{2.8}$$

If, in a moment connection, a contact force on the compression side counterbalances the applied tensile force no reduction in slip resistance is required.

2.1.6 Design for block tearing

Block tearing consists of failure in shear at the row of bolts along the shear face of the hole group accompanied by tensile rupture along the line of bolt holes on the tension face of the bolt group. Figure 2.6 shows the tearing block. For a symmetric bolt group subject to concentric loading the design block tearing resistance, $V_{eff,1,Rd}$ is given by:

$$V_{eff,1,Rd} = \frac{A_{nt} f_u}{\gamma_{M2}} + \frac{A_{nv} f_y}{\sqrt{3}\,\gamma_{M0}} \tag{2.9}$$

For a bolt group subject to eccentric loading the design block shear tearing resistance $V_{eff,2,Rd}$ is given by:

$$V_{eff,2,Rd} = 0,5\,\frac{A_{nt} f_u}{\gamma_{M2}} + \frac{A_{nv} f_y}{\sqrt{3}\,\gamma_{M0}} \tag{2.10}$$

where

A_{nt} is net area subjected to tension

A_{nv} is net area subjected to shear

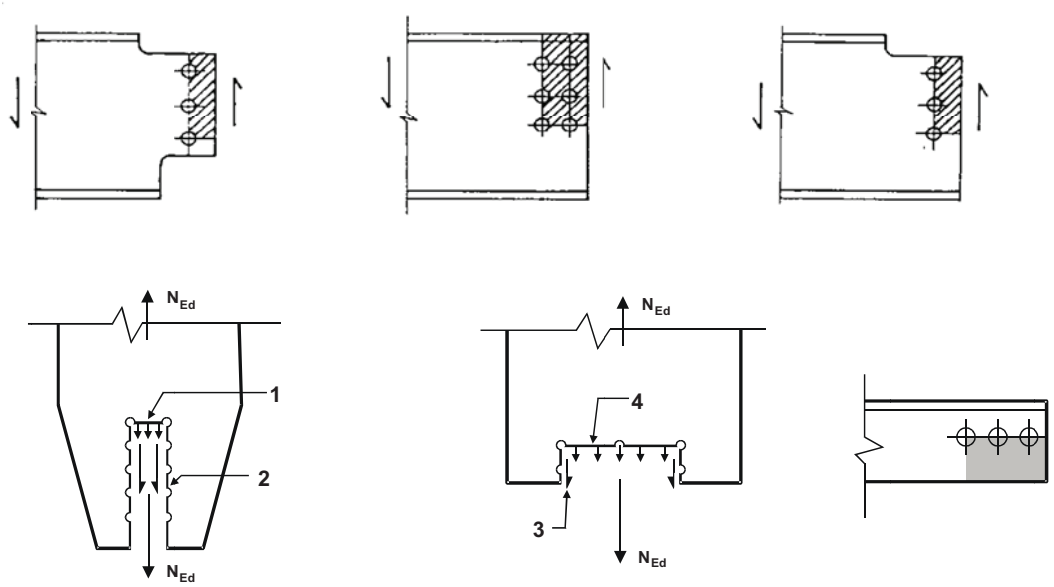

1 small tension force; 2 large shear force; 3 small shear force; 4 large tension force

Figure 2.6 Block tearing (Figure 3.9 in EN1993-1-8)

The eccentricity in joints and the effects of the spacing and edge distances of the bolts, should be taken into account in determining the design resistance of:

- unsymmetrical members;
- symmetrical members that are connected asymmetrically, such as angles connected by one leg.

A single angle in tension connected by a single row of bolts in one leg, see Figure 2.7, may be treated as concentrically loaded over an effective net section for which the design ultimate resistance should be determined as follows:

with one bolt:

$$N_{u,Rd} = \frac{2,0\left(e_2 - 0,5\, d_0\right) t f_u}{\gamma_{M2}} \tag{2.11}$$

with two bolts:

$$N_{u,Rd} = \frac{\beta_2 A_{net} f_u}{\gamma_{M2}} \tag{2.12}$$

with three or more bolts:

$$N_{u,Rd} = \frac{\beta_3 A_{net} f_u}{\gamma_{M2}} \tag{2.13}$$

where:

β_2 and β_3 are reduction factors dependent on the pitch p_1 as given in Table 2.7. For intermediate values of p_1 the value of β may be determined by linear interpolation;

A_{net} is the net area of the angle. For an unequal-leg angle connected by its smaller leg, A_{net} should be taken as equal to the net section area of an equivalent equal-leg angle of leg size equal to that of the smaller leg.

Table 2.7 Reduction factors β_2 and β_3 (Table 3.8 in EN1993-1-8)

Pitch	p_1	$\leq 2,5\, d_0$	$\geq 5\, d_0$
Two bolts	β_2	0,4	0,7
Three bolts or more	β_3	0,5	0,7

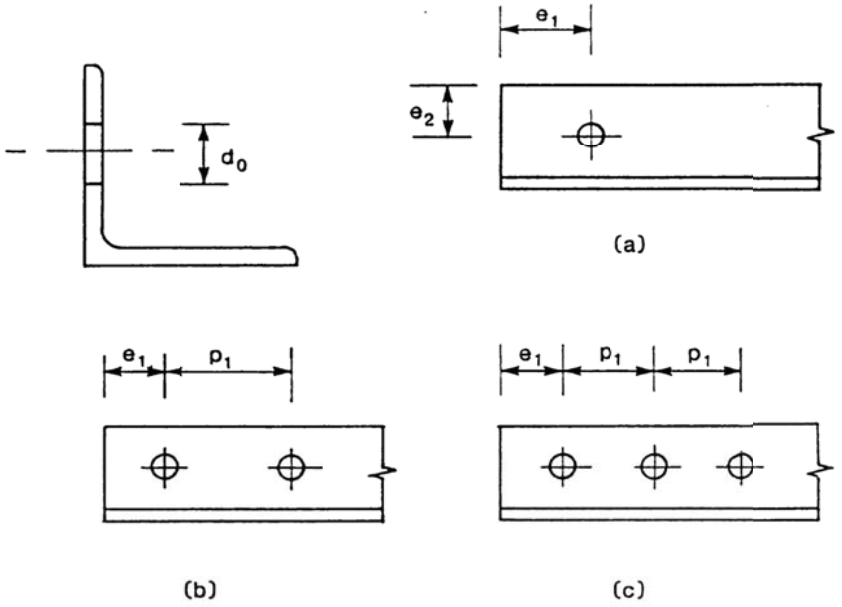

a) one bolt

b) two bolts

c) three bolts

Figure 2.7 Angles connected by one leg (Figure 3.9 in EN1993-1-8)

2.1.7 Connections made with pins

In the specific case of pin connections in which no rotation is required, it may be designed as single bolted connections, provided that the length of the pin is less than three times the diameter of the pin. For all other cases the design model is given in cl. 3.13 in EN1993-1-8. Wherever there is a risk of pins becoming loose, they should be secured.

2.1.8 Worked example - bolted connection of double angle bar

Design the bolted connection of tension element from double angle bar of section L 80 × 6, steel S 355. The element is loaded by tensile force N_{Ed} = 580 kN and is connected to gusset plate of thickness 8 mm, see Figure 2.8.

Try full thread bolts M20 Class 6.8.

First, the resistance of sections with hole is checked as follows:

$$N_{u,Rd} = \frac{0,9A_{net}f_u}{\gamma_{M2}} = \frac{0,9 \cdot 2 \cdot (935 - 22 \cdot 6) \cdot 510}{1,25} = 589,7 \text{ kN} > N_{Ed} = 580 \text{ kN}$$

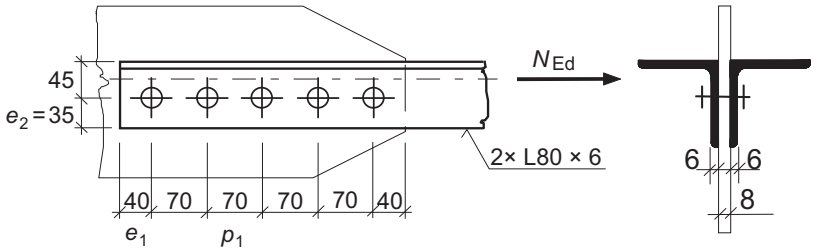

Figure 2.8 Bolted connection of double angle bar

The shear resistance of one bolt, for two shear planes and shear in bolt thread:

$$F_{v,Rd} = 2\frac{\alpha_v A_s f_{ub}}{\gamma_{M2}} = 2\cdot\frac{0,6\cdot 245\cdot 600}{1,25} = 141,1\ \text{kN}$$

The design bearing resistance of bolts is evaluated for end and inner bolts, see Figure 2.8. Factors k_1 and α_b will be calculated as follows:

Factor k_1 for end bolt:

$$k_1 = \min\left(2,8\frac{e_2}{d_0} - 1,7;\ 2,5\right) = \min\left(2,8\cdot\frac{35}{22} - 1,7;\ 2,5\right) = \min(2,75;\ 2,5) \quad \rightarrow \quad k_1 = 2,5$$

Factor k_1 for inner bolt:

$$k_1 = \min\left(2,8\frac{e_2}{d_0} - 1,7;\ 2,5\right) = \min\left(2,8\cdot\frac{35}{22} - 1,7;\ 2,5\right) = \min(2,75;\ 2,5) \quad \rightarrow \quad k_1 = 2,5$$

Factor α_b for end bolt:

$$\alpha_b = \min\left\{\begin{matrix}\frac{e_1}{3d_0}\\ \frac{f_{ub}}{f_u}\\ 1,0\end{matrix}\right\} = \min\left\{\begin{matrix}\frac{40}{3\cdot 22}\\ \frac{600}{360}\\ 1,0\end{matrix}\right\} = \min\left\{\begin{matrix}0,606\\ 1,176\\ 1,0\end{matrix}\right\} = 0,606$$

Factor α_b for inner bolt:

$$\alpha_b = \min\left\{\begin{matrix}\frac{p_1}{3d_0} - \frac{1}{4}\\ \frac{f_{ub}}{f_u}\\ 1,0\end{matrix}\right\} = \min\left\{\begin{matrix}\frac{70}{3\cdot 22} - \frac{1}{4}\\ \frac{600}{360}\\ 1,0\end{matrix}\right\} = \min\left\{\begin{matrix}0,811\\ 1,176\\ 1,0\end{matrix}\right\} = 0,811$$

The bearing action is decisive to the gusset plate since the 8 mm thick plate is thinner than the angles (12 mm thick). Hence, the bearing resistance of end bolt is:

$$F_{b,Rd} = \frac{k_1 \alpha_b d t f_u}{\gamma_{M2}} = \frac{2,5 \cdot 0,606 \cdot 20 \cdot 8 \cdot 510}{1,25} = 98,9 \text{ kN}$$

The bearing resistance of inner bolts is:

$$F_{b,Rd} = \frac{2,5 \cdot 0,811 \cdot 20 \cdot 8 \cdot 510}{1,25} = 132,4 \text{ kN}$$

Since the bearing resistance is lower than the shear resistance, the design is governed by bearing action. Adding up the end bolt and inner bolt bearing capacities, the resistance of the connection with 5 bolts is:

$$98,9 + 3.132,4 + 98,9 = 595,0 \text{ kN} > 580 \text{ kN} = N_{Ed}$$

Note:

In example above is taken the bearing resistance of inner and end bolt separately. It may be taken conservatively as the lower value of inner and end bolt (here the end bolt). With this option, the design resistance of the connection is $5 \cdot 98,9 = 494,5$ kN.

2.2 Welded connections

2.2.1 Geometry and dimensions

The provisions in this section apply to weldable structural steels conforming to EN 1993-1-1 and to material thicknesses of 4 mm and over. The provisions also apply to joints in which the mechanical properties of the weld metal are compatible with those of the parent metal. For welds in thinner material reference should be made to EN 1993 part 1.3 and for welds in structural hollow sections in material thicknesses of 2,5 mm and over the guidance is given in chapter 7 of EN 1993-1-8. Further guidance on stud welding can be found in EN ISO 14555 and EN ISO 13918. For stud welding reference should be made to EN 1994-1-1.

This guide covers the design of fillet welds, fillet welds all round, butt welds, plug welds and flare groove welds. Butt welds may be either full penetration butt welds or partial penetration butt welds. Both fillet welds all round and plug welds may be either in circular holes or in elongated holes. The most common types of joints and welds are illustrated in EN ISO 17659.

Fillet welds may be used for connecting parts where the fusion faces form an angle of between 60° and 120°. Angles smaller than 60° are also permitted. However, in such cases the weld should be considered to be a partial penetration butt weld. For angles greater than 120° the resistance of fillet welds should be determined by testing in accordance with EN 1990 Annex D: Design by testing. Fillet welds finishing at the ends or sides of parts should be returned continuously, full size, around the corner for a distance of at least twice the leg length of the weld, unless access or the configuration of the joint renders this impracticable. In the case of intermittent welds this rule applies only to the last intermittent fillet weld at corners. End returns should be indicated on the drawings.

Intermittent fillet welds should not be used in corrosive conditions. In an intermittent fillet weld, the gaps, L_1 or L_2, between the ends of each length of weld L_w should fulfil the requirement given in Figure 2.9. In an intermittent fillet weld, the gap, L_1 or L_2, should be taken as the smaller of the distances between the ends of the welds on opposite sides and the distance between the ends of the welds on the same side. In any run of intermittent fillet weld there should always be a length of weld at each end of the part connected. In a built-up member in which plates are connected by means of intermittent fillet welds, a continuous fillet weld should be provided on each side of the plate for a length at each end equal to at least three-quarters of the width of the narrower plate concerned, see Figure 2.9.

Fillet welds all round, comprising fillet welds in circular or elongated holes, may be used only to transmit shear or to prevent the buckling or separation of lapped parts. The diameter of a circular hole, or width of an elongated hole, for a fillet weld all round should not be less than four times the thickness of the part containing it. The ends of elongated holes should be semi-circular, except for those ends which extend to the edge of the part concerned. The centre to centre spacing of fillet welds all round should not exceed the value necessary to prevent local buckling.

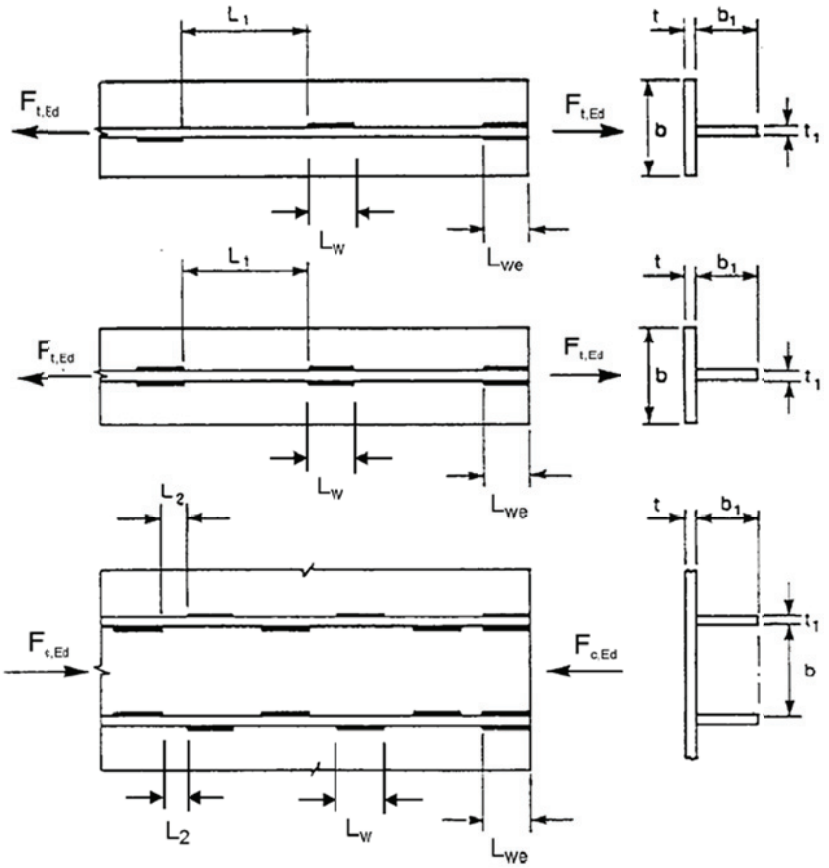

The smaller of: $L_{we} \geq 0{,}75\ b$ and $0{,}75\ b_1$

For build-up members in tension:

the smallest of $L_1 \leq 16\ t$ and $16\ t_1$ and 200 mm

For build-up members in compression or shear:

the smallest of $L_2 \leq 12\ t$ and $12\ t_1$ and $0{,}25\ b$ and 200 mm

Figure 2.9 Intermittent fillet welds (Figure 4.1 in EN 1993-1-8)

A full penetration butt weld is defined as a weld that has complete penetration and fusion of weld and parent metal throughout the thickness of the joint. A partial penetration butt weld is defined as a weld that has joint penetration which is less than the full thickness of the parent material. Intermittent butt welds should not be used. The design should calculate for eccentricity in single-sided partial penetration butt welds.

2.2.2 Design resistance of a fillet welds

The effective length of a fillet weld L_{eff} should be taken as the length over which the fillet is full-size. This may be taken as the overall length of the weld reduced by twice the effective throat thickness a. Provided that the weld is full size throughout its length including starts and terminations, no reduction in effective length need to be made for either the start or the termination of the weld. A fillet weld with an effective length less than 30 mm or less than 6 times its throat thickness, whichever is larger, should not be designed to carry load.

The effective throat thickness *a* of a fillet weld should be taken as the height of the largest triangle (with equal or unequal legs) that can be inscribed within the fusion faces and the weld surface, measured perpendicular to the outer side of this triangle, see Figure 2.10. The effective throat thickness of a fillet weld should not be less than 3 mm. In determining the design resistance of a deep penetration fillet weld, account may be taken of its additional throat thickness, see Figure 2.11, provided that preliminary tests show that the required penetration can consistently be achieved.

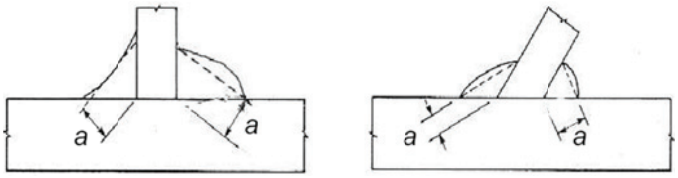

Figure 2.10 Throat thickness of a fillet weld (Figure 4.3 in EN 1993-1-8)

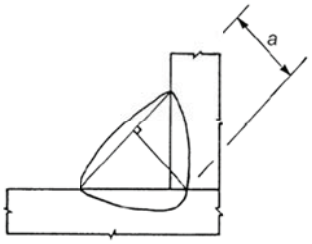

Figure 2.11 Throat thickness of a deep penetration fillet weld (Figure 4.4 in EN 1993-1-8)

In this method, the forces transmitted by a unit length of weld are resolved into components parallel and transverse to the longitudinal axis of the weld and normal and transverse to the plane of its throat. The design throat area A_w should be taken as $A_w = \sum a\, L_{eff}$ .The location of the design throat area should be assumed to be concentrated in the root. A uniform distribution of stress is assumed on the throat section of the weld, leading to the normal stresses and shear stresses shown in Figure 2.12. The normal stress $\sigma_{\parallel}$ parallel to the axis is not considered when verifying the design resistance of the weld. Welds between parts with different material strength grades should be designed using the properties of the material with the lower strength grade.

The design resistance of the fillet weld will be sufficient if the following are both satisfied:

$$\sqrt{\sigma_{\perp}^2 + 3\left(\tau_{\perp}^2 + \tau_{\parallel}^2\right)} \le \frac{f_u}{\beta_w \gamma_{M2}} \quad \text{and} \quad \sigma_{\perp} \le \frac{f_u}{\gamma_{M2}} \tag{2.14}$$

where:

f_u is the nominal ultimate tensile strength of the weaker part joined

β_w is the appropriate correlation factor taken from Table 2.8

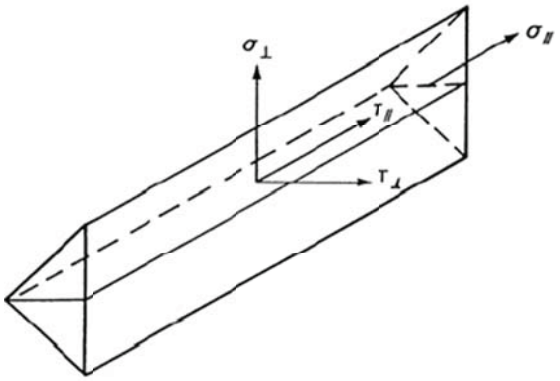

$\sigma_{\perp}$ is the normal stress perpendicular to the throat;

$\sigma_{\parallel}$ is the normal stress parallel to the axis of the weld;

$\tau_{\perp}$ is the shear stress in the plane of the throat perpendicular to the axis of the weld;

$\tau_{\parallel}$ is the shear stress in the plane of the throat parallel to the axis of the weld.

Figure 2.12 Stresses on the throat section of a fillet weld (Figure 4.5 in EN 1993-1-8)

Table 2.8 Correlation factor β_w for fillet welds (Tab 4.1 in EN 1993-1-8)

Standard and steel grade			Correlation factor β_w
EN 10025	**EN 10210**	**EN 10219**	
S 235 S 235 W	S 235 H	S 235 H	0,80
S 275 S 275 N/NL S 275 M/ML	S 275 H S 275 NH/NLH	S 275 H S 275 NH/NLH S 275 MH/MLH	0,85
S 355 S 355 N/NL S 355 M/ML S 355 W	S 355 H S 355 NH/NLH	S 355 H S 355 NH/NLH S 355 MH/MLH	0,90
S 420 N/NL S 420 M/ML		S 420 MH/MLH	1,00
S 460 N/NL S 460 M/ML S 460 Q/QL/QL1	S 460 NH/NLH	S 460 NH/NLH S 460 MH/MLH	1,00

The design resistance of a fillet weld all round should be determined using one of the methods given in cl. 4.5 of EN 1993-1-8.

2.2.3 Design resistance of butt welds

The design resistance of a full penetration butt weld should be taken as equal to the design resistance of the weaker of the parts connected, provided that the weld is made with a suitable consumable which will produce all weld tensile specimens having both a minimum yield strength and a minimum tensile strength not less than those specified for the parent metal.

The design resistance of a partial penetration butt weld should be determined using the method for a deep penetration fillet weld given in cl. 4.5.2 of EN 1993-1-8. The throat thickness of a partial penetration butt weld should not be greater than the depth of penetration that can be consistently achieved.

The design resistance of a T-butt joint, consisting of a pair of partial penetration butt welds reinforced by superimposed fillet welds, may be determined as for a full penetration butt weld, see cl. 4.7.1 of EN 1993-1-8, if the total nominal throat thickness, exclusive of the unwelded gap, is not less than the thickness t of the part forming the stem of the tee joint, provided that the unwelded gap is not more than (t / 5) or 3 mm, whichever is less, see Figure 2.13. The design resistance of a T-butt joint which does not meet the requirements given in clause 4.7.3 of EN 1993-1-8 should be determined using the method for a fillet weld or a deep penetration fillet weld given in cl. 4.5 of EN 1993-1-8 depending on the amount of penetration. The throat thickness should be determined in conformity with the provisions for fillet welds or partial penetration butt welds as relevant.

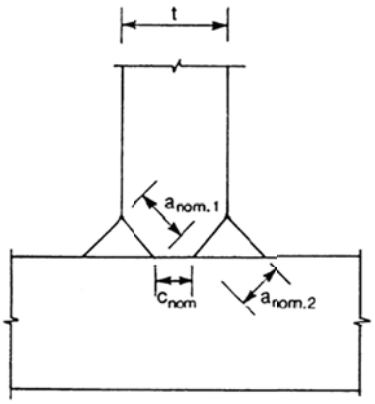

$a_{nom,1} + a_{nom,2} \geq t$

c_{nom} should be the smaller of t/5 and 3 mm

Figure 2.13 Effective full penetration of T-butt welds (Figure 4.6 in EN 1993-1-8)

2.2.4 Connections to unstiffened flanges

Where a transverse plate, or beam flange, is welded to a supporting unstiffened flange of an I, H or other section, see Figure 2.14, the applied force perpendicular to the unstiffened flange should not exceed any of the relevant design resistances of the web of the supporting member of I or H sections, for a transverse plate, and that of the supporting flange.

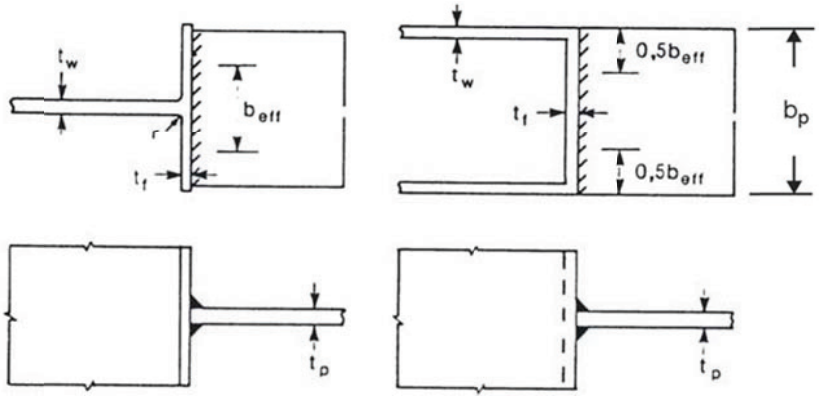

Figure 2.14 (Figure 4.8 in EN 1993-1-8) Effective width of an unstiffened T-joint

For an unstiffened I or H section the effective width beff should be obtained from:

$$b_{\text{eff}} = t_{\text{w}} + 2s + 7k\,t_{\text{f}} \tag{2.15}$$

where

$$k = \frac{t_{\text{f}}\,f_{\text{yf}}}{t_{\text{p}}\,f_{\text{yp}}}, \text{ but } k \le 1 \tag{2.16}$$

$f_{y,f}$ is the yield strength of the flange of the I or H section;

$f_{y,p}$ is the yield strength of the plate welded to the I or H section. The dimension s should be obtained from:

– for a rolled I or H section: $s = r$ (2.17)

– for a welded I or H section: $s = \sqrt{2}\,a$. (2.18)

The effective width b_{eff} is included in clause 4.10 in EN 1993-1-8 for an unstiffened flange of an I or H section and for other sections such as box sections or channel sections where the width of the connected plate is similar to the width of the flange.

2.2.5 Long joints

In lap joints the design resistance of a fillet weld should be reduced by multiplying it by a reduction factor β_{Lw} to allow for the effects of non-uniform distribution of stress along its length. The provisions do not apply when the stress distribution along the weld corresponds to the stress distribution in the adjacent base metal, as, for example, in the case of a weld connecting the flange and the web of a plate girder. In lap joints longer than 150a the reduction factor β_{Lw} should be taken as $\beta_{\text{Lw.1}}$ given by:

$$\beta_{\text{Lw}} = 1,2 - \frac{0,2L_{\text{j}}}{150a}, \text{ but } \beta_{\text{Lw}} \le 1 \tag{2.19}$$

where L_{j} is the overall length of the lap in the direction of the force.

2.2.6 Worked example - welded connection of double angle bar

Design the welded connection of tension elements from double angle bar of section L 80 × 6, steel S 235. Element is loaded by tensile force N_{Ed} = 400 kN and is connected to truss plate of thickness 8 mm, see Figure 2.15.

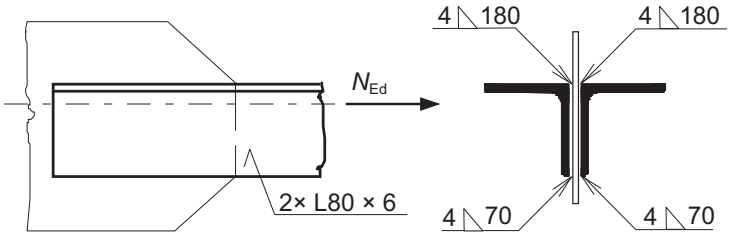

Figure 2.15 Welded connection of tension double angle bar

Try weld of throat thickness a = 4 mm.

The force acting on the cross-section will be distributed to the section area to be connected by the weld. The weld by adjacent leg is exposed to force:

$$F_{w1} = N_{Ed}\frac{e}{b} = 400 \cdot 10^3 \cdot \frac{21,7}{80} = 108,5 \text{ kN}$$

The weld by outlying leg is exposed to force:

$$F_{w2} = N_{Ed}\frac{b-e}{b} = 400 \cdot 10^3 \cdot \frac{80-21,7}{80} = 291,5 \text{ kN}$$

The weld is subject to longitudinal shear $\tau_{||}$ only:

$$\tau_{||} = \frac{F_w}{a\,\ell} \le \frac{f_u}{\sqrt{3}\;\beta_w\;\gamma_{M2}}$$

For welding of adjacent leg for both sides, the following length is needed:

$$\ell_1 = \frac{F_{w1}\sqrt{3}\beta_w\gamma_{M2}}{a\,f_u} = \frac{108,5 \cdot 10^3 \cdot \sqrt{3} \cdot 0,8 \cdot 1,25}{2 \cdot 4 \cdot 360} = 65,3 \text{ mm}$$

For welding of outlying leg, the following length is needed:

$$\ell_2 = \frac{F_{w2}\sqrt{3}\beta_w\gamma_{M2}}{a\,f_u} = \frac{291,5 \cdot 10^3 \cdot \sqrt{3} \cdot 0,8 \cdot 1,25}{2 \cdot 4 \cdot 360} = 175,3 \text{ mm}$$

The welds with throat thickness a = 4 mm require lengths of 70 and 180 mm.

2.2.7 Worked example - header plate simple connection

Design the short end plate connection of primary beam of cross-section IPE by bolts M16 Class 4.6, see Figure 2.16. The acting vertical shear force V_{Ed} = 48,8 kN. The primary beam is connected to column web of cross section HEB 260, steel S 235.

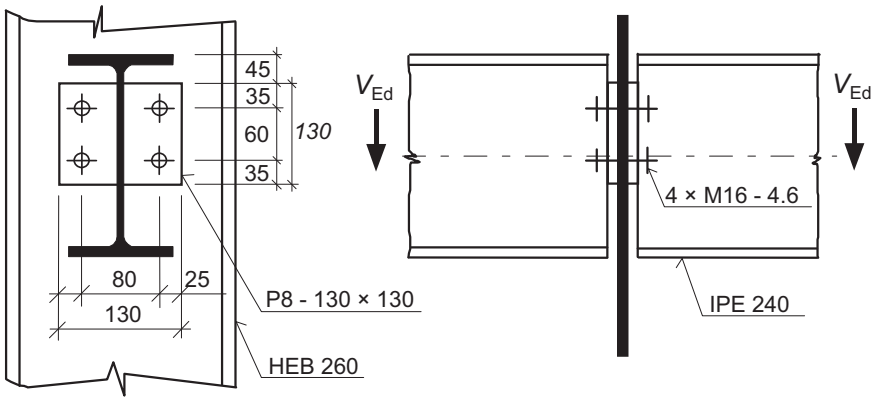

Figure 2.16 Header plate connection

The resistance of short end plate connections is governed by the shear resistance of the connected beam. The shear resistance of the beam section transferring shear to the end plate is:

$$V_{pl,Rd} = \frac{A_v f_y}{\sqrt{3}\ \gamma_{M0}} = \frac{6{,}2 \cdot\ 130 \cdot 235}{\sqrt{3}\ \cdot 1{,}00} = 109{,}4 \text{ kN} > 48{,}8 \text{ kN} = V_{Ed} \qquad \text{(satisfactory)}$$

The design resistance of one bolt in shear (M16, Class 4.6):

$$F_{v,Rd} = \frac{\alpha_v\ A_s\ f_{ub}}{\gamma_{M2}} = \frac{0{,}6 \cdot 157 \cdot 400}{1{,}25} = 30{,}1 \text{ kN}$$

The design resistance of four bolts is

$$4F_{v,Rd} = 4 \cdot 30{,}1 = 120{,}4 \text{ kN} > 48{,}8 \text{ kN} = V_{Ed} \qquad \text{(satisfactory)}$$

The design bearing resistance of four bolts is guided by column web t = 10,0 mm.

$$\alpha_b = \min\left\{\begin{matrix} \frac{e_1}{3d_0} \\ \frac{p_1}{3d_0} - \frac{1}{4} \\ \frac{f_{ub}}{f_u} \\ 1 \end{matrix}\right\} = \min\left\{\begin{matrix} \frac{35}{3 \cdot 18} \\ \frac{60}{3 \cdot 18} - \frac{1}{4} \\ \frac{400}{360} \\ 1 \end{matrix}\right\} = \min\left\{\begin{matrix} 0{,}648 \\ 0{,}861 \\ 1{,}111 \\ 1 \end{matrix}\right\} = 0{,}648$$

$$k_1 = \min\left\{\begin{matrix} 2,8\dfrac{e_2}{d_0} - 1,7 \\ 1,4\dfrac{e_2}{d_0} - 1,7 \\ 2,5 \end{matrix}\right\} = \min\left\{\begin{matrix} 2,8 \cdot \dfrac{25}{18} - 1,7 \\ 1,4 \cdot \dfrac{80}{18} - 1,7 \\ 2,5 \end{matrix}\right\} = \min\left\{\begin{matrix} 2,188 \\ 4,522 \\ 2,5 \end{matrix}\right\} = 2,188$$

$$F_{b,Rd} = 4\frac{k_1\ \alpha_b\ d\ t\ f_u}{\gamma_{M2}} = 4 \cdot \frac{2,188 \cdot\ 0,648 \cdot 16 \cdot 10 \cdot 360}{1,25} = 261,3\ \text{kN} > 97,6\ \text{kN} = 2 \cdot 48,8 = V_{Ed}$$

(satisfactory)

The resistance of the filled weld with 3 mm throat thickness is:

$$F_{W,Rd} = \frac{a\ L\ f_u}{\sqrt{3}\ \beta_W \gamma_{M2}} = \frac{2 \cdot 3 \cdot 130 \cdot 360}{\sqrt{3} \cdot 0,8 \cdot 1,25} = 162,1\ \text{kN} > 48,8\ \text{kN}$$ (satisfactory)

Overall, the connection design is satisfactory.

NOTE:

In presented simplified procedure, some resistances such as the end plate resistance in bending, the connection tying resistance and the ultimate resistance to horizontal forces are expected to be fulfilled by proper design practices. For more information, the reader is referred to (Jaspart et al., 2009) and (BCSA and SCI, 2002).

2.2.8 Worked example – fin plate connection

Examine the secondary beam to column connection by fin plate, see Figure 2.17. The connection transfers vertical shear force V_{Ed} = 30 kN. Steel S235 and fully threaded bolts M20 Class 5.6 are used for the design.

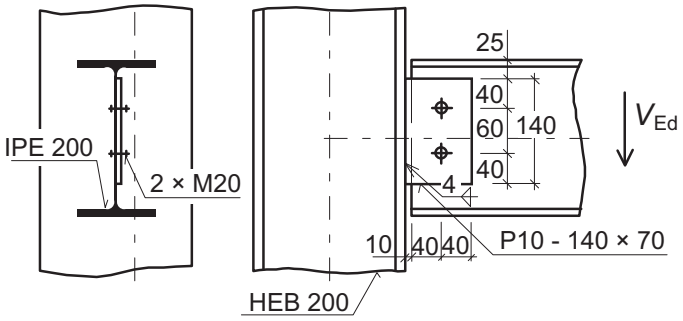

Figure 2.17 Fin plate connection

Design shear resistance of one fully treated bolt is:

$$F_{v,Rd} = \frac{\alpha_V A_S f_{ub}}{\gamma_{M2}} = \frac{0,6 \cdot 245 \cdot 500}{1,25} = 58,8 \text{ kN}$$

The design bearing resistance of bolts is evaluated by factors k_1 a α_b as governed by the fin plate:

$$k_1 = \min\left(2,8\frac{e_2}{d_0} - 1,7; 2,5\right) = \min\left(2,8 \cdot \frac{40}{22} - 1,7; 2,5\right) = \min(3,4; 2,5) = 2,5$$

$$\alpha_b = \min\left\{\begin{matrix} \frac{e_1}{3d_0} \\ \frac{p_1}{3d_0} - 0,25 \\ \frac{f_{ub}}{f_u} \\ 1 \end{matrix}\right\} = \min\left\{\begin{matrix} \frac{40}{3 \cdot 22} \\ \frac{60}{3 \cdot 22} - 0,25 \\ \frac{500}{360} \\ 1 \end{matrix}\right\} = \min\left\{\begin{matrix} 0,606 \\ 0,659 \\ 1,389 \\ 1 \end{matrix}\right\} = 0,606$$

The design bearing resistance of one bolt is:

$$F_{b,Rd} = \frac{k_1 \alpha_b d t f_u}{\gamma_{M2}} = \frac{2,5 \cdot 0,606 \cdot 20 \cdot 10 \cdot 360}{1,25} = 109,1 \text{ kN}$$

Analogous to the bearing resistance of the bolts, the bearing resistance of the beam web may be calculated by factors k_1 and α_b governed by the fin plate as follows:

$$\alpha_b = \min\left\{\begin{matrix} \frac{e_1}{3d_0} \\ \frac{p_1}{3d_0} - \frac{1}{4} \\ \frac{f_{ub}}{f_u} \\ 1 \end{matrix}\right\} = \min\left\{\begin{matrix} \frac{65}{3 \cdot 22} \\ \frac{60}{3 \cdot 22} - \frac{1}{4} \\ \frac{500}{360} \\ 1 \end{matrix}\right\} = \min\left\{\begin{matrix} 0,985 \\ 0,659 \\ 1,389 \\ 1 \end{matrix}\right\} = 0,659$$

$$F_{b,Rd} = \frac{k_1 \alpha_b d t f_u}{\gamma_{M2}} = \frac{2,5 \cdot 0,659 \cdot 20 \cdot 5,6 \cdot 360}{1,25} = 53,1 \text{ kN}$$

The resistance of connection with two bolts:

$$V_{Rd} = 2 \cdot \min\left(F_{v,Rd}; F_{b,Rd}\right) = 2 \cdot \min(58,8; 109,1; 53,1) = 106,2 \text{ kN} > 30 \text{ kN} = V_{Ed}$$

(satisfactory)

Eccentricity of acting shear force in bots creates a bending moment in welds:

$$M_{Ed} = V_{Ed}\, e = 30 \cdot 0,05 = 1,5 \text{ kNm}$$

The moments introduces stress σ_w is plane of the fin plate:

$$\sigma_W = \frac{M_{Ed}}{W_{el,W}} = \frac{M_{Ed}}{\frac{2\, a\, \ell^2}{6}} = \frac{1,5 \cdot 10^6}{\frac{2 \cdot 4 \cdot 140^2}{6}} = 57,4 \text{ MPa}$$

This stress is resolved into stress perpendicular and parallel to axes of weld throat calculated as follows:

$$\tau_\perp = \sigma_\perp = \frac{\sigma_W}{\sqrt{2}} = \frac{57,4}{\sqrt{2}} = 40,6 \text{ MPa}$$

$$\tau_\parallel = \frac{V_{Ed}}{2\, a\, \ell} = \frac{30 \cdot 10^3}{2 \cdot 4 \cdot 140} = 26,8 \text{ MPa}$$

The design resistance of the fillet weld is sufficient if the following are satisfied:

$$\sqrt{\sigma_\perp^2 + 3\left(\tau_\perp^2 + \tau_\parallel^2\right)} = \sqrt{40,6^2 + 3 \cdot \left(40,6^2 + 26,8^2\right)} = 93,5 \text{ MPa} < 360,0 \text{ MPa} =$$

$$= \frac{f_u}{\beta_W\, \gamma_{M2}} = \frac{360}{0,8 \cdot 1,25}$$

$$\sigma_\perp = 40,6 \text{ MPa} < \frac{f_u}{\gamma_{M2}} = \frac{360}{1,25} = 288 \text{ MPa} \qquad \text{(satisfactory)}$$

$$\tau_\parallel = \frac{V_{Ed}}{2\, a\, \ell} = \frac{30 \cdot 10^3}{2 \cdot 4 \cdot 140} = 26,8 \text{ MPa}$$

The design block tearing resistance of a fin plate is given by summing the resistance on critical area in tension and that in shear, see Figure 2.18:

$$V_{eff2,Rd} = \frac{0,5\, A_{nt} f_u}{\gamma_{M2}} + \frac{A_{nv} f_y}{\sqrt{3}\, \gamma_{M0}}$$

where
A_{nt} is net area of cross section carrying the tensile force and
A_{nv} is net area of cross section carrying the shear force:

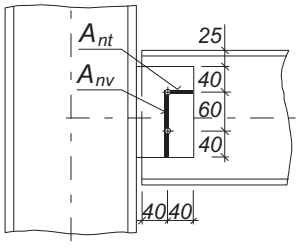

Figure 2.18 Critical sections on fin plate

$$A_{nv} = 10 \cdot \left(40 + 60 - 22 - \frac{22}{2}\right) = 670 \text{ mm}^2$$

$$A_{nt} = 10 \cdot \left(40 - \frac{22}{2}\right) = 290 \text{ mm}^2 \ .$$

The design block tearing resistance is:

$$V_{eff2,Rd} = \frac{0{,}5 \cdot 290 \cdot 360}{1{,}25} + \frac{670 \cdot 235}{\sqrt{3}\ 1{,}00} = 132{,}7 \text{ kN} > 30 \text{ kN} = V_{Ed} \qquad \text{(satisfactory)}$$

The shear resistance of gross area is:

$$V_{pl,Rd} = \frac{A_v f_y}{\sqrt{3}\ \gamma_{M0}} = \frac{10 \cdot 140 \cdot 235}{\sqrt{6} \cdot 1{,}00} = 189{,}9 \text{ kN} > 30 \text{ kN} = V_{Ed} \qquad \text{(satisfactory)}$$

For the beam web, the design block shear resistance is evaluated in a similar way as for the fin plate, see Figure 2.19, as:

$$A_{nt} = 5{,}6 \cdot \left(40 - \frac{22}{2}\right) = 162{,}4 \text{ mm}^2$$

$$A_{nv} = 5{,}6 \cdot \left(25 + 40 + 60 - 22 - \frac{22}{2}\right) = 515{,}2 \text{ mm}^2 \ .$$

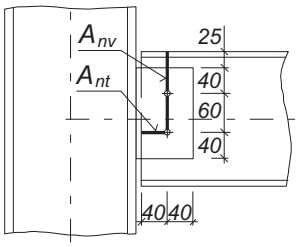

Figure 2.19 Critical sections on beam

The beam web shear resistance:

$$V_{eff2,Rd} = \frac{0{,}5 \cdot 162{,}4 \cdot 360}{1{,}25} + \frac{515{,}2 \cdot 235}{\sqrt{3}\ 1{,}00} = 93{,}3 \text{ kN} > 30 \text{ kN} = V_{Ed} \qquad \text{(satisfactory)}$$

The bending resistance is checked for Class 3 cross-section, which resistance is:

$$M_{el,Rd} = \frac{W_{el} f_y}{\gamma_{M0}} = \frac{\frac{10 \cdot 140^2}{6} \cdot 235}{1{,}00} = 7{,}7 \text{ kNm} > 1{,}5 \text{ kNm} = M_{Ed} \qquad \text{(satisfactory)}$$

Hence, the connection design is satisfactory.

NOTE:

In presented simplified procedure, some resistances such as the fin plate resistance in bending and its out-of-plane bending during erection, the connection tying resistance and the connection ultimate resistance to horizontal forces are expected to be fulfilled by proper design practices. For more information on the complete design procedure, the reader is referred to (Jaspart et al., 2009) and (BCSA and SCI, 2002).

2.3 Column bases

2.3.1 Design resistance

The calculation of the column base resistance, based on the plastic force equilibrium on the base plate and applied in EN1993-1-8:2006, is described in (Wald et al., 2008, 3-20).

Based on the combination of acting load, see Figure 2.20, three patterns may be distinguished:

Pattern 1 without tension in anchor bolts occurs due to high normal force loading. The collapse of concrete appears before developing stresses in the tension part.

Pattern 2 with tension in one anchor bolt row arises when the base plate is loaded by small normal force compared to the ultimate bearing capacity of concrete. During collapse the concrete bearing stress is not reached. The breaking down occurs because of yielding of the bolts or because of plastic mechanism in the base plate.

Pattern 3 with tension in both rows of anchor bolts occurs when the base plate is loaded by tensile normal force. The stiffness is guided by yielding of the bolts or because of plastic mechanism in the base plate. This pattern occurs often in base plates designed for tensile force only and may lead to contact of baseplate to the concrete block.

The connection is loaded by axial force N_{Ed} and bending moment M_{Ed}, see Figure 2.21. The position of the neutral axis is calculated according to the resistance of the tension part $F_{T,Rd}$. Then the bending resistance M_{Rd} is determined assuming a plastic distribution of the internal forces. For simplicity of the model, only the effective area is taken into account, see (Cestruco, 2003). The effective area A_{eff} under the base plate, which is taken as an active part of equivalent rigid plate, is calculated from an equivalent T-stub, with an effective width c. The compression force is assumed to act at the centre of the compressed part. The tensile force is located at the anchor bolts or in the middle when there are more rows or bolts. Like for another cross sections of the composite structures there should be a closer look at the resistance for the ultimate limit state ULS and to the elastic behaviour under the serviceability limit state SLS. In the ultimate limit state the failure load of the system is important, see (BCSA and SCI. 2013). Under service loads is checked the elastic behaviour and that the concrete cone will not fail. This would lead to cracks and with the time to a corrosion of the reinforcement of the concrete wall and finally to a failure of the construction.

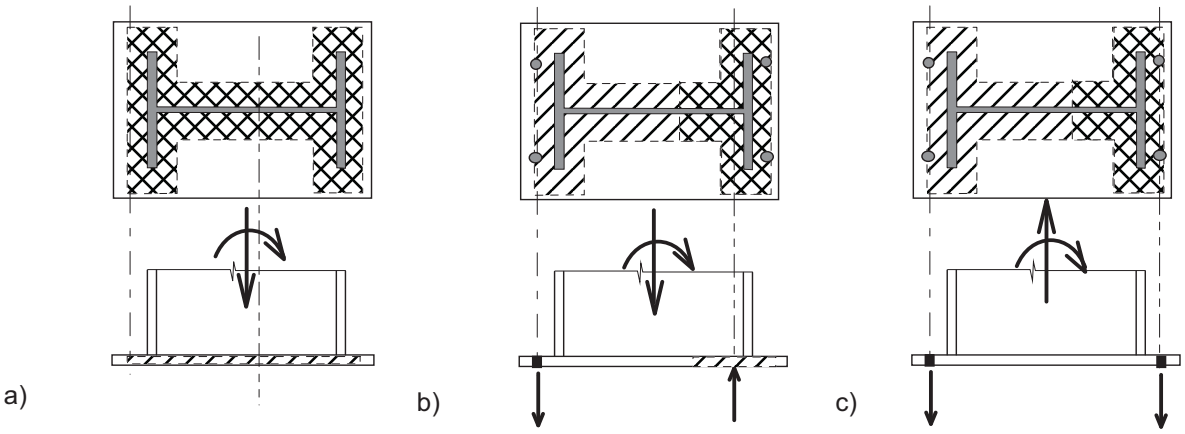

a) no tension in anchor bolts, b) one row of the anchor bolts in tension,
c) two rows of the anchor bolts in tension

Figure 2.20 The force equilibrium of the base plate

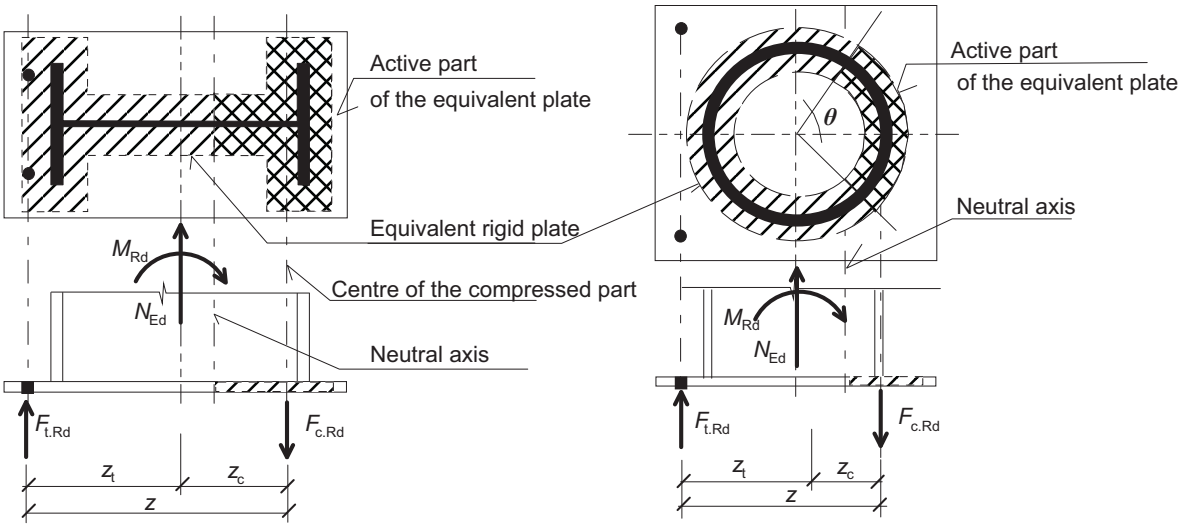

Figure 2.21 Force equilibrium for the column base, one row of the anchor bolts in tension

The equilibrium of forces is calculated according to Figure 2.21 as follows:

$$N_{Ed} = F_{c,Rd} + F_{t,Rd} \tag{2.20}$$

$$M_{\mathrm{Rd}} = F_{\mathrm{c,Rd}} \cdot z_{\mathrm{c}} + F_{\mathrm{t,Rd}} \cdot z_{\mathrm{t}} \tag{2.21}$$

where

$$F_{\mathrm{c,Rd}} = A_{\mathrm{eff}} \cdot f_{\mathrm{jd}} \tag{2.22}$$

A_{eff} is effective area under the base plate
z_{t} distance of tension part
z_{c} distance of compressed part

The resistance of the compressed part $F_{\mathrm{c,Rd}}$ and the resistance of the part in tension $F_{\mathrm{t,Rd}}$ are determined in next chapters. If the tensile force in the anchor bolts according to Figure 2.21 occur for

$$e = \frac{M_{\mathrm{Rd}}}{N_{\mathrm{Ed}}} \geq z_{\mathrm{c}} \tag{2.23}$$

formulas for tension and compressed part are derived

$$\frac{M_{\mathrm{Rd}}}{z} - \frac{N_{\mathrm{Ed}} \cdot z_{\mathrm{c}}}{z} \leq F_{\mathrm{c1,Rd}} \tag{2.24}$$

$$\frac{M_{\mathrm{Rd}}}{z} + \frac{N_{\mathrm{Ed}} \cdot z_{\mathrm{c1}}}{z} \leq F_{\mathrm{c,Rd}} \tag{2.25}$$

Then, the column base moment resistance M_{Rd} under a constant normal force N_{Ed} is expressed as follow:

with tension force in the anchor bolts

$$M_{Rd} = \min \begin{cases} F_{t,Rd} \cdot z + N_{Ed} \cdot z_c \\ F_{c,Rd} \cdot z - N_{Ed} \cdot z_t \end{cases} \tag{2.26}$$

without tension force, both parts are compressed

$$M_{Rd} = \min \begin{cases} F_{c1,Rd} \cdot z + N_{Ed} \cdot z_c \\ F_{c,Rd} \cdot z - N_{Ed} \cdot z_{c1} \end{cases} \tag{2.27}$$

The procedure is derived for open section of I/H cross section. For rectangular hollow section RHS may be taken directly with two webs. For circular/elliptical hollow sections CHS/EHS is the procedure modified, see (Horová et al., 2011), using sector coordinates. The effective area $A_{eff} = 2\ \theta\ r\ c$ depends on the angle θ. The lever arm and the resistance of the component in compression is

$$z_c = r \cdot \cos\frac{\theta}{2} \tag{2.28}$$

$$F_{c,Rd} = F_{c1,Rd} = \pi \cdot r \cdot c \tag{2.29}$$

2.3.2 Bending stiffness

The calculation of stiffness of the base plate, given in (Wald et al., 2008, 3-20), is compatible with beam to column stiffness calculation. The difference between these two procedures is in the fact that by the base plate joint the normal force has to be introduced. In Figure 2.22 there is the stiffness model which shows a way of loading, compression area under the flange, allocating of forces under the base plate, and a position of the neutral axes.

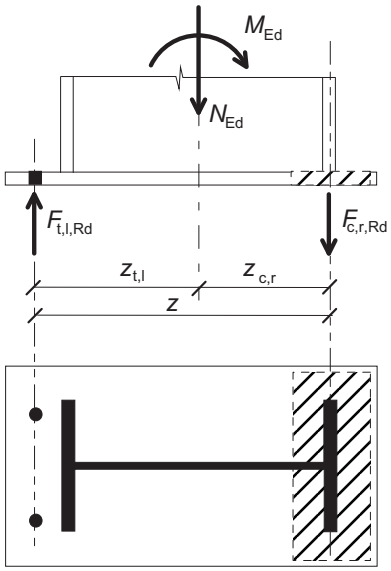

Figure 2.22 The stiffness model of the base plate connection of the column base

By the calculation of the stiffness the effective area is taken into account. The position of compression force $F_{c,Rd}$ is located at the centre of compression area. The tensile force $F_{t,Rd}$ is located at the anchor bolts. The rotational bending stiffness of the base plate is determined during proportional loading with constant eccentricity

$$e = \frac{M_{Ed}}{N_{Ed}} = \text{const.} \tag{2.30}$$

According to the eccentricity three possible patterns can arise, as for resistance, based on activation of anchor bolts, see (Wald et al., 2008, 3-20). For large eccentricity with tension in one row of anchor bolts, see Pattern 1 in Figure 2.23a, without tension in row of anchor bolts, small eccentricity, Pattern 2 in Figure 2.23b, and with tension in both row of anchor bolts, Pattern 3 in Figure 2.23c.

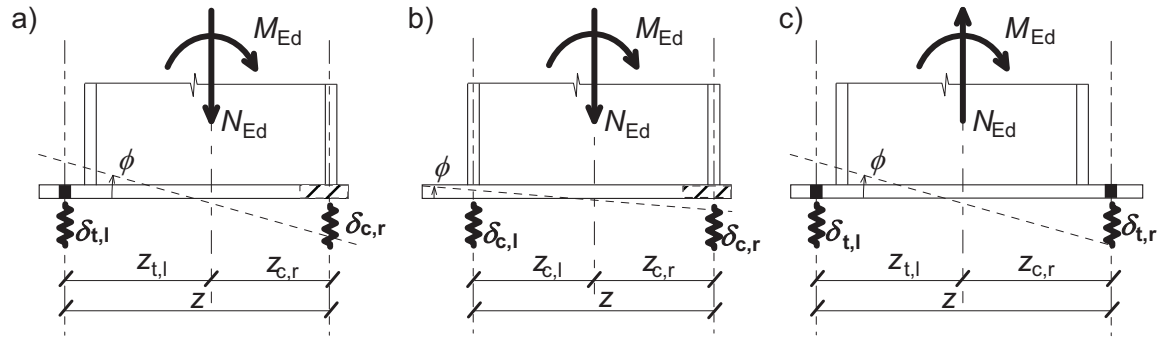

a) one anchor bolt row activated, b) no anchor bolt activated
c) both anchor bolt rows activated

Figure 2.23 The mechanical model of the base plate

Deformations δ_t and δ_c of components depend on the stiffness coefficient of tension part k_t and the compression part k_c.

$$\delta_{t,l} = \frac{\frac{M_{Ed}}{z} - \frac{N_{Ed} \cdot z_t}{z}}{E\, k_t} = \frac{M_{Ed} - N_{Ed} \cdot z_t}{E\, z\, k_t} \tag{2.31}$$

$$\delta_{c,r} = \frac{\frac{M_{Ed}}{z} - \frac{N_{Ed} \cdot z_t}{z}}{E\, k_c} = \frac{M_{Ed} - N_{Ed} \cdot z_t}{E\, z\, k_c} \tag{2.32}$$

where:

z_t distance of tension/compressed part

z level arm of internal forces

E modulus of elasticity the steel

The rotation of the base plate for proportional loading, see Figure 2.24, could be determined from formulas above

$$\phi = \frac{\delta_{t,l} + \delta_{c,r}}{z} = \frac{1}{E\,z^2} \cdot \left(\frac{M_{Ed} - N_{Ed} \cdot z_c}{k_t} + \frac{M_{Ed} + N_{Ed} \cdot z_t}{k_c} \right) \tag{2.33}$$

From the rotation the initial stiffness is derived

$$S_{j,ini} = \frac{E\,z^2}{\frac{1}{k_c} + \frac{1}{E\,z_t^2}} = \frac{E\,z^2}{\sum \frac{1}{k}} \tag{2.34}$$

Nonlinear part of the moment-rotation curve is given by coefficient μ, which express the ratio between the rotational stiffness in respect to the bending moment, see EN1993-1-8:2006

$$\mu = \frac{S_{j,ini}}{S_j} = \left(\kappa \frac{M_{Ed}}{M_{Ed}} \right)^{\zeta} \geq 1 \tag{2.35}$$

where

κ is coefficient introducing the beginning of non-linear part of curve, κ = 1,5

ξ is shape parameter of the curve, ξ = 2,7.

The procedure for evaluation of stiffens is derived for open section of I/H cross section. For rectangular hollow section RHS may be taken directly taking into account two webs. For circular/elliptical hollow sections CHS/EHS may be modified, see (Horová, et al., 2011).

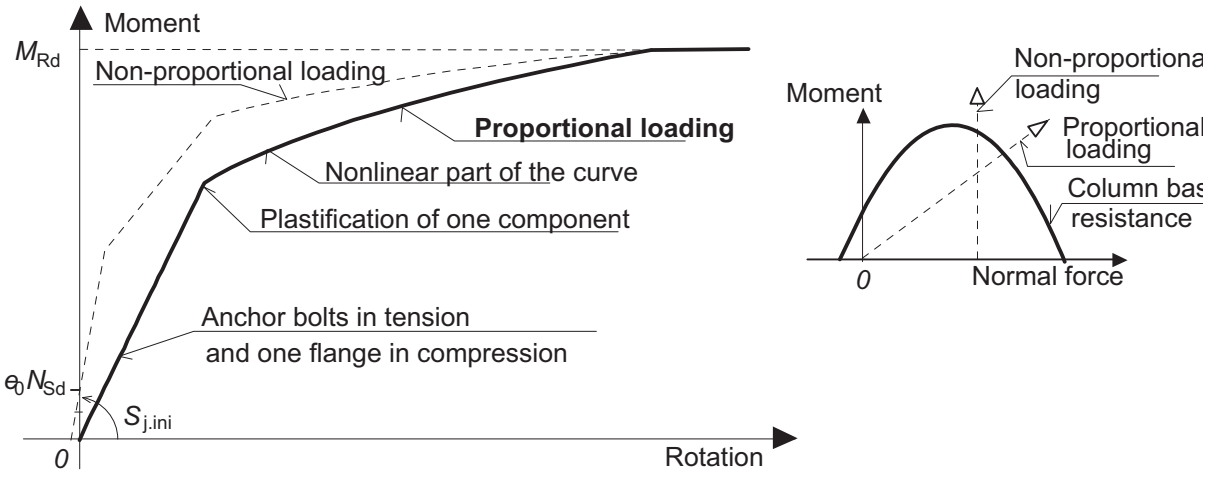

Figure 2.24 Moment rotation curve for proportional loading

2.3.3 Component base plate in bending and concrete in compression

The components concrete in compression and base plate in bending represent the behaviour of the compressed part of a steel to concrete connection. The resistance of these components depends primarily on the bearing resistance of the concrete block under the flexible base plate. The resistance of concrete is influenced by flexibility of base plate. In case of loading by an axial force, the stresses in concrete are not uniformly distributed, they are concentrated around the footprint of the column under the plate according to its thickness. For the design the flexible base plate is replaced by reducing the effective fully rigid plate. The grout layer between the base plate and concrete block influences the resistance and stiffness of the component. That is why this layer is also included into this component. Other important factors which influence the resistance are the concrete strength, the compression area, the location of the plate on the concrete foundation, the size of the concrete block and its reinforcement. The stiffness behaviour of column base connection subjected to bending moment is influenced mostly by elongation of anchor bolts. The component concrete in compression is mostly stiffer in comparison to the component anchor bolts in tension. The deformation of concrete block and base plate in compression is important in case of dominant axial compressive force. The strength of the component $F_{\mathrm{Rd,u}}$, expecting the constant distribution of the bearing stresses under the effective area, is given by

$$F_{\mathrm{Rd,u}} = A_{\mathrm{c0}}\, f_{\mathrm{jd}} \tag{2.36}$$

The design value of the bearing strength f_{jd} in the joint loaded by concentrated compression, is determined as follows. The concrete resistance is calculated according to cl. 6.7(2) in EN1992-1-1:2004 see Figure 2.25 is

$$F_{\mathrm{Rd,u}} = A_{\mathrm{c0}}\, f_{\mathrm{cd}} \sqrt{\frac{A_{\mathrm{c1}}}{A_{\mathrm{c0}}}} \le 3{,}0 A_{\mathrm{c0}} f_{\mathrm{cd}} \tag{2.37}$$

where

$$A_{\mathrm{c0}} = b_1 d_1 \tag{2.38}$$

where A_{c0} is the loaded area and A_{c1} the maximum spread area. The influence of height of the concrete block to its 3D behaviour is introduced by

$$h \ge b_2 - b_1 \quad \text{and} \quad h \ge d_2 - d_1 \tag{2.39}$$

$$3 b_1 \ge b_2 \quad \text{and} \quad 3 d_1 \ge d_2 \tag{2.40}$$

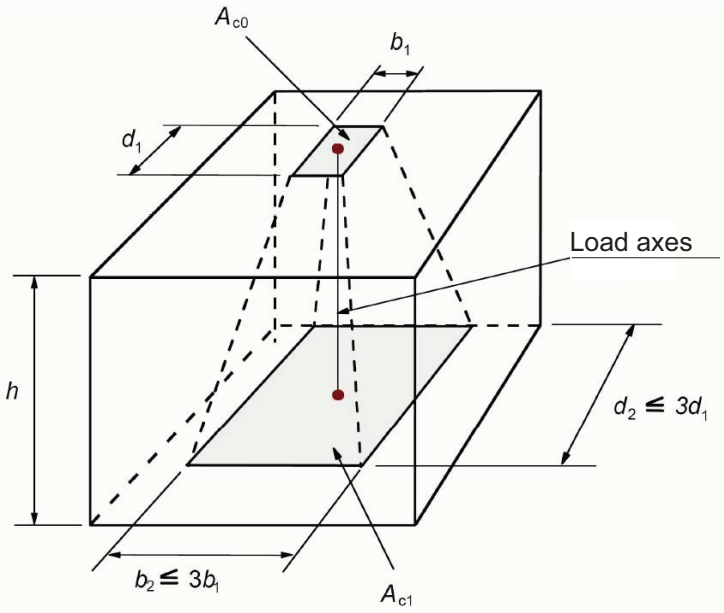

Figure 2.25 Concrete compressive strength for calculation of 3D concentration

From this geometrical limitation the following formulation is derived

$$f_{jd} = \frac{\beta_j F_{Rd,u}}{b_{eff}\, l_{ef}} = \frac{\beta_j A_{c0}\, f_{cd} \sqrt{\frac{A_{c1}}{A_{c0}}}}{A_{c0}} = \beta_j f_{cd}\, k_j \leq \frac{3A_{c0}\, f_{cd}}{A_{c0}} = 3,0\, f_{cd} \tag{2.41}$$

The factor β_j represents the fact that the resistance under the plate might be lower due to the quality of the grout layer after filling. The value 2/3 is used in the case of the characteristic resistance of the grout layer is at least 0,2 times the characteristic resistance of concrete and thickness of this layer is smaller than 0,2 times the smallest measurement of the base plate. In different cases, it is necessary to check the grout separately, see Figure 2.26. The bearing distribution under 45° is expected in these cases, see (Steenhuis et al., 2008).

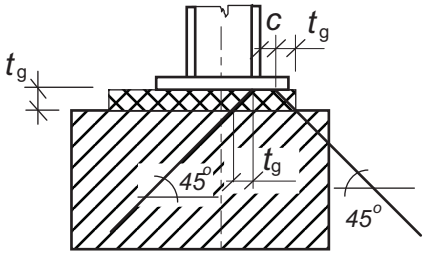

Figure 2.26 Modelling of grout

In case of the elastic deformation of the base plate is expected homogenous stress distribution in concrete block is expected under the flexible base plate based on the best engineering practice. The formula for the effective width c is derived from the equality of elastic bending moment resistance of the base plate and the bending moment acting on the base plate. Acting forces are shown in Figure 2.27.

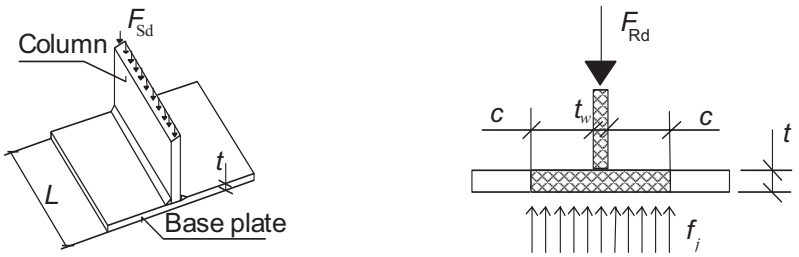

Figure 2.27 Base plate as a cantilever for check of its elastic deformation only

Elastic bending moment of the base plate per unit length is

$$M' = \frac{1}{6} t^2 \frac{f_y}{\gamma_{M0}} \tag{2.42}$$

and the bending moment per unit length on the base plate of span c and loaded by distributed load is

$$M' = \frac{1}{2} f_j c^2 \tag{2.43}$$

where f_j is concrete bearing strength from Eqn. (2.41) and the effective width c is

$$c = t \sqrt{\frac{f_y}{3 \cdot f_{jd} \cdot \gamma_{M0}}} \tag{2.44}$$

The flexible base plate, of the area A_p, is replaced by an equivalent rigid plate with area A_{eq}, see Figure 2.28. Then the resistance of the component, expecting the constant distribution of the bearing stresses under the effective area is given by

$$F_{Rd,u} = A_{eq} \cdot f_{jd} \tag{2.45}$$

The resistance F_{Rd} should be higher than the loading F_{Ed}

$$F_{Ed} \le F_{Rd,u} \tag{2.46}$$

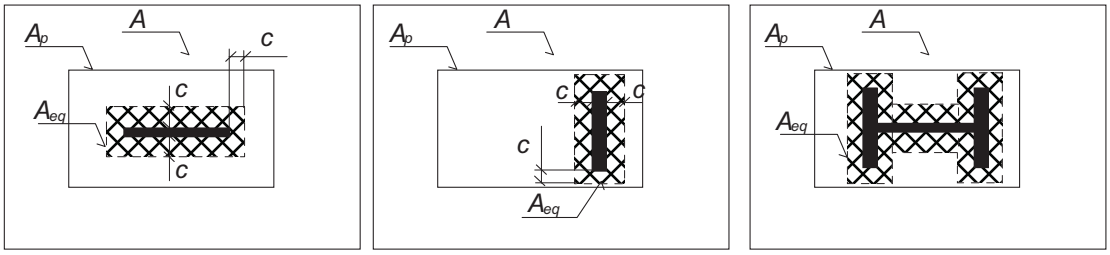

Figure 2.28 Effective area under the base plate

The proposed design model for stiffness of the components base plate in bending and concrete in compression is given also in (Steenhuis et al., 2008). The stiffness of the component is influenced by factors: the flexibility of the plate, the Young´s modulus of concrete, and the size of the concrete block. By loading with force, a flexible rectangular plate could be pressed down into concrete block. From the deformation of the component and other necessary values which are described above, the formula to calculate the stiffness coefficient is derived

$$k_c = \frac{E_c \cdot \sqrt{t \cdot L}}{0,72 \cdot E} \tag{2.47}$$

where

$a_{eq,el}$ is equivalent width of the T-stub

L is length of the T-stub

2.3.4 Component base plate in bending and anchor bolt in tension

The base plate in bending and anchor bolts in tension is modelled by the help of T-stub model based on the beam to column end plate connection model, see Figure 2.29. Though in its behaviour there are some differences. Thickness of the base plate is bigger to transfer compression into the concrete block. The anchor bolts are longer due to thick pad, thick base plate, significant layer of grout and flexible embedding into concrete block. The influence of a pad and a bolt head may be higher.

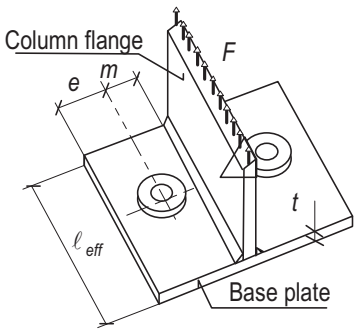

Figure 2.29 The T stub - anchor bolts in tension and base plate in bending

Due to longer free lengths of bolts, bigger deformations could arise. The anchor bolts, compare to bolts, are expecting to behave ductile. When it is loaded by tension, the base plate is often separated from the concrete surface, see Figure 2.30. By bending moment loading different behaviour should be expected. The areas of bolt head and pad change favourably distribution of forces on T-stub. This influence is not so distinctive during calculation of component stiffness. The all differences from end plate connections are involved in the component method, see EN1993-1-8:2006. The design model of this component for resistance as well for stiffness is given in (Wald et al., 2008, 21-50).

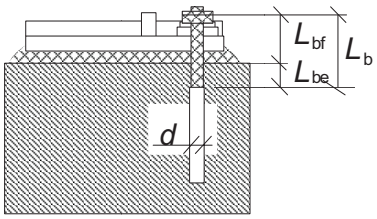

Figure 2.30 Length of anchor bolt

When the column base is loaded by bending moment as it is shown in Figure 2.31, anchor bolts transfer tensile forces. This case of loading leads to elongation of anchor bolts and bending of the base plate. Deformed bolts can cause failure as well as reaching of the yield strength of the base plate.

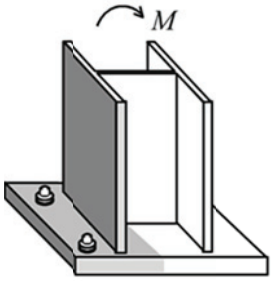

Figure 2.31 Tensile zone and equivalent T-stub in case of loading by bending moment

Column with connected base plate taken, as it is shown in Figure 2.32, into model of T-stub.

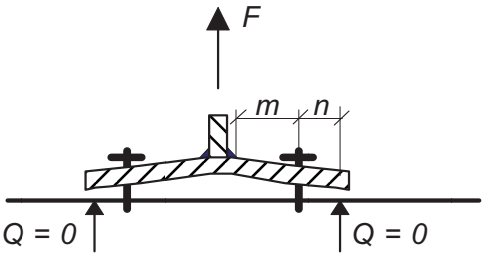

Figure 2.32 T-stub separated from the concrete block with no prying force

There are two models of deformation of the T-stub of the base plate according to presence of prying. In the case the base plate separated from the concrete foundation, there is no prying force Q, see Figure 2.33. In other case, the edge of the plate is in contact with concrete block, the bolts are loaded by additional prying force Q. This force is balanced just by the contact force at the edge of the T-stub, see Figure 2.33.

When there is contact between the base plate and the concrete block, beam theory is used to describe deformed shape of the T-stub.

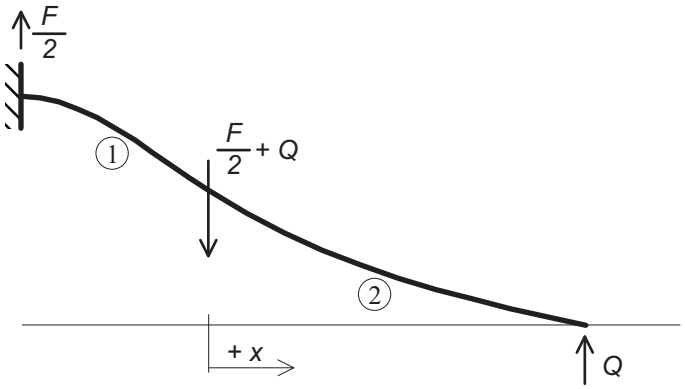

Figure 2.33 Beam model of T-stub and prying force Q

Deformed shape of the curve is described by differential equation

$$E\,I\,\delta'' = -M \tag{2.48}$$

After writing the above equation for both parts of the beam model 1 and 2, application of suitable boundary conditions, the equations could be solved. The prying force Q is derived just from these solved equations as

$$Q = \frac{F}{2} \cdot \frac{3\left(m^2 n\,A - 2L_b\,I\right)}{2\,n^2 A\left(3m + n\right) + 3\,L_b I} \tag{2.49}$$

When the base plate is in contact with concrete surface, the prying of bolts appears and on the contrary no prying forces occur in the case of separated base plate from the concrete block due to the deformation of long bolts. This boundary, between prying and no prying has to be determined. Providing that n = 1,25 m it may be expressed as

$$L_{b,\min} = \frac{8,82\,m^3 A_s}{l_{eff}\,t^3} < L_b \tag{2.50}$$

where

A_s is the area of the bolt
L_b is equivalent length of anchor bolt
l_{eff} is equivalent length of T-stub determined by the help of Yield line method, presented in following part of work

For embedded bolts length L_b is determined according to Figure 2.34 as

$$L_b = L_{bf} + L_{be} \tag{2.51}$$

where

L_{be} is 8 d effective bolt length

When the length of bolt $L_b > L_{b,min}$ there is no prying. Previous formulae is expressed for boundary thickness t_{lim}, see (Wald et al., 2008, 21-50), of the base plate as

$$t_{\text{lim}} = 2,066\,\text{m} \cdot \sqrt[3]{\frac{A_s}{l_{\text{eff}}\, L_b}} \tag{2.52}$$

If the base plate are loaded by compression force and by bending moment and not by tensile force it is recommended to neglect these prying forces. In other cases it needs to be checked.

The design resistance of a T-stub of flange in tension of effective length ℓ_{eff} is determined as minimum resistance of three possible plastic collapse mechanisms. For each collapse mechanism there is a failure mode. Following collapse modes, shown in Figure 2.33, is used for T-stub in contact with the concrete foundation, see in EN1993-1-8:2006.

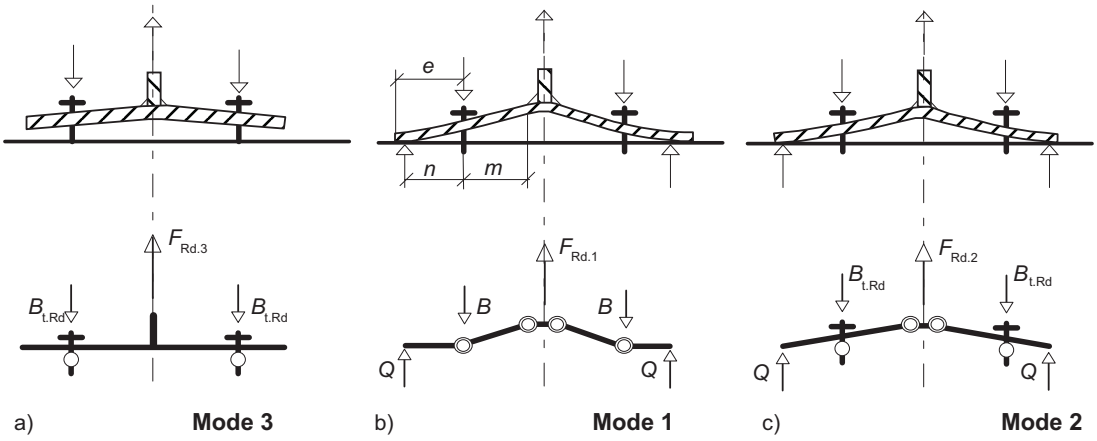

Figure 2.34 Failure modes of the T-stub in contact with the concrete foundation

Mode 1

According to this kind of failure the T-stub with thin base plate and high strength anchor bolts is broken. In the base plate plastic hinge mechanism with four hinges is developed.

$$F_{1,\text{Rd}} = \frac{4\, l_{\text{eff}}\, m_{\text{pl,Rd}}}{m} \tag{2.53}$$

Mode 2

This mode is a transition between failure Mode 1 and 3. At the same time two plastic hinges are developed in the base plate and the limit strength of the anchor bolts is achieved.

$$F_{2,\text{Rd}} = \frac{2\, l_{\text{eff}}\, m_{\text{pl,Rd}} + \sum B_{\text{t,Rd}} \cdot n}{m + n} \tag{2.54}$$

Mode 3

Failure mode 3 occurs by the T-stub with thick base plate and weak anchor bolts. The collapse is caused by bolt fracture.

$$F_{3,\text{Rd}} = \sum B_{\text{t,Rd}} \tag{2.55}$$

The design strength F_{Rd} of the T-stub is derived as the smallest of these three possible modes:

$$F_{Rd} = \min\left(F_{1,Rd}, F_{2,Rd}, F_{3,Rd}\right) \tag{2.56}$$

Because of the long anchor bolts and thick base plate different failure mode arises compare to an end plate connection. When the T-stub is uplifted from the concrete foundation, there is no prying, new collapse mode is obtained, see Figure 2.35. This particular failure mode is named Mode 1-2.

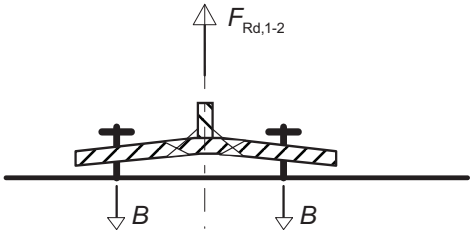

Figure 2.35 T-stub without contact with the concrete foundation, Mode 1-2

Mode 1-2

The failure results either from bearing of the anchor bolts in tension or from the yielding of the plate in bending, where a two hinges mechanism develops in the T-stub flange. This failure does not appear in beam to column connection because of the small deformation of the bolts in tension, see (Wald et al., 2008, 21-50).

$$F_{1\text{-}2,Rd} = \frac{2\, l_{eff}\, m_{pl,Rd}}{m+n} \tag{2.57}$$

The relationship between Mode 1-2 and modes of T-stub in contact with concrete is shown in Figure 2.36.

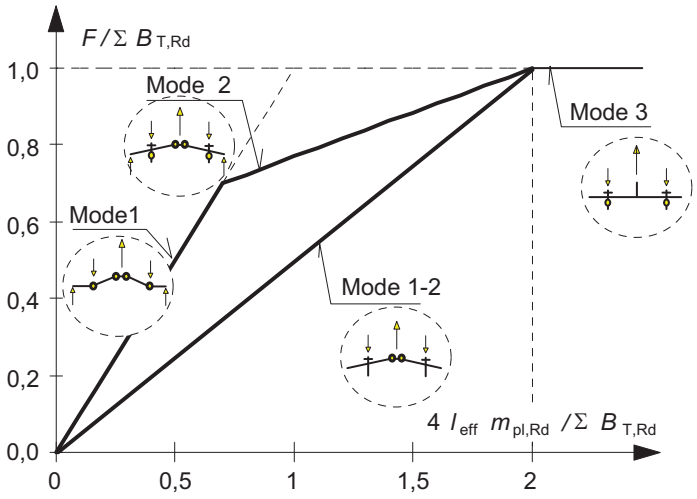

Figure 2.36 Failure mode 1-2

The boundary between the mode 1-2 and others is given in the same way like the boundary of prying and no prying – according to the limiting bolt length $L_{b,min}$.

During the Mode 1-2 large deformations of the base plate can develop. Finally these deformations could lead to contact between the concrete block and the edge of the T-stub (prying forces can arise even in this case). After loading Modes 1 or 2 should be obtained like the first. But for reaching this level of resistance, which is necessary to obtain these modes, very large deformations are required. And so high deformations are not acceptable for design. In conclusion, in cases where no prying forces develop, the design resistance of the T-stub is taken as

$$F_{\text{Rd}} = \min\left(F_{\text{1-2,Rd}}, F_{\text{3,Rd}}\right) \tag{2.58}$$

Equivalent length of T-stub

The equivalent length of T-stub l_{eff}, which is important for the resistance determination, is calculated by the help of the yield line method.

Two groups of yield line patterns called circular and non-circular yield lines are distinguished in EN1993-1-8: 2006, see Figure 2.37. The major difference between circular and non-circular patterns is related to contact between the T-stub and rigid foundation. The contact may occur only for non-circular patterns and prying force will develop only in this case. This is considered in the failure modes as follows:

Mode 1

The prying force does not have influence on the failure and development of plastic hinges in the base plate. Therefore, the formula applies to both circular and non-circular yield line patterns.

Mode 2

First plastic hinge forms at the web of the T-stub. Plastic mechanism is developed in the base plate and its edges come into contact with the concrete foundation. As a result, prying forces develop in the anchor bolts and bolt fracture is observed. Therefore, Mode 2 occurs only for non-circular yield line patterns, which allow development of prying forces.

Mode 3

This mode does not involve any yielding of the plate and applies therefore to any T-stub. In the design procedure, the appropriate effective length of the T-stub should be used for Mode 1

$$l_{\text{eff,1}} = \min\left(l_{\text{eff,cp}}; l_{\text{eff,np}}\right) \tag{2.59}$$

and for Mode 2

$$l_{\text{eff,2}} = \min\left(l_{\text{eff,np}}\right) \tag{2.60}$$

Table 2.9, Table 2.10, Figure 2.37 and Figure 2.38 from (Wald et al., 2008, 21-50), indicate the values of l_{eff} for typical base plates in cases with and without contact. For symbols see Figure 2.36.

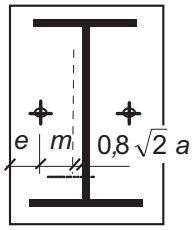

Figure 2.37 The effective length of T-stub for bolts inside the flanges

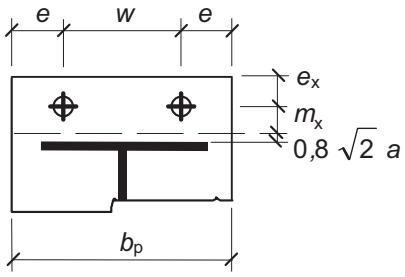

Figure 2.38 The effective length of T-stub for bolts outside the flanges

Table 2.9 The effective length l_{eff} of a T-stub with bolts inside the flanges

Prying case	No prying case
$l_1 = 2\ a\ m$ - (4 m - 1,25 e)	$l_1 = 2\ a\ m$ - (4 m + 1,25 e)
$l_2 = 2\ \pi\ m$	$l_2 = 4\ \pi\ m$
$l_{eff,1} = \min\ (l_1; l_2)$	$l_{eff,1} = \min\ (l_1; l_2)$
$l_{eff,2} = l_1$	$l_{eff,2} = l_1$

Table 2.10 Effective length l_{eff} for bolts outside the flanges

Prying case	No prying case
$l_1 = 4\ a\ m_x + 1{,}25\ e_x$	$l_1 = 4\ a\ m_x + 1{,}25\ e_x$
$l_2 = 2\ \pi\ m_x$	$l_2 = 2\ \pi\ m_x$
$l_3 = 0{,}5 b_p$	$l_3 = 0{,}5\ b_p$
$l_4 = 0{,}5\ w + 2\ m_x + 0{,}625\ e_x$	$l_4 = 0{,}5\ w + 2\ m_x + 0{,}625\ e_x$
$l_5 = e + 2\ m_x + 0{,}625\ e_x$	$l_5 = e + 2\ m_x + 0{,}625\ e_x$
$l_6 = \pi\ m_x + 2\ e$	$l_6 = 2\ \pi\ m_x + 4\ e$
$l_7 = \pi\ m_x + w$	$l_7 = 2\ (\pi\ m_x + w\ )$
$l_{eff,1} = \min\ (l_1\ ;\ l_2\ ;\ l_3\ ;\ l_4\ ;\ l_5\ ;\ l_6\ ;\ l_7)$	$l_{eff,1} = \min\ (l_1\ ;\ l_2\ ;\ l_3\ ;\ l_4\ ;\ l_5;\ l_6\ ;\ l_7)$
$l_{eff,2} = \min\ (l_1\ ;\ l_2\ ;\ l_3\ ;\ l_4\ ;\ l_5)$	$l_{eff,2} = \min\ (l_1\ ;\ l_2\ ;\ l_3\ ;\ l_4\ ;\ l_5)$

The prediction of the base plate stiffness is based on (Steenhuis et al., 2008). The stiffness of the component analogous to the resistance of the T-stub is influenced by the contact of the base plate and the concrete foundation (Wald et al., 2008, 3-20). The formula for deformation of the base plate loaded by the force in bolt F_b is

$$\delta_p = \frac{1}{2}\frac{F_b m^3}{3 E I} = \frac{2 F_b m^3}{E \cdot l_{eff}\, t^3} = \frac{2 F_b m^3}{E \cdot k_p} \tag{2.61}$$

and deformation of the bolt is

$$\delta_{\mathrm{p}} = \frac{F_{\mathrm{b}} L_{\mathrm{b}}}{E_{\mathrm{b}} A_{\mathrm{b}}} = \frac{F_{\mathrm{b}}}{E_{\mathrm{b}} k_{\mathrm{b}}} \tag{2.62}$$

The stiffness of the T-stub is written as

$$k_{\mathrm{T}} = \frac{F_{\mathrm{b}}}{E\left(\delta_{\mathrm{p}} + \delta_{\mathrm{b}}\right)} \tag{2.63}$$

In following conditions cases prying force are appearing in the T-stub

$$\frac{A_{\mathrm{s}}}{L_{\mathrm{b}}} \geq \frac{l_{\mathrm{eff,ini}}\, t^3}{8{,}82\, m^3} \tag{2.64}$$

Formulas for stiffness coefficient of the base plate and of the bolt are

$$k_{\mathrm{p}} = \frac{l_{\mathrm{eff,ini}}\, t^3}{m^3} = \frac{0{,}85\, l_{\mathrm{eff}}\, t^3}{m^3} \tag{2.65}$$

$$k_{\mathrm{b}} = 1{,}6\, \frac{A_{\mathrm{s}}}{L_{\mathrm{b}}} \tag{2.66}$$

In case of no prying, it means when

$$\frac{A_{\mathrm{s}}}{L_{\mathrm{b}}} \geq \frac{l_{\mathrm{eff,ini}}\, t^3}{8{,}82\, m^3} \tag{2.67}$$

Formulas are as following:

$$k_{\mathrm{p}} = \frac{F_{\mathrm{p}}}{E\, \delta_{\mathrm{p}}} = \frac{l_{\mathrm{eff,ini}}\, t^3}{2\, m^3} = \frac{0{,}425\, l_{\mathrm{eff}}\, t^3}{m^3} \tag{2.68}$$

$$k_{\mathrm{b}} = \frac{F_{\mathrm{p}}}{E\, \delta_{\mathrm{p}}} = 2{,}0\, \frac{A_{\mathrm{s}}}{L_{\mathrm{b}}} \tag{2.69}$$

The stiffness of the component of base plate in bending and bolts in tension is summarised from above simplified predictions as

$$\frac{1}{k_{\mathrm{T}}} = \frac{1}{k_{\mathrm{b,i}}} + \frac{1}{k_{\mathrm{p,i}}} \tag{2.70}$$

For base plates are used the bolt pads under the bolt nut to help to cover the tolerances. The impact of an area of the bolt pad/nut changes the geometrical characteristics of T-stub. The influence is taken into account by the help of equivalent moment of inertia $I_{\mathrm{p,bp}}$ and addition of stiffness k_{w} to the previous stiffness k_{p}.

2.3.5 Anchor bolts in shear

In most cases the shear force is transmitted via friction between the base plate and the grout. The friction capacity depends on the compressive normal force between the base plate and the grout and the friction coefficient. At increasing horizontal displacement the shear force increases till it reaches the friction capacity. At that point the friction resistance stays constant with increasing displacements, while the load transfer through the anchor bolts increases further. Because the grout does not have sufficient strength to resist the bearing stresses between the bolts and the grout, considerable bending of the anchor bolts may occur. The tests shows the bending deformation of the anchor bolts, the crumbling of the grout and the final cracking of the concrete. The analytical model for shear resistance of anchor bolts was derived in EN1993-1-8 cl 6.2.2, see (Gresnigt at al, 2008). Also, the preload in the anchor bolts contributes to the friction resistance. However, because of its uncertainty, e.g. relaxation and interaction with the column normal force, it was decided to neglect this action in current standard.

The design shear resistance $F_{v,Rd}$ may be derived as follows

$$F_{v,Rd} = F_{f,Rd} + F_{vb,Rd} \tag{2.71}$$

where

$F_{f,Rd}$ is the design friction resistance between base plate and grout layer

$$F_{f,Rd} = C_{f,d}\, N_{c,Sd} \tag{2.72}$$

$C_{f,d}$ is the coefficient of friction between base plate and grout layer. The following values may be used for sand-cement mortar $C_{f,d}$ = 0,20.

$N_{c,Sd}$ is the design value of the normal compressive force in the column. If the normal force in the column is a tensile force $F_{f,Rd}$ = 0

n is the number of anchor bolts in the base plate

$F_{vb,Rd}$ is the smallest of $F_{1,vb,Rd}$ and $F_{2,vb,Rd}$

$F_{1,vb,Rd}$ is the shear resistance of the anchor bolt and

$$F_{2,vb,Rd} = \frac{\alpha_b\, f_{ub}\, A_s}{\gamma_{M2}} \tag{2.73}$$

A_s is the tensile stress area of the bolt or of the anchor bolt

α_{bc} is a coefficient depending on the yield strength f_{yb} the anchor bolt

$$\alpha_{bc} = 0,44 - 0,0003\, f_{yb} \tag{2.74}$$

f_{yb} is the nominal yield strength the anchor bolt

where 235 N/mm^2 $\leq$ f_{yb} $\leq$ 640 N/mm^2

γ_{M2} is the partial safety factor for anchor bolt

2.3.6 Worked example - simple column base

Check the resistance of the column base, see Figure 2.39. The column of HE 200 B section, a concrete foundation size 850 × 850 × 900 mm, a base plate thickness 18 mm, steel S 235 and concrete *C* 12/15, γ_c = 1,50, γ_{M0} = 1,00.

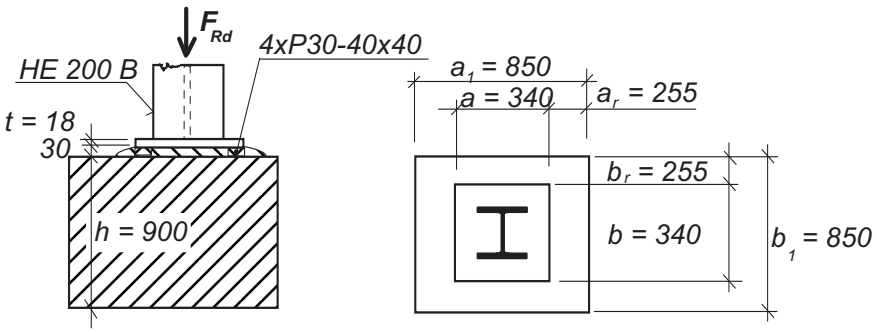

Figure 2.39 Designed simple column base

Concrete design strength

The minimum values for a_1 (or b_1) are taken into account

$$a_1 = b_1 = \min\begin{Bmatrix} a + 2a_r = 340 + 2 \cdot 255 = 850 \\ 3a = 3 \cdot 340 = 1020 \\ a + h = 340 + 900 = 1240 \end{Bmatrix} = 850 \text{ mm}$$

The condition $a_1 = b_1 = 850 > a = 340$ mm is satisfied, and therefore the stress concentration factor is

$$k_j = \sqrt{\frac{a_1 \cdot b_1}{a \cdot b}} = \sqrt{\frac{850 \cdot 850}{340 \cdot 340}} = 2,5$$

The concrete design strength is calculated from the equation

$$f_{jd} = \frac{\beta_j F_{Rd,u}}{b_{eff}\, l_{ef}} = \frac{\beta_j A_{c0}\, f_{cd} \sqrt{\frac{A_{c1}}{A_{c0}}}}{A_{c0}} = \beta_j f_{cd}\, k_j = 0,67 \cdot \frac{12,0}{1,5} \cdot 2,5 = 13,4 \text{ MPa}$$

Flexible base plate

The flexible base plate is replaced by a rigid plate, see the following picture Figure 2.40. The strip width is

$$c = t\sqrt{\frac{f_y}{3 \cdot f_{jd} \cdot \gamma_{M0}}} = 18\sqrt{\frac{235}{3 \cdot 13,4 \cdot 1,00}} = 43,5 \text{ mm}$$

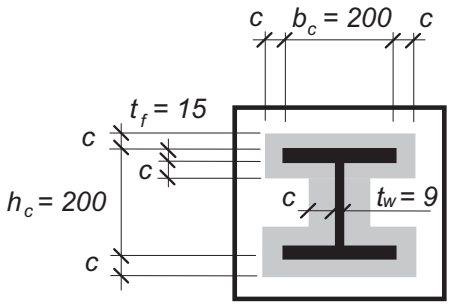

Figure 2.40 Effective area under the base plate

The effective area of the base plate of *H* shape is calculated as a rectangular area minus the central areas without contact such that;

$$A_{\text{eff}} = \min\left(b; b_{\text{c}} + 2c\right) \cdot \min\left(a; h_{\text{ef}} + 2c\right) - \max\left[\min\left(b; b_{\text{c}} + 2c\right) - t_{\text{w}} - 2c; 0\right] \cdot \max\left(h_{\text{c}} - 2t_{\text{f}} - 2c; 0\right)$$

$$A_{\text{eff}} = \left(200 + 2 \cdot 43,5\right) \cdot \left(200 + 2 \cdot 43,5\right) - \left(200 + 2 \cdot 43,5 - 9 - 2 \cdot 43,5\right) \cdot \left(200 - 2 \cdot 15 - 2 \cdot 43,5\right)$$

$$A_{\text{eff}} = 82\,369 - 15\,853 = 66\,516 \text{ mm}^2$$

Design resistance

The design resistance of the column base in compression is

$$N_{\text{Rd}} = A_{\text{eff}} \cdot f_{\text{jd}} = 66\,516 \cdot 13,4 = 891 \cdot 10^3 \text{ N}$$

Column footing

The design resistance of the column footing is higher than the resistance of the column base

$$N_{\text{pl,Rd}} = \frac{A_{\text{c}} \cdot f_{\text{y}}}{\gamma_{M0}} = \frac{7808 \cdot 235}{1,00} = 1\,835 \cdot 10^3 \quad N > N_{\text{Rd}}$$

where

A_{c} is area of the column. The column base is usually designed for column resistance, which is determined by column buckling resistance.

2.3.7 Worked example - fixed column base

In the following example the calculation of the moment resistance and the bending stiffness of the column base at Figure 2.41 is shown. The column HE 200 B of length 4 m is loaded by a normal force F_{Sd} = 500 kN. The concrete block C25/30 of size 1 600 × 1 600× 1000 mm is designed for particular soil conditions. The base plate is of 30 mm thickness and the steel strength is S235. Safety factors are considered as γ_{Mc} = 1,50; γ_{Ms} = 1,15, γ_{M0} = 1,00; and γ_{M2} = 1,25. The connection between the base plate and the concrete is carried out through four anchor bolt 22 mm diameter and f_{uk} = 470 MPa.

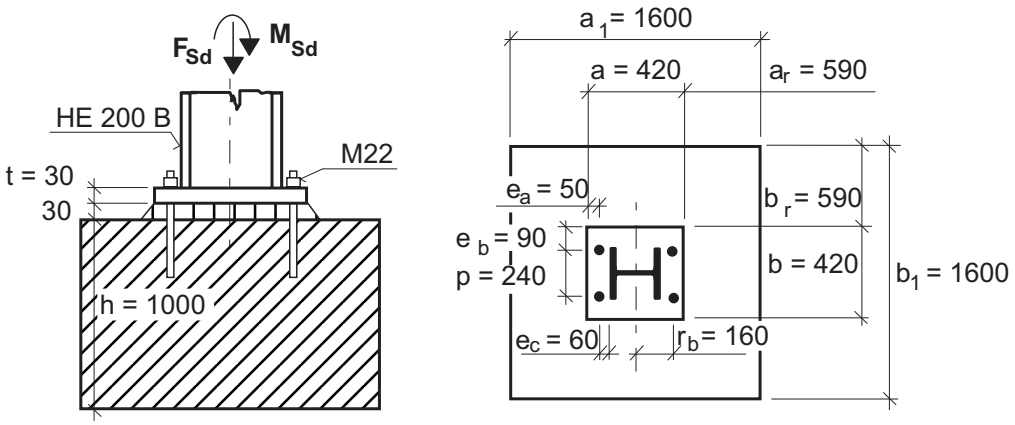

Figure 2.41 Designed fixed column base

Component base plate in bending and anchor bolts in tension

Lever arm, for fillet weld a_{wf} = 6 mm is

$$m = 60 - 0,8 \cdot a_{wf} \cdot \sqrt{2} = 60 - 0,8 \cdot 6 \cdot \sqrt{2} = 53,2 \text{ mm}$$

The minimum T-stub length in base plates where the prying forces not taken into account, is

$$l_{eff,1} = \min \left\{ \begin{array}{r} 4m + 1,25 e_a = 4 \cdot 53,2 + 1,25 \cdot 50 = 275,3 \\ 2\pi m = 2\pi \cdot 53,2 = 334,3 \\ b \cdot 0,5 = 420 \cdot 0,5 = 210 \\ 2m + 0,625 e_a + 0,5 p = 2 \cdot 53,2 + 0,625 \cdot 50 + 0,5 \cdot 240 = 257,7 \\ 2m + 0,625 e_a + e_b = 2 \cdot 53,2 + 0,625 \cdot 50 + 90 = 227,7 \\ 2\pi m + 4 e_b = 2\pi \cdot 53,2 + 4 \cdot 90 = 694,3 \\ 2\pi m + 2 p = 2\pi \cdot 53,2 + 2 \cdot 240 = 814,3 \end{array} \right\}$$

$$l_{eff,1} = 210 \text{ mm}$$

The effective length of headed studs L_b is taken as

$$L_b = \min\left(h_{eff}; 8 \cdot d\right) + t_g + t + \frac{t_n}{2} = 150 + 30 + 30 + \frac{19}{2} = 219,5 \text{ mm}$$

The resistance of T - stub with two headed studs is

$$F_{T,1\text{-}2,Rd} = \frac{2 L_{eff,1} t^2 f_y}{4 m \gamma_{M0}} = \frac{2 \cdot 210 \cdot 30^2 \cdot 235}{4 \cdot 53,2 \cdot 1,00} = 417,4 \text{ kN}$$

The resistance is limited by tension resistance of two headed studs M 22, the area in tension A_s = 303 mm.

$$F_{T,3,Rd} = 2 \cdot B_{t,Rd} = 2 \cdot \frac{0,9 \cdot f_{uk} A_s}{\gamma_{M2}} = 2 \cdot \frac{0,9 \cdot 470 \cdot 303}{1,25} = 205,1 \text{ kN}$$

The component stiffness coefficients for anchor bolts in tension and base plate in bending is calculated as

$$k_b = 2,0 \cdot \frac{A_s}{L_b} = 2,0 \cdot \frac{303}{219,5} = 2,8 \text{ mm}$$

$$k_p = \frac{0,425 \cdot L_{beff} \cdot t^3}{m^3} = \frac{0,425 \cdot 210 \cdot 30^3}{53,2^3} = 16,0 \text{ mm}$$

Component base plate in bending and concrete block in compression

To evaluate the compressed part resistance is calculated the connection factor as

$$a_1 = b_1 = \min \left\{ \begin{array}{c} a + 2a_r = 420 + 2 \cdot 590 = 1600 \\ 3a = 3 \cdot 420 = 1260 \\ a + h = 420 + 1000 = 1420 \end{array} \right\} = 1260 \text{ mm}$$

and $a_1 = b_1 = 1\,260 > a = b = 420$ mm

The above condition is fulfilled and

$$k_j = \sqrt{\frac{a_1 \cdot b_1}{a \cdot b}} = \sqrt{\frac{1260 \cdot 1260}{420 \cdot 420}} = 3,0$$

The grout is not influencing the concrete bearing resistance because

$$0,2 \cdot \min(a; b) = 0,2 \cdot \min(420; 420) = 84 \text{ mm} > 30 \text{ mm} = t_g$$

The concrete bearing resistance is calculated as

$$f_{jd} = \frac{2}{3} \cdot \frac{k_j f_{ck}}{\gamma_{Mc}} = \frac{2}{3} \cdot \frac{3,00 \cdot 25}{1,5} = 33,3 \text{ MPa}$$

From the force equilibrium in the vertical direction $F_{sd} = A_{eff} f_{jd} - F_{t,Rd}$ the area of concrete in compression A_{eff} in case of the full resistance of tension part is calculated

$$A_{eff} = \frac{F_{Sd} + F_{Rd,3}}{f_{jd}} = \frac{500 \cdot 10^3 + 205,1 \cdot 10^3}{33,3} = 21\,174 \text{ mm}^2$$

The flexible base plate is transferred into a rigid plate of equivalent area. The width of the strip c around the column cross section, see Figure 2.42, is calculated from

$$c = t \sqrt{\frac{f_y}{3 \cdot f_{jd} \cdot \gamma_{M0}}} = 30 \cdot \sqrt{\frac{235}{3 \cdot 33,3 \cdot 1,00}} = 46,0 \text{ mm}$$

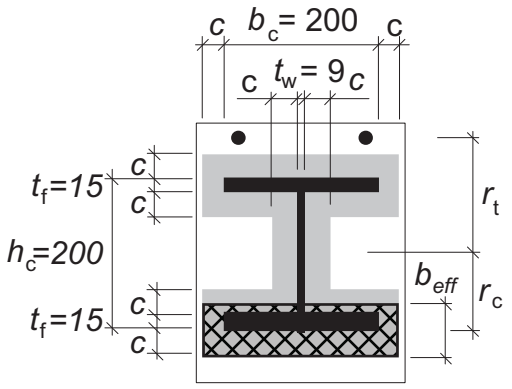

Figure 2.42 The effective area under the base plate

For equivalent width, see Figure 2.43,

$$a_{eq} = t_f + 2,5t = 15 + 2,5 \cdot 30 = 90\,\text{mm}$$

is the stiffness coefficient for base plate in bending and column in compression

$$k_c = \frac{E_c}{1,275 E_s} \cdot \sqrt{a_{eq} \cdot b_c} = \frac{31000}{1,275 \cdot 210000} \cdot \sqrt{90 \cdot 200} = 15,5\,\text{mm}$$

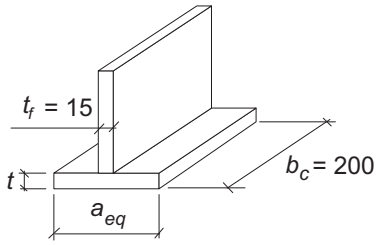

Figure 2.43 The T stub in compression

Base plate resistance

The active effective width is calculated as

$$b_{eff} = \frac{A_{eff}}{b_c + 2c} = \frac{21174}{200 + 2 \cdot 46,0} = 72,5\,\text{mm} < t_f + 2c = 15 + 2 \cdot 46,0 = 107,0\,\text{mm}$$

The lever arm of concrete to the column axes of symmetry is calculated as

$$r_c = \frac{h_c}{2} + c - \frac{b_{eff}}{2} = \frac{200}{2} + 46,0 - \frac{72,5}{2} = 109,8\,\text{mm}$$

The moment resistance of the column base is $M_{Rd} = F_{T,3,Rd} \cdot r_t + A_{eff} \cdot f_{jd} \cdot r_c$

$$M_{Rd} = 205,1 \cdot 10^3 \cdot 160 + 21174 \cdot 33,3 \cdot 109,8 = 110,2\,\text{kNm}$$

Under acting normal force $N_{Sd} = 500\,\text{kN}$ the moment resistance in bending is $M_{Rd} = 110,2\,\text{kN}$.

The end of column resistance

The design resistance in poor compression is

$$N_{\mathrm{pl,Rd}} = \frac{A \cdot f_{\mathrm{y}}}{\gamma_{\mathrm{M0}}} = \frac{7\,808 \cdot 235}{1,00} = 1\,835 \cdot 10^{3} \quad N > N_{\mathrm{Rd}} = 500\ \mathrm{kN}$$

The column bending resistance

$$M_{\mathrm{pl,Rd}} = \frac{W_{\mathrm{pl}} \cdot f_{\mathrm{yk}}}{\gamma_{\mathrm{M0}}} = \frac{642,5 \cdot 10^{3} \cdot 235}{1,00} = 151,0\ \mathrm{kNm}$$

The interaction of normal force reduces moment resistance

$$M_{\mathrm{Ny,Rd}} = M_{\mathrm{pl,Rd}} \frac{1 - \frac{N_{\mathrm{Sd}}}{N_{\mathrm{pl,Rd}}}}{1 - 0,5 \frac{A - 2\,b\,t_{\mathrm{f}}}{A}} = 151,0 \cdot \frac{1 - \frac{500}{1\,835}}{1 - 0,5 \frac{7\,808 - 2 \cdot 200 \cdot 15}{7\,808}} = 124,2\ \mathrm{kNm}$$

The column base is designed on acting force only, not for column resistance.

Base plate stiffness

The lever arm of component in tension z_{t} and in compression z_{c} to the column base neutral axes is

$$z_{\mathrm{t}} = \frac{h_{\mathrm{c}}}{2} + e_{\mathrm{c}} = \frac{200}{2} + 60 = 160\ \mathrm{mm}$$

$$z_{\mathrm{c}} = \frac{h_{\mathrm{c}}}{2} - \frac{t_{\mathrm{f}}}{2} = \frac{200}{2} - \frac{15}{2} = 92,5\ \mathrm{mm}$$

The stiffness coefficient of tension part, headed studs and T stub, is calculated as

$$k_{\mathrm{t}} = \frac{1}{\frac{1}{k_{\mathrm{b}}} + \frac{1}{k_{\mathrm{p}}}} = \frac{1}{\frac{1}{2,8} + \frac{1}{16,0}} = 2,4\ \mathrm{mm}$$

For the calculation of the initial stiffness of the column base the lever arm is evaluated

$z = z_{\mathrm{t}} + z_{\mathrm{c}} = 160 + 92,5 = 252,5\ \mathrm{mm}$ and

$$a = \frac{k_{\mathrm{c}} \cdot z_{\mathrm{c}} - k_{\mathrm{t}} \cdot z_{\mathrm{t}}}{k_{\mathrm{c}} + k_{\mathrm{t}}} = \frac{15,5 \cdot 92,5 - 2,4 \cdot 160}{15,5 + 2,4} = 58,6\ \mathrm{mm}$$

The bending stiffness is calculated for particular constant eccentricity

$$e = \frac{M_{\mathrm{Rd}}}{F_{\mathrm{Sd}}} = \frac{110,2 \cdot 10^{6}}{500 \cdot 10^{3}} = 220,4\ \mathrm{mm}$$

as

$$S_{j,ini} = \frac{e}{e+a} \cdot \frac{E_S z^2}{\mu \sum_i \frac{1}{k_i}} = \frac{220,4}{220,4+58,6} \cdot \frac{210\,000 \cdot 252,5^2}{1 \cdot \left(\frac{1}{2,4} + \frac{1}{15,5} \right)} =$$

$$= 37,902 \cdot 10^9 \text{ Nmm/rad} = 37\,902 \text{ kNm/rad}$$

Stiffness classification

The classification of the column base according to its bending stiffness is evaluated in comparison to column bending stiffness. For column length L_c = 4 m and its cross-section HE 200 B is relative bending stiffness

$$\overline{S}_{j,ini} = S_{j,ini} \cdot \frac{L_c}{E_S \cdot I_c} = 37,902 \cdot 10^9 \cdot \frac{4000}{210\,000 \cdot 56,96 \cdot 10^6} = 13,0$$

The designed column base is rigid for braced and semi-rigid for non-sway frames because

$$\overline{S}_{j,ini} = 13,0 > 12,0 = \overline{S}_{j,ini,EC3,n}; \overline{S}_{j,ini} = 13,0 < 30,0 = \overline{S}_{j,ini,EC3,n}.$$

References

BCSA and SCI. 2002. Joints in steel construction. Simple connections (Reprinted Edition) (P212), Volume 1: Design Methods (P205) and Volume 2: Practical Applications (P206/92), BCSA and SCI, ISBN 978-1-85942-072-0.

BCSA and SCI. 2013. Joints in Steel Construction Moment-Resisting Joints to Eurocode 3 (P398), BCSA and SCI, ISBN 978-1-85-942209-0.

Cestruco. 2003. Questions and Answers to Design of Structural Connections According to Eurocode 3, CTU, 138 p. ISBN 80-01-02754-6, URL: www.fsv.cvut.cz/cestruco.

EN 10025-2+A1:1996. Hot rolled products of structural steels - Part 2: Technical delivery conditions for non-alloy structural steels, CEN, Brussels.

EN 10025-2+A1:2004. Hot rolled products of structural steels - Part 5: Technical delivery conditions for structural steels with improved atmospheric corrosion resistance, CEN, Brussels.

EN 1992-1-1: 2004. AC:2008, AC2010, Eurocode 2: Design of concrete structures – Part 1-1: General rules and rules for buildings.

EN 1993-1-1: 2005. AC2006, AC 2009. Eurocode 3, Design of steel structures, Part 1.1, General rules and rules for buildings, European Committee for Standardization (CEN), Brussels, 91 p.

EN 1993-1-8: 2013. Eurocode 3, Design of steel structures, Part 1.8, General rules, Design of joints, European Committee for Standardization (CEN), ed. 2, Brussels, 2013, 133 p.

EN 1994-1-1: 2004. AC:2009. Eurocode 4: Design of composite steel and concrete structures – Part 1-1: General rules and rules for buildings. CEN, Brussels.

EN ISO 13918:2000. Welding - Studs and ceramic ferrules for arc stud welding, CEN, Brussels.

Gresnigt, N., Romeijn, A., Wald, F., Steenhuis M. 2008. Column Bases in Shear and Normal Force, Heron. 87-108.

Horová, K., Wald, F., Sokol, Z. 2011. Design of Circular Hollow Section Base Plates, in Eurosteel 2011 6th European Conference on Steel and Composite Structures. Brussels, 2011 (1) 249-254.

ISO 14555:2014. Welding – Arc stud welding of metallic materials, CEN, Brussels, 2014.

ISO 17659:2004. Welding - Multilingual terms for welded joints with illustrations, CEN, Brussels.

Jaspart, J.P., Demonceau, J.F., Renkin, S., Guillaume, M.L. 2009. European Recommendations for the Design of Simple Joints in Steel Structures, ECCS, 92 p., ISBN 92-9147-000-95.

Steenhuis, M., Wald, F., Sokol, Z., Stark, J.W.B. 2008. Concrete in Compression and Base Plate in Bending, Heron 53. 51-68.

Wald, F., Sokol, Z., Jaspart, J.P. 2008. Base Plate in Bending and Anchor Bolts in Tension, Heron 53. 21-50.

Wald, F., Sokol, Z., Steenhuis, M., Jaspart, J.P. 2008. Component Method for Steel Column Bases, Heron 53. 3-20.

CHAPTER 3

DESIGN OF MOMENT RESISTING JOINTS IN STEEL STRUCTURES

Jean-Pierre JASPART[1] and Klaus WEYNAND[2]

[1]Université de Liège, Belgium

[2]Feldmann & Weynand Ingenieure, Germany

3 Design of moment resisting joints in steel structures

3.1 Introduction

3.1.1 The traditional way in which joints are modelled for the design of a frame

Generally speaking, the process of designing building structures has been up to now made up of the following successive steps:

- frame modelling (including the choice of rigid or pinned joints);
- initial sizing of beams and columns;
- evaluation of internal forces and moments (load effects) for each ultimate limit state (ULS) and serviceability limit state (SLS) load combination;
- design checks of ULS and SLS criteria;
- iteration on member sizes until all design checks are satisfactory;
- design of joints to resist the relevant members end forces (either those calculated or the maximum ones able to be transmitted by the actual members); the design is carried out in accordance with the prior assumptions (frame modelling) on joint stiffness.

This approach was possible since designers were accustomed to considering the joints to be either pinned or rigid only. In this way, the design of the joints became a separate task from the design of the members. Indeed, joint design was often performed at a later stage, either by other personnel or by another company.

Recognising that most joints have an actual behaviour which is intermediate between that of pinned and rigid joints, Eurocode 3 and Eurocode 4 offers the possibility to account for this behaviour by opening up the way to what is presently known as the semi-continuous approach. This approach offers the potential for achieving better and more economical structures.

3.1.2 The semi-continuous approach

The rotational behaviour of actual joints is well recognised as being often intermediate between the two extreme situations, i.e. rigid or pinned.

Let us consider the bending moments and the related rotations at a joint (Figure 3.1).

When all the different parts in the joint are sufficiently stiff (i.e. ideally infinitely stiff), the joint is rigid, and there is no difference between the respective rotations at the ends of the members connected at this joint (Figure 3.1a). The joint experiences a single global rigid-body rotation which is the nodal rotation in the commonly used analysis methods for framed structures.

Should the joint be without any stiffness, then the beam will behave just as a simply supported beam, whatever the behaviour of the other connected member(s) (Figure 3.1b). This is a pinned joint.

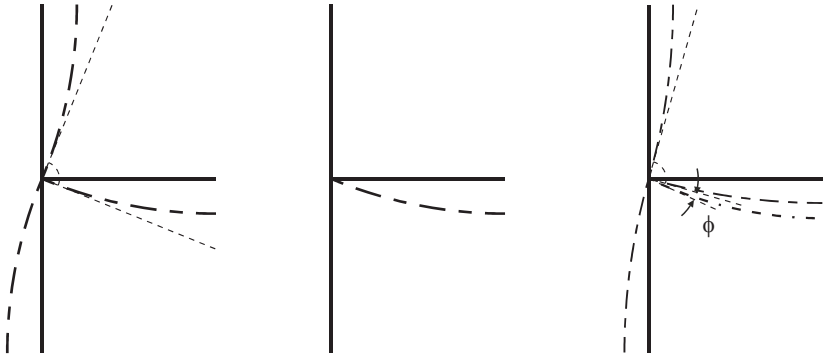

Figure 3.1 Classification of joints according to stiffness

For intermediate cases (non-zero and non-infinite stiffness), the transmitted moment will result in a difference between the absolute rotations of the two connected members (Figure 3.1c). The joint is semi-rigid in these cases.

The simplest mean for representing the concept is a rotational (spiral) spring between the ends of the two connected members. The rotational stiffness S_i of this spring is the parameter that links the transmitted moment M_i to the relative rotation ϕ, which is the difference between the absolute rotations of the two connected members.

When this rotational stiffness S_i is zero, or when it is relatively small, the joint falls back into the pinned joint class. In contrast, when the rotational stiffness S_i is infinite, or when it is relatively high, the joint falls into the rigid joint class. In all the intermediate cases, the joint belongs to the semi-rigid joint class.

For semi-rigid joints the loads will result in both a bending moment M_i and a relative rotation ϕ between the connected members. The moment and the relative rotation are related through a constitutive law depending on the joint properties. This is illustrated in Figure 3.2 where, for the sake of simplicity, an elastic response of the joint is assumed in view of the structural analysis to be performed.

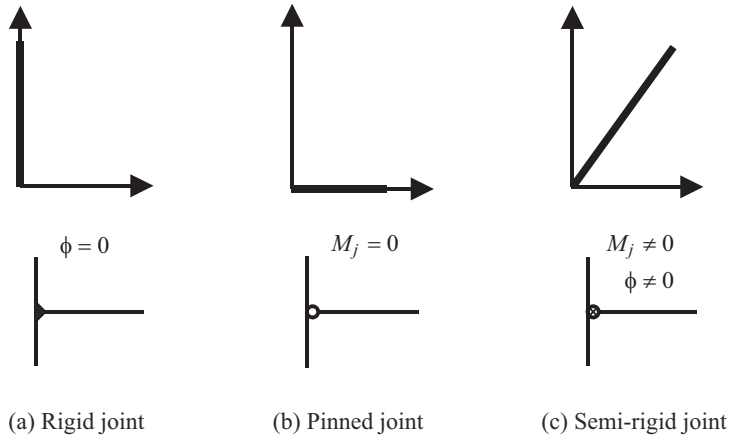

Figure 3.2 Modelling of joints (case of elastic global analysis)

3.1.3 Application of the "Static approach"

The verification of the joint resistance may, as for any other cross-section, be performed an elastic or a plastic basis.

In a pure elastic approach, the joints should be designed in such a way that the generalised Von Mises stress nowhere exceeds the elastic strength of the constitutive materials.

But steel generally exhibits significant ductility; the designer may therefore profit from this ability to deform steel plastically and so to develop "plastic" design approaches in which local stress plastic redistributions in the joint elements are allowed.

The use of plastic design approaches in steel construction is explicitly allowed in the Eurocodes. For joints and connections, reference has to be made to *Clause 2.5(1)* of EN 1993-1-8. Obviously, limitations to the use of such plastic approaches exist; there all relate to the possible lack of ductility of the steel material, on one side, and of some connections elements like bolts and welds, on the other hand. As far as steel material itself is concerned, the use of normalized steels according to Euronorms (for instance EN 10025) guarantees a sufficient material ductility. For the here above listed possibly non ductile joint elements, *EN1993-1-8* introduces specific requirements.

Clause 2.5(1) of EN 1993-1-8 is simply paraphrasing the so-called "static" theorem of the limit analysis. The application of this theorem to cross-sections, for instance in bending, is well known as it leads to the concept of bi-rectangular stress patterns and to the notion of plastic moment resistance for Class 1 or 2 cross-sections for which no limit of ductility linked to plate buckling phenomena has to be contemplated. For connections and joints, the implementation of the static theorem is probably less direct, but this does not at all prevent designers to use it.

The static theorem requires first the determination of an internal statically admissible distribution of stresses (for cross-sections) or forces (for connections and joints), i.e. of a set of stresses or forces in equilibrium with the external forces acting on the cross-section or on the joint/connection and resulting from the global structural analysis. The second requirement is to be plastically admissible; nowhere in the cross-section or joint/connection, plasticity resistance and ductility criteria should be violated.

A large number of statically and plastically admissible distributions may exist. In most of the cases, these ones will not respect the "kinematically admissible" criterion; in fact, only the actual distribution has the ability to satisfy the three requirements: equilibrium, plasticity and compatibility of displacements. But in fact, this is not a problem as long as local deformation capacity (ductility) is available at the places where plasticity develops in the cross-section or in the joint/connection. As long as this last condition is fulfilled, the static theorem ensures that the resistance of the cross-section or joint/connection associated to any statically and plastically is lower than the actual one (and therefore on the safe side). The closer the assumed distribution will be from the actual one, the closer the estimated resistance will be from the actual resistance.

3.1.4 Component approach

3.1.4.1 General

The characterisation of the response of the joints in terms of stiffness, resistance and ductility is a key aspect for design purposes. From this point of view, three main approaches may be followed:

- experimental;
- numerical;
- analytical.

The only practical one for the designer is usually the analytical approach. Analytical procedures enable a prediction of the joint response based on the knowledge of the mechanical and geometrical properties of the so-called "joint components".

In *EN1998-1-8*, a general analytical procedure, termed component method, is introduced. It applies to any type of steel or composite joints, whatever the geometrical configuration, the type of loading (axial force and/or bending moment, etc.) and the type of member cross-sections.

The method is a general and convenient procedure to evaluate the mechanical properties of joints subjected to various loading situations, including static and dynamic loading conditions, fire, earthquake, etc.

3.1.4.2 Introduction to the component method

A joint is generally considered as a whole and studied accordingly; the originality of the component method is to consider any joint as a set of individual basic components. For the particular joint shown in Figure 3.3a (joint with an extended end-plate connection assumed to be mainly subjected to bending), the relevant components (i.e. zones of transfer of internal forces) are the following:

- column web in compression;
- beam flange and web in compression;
- column web in tension;
- column flange in bending;
- bolts in tension;
- end-plate in bending;
- beam web in tension;
- column web panel in shear.

Each of these basic components possesses its own strength and stiffness either in tension, compression or shear. The column web is subject to coincident compression, tension and shear. This coexistence of several components within the same joint element can obviously lead to stress interactions that are likely to decrease the resistance of the individual basic components.

The application of the component method requires the following steps:

1. *Identification* of the active components in the joint being considered;
2. *Evaluation* of the stiffness and/or resistance characteristics for each individual basic component (specific characteristics - initial stiffness, design resistance, etc. - or whole deformability curve);
3. *Assembly* of all the constituent components and evaluation of the stiffness and/or resistance characteristics of the whole joint (specific characteristics - initial stiffness, design resistance, etc. - or whole deformability curve).
4. The assembly procedure is the step where the mechanical properties of the whole joint are derived from those of all the individual constituent components. That requires, according to the static theorem introduced in section 3.1.3, to define how the external forces acting on the joint distribute into internal forces acting on the components; and in a way that satisfies equilibrium and respects the behaviour of the components.

5. In EN 1993-1-8, guidelines on how to apply the component method for the evaluation of the initial stiffness and the design moment resistance of the joints are provided; the aspects of ductility are also addressed.
6. The application of the component method requires a sufficient knowledge of the behaviour of the basic components. Those covered for static loading by EN 1993-1-8 are listed respectively in Table 3.1. The combination of these components allows one to cover a wide range of joint configurations and should be largely sufficient to satisfy the needs of practitioners. Examples of such joints are given in Figure 3.3.

Table 3.1 List of components covered by EN 1993-1-8

No	Component	
1	Column web panel in shear	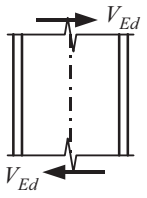
2	Column web in transverse compression	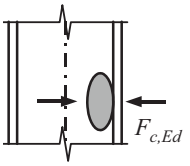
3	Column web in transverse tension	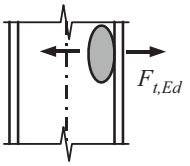
4	Column flange in bending	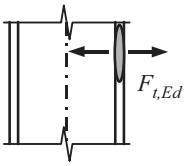
5	End-plate in bending	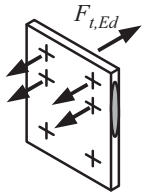
6	Flange cleat in bending	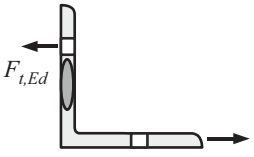

7	Beam or column flange and web in compression	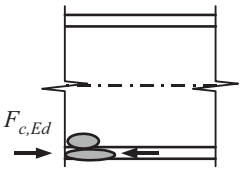
8	Beam web in tension	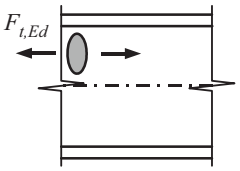
9	Plate in tension or compression	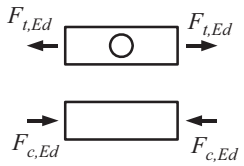
10	Bolts in tension	
11	Bolts in shear	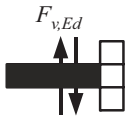
12	Bolts in bearing (on beam flange, column flange, end-plate or cleat)	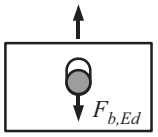

The Eurocodes give new and advanced options to design efficient and economic steel structures. The design of joints plays a major role in that process. Thus the detailing of joints and the methods of considering the joints properties in the frame analysis will significantly influence the costs of a steel structure. This has been demonstrated by various investigations.

However, the exploitation of the advanced possibilities is rather time consuming for the designer if no appropriate tools for a quick and easy design are available. Different opinions have been discussed in Europe concerning the development of the Eurocodes. On one side it is expected that the Eurocodes provide design methods which will allow safe, robust and economic solutions. Of course this requires more sophisticated approaches for the design rules. On the other side the users of the Eurocodes are requesting simple codes for practice. But this is in conflict with the major request to make steel structures more economic. It would be unfortunate to make standards too simple as there is the loss of many possibilities to take profit of the new and advanced options mentioned above.

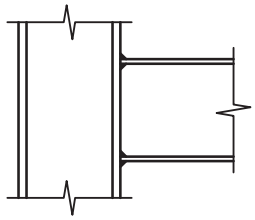

(a) Welded joint

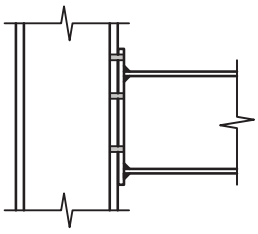

(b) Bolted joint with extended end-plate

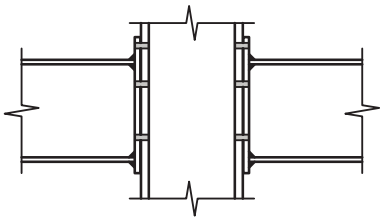

(c)Two joints with flush end-plates (Double-sided configuration)

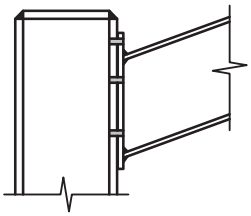

(d) Joint with flush end-plate

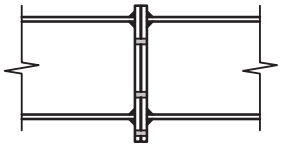

(e) End-plate type beam splice

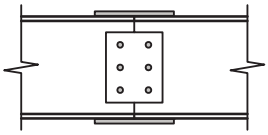

(f) Cover-joint type beam splice

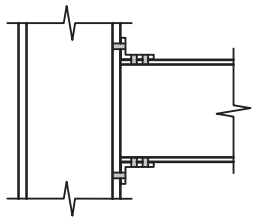

(g) Bolted joint with angle flange cleats

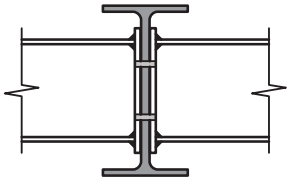

(h) Two beam-to-beam joints (Double-sided configuration)

Figure 3.3 Examples of steel beam-to-column joints, beam-to-beam joints and beam splices joints covered by EN 1993-1-8

The message is quite clear: there was and there still is a need for sophisticated standards which form an accepted basis to design steel structures. The component method is one of these, with its very wide scope of application. Based on the methods given in the standards simple design tools need to be developed and provided to practitioners. This is an optimal way to bring more economic solutions on the market with an acceptable effort needed by the designers.

3.1.4.3 Types of design tools for joints

Beside the need for background information the engineer requires simple design tools to be able to design joint in an efficient way. Three different types of design aids are

provided now in various countries by several institutions or companies. The most appropriate type depends on various aspects.

- Design tables

  Design tables are ready-to-use tables containing standardised joint layouts including dimension details and all relevant mechanical properties like resistance, stiffness and ductility. The use of tables is certainly the quickest way to design a joint. However, any change in the layout will require further calculations and tables are no more helpful. Here design sheets may be used.

- Design sheets

  Design sheets are set of simple design formulae. The aim is to allow a simple and rather quick hand calculation. Due to simplifications, the results could be more conservative or the range of validity more limited. Both design tables and design sheets can be published in handbooks.

- Software

  The most flexible way is the use of software. Of course it takes a few minutes to enter all joint details, but there will be only few limitations in the range of validity and any re-calculation, for example due to a change in the layout, is a matter of a few seconds.

The optimal use of the design tool in practice requires anyway from the user a minimum understanding of the component method approach and of its main principles in terms of component characterisation and assembly of components. And the best way to acquire this knowledge is to apply, at least one time in his or her professional life, EN 1993-1-8 models and rules to a specific joint. That is why a large part of the rest of the present chapter is devoted to the line-by-line application of the component method to a beam-to-column joint with an endplate connection.

3.2 Structural analysis and design

3.2.1 Introduction

The design of a frame and of its components consists of a two-step procedure involving a global frame analysis followed by individual cross-section and/or member design checks.

Global frame analysis is aimed at deriving the values of the internal forces and of the displacements in the considered structure when this one is subjected to a given set of loads. It is based on assumptions regarding the component behaviour (elastic or plastic) and the geometrical response (first-order or second-order theory) of the frame. Once the analysis is complete, i.e. all relevant internal forces and displacements are determined in the whole structure, then the design checks of all the frame components is performed. These ones consist in verifying whether the structure satisfies all the required design criteria under service loads (serviceability limit states – SLS) and under factored loads (ultimate limit states – ULS).

Globally speaking, four main analysis approaches may be contemplated according to Eurocode 3. They are reported in Table 3.2:

- linear elastic first order analysis;
- plastic (or elasto-plastic) first order analysis;
- linear elastic second order analysis;
- plastic (or elasto-plastic) second order analysis.

Table 3.2 Four main approaches for frame analysis

		Assumed material law (linear or non-linear)	
		Elastic	Plastic
Assumption in terms of geometrical effects (linearity or non-linearity)	1st order	Linear elastic first order analysis	Plastic (or elasto-plastic) first order analysis
	2nd order	Linear elastic second order analysis	Plastic (or elasto-plastic) second order analysis

The selection of the more appropriate one by the user is a quite important step which will strongly influence the number and the nature of the checks to be achieved further on, as already stated in section 3.1.1. This choice is however not free. Next paragraphs tend to summarise the recommendations of Eurocode 3 in this domain.

3.2.1.1 Elastic or plastic analysis and verification process

The selection of an elastic or plastic analysis and design process depends on the class of the member cross-sections (Class 1, 2, 3 or 4).

A class expresses the way on how the possible local plate buckling of cross-section walls subjected to compression may or not affect the resistance or the ductility of the cross-sections.

An elastic analysis is required for frames in all cases, except for frames constituted of Class 1 member cross-sections (at least at the locations of the plastic hinges) where a plastic (elasto-plastic) analysis may be performed.

The cross-section and/or member design checks are also depending on the cross-section class. Table 3.3 summarises the various possibilities offered by Eurocode 3.

Table 3.3 Selection between elastic and plastic (elasto-plastic) analysis and design process

Cross-section class	**Frame analysis**	**Cross-section/member verifications**	**Designation of the global approach (E = elastic; P = plastic)**
Class 1	Plastic	Plastic	P-P
	Elastic	Plastic	E-P
	Elastic	Elastic	E-E
Class 2	Elastic	Plastic	E-P
	Elastic	Elastic	E-E
Class 3 – Class 4	Elastic	Elastic	E-E

3.2.1.2 First order or second order analysis

Geometrical non-linearities may affect the response of members or the response of the full frame and lead respectively to local (flexural buckling, torsional buckling, lateral torsional buckling, etc.) or global (global sway instability) instability phenomena.

A structural analysis may be defined as the expression of the equilibrium between the external forces acting on the structure and the resulting internal forces in the member cross-sections. According to the geometry of the structure taken as a reference to express this equilibrium, one will speak about first order or second order analysis:

- in a first order analysis, reference is made to the initial undeformed shape of the structure;
- in a second order analysis, reference is made to the actual deformed shape of the structure.

Two types of second order are to be considered, respectively linked to so-called *P-*Δ effects and *P-*δ effects. *P-*Δ effects determine possible sway instability phenomena whereas *P-*δ effects govern the possible development of member instabilities. A full second order analysis will be characterised by an explicit consideration of all geometrical second order effects (sway and member). In this case, no member check has to be achieved further to the structural analysis.

Usually the designer prefers not to integrate the so-called *P-*δ effects (second order effects related to the member buckling) in the frame analysis and so to check member buckling phenomena further to the analysis, when verifying ULS. It just then remains to decide whether the *P-*Δ effects are to be or not considered. This is achieved through the verification of a specific criterion defining the "sway" or "non sway" character of the structure ("α_{cr}" criterion in EN 1993-1-1).

The description "non-sway frame" applies to a frame when its response to in-plane horizontal forces is so stiff that it is acceptable to neglect any additional forces or moments arising from horizontal displacements of its storeys. This means that the global second-order effects may be neglected. When the second order effects are not negligible, the frame is said to be a "sway frame".

Figure 3.4 summarises the choices offered to the designer, not only in terms of frame analysis, but also of type of cross-section and/or member verification at ULS further to the frame analysis.

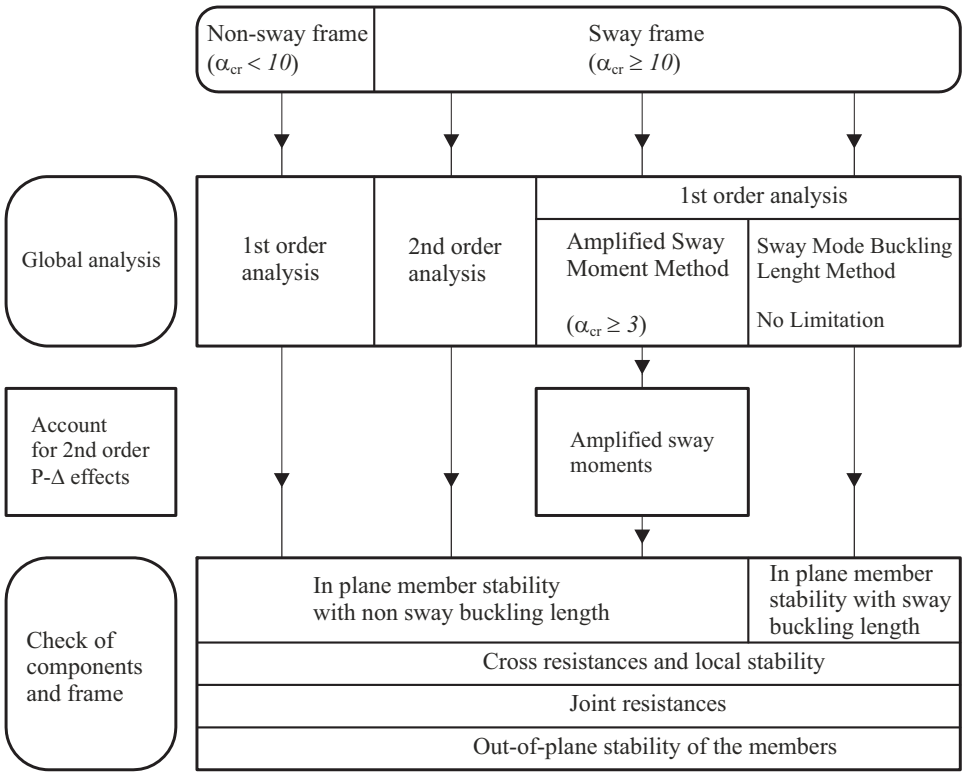

Figure 3.4 Various ways for the global analysis and design process

3.2.1.3 Integration of joint response into the frame analysis and design process

Traditionally frame analysis is performed by assuming joints as perfectly pinned or perfectly rigid. Further to the analysis, joints have therefore to be designed to behave accordingly. In Chapter 3.1 it has been pointed out that significant global economy may often result from what has been presented as a semi-continuous approach for structural joints.

A cross-section being nothing else than a particular cross-section, characterised by its own stiffness, resistance and ductility, the integration of the actual joint properties into the frame analysis and design process appears as natural. And it is the case. For instance, all what has been said in the previous sections remains unchanged at the condition that the meaning of the word "cross-section" is extended to "member or joint cross-section". From an operational point of view, the attention has however to be drawn to some specific concepts respectively named "joint modelling", "joint classification" and joint "idealisation". These ones are presented in the next sections.

3.2.2 Joint modelling

3.2.2.1 General

Joint behaviour affects the structural frame response and shall therefore be modelled, just like beams and columns are, for the frame analysis and design. Traditionally, the following types of joint modelling are considered:

- for rotational stiffness:
  - rigid
  - pinned
- for resistance:
  - full-strength
  - partial-strength
  - pinned

When the joint rotational stiffness is of concern, the wording rigid means that no relative rotation occurs between the connected members whatever is the applied moment. The wording pinned postulates the existence of a perfect (i.e. frictionless) hinge between the members. In fact these definitions may be relaxed, as explained in section 3.2.4 devoted to the joint classification. Indeed rather flexible but not fully pinned joints and rather stiff but not fully rigid joints may be considered as fairly pinned and fairly rigid respectively. The stiffness boundaries allowing one to classify joints as rigid or pinned are examined in section 3.2.4.

For what regards the joint resistance, a full-strength joint is stronger than the weaker of the connected members, what is in contrast with a partial-strength joint. In the daily practice, partial-strength joints are used whenever the joints are designed to transfer the internal forces and not to resist the full capacity of the connected members. A pinned joint transfers no moment. Related classification criteria are conceptually discussed in section 3.2.4.

Consideration of rotational stiffness and resistance joint properties leads to three significant joint modelling:

- rigid/full-strength;
- rigid/partial-strength;
- pinned.

However, as far as the joint rotational stiffness is considered, joints designed for economy may be neither rigid nor pinned but semi-rigid. There are thus new possibilities for joint modelling:

- semi-rigid/full-strength;
- semi-rigid/partial-strength.

With a view to simplification, EN 1993-1-8 accounts for these possibilities by introducing three joint models (Table 3.4):

- continuous:

  covering the rigid/full-strength case only;
- semi-continuous:

  covering the rigid/partial-strength, the semi-rigid/full-strength and the semi-rigid/partial-strength cases;
- simple:

  covering the pinned case only.

Table 3.4 Types of joint modelling

Stiffness	**Resistance**		
	Full-strength	Partial-strength	Pinned
Rigid	Continuous	Semi-continuous	*
Semi-rigid	Semi-continuous	Semi-continuous	*
Pinned	*	*	Simple
	* : Without meaning		

The following meanings are given to these terms:

- continuous:
  the joint ensures a full rotational continuity between the connected members;
- semi-continuous:
  the joint ensures only a partial rotational continuity between the connected members;
- simple:
  the joint prevents from any rotational continuity between the connected members.

The interpretation to be given to these wordings depends on the type of frame analysis to be performed. In the case of an elastic global frame analysis, only the stiffness properties of the joint are relevant for the joint modelling. In the case of a rigid-plastic analysis, the main joint feature is the resistance. In all the other cases, both the stiffness and resistance properties govern the manner the joints shall be modelled. These possibilities are illustrated in Table 3.5.

Table 3.5 Joint modelling and frame analysis

Modelling	**Type of frame analysis**		
	Elastic analysis	Rigid-plastic analysis	Elastic-perfectly plastic and elasto-plastic analysis
Continuous	Rigid	Full-strength	Rigid/full-strength
Semi-continuous	Semi-rigid	Partial-strength	Rigid/partial-strength Semi-rigid/full-strength Semi-rigid/partial-strength
Simple	Pinned	Pinned	Pinned

3.2.2.2 Modelling and sources of joint deformability

In some joints, as for instance in beam-to-column joints, EN 1993-1-8*, Sec. 5.3* differentiates the loading of the connection and that of the column web; what requires, from a theoretical point of view, that account be taken separately of both deformability sources when designing a building frame.

However doing so is only feasible when the frame is analysed by means of a sophisticated computer program which enables a separate modelling of both deformability sources. For most available software, the modelling of the joints has to be simplified by concentrating the sources of deformability into a single rotational spring located at the intersection of the axes of the connected members.

3.2.2.3 Simplified modelling according to Eurocode 3

For most applications, the separate modelling of the connection and of the web panel behaviour is neither useful nor feasible; therefore only the simplified modelling of the joint behaviour will be considered in the present document. This idea is the one followed by EN 1993-1-8. Table 3.6 shows how to relate the simplified modelling of typical joints to the basic wordings used for the joint modelling: simple, semi-continuous and continuous.

Table 3.6 Simplified modelling for joints according to EN 1993-1-8

Joint modelling	Beam-to-column joints major axis bending	Beam splices	Column bases
Simple	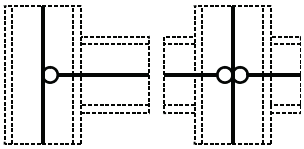	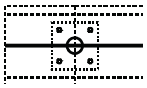	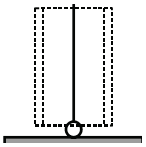
Semi-continuous	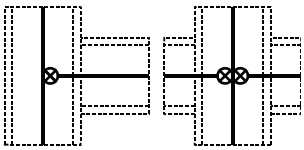	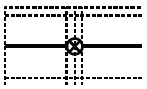	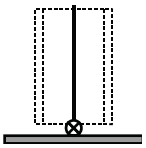
Continuous	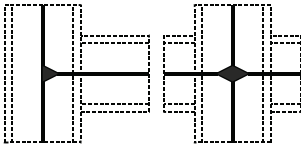	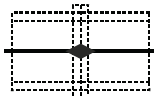	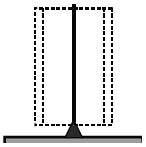

3.2.3 Joint idealization

The non-linear behaviour of the isolated flexural spring which characterises the actual joint response does not lend itself towards everyday design practice. However the moment-rotation characteristic curve may be idealised without significant loss of accuracy. One of the most simple idealisations possible is the elastic-perfectly plastic one (Figure 3.5a). This modelling has the advantage of being quite similar to that used traditionally for the modelling of member cross-sections subject to bending (Figure 3.5b).

The moment $M_{j,Rd}$ that corresponds to the yield plateau is termed design moment resistance in Eurocode 3. It may be understood as the *pseudo-plastic moment resistance* of the joint. Strain-hardening effects and possible membrane effects are henceforth neglected; that explains the difference in Figure 3.5 between the actual M-ϕ characteristic and the *yield plateau* of the idealised one.

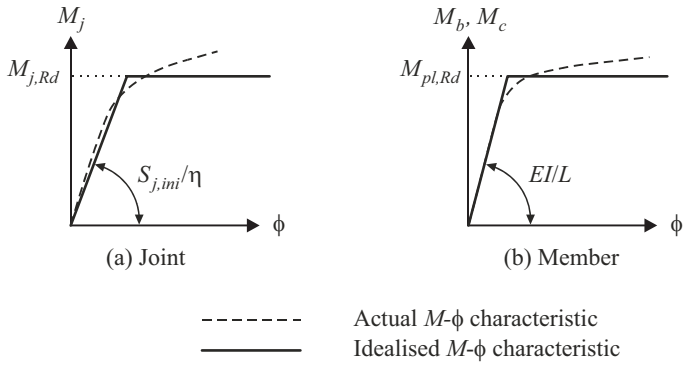

Figure 3.5 Bi-linearisation of moment-rotation curves

The value of the constant stiffness is discussed below.

In fact there are different possible ways to idealise a joint M-ϕ characteristic. The choice of one of them is subordinated to the type of frame analysis which is contemplated, as explained below.

3.2.3.1 Elastic idealisation for an elastic analysis

The main joint characteristic is the constant rotational stiffness.

Two possibilities are offered in Eurocode 3 Part 1-8, see Figure 3.6:

- *Elastic verification of the joint resistance* (Figure 3.6a) : the constant stiffness is taken equal to the initial stiffness $S_{j,ini} / \eta$; at the end of the frame analysis, it shall be checked that the design moment M_{Ed} experienced by the joint is less than the maximum elastic joint moment resistance defined as $2/3\ M_{j,Rd}$;
- *Plastic verification of the joint resistance* (Figure 3.6b): the constant stiffness is taken equal to a fictitious stiffness, the value of which is intermediate between the initial stiffness and the secant stiffness relative to $M_{j,Rd}$; it is defined as $S_{j,ini}$. This idealisation is aimed at "replacing" the actual non-linear response of the joint by an "equivalent" constant one; it is valid for M_{Ed} values less than or equal to $M_{j,Rd}$. EN 1993-1-8 recommends values of η reported in in Table 3.7.

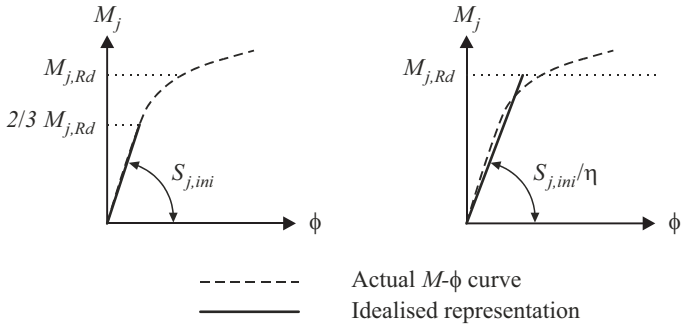

Figure 3.6 Linear representation of a *M*-ϕ curve

Table 3.7 Stiffness modification factors

Type of connection	Beam-to-column joints	Other types of joints (beam-to-beam joints, beam splices, column base joints)
Welded	2	3
Bolted end-plates	2	3
Bolted flange cleats	2	3,5
Base plates	-	3

3.2.3.2 Rigid-plastic idealisation for a rigid-plastic analysis

Only the design resistance $M_{j,Rd}$ is needed. In order to allow the possible plastic hinges to form and rotate in the joint locations, it shall be checked that the joint has a sufficient rotation capacity, see Figure 3.7.

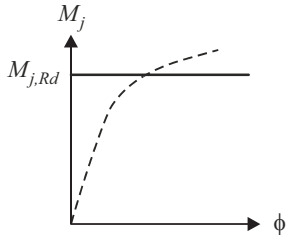

Figure 3.7 Rigid-plastic representation of a *M-ϕ* curve

3.2.3.3 Non-linear idealisation for an elastic-plastic analysis

The stiffness and resistance properties are of equal importance in this case. The possible idealisations range from bi-linear, tri-linear representations or a fully non-linear curve, see Figure 3.8. Again rotation capacity is required in joints where plastic hinges are likely to form and rotate.

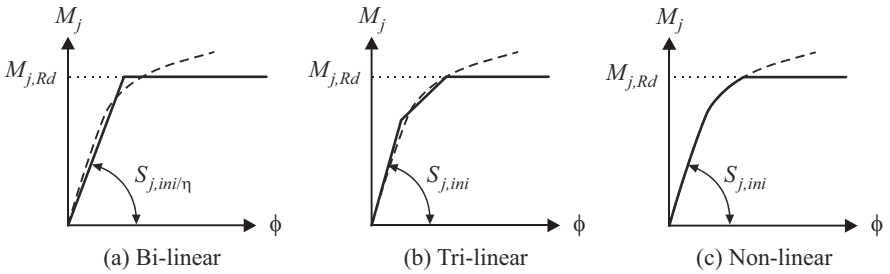

Figure 3.8 Non-linear representations of a *M-ϕ* curve

3.2.4 Joint classification

3.2.4.1 General

In section 3.2.2, it is shown that the joints need to be modelled for the global frame analysis and that three different types of joint modelling are introduced: simple, semi-continuous and continuous.

It has also been explained that the type of joint modelling to which it shall be referred is dependent both on the type of frame analysis and on the class of the joint in terms of stiffness and/or strength (Table 3.5).

Classification criteria are used to define the stiffness class and the strength class to which the joint belongs and also to determine the type of joint modelling which shall be adopted for analysis. They are described here below.

3.2.4.2 Classification based on mechanical joint properties

The stiffness classification is performed by comparing simply the design joint stiffness to two stiffness boundaries (Figure 3.9). For sake of simplicity, the stiffness boundaries have been derived so as to allow a direct comparison with the initial design joint stiffness, whatever the type of joint idealisation that is used afterwards in the analysis (Figure 3.6 and Figure 3.8).

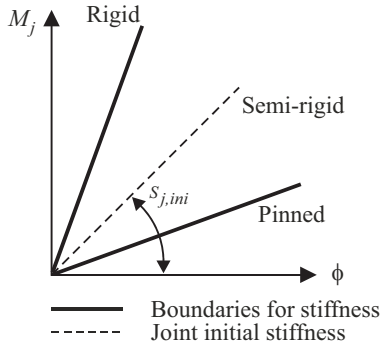

Figure 3.9 Stiffness classification boundaries

The strength classification simply consists in comparing the joint design moment resistance to "full-strength" and "pinned" boundaries (Figure 3.10).

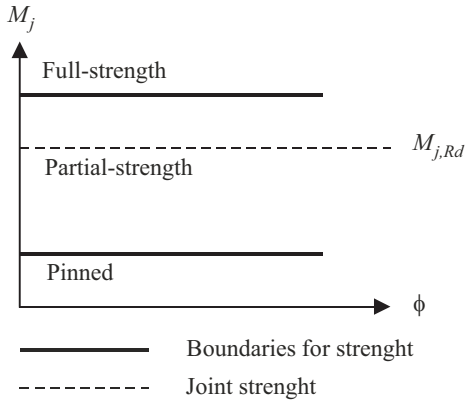

Figure 3.10 Strength classification boundaries

It is while stressing that a classification based on the experimental joint M-ϕ characteristics is not allowed, as design properties only are of concern.

3.2.5 Ductility classes

3.2.5.1 General concept

Experience and proper detailing result in so-called pinned joints which exhibit a sufficient rotation capacity to sustain the rotations imposed on them.

For moment resistant joints the concept of ductility classes is introduced to deal with the question of rotation capacity.

For most of these structural joints, the shape of the M-ϕ characteristic is rather bi-linear (Figure 3.11a). The initial slope $S_{j,ini}$ corresponds to the elastic deformation of the joint. It is followed by a progressive yielding of the joint (of one or some of the constituent components) until the design moment resistance $M_{j,Rd}$ is reached. Then a post-limit behaviour ($S_{j,post\text{-}lim}$) develops which corresponds to the onset of strain-hardening and possibly of membrane effects. The latter are especially important in components where rather thin plates are subject to transverse tensile forces as, for instance, in minor axis joints and in joints with columns made of rectangular hollow sections.

In many experimental tests (Figure 3.11a) the collapse of the joints at a peak moment $M_{j,u}$ has practically never been reached because of high local deformations in the joints involving extremely high relative rotations. In the others (Figure 3.11b) the collapse has involved an excessive yielding (rupture of the material) or, more often, the instability of one of the constituent components (ex: column web panel in compression or buckling of the beam flange and web in compression) or the brittle failure in the welds or in the bolts.

In some joints, the premature collapse of one of the components prevents the development of a high moment resistance and high rotation. The post-limit range is rather limited and the bi-linear character of the M_j-ϕ response is less obvious to detect (Figure 3.11c).

As explained in section 3.2.3, the actual M_j-ϕ curves are idealised before performing the global analysis. As for beam and column cross-sections, the usual concept of plastic hinge can be referred to for plastic global analysis.

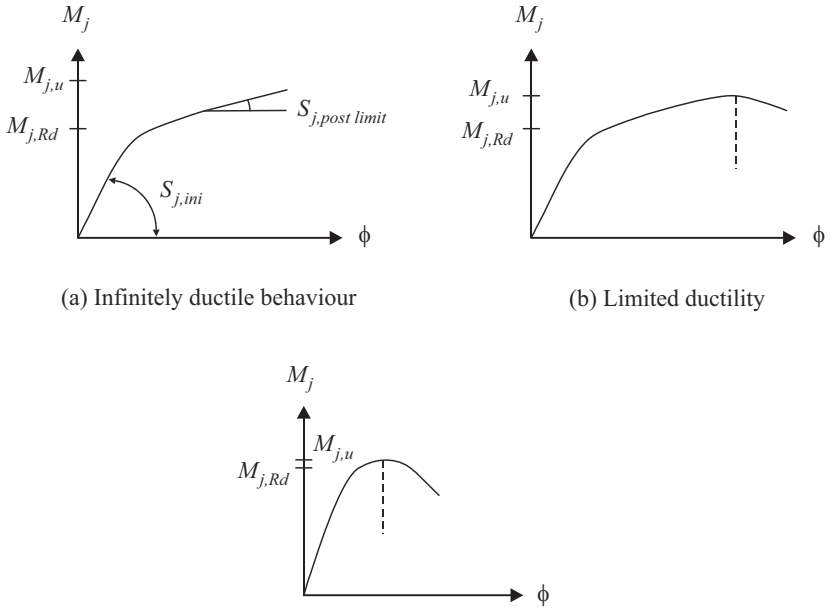

(a) Infinitely ductile behaviour

(b) Limited ductility

(c) Non-ductile behaviour

Figure 3.11 Shape of joint M-ϕ characteristics

The development of plastic hinges during the loading of the frame and the corresponding redistribution of internal forces in the frame require, from the joints where hinges are likely to occur, a sufficient rotation capacity. In other words, there must be a sufficiently long yield plateau ϕ_{pl} (Figure 3.12) to allow the redistribution of internal forces to take place.

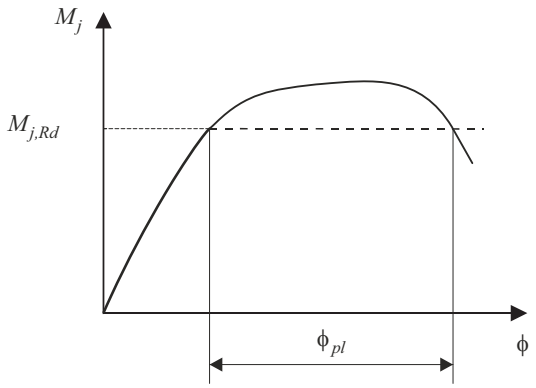

Figure 3.12 Plastic rotation capacity

For beam and column sections, deemed-to-satisfy criteria allow one to determine the class of the sections and therefore the type of global frame analysis which can be contemplated.

A strong similarity exists for what regards structural joints; moreover a similar classification may be referred to:

- *Class 1 joints*: $M_{j,Rd}$ is reached by full plastic redistribution of the internal forces within the joints and a sufficiently good rotation capacity is available to allow, without specific restrictions, a plastic frame analysis and design to be performed, if required;
- *Class 2 joints*: $M_{j,Rd}$ is reached by full plastic redistribution of the internal forces within the joints but the rotation capacity is limited. An elastic frame analysis possibly combined with a plastic verification of the joints has to be performed. A plastic frame analysis is also allowed as long as it does not result in a too high required rotation capacity in the joints where hinges are likely to occur. The available and required rotation capacities have therefore to be compared before validating the analysis;
- *Class 3 joints*: brittle failure (or instability) limits the moment resistance and does not allow a full redistribution of the internal forces in the joints. It is compulsory to perform an elastic verification of the joints.

As the moment design resistance $M_{j,Rd}$ is known whatever the collapse mode and the resistance level, no Class 4 has to be defined as for member sections.

3.2.5.2 Requirements for classes of joints

In *Eurocode 3*, the procedure given for the evaluation of the design moment resistance of any joint provides the designer with other information such as:

- the collapse mode;
- the internal forces in the joint at collapse.

Through this procedure, the designer knows directly whether the full plastic redistribution of the forces within the joint has been reached - the joint is then Class 1 or 2 - or not - the joint is then classified as Class 3.

For Class 1 or 2 joints, the knowledge of the collapse mode, and more especially of the component leading to collapse, gives an indication about whether there is adequate rotation capacity for a global plastic analysis to be permitted. The related criteria are expressed in EN 1993-1-8.

3.3 Worked example for joint characterisation

3.3.1 General data

The selected example is the beam-to-column joint in a typical steel frame shown in Figure 3.13. The detailing of the joint are also shown in this Figure. As type of connection an end-plate extended in the tensile zone was chosen. Four bolt rows are met in this joint. A steel grade of S 235 is used.

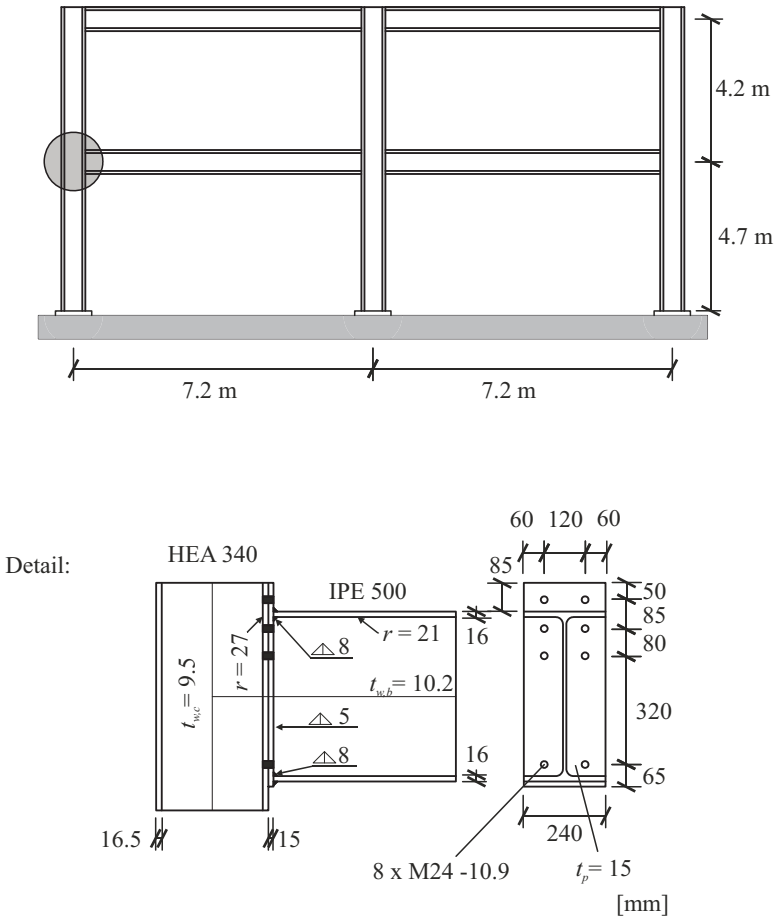

Figure 3.13 Joint in a steel building frame and joint detailing

The objective of this example is to characterise the joint in terms of resistance and stiffness when subjected to hogging moments. The prediction of the resistance in shear will also be addressed.

The partial safety factors (as recommended in the CEN version of Eurocode 3) are as follows:

$$\begin{aligned}\gamma_{M0} &= 1,00\\ \gamma_{M1} &= 1,00\\ \gamma_{M2} &= 1,25\\ \gamma_{Mb} &= 1,25\\ \gamma_{Mw} &= 1,25\end{aligned} \tag{3.1}$$

At the end, the joint will be classified, in view of its modelling in a structural analysis.

Here below, a detailed computation of the joint is realised according to the recommendations given in the EN 1993-1-8. The main steps described in *Figure 6.8* will be followed to compute the resistance in bending.

3.3.2 Determination of the component properties

a) Component 1 – Column web panel in shear

According to the catalogue of profiles, the shear area is equal to 4495 mm². So, the resistance of the column web panel in shear is equal to:

$$V_{wp,Rd} = \frac{0.9 \cdot 235 \cdot 4495}{1000\sqrt{3} \cdot 1.0} = 548,88\ \text{kN} \ \Rightarrow \ \frac{548,88}{1.0} = 548,88\ \text{kN} \tag{3.2}$$

b) Component 2 – Column web in compression

The effective width is equal to:

$$\begin{aligned}b_{eff,c,wc,2} &= t_{fb} + 2\sqrt{2} \cdot a_{fb} + 5\left(t_{fc} + s\right) + s_p\\ &= 16 + 2\sqrt{2} \cdot 8 + 5\left(16,5 + 27\right) + 15 + 3,69\\ &= 274,81\ \text{mm}\end{aligned} \tag{3.3}$$

In most of the cases, the longitudinal stress in the web of the column $\sigma_{com,Ed} \le 0.7\, f_{y,wc}$ and, so $k_{wc} = 1,0$. In the case of a single-sided joint, β can be safely taken as equal to 1,0. Accordingly:

$$\begin{aligned}\omega = \omega_1 &= \frac{1}{\sqrt{1 + 1,3\left(\frac{b_{eff,c,wc} t_{wc}}{A_{vc}}\right)^2}}\\ &= \frac{1}{\sqrt{1 + 1,3\left(274,81 \cdot 9,5 / 4495\right)^2}} = 0,834\end{aligned} \tag{3.4}$$

The estimation of the slenderness of the web is used for the definition of the reduction factor ρ.

$$\bar{\lambda}_p = 0,932\sqrt{\frac{b_{eff,c,wc} d_{wc} f_{y,wc}}{E t_{wc}^{\,2}}} = 0,932\sqrt{\frac{274,81 \cdot 243 \cdot 235}{210000 \cdot 9,5^2}} = 0,848 \tag{3.5}$$

$$\rho = \frac{\left(\bar{\lambda}_p - 0,2\right)}{\bar{\lambda}_p^{\,2}} = \frac{\left(0,848 - 0,2\right)}{0,848^2} = 0,901 \tag{3.6}$$

As ρ < 1,0, the resistance in compression will be limited by a local buckling phenomenon. At the end:

$$\begin{aligned} F_{c,wc,Rd} &= \frac{0,834 \cdot 1,0 \cdot 274,81 \cdot 9,5 \cdot 235}{1,0 \cdot 1000} = 511,67 \text{ kN} \\ &\leq \frac{0,834 \cdot 1,0 \cdot 0,901 \cdot 274,81 \cdot 9,5 \cdot 235}{1,0 \cdot 1000} = 460,9 \text{ kN} \end{aligned} \tag{3.7}$$

c) Component 3 – Column web in tension

The values of effective lengths need to be known for the estimation of the resistance of this component. These values are the same as those to be calculated for the component 4 „column flange in bending" (see section 3.3.2d). Four resistant loads have to be determined:

- individual bolt row resistances
- resistance of the group "rows 1 and 2"
- resistance of the group "rows 1, 2 and 3"
- resistance of the group "rows 2 and 3"

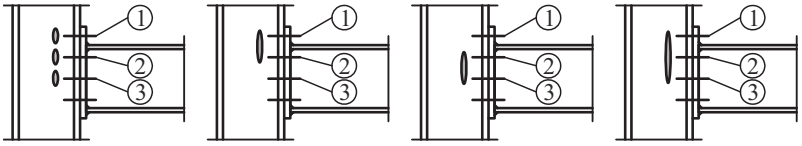

Figure 3.14 Bolt rows and groups of bolt rows

- In a first step, the behaviour of each individual bolt row is considered. At this level, the resistance of the bolt rows 1, 2 and 3 are identical:

$$F_{t,wc,Rd} = \frac{0,86 \cdot 247,1 \cdot 9,5 \cdot 235}{1,0 \cdot 1000} = 474 \text{ kN} \tag{3.8}$$

where: $b_{eff,c,wc} = l_{eff,CFB} = 247,1 \text{ mm}$

$$\omega = \frac{1}{\sqrt{1 + 1,3\left(247,1 \cdot 9,5 / 4495\right)^2}} = 0,86$$

The resistance of the group composed of bolt rows 1 and 2 is equal to:

$$F_{t,wc,Rd} = \frac{0,781 \cdot 332,1 \cdot 9,5 \cdot 235}{1,0 \cdot 1000} = 579,04 \text{ kN} \tag{3.9}$$

$$\text{where}: \; b_{\text{eff,c,wc}} = l_{\text{eff,CFB}} = (166,05 + 166,05) = 332,1 \text{ mm}$$

$$\omega = \frac{1}{\sqrt{1 + 1,3\left(332,1 \cdot 9,5 / 4495\right)^2}} = 0,781$$

For the group composed of bolt rows 1 to 3:

$$F_{\text{t,wc,Rd}} = \frac{0,710 \times 412,1 \times 9,5 \times 235}{1,0 \times 1000} = 653,21 \text{ kN} \tag{3.10}$$

$$\text{where}: \; b_{\text{eff,c,wc}} = l_{\text{eff,CFB}} = (166,05 + 82,5 + 163,55) = 412,1 \text{ mm}$$

$$\omega = \frac{1}{\sqrt{1 + 1,3\left(412,1 \cdot 9,5 / 4495\right)^2}} = 0,710$$

Finally, for the group composed of bolt rows 2 and 3:

$$F_{\text{t,wc,Rd}} = \frac{0,785 \cdot 327,1 \cdot 9,5 \cdot 235}{1,0 \cdot 1000} = 573,25 \text{ kN} \tag{3.11}$$

$$\text{where}: \; b_{\text{eff,c,wc}} = l_{\text{eff,CFB}} = (163,55 + 163,55) = 327,1 \text{ mm}$$

$$\omega = \frac{1}{\sqrt{1 + 1,3\left(327,1 \cdot 9,5 / 4495\right)^2}} = 0,785$$

d) Component 4 – Column flange in bending

For this component, the T-stub model is used. For the latter, the following parameters need to be determined:

$$\begin{aligned} m &= \frac{w_1}{2} - \frac{t_{\text{wc}}}{2} - 0,8 r_{\text{c}} = \frac{120}{2} - \frac{9,5}{2} - 0,8 \cdot 27 = 33,65 \text{ mm} \\ e &= \frac{b_{\text{c}}}{2} - \frac{w_1}{2} = \frac{300}{2} - \frac{120}{2} = 90 \text{ mm} \\ e_1 &= 50 \text{ mm} \\ e_{\min} &= \min\left(e; w_2\right) = \min\left(90; 60\right) = 60 \text{ mm} \end{aligned} \tag{3.12}$$

EN 1993-1-8*, Table 6.4* allows computing the effective lengths corresponding to different patterns of yielding lines and that, for the following cases:

- individual bolt rows
- group involving bolt rows 1 and 2
- group involving bolt rows 1, 2 and 3
- group involving bolt rows 2 and 3

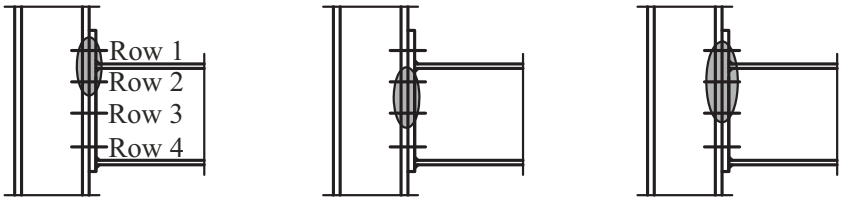

Figure 3.15 Bolt rows and groups of bolt rows

The contribution of bolt row 4 to the resistance in bending is limited, due to its close position to the centre of compression; accordingly, this contribution is neglected here. In this case bolt row 4 may be assumed to contribute with its full shear resistance to the design shear resistance of the joint. However, if needed, also bolt row 4 may be condisered to be in tension zone and hence, its contribution to the moment resistance could be taken into account.

Row 1 – Individual effective lengths:

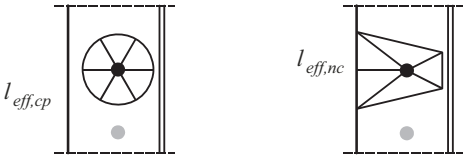

$$\begin{aligned} l_{\text{eff,cp}} &= 2\pi m = 2\pi \cdot 33,65 = 211,43 \text{ mm} \\ l_{\text{eff,nc}} &= 4m + 1,25e = 4 \cdot 33,65 + 1,25 \times 90 = 247,1 \text{ mm} \end{aligned} \tag{3.13}$$

Row 1 – Effective lengths as first bolt row of a group:

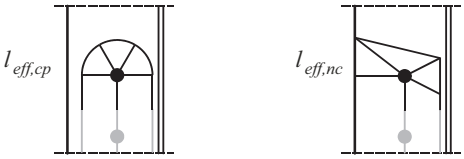

$$\begin{aligned} l_{\text{eff,cp}} &= \pi m + p = \pi \cdot 33,65 + 85 = 190,71 \text{ mm} \\ l_{\text{eff,nc}} &= 2m + 0,625e + 0,5p \\ &= 2 \cdot 33,65 + 0,625 \cdot 90 + 0,5 \cdot 85 = 166,05 \text{ mm} \end{aligned} \tag{3.14}$$

Row 2 – Individual effective lengths:

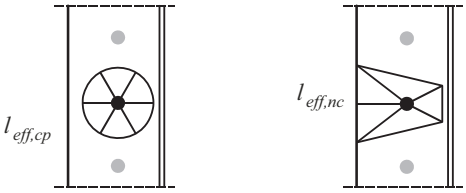

$$\begin{aligned} l_{\text{eff,cp}} &= 2\pi m = 2\pi \cdot 33,65 = 211,43 \text{ mm} \\ l_{\text{eff,nc}} &= 4m + 1,25e = 4 \cdot 33,65 + 1,25 \cdot 90 = 247,1 \text{ mm} \end{aligned} \tag{3.15}$$

Row 2 – Effective lengths as first bolt row of a group:

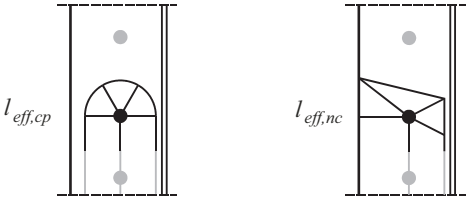

$$\begin{aligned} l_{\text{eff,cp}} &= \pi m + p = \pi \cdot 33,65 + 80 = 185,71 \text{ mm} \\ l_{\text{eff,nc}} &= 2m + 0,625e + 0,5p \\ &= 2 \cdot 33,65 + 0,625 \cdot 90 + 0,5 \cdot 80 = 163,55 \text{ mm} \end{aligned} \tag{3.16}$$

Row 2 – Effective lengths as last bolt row of a group:

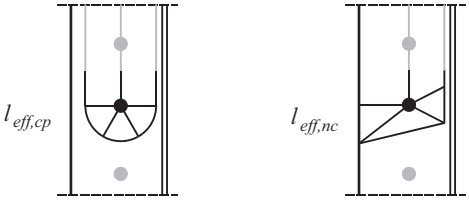

$$\begin{aligned} l_{\text{eff,cp}} &= \pi m + p = \pi \cdot 33,65 + 85 = 190,71 \text{ mm} \\ l_{\text{eff,nc}} &= 2m + 0,625e + 0,5p \\ &= 2 \cdot 33,65 + 0,625 \cdot 90 + 0,5 \cdot 85 = 166,05 \text{ mm} \end{aligned} \tag{3.17}$$

Row 2 – Effective lengths as internal bolt row of a group:

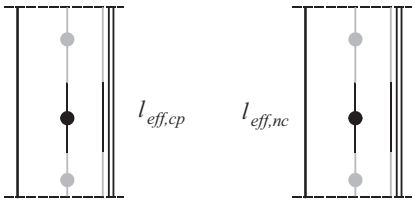

$$\begin{aligned} l_{\text{eff,cp}} &= 2p = 2 \cdot \frac{85+80}{2} = 165,0 \text{ mm} \\ l_{\text{eff,nc}} &= p = \frac{85+80}{2} = 82,5 \text{ mm} \end{aligned} \tag{3.18}$$

Row 3 – Individual effective lengths:

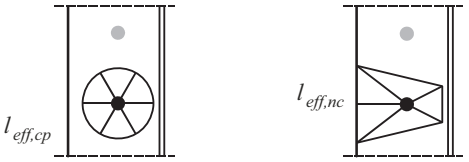

$$\begin{aligned} l_{\text{eff,cp}} &= 2\pi m = 2\pi \cdot 33,65 = 211,43 \text{ mm} \\ l_{\text{eff,nc}} &= 4m + 1,25e = 4 \cdot 33,65 + 1,25 \cdot 90 = 247,1 \text{ mm} \end{aligned} \tag{3.19}$$

Row 3 – Effective lengths as last bolt row of a group:

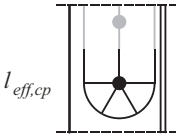

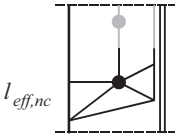

$$\begin{aligned} l_{\text{eff,cp}} &= \pi m + p = \pi \cdot 33,65 + 80 = 185,7 \text{ mm} \\ l_{\text{eff,nc}} &= 2m + 0,625e + 0,5p \\ &= 2 \cdot 33,65 + 0,625 \cdot 90 + 0,5 \cdot 80 = 163,55 \text{ mm} \end{aligned} \tag{3.20}$$

The resistances are then determined on the basis of the knowledge of the values of the effective lengths.

Individual resistances of bolt rows 1, 2 and 3:

Mode 1

$$F_{\text{T,1,Rd}} = \frac{4M_{\text{pl,1,Rd}}}{m} = \frac{4 \cdot 3381,76}{33,65} = 401,99 \text{ kN} \tag{3.21}$$

where: $M_{\text{pl,1,Rd}} = \dfrac{0,25 l_{\text{eff}} t_{\text{fc}}^2 f_{\text{y,c}}}{\gamma_{\text{M0}}}$

$$= \frac{0,25 \cdot 211,43 \cdot 16,5^2 \cdot 235}{1,0 \cdot 1000} = 3381,76 \text{ kNmm}$$

Mode 2

$$F_{T,2,Rd} = \frac{2 \cdot 3952,29 + 42,0625 \cdot 2 \cdot 254,16}{33,65 + 42,0625} = 386,80 \text{ kN} \tag{3.22}$$

where: $M_{pl,2,Rd} = \dfrac{0,25 l_{\text{eff,nc}} t_{\text{fc}}^2 f_{\text{y,c}}}{\gamma_{\text{M0}}}$

$$= \frac{0,25 \cdot 247,1 \cdot 16,5^2 \cdot 235}{1,0 \cdot 1000} = 3952,29 \text{ kNmm}$$

$$F_{\text{t,Rd}} = \frac{0,9 \cdot 1000 \cdot 353}{1,25 \cdot 1000} = 254,16 \text{ kN}$$

$$n = \min\left(e_{\text{min}}; 1,25m = 1,25 \cdot 33,65 = 42,0625\right)$$

$$= 42,0625 \text{ mm}$$

Mode 3

$$F_{\text{T,3,Rd}} = 2 \cdot 254,16 = 508,32 \text{ kN} \tag{3.23}$$

Resistance of the group with bolt rows 1 and 2:

In this example, the non-circular yield pattern are decisive.

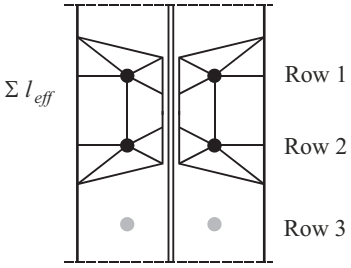

Mode 1

$$F_{T,1,Rd} = \frac{4 \cdot 5311,84}{33,65} = 631,42 \text{ kN} \tag{3.24}$$

where: $M_{pl,1,Rd} = \frac{0,25(166,05 + 166,05) \cdot 16,5^2 \cdot 235}{1,0 \cdot 1000}$

$= 5311,84$ kNmm

Mode 2

$$F_{T,2,Rd} = \frac{2 \cdot 5311,84 + 42,0625 \cdot 4 \cdot 254,16}{33,65 + 42,0625} = 705,12 \text{ kN} \tag{3.25}$$

where: $M_{pl,2,Rd} = \frac{0,25(166,05 + 166,05) \cdot 16,5^2 \cdot 235}{1,0 \times 1000}$

$= 5311,84$ kNmm

Mode 3

$$F_{T,3,Rd} = 4 \cdot 254.16 = 1016,64 \text{ kN} \tag{3.26}$$

Resistance of the group with bolt rows 1 to 3:

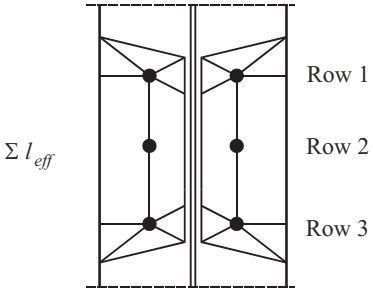

Mode 1

$$F_{T,1,Rd} = \frac{4 \cdot 6591,41}{33,65} = 783,53 \text{ kN} \tag{3.27}$$

where: $M_{pl,1,Rd} = \frac{0,25\left(166,05 + 82,5 + 163,55\right) \cdot 16,5^2 \cdot 235}{1,0 \cdot 1000}$

$= 6591,41 \text{ kNmm}$

Mode 2

$$F_{T,2,Rd} = \frac{2 \cdot 6591,41 + 42,0625 \cdot 6 \cdot 254,16}{33,65 + 42,0625} = 1021,32 \text{ kN} \tag{3.28}$$

where: $M_{pl,2,Rd} = \frac{0,25\left(166,05 + 82,5 + 163,55\right) \cdot 16,5^2 \cdot 235}{1,0 \cdot 1000}$

$= 6591,41 \text{ kNmm}$

Mode 3

$$F_{T,3,Rd} = 6 \cdot 254,16 = 1524,96 \text{ kN} \tag{3.29}$$

Resistance of the group with bolt rows 2 to 3:

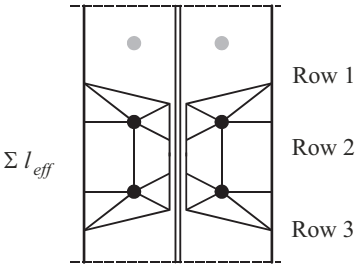

Mode 1

$$F_{T,1,Rd} = \frac{4 \cdot 5231,86}{33,65} = 621,92 \text{ kN} \tag{3.30}$$

where: $M_{pl,1,Rd} = \frac{0,25\left(163,55 + 163,55\right) \cdot 16,5^2 \cdot 235}{1,0 \cdot 1000}$

$= 5231,86 \text{ kNmm}$

Mode 2

$$F_{T,2,Rd} = \frac{2 \cdot 5231,86 + 42,0625 \cdot 4 \cdot 254,16}{33,65 + 42,0625} = 703,00 \text{ kN} \tag{3.31}$$

where: $M_{pl,2,Rd} = \frac{0,25\left(163,55 + 163,55\right) + 16,5^2 \cdot 235}{1,0 \cdot 1000}$

$= 5231,86 \text{ kNmm}$

Mode 3

$$F_{T,3,Rd} = 4 \cdot 254,16 = 1016,64 \text{ kN} \tag{3.32}$$

e) Component 5 – End-plate in bending

Reference is again made to the equivalent T-stub model. Accordingly, the following parameters need to be determined:

$$\begin{aligned}
e_x &= 50 \text{ mm} \\
m_x &= u_2 - 0,8a_f\sqrt{2} - e_x = 85 - 0,8 \cdot 8\sqrt{2} - 50 = 25,95 \text{ mm} \\
w &= 120 \text{ mm} \\
e &= 60 \text{ mm} \\
m &= \frac{w}{2} - \frac{t_{wb}}{2} - 0,8a_{fb}\sqrt{2} = 60 - 5,1 - 0,8 \cdot 5\sqrt{2} = 49,29 \text{ mm} \\
m_2 &= e_x + e_{1\text{-}2} - u_2 - t_{fb} - 0,8a_{fb}\sqrt{2} \\
&= 50 + 85 - 85 - 16 - 0,8 \cdot 8\sqrt{2} = 24,95 \text{ mm} \\
n_x &= \min\left(e_x;\ 1,25m_x = 1,25 \cdot 25,95 = 32,44\right) = 32,44 \text{ mm}
\end{aligned} \tag{3.33}$$

As previously done, the reduced effect of bolt row 4 is neglected for the estimation of the resistance in bending. The values of the effective lengths are extracted from Table 6.6 of Part 1-8; only group 2-3 is considered here as the presence of the beam flange does not allow developing yield lines between bolt row 1 and bolt row 2. Bolt row 2 needs the estimation of a α coefficient as this bolt row is close to the beam flange; the two following parameters are needed for the estimation of this parameter (see EN 1993-1-8, *Fig. 6.11*):

$$\left.\begin{aligned}
\lambda_1 &= \frac{m}{m + e} = \frac{49,24}{49,24 + 60} = 0,45 \\
\lambda_2 &= \frac{m_2}{m + e} = \frac{24,95}{49,24 + 60} = 0,23
\end{aligned}\right\} \rightarrow \alpha = 7,21 \tag{3.34}$$

Row 1 – Individual effective lengths:

$$\begin{aligned}
l_{\text{eff,cp,1}} &= 2\pi m_x = 2\pi \cdot 25,95 = 163,05 \text{ mm} \\
l_{\text{eff,cp,2}} &= \pi m_x + w = \pi \cdot 25,95 + 120 = 201,52 \text{ mm} \\
l_{\text{eff,cp,3}} &= \pi m_x + 2e = \pi \cdot 25,95 + 2 \cdot 60 = 201,52 \text{ mm} \\
l_{\text{eff,nc,1}} &= 4m_x + 1,25e_x = 4 \cdot 25,95 + 1,25 \cdot 50 = 166,3 \text{ mm} \\
l_{\text{eff,nc,2}} &= e + 2m_x + 0,625e_x = 60 + 2 \cdot 25,95 + 0,625 \cdot 50 = 143,15 \text{ mm} \\
l_{\text{eff,nc,3}} &= 0,5b_p = 0,5 \cdot 240 = 120 \text{ mm} \\
l_{\text{eff,nc,4}} &= 0,5w + 2m_x + 0,625e_x \\
&= 0,5 \cdot 120 + 2 \cdot 25,95 + 0,625 \cdot 50 = 143,15 \text{ mm}
\end{aligned} \tag{3.35}$$

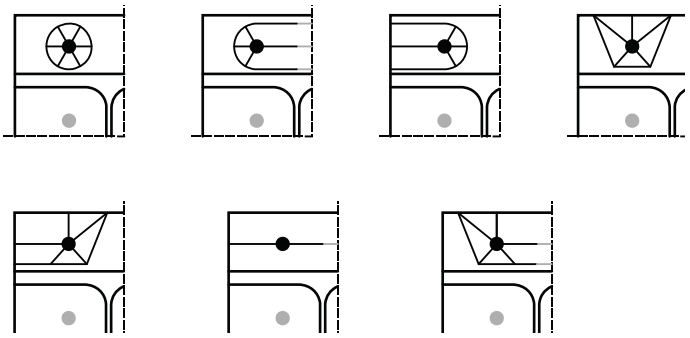

Row 2 – individual effective lengths:

$$\begin{aligned}
l_{\text{eff,cp}} &= 2\pi m = 2\pi \cdot 49,24 = 309,40 \text{ mm} \\
l_{\text{eff,nc}} &= \alpha m = 7,21 \cdot 49.24 = 355,02 \text{ mm}
\end{aligned} \tag{3.36}$$

Row 2 – effective lengths as first row of a group:

$$\begin{aligned}
l_{\text{eff,cp}} &= \pi m + p = \pi \cdot 49,24 + 80 = 234,69 \text{ mm} \\
l_{\text{eff,nc}} &= 0,5p + \alpha m - \left(2m + 0,625e\right) \\
&= 0,5 \cdot 80 + 7,21 \cdot 49,24 - \left(2 \cdot 49,24 + 0,625 \cdot 60\right) = 259,04 \text{ mm}
\end{aligned} \tag{3.37}$$

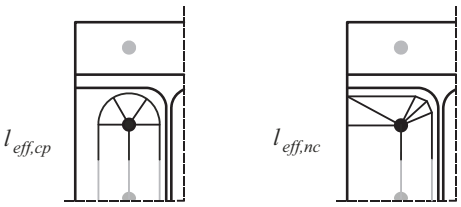

Row 3 – individual effective lengths:

$$\begin{aligned} l_{\text{eff,cp}} &= 2\pi m = 2\pi \cdot 49,24 = 309,40 \text{ mm} \\ l_{\text{eff,nc}} &= 4m + 1,25e = 4 \cdot 49,24 + 1,25 \cdot 60 = 271,96 \text{ mm} \end{aligned} \tag{3.38}$$

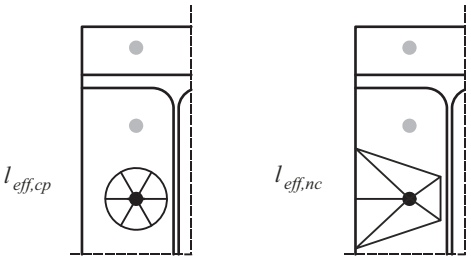

Row 3 – effective lengths as last row of a group:

$$\begin{aligned} l_{\text{eff,cp}} &= \pi m + p = \pi \cdot 49,24 + 80 = 234,69 \text{ mm} \\ l_{\text{eff,nc}} &= 2m + 0,625e + 0,5p \\ &= 2 \cdot 49,24 + 0,625 \cdot 60 + 0,5 \cdot 80 = 175,98 \text{ mm} \end{aligned} \tag{3.39}$$

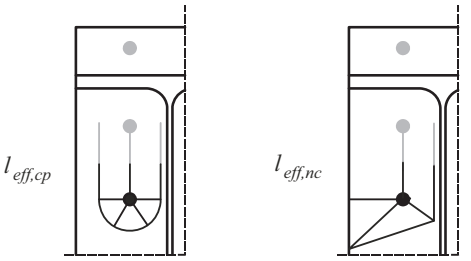

The corresponding resistances are then estimated.

Individual resistances of row 1:

Mode 1

$$F_{\text{T,1,Rd}} = \frac{4M_{\text{pl,1,Rd}}}{m_{\text{x}}} = \frac{4 \cdot 1586,25}{25,95} = 244,51 \text{ kN} \tag{3.40}$$

where: $M_{\text{pl,1,Rd}} = \dfrac{0,25 \cdot 120 \cdot 15^2 \cdot 235}{1.0 \cdot 1000} = 1586,25 \text{ kNmm}$

Mode 2

$$\begin{aligned} F_{\text{T,2,Rd}} &= \frac{2M_{\text{pl,2,Rd}} + n_{\text{x}} \sum F_{\text{t,Rd}}}{m_{\text{x}} + n_{\text{x}}} \\ &= \frac{2 \cdot 1586,25 + 32,44 \cdot 2 \cdot 254,16}{25,95 + 32,44} = 336,74 \text{ kN} \end{aligned} \tag{3.41}$$

where: $M_{pl,2,Rd} = \frac{0,25 \cdot 120 \cdot 15^2 \cdot 235}{1,0 \cdot 1000} = 1586,25\,\text{kNmm}$

Mode 3

$$F_{T,3,Rd} = 2 \cdot 254,16 = 508,32\,\text{kN} \tag{3.42}$$

Individual resistances of row 2:

Mode 1

$$F_{T,1,Rd} = \frac{4 \cdot 4089,88}{49,24} = 332,24\,\text{kN} \tag{3.43}$$

where: $M_{pl,1,Rd} = \frac{0,25 \cdot 309,40 \cdot 15^2 \cdot 235}{1,0 \cdot 1000} = 4089,88\,\text{kNmm}$

Mode 2

$$F_{T,2,Rd} = \frac{2 \cdot 4692,92 + 60 \cdot 2 \cdot 254,16}{49,24 + 60} = 365,11\,\text{kN} \tag{3.44}$$

where: $M_{pl,2,Rd} = \frac{0,25 \cdot 355,02 \cdot 15^2 \cdot 235}{1,0 \cdot 1000} = 4692,92\,\text{kNmm}$

Mode 3

$$F_{T,3,Rd} = 2 \cdot 254,16 = 508,32\,\text{kN} \tag{3.45}$$

Individual resistances of row 3:

Mode 1

$$F_{T,1,Rd} = \frac{4 \cdot 3594,97}{49,24} = 292,04\,\text{kN} \tag{3.46}$$

where: $M_{pl,1,Rd} = \frac{0,25 \cdot 271,96 \cdot 15^2 \cdot 235}{1,0 \cdot 1000} = 3594,97\,\text{kNmm}$

Mode 2

$$F_{T,2,Rd} = \frac{2 \cdot 3594,97 + 60 \cdot 2 \cdot 254,16}{49,24 + 60} = 345,01\ \text{kN} \tag{3.47}$$

where: $M_{pl,2,Rd} = \dfrac{0,25 \cdot 271,96 \cdot 15^2 \cdot 235}{1,0 \cdot 1000} = 3594,97\ \text{kNmm}$

Mode 3

$$F_{T,3,Rd} = 2 \cdot 254,16 = 508,32\ \text{kN} \tag{3.48}$$

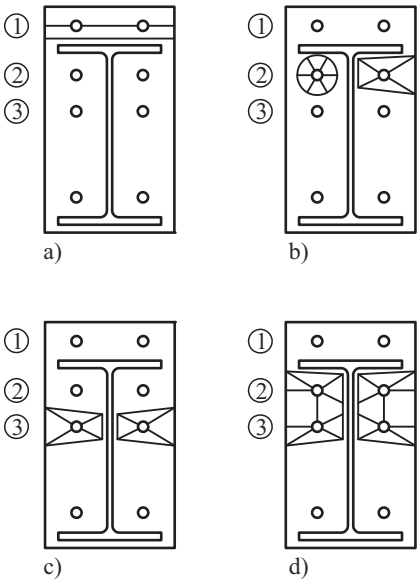

Group resistance - rows 2 and 3:

Mode 1

$$F_{T,1,Rd} = \frac{4 \cdot 5750,42}{49,24} = 467,13\ \text{kN} \tag{3.49}$$

where: $M_{pl,1,Rd} = \dfrac{0,25\left(259.04 + 175,98\right)15^2 \cdot 235}{1,0 \times 1000} = 5750,42\ \text{kNmm}$

Mode 2

$$F_{T,2,Rd} = \frac{2 \cdot 5750,42 + 60 \cdot 4 \cdot 254,16}{49,24 + 60} = 663,67\ \text{kN} \tag{3.50}$$

where: $M_{pl,2,Rd} = \dfrac{0,25\left(259,04+175,98\right)15^2 \cdot 235}{1,0 \cdot 1000} = 5750,42 \text{ kNmm}$

Mode 3

$$F_{T,3,Rd} = 4 \cdot 254,16 = 1016,64 \text{ kN} \tag{3.51}$$

f) Component 6 – Flange and web of the beam in compression

This resistance is estimated as follows, on the basis of properties extracted from the catalogue of profiles:

$$F_{c,fb,Rd} = \frac{515,59}{0,5-0,016} = 1065,3 \text{ kN} \tag{3.52}$$

g) Component 7 – Beam web in tension

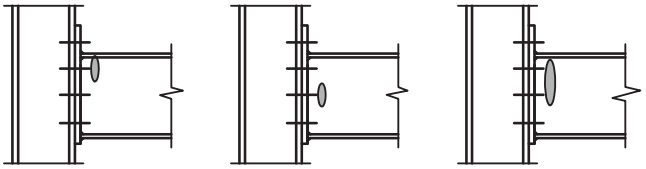

a) b) c)

This component has to be considered for bolt rows 2 and 3 only. The individual resistances of rows 2 and 3 (case a and b of the figure) and the group resistance (case c of the figure) are given here after:

Individual resistance of row 2:

$$F_{t,wb,Rd} = \frac{309,40 \cdot 10,2 \cdot 235}{1,0 \cdot 1000} = 741,63 \text{ kN} \tag{3.53}$$

Individual resistance of row 3:

$$F_{t,wb,Rd} = \frac{271,96 \cdot 10,2 \cdot 235}{1,0 \cdot 1000} = 651,89 \text{ kN} \tag{3.54}$$

Group resistance - rows 2 and 3:

$$F_{t,wb,Rd} = \frac{\left(259,04+175,98\right) \cdot 10,2 \cdot 235}{1,0 \cdot 1000} = 1042,74 \text{ kN} \tag{3.55}$$

3.3.3 Assembling of the components

Load which can be supported by row 1 considered individually

Column flange in bending: 401,99 kN

Column web in tension: 474,00 kN

End-plate in bending: 244,51 kN

$F_{1,min} = 244,51$ kN

Load which can be supported by row 2 considered individually

Column flange in bending: 401,99 kN

Column web in tension: 474,00 kN

End-plate in bending: 332,24 kN

Beam web in tension: 741,63 kN

$F_{2,min} = 332,24$ kN

Load which can be supported by row 3 considered individually

Column flange in bending: 401,99 kN

Column web in tension: 474,00 kN

End-plate in bending: 292,04 kN

Beam web in tension: 651,89 kN

$F_{3,min} = 292,04$ kN

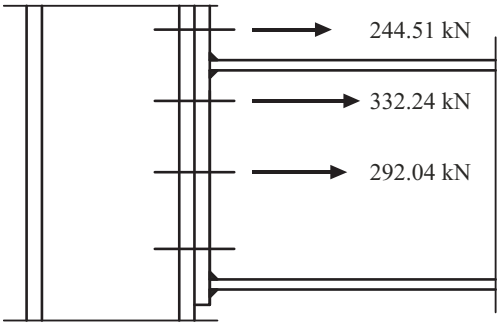

Figure 3.16 Loads which can be supported individually by the rows

Account for the group effects (group between rows 1-2 only)

The sum of the individual resistances of rows 1 and 2 is equal to:

$$F_{1,min} + F_{2,min} = 244,51 + 332,24 = 576,75\,\text{kN} \tag{3.56}$$

This value is compared to the load which can be supported by bolt rows 1 and 2 acting as a group:

Column flange in bending: 631,42 kN

Column web in tension: 579,04 kN

$F_{1+2,min} =$ 579,04 kN

As the group resistance is higher than the sum of the individual resistances, the individual resistances of rows 1 and 2 will be reached (i.e. the maximum load which can be supported by these rows is not affected by the considered group effect).

Account for group effects (group between rows 1-2-3 only)

The sum of the individual resistances of rows 1-2-3 is equal to:

$$F_{1,\min} + F_{2,\min} + F_{3,\min} = 244,51 + 332,24 + 292,04 = 868,79\ \text{kN} \tag{3.57}$$

This value is compared to the load which can be supported by rows 1-2-3 acting as a group:

Column flange in bending: 783,53 kN

Column web in tension: 653,21 kN

$F_{1+2+3,\min} =$ 653,21 kN

The group resistance is smaller than the sum of the individual resistances. Accordingly, the individual resistances in each row cannot be reached and a reduction of the loads which can be supported as to be taken into account. The load which can be supported by bolt row 3 is estimated as follows:

$$F_{3,\min,\text{red}} = F_{1+2+3,\min} - F_{1,\min} - F_{2,\min} = 653,21 - 244,51 - 332,24 = 76,46\ \text{kN} \tag{3.58}$$

Account for the group effects (group between rows 2-3 only)

The sum of the individual resistances of rows 2-3, taking into account of the reduction estimated in the previous section, is equal to:

$$F_{2,\min} + F_{3,\min,\text{red}} = 332,24 + 76,46 = 408,7\ \text{kN} \tag{3.59}$$

This value is compared to the load which can be supported by the group formed between rows 2 and 3 estimated as follows:

Column flange in bending: 621,92 kN

Column web in tension: 573,25 kN

End-plate in bending: 467,13 kN

Beam web in tension: 1042,7 kN

$F_{2+3,\min} =$ 467,13 kN

As the resistance of the group is higher than the sum of the individual resistances, it is assumed that each individual resistance can be reached.

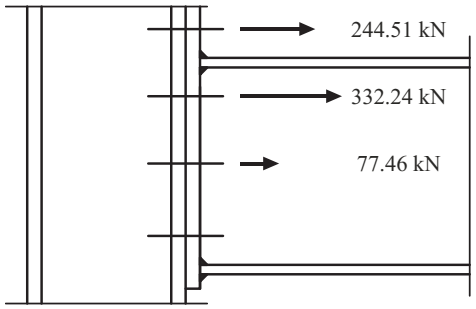

Figure 3.17 Maximum loads which can be supported by the rows, taking into account the group effects

In order to ensure equilibrium of the internal forces in the joint, one has to compare the resistance values of the bolt rows in tension with the other components. The sum of the maximal tensile resistances of rows 1, 2 and 3, taking into account of the group effects, is equal to:

$$F_{1,min} + F_{2,min} + F_{3,min,red} = 244,51 + 332,24 + 76,46 = 653,17 \text{ kN} \tag{3.60}$$

This value has now to be compared to the following loads:

Column web panel in shear:	548,88 kN
Column web in compression:	460,90 kN
Beam flange and beam web in compression:	1065,3 kN
$F_{glob,min}$ =	460,90 kN

Accordingly, the resistance of the column web in compression limits the maximal loads which can be supported by the rows. The loads in the latter have to be reduced, starting from bolt row 3:

$$\begin{aligned} &F_{1,min} + F_{2,min} = 244,51 + 332,24 = 576,75 \text{ kN} > F_{glob,min} = 460,90 \text{ kN} \\ &\Rightarrow F_{3,min,red} = 0 \text{ kN} \\ &F_{2,min,red} = F_{glob,min} - F_{1,min} = 460,9 - 244,51 = 216,39 \text{ kN} \end{aligned} \tag{3.61}$$

Because the resistance of the bolt row 2 is limited by a "global" component (here: column web in compression), bolt row 3 cannot be considered to contribute to the design moment resistance of the joint. The final summary of the loads which can be supported by the rows is shown in Figure 3.18.

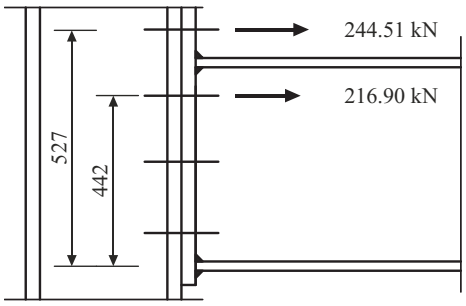

Figure 3.18 Final loads which can be supported by the rows

3.3.4 Determination of the design moment resistance

The design bending resistance is estimated as follows:

$$M_{j,Rd} = 244,5 \cdot 0,527 + 216,4 \cdot 0,442 = 224,5\,\text{kNm} \tag{3.62}$$

3.3.5 Determination of the rotational stiffness

The first step consists in estimating stiffness coefficients for the different components of the joint, according to EN 1993-1-8*, Table 6.11*. These coefficients are given in Table 3.8. The formulae as given in EN 1993-1-8*, Table 6.11* are not repeated in the table.

Table 3.8 Stiffness coefficients

Components	Stiffness coefficients
Column web panel in shear	$k_1 = \dfrac{0,38 \cdot 4495}{1,0\left(500 - \dfrac{16}{3} + 85 - 50 - \dfrac{85}{2}\right)10^{-3}} = 3,53$
Column web in compression	$k_2 = \dfrac{0,7 \cdot 274,81 \cdot 9,5}{243} = 7,52$
Column web in tension	$k_{3,1} = \dfrac{0,7 \cdot 166,05 \cdot 9,5}{243} = 4,54$ $k_{3,2} = \dfrac{0,7 \cdot 82,5 \cdot 9,5}{243} = 2,26$ $k_{3,3} = \dfrac{0,7 \cdot 163,55 \cdot 9,5}{243} = 4,48$ Contribution from row 4 neglected
Column flange in bending	$k_{4,1} = \dfrac{0,9 \cdot 166,05 \cdot 16,5^3}{33,65^3} = 17,62$ $k_{4,2} = \dfrac{0,9 \cdot 82,5 \cdot 16,5^3}{33,65^3} = 8,75$ $k_{4,3} = \dfrac{0,9 \cdot 163,55 \cdot 16,5^3}{33,65^3} = 17,35$
End-plate in bending	$k_{5,1} = \dfrac{0,9 \cdot 120 \cdot 15^3}{25,95^3} = 20,86$ $k_{5,2} = \dfrac{0,9 \cdot 234,69 \cdot 15^3}{49,24^3} = 5,97$ $k_{5,3} = \dfrac{0,9 \cdot 175,98 \cdot 15^3}{49,24^3} = 4,48$
Beam web and beam flange in compression	$k_6 = \infty$
Bolts in tension	$k_{10} = \dfrac{1,6 \cdot 353}{15 + 16,5 + (15+19)/2} = 11,65$

In a second step, the component assembling is realised in agreement with the recommended rules given in EN 1998-1-8*, Sec. 6.3.3.1*. The effective stiffness coefficient of each bolt row is obtained as follows:

$$\begin{aligned} k_{\text{eff},1} &= \frac{1}{\frac{1}{4,54}+\frac{1}{17,62}+\frac{1}{11,65}+\frac{1}{20,86}} = 2,43 \quad \text{and} \quad h_1 = 527\,\text{mm} \\ k_{\text{eff},2} &= \frac{1}{\frac{1}{2,26}+\frac{1}{8,75}+\frac{1}{11,65}+\frac{1}{5,97}} = 1,23 \quad \text{and} \quad h_2 = 442\,\text{mm} \\ k_{\text{eff},3} &= \frac{1}{\frac{1}{4,48}+\frac{1}{17,35}+\frac{1}{11,65}+\frac{1}{4,48}} = 1,70 \quad \text{and} \quad h_3 = 362\,\text{mm} \end{aligned} \tag{3.63}$$

The equivalent stiffness coefficient related to the tensile part of the joint is determined as follows:

$$\begin{aligned} z_{eq} &= \frac{2,43\cdot 527^2 + 1,23\cdot 442^2 + 1,70\cdot 362^2}{2,43\cdot 527 + 1,23\cdot 442 + 1,70\cdot 362} = 466,44\,\text{mm} \\ \Rightarrow k_{eq} &= \frac{2,43\cdot 527 + 1,23\cdot 442 + 1,7\cdot 362}{466,44} = 5,23\,\text{mm} \end{aligned} \tag{3.64}$$

The joint stiffness is then computed through the use of EN 1993-1-8*, Eq. 6.27*:

$$S_{\text{j,ini}} = \frac{210000\cdot 466,44^2}{\frac{1}{5,23}+\frac{1}{7,52}\cdot\frac{1}{3,53}}10^{-6} = 75,214\,\text{MNm/rad} \tag{3.65}$$

3.3.6 Computation of the resistance in shear

The shear load is supported by the four bolt rows. The latter being assumed as non-prestressed, the resistance in shear will be limited by the resistance of the bolt shanks in shear or by the bearing resistances of the connected plates (i.e. column flange or end-plate). In the previous case, the use of the design rules for these failure modes as recommended in EN 1993-1-8*, Table 3.4* was described; through these rules, it is possible to demonstrate that the failure mode to be considered is the mode "bolts in shear":

$$F_{\text{v,Rd}} = \frac{\alpha_{\text{v}} f_{\text{ub}} A_{\text{s}}}{\gamma_{\text{M2}}} = \frac{0,5\cdot 1000\cdot 353}{1,25}10^{-3} = 141,2\,\text{kN} \tag{3.66}$$

Height bolt contributes to the shear resistance. However, as indicated here above, half of them support tensile loads to contribute to the bending resistance. Accordingly, their contribution to the shear resistance has to be limited to take into account of these tensile loads; it is recommended in EN 1993-1-8 to multiply the shear resistance of the bolts by the factor 0,4/1,4.

The resistance of the joint to shear force is then obtained through the following formula:

$$V_{Rd} = 4F_{v,Rd}\left(1 + \frac{0,4}{1,4}\right) = 726,2\ \text{kN} \tag{3.67}$$

3.4 Design strategies

3.4.1 Design opportunities for optimisation of joints and frames

3.4.1.1 Introduction

This chapter describes the various approaches which can be used to design steel frames with due attention being paid to the behaviour of the joints. In practice, this design activity is normally performed by one or two parties, according to one of the following ways:

- an engineering office (in short *engineer*) and a steel fabricator (in short *fabricator*), referred as *Case A*;
- an engineering office (*engineer*) alone, referred as *Case B1*;
- a steel fabricator (*fabricator*) alone, referred as *Case B2.*

At the end of this design phase, fabrication by the steel fabricator takes place.

The share of responsibilities for design and fabrication respectively is given in Table 3.9 for these three cases.

Table 3.9 Parties and their roles in the design/fabrication process of a steel structure

Role	Case A	Case B1	Case B2
Design of members	Engineer	Engineer	Fabricator
Design of joints	Fabricator	Engineer	Fabricator
Fabrication	Fabricator	Fabricator	Fabricator

The design process is ideally aimed at ascertaining that a given structure fulfils architectural requirements, on the one hand, and is safe, serviceable and durable for a minimum of global cost, on the other hand. The parties involved in the design activities also care about the cost of these latter, with a view to optimising their respective profits.

In *Case A*, the engineer designs the members while the steel fabricator designs the joints. It is up to the engineer to specify the mechanical requirements to be fulfilled by the joints. The fabricator has then to design the joints accordingly, keeping in mind the manufacturing aspects also. Due to the disparity in the respective involvements of both parties, the constructional solution adopted by the fabricator for the joints may reveal to be sub-optimal; indeed it is dependent on the beam and column sizing that is made previously by the engineer. The latter may for instance aim at minimum shape sizes, with the consequence that the joints then need stiffeners in order to achieve safety and serviceability requirements. If he chooses larger shapes, then joints may prove to be less elaborated and result in a better economy of the structure as a whole (Figure 3.19).

In *Case B1*, the engineer designs both the members and the joints. He is thus able to account for mechanical joint properties when designing members. He can search for global cost optimisation too. It may happen however that the engineer has only a limited knowledge of the manufacturing requisites (machinery used, available materials, bolt grades and spacing, accessibility for welding, etc.); then this approach may contribute to some increase in the fabrication costs.

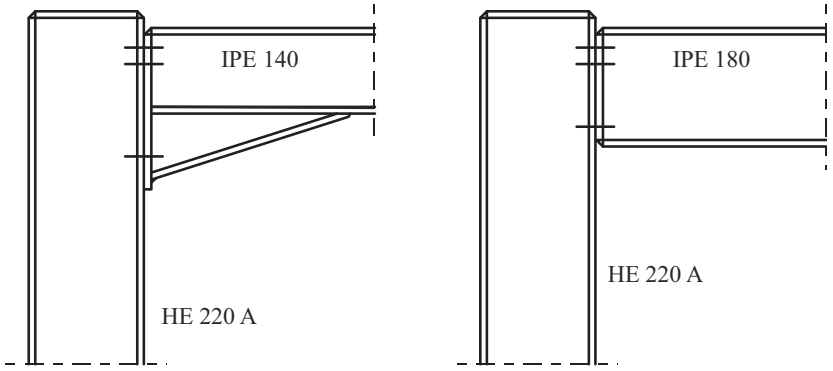

(a) Bolted end-plate with haunch (b) Bolted flush end-plate

Figure 3.19 Two solutions: different economy

Case B2 is ideal with regard to global economy. Indeed the design of both members and joints are in the hands of the fabricator who is presumably well aware of all the manufacturing aspects.

Before commenting on these various approaches, it is necessary to introduce some wording regarding joints.

A joint is termed simple, *semi-continuous or continuous*. This wording is general; it is concerned with resistance, with stiffness or with both. Being a novelty for most readers, some detailed explanations are given in section 3.2.2 on joints. In two circumstances only - that are related to the methods of global frame analysis -, this wording leads to more commonly used terms:

1. In an elastic global frame analysis, only the stiffness of the joints is involved. Then, a simple joint is a *pinned* joint, a continuous joint is a *rigid* joint while a semi-continuous is a *semi-rigid* joint;
2. In a rigid-plastic analysis, only the resistance of the joints is involved. Then, a simple joint is a *pinned* joint, a continuous joint is a *full-strength* joint while a semi-continuous joint is *a partial-strength* joint.

The various cases described above are commented on in the present chapter. For the sake of simplicity, it is assumed that global frame analysis is conducted based on an elastic method of analysis. This assumption is however not at all a restriction; should another kind of analysis be performed, similar conclusions would indeed be drawn.

For the design of steel frames, the designer can follow one of the following design approaches:

- *Traditional design approach:*
  The joints are presumably either simple or continuous. The members are designed first; then the joints are. Such an approach may be used in any Case A, B1 or B2; it is of common practice in almost all the European countries.
- *Consistent design approach:*
  Both member and joint properties are accounted for when starting the global

frame analysis. This approach is normally used in Cases B1 and B2, and possibly in Case A.

- *Intermediate design approach:*
  Members and joints are preferably designed by a single party (Case B1 or B2).

3.4.1.2 Traditional design approach

In the traditional design approach, any joint is assumed to be either simple or continuous. A simple joint is capable of transmitting the internal forces got from the global frame analysis but does not develop a significant moment resistance which might affect adversely the beam and/or column structural behaviour. A continuous joint exhibits only a limited relative rotation between the members connected as long as the applied bending moment does not exceed the bending resistance of the joint.

The assumption of simple and/or continuous joints results in the share of design activities into two more or less independent tasks, with limited data flow in between. The traditional design approach of any steel frame consists of eight steps (Figure 3.20).

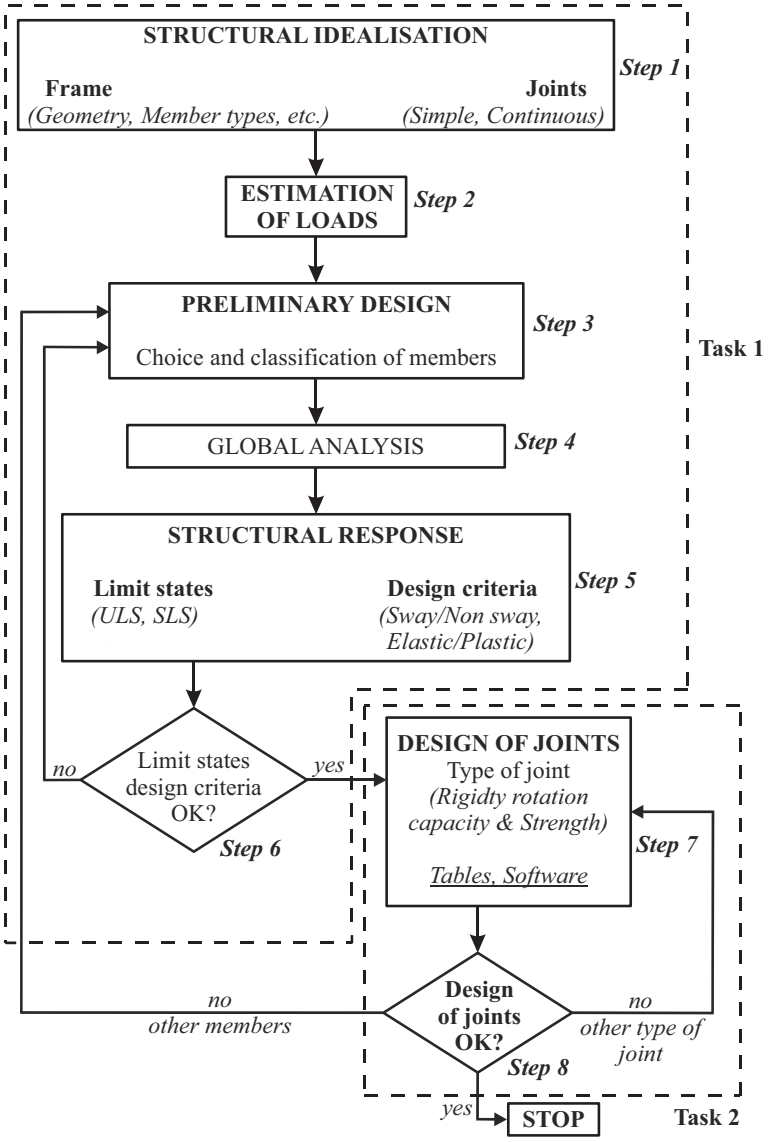

Figure 3.20 Traditional design approach (simple/continuous joints)

Step 1: The structural idealisation is a conversion of the real properties of the frame into the properties required for frame analysis. Beams and columns are normally modelled as bars. Dependent on the type of frame analysis which will be applied, properties need to be assigned to these bars. For example, if an elastic analysis is used, only the stiffness properties of the members are relevant; the joints are pinned or rigid and are modelled accordingly (Figure 3.21).

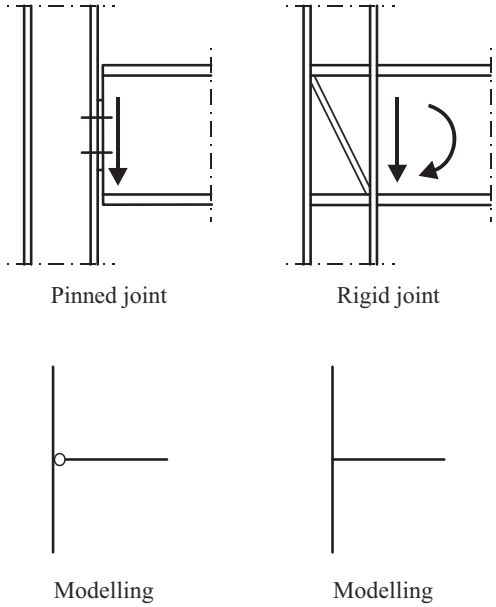

Figure 3.21 Modelling of pinned and rigid joints (elastic global analysis)

Step 2: Loads are determined based on relevant standards.

Step 3: The designer normally performs the preliminary design - termed pre-design in short - of beams and columns by taking advantage of his own design experience from previous projects. Should he have a limited experience only, then simple design rules can help for a rough sizing of the members. In the pre-design, an assumption shall be made concerning the stress distribution within the sections (elastic, plastic), on the one hand, and, possibly, on the allowance for plastic redistribution between sections, on the other hand. Therefore classes need to be assumed for the structural shapes composing the frame; the validity of this assumption shall be verified later in Step 5.

Step 4: The input for global frame analysis is dependent on the type of analysis. In an elastic analysis, the input is the geometry of the frame, the loads and the flexural stiffness of the members. In a rigid-plastic analysis, the input is the geometry of the frame, the loads and the resistance of the members. An elastic-plastic analysis requires both resistance and flexural stiffness of the members. Whatever the type of global frame analysis, the distribution and the magnitude of the internal forces and displacements are the output (however rigid-plastic analysis does not allow for any information regarding displacements).

Step 5: Limit state verifications consist normally in checking the displacements of the frame and of the members under service loading conditions (Serviceability Limit States, in short SLS), the resistance of the member sections (Ultimate Limit States, in short ULS), as well as the frame and member stability (ULS). The assumptions made regarding the section classes (see Step 3) are checked also.

Step 6: The adjustment of member sizing is to be carried out when the limit state verifications fail, or when undue under-loading occurs in a part of the structure. Member

sizing is adjusted by choosing larger shapes in the first case, smaller ones in the second case. Normally the designer's experience and know-how form the basis for the decisions made in this respect.

Steps 7/8: The member sizes and the magnitude of the internal forces that are experienced by the joints are the starting point for the design of joints. The purpose of any joint design task is to find a conception which allows for a safe and sound transmission of the internal forces between the connected members. Additionally, when a simple joint is adopted, the fabricator shall verify that no significant bending moment develops in the joint. For a continuous joint, the fabricator shall check whether the joint satisfies the assumptions made in Step 1 (for instance, whether the joint stiffness is sufficiently large when an elastic global frame analysis is performed). In addition, the rotation capacity shall be appropriate when necessary.

The determination of the mechanical properties of a joint is called *joint characterisation* (see section 3.2.3). To check whether a joint may be considered as simple or continuous, reference will be made to *joint classification* (see section 3.2.4.2).

Rules for joint characterisation in compliance with Eurocode 3 are available (see section 3.1.4 and application in 3.3), but design tools can be very helpful during the design process because they enlighten drastically the design tasks. In many cases the designer may select the joints out of tables which provide the strength and stiffness properties of the relevant joints, as well as, when necessary, the rotation capacity. Dedicated software may be an alternative to the latter; they require the whole layout of the joint as input and provide strength, stiffness and rotational capacity as output. Computer based design proceeds interactively by trial and error; for instance, the designer first tries a simple solution and improves it by adjusting the joint layout until the strength and stiffness criteria are fulfilled.

The mechanical properties of a joint shall be consistent with those required by the modelling of this joint in view of global frame analysis. Either the design of the joint and/or that of the members may need to be adjusted. In any case, some steps of the design approach need to be repeated.

3.4.1.3 Consistent design approach

In the consistent design approach, the global analysis is carried out in full consistency with the presumed real joint response (Figure 3.22).

It is therefore different from the traditional design approach described in section 3.4.1.2 in several respects:

- *Structural conception:*
  In the structural conception phase, the real mechanical behaviour of the joints is modelled;
- *Preliminary design:*
  In the pre-design phase, joints are selected by the practitioner based on his experience. Proportions for the joint components are determined: end-plate or cleat dimensions, location of bolts, number and diameter of bolts, sizes of column and beam flanges, thickness and depth of column web, etc.;
- *Determination of the mechanical properties:*
  In Step 4, the structural response of both the selected members and joints is determined. First the joints are characterised (see section 3.2.3) with the possible consequence of having a non-linear behaviour. This characterisation is followed by an idealisation, for instance according to a linear or bi-linear joint response curve (see section 3.2.3), which becomes a part of the input for global frame analysis;

- *Global frame analysis*:
  For the purpose of global frame analysis, any joint structural response is assigned to a relevant spring in the frame model. This activity is called *modelling* (see section 3.2.2).

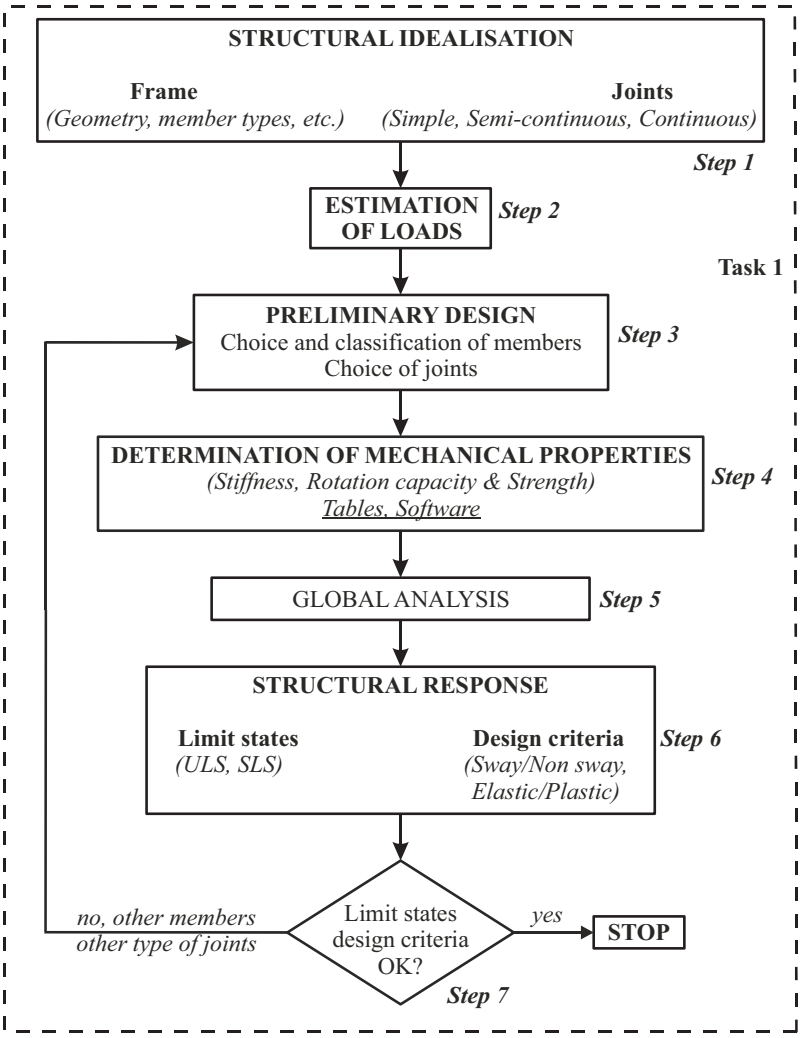

Figure 3.22 Consistent design approach

3.4.1.4 Intermediate design approaches

The two design approaches described in section 3.4.1.2 (for frames with simple or continuous joints) and in section 3.4.1.3 (for frames with semi-continuous joints) correspond to extreme situations. Intermediate approaches can be used. For example, the procedure given in Figure 3.20 can also be applied for semi-continuous joints. In that case, during the first pass through the design process, the joints are assumed to behave as simple or continuous joints. Joints are then chosen, the real properties of which are then accounted for in a second pass of the global analysis (i.e. after Step 8). The design process is then pursued similarly to the one described in Figure 3.22. But for sure such a way to proceed is not recommended as it involves iterations and so extra calculation costs.

More "clever" applications of intermediate design approaches are commented on in (Maquoi et al., 1997).

3.4.1.5 Economical considerations

Savings of fabrication and erection costs

a) Optimal detailing of rigid joints

A first very efficient strategy can be summarized as follows: "Optimise the joint detailing such that the joint stiffness comes close to the 'rigid' classification boundary but remains higher". This is illustrated in Figure 3.23.

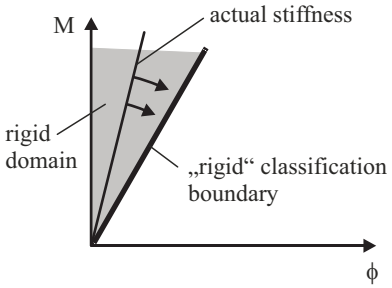

Figure 3.23 Optimization of rigid joints

The actual stiffness of a joint as well the classification boundary for rigid joints can be calculated according to Eurocode 3. The classification boundary is the minimum stiffness required to model a joint as rigid. If the actual joint stiffness is significantly higher, e.g. due to stiffeners, it should be checked whether it is not possible to omit some of the stiffeners while still fulfilling the criterion for rigid joints. This will not change the overall design at all, but it will directly reduce the fabrication costs of the joints (e.g. less welding). This procedure is used in the example described below:

The joints of a typical portal frame (see Figure 3.24) were designed using traditional design practice.

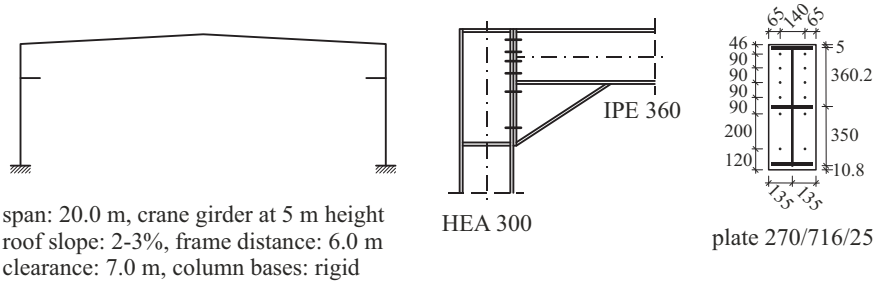

Figure 3.24 Example for the optimization of rigid joints

To classify the joints as rigid, EC 3 requires for the given unbraced frame that:

$$S_{j,ini} \geq 25 \frac{EI_b}{L_b} = 85\,628 \text{ kNm/rad} \tag{3.68}$$

According to EN 1993-1-8 the joint characteristics in *Fig. 9.6* are calculated as follows:

- design moment resistance $M_{j,Rd} = 281,6$ kNm
- initial stiffness $S_{j,ini} = 144\,971$ kNm/rad

Hence the joint is classified as rigid. But in order to optimise the joint, the detailing of the joint is modified step by step as follows:

1. omit the stiffeners at compression side,
2. in addition, omit the stiffeners at tension side,
3. in addition, omit the lowest bolt row in tension.

For all variations it is requested that the joint may still be classified as rigid, i.e. the initial stiffness of the joint should be higher than 85 628 kNm/rad. Table 3.10 gives the resistance and stiffness for all variations. It is seen that the design moment resistance is less than the applied moment and the joint behaves as a rigid one. The different joint detailings will have no influence on the design of the member as the joint remains rigid. Therefore, differences in the fabrication costs of the joint give direct indication of economic benefits. The fabrication costs (material and labour) are given for all investigated solutions in Table 3.10 as a percentage of the fabrication costs of the original joint layout. Beside the reduction of fabrication costs, the modified joints are seen to be more ductile. Another possibility to optimize the stiffness is the use of thinner plates. This can also lead to a more ductile behaviour. Other advantages are: smaller weld, the preparation of hole drilling is easier or hole punching becomes possible.

Table 3.10 Variations in joint detailing and relative savings in fabrication costs

Variations	$M_{j,Rd}$ **[kNm]**	$S_{j,ini}$ **[kNm]**	**Stiffness classification**	**Relative fabrication costs *)**	**Saving**
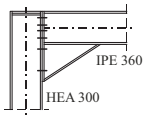	255,0	92 706	rigid	87 %	13 %
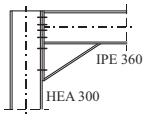	250,6	89 022	rigid	73 %	27 %
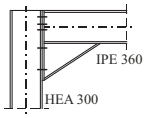	247,8	87 919	rigid	72 %	28 %
*) fabrication costs of the joints relative to those of the configuration shown in Figure 3.24					

b) Economical benefits from semi-rigid joints

A second strategy to profit from the extended possibilities in design can be expressed as follows: "*Use semi-rigid joints in order to have any freedom to optimise the global frame and joint design*".

The ideal assumption that the joints are rigid can lead often to situations where it is not possible to work without stiffeners. In consequence the joints are very expensive due to high fabrication costs (e.g. welding). In this case more economical solutions can be found by 'crossing the rigid classification boundary' to semi-rigid joints (see Figure 3.25 Optimisation with semi-rigid joints).

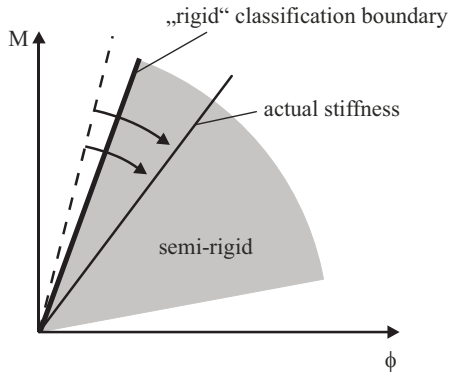

Figure 3.25 Optimisation with semi-rigid joints

The layout of the joints is then chosen for economy. Usually, this leads to more flexible, i.e. semi-rigid joints. The joint behaviour has to be taken into account in the frame analysis. This is possible by modelling the joints with rotational springs at beam ends. Their behaviour influences the global response of the frame, i.e. moment redistributions and displacements. As a consequence the size of the members may increase in comparison with a design with rigid joints. The decrease of the fabrication cost for the joints on one side has to be compared with the increase of the weight of the structure due to larger profiles on the other side. The optimum solution can only be found when a detailed calculation of the costs is carried out. Beside the positive effect in view of economy the use of joint without stiffeners provides more advantages: it becomes more easy to connect secondary beams, service pipes may be installed between the column flanges, easier coating and less problems with corrosion. The steel construction can appear more aesthetic and lighter and again, joint without stiffeners are usually more ductile. With respect to ultimate limit state design this is an important aspect as well, for instance in the case of seismic or robust requirements.

Savings of material costs

In the previous section, strategies where discussed when a frame is designed with so-called moment connections. This is usually required for unbraced frames. However for braced frames simple joints are normally more economic. However the moment diagram for the (simple supported) beams leads to beam sizes which are optimized for the mid-span moment, but ‘oversized’ at their ends. Further - due to the fact that the joints do not transfer any moment (this is the assumption for the frame analysis) - it becomes sometimes necessary to install additional temporary bracings during erection. However in many cases, joints which are assumed to behave as nominally pinned (e.g. flush end-plates) can be treated as semi-rigid joint. The strategy therefore is: “*Simple joints may have some inherent stiffness and may transfer moments - take profit from that actual behaviour*”.

This can improve the distribution of moments and reinforce the frame, i.e. lighter members (also for the bracing systems) without any change in joint detailing. And - as a consequent step - a further strategy is as follows: “*Check if small reinforcements of simple joints may strongly reinforce the frame*”

Sometimes it will be possible to reinforce simple joints without a large increase of fabrication cost (e.g. flush end-plates instead of a short end-plates). As those joints can transfer significant moments, the bending diagram is more balanced and the dimensions of the members can be lighter. Here again, increase of fabrication costs for the joints and decrease of weight of the structure are two competing aspects and a check of balance is necessary. However recent investigations show that the most economical solutions can be found if the contributions of the stiffness and resistance of the joints are considered, i.e. semi-rigid joints are used.

Summary and conclusions

With respect to joint design basically two different strategies can be identified when minimum costs of steel structures are of interest:

- simplification of the joint detailing, i.e. reduction of fabrication costs. Typically this is relevant for unbraced frames when the joints transfer significant moments (traditionally rigid joints);
- reduction of profile dimensions, i.e. reduction of material costs. Typically this is relevant for braced frames with simple joints.

In general both strategies would lead to the use of semi-rigid joints. In case of rigid joints an economic solution may already be found if the stiffness of the joint is close to the classification boundary.

Economy studies in various countries have shown possible benefits from the use of the concept of semi-rigid joints. More significant savings can be achieved when moment connections are optimized in view of economy. It is remarkable that all studies came to similar values when the saving due to the use of the new concept is compared to traditional design solutions. However it should be understood that the savings depend on the preferences of the steel fabricators to design the joints and how the cost are calculated. From the different studies it can be concluded that the possible savings due to semi-rigid design can be 20 - 25 % in case of unbraced frames and 5 - 9 % in case of braced frames. With the assumption that the costs of the pure steel frames are about 10% of the total costs for office buildings and about 20 % for industrial buildings, the reduction of the total building costs could be estimated to 4-5% for unbraced frames. For braced systems savings of 1-2 % are possible.

Of course the results of the investigations presented in this paper cannot be compared directly; particularly because different types of frames are used. However the following conclusion can be drawn as shown in Figure 3.26: the costs for material and fabrication (labour) are dependent on the relative stiffness of the joints. While the material costs decrease (curve A), the labour costs increase (curve B) with an increasing joint stiffness. For the total costs which are the sum of these both curves, a minimum can be found and from this, an "optimum joint stiffness". In many cases the value (which leads to an optimized design of the structure with respect to minimum total costs) is neither pinned nor rigid. Following the tendency of the last decades, it is obvious that the labour costs are increasing in comparison to the material costs (see dashed curve B*). From Figure 3.26 it becomes clear that as a consequence there is a progressive evolution of the "optimum joints stiffness" towards more flexible joints. Hence to find economical solutions for steel structures the use of semi-rigid joints will become more and more interesting.

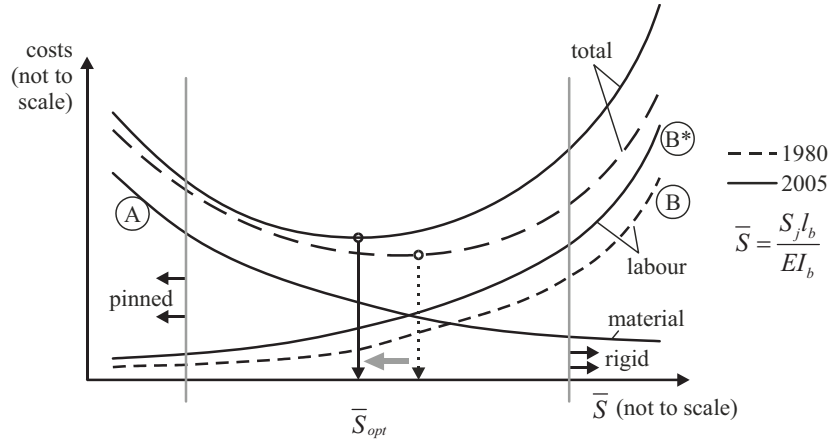

Figure 3.26 Costs of steel structures depending on the relative joint stiffness

References and further reading

ECCS Technical Committee 11 Composite construction. 1999. Design of composite joints for buildings, ECCS Publication n°109.

EN 1993 1-1: 2005. Eurocode 3: Design of Steel Structures Part 1-1: General rules and rules for buildings, CEN.

EN 1993 1-8: 2005. Eurocode 3: Design of Steel Structures Part 1-8: Design of joints, CEN.

Ivanyi, M., Baniotopoulos, C. C. 2000. Semi-Rigid Connections in Structural Steelwork, CISM Courses and Lectures N°419, SpringerWienNewYork.

Jaspart, J. P., Demonceau, J. F., Renkin, S., Guillaume, L. S. 2009. European Recommendations for the design of simple joints in steel structures, ECCS Technical Committee 10 Structural Connections, ECCS Publication n°126.

Maquoi, R., Chabrolin, B., Jaspart, J. P. 1997. Frame design including joint behaviour, ECSC Report 18563, Office for Official Publications of the European Communities, Luxembourg, (http://hdl.handle.net/2268/30506).

Simoes da Silva, L., Simoes, R., Gervasio, H. 2010. Design of Steel Structures, ECCS Eurocode Design Manual, ECCS, 1st edition.

CHAPTER 4

COLD-FORMED STEEL DESIGN ESSENTIALS

Dan DUBINĂ

Politehnica University Timisoara, Romania

4 Cold-formed steel design essentials

4.1 Introduction

The use of cold-formed steel structures is increasing throughout the world with the production of more economic steel coils particularly in coated form with zinc or aluminium/zinc coatings. These coils are subsequently formed into thin-walled sections by the cold-forming process. They are commonly called "Light gauge sections" since their thickness has been normally less than 3 mm. However, recent developments have allowed sections up to 25 mm to be cold-formed, and open sections up to approximately 8 mm thick are becoming common in building construction. The steel used for these sections may have a yield stress ranging from 250 MPa to 550 MPa. The higher yield stress steels are also becoming more common as steel manufacturers produce high strength steel more efficiently.

The use of thinner sections and high strength steels leads to design problems for structural engineers which may not normally be encountered in routine structural steel design. Structural instability of sections is most likely to occur as a result of the thickness of the sections, leading to reduced buckling loads (and stresses), and the use of higher strength steel typically makes the buckling stress and yield stress of the thin-walled sections approximately equal. Further, the shapes which can be cold-formed are often considerably more complex than hot-rolled steel shapes such as I-sections and unlipped channel sections. Cold-formed sections commonly have mono-symmetric or point-symmetric shapes, and normally have stiffening lips on flanges and intermediate stiffeners in wide flanges and webs. Both simple and complex shapes can be formed for structural and non-structural applications. Special design standards have been developed for these sections.

In Europe, the ECCS Committee TC7 originally produced the European Recommendations for the design of light gauge steel members in 1987 (ECCS_49, 1987). This European document has been further developed and published in 2006 as the European Standard Eurocode 3: Design of steel structures. Part 1-3: General Rules. Supplementary rules for cold-formed thin gauge members and sheeting (EN1993-1-3, 2006).

The market share of cold-formed structural steelwork continues to increase in the developed world. The reasons for this include the improving technology of manufacture and corrosion protection which leads, in turn, to the increase competitiveness of resulting products as well as new applications. Recent studies have shown that the coating loss for galvanised steel members is sufficiently slow, and indeed slows down to effectively zero, that a design life in excess of 60 years can be guaranteed.

The range of use of cold-formed steel sections specifically as load-bearing structural components is very wide, encompassing residential, office and industrial buildings, the automobile industry, shipbuilding, rail transport, the aircraft industry, highway engineering, agricultural and industry equipment, office equipment, chemical, mining, petroleum, nuclear and space industries.

Cold-formed members and profiled sheets are steel products made from coated or uncoated hot-rolled or cold-rolled flat strips or coils. Within the permitted range of tolerances, they have constant or variable cross-section. They are normally manufactured by one of two processes that are:

- roll forming;
- folding and press braking.

The first technology applies for large production of sections, while the second for small quantities and also for specific shapes.

Cold-formed structural members can be classified into two major types:

- individual structural framing members (Figure 4.1);
- profiled sheets and linear trays (Figure 4.2).

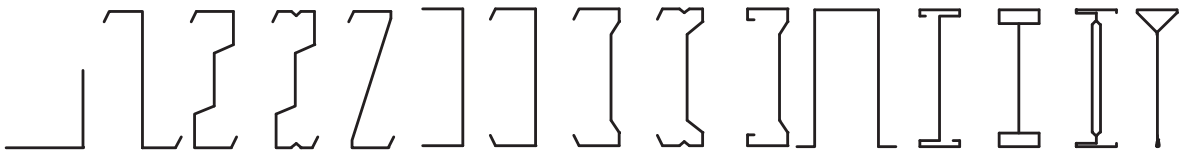

a) single open sections

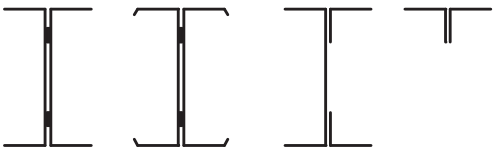

b) open built-up section

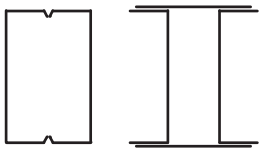

c) Closed built-up sections

Figure 4.1 Typical forms of sections for cold-formed structural members

In order to increase the stiffness of both cold-formed steel sections and sheeting, edge and intermediate stiffeners are used (Figure 4.3); they can be easily identified in examples from Figure 4.1 and Figure 4.2.

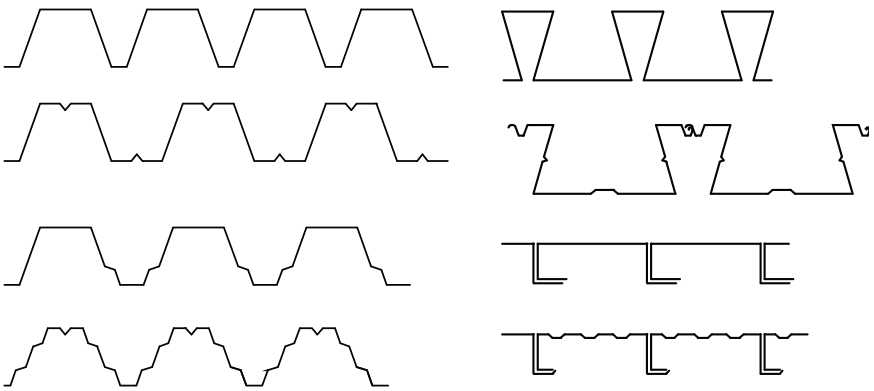

Figure 4.2 Profiled sheets and linear trays

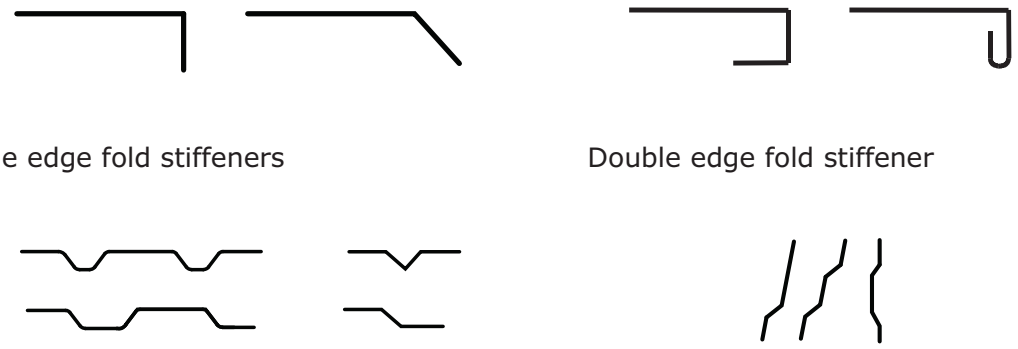

Single edge fold stiffeners | Double edge fold stiffener

Intermediate flange stiffeners | Intermediate web stiffeners

Figure 4.3 Typical forms of stiffeners for cold-formed members and sheeting

In general, cold-formed steel sections provide the following advantages in building construction (Yu, 2000):

- as compared with thicker hot-rolled shapes, cold-formed steel members can be manufactured for relatively light loads and/or short spans;
- nestable sections can be produced, allowing for compact packaging and shipping;
- unusual sectional configurations can be produced economically by cold-forming operations and consequently favourable strength-to-weight ratios can be obtained;
- load-carrying panels and decks can provide useful surfaces for floor, roof, and wall construction, and in other cases they can also provide enclosed cells for electrical and other conduits;
- load-carrying panels and decks not only withstand loads normal to their surfaces, but they can also act as shear diaphragms to resist force in their own planes if they are adequately interconnected to each other and to supporting members.

Compared with other materials such timber and concrete, the following qualities can be realised for cold-formed steel structural members.

- lightness, high strength and stiffness; non-combustibility;
- ability to provide long spans, up to 12 m (Rhodes, 1991);
- ease of prefabrication and mass production;
- fast and easy erection and installation; recyclable material;
- substantial elimination of delays due to weather;
- more accurate detailing; formwork unnecessary; uniform quality;
- non-shrinking and non-creeping at ambient temperatures;
- termite-proof and rot-proof; economy in transportation and handling.

The combination of the above-mentioned advantages can result in cost saving in construction.

4.2 Peculiar problems in cold-formed steel design

4.2.1 Peculiar characteristics of cold-formed steel sections (Dubina et al., 2012)

Compared to hot-rolled steel sections, the manufacturing technology of cold-formed steel sections induces some peculiar characteristics. First of all, cold-forming leads to a modification of the stress-strain curve of the steel. With respect to the virgin material, cold-rolling provides an increase of the yield strength and, sometimes, of the ultimate strength that is important in the corners and still appreciable in the flanges, while press braking leave these characteristics nearly unchanged in the flanges. Obviously, such effects do not appear in case of hot-rolled sections, as shown in Table 4.1.

Table 4.1 Influence of manufacturing process on the basic strengths of hot and cold-formed profiles

Forming method		Hot rolling	Cold forming	
			Cold rolling	Press braking
Yield strength	Corner	-	High	High
	Flange	-	Moderate	-
Ultimate strength	Corner	-	High	High
	Flange	-	Moderate	-

The increase of the yield strength is due to strain hardening and depends on the type of steel used for cold rolling. On the contrary, the increase of the ultimate strength is related to strain aging that is accompanied by a decrease of the ductility and depends on the metallurgical properties of the material.

Design codes provide formulas to evaluate the increase of yield strength of cold-formed steel sections, compared to that of the basic material.

Hot-rolled profiles are affected by residual stresses, which result from air cooling after hot-rolling. These stresses are mostly of membrane type, they depend on the shape of sections and have a significant influence on the buckling strength. Therefore, residual stresses are the main factor which causes the design of hot-rolled sections to use different buckling curves in European design codes (EN1993-1-1, 2005).

In the case of cold-formed sections the residual stresses are mainly of flexural type, as Figure 4.4 demonstrates, and their influence on the buckling strength is less important than membrane residual stresses as Table 4.2 shows.

On the other hand, cold rolling produce different residual stresses in the section when compared with press braking, as shown in Table 4.2, so the section strength may be different in cases where buckling and yielding interact.

Experimental evidence shows more complex actual distributions of residual stresses. Figure 4.5 (a to c) presents the distribution of measured residual stress for a cold-formed steel angle, channel and lipped channel (Rondal et al., 1994).

The European buckling curves have been calibrated using test results on hot formed (rolled and welded) steel sections, obtained during a large experimental program in Europe in the 1960's. These curves are based on the well-known Ayrton-Perry formula, in

which the imperfection factor α was correspondingly calibrated (Rondal and Maquoi, 1979a, Rondal and Maquoi, 1979b).

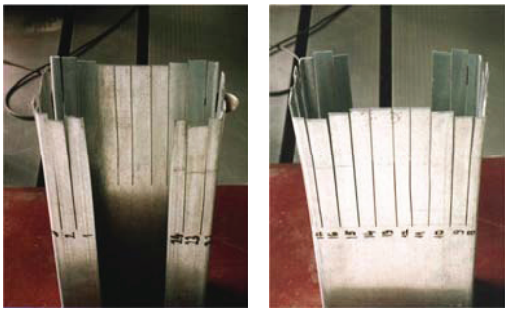

Figure 4.4 Evidence of flexural residual stresses in a lipped channel cold-formed steel section

Table 4.2 Type magnitude of residual stresses in steel sections

Forming method	Hot rolling	Cold forming	
		Cold rolling	Press braking
Membrane residual stresses	High	Low	Low
Flexural residual stresses	Low	High	Low

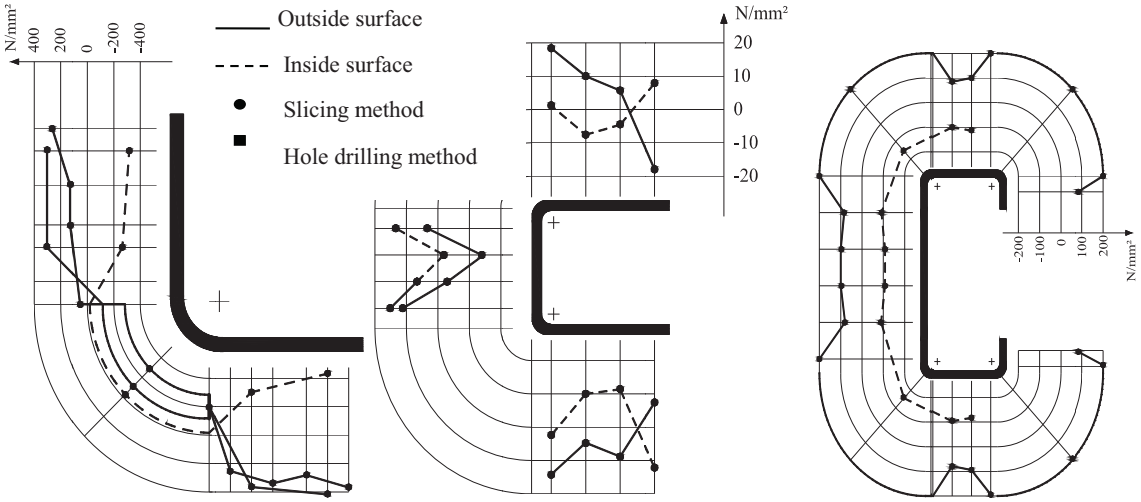

Figure 4.5 Measured residual stress in cold-formed steel sections: cold-rolled angle; cold-rolled C profile and press braked U profile

Due to the fact the mechanical properties of cold-formed sections – e.g. cold-forming effect and residual stresses – are different to those of hot-rolled ones, different buckling curves should be justified (Dubina, 1996). Nowadays both numerical and experimental approaches are available to calibrate appropriate α factors for cold-formed sections (Dubina, 2001) but, for the sake of simplicity of the design process, the same buckling curves as for hot formed sections are still used (EN1993-1-1 and EN1993-1-3).

4.2.2 Peculiar problems of cold-formed steel design

The use of thin-walled sections and cold-forming manufacturing effects can results in special design problems not normally encountered when tick hot-rolled sections are used. A brief summary of some special problems in cold-formed steel design are reviewed in the following.

4.2.2.1 Buckling strength of cold-formed steel members

Steel sections may be subject to one of four generic types of buckling, namely local, global, distortional and shear. Local buckling is particularly prevalent in cold-formed steel sections and is characterised by the relatively short wavelength buckling of individual plate element. The term "global buckling" embraces Euler (flexural) and flexural-torsional buckling of columns and lateral-torsional buckling of beams. It is sometimes termed "rigid-body" buckling because any given cross-section moves as a rigid body without any distortion of the cross-section. Distortional buckling, as the term suggests, is buckling which takes place as a consequence of distortion of the cross-section. In cold-formed sections, it is characterised by relative movement of the fold-lines. The wavelength of distortional buckling is generally intermediate between that of local buckling and global buckling. It is a consequence of the increasing complexity of section shapes that local buckling calculation are becoming more complicated and that distortional buckling takes on increasing importance.

Local and distortional buckling can be considered as "sectional" modes, and they can interact with each other as well as with global buckling (Dubina, 1996). Figure 4.6 shows single and interactive (coupled) buckling modes for a lipped channel section in compression.

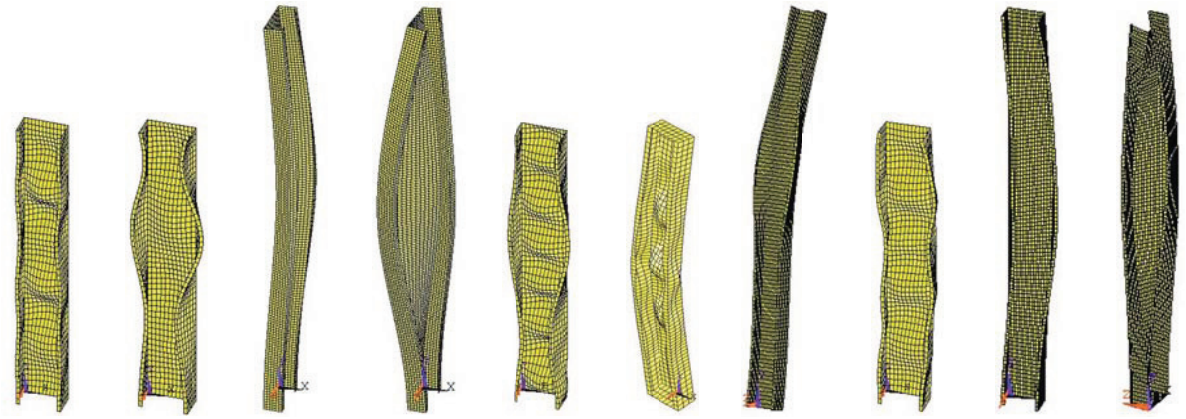

a b c d e f g h i j

Figure 4.6 Buckling modes for a lipped channel in compression
Single modes: (a) local (L); (b) distortional (D); (c) flexural (F);
(d) flexural-torsional (FT); Coupled (interactive) modes: (e) L + D; (f) F + L;
(g) F + D; (h) FT + L; (i) FT + D; (j) F + FT (Dubina, 2004)

The results have been obtained using a Linear Buckling FEM analysis (LBA). For given geometrical properties of member cross-section, the different buckling modes depend by the buckling length, as shown in Figure 4.7 (Hancock, 2001).

The curves shown in Figure 4.7 have been obtained using an elastic Finite Strip (FS) software, analysing and describing the change of buckling strength versus buckle half-wavelength.

A first minimum (Point A) occurs in the curve at a half-wavelength of 65 mm and represents local buckling in the mode shown. The local mode consists mainly of deformation of the web element without movement of the line junction between the flange and lip stiffener. A second minimum also occurs at a point B at a half-wavelength of 280 mm in the mode shown. This mode is the distortional buckling mode since movement of the line junction between the flange and lip stiffener occurs without a rigid body rotation or translation of the cross-section. In some papers, this mode is called a

local-torsional mode. The distortional buckling stress at point B is slightly higher than the local buckling stress at point A, so that when a long length fully braced section is subjected to compression, it is likely to undergo local buckling in preference to distortional buckling. The section buckles in a flexural or flexural-torsional buckling mode at long wavelengths, such as at points C, D and E. For this particular section, flexural-torsional buckling occurs at half-wavelengths up to approximately 1800 mm beyond which flexural buckling occurs.

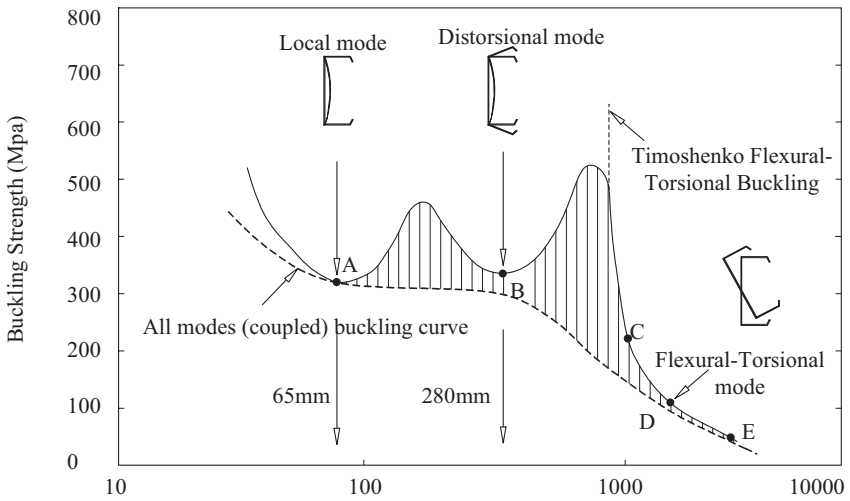

Figure 4.7 Buckling strength versus half-wavelength for a lipped channel in compression (Hancock, 2001)

The dashed line in Figure 4.7, added to the original figure, qualitatively shows the pattern of *all modes* or *coupled mode*.

The effect of interaction between sectional and global buckling modes results in increasing sensitivity to imperfections, leading to the erosion of the theoretical buckling strength (see hachured zones in Figure 4.7). In fact, due to the inherent presence of imperfection, buckling mode interaction always occurs in case of thin-walled members.

Figure 4.8 shows the difference in behaviour of a *thick-walled* slender bar in compression (Figure 4.8a), and a *thin-walled* bar (Figure 4.8b); they are assumed, theoretically, to have the same value of their gross areas. Both cases of an ideal perfect bar and a geometric imperfect bar are presented.

Looking at the behaviour of a *thick-walled* bar it can be seen that it begins to depart from the elastic curve at point B when the first fibre reaches the yield stress, N_{el}, and it reaches its maximum (ultimate) load capacity, N_u, at point C; after which the load drops gradually and the curve approaches the theoretical rigid-plastic curve asymptotically. The elastic theory is able to define the deflections and stresses up to the point of first yield and the load at which first yield occurs. The position of the rigid-plastic curve determines the absolute limit of the load carrying capacity, above which the structure cannot support the load and remain in a state of equilibrium. It intersects the elastic line as if to say "thus far and no further" (Murray, 1985).

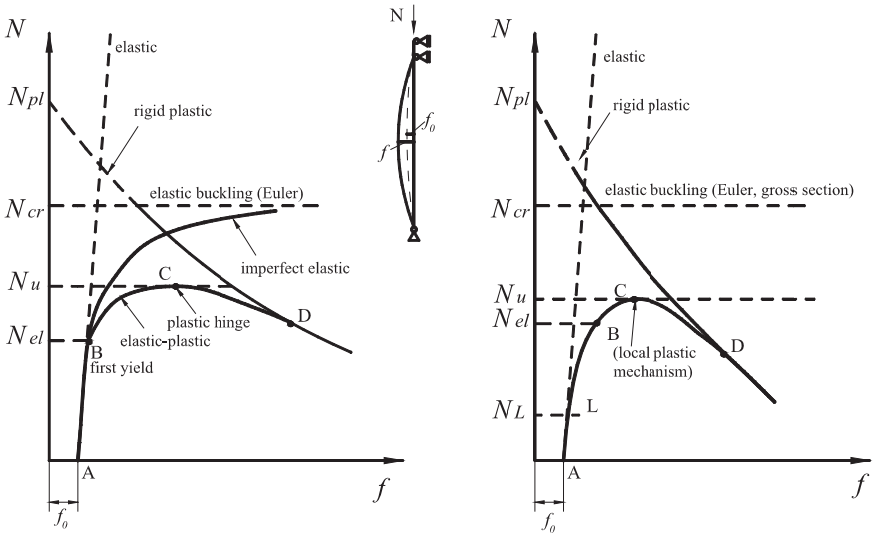

Figure 4.8 Behaviour of (a) slender thick-walled and (b) thin-walled compression bar

In case of a thin-walled bar, sectional buckling, e.g. local or distortional buckling, may occur prior to the initiation of plastification. Sectional buckling is characterised by the stable post-critical path and the bar does not fail as a result of this, but significantly lose stiffness. Yielding starts at the corners of cross-section prior to failure of the bar, when sectional buckling mode changes into a local plastic mechanism quasi-simultaneously with the occurrence of global buckling (Dubina, 2000). Figure 4.9, obtained by advanced FEM simulation, clearly shows the failure mechanism of a lipped channel bar in compression (Ungureanu and Dubina, 2004).

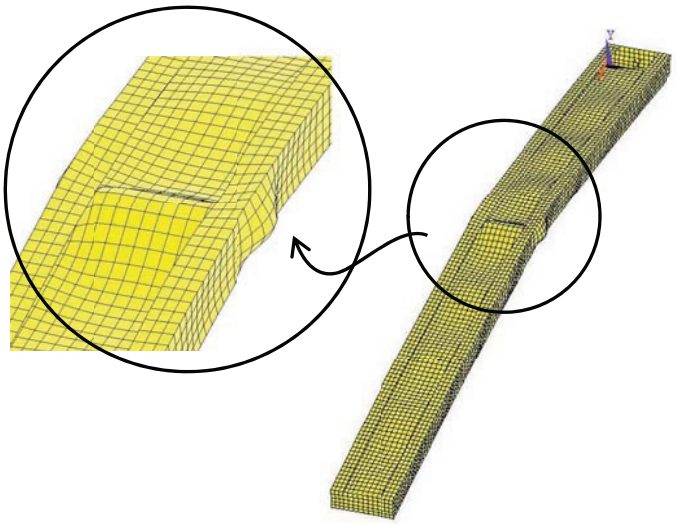

Figure 4.9 Failure mode of a lipped channel in compression (Ungureanu and Dubina, 2004)

Figure 4.10 shows the comparison between the buckling curves of a lipped channel member in compression, calculated according to EN1993-1-3, considering the fully effective cross-section (i.e. no local buckling effect) and the reduced (effective) cross-section (i.e. when local buckling occurs and interacts with global buckling).

However the effectiveness of thin-walled sections, expressed in terms of load carrying capacity and buckling strength of compression walls of beam and columns can be improved considerably by the use of edge stiffeners or intermediate stiffeners.

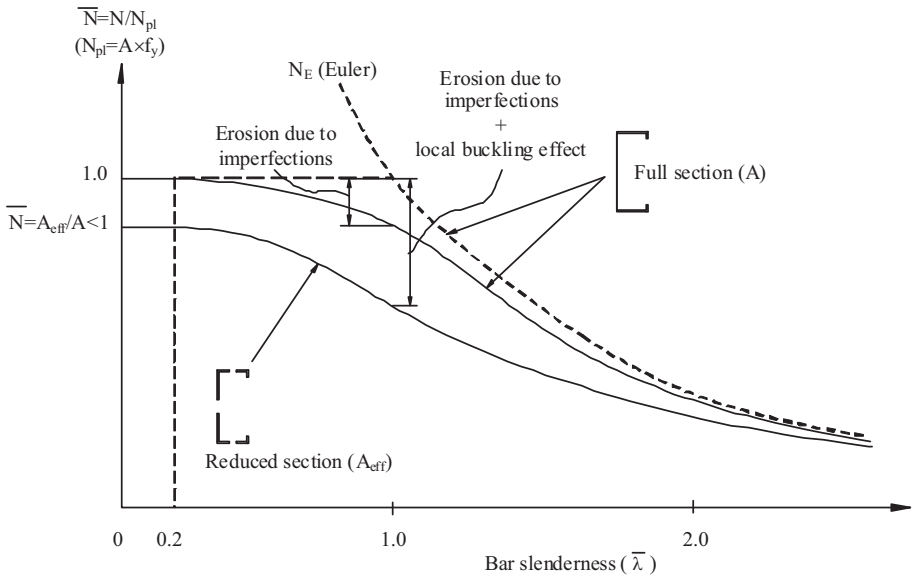

Figure 4.10 Effect of local buckling on the member capacity

4.2.2.2 Web crippling

Web crippling at points of concentrated load and supports can be a critical problem in cold-formed steel structural members and sheeting for several reasons. These are:

- in cold-formed steel design, it is often not practical to provide load bearing and end bearing stiffeners. This is always the case in continuous sheeting and decking spanning several support points;
- the depth-to-thickness ratios of the webs of cold-formed members are usually larger than for hot-rolled structural members;
- in many cases, the webs are inclined rather than vertical;
- the intermediate element between the flange, onto which the load is applied, and the web of a cold-formed member usually consists of a bend of finite radius. Hence the load is applied eccentrically from the web.

Special provisions are included in design codes to guard against failure by web crippling.

4.2.2.3 Torsional rigidity

Cold-formed sections are normally thin and consequently they have low torsional stiffness. Many of the sections produced by cold-forming are mono-symmetric and their shear centres are eccentric from their centroids as shown in Figure 4.11a. Since the shear centre of a thin-walled beam is the axis through which it must be loaded to produce flexural deformation without twisting, then any eccentricity of the load from this axis will generally produce considerable torsional deformations in a thin-walled beam as shown in Figure 4.11a. Consequently, thin-walled beams usually require torsional restraints either at intervals or continuously along the length to prevent torsional deformations. Often, this is the case for beams such as Z- and C- purlins which may undergo flexural-torsional buckling because of their low torsional stiffness, if not properly braced.

In addition, for columns axially loaded along their centroid axis, the eccentricity of the load from the shear centre axis may cause buckling in the flexural-torsional mode as shown in Figure 4.11b at a lower load than the flexural buckling mode also shown in Figure 4.11b. Hence the checking for the flexural-torsional mode of buckling is necessary for such mono-symmetric columns.

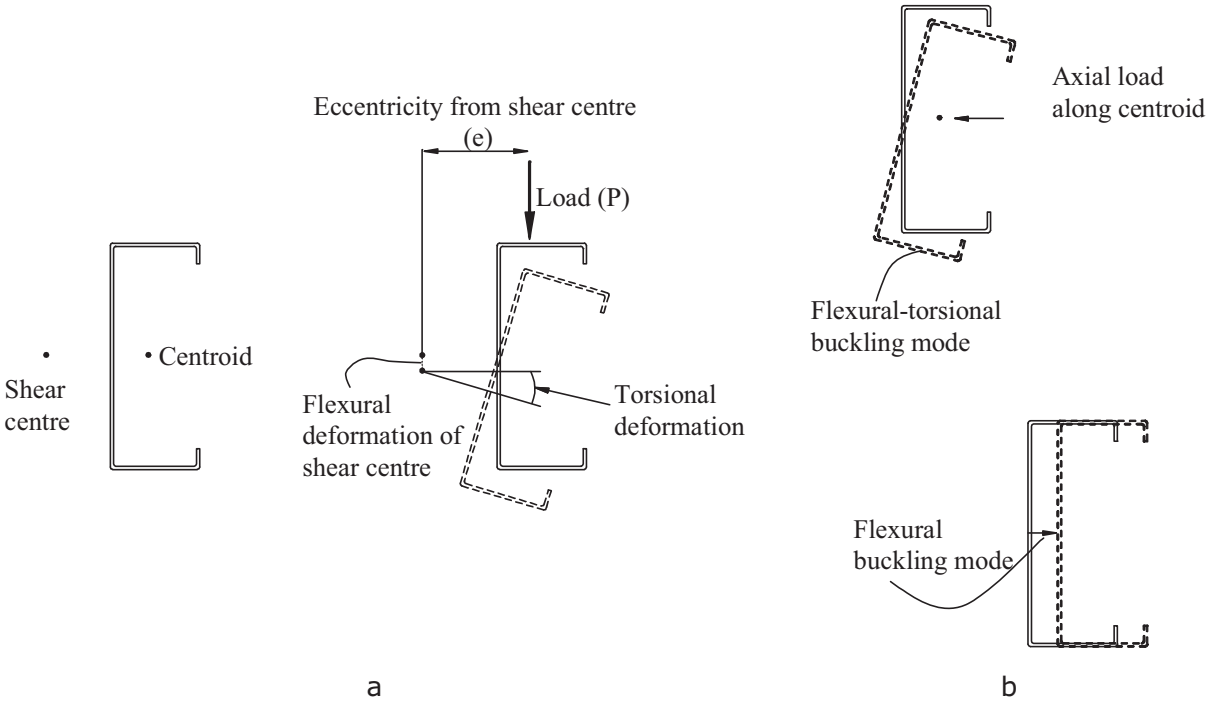

Figure 4.11 Torsional deformations: (a) eccentrically loaded lipped channel beam; (b) axially loaded lipped channel column

4.2.2.4 Ductility and plastic design

Due to sectional buckling mainly (cold-formed sections are of class 4 or class 3, at the most), but also due to the effect of cold-forming by strain hardening, cold-formed steel sections possess low ductility and are not generally allowed for plastic design. The previous discussion related to Figure 4.8 revealed the low inelastic capacity reserve for these sections, after yielding initiated. However, for members in bending, design codes allow to use the inelastic capacity reserve in the part of the cross-section working in tension.

Because of their reduced ductility, cold-formed steel sections cannot dissipate energy in seismic resistant structures. However, cold-formed sections can be used in seismic resistant structures because there are structural benefits to be derived from their reduced weight, but only elastic design is allowed and no reduction of the shear seismic force is possible. Hence, in seismic design, a reduction factor q = 1 has to be assumed as stated in EN1998-1:2004.

4.2.2.5 Connections

Conventional methods for connections used in steel construction, such as bolting and arc-welding are available for cold-formed steel sections but are generally less appropriate because of the wall thinness, and special techniques more suited to thin materials are often employed. Long-standing methods for connecting two thin elements are blind rivets

and self-drilling, self-tapping screws. Fired pins are often used to connect thin materials to a ticker supporting member. More recently, press-joining or clinching technologies (Predeschi et al., 1997) have been developed, which require no additional components and cause no damage to the galvanising or other metallic coating. This technology has been adopted from the automotive industry and is successfully used in building construction. "Rosette" system is another innovative connecting technology (Makelainen and Kesti, 1999), applicable to cold-formed steel structures.

Therefore, connection design is more complex and challenging to the engineers.

4.2.2.6 Design codification framework

EN1993-1-3 provides specific design requirements and rules for cold-formed thin gauge members and sheeting. It applies to cold-formed steel products made from coated or uncoated thin gauge hot or cold-rolled sheet or strip, that have been cold-formed by such processes as cold-rolled forming or press-braking. However, the cold-formed steel design is supported not only by EN1993-1-3, but also by the other parts of EN1993 (see Figure 4.12) such as EN1993-1-1, 1-2, 1-5, 1-6, 1-7 1-8 and others. The execution of steel structures, including cold-formed thin gauge members and sheeting, is covered in EN1090. The calculation rules given in this standard are only valid if the tolerances of the cold-formed members comply with EN1090-2:2008 specific provisions.

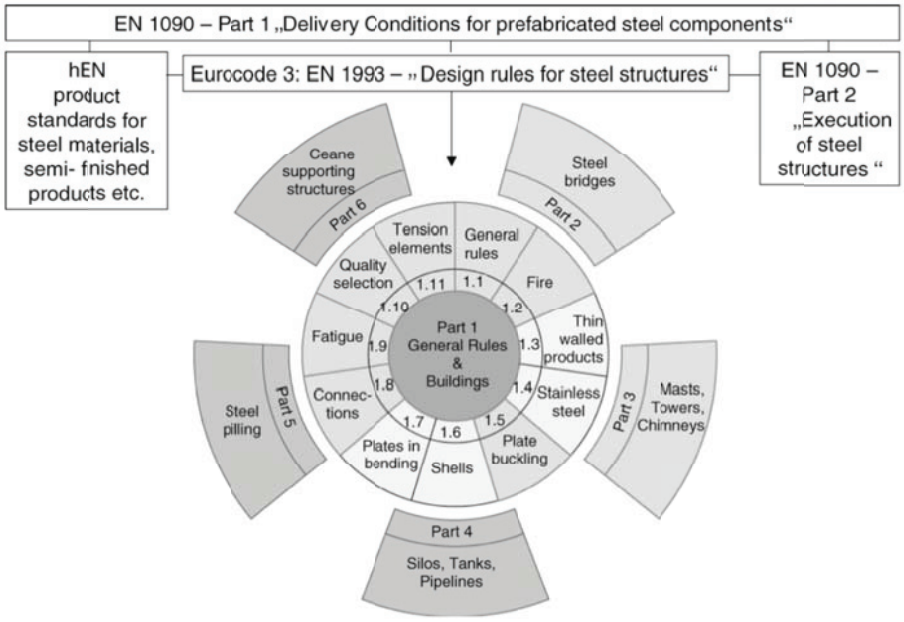

Figure 4.12 Standard system for steel structures (Sedlacek and Müller, 2006)

This European Standard EN1090 specifies requirements for execution of steel structures, in order to ensure adequate levels of mechanical resistance and stability, serviceability and durability. The requirements are expressed in terms of execution classes.

The structure shall be designed such that deterioration over its design working life does not impair the performance of the structure below that intended, having due regard to its environment and the anticipated level of maintenance. In order to achieve an adequately durable structure, the following should be taken into account (see EN1990):

- the intended or foreseeable use of the structure;
- the required design criteria;

- the expected environmental conditions;
- the composition, properties and performance of the materials and products;
- the properties of the soil and the choice of the structural system;
- the shape of members and the structural detailing;
- the quality of workmanship, and the level of control;
- the particular protective measures;
- the intended maintenance during the design working life.

The environmental conditions shall be identified at the design stage so that their significance can be assessed in relation to durability and adequate provisions can be made for protection of the materials used in the structure.

The effects of deterioration of material, corrosion and fatigue where relevant should be taken into account by appropriate choice of material, or by structural redundancy and by the choice of an appropriate corrosion protection system.

Cold-formed steel structures are, usually, thin-walled. This means, in the design for Ultimate Limit State, the stability criteria must be of concern. Also, since the structures will be slender, particular attention has to be paid to Serviceability Limit State criteria, e.g. for deflection limits and vibrations. On the other hand, the complex shapes of cross-sections and the special connecting technologies, might involve testing in design, either to check the solutions, either to calibrate the design formulas or to model safety coefficients. On this purpose the Annex D of EN1990 and Chapter 9 of EN1993-1-3:2006 will be considered. The code provisions are limited to steel in the thickness range 1,0 – 8,0 mm for members, and 0,5 – 4,0 mm for sheeting. Thicker material may also be used provided the load-bearing capacity is determined by testing.

EN1993-1-3 includes in Chapter 10 design criteria for the following particular applications: Beams restrained by sheeting, Linear trays restrained by sheeting, Stressed skin design and Perforated sheeting. The design provisions for these particular applications are often complex but may be useful for design engineers since they include detailed methodologies not available in other standards or specifications.

As application support of this code, the European Convention for Constructional Steel Work, ECCS, published in 2008 "Worked examples according to EN1993-1-3" (ECCS_123, 2008). Previously, in 2000, ECCS also edited worked examples on the same topic (ECCS_114, 2000). In 1995 the European Convention for Constructional Steelwork – ECCS published the European Recommendations for the Application of Metal Sheeting acting as a Diaphragm (ECCS_88, 1995). Recently, the ECCS Design Manual entitled "Design of Cold-Formed Steel Structures" (Dubina et al., 2012) has been published.

4.2.2.7 Fire resistance

Due to the small values of section factor (i.e. the ratio of the heated volume to the cross-sectional area of the member) the fire resistance of unprotected cold-formed steel sections is reduced. For the same reason fire protection with intumescent coating is not efficient.

Sprayed cementations or gypsum based coatings, while very efficient for other applications are, generally, not usable for galvanised cold-formed steel sections. However, cold-formed steel sections can be employed as beams concealed behind a suspended ceiling. In load bearing applications, fire resistance periods of 30 minutes can usually be achieved by one layer of "special" fire resistant plasterboard, and 60 minutes by two layers of this plasterboard, which possesses low shrinkage and high integrity properties in fire. Planar protection to floors and walls provides adequate fire resistance

to enclosed sections, which retain a significant proportion of their strength, even at temperatures of 500 °C.

In light gauge steel framing, the board covering of walls and floors can protect the steel against fire for up to 120 minutes, depending on the board material and the number of boards. The choice of insulation material, mineral wool or rock wool is also crucial to fire strength.

Box protection of individual cold-formed steel sections used as beams and columns is provided in much the same way as with hot-rolled sections.

Non-load bearing members require less fire protection, as they only have to satisfy the "insulation" criterion in fire conditions. Ordinary plasterboard may be used in such cases.

4.2.2.8 Corrosion

The main factor governing the corrosion resistance of cold-formed steel sections is the type and thickness of the protective treatment applied to the steel rather than the base metal thickness. Cold-formed steel has the advantage that the protective coatings can be applied to the strip during manufacture and before roll forming. Consequently, galvanised strip can be passed through the rolls and requires no further treatment.

Steel profiles are typically hot dip galvanised with 275 gram of zinc per square meter (Zn 275), corresponding to a zinc thickness of 20 μm on each side. The galvanising layer is sufficient to protect the steel profiles against corrosion during the entire life of a building, if constructed in the correct manner. The most severe effects of corrosion on the steel occur during transport and outdoors storage. When making holes in hot dip galvanised steel framing members, normally no treatment is needed afterwards since the zinc layer possesses a healing effect, i.e. transfers to unprotected surfaces.

Hot dip galvanising is sufficient to protect the steel profiles against corrosion during the life of a building. The service life of hot dip galvanised steel studs was studied by British Steel and others (Burling, 1990). The loss in zinc weight will be around 0,1 g/m^2 per year indoors. A similar study was also carried out for steel floors above crawl spaces with plastic sheeting on the ground. Results showed that a zinc weight of 275 g/m^2 is sufficient to provide a durability of around 100 years.

4.2.2.9 Sustainability of cold-formed steel construction

Burstrand (2000) presents the reasons in choosing light gauge steel framing from an environmental point of view:

- light gauge steel framing is a dry construction system without organic materials. Dry construction significantly reduces the risk of moisture problems and sick building syndrome;
- steel, gypsum and mineral wool are closed cycle materials;
- Every material used in light gauge steel framing (steel, gypsum and mineral wool) can be recycled to 100%;
- it is possible to disassemble the building components for re-use;
- light gauge steel framing means less energy consumption during production than equivalent housing with a framework of concrete poured on-site;
- light gauge steel framing only uses about a fourth of the amount of raw materials used for equivalent masonry-concrete homes;
- less waste means a cleaner work site and a low dead weight of building components ensures a good working environment;
- low dead weight leads to reduced transport needs.

4.3 Resistance of cross-sections

4.3.1 Introduction

The individual components of cold-formed steel members are usually so thin with respect to their widths that they buckle at stress levels less than the yield point when subjected to compression, shear, bending or bearing. Local buckling of such elements is therefore one of the major considerations in cold-formed steel design.

It is well known that, compared to other kinds of structures, thin plates are characterised by a stable post-critical behaviour. Consequently, cold-formed steel sections, which can be regarded as an assembly of thin plates along the corner lines, will not necessarily fail when their local buckling stress is reached and they may continue to carry increasing loads in excess of that at which local buckling occurs.

In order to account for local buckling, when the resistance of cross-sections and members is evaluated and checked for design purposes, the effective section properties have to be used. However, for members in tension the full section properties are used. The appropriate use of full and effective cross-section properties is explained in this section.

Local buckling of individual walls of cold-formed steel sections is a major design criterion and, consequently, the design of such members should provide sufficient safety against failure by local instability with due consideration given to the post-buckling strength of structural components (e.g. walls).

When speaking about the "resistance of cross-sections", the following design actions are to be considered:

- axial tension;
- axial compression;
- bending moment;
- combined bending and axial tension;
- combined bending and axial compression;
- torsional moment;
- shear force;
- local transverse forces;
- combined bending moment and shear force;
- combined bending moment and local transverse force.

Both local buckling and distortional buckling (sectional instability modes) effects on the cross-section strength have to be considered when compression stresses are induced by the given action scenarios.

In principle, there is no difference in calculation the resistance of cross-sections of cold-formed thin-walled steel members compared with hot-rolled sections. However, since, currently cold-formed steel sections are class 4 sections, the resistance of sections in compression, bending and combined compression and bending have to be calculated using the properties of effective cross-section.

4.3.2 Flange curling

In beams that have unusually wide and thin but stable flanges, i.e. primarily tension flanges with large *b*/*t* ratios, there is a tendency for these flanges to curl under bending. That is, the portion of these flanges most remote from the web (edges of I beams, centre portions of flanges of box or hat beams) tend to deflect toward the neutral axis, as illustrated in Figure 4.13.

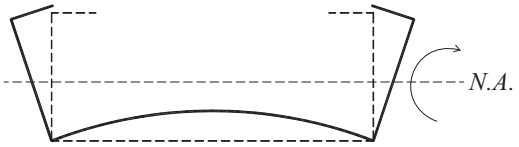

Figure 4.13 Flange curling of channel section beam

The curling is due to the effect of longitudinal curvature of the beam and bending stress in flanges. The first study of this phenomenon was presented by George Winter (1940). The phenomenon can be easily explained with reference to the behaviour of a wide flange I-beam in pure bending (see Figure 4.14). The transverse component p of the flange force ($\sigma_a \cdot t$) per unit width can be determined by:

$$p = \frac{\sigma_a \cdot t \cdot d\phi}{dl} = \frac{\sigma_a \cdot t}{\rho} = \frac{\sigma_a \cdot t}{E \cdot I / M} \tag{4.1}$$

where:

σ_a is the average (mean) bending stress in flange;

E is the modulus of elasticity;

I is the second moment of the beam area;

b_f, h, t, dl, $d\phi$ and ρ as shown in Figure 4.14.

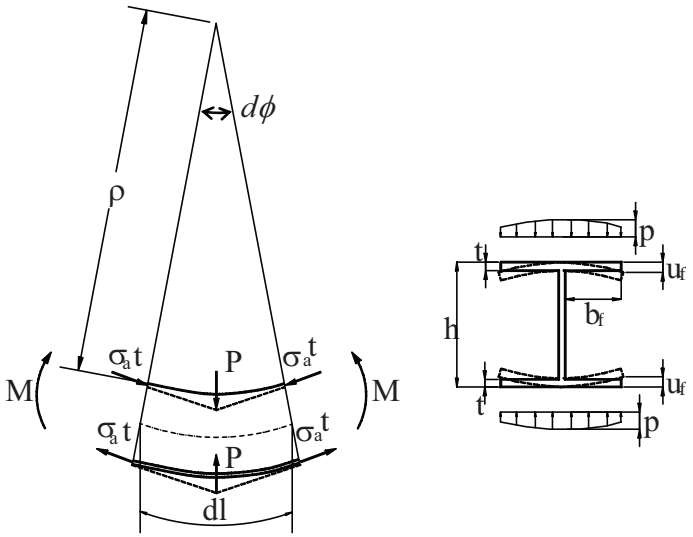

Figure 4.14 Flange curling of I-beam subjected to bending

If the value of the transverse component p is considered to be a uniformly distributed load applied on the flange, the deflection of curling at the outer edge of the flange, u, can be computed considering flange as a cantilever plate (Yu, 2000):

$$u_f = \frac{p \cdot b_f^4}{8 \cdot D} = 3 \cdot \left(\frac{\sigma_a}{E}\right)^2 \cdot \left(\frac{b_f^4}{t^2 \cdot d}\right) \cdot (1 - \nu^2) \tag{4.2}$$

where:

u_f is the flange deflection of outer edge;

D is the flexural rigidity of plate, $D = E\,t^2/12(1 - \nu^2)$;

ν is the Poisson's ratio.

The ECCS Recommendations (ECCS_49, 1987; the predecessor of EN1993–1–3) provide the following formula for calculating the curling displacement, applicable to both compression and tensile flanges, both with and without stiffeners:

$$u_f = 2 \cdot \frac{\sigma_a^2 \cdot b_f^4}{E^2 \cdot t^2 \cdot z} \tag{4.3}$$

In Eqn. (4.3), b_f is one half of the distance between webs in box and hat sections, or the width of the portion flange projecting from the web (see Figure 4.15), z is the distance of flange under consideration from neutral axis (N.A.), while the other notations are defined as in Eqn. (4.2).

When the actual stress in the flange has been calculated for the effective cross–section, the mean value of the stress, σ_a, is obtained by multiplying the stress for the effective cross–section by the ratio of the effective flange area to the gross flange area.

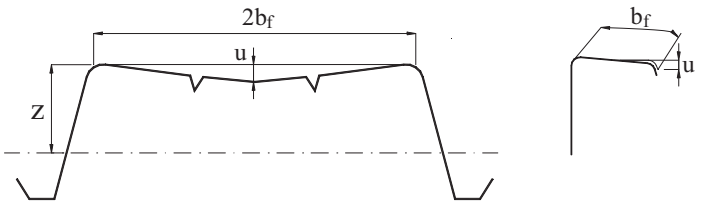

Figure 4.15 Geometrical parameters of flange curling

Flange curling is in general highly dependent on the flange width-to-thickness ratio, but also varies significantly with web depth and, indeed, the general geometry of the section. Beams with shallow webs and small tension elements are particularly prone to flange curling.

Flange curling can be neglected in calculations if the deflection us is not greater than 5% of the depth of cross-section.

4.3.3 Shear lag

For the beams of usual shapes, the normal stresses are induced in the flanges through shear stresses transferred from the web to the flange. These shear stresses produce shear strains in the flange which, for ordinary dimensions, have negligible effects. However, if the flanges are unusually wide (relative to their length) these shear strains

have the effect of decreasing the normal bending stresses in the flange with increasing distance from the web. This phenomenon is known as shear leg (see Figure 4.16).

The simplest way of accounting for this stress variation in design is to replace the non-uniformly stressed flange, of actual width b_f ($b \approx 2 \cdot b_f$), by a reduced (effective) width subjected to uniform stress (Winter, 1970).

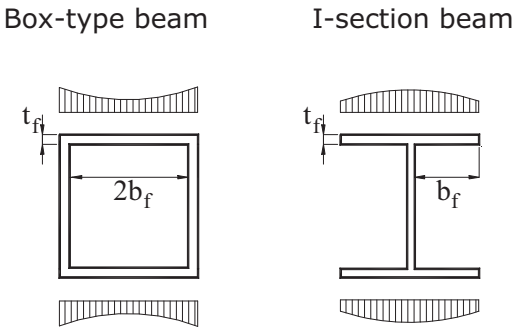

Figure 4.16 Normal bending stress distribution in both compression and tension flanges of short beams due to shear lag

Shear lag is important for beams with large flanges subjected to concentrated loads on fairly short spans; the smaller the span-to-width ratio, the larger the effect. For beams supporting uniform loads, shear leg is usually negligible except when the L/b_f ratio is less than about 10, as shown in Figure 4.17.

Where the span of the beam, L, is less than $30b_f$ and the beam supports a concentrated load, or several loads spaced greater than $2b_f$, the effective design width of a flange, whether in tension or compression, shall be limited to the values given in Table 4.3. These values were obtained by Winter in early 1940s (Winter, 1940), and actually are included in American (AISI S100-07) and Australian/New Zealand design codes (AS/NZS-4600:2005).

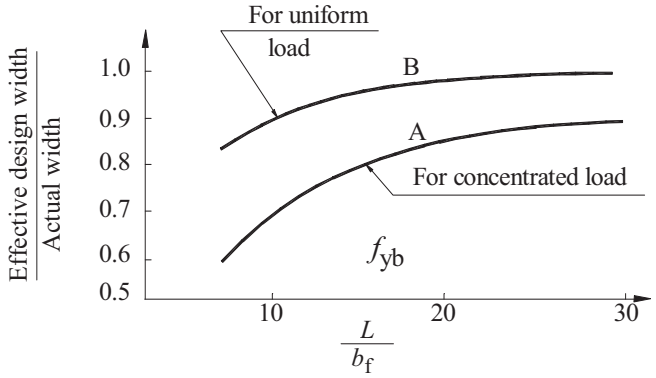

Figure 4.17 Analytical curves for determining effective width of flange of short span beams (Winter, 1940)

Table 4.3 Maximum ratio of effective design width to actual width for short wide flange beams

L/b_1	Ratio	L/b_1	Ratio
30	1,00	14	0,82
25	0,96	12	0,78
20	0,91	10	0,73
18	0,89	8	0,67
16	0,86	6	0,55

where, L is the full span for simple beams; or distance between inflection points for continuous beams; or twice the length of cantilever beam.

The values of effective width ratios given in Table 4.5 are those corresponding to Curve A of Figure 4.17. For uniform load, it can be seen from Curve B of Figure 4.17 that the

width reduction due to shear lag for any practicable width-span ratio is so small as to be effectively negligible.

According to EN1993-1-5, the effect of shear lag shall be taken into account in flanges of flexural members if the length *Le* between the points of zero bending moment is less than $50b_f$.

The phenomenon of shear lag is of considerable consequence in naval architecture and aircraft design. However, in cold-formed steel construction, beams are infrequently so wide that significant reductions are required.

4.3.4 Sectional buckling modes in thin-walled sections

4.3.4.1 Local and distortional buckling

Sectional instability modes refer to local and distortional buckling. Local buckling of a plane element (e.g. a wall of a cold-formed steel section) when both edges remain straight in the longitudinal direction, as shown in Figure 4.18 and Figure 4.19, is characterised by half-wavelengths comparable with the element width.

Distortional buckling of sections involves rotation of the lip/flange components about the flange/web junction as shown in Figure 4.18. Distortional buckling is also known as "stiffener buckling" or "local-torsional buckling". In this case, the web and lip/flange distortional buckling occur at the same half-wavelength which is larger than the local buckling half-wavelength. In members with intermediately stiffened elements distortional buckling is characterized by a displacement of the intermediate stiffer normal to the plane of the element (see Figure 4.19).

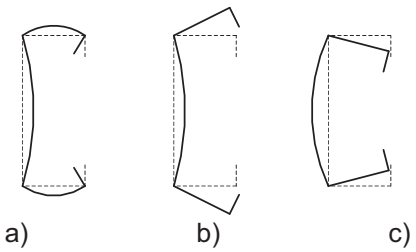

Figure 4.18 Local and distortional buckling of a lipped channel section in compression

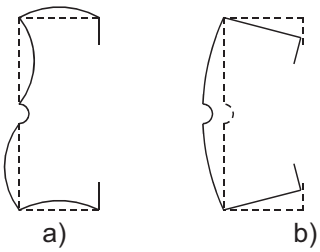

Figure 4.19 Local and distortional buckling of a lipped channel with web intermediate stiffener

Local buckling is a phenomenon which characterises the behaviour of thin plates, and is solved accordingly. Distortional buckling is treated either as a problem of elastic critical buckling of a long sheet (e.g. the flange/lip assembly) on an elastic foundation (see EN1993-1-3) or as a problem of lateral-torsional buckling of a flange/lip section column (Schafer and Peköz, 1999).

4.3.4.2 Buckling of thin flat walls in compression

Considering the compression wall in the pre-buckling phase stresses are uniformly distributed (see Figure 4.20a), while after buckling they become non-uniform (see Figure 4.20b) and continuously concentrate near the supported edges as the load increases, until the yield strength is reached (see Figure 4.20c) and the plate starts to fail.

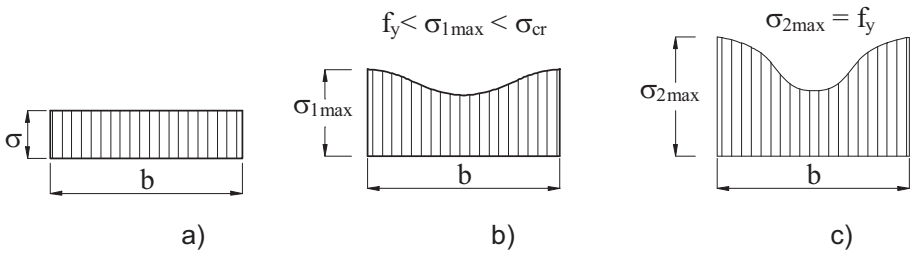

Figure 4.20 Consecutive stress distribution in stiffened compression elements: (a) pre-critical stage; (b) intermediate post-critical stage; (c) ultimate post-critical stage

The elastic post-buckling behaviour of a plate can be analysed by using the large deflection theory.

However, it has been found that the solution of the differential equation for large deflections has little application in practical design because of its complexity. For this reason, the concept of "effective width" was introduced by von Karman et al. in 1932. In this approach, instead of considering the non-uniform distribution of stress, $\sigma_x(y)$, over the entire width of the plate b_f it was assumed that the total load, P, is carried by a fictitious effective width, b_{eff}, subjected to a uniformly distributed stress equal to the edge stress, σ_{max}, as shown in Figure 4.21. The width b_{eff} is selected so that the area under the curve of the actual non-uniform stress distribution is equal to the sum of the two parts of the equivalent rectangular shaded area with a total width b_{eff} and an intensity of stress equal to the edge stress σ_{max}, that is:

$$P = \sigma_{med} \cdot b \cdot t = \int_0^b \sigma_x(y) \cdot t \cdot dy = \sigma_{max} \cdot b_{eff} \cdot t \tag{4.4}$$

The magnitude of effective width, b_{eff}, changes as the magnitude of σ_{max}, changes (see Figure 4.22). Therefore the minimum effective width results when σ_{max} equals to f_y (see Figure 4.20c).

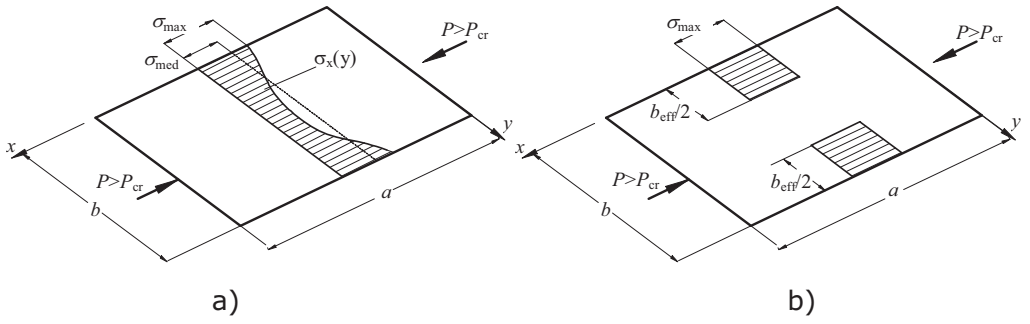

Figure 4.21 Stress distribution in simply supported plate, uniaxially compressed: (a) actual stress distribution; (b) equivalent stress distribution based on the "effective width" approach

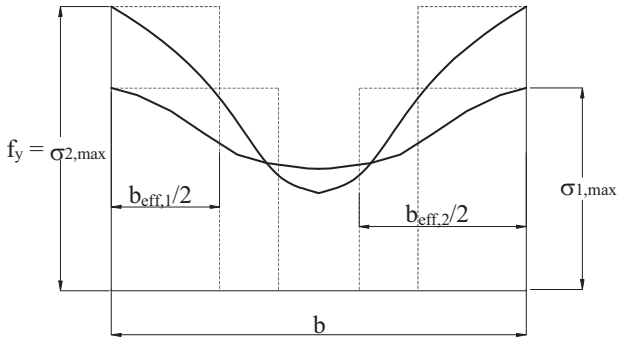

Figure 4.22 Change of effective width in terms of maximum edge stress

In the limit $\sigma_{max}=f_y$, it may also be considered that the effective width b_{eff} represents a particular width of the plate for which the plate strength is achieved when the applied stress ($\sigma_{max}=f_y$) causes buckling. Therefore for a long plate, the value of b_{eff} to be used for strength design may be determined from Eqn. (4.6) as follows:

$$\sigma_{\max} = f_y = \frac{k_\sigma \cdot \pi^2 \cdot E}{12 \cdot (1-\nu^2) \cdot (b_{eff} / t)^2} = \sigma_{cr,eff} \tag{4.5}$$

or

$$b_{eff} = \frac{\sqrt{k_\sigma} \cdot \pi}{\sqrt{12 \cdot (1-\nu^2)}} \cdot t \cdot \sqrt{\frac{E}{f_y}} \tag{4.6}$$

or

$$b_{eff} = C \cdot t \cdot \sqrt{\frac{E}{f_y}} \tag{4.7}$$

where

$$C = \sqrt{k_\sigma \cdot \pi^2 / 12 \cdot (1-\nu^2)} \tag{4.8}$$

is a constant for a given type of plate element, depending of the value of buckling coefficient, k_σ.

If k_σ = 4 and ν = 0,3, C = 1,9, Eqn. (4.7) becomes:

$$b_{eff} = 1,9 \cdot t \cdot \sqrt{\frac{E}{f_y}} \tag{4.9}$$

which represents the von Karman formula for the design of stiffened elements as derived in 1932.

Since the critical elastic buckling stress of the complete plate is given by,

$$\sigma_{cr} = \frac{k_\sigma \cdot \pi^2 \cdot E}{12 \cdot (1 - \nu^2) \cdot (b / t)^2} \tag{4.10}$$

then, by substitution

$$\frac{b_{eff}}{b} = \sqrt{\frac{\sigma_{cr}}{f_y}} \tag{4.11}$$

The relative or reduced plate slenderness, $\bar{\lambda}_p$, is defined as:

$$\bar{\lambda}_p = \sqrt{\frac{f_y}{\sigma_{cr}}} = \frac{1,052}{\sqrt{k}} \cdot \frac{b}{t} \cdot \sqrt{\frac{f_y}{E}} = \frac{b / t}{28,4 \cdot \varepsilon \cdot \sqrt{k}} \tag{4.12}$$

where $\varepsilon = \sqrt{235 / f_y}$

At the end, the effective width, b_{eff}, of a thin wall (e.g. plate) in compression, of width b, is calculated with the following formula:

$$b_{eff} = \rho \cdot b \tag{4.13}$$

where

$$\rho = \frac{b_{eff}}{b} = \frac{1}{\bar{\lambda}_p} \leq 1 \tag{4.14}$$

and is the reduction factor of the plate within the post-buckling range.

Eqn. (4.13) is in fact another form of the initial von Karman formula given by Eqn. (4.6). Eqn. (4.11) gives the effective width in the ultimate limit state. In the intermediate post-buckling stage, when $\sigma_{cr} < \sigma_{max} < f_y$, the effective width can be obtained from:

$$b_{eff} = C \cdot t \cdot \sqrt{\frac{E}{\sigma_{\max}}} \tag{4.15}$$

or

$$\frac{b_{eff}}{b} = \sqrt{\frac{\sigma_{cr}}{\sigma_{\max}}} \tag{4.16}$$

with the corresponding relative slenderness of the plate defined as,

$$\bar{\lambda}_p = \sqrt{\frac{\sigma_{\max}}{\sigma_{cr}}} \tag{4.17}$$

Eqn. (4.8) for C, which for plates simply supported on both longitudinal edges (i.e. k_σ=4) leads to the value of 1,9, was confirmed by test of plates with large b/t ratios.

Consequently, for plates with intermediate *b*/*t* ratios, in 1946 Winter proposed to replace the expression for *C* with:

$$C = 1,9 \cdot \left[1 - 0,415 \cdot \left(\frac{t}{b} \right) \cdot \sqrt{\frac{E}{f_y}} \right] \tag{4.18}$$

which leads to the well-known effective width equation

$$\rho = \frac{b_{eff}}{b} = \sqrt{\frac{\sigma_{cr}}{f_y}} \cdot \left(1 - 0,22 \cdot \sqrt{\frac{\sigma_{cr}}{f_y}} \right) \leq 1 \tag{4.19}$$

or, in terms of relative plate slenderness, $\overline{\lambda}_p$,

$$\rho = \frac{b_{eff}}{b} = \frac{1}{\overline{\lambda}_p} \cdot \left(1 - \frac{0,22}{\overline{\lambda}_p} \right) \tag{4.20}$$

The effective width depends on both edge stress σ_{max} and *b/t* ratio. The plate is fully effective when ρ = 1, i.e. $b = b_{eff}$. It is easy to show that this happens when $\overline{\lambda}_p \leq 0,673$ (see Figure 4.23) or

$$\frac{b}{t} < \left(\frac{b}{t} \right)_{\text{lim}} = 16,69 \cdot \varepsilon \cdot \sqrt{k_\sigma} \tag{4.21}$$

with

$$\varepsilon = \sqrt{235 / f_y} \tag{4.22}$$

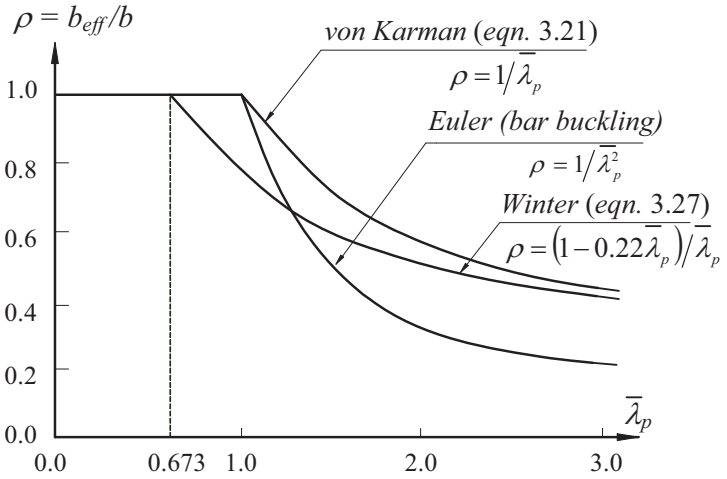

Figure 4.23 Reduction factor, ρ, vs. relative plate slenderness, $\overline{\lambda}_p$, relationship

If k_σ=4 and k_σ=0,425 are substituted into Eqn. (4.21) for simply supported edge stiffened or web type plate elements, and for unstiffened plate elements with a free

longitudinal edge, or flange type elements, respectively, the following limiting *b/t* ratios are obtained:

- web type elements

$$\left(\frac{b}{t}\right)_{\lim} = 38,3 \cdot \varepsilon \tag{4.23}$$

- flange type elements

$$\left(\frac{b}{t}\right)_{\lim} = 12,5 \cdot \varepsilon \tag{4.24}$$

The limiting *b/t* ratios for the usual steel grades S235, S275 and S355 are shown in Table 4.4.

The effective or equivalent width method leads to simple design rules and gives an indication of the behaviour of the plate as the ultimate condition is approached.

The Winter formula (4.20) for the effective width is actually used in the major design code provisions for thin-walled steel structures (EN1993-1-3:2006, AISI S100-07, AS/NZS 4600:2005). Despite its semi-empirical nature, the Winter formula leads to quite satisfactory results for stiffened (web type) plate elements. However, for unstiffened (flange type) plate elements, this formula used with a buckling coefficient equal to 0,425 or 0,43 is too conservative both for strength and stiffness.

The effective widths of compression elements shall be obtained from Table 4.5 for doubly supported compression elements or Table 4.6 for outstand compression elements (EN1993-1-5:2006).

The notional flat width b_p of a plane element shall be determined as specified in EN1993-1-3:2006. In the case of plane elements in sloping webs, the appropriate slant height shall be used.

Table 4.4 $(b/t)_{lim}$ values for stiffened and unstiffened plate elements

Steel grade	f_y (N/mm^2)	Type of plate element	
		Stiffened	Unstiffened
S235	235	38	12,5
S275	275	35	11,5
S355	355	31	10

The reduction factor ρ used in Table 4.5 and Table 4.6 to determine b_{eff} shall be based on the largest compressive stress $\sigma_{com,Ed}$ in the relevant element (calculated on the basis of the effective cross-section and taking account of possible second order effects), when the resistance of the cross-section is reached.

If $\sigma_{com,Ed} = f_{yb} / \gamma_{M0}$ the reduction factor ρ should be obtained according to EN1993-1-5, from the following:

- internal compression elements:

$$\rho = 1 \quad \text{for} \quad \bar{\lambda}_p \le 0,5 + \sqrt{0,085 - 0,055\psi} \tag{4.25a}$$

$$\rho = \frac{\bar{\lambda}_p - 0,055\,(3+\psi)}{\bar{\lambda}_p^2} < 1,0 \quad \text{for} \quad \bar{\lambda}_p > 0,5 + \sqrt{0,085 - 0,055\psi} \tag{4.25b}$$

Table 4.5 Internal compression elements

Stress distribution (compression positive)	**Effective width b_{eff}**
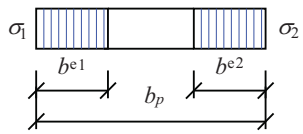	$\psi = 1$ $b_{eff} = \rho \cdot b_p$ $b_{e1} = 0,5 \cdot b_{eff}$; $b_{e2} = 0,5 \cdot b_{eff}$
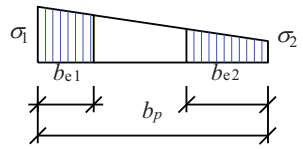	$1 > \psi \ge 0$ $b_{eff} = \rho \cdot b_p$ $b_{e1} = \frac{2}{5-\psi} \cdot b_{eff}$; $b_{e2} = b_{eff} - b_{e1}$
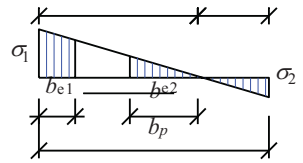	$\psi < 0$ $b_{eff} = \rho \cdot b_c = \rho b_p / (1-\psi)$ $b_{e1} = 0,4 \cdot b_{eff}$; $b_{e2} = 0,6 b_{eff}$

$\psi = \sigma_2 / \sigma_1$	**1**	**1> ψ >0**	**0**	**0> ψ >-1**	**-1**	**-1> ψ >-3**
Buckling factor, k_σ	**4,0**	**8,2/(1,05+ ψ)**	**7,81**	**7,81-6,29 ψ +9,78 ψ^2**	**23,9**	**5,98(1- ψ)²**

- outstand compression elements (flange type):

$$\rho = 1 \quad \textit{for} \quad \bar{\lambda}_p \le 0,748 \tag{4.26a}$$

$$\rho = \frac{\bar{\lambda}_p - 0,188}{\bar{\lambda}_p^2} < 1,0 \quad \text{for} \quad \bar{\lambda}_p > 0,748 \tag{4.26b}$$

in which the plate slenderness $\bar{\lambda}_p$ is given by:

$$\bar{\lambda}_p = \sqrt{\frac{f_{yb}}{\sigma_{cr}}} = \frac{b_p/t}{28,4 \cdot \varepsilon \cdot \sqrt{k_\sigma}} \tag{4.27}$$

where:

k_σ is the relevant buckling factor from Table 4.5 and Table 4.6;

ε is the ratio $\sqrt{235 / f_y}$ with f_{yb} in N/mm^2;

ψ is the stress ratio;

t is the thickness;

σ_{cr} is the elastic critical plate buckling stress.

Table 4.6 Outstand compression elements

<table>
<tr><th colspan="3">Stress distribution
(compression positive)</th><th colspan="3">Effective width b_{eff}</th></tr>
<tr><td colspan="3"> 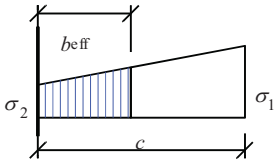

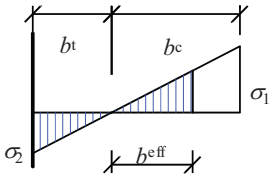
</td><td colspan="3">$1 > \psi \geq 0$
$b_{eff} = \rho \cdot c$

$\psi < 0$
$b_{eff} = \rho \cdot b_c = \rho b_p / (1 - \psi)$</td></tr>
<tr><td>$\psi = \sigma_2 / \sigma_1$</td><td>1</td><td>0</td><td>-1</td><td colspan="2">$-1 > \psi > -3$</td></tr>
<tr><td>Buckling factor, k_σ</td><td>0,43</td><td>0,57</td><td>0,85</td><td colspan="2">$0,57 - 0,21\ \psi + 0,07\ \psi^2$</td></tr>
<tr><td colspan="3"> 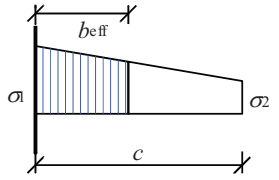

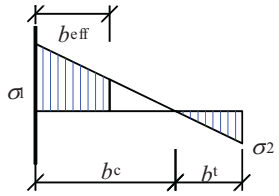
</td><td colspan="3">$1 > \psi \geq 0$
$b_{eff} = \rho \cdot c$

$\psi < 0$
$b_{eff} = \rho \cdot b_c = \rho b_p / (1 - \psi)$</td></tr>
<tr><td>$\psi = \sigma_2 / \sigma_1$</td><td>1</td><td>$1 > \psi > 0$</td><td>0</td><td>$0 > \psi > -1$</td><td>-1</td></tr>
<tr><td>Buckling factor, k_σ</td><td>0,43</td><td>$0,578/(\psi + 0,24)$</td><td>1,70</td><td>$0,57 - 0,21\ \psi + 0,07\ \psi^2$</td><td>23,8</td></tr>
</table>

If $\sigma_{com,Ed} < f_{yb}/\gamma_{M0}$ the reduction factor ρ should be determined in a similar manner, but the reduced plate slenderness $\bar{\lambda}_{p.red}$ is given by:

$$\bar{\lambda}_{p.red} = \bar{\lambda}_p \cdot \sqrt{\frac{\sigma_{com,Ed}}{f_{yb} / \gamma_{M0}}} \tag{4.28}$$

However, when verifying the design buckling resistance of a member or performing a second order system analysis, for calculating the values of $A_{eff}f$, e_N and W_{eff} the plate slenderness $\bar{\lambda}_p$ of an element should be based either on its yield strength f_y or on $\sigma_{com,Ed}$ based on a 2nd order system analysis.

The application of the second approach generally requires an iterative procedure for the second order calculation in which the internal forces and moments are determined with the effective cross-sections defined with the internal forces and moments determined from the previous iteration. For effective width calculation at the serviceability limit states the reduction factor ρ should be determined in a similar manner, but using the reduced plate slenderness $\bar{\lambda}_{p.ser}$ given by:

$$\bar{\lambda}_{p.ser} = \bar{\lambda}_p \cdot \sqrt{\frac{\sigma_{com,Ed,ser}}{f_{yb}}} \tag{4.29}$$

where:

$\sigma_{com,Ed,ser}$ is the largest compressive stress in the relevant element (calculated on the basis of the effective cross-section) under the serviceability limit state loading.

EN1993-1-3 contains detailed rules for evaluation of effective properties of cross-sections with edge and/or intermediate stiffeners of compression and/or bending stresses.

In determining the effective width of a flange element subject to stress gradient, the stress ratio ψ used in Table 4.5 and Table 4.6 may be based on the properties of the gross cross-section.

In determining the effective width of a web element the stress ratio ψ used in Table 4.5 may be obtained using the effective area of the compression flange but the gross area of the web.

4.3.4.3 Distortional buckling

Intuition for local buckling behaviour is relatively straightforward: as width-to-thickness (*b/t*) ratios increase, the local buckling critical stress becomes lower. This fact serves the engineer well in designing for local buckling. A similar intuition for distortional buckling is not as straightforward.

Distortional buckling of compression members with C cross-sections is governed by the rotational stiffness at the web/flange junction; deeper webs are more flexible and thus provide less rotational stiffness to the web/flange juncture. This results in earlier distortional buckling for deep webs. If the flange is narrow, local buckling of the web occurs at wavelengths close to distortional buckling of the flange and the distortional mode forms at lower stresses than local buckling. If the flange is excessively wide, local buckling is not the concern, but rather the size of the stiffener require to keep the flange in place is the concern. For practical stiffener lengths, wide flange also lead to low

distortional stresses. Longer lips are beneficial against flange distortion but become too sensitive for local buckling.

The wavelength of distortional buckling is generally intermediate between those of local and overall modes, like Figure 4.24 shows.

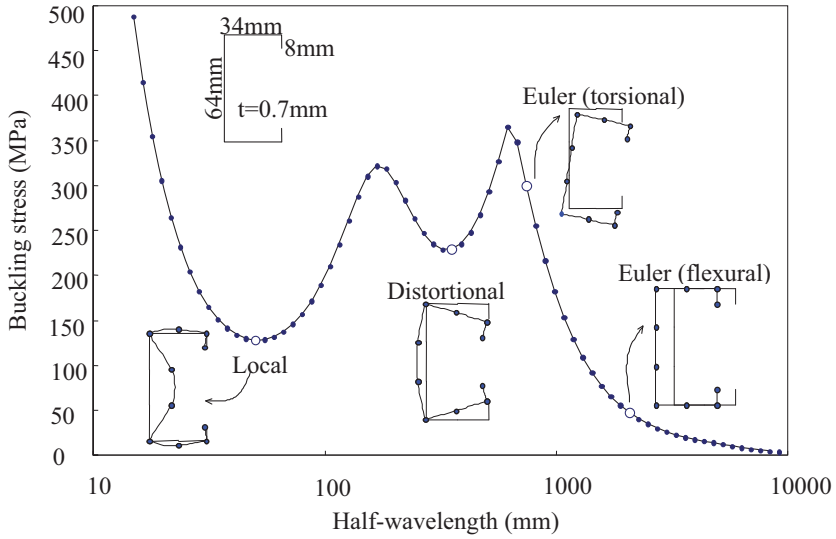

Figure 4.24 Elastic buckling modes vs. half-wavelengths curve for a lipped channel column (Finite Strip Analysis by Schafer, 2001)

Manual calculation methods for predicting the elastic distortional buckling stress of simple sections such as C- and rack-sections have been presented, e.g. by Lau and Hancock (1987) and Schafer and Peköz (1999). However, manual calculation methods for distortional buckling are relatively cumbersome. Numerical methods, such as the finite element method (FEM), or the finite strip method (FSM) have been found to be efficient methods for determining elastic buckling stresses for both local and distortional buckling. The finite strip method has proved to be a useful approach because it has a short solution time compared to the finite element method and does not require discretisation in the longitudinal direction. The finite strip method assumes simply supported end boundary conditions and is applicable to longer sections where multiple half-waves occur along the section length.

Generalized Beam Theory (GBT) is an extension of conventional engineering beam theory, allowing cross-section distortion to be considered (Silvestre and Camotim, 2002a Silvestre and Camotim, 2002b, Silvestre and Camotim, 2003). It has a short solution time and the method is applicable for both pin-ended and fixed-ended members. A user friendly GBT program has been developed at the Technical University of Lisbon called GBTUL (http://www.civil.ist.utl.pt/gbt/), which performs elastic buckling and vibration analyses of prismatic thin-walled members.

An alternative program to perform the elastic buckling analysis of thin-walled members is CUFSM (http://www.ce.jhu.edu/bschafer/cufsm/). CUFSM employs the semi-analytical finite strip method to provide solutions for the cross-section stability of thin-walled members (Schafer and Ádány, 2006).

EN1993-1-3:2006 does not provide explicit provisions for distortional buckling. However, a calculation procedure can be obtained from the interpretation of the rules given in the code for plane elements with edge or intermediate stiffeners in compression.

The design of compression elements with either edge or intermediate stiffeners is based on the assumption that the stiffener behaves as a compression member with continuous partial restraint. This restraint has a spring stiffness that depends on the boundary conditions and the flexural stiffness of the adjacent plane elements of the cross-section. The spring stiffness of the stiffener may be determined by applying a unit load per unit length to the cross-section at the location of the stiffener, as illustrated in Figure 4.25. The rotational spring stiffness C_θ characterizes the bending stiffness of the web part of the section. The spring stiffness K per unit length may be determined from:

$$K = u / \delta \tag{4.30}$$

where δ is the deflection of the stiffener due to the unit load u.

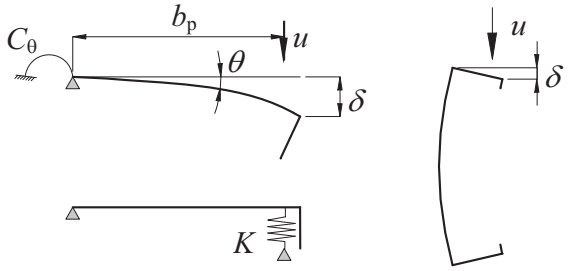

Figure 4.25 Determination of the spring stiffness *K* according to EN1993-1-3

The elastic critical buckling stress for a long strut on an elastic foundation, in which the preferred wavelength is free to develop, is given by Timoshenko and Gere (1961):

$$\sigma_{cr} = \frac{\pi^2 \cdot E \cdot I_s}{A_s \cdot \lambda^2} + \frac{I}{A_s \cdot \pi^2} K \cdot \lambda^2 \tag{4.31}$$

where

A_s and I_s are the effective cross-sectional area and second moment of area of the stiffener according to EN1993-1-3, as illustrated in Figure 4.26 for an edge stiffener;

$\lambda = L / m$ is the half-wavelength; m is the number of half-wavelengths.

The preferred half-wavelength of buckling for a long strut can be derived from Eqn. (4.31) by minimizing the critical stress:

$$\lambda_{cr} = \sqrt[4]{\frac{E \cdot I_s}{K}} \tag{4.32}$$

For an infinitely long strut, the critical buckling stress can be derived, after substitution, as:

$$\sigma_{cr} = \frac{2 \cdot \sqrt{K \cdot E \cdot I_s}}{A_s} \tag{4.33}$$

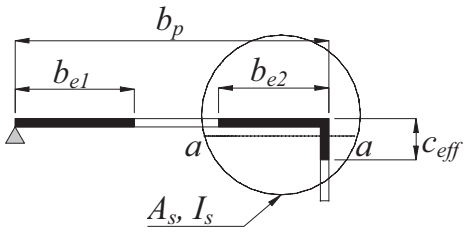

Figure 4.26 Effective cross-sectional area of an edge stiffener

Eqn. (4.33) is given in EN1993-1-3; thus, this method does not consider the effect of column length but assumes that it is sufficiently long for integer half-waves to occur. In the case of intermediate stiffeners, the procedure is similar, but the rotational stiffness due to adjacent plane elements is ignored and the stiffened plane element is assumed to be simply supported.

In fact, for elements with edge or intermediate stiffeners, the design against distortional buckling is limited to the checking of stiffener effectiveness. For more complete analysis, the code gives freedom for the designer to use numerical methods.

4.3.5 Design against local and distortional buckling according to EN1993-1-3

4.3.5.1 General scheme

According to EN1993-1-3, the followings general provisions must be considered when a section is designed against local or distortional buckling:

- the effects of local and distortional buckling shall be taken into account in determining the resistance and stiffness of cold-formed members and sheeting;
- local buckling effects may be accounted for by using effective cross-sectional properties, calculated on the basis of the effective widths of those elements that are prone to local buckling;
- the possible shift of the centroid axis of the effective cross-section relative to the centroid axis of the gross cross-section shall be taken into account;
- in determining resistance to local buckling, the yield strength f_y should be taken as f_{yb};
- in determining the resistance of a cross-section, the effective width of a compression element should be based on the compressive stress $\sigma_{com,Ed}$ in the element when the cross-section resistance is reached;
- two cross-sections are used in design: gross cross-section and effective cross-section of which the latter varies as a function of loading (compression, major axis bending etc.);
- for serviceability verifications, the effective width of a compression element should be based on the compressive stress $\sigma_{com,Ed,ser}$ in the element under the serviceability limit state loading;
- distortional buckling shall be taken into account where it constitutes the critical failure mode.

4.3.5.2 Plane elements with edge or intermediate stiffeners

The design of compression elements with edge or intermediate stiffeners shall be based on the assumption that the stiffener behaves as a compression member with continuous partial restraint, with a spring stiffness that depends on the boundary conditions and flexural stiffness of the adjacent plane elements.

The spring stiffness of a stiffener should be determined by applying a unit load per unit length u as illustrated in Figure 4.27. The spring stiffness K per unit length may be determined from:

$$K = u / \delta \tag{4.34}$$

where:

δ is the deflection of the stiffener due to the unit load u acting at the centroid (b_1) of the effective part of the stiffened part of the cross-section.

In determining the values of the rotational spring stiffnesses C_θ, $C_{\theta 1}$ and $C_{\theta 2}$ from the geometry of the cross-section, account should be taken of the possible effects of other stiffeners that exist in the same element, or on any other element of the cross-section that is subject to compression.

For an edge stiffener, the deflection δ should be obtained from:

$$\delta = \theta \cdot b_p + \frac{u \cdot b_p^3}{3} \cdot \frac{12 \cdot \left(1 - \nu^2\right)}{E \cdot t^3} \tag{4.35}$$

with

$$\theta = u \cdot b_p / C_\theta \tag{4.36}$$

In the case of the edge stiffeners of lipped C-sections and lipped Z-sections, C_θ should be determined with the unit loads u applied as shown in Figure 4.27c.

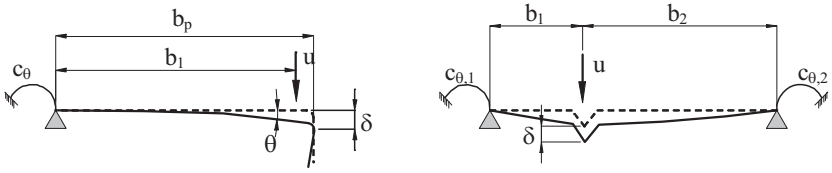

a) Actual system

b) Equivalent system

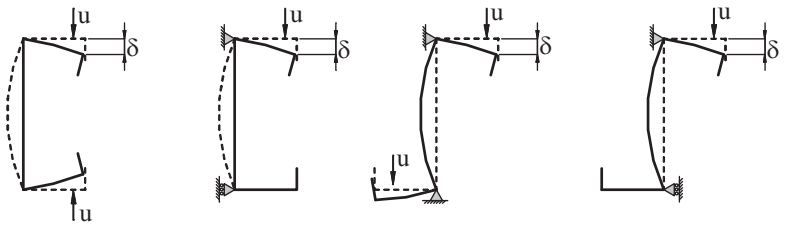

Compression Bending Bending Compression

c) Calculation of δ for C and Z sections

Figure 4.27 Determination of spring stiffness

This results in the following expression for the spring stiffness K_1 for the flange 1:

$$K_1 = \frac{E \cdot t^3}{4 \cdot (1 - \nu^2)} \cdot \frac{1}{b_1^2 \cdot h_w + b_1^3 + 0,5 \cdot b_1 \cdot b_2 \cdot h_w \cdot k_f} \tag{4.37}$$

where

b_1 is the distance from the web-to-flange junction to the gravity centre of the effective area of the edge stiffener (including the effective part b_{e2} of the flange) of flange 1 (see Figure 4.27a);

b_2 is the distance from the web-to-flange junction to the gravity centre of the effective area of the edge stiffener (including the effective part of the flange) of flange 2;

h_w is the web depth;

$k_f = 0$ if flange 2 is in tension (e.g. for a beam in bending about the y-y axis);

$k_f = A_{s2}/A_{s1}$ if flange 2 is in compression (e.g. for a member in axial compression);

$k_f = 1$ for a symmetric section in compression;

A_{s1} and A_{s2} are the effective area of the edge stiffener (including the effective part b_{e2} of the flange, see Figure 4.27b) of flange 1 and flange 2 respectively.

For an intermediate stiffener, the values of the rotational spring stiffnesses $C_{\theta 1}$ and $C_{\theta 2}$ may conservatively be taken as equal to zero, and the deflection δ may be obtained from:

$$\delta = \theta \cdot b_p + \frac{u \cdot b_1^2 \cdot b_2^2}{3 \cdot (b_1 + b_2)} \cdot \frac{12 \cdot (1 - \nu^2)}{E \cdot t^3} \tag{4.38}$$

The reduction factor χ_d for the distortional buckling resistance (flexural buckling of a stiffener) should be obtained from the relative slenderness $\bar{\lambda}_d$ from:

$$\chi_d = 1 \quad \text{if} \quad \bar{\lambda}_d \le 0,65 \tag{4.39a}$$

$$\chi_d = 1,47 - 0,723\bar{\lambda}_d \quad \text{if} \quad 0,65 < \bar{\lambda}_d \le 1,38 \tag{4.39b}$$

$$\chi_d = \frac{0,66}{\bar{\lambda}_d} \quad \text{if} \quad \bar{\lambda}_d \ge 1,38 \tag{4.39c}$$

and

$$\bar{\lambda}_d = \sqrt{f_{yb} / \sigma_{cr,s}} \tag{4.39d}$$

where:

$\sigma_{cr,s}$ is the elastic critical stress for the stiffener(s)

In the case of a plane element with an edge and intermediate stiffener(s), in the absence of a more accurate method the effect of the intermediate stiffener(s) may be neglected.

The cross-section of an edge stiffener should be taken as comprising the effective portions of the stiffener (element *c* or elements *c* and *d* as shown in Figure 4.28) plus the adjacent effective portion, b_{e2}, of the plane element b_p.

An edge stiffener shall not be taken into account in determining the resistance of the plane element to which it is attached unless the following conditions are met:

- the angle between the stiffener and the plane element is between 45° and 135°;
- the outstand width *c* is not less than 0,2*b*, where *b* and *c* are as shown in Figure 4.28;
- the *b*/*t* ratio is not more than 60^0 for a single edge fold stiffener, or 90^0 for a double edge fold stiffener.

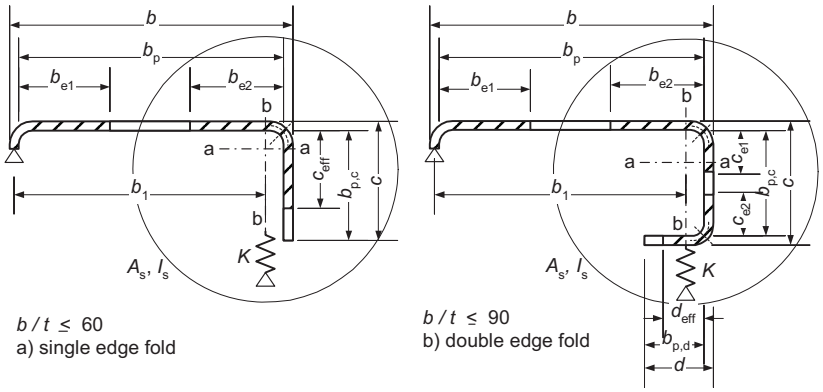

Figure 4.28 Edge stiffeners

The procedure, which is illustrated in Figure 4.29 and presented schematically in Figure 4.30 and Figure 4.31 , should be carried out in steps as follows:

Step 1: Obtain an initial effective cross-section for the stiffener using effective widths determined by assuming that the stiffener gives full restraint and that $\sigma_{com,Ed} = f_{yb} / \gamma_{M0}$;

Step 2: Use the initial effective cross-section of the stiffener to determine the reduction factor for distortional buckling (flexural buckling of the stiffener), allowing for the effects of the continuous spring restraint;

Step 3: Optionally iterate to refine the value of the reduction factor for buckling of the stiffener.

Initial values of the effective widths b_{e1} and b_{e2} shown in Figure 4.28 should be determined from §§4.3.4.2 by assuming that the plane element b_p is supported on both longitudinal edges (see Table 4.5).

Initial values of the effective widths c_{eff} and d_{eff} shown in Figure 4.28 should be obtained as follows:

- for a single edge fold stiffener:

$$c_{eff} = \rho \cdot b_{p,c} \tag{4.40a}$$

with ρ obtained from §§4.3.4.2, except using a value of the buckling factor k_σ given by:

- if $b_{p,c} / b_p \le 0,35$

$$k_\sigma = 0,5 \tag{4.40b}$$

- if $0,35 < b_{p,c} / b_p \le 0,6$

$$k_\sigma = 0,5 + \sqrt[3]{\left(b_{p,c} / b_p - 0,35\right)^2} \tag{4.40c}$$

- for a double edge fold stiffener:

$$c_{eff} = \rho \cdot b_{p,c} \tag{4.40d}$$

with ρ obtained from §§4.3.4.2, except using a value of the buckling factor k_σ for a doubly supported element as show in Table 4.5, and

$$d_{eff} = \rho \cdot b_{p,c} \tag{4.40e}$$

with ρ obtained from §§4.3.4.2, except using a value of the buckling factor k_σ for outstand element as show in Table 4.6.

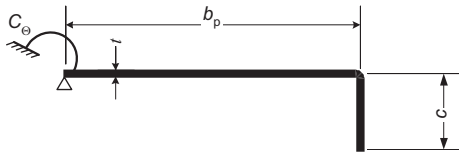	a) Gross cross-section and boundary conditions
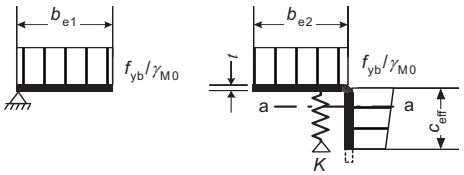	b) **Step 1**: Effective cross-section for $K = \infty$ based on $\sigma_{com,Ed} = f_{yb} / \gamma_{M0}$
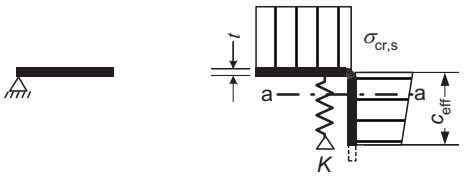	c) **Step 2**: Elastic critical stress $\sigma_{cr,s}$ for effective area of stiffener A_s from Step 1
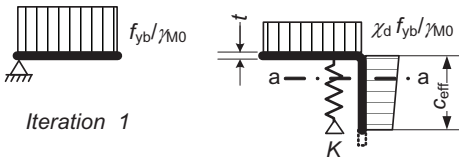	d) Reduced strength $\chi_d f_{yb}/\gamma_{M0}$ for effective area of stiffener A_s, with reduction factor χ_d based on $\sigma_{cr,s}$
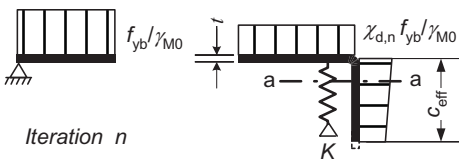	e) **Step 3**: Optionally repeat Step 1 by calculating the effective width with a reduced compressive stress $\sigma_{com,Ed,I} = \chi_d f_{yb} / \gamma_{M0}$ with χ_d from previous iteration, continuing until $\chi_{d,n} \approx \chi_{d,(n-1)}$ but $\chi_{d,n} \leq \chi_{d\ d,(n-1)}$
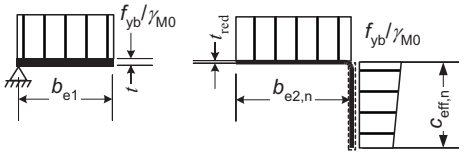	f) Adopt an effective cross-section with b_{e2} , c_{eff} and reduced thickness t_{red} corresponding to $\chi_{d,n}$

Figure 4.29 Compression resistance of a flange with an edge stiffener

The effective cross-sectional area of the edge stiffener A_s should be obtained from:

$$A_s = t\,(b_{e2} + c_{eff}) \tag{4.41a}$$

$$A_s = t\,(b_{e2} + c_{e1} + c_{e2} + d_{eff}) \tag{4.41b}$$

The elastic critical buckling stress $\sigma_{cr,s}$ for an edge stiffener should be obtained from:

$$\sigma_{cr,s} = \frac{2 \cdot \sqrt{K \cdot E \cdot I_s}}{A_s} \tag{4.42}$$

where:

K is the spring stiffness per unit length;

I_s is the effective second moment of area of the stiffener, taken as that of its effective area A_s about the centroid axis a - a of its effective cross-section, see Figure 4.28.

The reduction factor χ_d for the distortional buckling (flexural buckling of a stiffener) resistance of an edge stiffener should be obtained from the value of $\sigma_{cr,s}$ using the method given before.

If $\chi_d < 1$ the effective area calculation may be refined iteratively, starting with modified values of ρ obtained using the formulas from §§4.3.4.2 with $\sigma_{com,Ed,i}$ equal to $\chi_d f_{yb}/\gamma_{M0}$:

$$\overline{\lambda}_{p,red} = \overline{\lambda}_p \cdot \sqrt{\chi_d} \tag{4.43}$$

The reduced effective area of the stiffener $A_{s,red}$ allowing for flexural buckling should be taken as:

$$A_{s,red} = \chi_d \cdot A_s \cdot \frac{f_{yb} / \gamma_{M0}}{\sigma_{com,Ed}} \quad \text{but} \quad A_{s,red} \le A_s \tag{4.44}$$

where

$\sigma_{com,Ed}$ is compressive stress at the centreline of the stiffener calculated on the basis of the effective cross-section.

4.3.5.3 Design example

Figure 4.30 and Figure 4.31 present schematically the calculation of effective section properties for cold-formed steel sections under bending or compression.

In determining effective section properties, the reduced effective area $A_{s,red}$ should be represented by using a reduced thickness $t_{red} = t \cdot A_{red} / A_s$ for all the elements included in A_s.

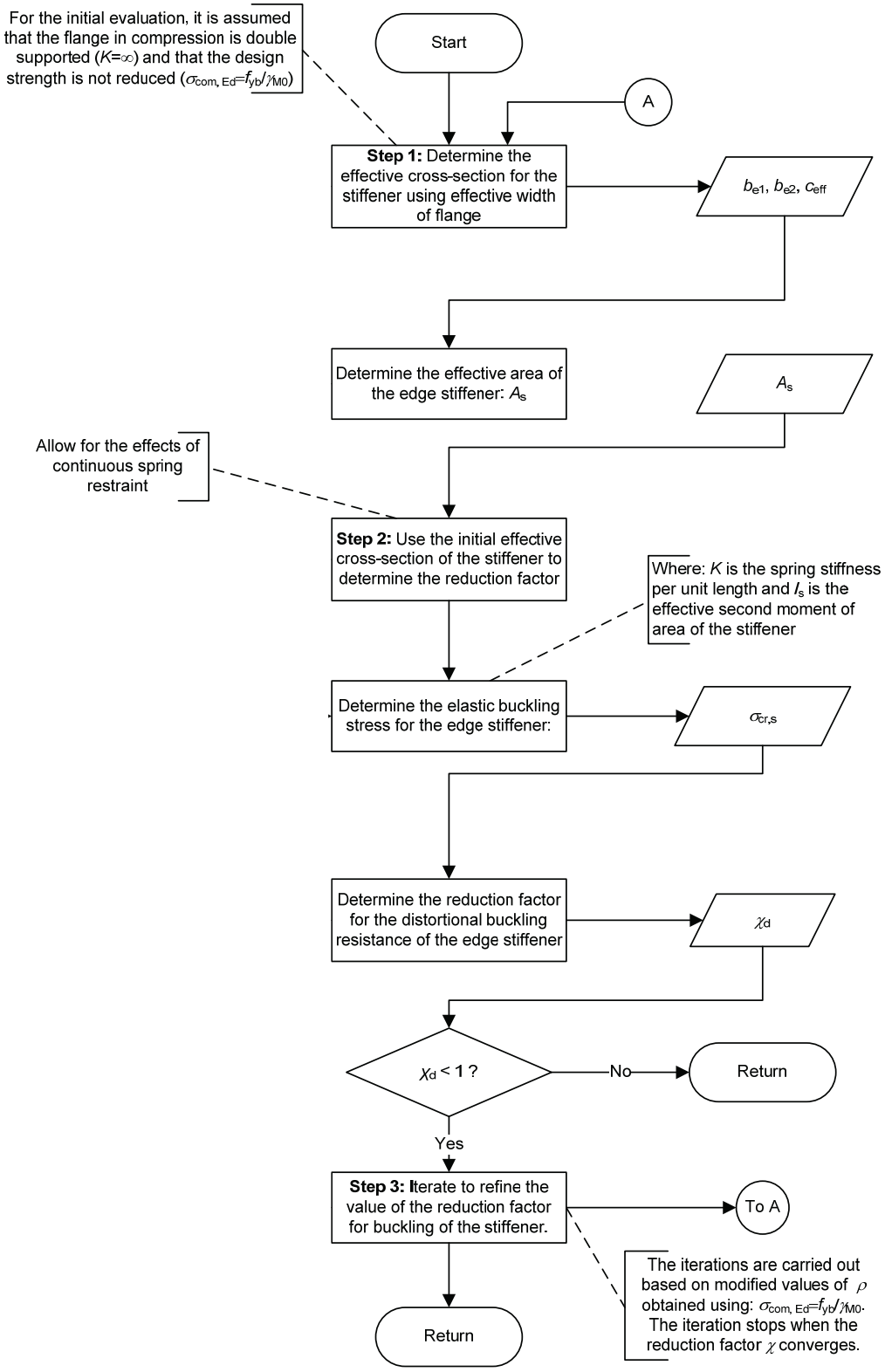

Figure 4.30 Effective section properties of the flange and lip in compression – General (iterative) procedure (SF038a-EN-EU, AccessSteel 2006)

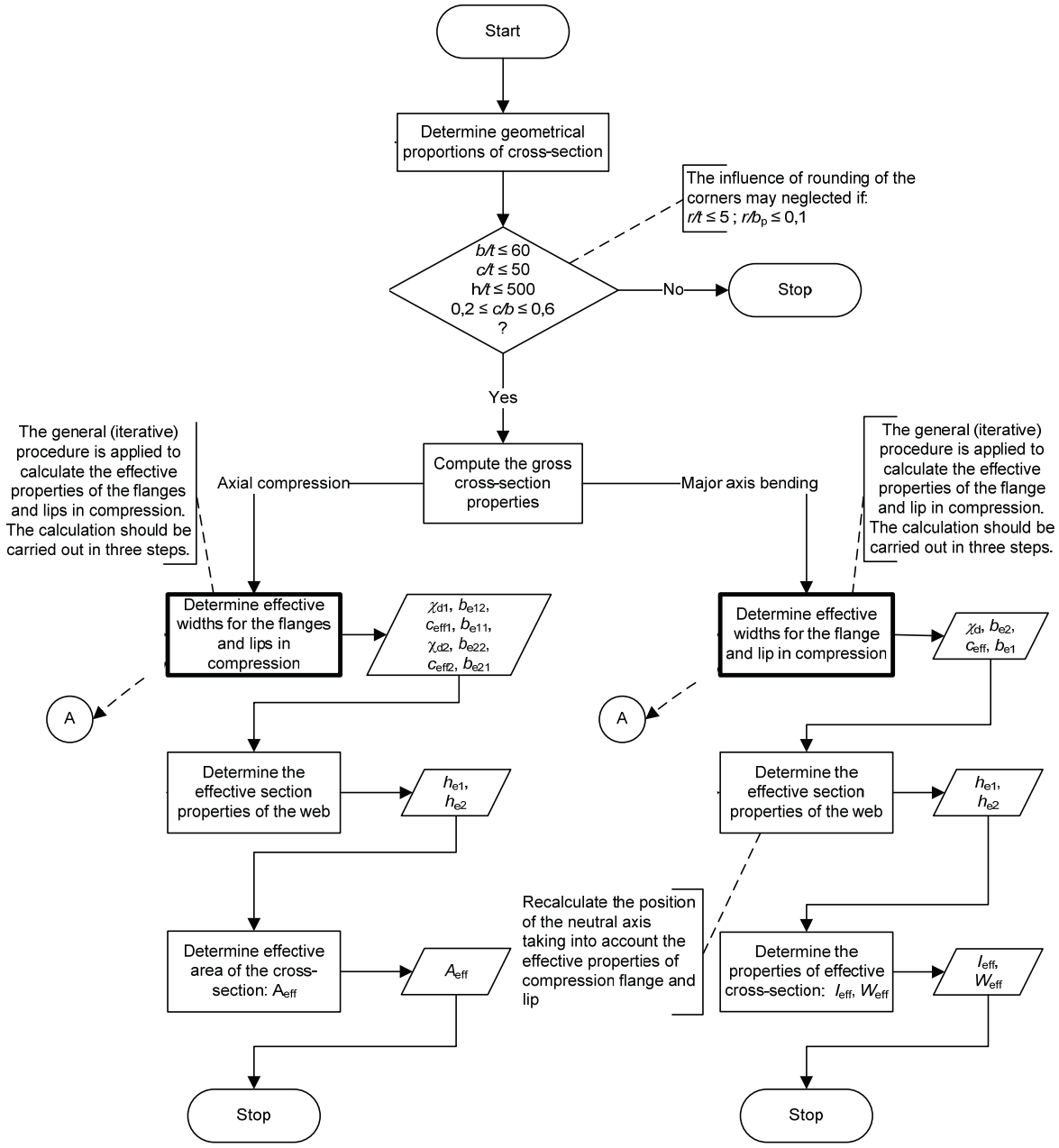

Figure 4.31 Calculation of effective section properties for cold-formed steel sections under compression or bending (SF038a-EN-EU, AccessSteel 2006)

Basic Data

The dimensions of the cross-section and the material properties are:

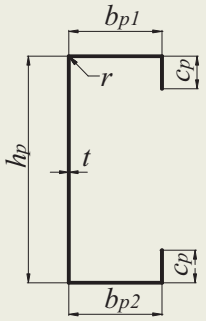

Total height	$h = 150$ mm
Total width of flange in compression	$b_1 = 47$ mm
Total width of flange in tension	$b_2 = 41$ mm
Total width of edge fold	$c = 16$ mm
Internal radius	$r = 3$ mm
Nominal thickness	$t_{nom} = 1$ mm
Steel core thickness (§§2.4.2.3)	$t = 0,96$ mm
Basic yield strength	$f_{yb} = 350$ N/mm^2
Modulus of elasticity	$E = 210\,000$ N/mm^2
Poisson's ratio	$\nu = 0,3$
Partial factor	$\gamma_{M0} = 1,00$
Web height	$h_p = h - t_{nom} = 150 - 1 = 149$ mm
Width of flange in compression	$b_{p1} = b_1 - t_{nom} = 47 - 1 = 46$ mm
Width of flange in tension	$b_{p2} = b_2 - t_{nom} = 41 - 1 = 40$ mm
Width of edge fold	$c_p = c - t_{nom}/2 = 16 - 1/2 = 15,5$mm

Checking of geometrical proportions

The design method of EN1993-1-3 can be applied if the following conditions are satisfied:

$b/t \le 60$	$b_1/t = 47/0,96 = 48,96 < 60$	– OK
$c/t \le 50$	$c/t = 16/0,96 = 16,67 < 50$	– OK
$h/t \le 500$	$h/t = 150/0,96 = 156,25 < 500$	– OK

In order to provide sufficient stiffness and to avoid primary buckling of the stiffener itself, the size of stiffener should be within the following range:

$0,2 \le c/b \le 0,6$	$c/b_1 = 16/47 = 0,34$	$0,2 < 0,34 < 0,6$ – OK
	$c/b_2 = 16/41 = 0,39$	$0,2 < 0,39 < 0,6$ – OK

The influence of rounding of the corners is neglected if (§§3.2.1, Eqn. (3.2)):

$r/t \le 5$	$r/t = 3/0,96 = 3,125 < 5$	– OK
$r/b_p \le 0,10$	$r/b_{p1} = 3/47 = 0,06 < 0,10$	– OK
	$r/b_{p2} = 3/41 = 0,07 < 0,10$	– OK

Gross cross-section properties

$$A_{br} = t\left(2c_p + b_{p1} + b_{p2} + h_p\right) = 0,96 \times \left(2 \times 15,5 + 46 + 40 + 149\right) = 255,36 \text{ mm}^2$$

Position of the neutral axis with respect to the flange in compression:

$$z_{b1} = \frac{\left[c_p\left(h_p - c_p/2\right) + b_{p2}h_p + h_p^2/2 + c_p^2/2\right]t}{A_{br}} = 72,82 \text{ mm}$$

Effective section properties of the flange and lip in compression

The general (iterative) procedure is applied to calculate the effective properties of the compressed flange and the lip (plane element with edge stiffener). The calculation should be carried out in three steps (§§3.7.3.2.2):

Step 1: Obtain an initial effective cross-section for the stiffener using effective widths of the flange determined by assuming that the compressed flange is doubly supported, the stiffener gives full restraint ($K = \infty$) and that design strength is not reduced ($\sigma_{com,Ed} = f_{yb} / \gamma_{M0}$).

Effective width of the compressed flange

The stress ratio: $\psi = 1$ (uniform compression), so the buckling factor is $k_\sigma = 4$ for internal compression element

$$\varepsilon = \sqrt{235/f_{yb}}$$

The relative slenderness:

$$\bar{\lambda}_{p,b} = \frac{b_{p1}/t}{28,4\,\varepsilon\sqrt{k_\sigma}} = \frac{46/0,96}{28,4 \times \sqrt{235/350} \times \sqrt{4}} = 1,03$$

The width reduction factor is:

$$\rho = \frac{\bar{\lambda}_{p,b} - 0,055\left(3 + \psi\right)}{\bar{\lambda}_{p,b}^{\ 2}} = \frac{1,03 - 0,055 \times \left(3 + 1\right)}{1,03^2} = 0,764 < 1$$

The effective width is:

$$b_{eff} = \rho\, b_{p1} = 0,764 \times 46 = 35,14 \text{ mm}$$

$$b_{e1} = b_{e2} = 0,5 b_{eff} = 0,5 \times 35,14 = 17,57 \text{ mm}$$

Effective width of the edge fold

The buckling factor is:

if $c_p/b_{p1} \le 0,35$: $k_\sigma = 0,5$

if $0,35 < c_p/b_{p1} \le 0,6$: $k_\sigma = 0,5 + 0,83\sqrt[3]{\left(c_p/b_{p1} - 0,35\right)^2}$

$c_p/b_{p1} = 15,5/46 = 0,337 < 0,35$ so $k_\sigma = 0,5$

The relative slenderness (§§3.7.2, Eqn. (3.38)):

$$\bar{\lambda}_{p,c} = \frac{c_p/t}{28,4\,\varepsilon\sqrt{k_\sigma}} = \frac{15,5/0,96}{28,4\times\sqrt{235/350}\times\sqrt{0,5}} = 0,981$$

The width reduction factor is:

$$\rho = \frac{\bar{\lambda}_{p,c} - 0,188}{\bar{\lambda}_{p,c}^{\,2}} = \frac{0,981 - 0,188}{0,981^2} = 0,824\,,\ \rho \le 1$$

The effective width is (§§3.7.3.2.2, Eqn. (3.47)):

$c_{eff} = \rho\, c_p = 0,824\times 15,5 = 12,77$ mm

Effective area of the edge stiffener (§§3.7.3.2.2, Eqn. (3.48)):

$A_s = t\left(b_{e2} + c_{eff}\right) = 0,96\times\left(17,57 + 12,77\right) = 29,126\ \text{mm}^2$

Step 2: Use the initial effective cross-section of the stiffener to determine the reduction factor, allowing for the effects of the continuous spring restraint.

The elastic critical buckling stress for the edge stiffener is

$$\sigma_{cr,s} = \frac{2\sqrt{K\,E\,I_s}}{A_s}$$

where:

K is the spring stiffness per unit length (§§3.7.3.1, Eqn. (3.44)):

$$K = \frac{E\,t^3}{4(1-\nu^2)}\cdot\frac{1}{b_1^{\,2}\,h_p + b_1^{\,3} + 0,5\,b_1\,b_2\,h_p\,k_f}$$

with:

b_1 – distance from the web to the centre of the effective area of the stiffener in compression (upper flange)

$$b_1 = b_{p1} - \frac{b_{e2}t\,b_{e2}/2}{(b_{e2}+c_{eff})t} = 46 - \frac{17,57\times 0,96\times 17,57/2}{(17,57+12,77)\times 0,96} = 40,913\ mm$$

$k_f = 0$ for bending about the *y-y* axis

$K = 0,161\ \text{N/mm}^2$

I_s is the effective second moment of area of the stiffener:

$$I_s = \frac{b_{e2}\,t^3}{12} + \frac{c_{eff}^{\,3}\,t}{12} + b_{e2}\,t\left[\frac{c_{eff}^{\,2}}{2\left(b_{e2}+c_{eff}\right)}\right]^2 + c_{eff}\,t\left[\frac{c_{eff}}{2} - \frac{c_{eff}^{\,2}}{2\left(b_{e2}+c_{eff}\right)}\right]^2$$

$\Rightarrow I_s = 457,32\ \text{mm}^4$

so, the elastic critical buckling stress for the edge stiffener is

$$\sigma_{cr,s} = \frac{2\times\sqrt{0,161\times 210000\times 457,32}}{29,126} = 270,011\ \text{N/mm}^2$$

Thickness reduction factor χ_d for the edge stiffener

The relative slenderness:

$\bar{\lambda}_d = \sqrt{f_{yb}/\sigma_{cr,s}} = \sqrt{350/270,011} = 1,139$

The reduction factor will be:

if $\bar{\lambda}_d \le 0,65$ $\chi_d = 1,0$

if $0,65 < \bar{\lambda}_d < 1,38$ $\chi_d = 1,47 - 0,723\,\bar{\lambda}_d$

if $\bar{\lambda}_d \ge 1,38$ $\chi_d = 0,66/\bar{\lambda}_d$

$\Rightarrow 0,65 < \bar{\lambda}_d = 1,139 < 1,38$ so $\chi_d = 1,47 - 0,723 \times 1,139 = 0,646$

Step 3:

As the reduction factor for buckling of the stiffener is χ_d < 1, iterate to refine the value of the reduction factor for buckling of the stiffener.

The iterations are carried out based on modified values of ρ obtained using:

$\sigma_{com,Ed,i} = \chi_d f_{yb}/\gamma_{M0}$ and $\bar{\lambda}_{p,red} = \bar{\lambda}_p\sqrt{\chi_d}$

The iteration stops when the reduction factor χ converges.

Initial values (iteration 1): Final values (iteration n):

$\chi_d = 0,646$ $\chi_d = \chi_{d,n} = 0,614$

$b_{e2} = 17,57\ mm$ $b_{e2} = b_{e2,n} = 20,736\ mm$

$c_{eff} = 12,77\ mm$ $c_{eff} = c_{eff,n} = 12,77\ mm$

Final values of effective properties for flange and lip in compression are:

$\chi_d = 0,614$ $b_{e2} = 20,736$ mm $c_{eff} = 12,77$ mm

and $b_{e1} = 17,57$ mm

$t_{red} = t\chi_d = 0,96 \times 0,614 = 0,589$ mm

Effective section properties of the web

The position of the neutral axis with regard to the flange in compression:

$$h_c = \frac{c_p\left(h_p - c_p/2\right) + b_{p2}\,h_p + h_p^2/2 + c_{eff}^2\,\chi_d/2}{c_p + b_{p2} + h_p + b_{e1} + \left(b_{e2} + c_{eff}\right)\chi_d} \qquad h_c = 79,5 \text{ mm}$$

The stress ratio:

$$\psi = \frac{h_c - h_p}{h_c} = \frac{79,5 - 149}{79,5} = -0,874$$

The buckling factor:

$k_\sigma = 7,81 - 6,29\psi + 9,78\psi^2 \quad k_\sigma = 20,76$

The relative slenderness:

$$\bar{\lambda}_{p,h} = \frac{h_p/t}{28,4\,\varepsilon\sqrt{k_\sigma}} = \frac{149/0,96}{28,4\times\sqrt{235/350}\times\sqrt{20,76}} = 1,464$$

The width reduction factor is:

$$\rho = \frac{\bar{\lambda}_{p,h} - 0,055(3+\psi)}{\bar{\lambda}_{p,h}^{\,2}} = \frac{1,464 - 0,055\times(3-0,874)}{1,464^2} = 0,629$$

The effective width of the zone in compression of the web is:

$h_{eff} = \rho\, h_c = 0,629\times 79,5 = 50\ \text{mm}$

Near the flange in compression:

$h_{e1} = 0,4h_{eff} = 0,4\times 50 = 20\ \text{mm}$

Near the neutral axis:

$h_{e2} = 0,6h_{eff} = 0,6\times 50 = 30\ \text{mm}$

The effective width of the web near the flange in compression:

$h_1 = h_{e1} = 20\ m\text{m}$

Near the flange in tension:

$h_2 = h_p - (h_c - h_{e2}) = 149 - (79,5 - 30) = 99,5\ \text{mm}$

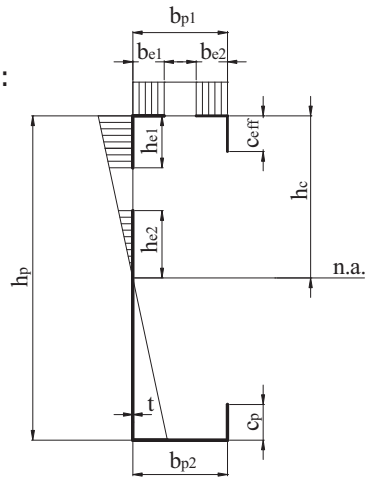

Effective section properties

Effective cross-section area:

$A_{eff} = t[c_p + b_{p2} + h_1 + h_2 + b_{e1} + (b_{e2} + c_{eff})\chi_d]$

$A_{eff} = 0,96\times\left[15,5 + 40 + 20 + 99,5 + 17,57 + (20,736 + 12,77)\times 0,614\right]$

$A_{eff} = 204,62\ \text{mm}^2$

Position of the neutral axis with regard to the flange in compression:

$$z_c = \frac{t\left[c_p\left(h_p - c_p/2\right) + b_{p2}h_p + h_2\left(h_p - h_2/2\right) + h_1^{\,2}/2 + c_{eff}^{\,2}\chi_d/2\right]}{A_{eff}}$$

$z_c = 85,75\ \text{mm}$

Position of the neutral axis with regard to the flange in tension:

$z_t = h_p - z_c = 149 - 85,75 = 63,25\ \text{mm}$

Second moment of area:

$$I_{eff,y} = \frac{h_1^3 t}{12} + \frac{h_2^3 t}{12} + \frac{b_{p2} t^3}{12} + \frac{c_p^3 t}{12} + \frac{b_{e1} t^3}{12} + \frac{b_{e2}(\chi_d t)^3}{12} + \frac{c_{eff}^3(\chi_d t)}{12} +$$
$$+c_p\, t(z_t - c_p/2)^2 + b_{p2} t z_t^2 + h_2 t(z_t - h_2/2)^2 + h_1 t(z_c - h_1/2)^2 +$$
$$+b_{e1} t\, z_c^2 + b_{e2}(\chi_d t)\, z_c^2 + c_{eff}(\chi_d t)(z_c - c_{eff}/2)^2$$

$$I_{eff,y} = 668103 \text{ mm}^4$$

Effective section modulus:

- with regard to the flange in compression

$$W_{eff,y,c} = \frac{I_{eff,y}}{z_c} = \frac{668103}{85,75} = 7791 \text{ mm}^3$$

- with regard to the flange in tension

$$W_{eff,y,t} = \frac{I_{eff,y}}{z_t} = \frac{668103}{63,25} = 10563 \text{ mm}^3$$

4.4 Resistance of bar members

4.4.1 Introduction

In the previous chapter, the behaviour and resistance of cross-sections of thin-walled cold-formed steel members under different stress states have been analysed. Therefore, this chapter, the problems in which the length and end-supports or other structural links and restraints of bar members become additional parameters to those characterising the resistance of the cross-sections, particularly the design against instability as well as serviceability conditions are addressed.

The instability behaviour of bar members is generally characterised by stable post-critical modes. However the interaction of two stable symmetric post-critical modes may generate an unstable coupled asymmetric mode, rendering the member highly sensitive to imperfections. In such cases significant erosion of critical load occurs.

A characteristic of behaviour of thin walled slender members is the coupling or interaction of instability modes, as presented in §§4.2.2.1.

Coupling due to design implies that the geometric dimensions of a structure are chosen such that two or more buckling modes are simultaneously possible (see Dubina, 2001). For this case, the optimisation based on the simultaneous mode design principle plays a very important role and the attitude of the designer towards this principle is decisive. This type of coupling is the most interesting in practice. However, since in such cases the sensitivity to imperfections is maximum, and the erosion of theoretical ultimate load corresponding to the coupling point is, as a consequence, maximum too. Really accurate methods need to be used to predict that.

4.4.2 Compression members

4.4.2.1 Interactive buckling of class 4 members

To take into account the interaction between local and global buckling of thin-walled sections (class 4), the calculation of the load bearing capacity is based upon the effective cross-section, calculated for uniform compression. For practical reasons, the same approach is applied in EN1993-1-3 for thin-walled cold-formed sections. In fact, the same buckling curves, based on hot-rolled section tests are used for cold-formed sections too, even though the behaviour of cold-formed sections is different due to the different fabrication process, which affects the nature and influence of imperfections.

A member is subjected to concentric compression if the line of action of the applied load goes through the neutral axis of the effective cross-section. If this line does not coincide with the centroid of the gross cross-section, bending moments corresponding to the shift of the centroid axes (see Figure 4.32) should be taken into account.

To take the effect of local buckling into account, the strength of the cross-section is expressed as:

$$N = A_{eff} f_y \tag{4.45}$$

where A_{eff} is the effective area of cross-section, calculated using the effective width approach.

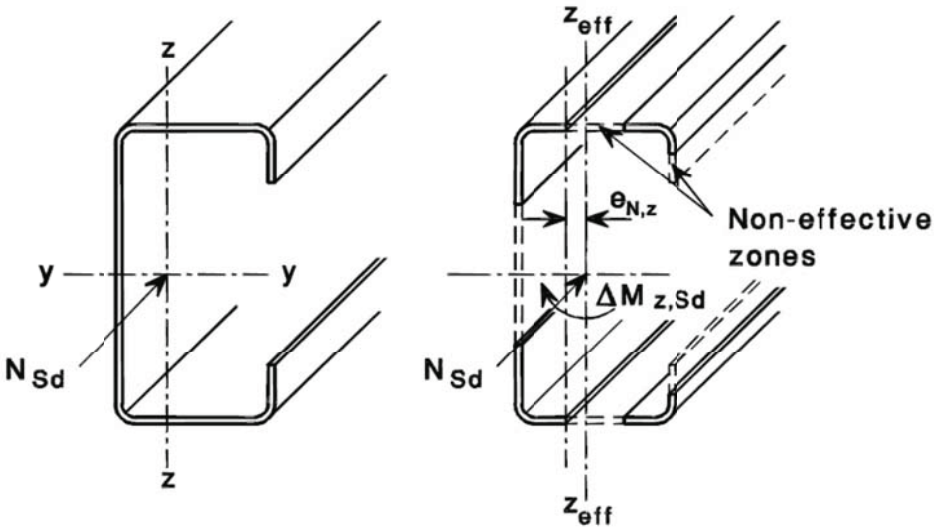

Figure 4.32 Shift of neutral axis due to effective cross-section

Introducing $A_{eff}=Q \cdot A$, where A is the area of the gross cross-section and Q is a reduction factor calculated on the basis of the effective width principle, the strength of the effective or reduced cross-section can be written as:

$$N = A_{eff} f_y = Q\ A\ f_y \tag{4.46}$$

and, as a consequence, the Ayrton-Perry equation can be written as:

$$(Q - \overline{N})(1 - \overline{\lambda}^2 \overline{N}) = \alpha(\overline{\lambda} - 0,2)\overline{N} \tag{4.47}$$

with $\overline{N} = N / QAf_y$ and

$$\overline{\lambda} = \sqrt{\frac{A_{eff} f_y}{N_{cr}}} = \frac{\lambda}{\lambda_1}\sqrt{Q} \tag{4.48}$$

Eqn. (4.48) represents the Ayrton-Perry formula for Local-Overall Interactive Buckling.

There are also other approaches available to account for the interactive buckling of thin-walled members which, in some way, are replicating better the nature of the interactive phenomenon. Two of these approaches are summarised in the following.

4.4.2.2 Design according to EN1993-1-3

The provisions in EN1993-1-1 (§§6.3.1 of the code) for buckling resistance of uniform members with cross-sections of Class 4 in compression have to be combined with the relevant provisions of §§6.2.1 of EN1993-1-3.

A member in compression should be verified against buckling using the following equation:

$$\frac{N_{Ed}}{N_{b.Rd}} \le 1 \tag{4.49}$$

where

N_{Ed} is the design value of the compression force;

$N_{b.Rd}$ is the design buckling resistance of the compression member.

The design buckling resistance of a compression member with Class 4 cross-section should be taken as:

$$N_{b.Rd} = \frac{\chi A_{eff} f_y}{\gamma_{M1}} \tag{4.50}$$

where

χ is the reduction factor for the relevant buckling mode.

For members with non-symmetric class 4 sections, the additional moment ΔM_{Ed} should be taken into account due to the eccentricity of the centroid axis of the effective section, (see §§6.2.2.5(4) of EN1993-1-1 and the interaction should be carried out according to §§6.3.3 of EN1993-1-1).

For axial compression members, the value of χ for the appropriate non-dimensional slenderness $\overline{\lambda}$ should be determined from the relevant buckling curve according to:

$$\chi = \frac{1}{\phi + \sqrt{\phi^2 - \bar{\lambda}^2}} \quad \text{but} \quad \chi \le 1 \tag{4.51}$$

where

$$\phi = 0,5\left[1 + \alpha\left(\bar{\lambda} - 0,2\right) + \bar{\lambda}^2\right]$$

and

$\bar{\lambda} = \sqrt{\frac{A_{eff} f_y}{N_{cr}}}$ for class 4 cross-sections.

α is the imperfection factor;

N_{cr} is the elastic critical force for the relevant buckling mode based on the gross cross-sectional properties.

$$N_{cr} = \frac{\pi^2 EI}{L^2} \tag{4.52}$$

The imperfection factor α corresponding to the appropriate buckling curve should be obtained from Table 4.7 and Table 4.8.

Table 4.7 Imperfection factors for buckling curves

Buckling curve	a_0	**a**	**b**	**c**	**d**
Imperfection factor	0,13	0,21	0,34	0,49	0,76

The design buckling resistance $N_{b.Rd}$ for flexural buckling should be obtained from EN1993-1-1 using the appropriate buckling curve according to the type of cross-section, axis of buckling and yield strength used.

For slenderness $\bar{\lambda} \le 0,2$ or for $N_{Ed} / N_{cr} \le 0,04$, the buckling effects may be ignored and only cross-sectional strength checks are required.

For flexural buckling, the appropriate buckling curve should be obtained from Table 4.8 The buckling curve for a cross-section not included in Table 4.8 may be obtained by analogy.

The buckling resistance of a closed built-up cross-section should be determined using either:

- buckling curve *b* in association with the basic yield strength f_{yb} of the flat sheet material out of which the member is made by cold-forming;
- buckling curve *c* in association with the average yield strength f_{ya} of the member after cold forming, provided that $A_{eff} = A$.

The appropriate non-dimensional slenderness $\bar{\lambda}$ could be written as:

$$\overline{\lambda} = \sqrt{\frac{A_{eff} f_y}{N_{cr}}} = \frac{L_{cr}}{i} \frac{\sqrt{\frac{A_{eff}}{A}}}{\lambda_1} \tag{4.53}$$

where

L_{cr} is the buckling length in the buckling plane considered;

i is the radius of gyration about the relevant axis, determined using the properties of the gross cross-section;

$$\lambda_1 = \pi \sqrt{\frac{E}{f_y}}$$

The corresponding values of the imperfection factor α are shown in Table 4.7.

For members with mono-symmetric open cross-sections, as shown Figure 4.33, account should be taken of the possibility that the resistance of the member to flexural-torsional buckling might be less than its resistance to flexural buckling.

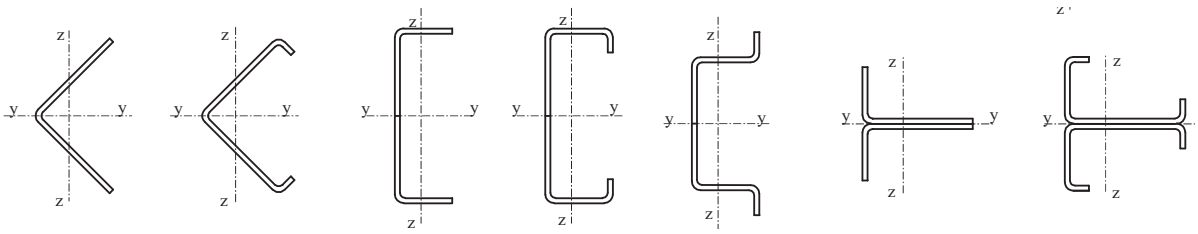

Figure 4.33 Mono-symmetric cross-sections susceptible to torsional-flexural buckling

For members with point-symmetric open cross-sections (e.g. cruciform section or Z-purlin with equal flanges), account should be taken of the possibility that the resistance of the member to torsional buckling might be less than its resistance to flexural buckling.

For members with non-symmetric open cross-sections the problem, even more complex, is quite similar.

The design buckling resistance $N_{b.Rd}$ for torsional or flexural-torsional buckling should be obtained using Eqn. (4.50) and the relevant buckling curve for buckling about the z–z axis obtained from Table 4.8; however, the y–y axis is relevant for determining the flexural buckling strength of plain and lipped angles.

The elastic critical force $N_{cr,T}$ for torsional buckling and $N_{cr,FT}$ for flexural-torsional buckling of a simply supported column should be determined using Eqn. (4.54) and (4.55), respectively.

Table 4.8 Appropriate buckling curve for various types of cross-section

Type of cross-section	Buckling about axis	Buckling curve
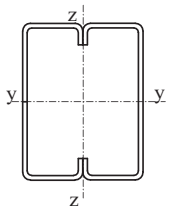 if f_{yb} is used	any	*b*
if f_{ya} is used *)	any	*c*
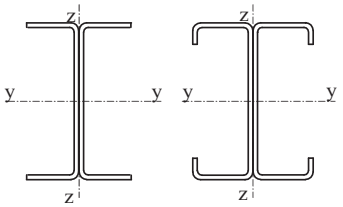	y –y	*a*
	z – z	*b*
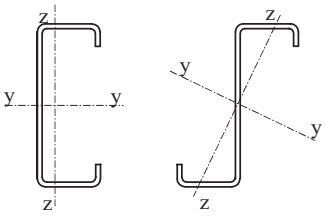	any	*b*
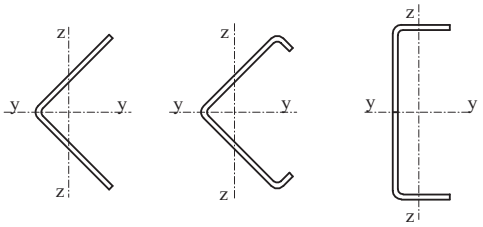	any	*c*
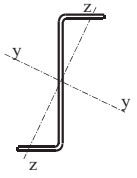 or other cross-section		

*) The average yield strength f_{ya} should not be used unless $A_{eff} = A_g$

$$N_{cr,T} = \frac{1}{i_o^2}\left(GI_t + \frac{\pi^2 EI_w}{L_{cr,T}^2}\right) \tag{4.54}$$

$$N_{cr,FT} = \frac{N_{cr,y}}{2\,\beta}\left[1 + \frac{N_{cr,T}}{N_{cr,y}} - \sqrt{(1 + \frac{N_{cr,T}}{N_{cr,y}})^2 - 4\,\beta\frac{N_{cr,T}}{N_{cr,y}}}\right] \tag{4.55}$$

where,

G is the shear modulus;

It is the torsion constant of the gross cross-section;

I_w is the warping constant of the gross cross-section;

i_y is the radius of gyration of the gross cross-section about the y-y axis;

i_z is the radius of gyration of the gross cross-section about the z-z axis;

$L_{cr,T}$ is the buckling length of the member for torsional buckling;

y_o, z_o are the shear centre coordinates with respect to the centroid of the gross cross-section (z_o = 0 for a cross-section symmetric with respect to the y-y axis);

i_o is the polar radius of gyration given by

$$i_o^2 = i_y^2 + i_z^2 + y_o^2 + z_o^2 \tag{4.56}$$

$N_{cr,y}$ is the critical load for flexural buckling about the y-y axis;

β is a factor given by

$$\beta = 1 - (y_o / i_o)^2 \tag{4.57}$$

In case of doubly symmetric cross-sections (i.e. y_o = z_o = 0), there are no flexural-torsional modes, so, all modes, i.e. $N_{cr,y}$, $N_{cr,z}$ and $N_{cr,T}$ are uncoupled.

For cross-sections that are symmetrical about the y–y axis (e.g. z_o = 0), the elastic critical force $N_{cr,FT}$ for flexural- torsional buckling should be determined using Eqn. (4.55).

For practical connections at each end, the value of l_T / L_T may be taken as follows:

- 1,0 for connections that provide partial restraint against torsion and warping, see Figure 4.34(a);
- 0,7 for connections that provide significant restraint against torsion and warping, see Figure 4.34(b).

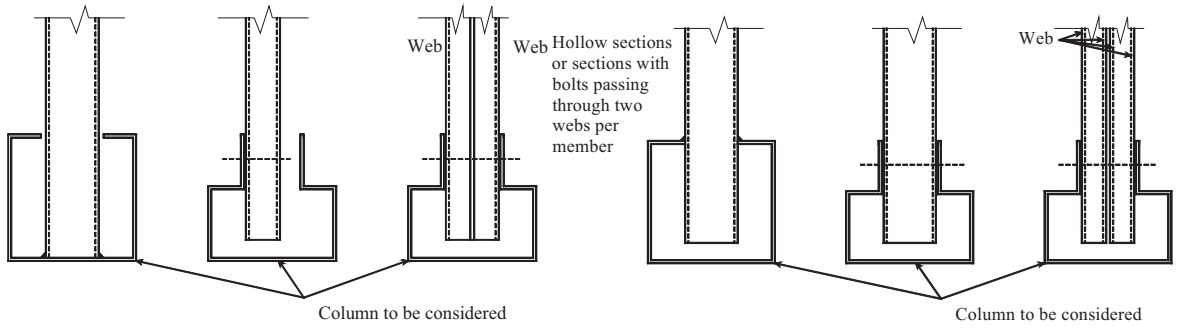

a) Connections capable of giving partial torsional and warping restraint

b) Connections capable of giving significant torsional and warping restraint

Figure 4.34 Torsional and warping restraint for practical connections

The buckling length l_T for torsional or flexural-torsional buckling should be determined taking into account the degree of torsional and warping restraint at each end of the member length L_T.

4.4.2.3 Design example

The following example deals with the design of an internal wall stud in compression. The stud has pinned end conditions and is composed of two thin-walled cold-formed back-to-back lipped channel sections. The connection between the channels is assumed to be rigid (a welded connection, for example). No restraints against buckling are applied between the ends.

Figure 4.35 and Figure 4.36 present schematically the design of a cold-formed steel member in compression.

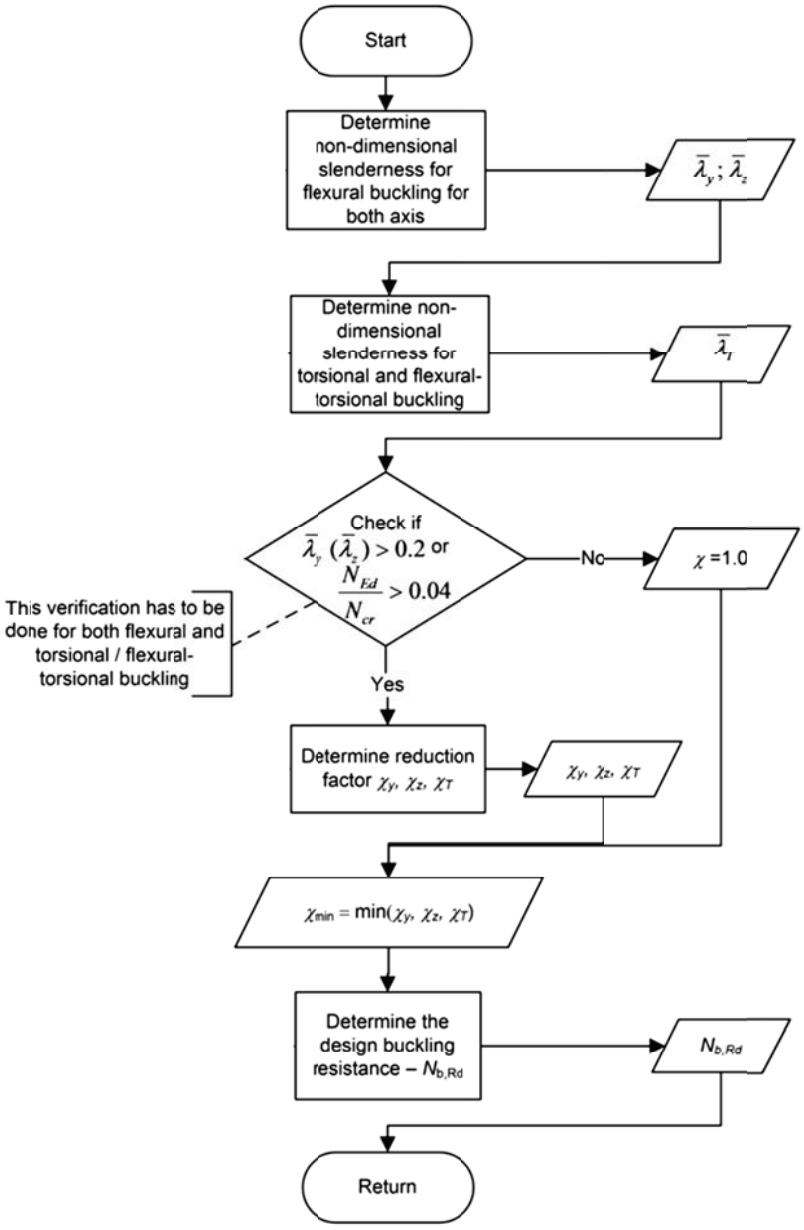

Figure 4.35 Calculate the design buckling resistance of a member in compression – $N_{b,Rd}$ (SF039a-EN-EU, Access Steel 2006)

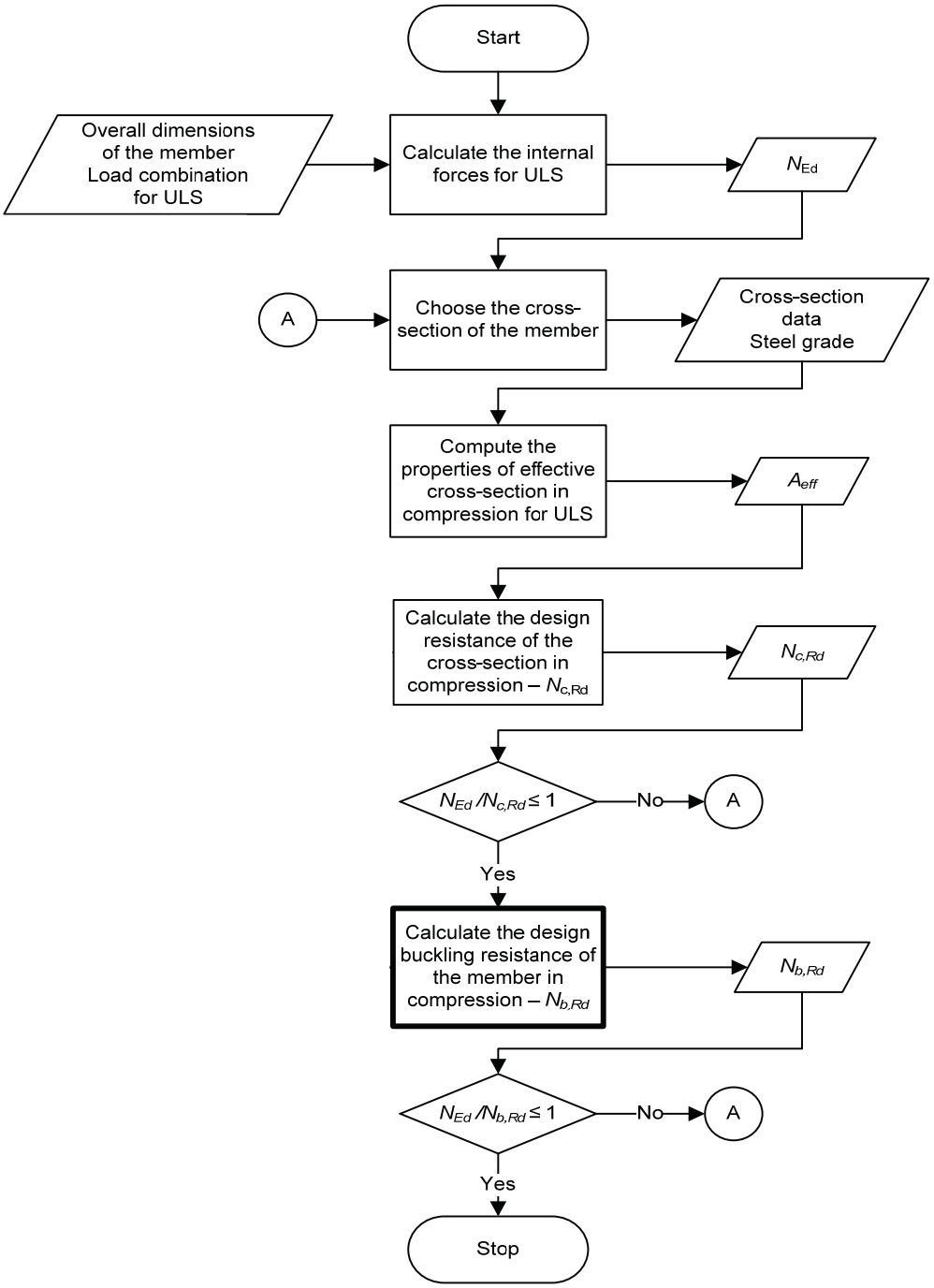

Figure 4.36 Design of a cold-formed steel member in compression (SF039a-EN-EU, Access Steel 2006)

Basic Data *(see Figure 4.37)*

Height of column	H = 3,0 m	
Span of floor	L = 6,00 m	
Spacing between floor joists	S = 0,6 m	
Distributed loads applied to the floor:		
- dead load:	1,5 kN/m	q_G = 1,5 x 0,6 = 0,9kN/m
- imposed load:	3,0 kN/m	q_Q = 3,0 x 0,6 = 1,8kN/m
Ultimate Limit State concentrated load from upper level and roof:		Q = 7,0 kN
The dimensions of a lipped channel section and the material properties are:		
Total height	h = 150 mm	
Total width of flange	b = 40 mm	
Total width of edge fold	c = 15 mm	
Internal radius	r = 3 mm	
Nominal thickness	t_{nom} = 1,2 mm	
Steel core thickness	t = 1,16 mm	
Steel grade	S350GD+Z	
Basic yield strength	f_{yb} = 350 N/mm^2	
Modulus of elasticity	E = 210000 N/mm^2	
Poisson's ratio	$\nu = 0,3$	
Shear modulus	$G = \frac{E}{2(1+\nu)} = 81000$ N/mm^2	
Partial factors	γ_{M0} = 1,0, γ_{M1} = 1,0, γ_G = 1,35, γ_Q = 1,50	

The applied concentrated load on the external column (compression) at the Ultimate Limit State is

$$N_{Ed} = \left(\gamma_G q_G + \gamma_Q q_Q\right) L/2 + Q = \left(1,35 \times 0,9 + 1,50 \times 1,80\right) \times 5/2 + 7 = 16,79\text{kN}$$

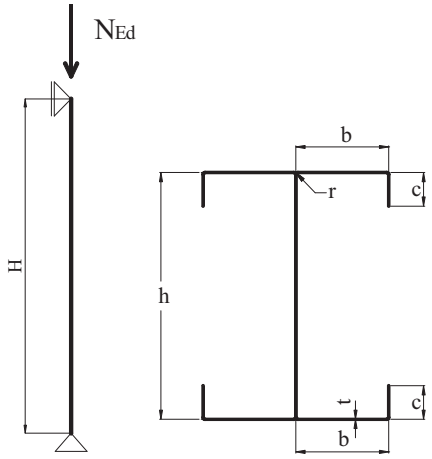

Figure 4.37 Overall dimensions of internal wall stud and cross-section

Properties of the gross cross-section

Area of gross cross-section:

$$A = 592\ \text{mm}^2$$

Radii of gyration:

$$i_y = 57,2\ \text{mm}\ ;\ i_z = 18\ \text{mm}$$

Second moment of area about

y-y: $I_y = 1,936 \times 10^6\ \text{mm}^4$

z-z: $I_z = 19,13 \times 10^4\ \text{mm}^4$

Warping constant:

$$I_w = 4,931 \times 10^8\ \text{mm}^6$$

Torsion constant:

$$I_t = 266\ \text{mm}^4$$

Effective section properties of the cross-section. Effective area of the cross-section when subjected to compression only:

$$A_{eff} = 322\ \text{mm}^2$$

Resistance check of the cross-section

The following criterion should be met:

$$\frac{N_{Ed}}{N_{c,Rd}} \le 1$$

where:

$$N_{c,Rd} = A_{eff} f_{yb} / \gamma_{M0}$$

The cross-section is doubly symmetric and so the shift of the centroidal *y–y* axis is

$$e_{Ny} = 0$$

The resistance check is:

$$\frac{16,79 \times 10^3}{322 \times 350/1,0} = 0,149 < 1 \qquad \text{– OK}$$

Buckling resistance check

Members which are subjected to axial compression should:

$$\frac{N_{Ed}}{N_{b,Rd}} \le 1$$

$N_{b.Rd} = \dfrac{\chi A_{eff} f_y}{\gamma_{M1}}$, where χ is the reduction factor for the relevant buckling mode.

$\chi = \dfrac{1}{\phi + \sqrt{\phi^2 - \bar{\lambda}^2}}$ but $\chi \le 1,0$,

$\phi = 0,5\left[1 + \alpha\left(\bar{\lambda} - 0,2\right) + \bar{\lambda}^2\right]$

α – imperfection factor

The non-dimensional slenderness is: $\bar{\lambda} = \sqrt{\dfrac{A_{eff} f_{yb}}{N_{cr}}}$

Determination of the reduction factors χ_y, χ_z, χ_T

Flexural buckling

$\bar{\lambda}_F = \sqrt{\dfrac{A_{eff} f_{yb}}{N_{cr}}} = \dfrac{L_{cr}}{i}\dfrac{\sqrt{A_{eff}/A}}{\lambda_1}$

N_{cr} – the elastic critical force for the relevant buckling mode.

The buckling length:

$L_{cr,y} = L_{cr,z} = H = 3000$ mm

$\lambda_1 = \pi\sqrt{\dfrac{E}{f_{yb}}} = \pi \times \sqrt{\dfrac{210000}{350}} = 76,95$

Buckling about *y–y* axis:

$\bar{\lambda}_y = \dfrac{L_{cr,y}}{i_y}\dfrac{\sqrt{A_{eff}/A}}{\lambda_1} = \dfrac{3000}{57,2} \times \dfrac{\sqrt{322/592}}{76,95} = 0,503$

$\alpha_y = 0,21$ – buckling curve *a* (§§4.2.1.2, Table 4.1)

$\phi_y = 0,5\left[1 + \alpha_y\left(\bar{\lambda}_y - 0,2\right) + \bar{\lambda}_y^{\,2}\right] =$

$= 0,5 \times \left[1 + 0,21 \times \left(0,503 - 0,2\right) + 0,503^2\right] = 0,658$

$\chi_y = \dfrac{1}{\phi_y + \sqrt{\phi_y^{\,2} - \bar{\lambda}_y^{\,2}}} = \dfrac{1}{0,658 + \sqrt{0,658^2 - 0,503^2}} = 0,924$

Buckling about *z–z* axis:

$\bar{\lambda}_z = \dfrac{L_{cr,z}}{i_z}\dfrac{\sqrt{A_{eff}/A}}{\lambda_1} = \dfrac{3000}{18} \times \dfrac{\sqrt{322/592}}{76,95} = 1,597$

$\alpha_z = 0,34$ – buckling curve *b* (§§4.2.1.2, Table 4.1)

$$\phi_z = 0,5\left[1 + \alpha_z\left(\bar{\lambda}_z - 0,2\right) + \bar{\lambda}_z^{\,2}\right] =$$
$$= 0,5 \times \left[1 + 0,34 \times \left(1,597 - 0,2\right) + 1,597^2\right] = 2,013$$

$$\chi_z = \frac{1}{\phi_z + \sqrt{\phi_z^{\,2} - \bar{\lambda}_z^{\,2}}} = \frac{1}{2,013 + \sqrt{2,013^2 - 1,597^2}} = 0,309$$

Torsional buckling:

$$N_{cr,T} = \frac{1}{i_o^{\,2}}\left(GI_t + \frac{\pi^2 EI_w}{l_T^{\,2}}\right)$$

where:

$$i_o^{\,2} = i_y^{\,2} + i_z^{\,2} + y_o^{\,2} + z_o^{\,2}$$

y_o, z_o – the shear centre coordinates with respect to the centroid of the gross cross-section: $y_o = z_o = 0$

$$i_o^{\,2} = 57,2^2 + 18^2 + 0 + 0 = 3594 \text{ mm}^2$$

$$l_T = H = 3000 \text{ mm}$$

The elastic critical force for torsional buckling is:

$$N_{cr,T} = \frac{1}{3594} \times \left(81000 \times 266 + \frac{\pi^2 \times 210000 \times 4,931 \times 10^8}{3000^2}\right) = 37,59 \times 10^3 \text{ N}$$

The elastic critical force will be:

$$N_{cr} = N_{cr,T} = 37,59 \text{ kN}$$

The non-dimensional slenderness is:

$$\bar{\lambda}_T = \sqrt{\frac{A_{eff} f_{yb}}{N_{cr}}} = \sqrt{\frac{322 \times 350}{37,59 \times 10^3}} = 1,731$$

$\alpha_T = 0.34$ – buckling curve *b*

$$\phi_T = 0,5\left[1 + \alpha_T\left(\bar{\lambda}_T - 0,2\right) + \bar{\lambda}_T^{\,2}\right] =$$
$$= 0,5 \times \left[1 + 0,34 \times \left(1,731 - 0,2\right) + 1,731^2\right] = 2,258$$

The reduction factor for torsional buckling is:

$$\chi_T = \frac{1}{\phi_T + \sqrt{\phi_T^{\,2} - \bar{\lambda}_T^{\,2}}} = \frac{1}{2,258 + \sqrt{2,258^2 - 1,731^2}} = 0,270$$

$$\chi = \min(\chi_y; \chi_z; \chi_T) = \min(0,924; 0,309; 0,270) = 0,270$$

$$N_{b.Rd} = \frac{\chi A_{eff} f_y}{\gamma_{M1}} = \frac{0,270 \times 322 \times 350}{1,00} = 30429 \text{ N} = 30,429 \text{ kN}$$

$$\frac{N_{Ed}}{N_{b,Rd}} = \frac{16,79}{30,429} = 0,552 \le 1 \text{ – OK}$$

4.4.3 Buckling strength of bending members

4.4.3.1 General approach

In the case of unrestrained beams, out-of-plane lateral-torsional (LT) buckling may affect the beam capacity. Since, particularly in the case of open-section thin-walled slender beams, LT buckling can be very dangerous, a proper design – calculation and preventive constructional measures – must be able to guard against this phenomenon.

In case of class 4 cross-sections, interaction between local or sectional buckling modes with lateral-torsional buckling might occur. Figure 4.38 shows the theoretical uncoupled buckling modes of a lipped channel section beam in bending obtained using CUFSM 3.12 (www.ce.jhu.edu/ bschafer/cufsm). To take local buckling into account, the effective cross-section of the beam will be considered, and the lateral-torsional buckling curve takes the shape shown in Figure 4.39.

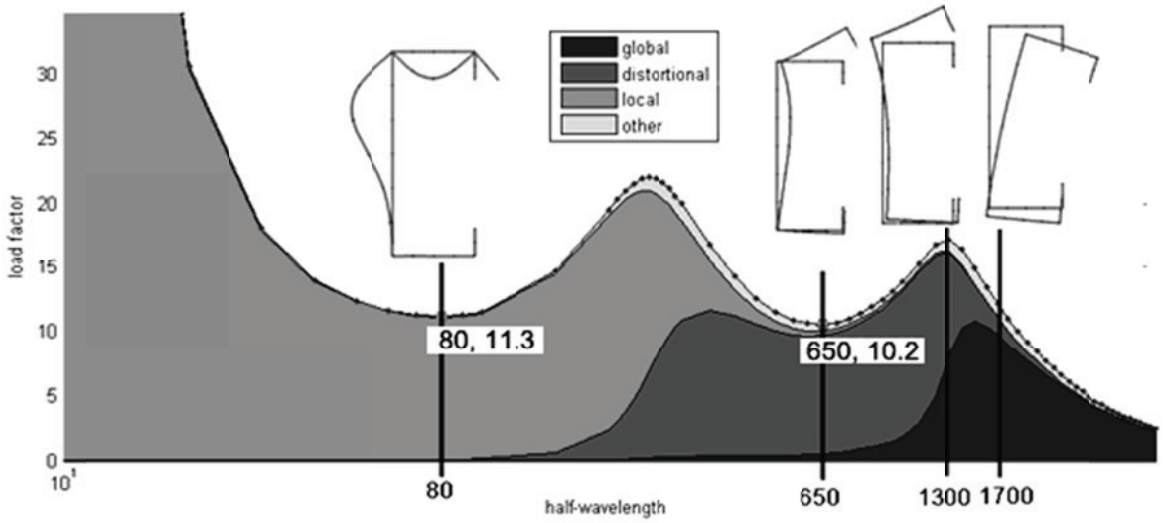

Figure 4.38 Lateral-torsional buckling curve for a class 4 cross-section beam (interaction local – *LT* buckling) – CUFSM 3.12 (www.ce.jhu.edu/bschafer/cufsm)

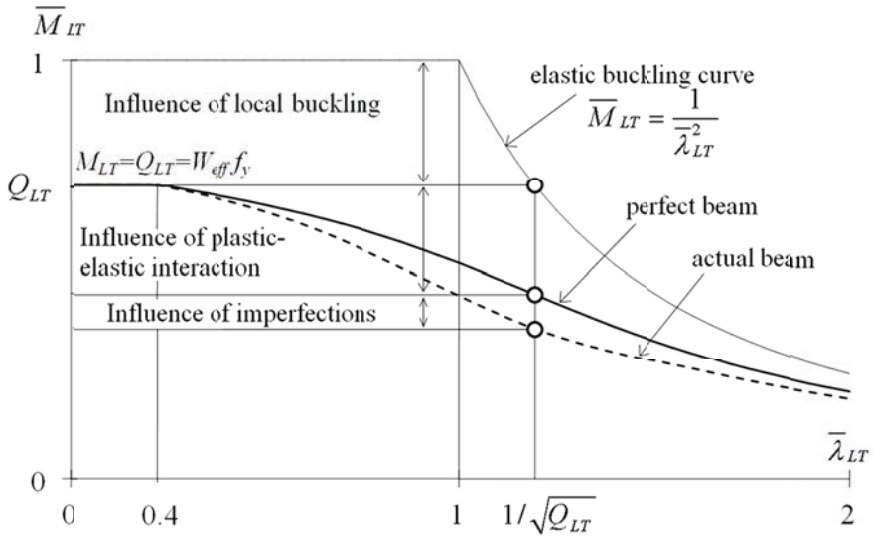

Figure 4.39 Buckling modes for a lipped channel beam

4.4.3.2 Design according to EN1993-1-3

Lateral-torsional buckling of members subject to bending

The design buckling resistance moment of a member that is susceptible to lateral-torsional buckling should be determined according to EN 1993-1-1, §§6.3.2.2 using the lateral buckling curve *b*.

This method should not be used for sections that have a significant angle between the principal axes of the effective cross-section, compared to those of the gross cross-section.

A laterally unrestrained member subject to major axis bending should be verified against lateral-torsional buckling as follows:

$$\frac{M_{Ed}}{M_{b.Rd}} \leq 1 \tag{4.58}$$

where

M_{Ed} is the design value of the moment;

$M_{b.Rd}$ is the design buckling resistance moment.

Beams with sufficient restraint to the compression flange are not susceptible to lateral-torsional buckling. In addition, beams with certain types of cross-sections, such as square or circular hollow sections, fabricated circular tubes or square box sections are generally not susceptible to lateral-torsional buckling, because of their high torsion rigidity GI_T.

The design buckling resistance moment of a laterally unrestrained beam should be taken as:

$$M_{b,Rd} = \chi_{LT} W_y f_y / \gamma_{M1} \tag{4.59}$$

where:

W_y is the appropriate section modulus as follows:

$W_y = W_{el,y}$ is for class 3 cross-section;

$W_y = W_{eff,y}$ is for class 4 cross-section;

In determining W_y, holes for fasteners at the beam ends need not to be taken into account.

χ_{LT} is the reduction factor for lateral-torsional buckling,

$$\chi_{LT} = \frac{1}{\phi_{LT} + \left(\phi_{LT}^{\ 2} - \overline{\lambda}_{LT}^{2}\right)^{0,5}} \quad \text{but} \quad \chi_{LT} \leq 1 \tag{4.60}$$

with:

$$\phi_{LT} = 0,5\left[1 + \alpha_{LT}\left(\overline{\lambda}_{LT} - 0,2\right) + \overline{\lambda}_{LT}^{2}\right]$$

α_{LT} is the imperfection factor corresponding to buckling curve *b*, α_{LT} = 0,34

$$\bar{\lambda}_{LT} = \sqrt{\frac{W_y f_y}{M_{cr}}}$$

M_{cr} is the elastic critical moment for lateral-torsional buckling. M_{cr} is based on gross cross-sectional properties and takes into account the loading conditions, the real moment distribution and the lateral restraints. For details see EN1993-1-1, §§6.3.2.

For slenderness $\bar{\lambda}_{LT} \le 0,4$ or for $M_{Ed} / M_{cr} \le 0,16$, lateral-torsional buckling effects may be ignored and only cross-sectional checks are required.

Simplified assessment methods for beams with restraints in building

Members with discrete lateral restraint to the compression flange (see Figure 4.40) are not susceptible to lateral-torsional buckling if the length L_c between restraints or the resulting slenderness $\bar{\lambda}_f$ of the equivalent compression flange satisfies:

$$\bar{\lambda}_f = \frac{k_c L_c}{i_{f,z} \lambda_1} \le \bar{\lambda}_{c0} \frac{M_{c,Rd}}{M_{y.Ed}} \tag{4.61}$$

where

$M_{y,Ed}$ is the maximum design value of the bending moment within the restraint spacing;

$$M_{c,Rd} = W_y \frac{f_y}{\gamma_{M0}}$$

W_y is the appropriate section modulus corresponding to the compression flange;

k_c is a slenderness correction factor for moment distribution between restraints, as shown in Table 4.9;

$i_{f,z}$ is the radius of gyration of the equivalent compression flange composed of the compression flange plus 1/3 of the compressed part of the web area, about the minor axis of the section;

$\bar{\lambda}_{c,0}$ is a slenderness limit for the equivalent compression flange defined above.

A recommended value is $\bar{\lambda}_{c,0} = \bar{\lambda}_{LT,0} + 0,1$, where $\bar{\lambda}_{LT,0} = 0,4$;

$$\lambda_1 = \pi \sqrt{\frac{E}{f_y}} = 93,9\varepsilon, \quad \varepsilon = \sqrt{\frac{235}{f_y}} \ (f_y \text{ in N/mm}^2)$$

Also, purlins and side rails acting as secondary beams are often restrained by the building envelope (e.g. trapezoidal sheeting, sandwich panels, OSB panels, etc.), and may be considered as members with discrete lateral restraint to the compression flange.

For class 4 cross-sections $i_{f,z}$ may be taken as:

$$i_{f,z} = \sqrt{\frac{I_{eff,f}}{A_{eff,f} + \frac{1}{3}A_{eff,w,c}}} \tag{4.62}$$

where

$I_{eff,f}$ is the effective second moment of area of the compression flange about the minor axis of the section;

$A_{eff,f}$ is the effective area of the compression flange;

$A_{eff,w,c}$ is the effective area of the compressed part of the web.

If the slenderness of the compression flange $\overline{\lambda}_f$ exceeds the limit $\overline{\lambda}_{c,0} = \overline{\lambda}_{LT,0} + 0,1$, the design buckling resistance moment may be taken as:

$$M_{b,Rd} = k_{fl}\chi M_{c,Rd} \quad \text{but} \quad M_{b,Rd} \le M_{c,Rd} \tag{4.63}$$

where

χ is the reduction factor of the equivalent compression flange determined with $\overline{\lambda}_f$;

k_{fl} is the modification factor accounting for the conservatism of the equivalent compression flange method. The value k_{fl} = 1,10 is recommended.

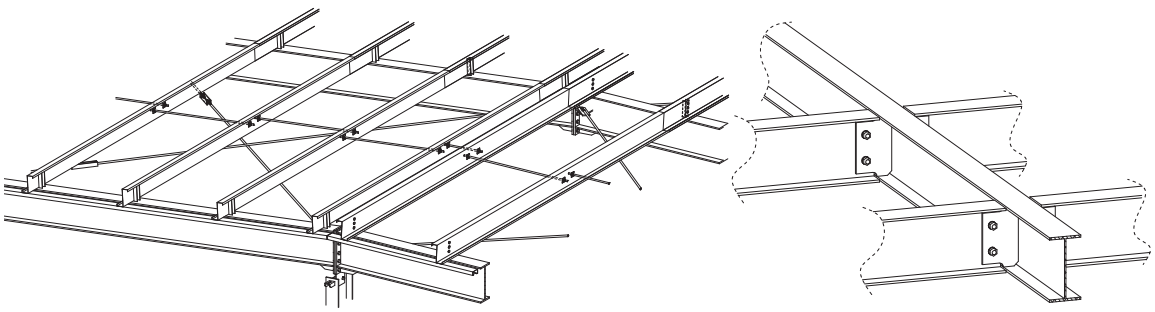

(a) anti-sag bars for Z-purlins and Z-purlins for roof beams

(b) secondary beams

Figure 4.40 Members with discrete lateral restraint

The buckling curves to be used to calculate the design buckling resistance moment using Eqn. (4.63) should be taken as curve *c*.

Table 4.9 Correction factor k_c

Moment distribution	k_c	Moment distribution	k_c
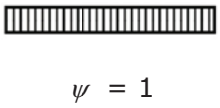 $\psi = 1$	1,0	 $-1 \le \psi \le 1$	$\frac{1}{1,33 - 0,33\psi}$
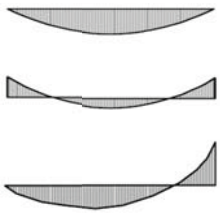	0,94	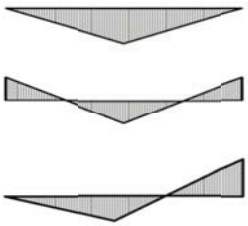	0,86
	0,90		0,77
	0,91		0,82

4.4.3.3 Design example

The following example presents the design of an unrestrained cold-formed steel beam in bending at the Ultimate Limit State. The beam to be designed, has pinned end conditions and is composed of two thin-walled cold-formed steel back-to-back lipped channel sections. The connection between the channels is assumed to be rigid.

Figure 4.42 and Figure 4.43 present schematically the design of a cold-formed steel member in bending.

Basic Data *(see Figure 4.41)*

Span of beam	L = 4,5 *m*
Spacing between beams	S = 3,0 *m*
Distributed loads applied to the joist:	
self-weight of the beam	$q_{G,beam}$ = 0,14 kN/m
weight of the floor and finishing	0,6 kN/m^2
	$q_{G,slab}$ = 0,55 x 3,0 = 1,65 kN/m
total dead load	$q_G = q_{G,beam} + q_{G,slab}$ =1,79 kN/m
imposed load	1,50 kN/m
	q_Q = 1,50 x 3,0 = 4,50 kN/m

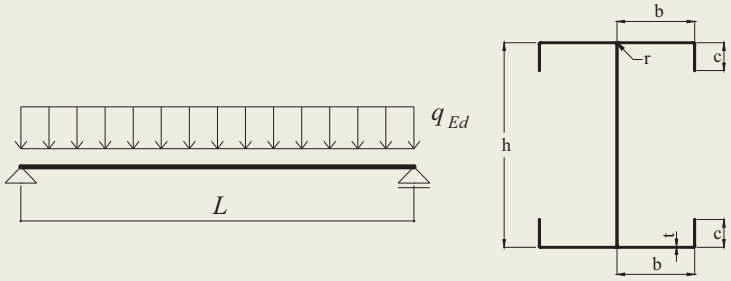

Figure 4.41 Overall dimensions of beam and of the cross-section

The dimensions of the cross-section and the material properties are:

Total height	h = 250 mm
Total width of flanges	b = 70 mm
Total width of edge fold	c = 25 mm
Internal radius	r = 3 mm
Nominal thickness	t_{nom} = 3,0 mm
Steel core thickness	t = 2,96 mm
Steel grade	*S350GD + Z*
Basic yield strength	f_{yb} = 350 N/mm^2
Modulus of elasticity	E = 210 000 N/mm^2
Poisson's ratio	$\nu = 0,3$
Shear modulus	$G = \frac{E}{2(1+\nu)} = 81\,000$ N/mm^2
Partial factors	γ_{M0} = 1,0, γ_{M1} = 1,0, γ_G = 1,35, γ_Q = 1,50

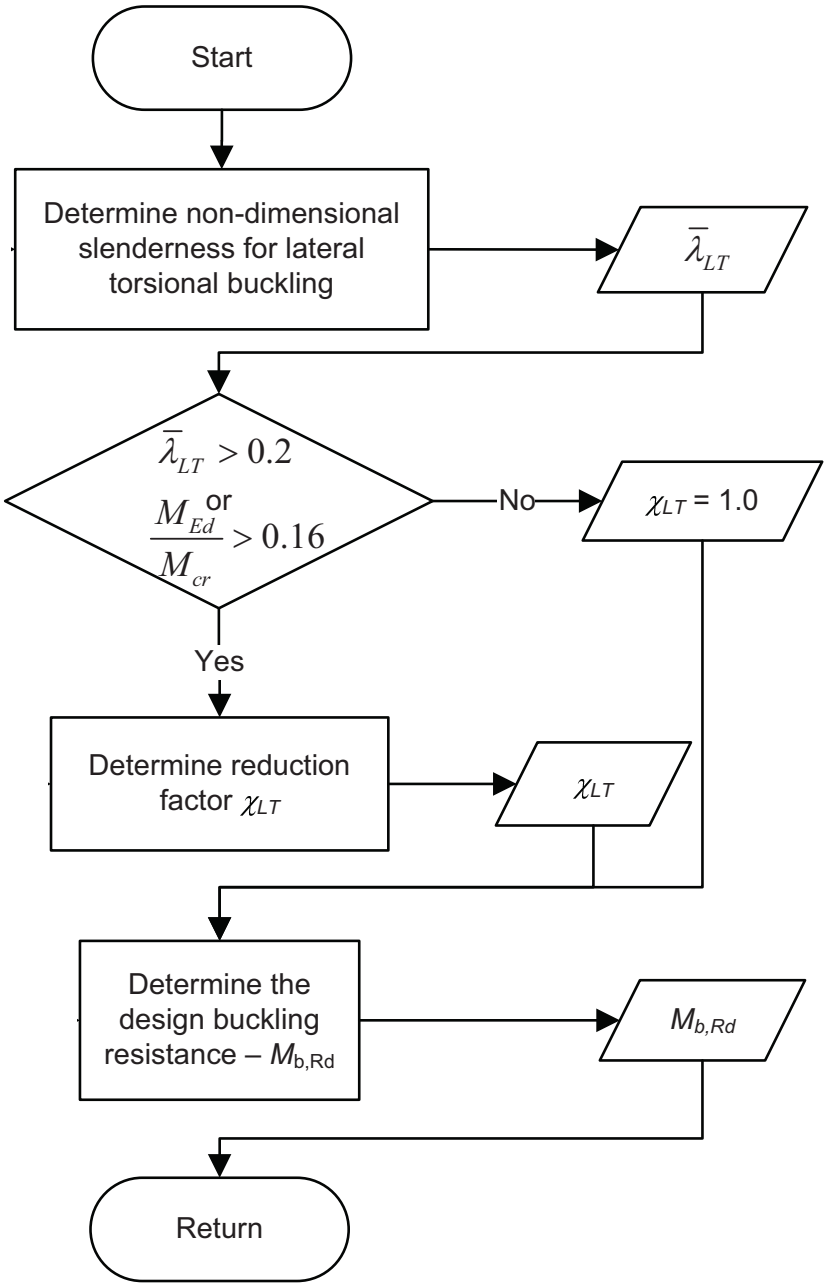

Figure 4.42 Calculate the design buckling resistance of a member in bending – $M_{b,Rd}$

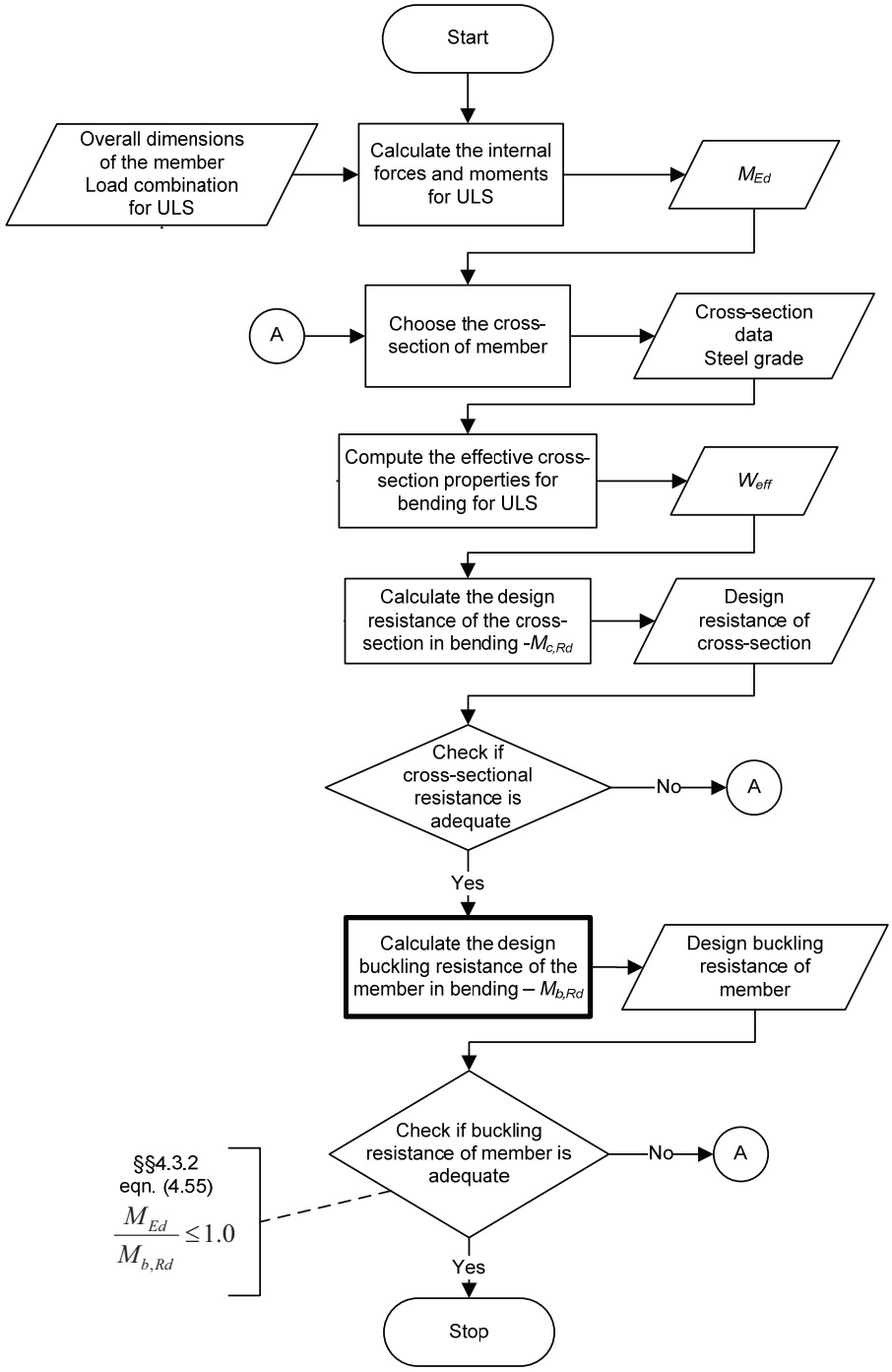

Figure 4.43 Design of a cold-formed steel member in bending

Design of the beam for Ultimate Limit State

Properties of the gross cross-section

Second moment of area about strong axis y–y: $I_y = 2302,15 \times 10^4$ mm^4

Second moment of area about weak axis z–z:

$I_z = 244,24 \times 10^4$ mm^4

Radii of gyration: $i_y = 95,3$ mm ; $i_z = 31$ mm

Warping constant: $I_w = 17692,78 \times 10^6$ mm^6

Torsion constant: $I_t = 7400$ mm^4

Effective section properties at the ultimate limit state

Second moment of area of cold-formed lipped channel section subjected to bending about its major axis: $I_{eff,y} = 22688890$ mm^4

Position of the neutral axis:

- from the flange in compression: $z_c = 124,6$ mm
- from the flange in tension: $z_t = 122,4$ mm

Effective section modulus:

- with respect to the flange in compression:

$$W_{eff,y,c} = \frac{I_{eff,y}}{z_c} = \frac{22688890}{124,6} = 182094 \text{ mm}^3$$

- with respect to the flange in tension:

$$W_{eff,y,t} = \frac{I_{eff,y}}{z_t} = \frac{22688890}{122,4} = 185367 \text{ mm}^3$$

$$W_{eff,y} = \min\left(W_{eff,y,c}, W_{eff,y,t}\right) = 182094 \text{ mm}^3$$

Applied loading on the beam at ULS

$q_d = \gamma_G q_G + \gamma_Q q_Q = 1,35 \times 1,79 + 1,50 \times 4,5 = 9,17$ kN/m

Maximum applied bending moment (at mid-span) about the major axis *y-y*:

$M_{Ed} = q_d L^2 / 8 = 9,17 \times 4,5^2 / 8 = 23,21$ kNm

Check of bending resistance at ULS

Design moment resistance of the cross-section for bending

$M_{c,Rd} = W_{eff,y} f_{yb} / \gamma_{M0} = 182094 \times 10^{-9} \times 350 \times 10^3 / 1,0 = 63,73$ kNm

Verification of bending resistance

$$\frac{M_{Ed}}{M_{c,Rd}} = \frac{23,21}{63,73} = 0,364 < 1 \text{ – OK}$$

Determination of the reduction factor χ_{LT}

Lateral-torsional buckling

$$\chi_{LT} = \frac{1}{\phi_{LT} + \sqrt{\phi_{LT}^2 - \bar{\lambda}_{LT}^2}} \qquad \text{but} \qquad \chi_{LT} \le 1,0$$

$$\phi_{LT} = 0,5\left[1 + \alpha_{LT}\left(\bar{\lambda}_{LT} - 0,2\right) + \bar{\lambda}_{LT}^2\right]$$

$\alpha_{LT} = 0,34$ – buckling curve *b*

The non-dimensional slenderness is:

$$\bar{\lambda}_{LT} = \sqrt{\frac{W_{eff,y,\min} f_{yb}}{M_{cr}}}$$

M_{cr} – the elastic critical moment for lateral-torsional buckling

$$M_{cr} = C_1 \frac{\pi^2 EI_z}{L^2}\sqrt{\frac{I_w}{I_z} + \frac{L^2 GI_t}{\pi^2 EI_z}}$$

where $C_1 = 1,127$ for a simply supported beam under uniform loading

$$M_{cr} = 1,127 \times \frac{\pi^2 \times 210000 \times 244,24 \times 10^4}{4500^2} \times \\ \times \sqrt{\frac{17692,78 \times 10^6}{244,24 \times 10^4} + \frac{4500^2 \times 81000 \times 7400}{\pi^2 \times 210000 \times 244,24 \times 10^4}}$$

$$M_{cr} = 27,66 \text{ kNm}$$

$$\bar{\lambda}_{LT} = \sqrt{\frac{W_{eff,y,\min} f_{yb}}{M_{cr}}} = \sqrt{\frac{182094 \times 350}{27,66 \times 10^6}} = 1,518$$

$$\phi_{LT} = 0,5\left[1 + \alpha_{LT}\left(\bar{\lambda}_{LT} - 0,2\right) + \bar{\lambda}_{LT}^2\right] = \\ = 0,5 \times \left[1 + 0,34 \times \left(1,437 - 0,2\right) + 1,437^2\right] = 1,743$$

$$\chi_{LT} = \frac{1}{\phi_{LT} + \sqrt{\phi_{LT}^2 - \bar{\lambda}_{LT}^2}} = \frac{1}{1,743 + \sqrt{1,734^2 - 1,437^2}} = 0,369$$

Check of buckling resistance at ULS

Design moment resistance of the cross-section for bending:

$$M_{b,Rd} = \chi_{LT} W_{eff,y} f_{yb} / \gamma_{M1} = 0,369 \times 182091 \times 10^{-9} \times 350 \times 10^3 / 1,0 = 23,52 \text{ kNm}$$

Verification of buckling resistance:

$$\frac{M_{Ed}}{M_{b,Rd}} = \frac{23,21}{23,52} = 0,987 < 1 \text{ – OK}$$

4.4.4 Buckling of members in bending and axial compression

4.4.4.1 General approach

In practical situations axial compression forces in columns are accompanied by bending moments acting about the major and minor axes of the cross-section. Usually, members in such loading conditions are called beam-columns. The design for axial compression force and bending moment varying along the length of the member through an exact analysis is complicated. For class 1 to 3 sections the overall buckling modes, e.g. flexural (F) and lateral – torsional (LT) buckling, can interact. In case of members in compression it is more likely that the interaction F + FT to be a problem of unsymmetrical and mono-symmetric cross-sections. In case of eccentric compression or members in bending and compression, when no lateral restrains are provided, such a coupled buckling mode can often occur due to inherent imperfections, even for symmetrical sections. Additionally, for the case of class 4 cross-sections, where wall/thickness ratios are large, prone to local (L) buckling (e.g. local and/or distortional), the interaction could be even more complex (e.g. L+F+LT or D+F+LT).

4.4.4.2 Design according to EN1993-1-1 and EN1993-1-3

Two different formats of the interaction formulae are provided in EN 1993–1–1, called Method 1 and Method 2. The main difference between them is the presentation of the different structural effects, either by specific coefficients in Method 1 or by one compact interaction factor in Method 2. This makes Method 1 more adaptable to identifying and accounting for the structural effects, while Method 2 is mainly focussed on the direct design of standard cases.

Method 1 (Annex A of EN 1993–1–1) contains a set of formulae that favours transparency and provides a wide range of applicability together with a high level of accuracy and consistency.

Method 2 (Annex B of EN 1993–1–1) is based on the concept of global factors, in which simplicity prevails against transparency. This approach appears to be the more straightforward in terms of a general format.

Both methods use the same basis of numerically calculated limit load results and test data for calibration and validation of the different coefficients. In this respect, the new interaction equations follow the format of those in the previous Eurocode 3 in principle. Both methods follow similar paths, namely the adaptation of the flexural-buckling formulae to lateral-torsional buckling by modified interaction factors calibrated using the limit-load results.

This leads to a design concept which differentiates between the two cases of buckling behaviour of members, firstly those which are susceptible to torsional deformations, and secondly those which are not. Members not susceptible to torsional deformations fail in flexural buckling, by in-plane or spatial deflection. These are closed sections, e.g. RHS, or open sections appropriately restrained against torsional deformations, as frequently found in building structures. Members susceptible to torsional deformations fail by lateral-torsional buckling, such as slender open sections. Accordingly, two sets of design formulae are provided, each covering a specified field of practical design situations.

As explained before, both sets of formulae are based on a second-order in-plane theory. Therefore, they rely on several common concepts, such as the equivalent moment concept, the definition of buckling length and the amplification concept.

Members which are subjected to combined bending and axial compression should satisfy:

$$\frac{N_{Ed}}{\chi_y N_{Rk} / \gamma_{M1}} + k_{yy} \frac{M_{y,Ed} + \Delta M_{y,Ed}}{\chi_{LT} M_{y,Rk} / \gamma_{M1}} + k_{yz} \frac{M_{z,Ed} + \Delta M_{z,Ed}}{M_{z,Rk} / \gamma_{M1}} \leq 1,0 \tag{4.64}$$

$$\frac{N_{Ed}}{\chi_z N_{Rk} / \gamma_{M1}} + k_{zy} \frac{M_{y,Ed} + \Delta M_{y,Ed}}{\chi_{LT} M_{y,Rk} / \gamma_{M1}} + k_{zz} \frac{M_{z,Ed} + \Delta M_{z,Ed}}{M_{z,Rk} / \gamma_{M1}} \leq 1,0 \tag{4.65}$$

where

N_{Ed}, $M_{y.Ed}$ and $M_{z.Ed}$ are the first order design values of the compression force and the maximum moments about the y–y and z–z axis along the member, respectively.

$\Delta M_{y,Ed}$, $\Delta M_{z,Ed}$ are the moments due to the shift of the centroid axis for class 4 sections (see Table 4.10)

χ_y and χ_z are the reduction factors due to flexural buckling;

χ_{LT} is the reduction factor due to lateral torsional buckling. For members not susceptible to torsional deformation χ_{LT} = 1,0;

k_{yy}, k_{yz}, k_{zy}, k_{zz} are interaction factors.

The interaction factors k_{yy}, k_{yz}, k_{zy}, k_{zz} depend on the method which is chosen, being derived from two alternative approaches: (1) Alternative method 1 – see Tables 4.7 and 4.8 (Annex A of EN1993-1-1) and (2) Alternative method 2 – see Tables 4.9, 4.10 and 4.11 (Annex B of EN1993-1-1).

Table 4.10 Values for $N_{Rk} = f_y \cdot A_i$, $M_{i,Rk} = f_y W_i$ and $\Delta M_{i,Ed}$

Class	1	2	3	4
A_i	A	A	A	A_{eff}
W_y	$W_{pl,y}$	$W_{pl,y}$	$W_{el,y}$	$W_{eff,y}$
W_z	$W_{pl,z}$	$W_{pl,z}$	$W_{el,z}$	$W_{eff,z}$
$\Delta M_{y,Ed}$	0	0	0	$e_{N,y} N_{Ed}$
$\Delta M_{z,Ed}$	0	0	0	$e_{N,z} N_{Ed}$

4.4.4.3 Design example

The following example presents the design of a cold-formed steel built-up column in compression and bending, as component of a pitched roof cold-formed steel portal frame consisting of back-to-back lipped channel sections and bolted joints. Pinned supports are considered at the column bases. The ridge and eave connections are assumed to be rigid.

Figure 4.44 and Figure 4.45 present schematically the design of a cold-formed steel member in combined compression and uniaxial bending.

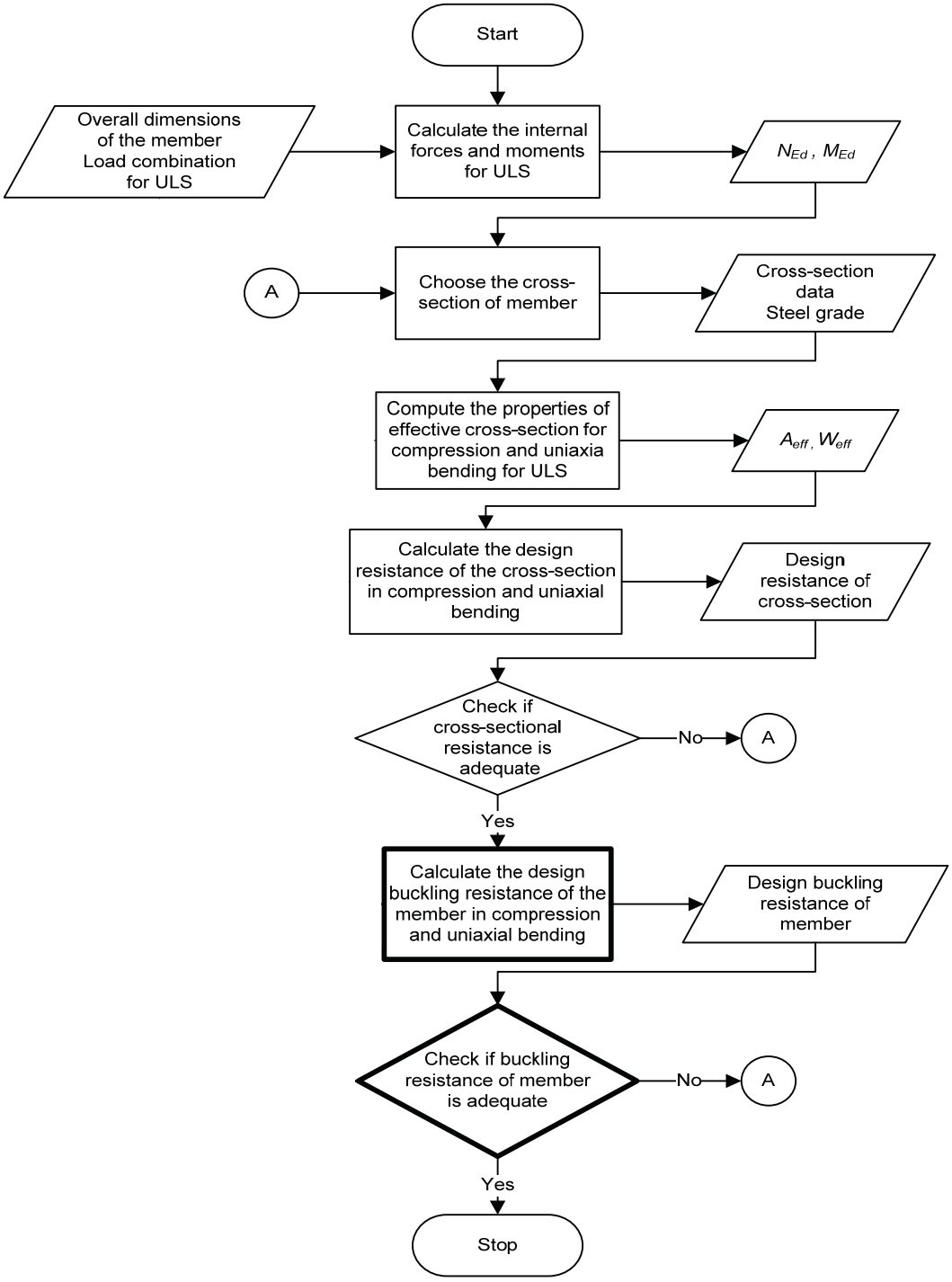

Figure 4.44 Design of a cold-formed steel member in combined compression and uniaxial bending (SF042a-EN-EU, Access Steel 2006)

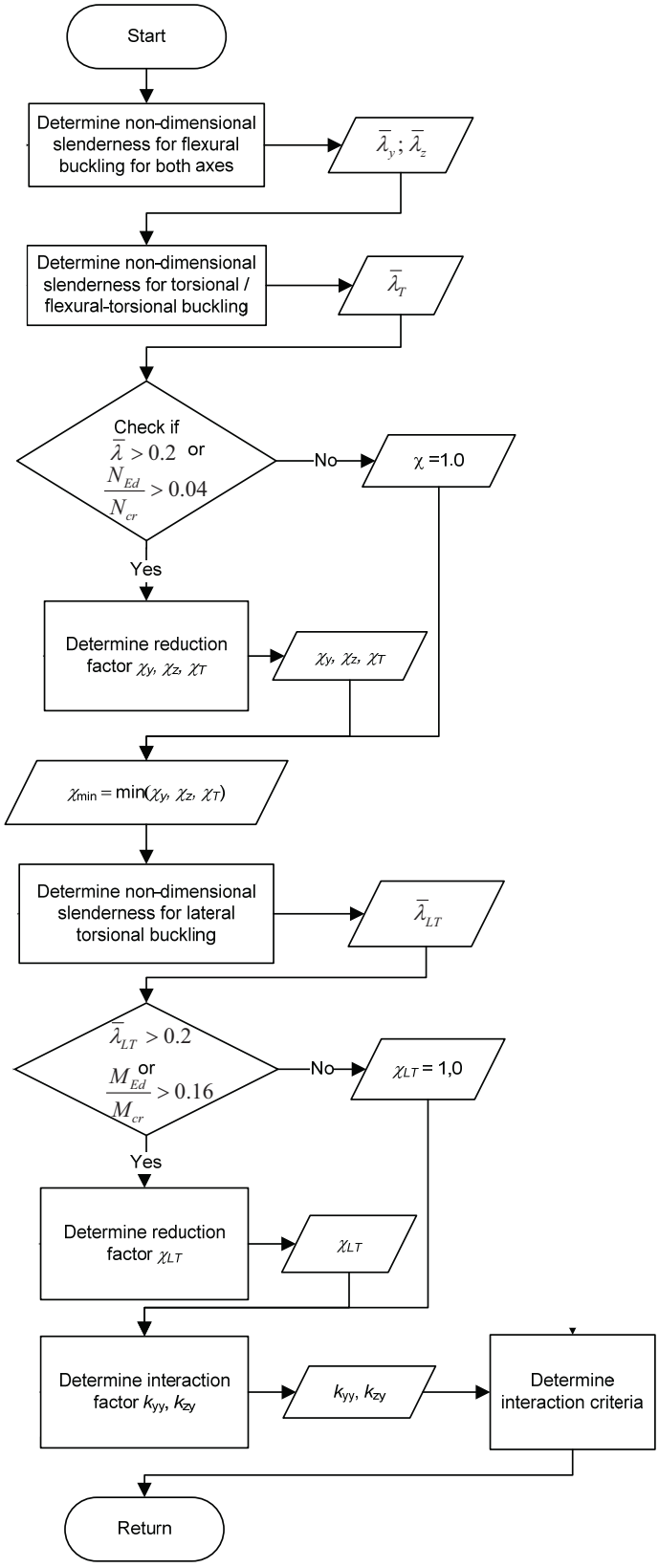

Figure 4.45 Calculate the design buckling resistance of the member in compression and UNIAXIAL bending (SF042a-EN-EU, Access Steel 2006)

Basic Data

Height of column:	H = 4,00 m
Span:	L = 12,00 m
Bay:	T = 4,00 m
Roof angle:	10°

The dimensions of one lipped channel section and the material properties are:

Total height	h = 350 mm
Total width of flange	b = 96 mm
Total width of edge fold	c = 32 mm
Internal radius	r = 3 mm
Nominal thickness	t_{nom} = 3,0 mm
Steel core thickness	t = 2,96 mm
Steel grade	*S350GD + Z*
Basic yield strength	f_{yb} = 350 N/mm^2
Modulus of elasticity	E = 210 000 N/mm^2
Poisson's ratio	$\nu = 0,3$
Shear modulus	$G = \frac{E}{2(1+\nu)} = 81\,000$ N/mm^2
Partial factors	γ_{M0} = 1,0, γ_{M1} = 1,0, γ_G = 1,35, γ_Q = 1,50

Distributed loads applied to the frame:

- self-weight of the structure (applied by the static computer program)
- dead load – the roof structure: 0,20 kN/m^2

  q_G = 0,2 x 4,0 = 0,8 kN/m
- snow load: 1,00 kN/m^2

  q_s = 1,00 x 4,00 kN/m

Only one load combination at the Ultimate Limit State was considered in the analysis. The uniform distributed load on the frame, according to §§2.3.1 (see Flowchart 2.1) is:

$$\left(\gamma_G q_G + \gamma_Q q_Q\right) T = \left(1,35 \times 0,2 + 1,50 \times 1,00 \times \cos 10^\circ\right) \times 4 \cong 7,00 \text{ kN/m}$$

Properties of the gross cross-section

Area of gross cross-section:	$A = 3502$ mm^2
Radii of gyration:	$i_y = 133,5$ mm ; $i_z = 45,9$ mm
Second moment of area about strong axis *y-y*:	$I_y = 6240,4 \times 10^4$ mm^4
Second moment of area about weak axis *z-z*:	$I_z = 737,24 \times 10^4$ mm^4

Warping constant: $I_w = 179274 \times 10^6$ mm^6

Torsion constant: $I_t = 10254,8$ mm^4

Effective section properties of the cross-section

Effective area of the cross-section when subjected to compression only:

$A_{eff,c} = 1982,26$ mm^2

Second moment of area of effective cross-section about strong axis *y–y*:

$I_{eff,y} = 5850,85 \times 10^4$ mm^4

Effective section modulus in bending:

- with respect to the flange in compression: $W_{eff,y,c} = 319968$ mm^3
- with respect to the flange in tension: $W_{eff,y,t} = 356448$ mm^3

$W_{eff,y,\min} = \min\left(W_{eff,y,c}, W_{eff,y,t}\right) = 319968$ mm^3

The built-up column has to be designed for the relevant values in N_{Ed} and M_{Ed} diagrams displayed in Figure 4.46, respectively i.e.:

- the axial force (compression): $N_{Ed} = -44,82$ kN;
- the maximum bending moment: $M_{y,Ed} = -68,95$ kNm

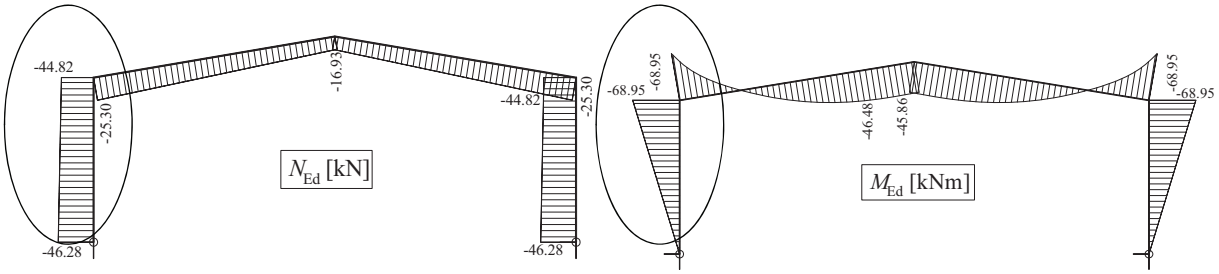

Figure 4.46 N_{Ed} and $M_{y,Ed}$ diagrams

Resistance check of the cross-section

The following criterion should be met:

$$\frac{N_{Ed}}{N_{c,Rd}} + \frac{M_{y,Ed} + \Delta M_{y,Ed}}{M_{cy,Rd,com}} \le 1$$

where:

$N_{c,Rd} = A_{eff} f_{yb} / \gamma_{M0}$

$M_{cz,Rd,com} = W_{eff,com} f_{yb} \; / \; \gamma_{M0}$

$\Delta M_{y,Ed} = N_{Ed} e_{Ny}$

e_{Ny} – is the shift of the centroidal *y–y* axis; but as the cross-section is doubly symmetric: $e_{Ny} = 0$ (§§3.8.9)

The resistance check is:

$$\frac{44,82 \times 10^3}{1982 \times 350/1,0} + \frac{68,95 \times 10^6 + 0}{319968 \times 350/1,0} = 0,680 < 1 \quad \text{– OK}$$

Buckling resistance check

Members which are subjected to combined axial compression and uniaxial bending should satisfy:

$$\frac{N_{Ed}}{\chi_y \frac{N_{Rk}}{\gamma_{M1}}} + k_{yy} \frac{M_{y,Ed} + \Delta M_{y,Ed}}{\chi_{LT} \frac{M_{y,Rk}}{\gamma_{M1}}} \le 1$$

$$\frac{N_{Ed}}{\chi_z \frac{N_{Rk}}{\gamma_{M1}}} + k_{zy} \frac{M_{y,Ed} + \Delta M_{y,Ed}}{\chi_{LT} \frac{M_{y,Rk}}{\gamma_{M1}}} \le 1$$

where:

$N_{Rk} = f_{yb} A_{eff} = 350 \times 1982 = 693,7 \times 10^3$ N $= 693,7$ kN

$M_{y,Rk} = f_{yb} W_{eff,y,\min} = 350 \times 319968 = 112 \times 10^6$ Nmm $= 112$ kNm

$\Delta M_{y,Ed}$ – additional moment due to the shift of the centroidal axes;

$\Delta M_{y,Ed} = 0$

$$\chi = \frac{1}{\phi + \sqrt{\phi^2 - \bar{\lambda}^2}} \quad \text{but} \quad \chi \le 1,0$$

$$\phi = 0,5\left[1 + \alpha\left(\bar{\lambda} - 0,2\right) + \bar{\lambda}^2\right]$$

α – imperfection factor

The non-dimensional slenderness is:

$$\bar{\lambda} = \sqrt{\frac{A_{eff} f_{yb}}{N_{cr}}}$$

N_{cr} – the elastic critical force for the relevant buckling mode

Determination of the reduction factors χ_y, χ_z, χ_T

Flexural buckling

$$\bar{\lambda}_F = \sqrt{\frac{A_{eff} f_{yb}}{N_{cr}}} = \frac{L_{cr}}{i} \frac{\sqrt{A_{eff}/A}}{\lambda_1}$$

The buckling length:

$$L_{cr,y} = L_{cr,z} = H = 4000 \text{ mm}$$

$$\lambda_1 = \pi \sqrt{\frac{E}{f_{yb}}} = \pi \times \sqrt{\frac{210000}{350}} = 76,95$$

Buckling about *y–y* axis

$$\bar{\lambda}_y = \frac{L_{cr,y}}{i_y} \frac{\sqrt{A_{eff}/A}}{\lambda_1} = \frac{4000}{133,5} \times \frac{\sqrt{1982,26/3502}}{76,95} = 0,293$$

$\alpha_y = 0,21$ – buckling curve *a*

$$\phi_y = 0,5\left[1 + \alpha_y \left(\bar{\lambda}_y - 0,2\right) + \bar{\lambda}_y^{\,2}\right] =$$
$$= 0,5 \times \left[1 + 0,21 \times \left(0,293 - 0,2\right) + 0,293^2\right] = 0,553$$

$$\chi_y = \frac{1}{\phi_y + \sqrt{\phi_y^{\,2} - \bar{\lambda}_y^{\,2}}} = \frac{1}{0,553 + \sqrt{0,553^2 - 0,293^2}} = 0,978$$

Buckling about *z–z* axis

$$\bar{\lambda}_z = \frac{L_{cr,z}}{i_z} \frac{\sqrt{A_{eff}/A}}{\lambda_1} = \frac{4000}{45,9} \times \frac{\sqrt{1982,26/3502}}{76,95} = 0,852$$

$\alpha_z = 0.34$ – buckling curve *b*

$$\phi_z = 0,5\left[1 + \alpha_z \left(\bar{\lambda}_z - 0,2\right) + \bar{\lambda}_z^{\,2}\right] =$$
$$= 0,5 \times \left[1 + 0,34 \times \left(0,852 - 0,2\right) + 0,852^2\right] = 0,974$$

$$\chi_z = \frac{1}{\phi_z + \sqrt{\phi_z^{\,2} - \bar{\lambda}_z^{\,2}}} = \frac{1}{0,974 + \sqrt{0,974^2 - 0,852^2}} = 0,692$$

Torsional buckling

$$N_{cr,T} = \frac{1}{i_o^{\,2}} \left(GI_t + \frac{\pi^2 EI_w}{l_T^{\,2}} \right)$$

where:

$$i_o^2 = i_y^2 + i_z^2 + y_o^2 + z_o^2$$

y_o, z_o – the shear centre coordinates with respect to the centroid of the gross cross-section: $y_o = z_o = 0$

$$i_o^2 = 133,5^2 + 45,9^2 + 0 + 0 = 19929,1 \text{ mm}^2$$

$$l_T = H = 4000 \text{ mm}$$

The elastic critical force for torsional buckling is:

$$N_{cr,T} = \frac{1}{19929,1} \times \left(81000 \times 10254,8 + \frac{\pi^2 \times 210000 \times 179274 \times 10^6}{4000^2} \right) =$$
$$= 1206,96 \times 10^3 \text{ N}$$

The non-dimensional slenderness is:

$$\bar{\lambda}_T = \sqrt{\frac{A_{eff} f_{yb}}{N_{cr}}} = \sqrt{\frac{1982,26 \times 350}{1206,96 \times 10^3}} = 0,758$$

$\alpha_T = 0,34$ – buckling curve *b*

$$\phi_T = 0,5 \left[1 + \alpha_T \left(\bar{\lambda}_T - 0,2 \right) + \bar{\lambda}_T^2 \right] =$$
$$= 0,5 \times \left[1 + 0,34 \times \left(0,758 - 0,2 \right) + 0,758^2 \right] = 0,882$$

The reduction factor for torsional and flexural-torsional buckling is:

$$\chi_T = \frac{1}{\phi_T + \sqrt{\phi_T^2 - \bar{\lambda}_T^2}} = \frac{1}{0,882 + \sqrt{0,882^2 - 0,758^2}} = 0,750$$

Determination of the reduction factor χ_{LT}

Lateral-torsional buckling

$$\chi_{LT} = \frac{1}{\phi_{LT} + \sqrt{\phi_{LT}^2 - \bar{\lambda}_{LT}^2}} \quad \text{but} \quad \chi_{LT} \le 1,0$$

$$\phi_{LT} = 0,5 \left[1 + \alpha_{LT} \left(\bar{\lambda}_{LT} - 0,2 \right) + \bar{\lambda}_{LT}^2 \right]$$

$\alpha_{LT} = 0,34$ – buckling curve *b*

The non-dimensional slenderness is:

$$\bar{\lambda}_{LT} = \sqrt{\frac{W_{eff,y,\min} f_{yb}}{M_{cr}}}$$

M_{cr} – the elastic critical moment for lateral-torsional buckling

$$M_{cr} = C_1 \frac{\pi^2 E I_z}{L^2} \sqrt{\frac{I_w}{I_z} + \frac{L^2 G I_t}{\pi^2 E I_z}}$$

where $C_1 = 1,77$ for a simply supported beam under uniform loading

$$M_{cr} = 1,77 \times \frac{\pi^2 \times 210000 \times 737,24 \times 10^4}{4000^2} \times \\ \times \sqrt{\frac{179274 \times 10^6}{737,24 \times 10^4} + \frac{4000^2 \times 81000 \times 10254,8}{\pi^2 \times 210000 \times 737,24 \times 10^4}}$$

$$M_{cr} = 282,27 \text{ kNm}$$

$$\bar{\lambda}_{LT} = \sqrt{\frac{W_{eff,y,\min} f_{yb}}{M_{cr}}} = \sqrt{\frac{319968 \times 350}{268,27 \times 10^6}} = 0,646$$

$$\phi_{LT} = 0,5\left[1 + \alpha_{LT}\left(\bar{\lambda}_{LT} - 0,2\right) + \bar{\lambda}_{LT}{}^2\right] = \\ = 0,5 \times \left[1 + 0,34 \times \left(0,646 - 0,2\right) + 0,646^2\right] = 0,784$$

$$\chi_{LT} = \frac{1}{\phi_{LT} + \sqrt{\phi_{LT}{}^2 - \bar{\lambda}_{LT}{}^2}} = \frac{1}{0,784 + \sqrt{0,784^2 - 0,646^2}} = 0,814$$

Determination of interaction factors k_{yy} and k_{zy} – Method 1

$$k_{yy} = C_{my} C_{mLT} \frac{\mu_y}{1 - \frac{N_{Ed}}{N_{cr,y}}}; \; k_{zy} = C_{my} C_{mLT} \frac{\mu_z}{1 - \frac{N_{Ed}}{N_{cr,y}}}$$

where:

$$\mu_y = \frac{1 - \frac{N_{Ed}}{N_{cr,y}}}{1 - \chi_y \frac{N_{Ed}}{N_{cr,y}}}; \qquad \mu_z = \frac{1 - \frac{N_{Ed}}{N_{cr,z}}}{1 - \chi_z \frac{N_{Ed}}{N_{cr,z}}}$$

$$N_{cr,y} = \frac{\pi^2 E I_y}{L_{cr,y}^2} = \frac{\pi^2 \times 210000 \times 6240,4 \times 10^4}{4000^2} = 8083,72 \times 10^3 \text{ N} = 8083,72 \text{ kN}$$

$$N_{cr,z} = \frac{\pi^2 E I_z}{L_{cr,z}^2} = \frac{\pi^2 \times 210000 \times 737.24 \times 10^4}{4000^2} = 955 \times 10^3 \text{ N} = 955 \text{ kN}$$

$$\mu_y = \frac{1 - \frac{N_{Ed}}{N_{cr,y}}}{1 - \chi_y \frac{N_{Ed}}{N_{cr,y}}} = \frac{1 - \frac{44,82}{8083,72}}{1 - 0,978 \times \frac{44,82}{8083,72}} = 1,00$$

$$\mu_z = \frac{1 - \frac{N_{Ed}}{N_{cr,z}}}{1 - \chi_z \frac{N_{Ed}}{N_{cr,z}}} = \frac{1 - \frac{44,82}{955}}{1 - 0,692 \times \frac{44,82}{955}} = 0,985$$

$$C_{my} = C_{my,0} + \left(1 - C_{my,0}\right) \frac{\sqrt{\varepsilon_y} a_{LT}}{1 + \sqrt{\varepsilon_y} a_{LT}}; \; C_{mLT} = C_{my}^2 \frac{a_{LT}}{\sqrt{\left(1 - \frac{N_{Ed}}{N_{cr,z}}\right)\left(1 - \frac{N_{Ed}}{N_{cr,T}}\right)}}$$

$$C_{my,0} = 1 + 0,03\frac{N_{Ed}}{N_{cr,y}} = 1 + 0,03 \times \frac{44,82}{8083,72} = 1,0002$$

$$\varepsilon_y = \frac{M_{y,Ed}}{N_{Ed}}\frac{A_{eff}}{W_{eff,y,\min}} = \frac{68,95 \times 10^6}{44,82 \times 10^3} \times \frac{1982,26}{319968} = 9,53$$

$$a_{LT} = 1 - \frac{I_t}{I_y} = 1 - \frac{10254,8}{6240,4 \times 10^4} = 1$$

$$C_{my} = 1,0002 + \left(1 - 1,0002\right) \times \frac{\sqrt{9,53} \times 1}{1 + \sqrt{9,53} \times 1} = 1$$

$$C_{mLT} = 1^2 \times \frac{1}{\sqrt{\left(1 - \frac{44,82}{955}\right) \times \left(1 - \frac{44,82}{1206,96}\right)}} = 1,090$$

The interaction factors are:

$$k_{yy} = C_{my}C_{mLT}\frac{\mu_y}{1 - \frac{N_{Ed}}{N_{cr,y}}} = 1 \times 1,090 \times \frac{1}{1 - \frac{44,82}{8083,72}} = 1,096$$

$$k_{zy} = C_{my}C_{mLT}\frac{\mu_z}{1 - \frac{N_{Ed}}{N_{cr,y}}} = 1 \times 1,090 \times \frac{0,985}{1 - \frac{44,82}{8083,72}} = 1,080$$

Buckling resistance check

$$\frac{N_{Ed}}{\chi_y \frac{N_{Rk}}{\gamma_{M1}}} + k_{yy}\frac{M_{y,Ed} + \Delta M_{y,Ed}}{\chi_{LT}\frac{M_{y,Rk}}{\gamma_{M1}}} = \\ = \frac{44,82}{0,978 \times \frac{693,7}{1,0}} + 1,096 \times \frac{68,95 + 0}{0,814 \times \frac{112}{1,0}} = 0,895 < 1 \quad \text{– OK}$$

$$\frac{N_{Ed}}{\chi_z \frac{N_{Rk}}{\gamma_{M1}}} + k_{zy}\frac{M_{y,Ed} + \Delta M_{y,Ed}}{\chi_{LT}\frac{M_{y,Rk}}{\gamma_{M1}}} = \\ = \frac{44,82}{0,692 \times \frac{693,7}{1,0}} + 1,080 \times \frac{68,95 + 0}{0,814 \times \frac{112}{1,0}} = 0,910 < 1 \quad \text{– OK}$$

As an alternative, the interaction formula may be used:

$$\left(\frac{N_{Ed}}{N_{b,Rd}}\right)^{0.8} + \left(\frac{M_{Ed}}{M_{b,Rd}}\right)^{0.8} \le 1,0$$

$$\chi = \min(\chi_y, \chi_z, \chi_T) = \min(0,978; 0,692; 0,750) = 0,692$$

$$N_{b.Rd} = \frac{\chi A_{eff} f_y}{\gamma_{M1}} = \frac{0,692 \times 1982,26 \times 350}{1,00} = 480,10 \times 10^3 \text{N} = 480,10 \text{ kN}$$

$$M_{b,Rd} = \chi_{LT} W_{eff,y} f_{yb} / \gamma_{M1} = 0,814 \times 319968 \times 10^{-9} \times 350 \times 10^{3} / 1,0 = 91,16 \text{ kNm}$$

$$\left(\frac{N_{Ed}}{N_{b,Rd}}\right)^{0,8} + \left(\frac{M_{Ed}}{M_{b,Rd}}\right)^{0,8} = \left(\frac{44,82}{480,1}\right)^{0,8} + \left(\frac{68,95}{91,16}\right)^{0,8} = 0,950 \le 1,0$$

4.4.5 Beams restrained by sheeting

4.4.5.1 General approach

Purlins and side rails acting as secondary beams supported by primary beams (e.g. rafters) or columns are often restrained by the building envelope (e.g. trapezoidal sheeting, cassettes, sandwich panels, OSB panels, etc.). Similarly, floor joists are restrained by the dry floor deck or the reinforced concrete slab.

Currently, Z- and C-sections are used as purlins or rails which, due to their shapes can be sensitive to lateral-torsional buckling, so it is important to take advantage of sheeting, if effective. Figure 4.47 shows, schematically, the position of a Z-section purlin on a sloped roof, while Figure 4.48 presents the composition of a roof panel.

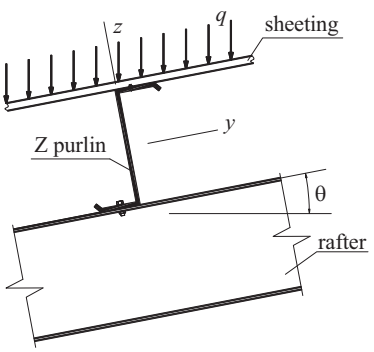

Figure 4.47 Sloped Z-section roof system

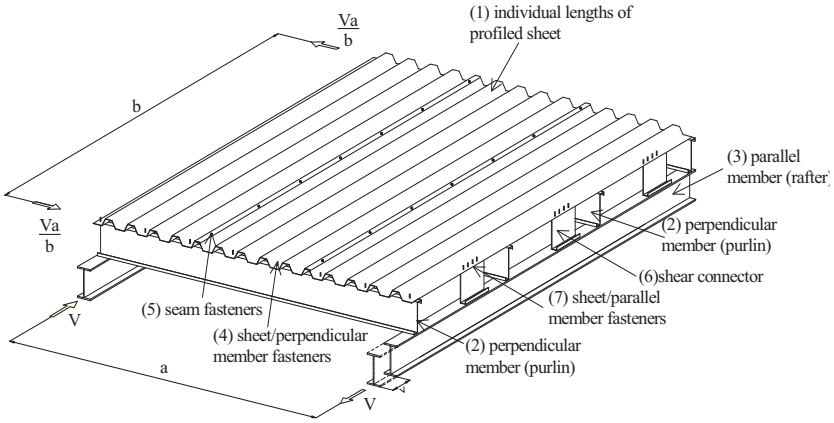

Figure 4.48 Arrangement of an individual shear panel (ECCS_88, 1995)

The restraining effect of sheeting has to be considered for an effective design of purlin-sheeting systems. It is generally assumed that the sheeting can provide the necessary in-plane stiffness and capacity to carry the component of the load in the plane of the sheeting (see Figure 4.49), while the purlin resists to normal component. In fact, the sheeting may provide not only lateral restraint but can also partially restrain the twisting of purlins, taking account of the flexural stiffness of the sheeting if substantial (e.g. as for trapezoidal sheeting) and properly connected to the purlin.

According to EN1993-1-3, if trapezoidal sheeting is connected to a purlin and the condition expressed by the Eqn. (4.66) is met, the purlin at the connection may be regarded as being laterally restrained in the plane of the sheeting:

$$S \ge \left(EI_w \frac{\pi^2}{L^2} + GI_t + EI_z \frac{\pi^2}{L^2} 0,25 h^2 \right) \frac{70}{h^2} \tag{4.66}$$

where

S is the portion of the shear stiffness provided by the sheeting for the examined member connected to the sheeting at each rib. If the sheeting is connected to a purlin every second rib only, then *S* should be replaced by 0,20 *S*;

I_w is the warping constant of the purlin;

I_t is the torsion constant of the purlin;

I_z is the second moment of area of the cross-section about the minor axis of the cross-section of the purlin;

L is the span of the purlin;

h is the height of the purlin.

To evaluate the restraining effect of sheeting, in EN1993-1-3 the free flange is considered as a beam on an elastic foundation, as shown in Figure 4.49, where q_{Ed} is the vertical load, *K* is the stiffness of an equivalent lateral linear spring and k_h is the equivalent lateral load factor.

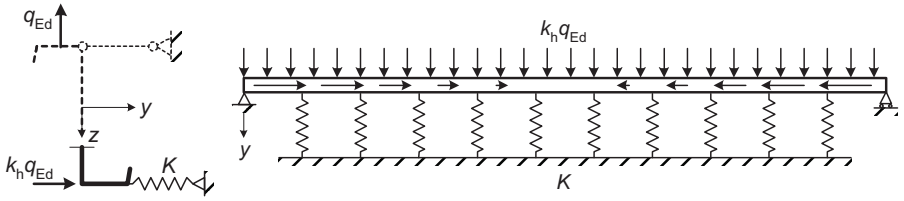

As a simplification replace the rotational spring C_D by a lateral spring of stiffness *K*

Free flange of purlin modelled as a beam on an elastic foundation. Model representing effect of torsion and lateral bending (including cross-section distortion) on single span under with uplift loading

Figure 4.49 Modelling laterally braced purlins rotationally restrained by sheeting

The equivalent lateral spring stiffness for the strength and stability check is obtained by a combination of:

1. rotational stiffness of the connection between the sheeting and the purlin C_D, (see Figure 4.50);
2. distortion of the cross-section of the purlin, K_B, as shown in Figure 4.51;
3. bending stiffness of the sheeting, $C_{D,C}$, perpendicular to the span of the purlin (see Figure 4.52).

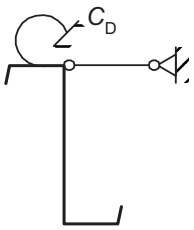

Figure 4.50 Torsional and lateral restraining of purlin by sheeting

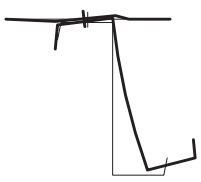

Figure 4.51 Distortion of purlin

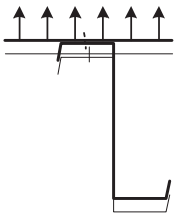

Figure 4.52 Bending of the purlin

The composed distortion-torsion-bending effect is shown in Figure 4.53:

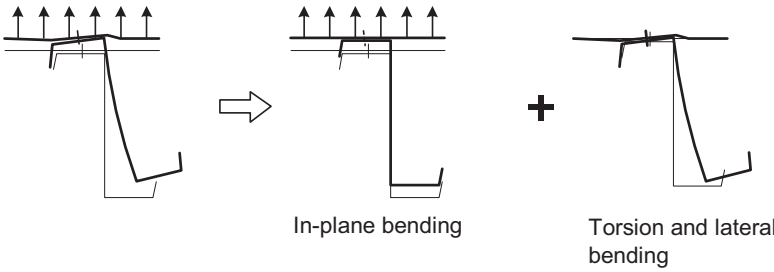

Figure 4.53 Deformation of purlin restrained by sheeting

According to EN1993-1-3, the partial torsional restraint may be represented by a rotational spring with a spring stiffness C_D, which can be calculated based on the stiffness of the sheeting and the connection between the sheeting and the purlin, as follows,

$$\frac{1}{C_D} = \frac{1}{C_{D,A}} + \frac{1}{C_{D,C}} \tag{4.67}$$

where:

$C_{D,A}$ is the rotational stiffness of the connection between the sheeting and the purlin;

$C_{D,C}$ is the rotational stiffness corresponding to the flexural stiffness of the sheeting.

Both $C_{D,A}$ and $C_{D,C}$ are specified in Section 10.1.5 of EN1993-1-3. Alternatively, the $C_{D,A}$ stiffness and $C_{D,C}$ stiffness values can be obtained experimentally applying the recommendation in Annex A5 of EN1993-1-3.

The model presented above can be also used for other types of claddings. For instance, Figure 4.54 shows the model adopted to represent the sandwich panel-purlin interaction.

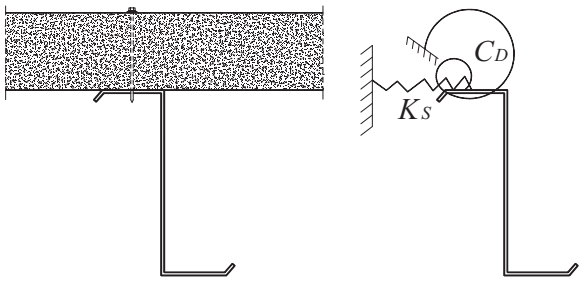

Figure 4.54 Model adopted for sandwich panel – purlin interaction (Davies, 2001)

The restraints of the sheeting to the purlin have important influence on the buckling behaviour of the purlin. Figure 4.55 shows the buckling curves of a simply supported Z-purlin beam (h=202 mm, b=75 mm, c=20 mm and t=2,3 mm) with various different lateral restraints applied at the junction between the web and the compression flange when subjected to pure bending (Martin and Purkiss, 2008). One observes that, when the translational displacement of the compression flange is restrained, the purlin does not buckle lateral-torsionally, while when the rotation of the compression flange is restrained,

the critical stresses of the local buckling and distortional buckling modes are increased significantly.

However, when the restraints are applied at the junction between the web and the tension flange, it is only the rotational restraint that influences the lateral–torsional buckling of the purlin (see Figure 4.56).

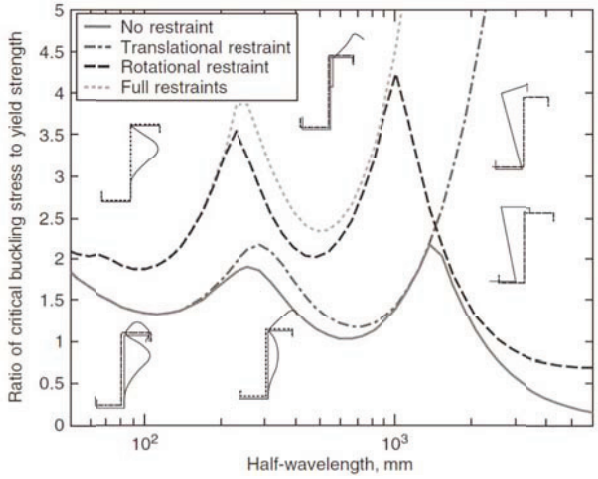

Figure 4.55 Buckling curves of a simply supported zed section beam with different restraint applied at the junction between web and compression flange subjected to pure bending (h=202 mm, b=75 mm, c=20 mm, t =2,3mm) (Martin and Purkiss, 2008)

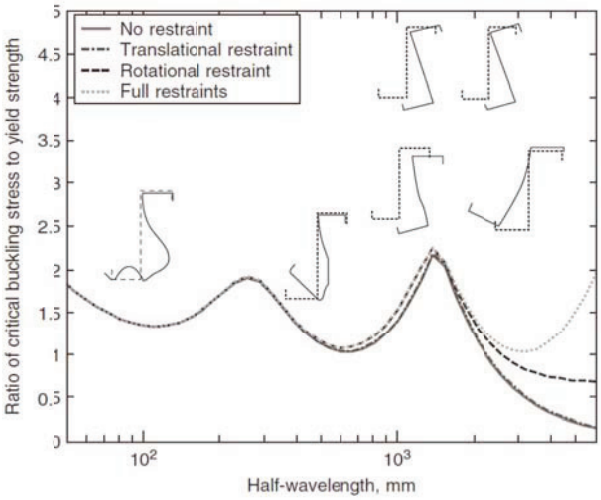

Figure 4.56 Buckling curves of a simply supported zed section beam with different restraint applied at the junction between web and tension flange subjected to pure bending (h=202 mm, b=75 mm, c=20 mm, t =2,3mm) (Martin and Purkiss, 2008)

4.5 Connections

4.5.1 Introduction

Connections are an important part of every structure, not only from the point of view of structural behaviour, but also in relation to the method of production. It has been shown that, for a structure made of hot-rolled sections, the connections account for a minimum of 50% of the total value of constructional steelwork (Fenster et al., 1992). There is no reason to believe that the percentage will be much lower for cold-formed steel structures (Yu et al., 1993). Connections in cold-formed steel structures are used for:

1. connecting steel sheets to supporting structure (thin-to-thick), e.g. roof sheeting to purlins, cladding sheeting to side-rails etc.;
2. interconnecting two or more sheets (thin-to-thin), e.g. seam fastening of sheeting;
3. assembling bar members (thin-to-thin or thick-to-thick), e.g. for framed structures, trusses etc.

In comparison with hot-rolled sections, the behaviour of connections in cold-formed steel elements is influenced by the reduced stiffness of thin walls. Therefore, additional effects are, for example, the tilting of the fastener in hole bearing failure under the shear distortion of the sheet when the fastener is loaded in tension and the sheet is pulled over the head of the fastener. This is the reason why specific technologies and related design procedures, either by calculation or calculation assisted by testing, have been developed for cold-formed steel structures.

A variety of joining methods is available for these structures. They can be classified as follows (Toma et al., 1993; Yu, 2000):

- fastenings with mechanical fasteners;
- fastenings based on welding;
- fastenings based on adhesive bonding.

Fasteners for light gauge steelwork can be also classified into three main groups depending on the thickness of the parts being connected. These groupings and some typical types of fasteners within each group are shown in Table 4.11.

Table 4.11 Some typical application of different type of fasteners

Thin-to-thin	Thin-to-thick or thin-to-hot rolled	Thick-to-thick or thick-to-hot rolled
○ self-drilling, self-tapping screws; ○ blind rivets; ○ press-joints; ○ single-flare V welds; ○ spot welds; ○ seam welding; ○ adhesive bonding.	○ self-drilling, self-tapping screws; ○ fired pins; ○ bolts; ○ arc spot puddle welds; ○ adhesive bonding.	○ bolts; ○ arc welds.

The selection of the most suitable types of fastener for a given application is governed by several factors (Davies, 1991):

a) load-bearing requirements: strength; stiffness; ductility (deformation capacity);
b) economic requirements: number of fasteners required; cost of labour and materials; skill required in fabrication; design life; maintenance; ability to be dismantled; durability; resistance to aggressive environments;
c) water tightness;
d) appearance (architectural aspect).

Although the structural engineers tend to be primarily concerned with the most economical way of meeting the load-bearing requirements, in many applications other factors may be equally important.

4.5.2 Fastening techniques of cold-formed steel constructions

4.5.2.1 Mechanical fasteners

Fasteners for sheets of sections and sandwich panels are discussed separately. Most fasteners can be used in almost all kinds of cold-formed steel applications (like screws),

others are appropriate for specific applications, only. Table 4.12 gives a general overview of the application of different mechanical fasteners in cold-formed steel sections.

In recent years, the press-joining technology (Predeschi et al., 1997), originating from the automotive industry, and the "Rosette" system (Makelainen and Kesti, 1999) have augmented the family of mechanical fasteners for thin-walled steel constructions.

Bolts with nuts are threaded fasteners which are assembled in drilled holes through the material elements to be joined. Thin members will necessitate the use of bolts threaded close to the head. Head shapes may be hexagonal, cup, countersunk, or hexagonal flanged. The nuts should normally be hexagonal. For thin-walled sections bolt diameters are usually M5 to M16. The preferred property classes are 8.8 or 10.9.

Bolts with nuts are used for connections in cold-formed steel framed and truss structures, and for purlin-to-rafter or purlin-to-purlin attachment by sleeved or overlapping purlin (see Figure 4.57).

Table 4.12 Usual mechanical fasteners for common applications (Yu et al., 1993)

Thin -to-thick	Steel -to-wood	Thin -to-thin	Fasteners	Remark
X		X	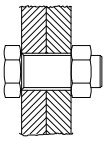	Bolts M5-M16
X			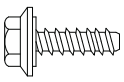	Self-tapping screw ϕ6,3 with washer $\geq$ 16 mm, 1 mm thick with elastomer
	X	X	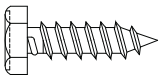	Hexagon head screw ϕ6,3 or ϕ6,5 with washer $\geq$ 16 mm, 1 mm thick with elastomer
X		X	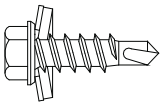	Self-drilling screws with diameters: ϕ4,22 or ϕ4,8 mm ϕ5,5 mm ϕ6,3 mm
		X	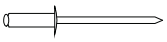	Blind rivets with diameters: ϕ4,0 mm ϕ4,8 mm ϕ6,4 mm
X			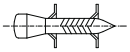	Shot (fired) pins
X				Nuts

Tests have revealed the following basic types of failure for thin steel bolted connections working in shear and tension:

a) failure modes in shear:
   - shearing of the bolt: rupture (Figure 4.57a) or crushing (Figure 4.57b);

- bearing (yield) and/or piling of thinner material (Figure 4.57c). When both materials are thin, yielding of both sheets may occur together with bolt tilting (Figure 4.57d);
- tearing of the sheet in the net sections (Figure 4.57e);
- end failure by shearing of thin material (Figure 4.57f);

b) failure modes in tension:

- tension failure or rupture of bolt (Figure 4.58a);
- pull-through failure (Figure 4.58b).

The two main types of screws are self-tapping and self-drilling screws. Most screws will be combined with washers to improve the load-bearing capacity of the fastening or to make the fastening self-sealing. Some types have plastic heads or plastic caps, which are available for additional corrosion resistance and/or colour matching.

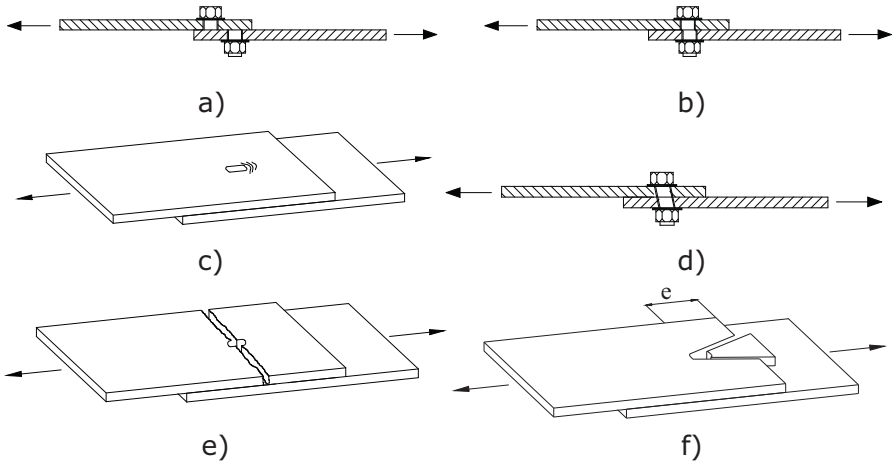

Figure 4.57 Failure modes of bolted connections in shear

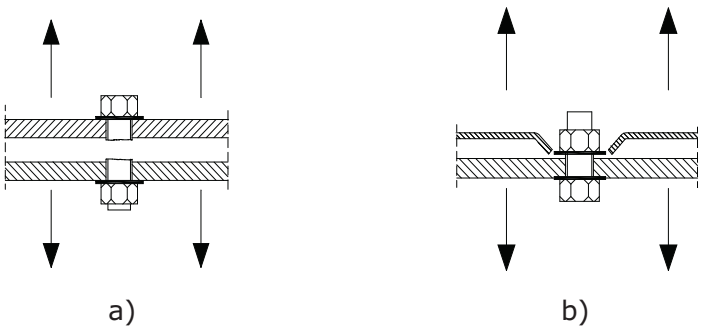

Figure 4.58 Failure modes for bolted connections in tension

Self-tapping screws. Self-tapping screws tap their counterthread in a prepared hole. They can be classified as thread-forming and thread-cutting.

Self-drilling screws. Self-drilling screws drill their own holes and form their mating threads in one operation. This type of screw serves to fasten thin sheets to thin sheets.

Self-drilling screws are normally fabricated from heat-treated carbon steel (plated with zinc for corrosion protection and lubrication) or from stainless steel (with carbon-steel drill point and plated with zinc for lubrication).

Self-tapping and self-drilling screws are usually combined with washers. The washers increase the load-bearing capacity and/or the sealing ability. Elastomeric or combined metal-elastomeric washers cause a marked reduction in the strength and stiffness of the connections.

The failure modes of screwed connections in shear are generally similar to those of bolted connections. However, due to the fact that the connected materials are usually thin (or at least one of the connected parts is thin), usually does not fail in shear. Bearing, pulling, tearing and/or shearing of the material connected by screws and working in shear are possible failure modes. Also, the tilting and pulling out of the fastener may occur (see Figure 4.59).

Figure 4.59 Tilting and pull-out of fastener (inclination failure)

In what concerns the behaviour in tension, compared with bolted connections, there are three supplementary failure modes characteristic for screwed connections, i.e. (1) pull-out (see Figure 4.60a); (2) pull-over (see Figure 4.60b) and distortion of thinner material (see Figure 4.60c).

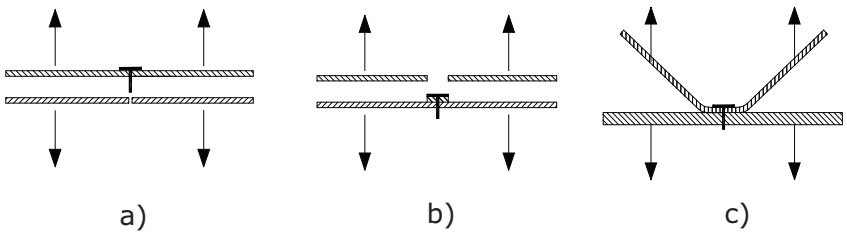

Figure 4.60 Supplementary failure modes for screwed fastening in tension: a) pull-out; b) pull-over; c) gross distortion of sheeting

Failure modes of mechanical fastener in tension are not easy to understand. Usually, failure occurs in combinations of two or even three modes. The following supplementary comments may be helpful to the reader:

a) tensile failure of the fastener itself. This failure mode is only likely to occur when the sheeting is excessively thick or when an unsuitable or faulty fastener is used;
b) pull-out of the fastener. This failure mode may occur when the support member is insufficiently thick or when there is insufficient thread engagement;
c) pull-over of the sheeting. In this mode, the sheeting tears around the fastener head of the washer;
d) pull-through of the sheeting. Here, the sheeting distorts sufficiently to pull through from under the head of the fastener and its washer. This is the most frequent mode of failure and is always accompanied by a significant amount of sheet distortion and possibly also distortion of the washer. It is with this and the next mode of failure that the profile geometry starts to become important;
e) gross distortion of the sheeting. This mode of failure is almost entirely a function of the profile geometry rather than the fastener and to some extent, this mode is present in almost all tests of fasteners in tension. It is not at all clear how to define a serviceability or failure limit for this case. This assessment is largely the discretion of the person carrying out the tests.

Rivets

Blind rivets and tubular rivets are often used in cold-formed steel constructions by extension of their applications in automotive and aircraft industries. A blind rivet is a mechanical fastener capable of joining work pieces together where access is limited to one side only. Typically, blind rivets are installed using a locking mechanism which expands the rivet shank. The rivets are installed in predrilled holes. They are used for thin-to-thin fastenings.

Based on the locking method, blind rivets can be classified into pull-stem rivets, explosive rivets and drive-pin rivets (Yu, 2000):

1. pull-stem rivets. As shown in Figure 4.61(a), pull-stem rivets can be classified into three types:
   - self-plugging rivets. The stem is pulled into but not through the rivet body and the projecting end is removed in a separate operation;
   - pull-through rivets. A mandrel or stem is pulled completely out, leaving a hollow rivet;
   - crimped-mandrel rivets. A part of the mandrel remains as a plug in the rivet body. There are two alternatives: open end (Pull through) and closed end (Pull break);
2. explosive rivets. (Figure 4.61b) Explosive rivets have a chemical charge in the body. The blind end is expanded by applying heat to the river head;
3. drive-pin rivets. (Figure 4.61c) Drive-pin rivets are two piece rivets consisting of a rivet body and a separate pin installed from the head side of the rivet. The pin, which can be driven into the rivet body by a hammer, flares out of the slotted ends on the blind side.

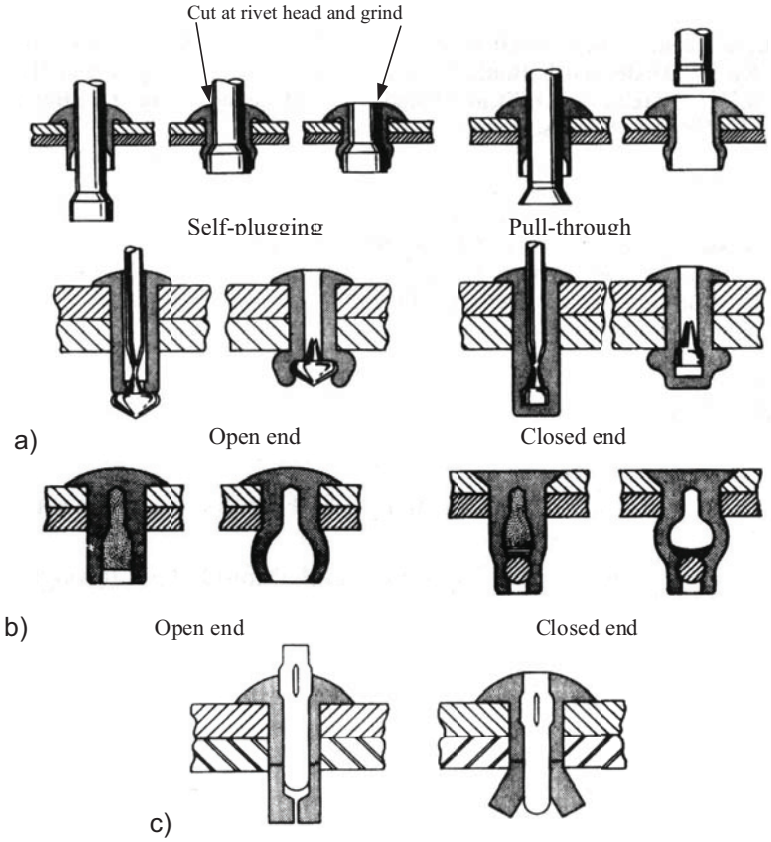

Figure 4.61 Different types of blind rivets (Yu, 2000)

Tubular rivets are also often used to fasten sheet metal. The strength in shear or compression is comparable to that of solid rivets. Nominally body diameter range from 0,8 to 7,9 mm. The corresponding minimum lengths range from 0,8 to 6,4 mm. When tubular rivets are used to join heavy and thin-gauge stock, the rivet head should be on the side of thin sheet.

Failure of riveted connections is similar to those of screwed connections. Generally speaking, for all kinds of mechanical fasteners it is desirable that the mode of failure of a connection is ductile. It follows that shear failure of the fastener itself is undesirable and should be avoided. In general, this mode will only occur if the diameter of the fastener is thin compared to the thickness of connected sheets. Aluminium blind rivets are particularly prone to shear failure and are only suitable for load-bearing applications in relatively thin material (t < 0,7 mm approx.) (Davies, 1991).

For other modes of failure, as a very rough guide, adequate deformation capacity of connections may be taken to be (Davies, 1991):

- for seam fasteners between adjacent cladding elements: 0,5 mm;
- for all other connections: 3,0 mm.

Shot (fired) pins.

Shot pins are fasteners driven through the material to be fastened into the base metal structure. Depending on the type of the driving energy, there are:

- powder actuated fasteners, which are installed with tools containing cartridges filled with propellant that is ignited (minimum thickness of substructure 4 mm);
- air-driven fasteners, which are installed with tools powered by compressed air (minimum thickness of substructure 3 mm).

Figure 4.62 shows examples of shot fired pins. The failure modes and design of shot pin connections are similar to those of screwed connections.

Seam locking. Seam locking is used in structural applications as longitudinal connections between adjacent (flat) sheets. Single or double fold locking can be used.

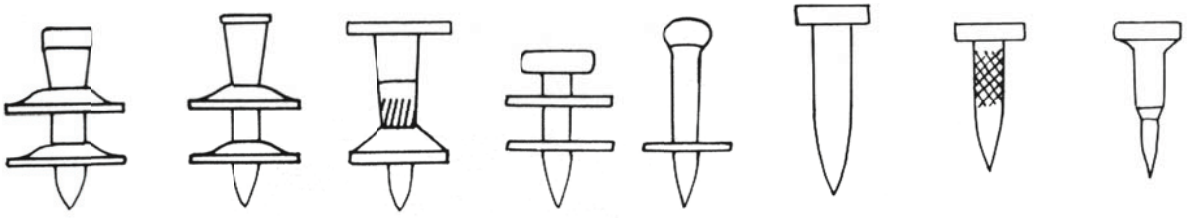

Five types of powder actuated fasteners

Three types of air driven fasteners

Figure 4.62 Shot fired pins

Special mechanical fastenings

a) nuts

A number of systems is available where a nut will be fastened to one of the connected parts. Such systems can be used when loose nuts cannot be applied or when it is not possible to make a sufficiently strong fastening with screws. The thickness of the

parts to be fastened will not limit the application. Figure 4.63 shows a number of examples featuring loose nuts (Yu et al., 1993).

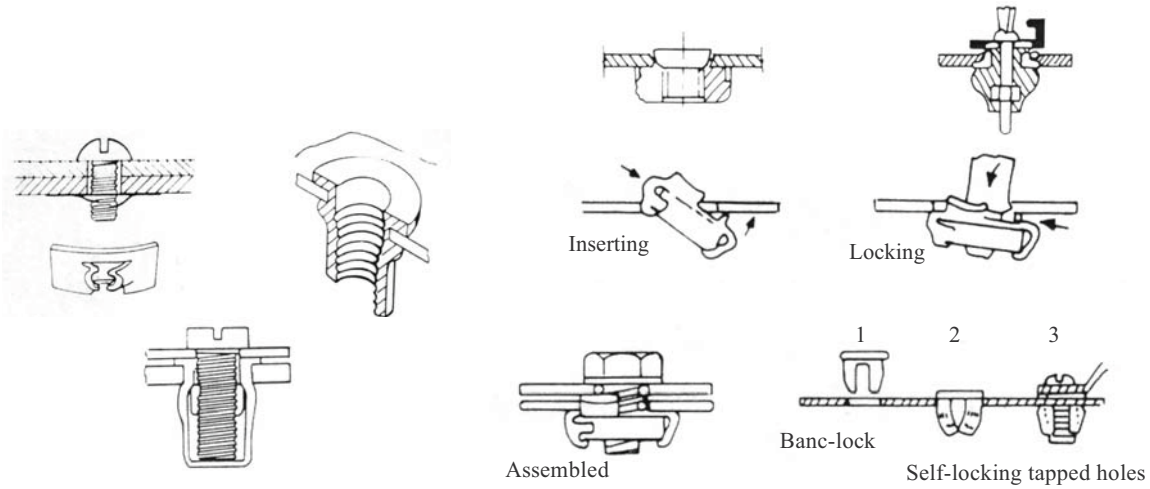

Figure 4.63 Nut systems (Yu et al., 1993)

b) Press joints (Clinched connections)

Press joining is a relatively new technique for joining cold-formed steel sections (Predeschi et al., 1997). Press joining is a single-step process which requires a tool consisting of a punch and expanding die as shown in Figure 4.64. The tool parts have a rectangular profile and the punch tapers along the line of cut. The die has a fixed anvil with spring plates on either side. Although the process is a single action, it consists of two phases. In the first phase, the punch moves towards the die and forms a double cut in the two steel sheets. In the second phase, the pressed sheets are flattened against an anvil in order to spread the sheets laterally and form a permanent connection.

The advantages of press joining in the context of construction are (Davies and Jiang, 1996):

- the joint is formed using the material of the sheets to be connected and no additional items are required;
- it does not destroy protective coatings such as galvanising;
- it is very rapid, taking less than one second to form a joint;
- it is very efficient, requiring about 10% of the energy for spot welding;
- multipoint joining tools can produce several joints simultaneously;
- the joint can be made air and water tight.

Press joining can be used for fabrication of beams, studs, trusses and other structural systems.

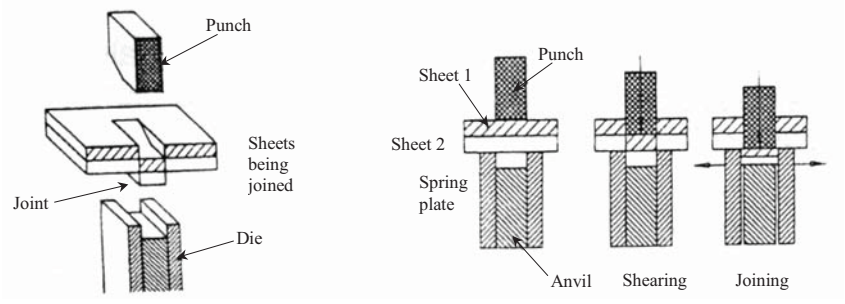

Figure 4.64 Press joining

c) "Rosette" system

The "Rosette" is another joining method which is particularly suited to the fabrication of light gauge steel frames (Makelainen and Kesti, 1999). A Rosette joint is made between a preformed hole in one of the parts to be joined and a collared hole in the other. The parts are snapped together and then a special hydraulic tool is used to pull back the collar and crimp it over the non-collared part of the connection, as shown in Figure 4.65. A Rosette typically has a nominal diameter of 20 mm and a strength several times that of a press joint or conventional mechanical connection such as screw or blind rivet.

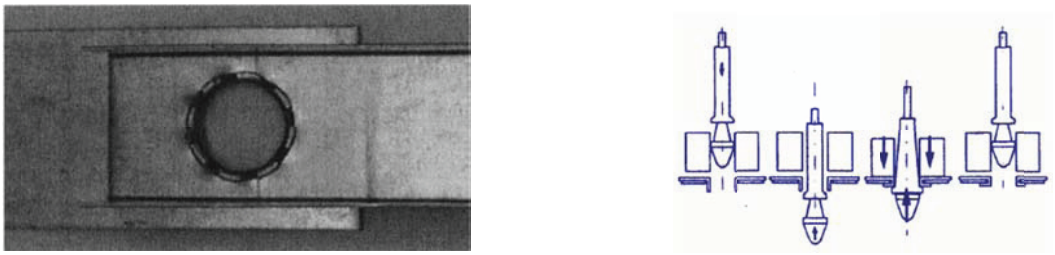

Figure 4.65 Rosette-joint and rosette-joining process (Makelainen and Kesti, 1999)

Design codes do not contain provisions for special fasteners. Their design is mainly based on testing and guidelines offered by fabricators.

Design of connection with conventional mechanical fasteners (e.g. bolts, screws, rivets and short (fired) pins) are generally designed according to specifications of EN1993-1-3, §§8.3. Connections of special fasteners are designer assisted by testing, following the guidance of §9 and Annex A of EN1993-1-3.

The general format for the design checking is:

$$F_{i,Ed} \leq F_{i,Rd} \tag{4.68}$$

where:

$F_{i,Ed}$ is the design stress for the fastener, corresponding to failure mode *i*;

$F_{i,Rd}$ is the design strength for the fastener, corresponding to failure mode *i*.

4.5.2.2 Welding

The most common weld type to connect sheet-to-sheet or cross-section-to-cross-section is the fillet weld. Groove (or butt) welds are commonly used during the roll-forming process to connect flat sheet of one coil to the subsequent coil. Arc spot welds, commonly called puddle welds, are used extensively to attach deck and panels to bar joists or hot-rolled shapes.

Welding electrodes should appropriately match the strength of the base metals. The following welding processes may be used for cold-formed steel construction: shielded metal arc welding (SMA); gas metal arc welding (GMA); flux cored arc welding (FCA); gas tungsten arc welding (GTA) also known as tungsten-inert gas welding (TIG) and submerged arc welding (SA).

An alternative to the GTA (TIG) process is plasma welding. Plasma is produced between a tungsten electrode and the base material. In comparison with the GTA (TIG) process, the energy input during the welding procedure is more concentrated.

The usual types of arc welds used to connect steel members are shown in Figure 4.66.

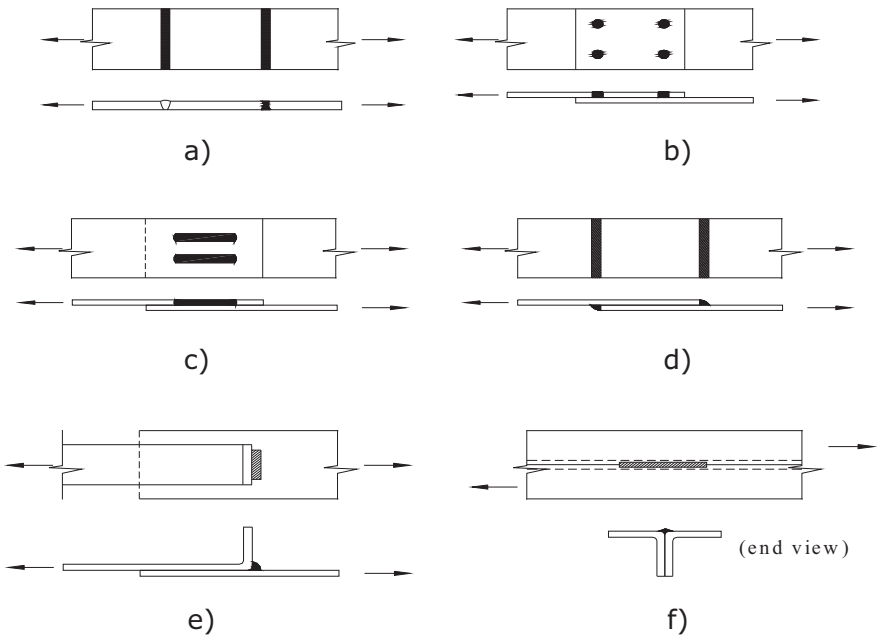

Figure 4.66 Types of arc (fusion) welds (Yu, 2000): (a) Grove welds in butt joints; (b) Arc spot weld (puddle weld); (c) Plug and slot welds; (d) Fillet welds; (e) Flare bevel grove weld; (f) Flare V-grove weld

Grove or butt welds may be difficult to produce in thin sheet and are therefore not as common as fillet, spot and slot welds. Arc spot and slot welds are commonly used for welding cold-formed steel decks and panels to their supporting frames. Flare bevel grooved welds and flare V-grove welds are used to produce built-up sections.

Resistance welding is done without open arc. In contrary to the open arc welding process there is no need of protection of the molten metal by shielding gas slag.

During this procedure, special electrodes led the welding current locally with high density to the base material. The workpiece is being so strongly heated that it turns into plastic condition and starts to melt. In this condition a pressure transferred by the electrodes to the workpiece leads to a local connection of the construction pieces. Figure 4.67 shows the available resistance welding procedures.

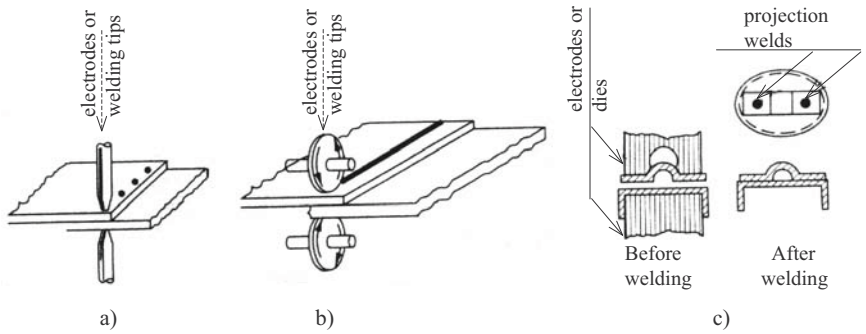

Figure 4.67 Resistance welding procedures: (a) spot welding; (b) seam welding; (c) projection welding

EN1993-1-3, in section 8.4 and 8.5 provides detailed specifications for "spot" and "lap" joints.

4.5.2.3 Fastening based on adhesive bonding

For fastening by means of bonding it is important to realise that a bonded connection possesses good shear resistance and mostly poor peeling resistance (see Figure 4.68). For that reason, a combination of bonding and mechanical fastening is occasionally chosen. Adhesives used for thin-walled steels are as follows:

- epoxy adhesive types – best hardening will appear under elevated temperature (typically 80 – 120°C);
- acrylic adhesive types – more flexible than the epoxy types.

Two advantages of bonded connections are a uniform distribution of forces over the connection and a high resistance to repeated loading. Some disadvantages are that the surface should be flat and clean and there is a hardening time.

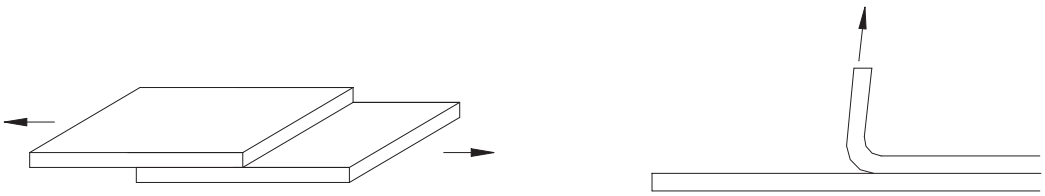

Figure 4.68 Shear and peeling of connections by means of adhesive bonding

4.5.3 Mechanical properties of connections

The important mechanical properties of connections are strength (capacity), rigidity, and deformation capacity or ductility (see Figure 4.69).

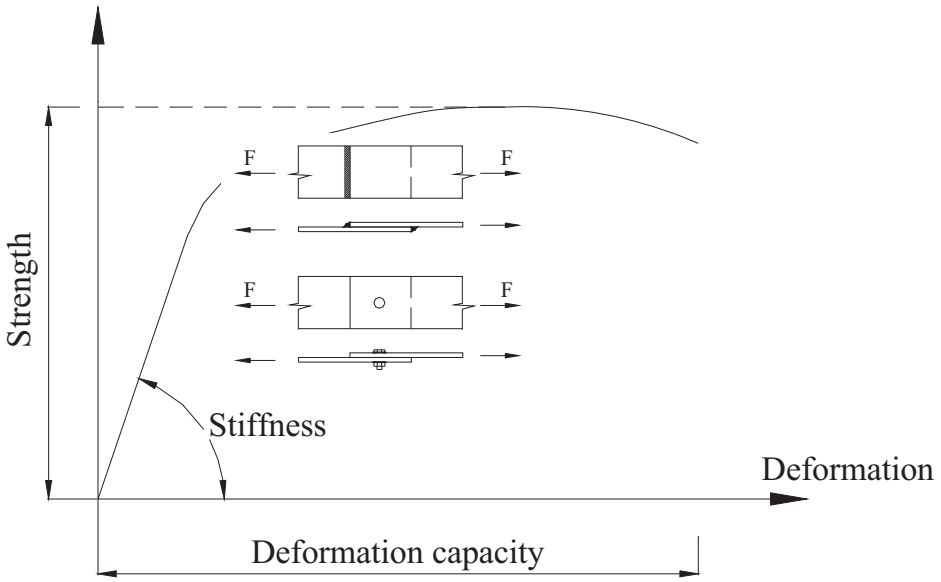

Figure 4.69 Main feature of connection response

Strength

Connection must possess the necessary strength to ensures the reliable transfer of internal forces, in Ultimate Limit State stage, in between connected elements.

The strength of the connections mainly depends on:

- the type of the fastener, and
- the properties of the connected elements e.g. thickness and yield stress.

The most reliable strength values are determined by testing. However, design codes, like EN1993-1-3:2006, for instance, but also the North American Specifications AISI S100-07 and AS/NZS 4600:2005 provide formulas to determine the shear and tension resistance of most common fastener types together with their range of application.

In case of special fasteners techniques, like press joining, "Rosette" or loose nuts, design procedures are provided by fabricators.

Stiffness

The stiffness of a connection is important because it determines the overall stiffness of the structures or its components. Moreover, the stiffness of the connections will influence the force distribution within the structure. Especially when the connection is a part of a bracing structure, the stiffer the connection the lower the bracing force will be (Yu et al., 1993).

Traditionally, bolted and screwed connections in cold-formed steel framing and trusses are considered either rigid (continuous framing) or pinned. Experimental research and numerical studies performed in last decade have provided evidence of the semi-rigid character of the behaviour of these connections. As direct consequence of semi-rigidity, these connections have partial moment resistance or semi-continuous.

In case of thin-walled steel structures the real behaviour of connections should be taken into account because, if neglected, it could lead either to unsafe or uneconomic design.

For the cases not covered by such formulas, testing procedures are available (Annex A: Testing procedures of EN1993-1-3:2006).

Special systems are available where cold-formed sections interlock to form a connection with a good bending and shear rigidity. This is particularly the case for pallet rack frames.

Deformation capacity

Deformation capacity or ductile behaviour of connections is required in order to allow local redistribution of forces without detrimental effects. Otherwise brittle fracture might be caused by local overloading. A proper detailing and fastener selection is vital in order to ensure sufficient deformation capacity of the connection, particularly in seismic actions.

4.5.4 Design of connections

In this section the principles of design procedures according to EN1993-1-3:2006 and EN 1993-1-8:2005 will be presented, accompanied by design examples.

EN1993-1-8:2005 distinguishes between connections and joints. For this reason the following basic definitions must be considered:

Connection: location at which two or more elements meet. For design purposes it is the assembly of the basic components required to represent the behaviour during the transfer of the relevant internal forces and moments at the connection.

Joint: zone where two or more members are interconnected. For design purposes it is the assembly of the basic components required to represent the behaviour during the transfer of the relevant internal forces and moments between the connected members.

Joint configuration: type or layout of the joint or joints in a zone within which the axes of two or more inter-connected members intersect.

However, in case of cold-formed steel framing, generally no significant distinction can be made between joint and connection.

The resistance of a joint shall be determined on the basis of the resistance of the individual fasteners, welds and other components of the joint. For cold-formed steel structures, elastic analysis is recommended for the design of joints. Alternatively, for special cases, elastic-plastic analysis of the joint may be used provided it takes account of the load-deformation characteristics of the components of the joint.

Where fasteners with different stiffness are used to carry a shear load, the fastener with the highest stiffness should be designed to carry the design load.

Design of connections for cold-formed steel may be based on calculation procedures and specific test results. Testing procedures to produce experimental results to be used in the design procedure presented in this book will be based on the provisions of Chapter 9 and Annex A of EN1993-1-3. Alternatively, design data provided by fabricators for specific type of fasteners may also be used.

The following general design assumptions have to be considered when designing structural connections in cold-formed steel constructions:

a) joints shall be designed on the basis of a realistic assumption of the distribution of internal forces and moments, having regard to relative stiffness within the joint. This distribution shall be representative of the load paths through the elements of

the joint. It shall be ensured that equilibrium is maintained with the applied external forces and moments;

b) allowance may be made for the ductility of steel in facilitating the redistribution of internal forces generated within a joint. Accordingly, residual stresses and stresses due to tightening of fasteners and normal accuracy of fit-up need not be considered;

c) ease of fabrication and erection shall be taken into account in the detailing of connections and splices. Attention shall be paid to the clearance necessary for tightening the fasteners, the requirements of welding procedures, and the need for subsequent inspection, surface treatment and maintenance;

d) the determination of any structural property of fastener or joint shall be based on design assisted by testing; e.g. a design model should be calibrated/validated by relevant tests according to Annex D of EN1990:2002.

Usually, members connecting in a joint shall be arranged so that their centroid axes meet in a point. If there is an eccentricity at the intersection of connected members, the members and connections shall be designed accounting for the resulting moments.

In the case of joints of angles or tees attached by either a single line of bolts or two lines of bolts, possible eccentricities should be taken into account. In-plane and out-of-plane eccentricities should be determined by considering the relative positions of the centroid axes of the members and of the setting out lines in the plane of the connection.

Where a connection is subjected to impact or vibration, either preloaded bolts, bolts with looking devices or welding shall be used.

When a connection loaded in shear is subjected to reversal of stresses (unless such stresses are due solely to wind) or where for some special reasons slipping of bolts is not acceptable, either preloaded bolts, fit bolts or welding should be used. However, while available, preloaded bolts are not widely used in cold-formed steel framing.

4.6 Conceptual design of Cold formed steel structures

4.6.1 Introduction

When designing cold-formed steel building structures, the designer has to manage four peculiar problems which characterise the behaviour and performance of thin-walled sections. These peculiarities refer mainly to:

- stability and local strength of sections;
- connecting technology and related design procedures;
- reduced ductility with reference to ductility, plastic design and seismic resistance;
- fire resistance.

If compares with conventional steel construction, the fact of structural members of a cold formed steel –structure are, in general, of class 4, in involves to work with effective cross sections of members in compression bending. The overall stability of these structures, their sensitivity to imperfections and to 2nd order effects must carefully controlled by proper analyses and design.

4.6.2 Case study: Wall Stud Modular System (WSMS) for residential and non-residential buildings

Under coordination of author, BRITT Ltd. Company in Timisoara, Romania created in co-operation with the "Politehnica" University of Timisoara and Research Centre for Advanced and Fundamental Technical Sciences of Romanian Academy, also from Timisoara, a modular system of cold-formed steel structures for residential and non-residential buildings (WSMS). The beneficiary of the system is Romanian Branch of Sweden Company LINDAB. The system was created for 2 or 3 bays, which means a length of 12m or 18m. However, two or three modules can be completed to obtain larger buildings

Structural layout

The main idea in designing the WSMS was to combine the "wall stud" system, used for steel framed housing, with a "light roof" solution, used for industrial hall type buildings. Figure 4.70 shows the basic components of the system.

The modular system presented in this paragraph is made by cold-formed built-up C section units connected with self drilling-self taping screws. The structure is designed by modules, to be installed bay-by-bay, using the so-called "stick" technique, easier to transport and to build pre-erected units (panels, trusses) on the site. Prefabrication in modules is also possible. The "wall stud" panels are adaptable, according to the shape and dimensions of openings. All structural and non-structural components are made of cold-formed steel LINDAB sections (f_y = 350N/mm^2).

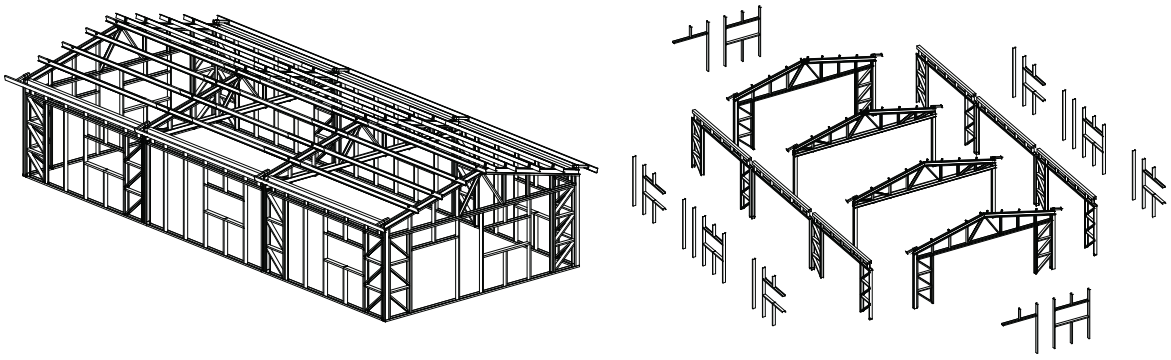

a) b)

Figure 4.70 a) Main frame structure for a WSMS; b) Expanded basic components of a WSMS

The façade as well as the choice of foundation are decided by the customer in co-operation with the retailer and according to technical specifications given by designer. The cladding for both roof and walls are made by trapezoidal steel sheets of LINDAB type. For roof, the stratification of the cladding from outer to inner layers is composed by: LTP45/0.5 trapezoidal steel sheets for the exterior layer, thermal insulation and LVP20/0.4 trapezoidal steel sheets for the interior one, while for walls LTP45/0.5 trapezoidal steel sheets for the exterior layer, thermal insulation and LVP20/0.4 trapezoidal steel sheets for the interior one. Steel sheets are fastened to purlins in alternate troughs using SD6T self drilling-self taping screws and seam fasteners are SD3T screws placed at intervals of 30 cm. Purlins are Z150/2.5 beams, placed at 1000 mm intervals and connected to main beams using U60x40x4 cold formed connecting elements.

Design cases. Loading conditions and design criteria

In this paragraph are presented the characteristics of dead, snow, wind and seismic loads used to design the Wall Stud Modular System. As specified, Romanian territory is characterised by heavy snow and moderate to high seismic risk.

The seismic loads were estimated accordingly to Romanian Standard, in use at that time (P100-2004), but the setting of design elastic spectra approximately corresponds to design spectra on subsoil type D from EN1998-1. Because the structure is made of class four sections, the behaviour "*q*" has to be taken equal to 1 (see also Section 11.2.2). This means that during the earthquake the structure remains in elastic range and energy dissipation is not considered.

The design values were selected to cover two different climatic zones, which are presented below.

Load cases

- dead load on roof: G_k = 0,25 kN/m^2 (γ_G=1,35);
- snow load: Zone I: S_k = 1,5 kN/m^2 (γ_Q=1,5);
- Zone II: S_k = 0,9 kN/m^2 (γ_Q=1,5) ;
- wind load: Zone I: the basic wind speed is v=30m/s and leads to a design wind pressure of w_k=0,704 kN/m2 (γ_Q=1,5); Zone II: the basic wind speed is v=22m/s and leads to a design wind pressure of w_k=0,348kN/m^2 (γ_Q=1,5);
- seismic load: Zone I: ground acceleration a_g=0,20g and constant spectral acceleration branch Tc=1,5s;
- Zone II: ground acceleration a_g=0,16g and constant spectral acceleration branch Tc=1,0s.

The load combinations accordingly to EN 1998-1 have been considered and 3D static and dynamic analyses have been performed. In phase of conceptual design the global performance of the structure under dynamic horizontal action (e.g. wind, earthquake) was controlled by means of eigenmodes of vibrations. The periods for the first three eigenmodes of vibration, corresponding to transversal (X) direction were T_1=0,396s, T_2=0,283s, T_3=0,157s, and clearly show that the structural behaviour is determined by the constant acceleration branch from the design spectra. The 3D model comprises main frames, with built-up sections in columns and trusses, the wall-stud panels and the roof structure with purlins and sheeting panels (diaphragm effect is considered), able to carry both vertical and horizontal loads.

The diaphragm effect was introduced via equivalent bracings (see Figure 4.71) for the roof cladding. The size equivalent bracings, in this specific case, is of 6 mm diameter.

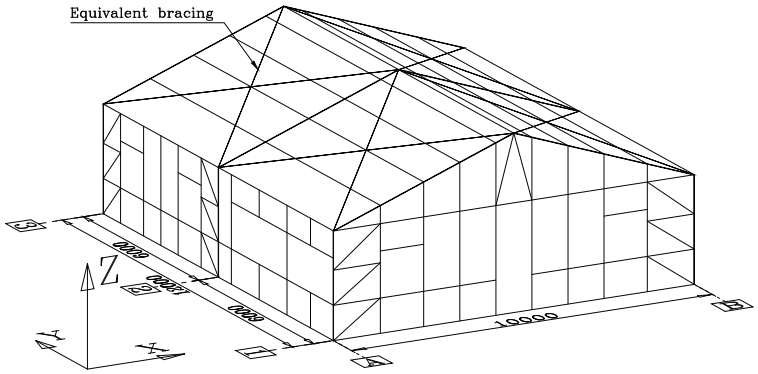

Figure 4.71 Equivalent braces in the roof to simulate the diaphragm acction of the envelope

Static analysis from fundamental load combinations has been carried out and completed by spectral analyses corresponding to the seismic area were the building is located. The seismic calculation was based on spectral analysis and has been carried out using the same computer program. In this case, due to the slenderness of cold-formed steel sections (class 4), no reduction of base seismic shear force was introduced in design (q=1).

Structural detailing

The main members of the framing are displayed in Figure 4.72.

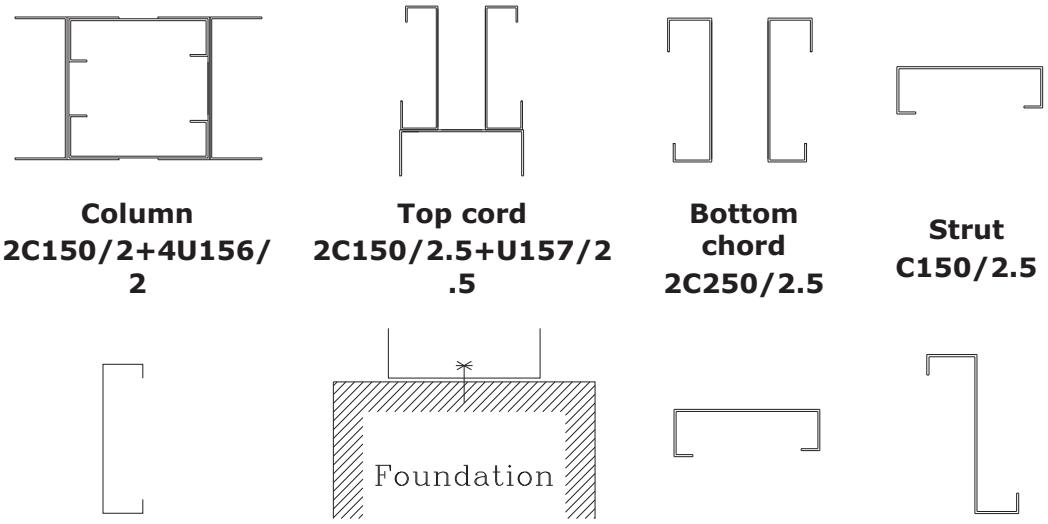

Figure 4.72 Typical dimensions of structural elements

The following figures are presenting structural details for eaves, ridge, base – column connection and base connection of a bracing panel (see Figure 4.73a to Figure 4.73d).

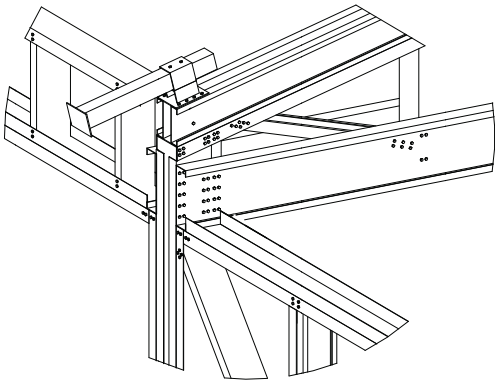

Figure 4.73a Eaves connection

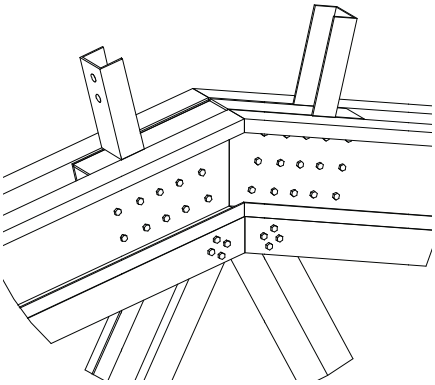

Figure 4.73bRidge connection

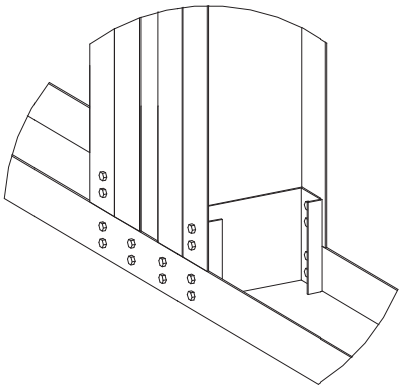

Figure 4.73c Base – column connection

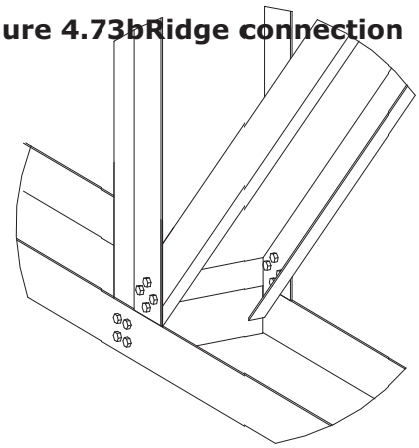

Figure 4.73d Base connection of a bracing panel

Figure 4.74 and Figure 4.75 are showing some representative images for this modular system during erection and completion. In case of the structure in Figure 4.74a, two modules of 15m length have been connected to obtain a building of 30m.

a) b)

Figure 4.74 WSMS Main frames during erection

Figure 4.75 WSMS after completion (two different span modules coupled)

4.6.3 Concluding remarks

The modular systems presented in this paragraph are made by cold-formed single and built-up C section members and with some particular screwed connection details. These structures show very good technical and economical performances. The structure is designed by modules, to be installed bay-by-bay, using "stick" technique or prefabricated subassemblies.

Taking into account the variety of dimensions for spans, bays, number of bays and eaves height result a total amount of 40 modular buildings. The structures are very light and easy to erected (7-10 days).

Figure 4.76 shows the theoretical weight performances for a 12m building (steel consumption for the main frame structure, e.g. without purlins and adaptable wall panels) obtained for the modular system situated in to different climatic location (with quite heavy snow and seismic load!). Figure 4.77 show the distribution of cost per components of the building.

a)

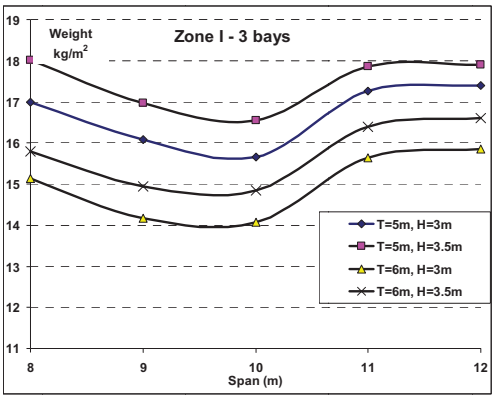

b)

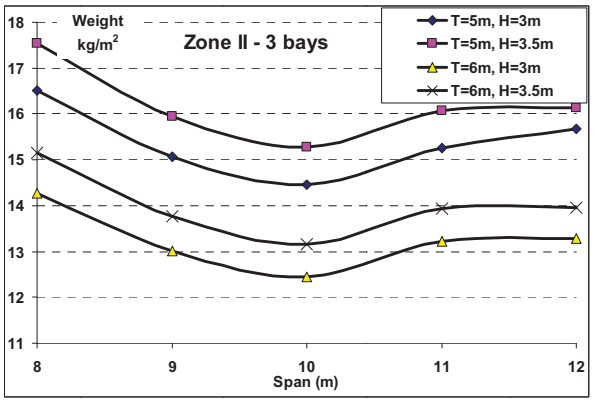

Figure 4.76 Weight performances of the system

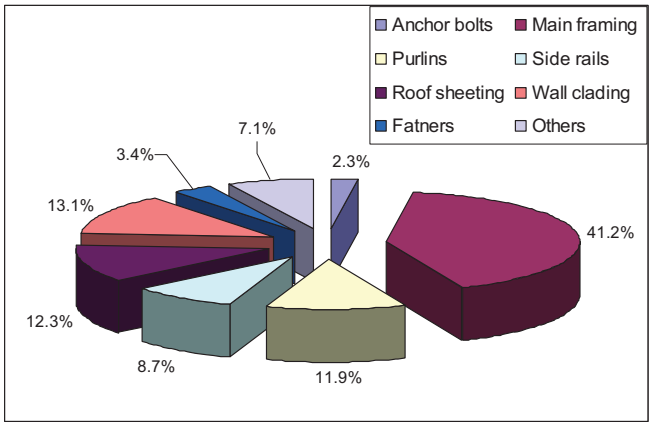

Figure 4.77 Cost distribution for components of WSMS

References

AISI S100-07: 2007. North American specification for the design of cold-formed steel structural members American Iron and Steel Institute, Washington, D.C.

AS/NZS 4600: 2005. Cold-formed Steel Structures. Australian Standard / New Zealand Standard, Sydney, Australia.

Burling, P.M. et al. 1990. Building with British steel. No. 1 1990, British Steel plc, England.

Burstand, H. 2000. Light gauge steel framing for housing, SBI – Swedish Institute of Steel Construction, Publication 170, Stockholm, Sweden.

Davies, J.M. 1991. Connections for cold-formed steelwork. In: Design of Cold-Formed Steel Members (Rhodes J, Editor). Elsevier Applied Science, London and New York.

Davies, J.M. 2001. Lightweight sandwich construction. Oxford, London, Edinburgh (UK). Blackwell Science Ltd.

Davies, J.M., Jiang, C. 1996. Design of thin-walled columns for distortional buckling. Coupled Instabilities of Metal Structures – CIMS'96, Imperial College Press, London, 165-172.

Dubina, D. 1996. Coupled instabilities in bar members – General Report. Coupled Instabilities in Metal Structures – CISM'96 (Rondal J, Dubina D, Gioncu V, Eds.). Imperial College Press, London, 119-132.

Dubina, D. 2000. Recent research advances and trends on coupled instability of bar members, General Report – Session 3: Bar Members. Coupled Instabilities in Metal Structures - CIMS'2000 (Camotin D, Dubina D, Rondal J, Eds.). Imperial Colleague Press, London, 131-144.

Dubina, D. 2001. The ECBL approach for interactive buckling of thin-walled steel members. Steel & Composite Structures. 1(1):75-96.

Dubina D. 2004. Foreword to Special Issue on Cold-Formed Structures: Recent Research Advances in Central and Eastern Europe, Thin Walled Structures, Vol. 42, No 2, February 2004, 149-152.

Dubina, D., Ungureanu, V., Landolfo, R. 2012. Design of cold-formed steel structures. Eurocode 3: Design of Steel Structures Part 1-3 – Design of Cold-formed Steel Structures, Published by ECCS – European Convention for Constructional Steelwork, ISBN (ECCS): 978-92-9147-107-2.

ECCS_49, 1987. European recommendations for design of light gauge steel members, Publication P049, European Convention for Constructional Steelwork, Brussels, Belgium.

ECCS_88, 1995. European recommendations for the application of metal sheeting acting as a diaphragm, Publication P088, European Convention for Constructional Steelwork, Brussels, Belgium.

ECCS_114, 2000. Preliminary worked examples according to Eurocode 3 Part 1.3, Publication P114, European Convention for Constructional Steelwork, Brussels, Belgium.

ECCS_123, 2008. Worked examples according to EN1993-1-3. European Convention for Constructional Steelwork, Brussels, Belgium.

EN 1090: 2008. Execution of steel structures and aluminium structures - Part 2: Technical requirements for steel structures. European Committee for Standardization, Brussels, Belgium.

EN 1990: 2002. Eurocode – Basis of structural design. European Committee for Standardization, Brussels, Belgium.

EN 1993-1-1: 2005. Eurocode 3: Design of steel structures - Part 1-1: General rules and rules for buildings. European Committee for Standardization, Brussels, Belgium (including EN1993-1-1:2005/AC, 2009).

EN 1993-1-3: 2006. Eurocode 3: Design of steel structures. Part 1-3: General Rules. Supplementary rules for cold-formed thin gauge members and sheeting. European Committee for Standardization, Brussels, Belgium (including EN1993-1-3:2006/AC, 2009).

EN 1993-1-5: 2006. Eurocode 3: Design of steel structures - Part 1-5: Plated structural elements. European Committee for Standardization, Brussels, Belgium (including EN1993-1-5: 2006/AC, 2009).

EN 1993-1-8: 2005. Eurocode 3: Design of steel structures. Part 1-8: Design of joints. European Committee for Standardization, Brussels, Belgium.

EN 1998-1: 2004. Eurocode 8 – Design of structures for earthquake resistance - Part 1: General rules, seismic actions and rules for buildings. European Committee for Standardization, Brussels, Belgium.

Fenster, S.M.C., Girardier, E.V., Owens, G.W. 1992. Economic design and the importance of standardised connections. In Constructional Steel Design: World Developments (Dowling PJ et al., Eds.). Elsevier Applied Science, Barking, Essex, UK, 541-550.

Hancock, G.J., Murray, T.M., Ellifritt, D.S. 2001. Cold-formed steel structures to the AISI specification, Marcel Dekker, Inc., New York.

Lau, S.C.W., Hancock, G.J.(1987. Distortional buckling formulas for channel columns. Journal of Structural Engineering, ASCE, Vol. 113, No. 5, 1063-1078.

Makelainen, P., Kesti, J. 1999. Advanced method for lightweight steel joining. Journal of Constructional Steel Research, Vol. 49, No. 2, 107-116.

Martin, L.H., Purkiss, J.A. 2008. Structural design of steelwork to EN 1993 and EN 1994. 3rd Edition, Butterworth-Heinemann – imprint of Elsevier, UK.

Murray, N.W. 1985. Introduction to the theory of thin-walled structures. Claredon Press, Oxford.

P 100-1. 2004. Romanian Seismic Design Code, Part I, Design Rules for Buildings (In Romanian), Ministry of Constructions and Tourism, Order No. 489/5.04.2005.

Predeschi, R.F., Sinha, D.P., Davies, R. 1997. Advance connection Techniques for cold-formed steel structures. Journal of Structural Engineering (ASCE), 2(123), 138-144.

Rhodes, J. (Ed.) 1991. Design of cold-formed steel members, Elsevier Applied Science, London and New York.

Rondal, J., Dubina, D., Bivolaru, D. 1994. Residual stresses and the behaviour of cold-formed steel structures. Proceedings of 17th Czech and Slovak International Conference on Steel Structures and Bridges, Bratislava, Slovakia, September 7-9, 193-197.

Rondal, J., Maquoi, R. 1979a. Formulation d'Ayrton-Perry pour le flambement des barres métalliques, Construction Métallique, 4, 41-53.

Rondal, J., Maquoi, R. 1979b. Single equation for SSRC column strength curves, ASCE J. Struct. Div., Vol. 105, No. ST1, 247-250.

Schafer, B., Peköz, T. 1999. Local and distortional buckling of cold-formed steel members with edge stiffened flanges. light-weight steel and aluminium structures, Proceedings of the 4th Int. Conf. on Steel and Aluminium Structures, ICSAS'99, Espoo, Finland, 89-97.

Schafer, B.W. 2001. Direct strength prediction of thin-walled beams and columns, Research Report, John Hopkins University, USA.

Schafer, B.W., Ádány, S. 2006. Buckling analysis of cold-formed steel members using CUFSM: conventional and constrained finite strip methods. Eighteenth International Specialty Conference on Cold-Formed Steel Structures, Orlando, FL. October 2006.

Sedlacek, G., Müller, C. 2006. The European standard family and its basis. Journal of Constructional Steel Research, 62(2006), 1047-1059.

Silvestre, N., Camotim, D. 2002a. First-order generalised beam theory for arbitrary orthotropic materials. Thin-Walled Structures, Elsevier 40 (9) 755-789.

Silvestre N, Camotim, D. 2002b. Second-order generalised beam theory for arbitrary orthotropic materials. Thin-Walled Structures, Elsevier, 40 (9) 791-820.

Silvestre N, Camotim, D. 2003. Nonlinear Generalized Beam Theory for Cold-formed Steel Members. International Journal of Structural Stability and Dynamics. 3 (4) 461-490.

Timoshenko, S.P., Gere, J.M. 1961. Theory of elastic stability. McGraw-Hill, New York.

Toma, T., Sedlacek, G., Weynand, K. 1993. Connections in Cold-Formed Steel. Thin Walled Structures, 16, 219-237.

Ungureanu, V., Dubina, D. 2004. Recent research advances on ECBL approach. Part I: Plastic-elastic interactive buckling of cold-formed steel sections. Thin-walled Structures, 42(2), 177-194.

Von Karman, T., Sechler, E.E., Donnel, L.H. 1932. Strength of thin plates in compression. Trans ASME, 54-53.

Winter, G. 1940. Stress distribution in and equivalent width of flanges of wide thin-wall steel beams, NACA Technical, Note 784, 1940.

Winter, G. 1970. Commentary on the 1968 Edition of the specification for the design of cold-formed steel structural members. American Iron and Steel Institute, New York, NY.

Yu, W.-W. 2000. Cold-formed steel design (3rd Edition), John Willey & Sons, New York.

Yu, W.-W., Toma, T., Baehre, R., Eds. 1993. Cold-Formed Steel in Tall Buildings, Chapter 5: Connections in Cold Formed Steel (Author: Toma T), 95-115. Council on Tall Buildings and Urban Habitat. Committee S37. McGraw-Hill, New York, 1993, 184 p.

CHAPTER 5

SEISMIC DESIGN OF STEEL STRUCTURES ACCORDING TO EN 1998-1

Raffaele Landolfo

University of Naples Federico II, Italy

5 Seismic design of steel structures according to EN 1998-1

5.1 Introduction

EN 1998-1 (2005) applies to the seismic design of building structures. However, this code includes also the general provisions for the other parts of EC8, covering the following aspects: seismic performance levels, types of seismic action, types of structural analysis, general concepts and rules which should be applied to all types of structures beyond those generally used for buildings.

It is subdivided into 10 sections as follows:

- section 1 reports the generality about normative references and symbols;
- section 2 provides the seismic performance requirements and compliance criteria;
- section 3 gives the rules to represent the seismic actions and their combination with other design actions;
- section 4 describes the general design rules specifically conceived for building structures;
- from section 5 to 9 the code provides specific rules for structures made of each type of building materials (namely concrete, steel, composite steel-concrete, timber and masonry buildings);
- section 10 gives the fundamental requirements and design rules for base isolation of buildings.

The main aspects of EN 1998-1 (2005) relevant to the seismic design of steel buildings are described hereinafter. The chapter concludes with explanatory worked examples for the use of EC8 in the preliminary design of both a six-storey moment resisting frame and a multi-storey building with concentrically braced frames.

5.2 Performance requirements and compliance criteria

In EN 1998-1 (2005) two performance levels should be accounted for the seismic design of building structures, which corresponds to the following objectives:

- the protection of human lives under rare seismic actions, by preventing the local or global collapse of the structure and preserving the structural integrity with a residual load capacity;
- the limitation of both structural and non-structural damage in case of frequent seismic events.

The former performance level is achieved by applying capacity design rules based on the hierarchy of strength concept. The second performance level is accomplished by limiting the lateral interstorey drifts of the structure within levels acceptable for the integrity of both non-structural (i.e. infill walls, claddings, plants, etc.) and structural elements.

According to the Community principles allocating national competence on issues of safety and economy, the Eurocode 8 refers to national annex the determination of the hazard

levels corresponding to the two performance levels above described. However, as also reported in Figure 5.1, for ordinary structures EC8 recommends the following:

- a seismic action having 10% exceedance probability in 50 years (namely a mean return period equal to 475 years) for the ultimate limit state (i.e. collapse prevention). At this limit state the design seismic action for structures of ordinary importance over rock is termed "reference" seismic action;
- a seismic action having 10% exceedance probability in 10 years (namely a mean return period equal to 95 years) for the serviceability limit state (i.e. damage limitation).

In case of essential or large occupancy facilities the code recommends to guarantee an enhanced performance than the case of ordinary structures. This objective is achieved by modifying the hazard level (namely the mean return period) for both collapse prevention and damage limitation. In particular, it is recommended to increase the reference seismic action at both performance levels by the importance factor γ_I. At the collapse prevention level the recommended value of γ_I ranges from 1,4 (for essential buildings) to 1,2 (for large occupancy buildings). In addition, the code allows using γ_I = 0,8 for buildings of reduced importance for public safety. The appropriate values of γ_I for the main building categories are reported in Table 5.1.

Damage Limitation Requirement	No Collapse Requirement
Damage Limitation State (DLS)	**Ultimate Limit State (ULS)**
• For ordinary structures this requirement should be met for a seismic action with 10 % probability of exceedance in 10 years • Return Period= 95 years • Performance level required: - Resist the design seismic action without damage - Avoid limitations of use and high repair costs	• For ordinary structures this requirement should be met for a reference seismic action with 10 % probability of exceedance in 50 years • Return Period= 475 years • Performance level required: - Resist the design seismic action without local or global collapse - Preserve structural integrity and residual load bearing capacity after the seismic event

Figure 5.1 Performance levels according to EN1998-1.

Table 5.1 Importance factors for each building category.

Importance class	Buildings	γ_I
I	Buildings of minor importance for public safety, e.g. agricultural buildings, etc.	0,8
II	Ordinary buildings, not belonging in the other categories.	1,0
III	Buildings whose seismic resistance is of importance in view of the consequences associated with a collapse, e.g. schools, assembly halls, cultural institutions, etc.	1,2
IV	Buildings whose integrity during earthquakes is of vital importance for civil protection, e.g. hospitals, fire stations, power plants, etc.	1,4

5.3 Seismic action

In EN 1998-1 (2005) the seismic action is represented by an elastic acceleration response spectrum. The code assumes the same spectral shape for both damage limitation and collapse prevention limit states. In order to consider different hazard levels, a factor ν is provided to obtain the seismic demand at serviceability limit state. The latter is derived multiplying by ν the ordinates of the elastic acceleration response spectrum at ultimate limit state. The value of ν depends on two aspects: i) the local seismic hazard conditions; ii) the protection of property objective. The recommended values for ν are equal to 0,4 and 0,5 for ordinary and large-occupancy buildings, respectively.

The elastic response spectrum of the design seismic action (namely that corresponding to collapse prevention) is characterized by the reference ground acceleration on rock, a_{gR}, which should be provided by national seismic-zoning maps. The spectrum is shown in Figure 5.2 and it is constituted by three main regions having constant properties, namely the spectral acceleration (for period T from T_B to T_C), the spectral pseudo-velocity (for period T from T_C to T_D) and spectral displacement (for period $T > T_D$). The amplitude and the period of these zones depend on the soil type. In the EN1998-1(2005) five standard soil types are considered, as follows:

- type A: rock, with an average shear wave velocity v_s in the top 30m, larger than 800m/s;
- type B: very dense sand or gravel, or very stiff clay, with v_s ranging within 360 to 800m/s;
- type C: medium-dense sand or gravel, or stiff clay, with v_s ranging within 180m/s to 360m/s;
- type D: loose-to-medium sand or gravel, or soft-to-firm clay, with v_s lesser than 180m/s;
- type E: 5m to 20m thick soil with v_s lesser than 360 m/s, underlain by rock.

The entire elastic spectrum is anchored to the mapped "reference" acceleration on rock multiplied by: a) the importance factor γ_I; b) the soil factor $S \geq 1$ accounting for the dynamic amplification effects on spectral values due to soil conditions; c) a damping correction factor η equal to $\sqrt{10/(5+\xi)}$, being ξ the viscous damping ratio expressed as a percentage.

Assuming $\gamma_I = 1$, the equations to obtain the elastic acceleration response spectra are given as follows:

$$
\begin{aligned}
&0 < T < T_B && S_d(T) = a_g \cdot S \cdot \left(1 + \frac{T}{T_B} \cdot (\eta \cdot 2,5 - 1)\right) \\
&T_B < T < T_C && S_d(T) = a_g \cdot S \cdot 2,5 \\
&T_C < T < T_D && S_d(T) = a_g \cdot S \cdot 2,5 \cdot \left(\frac{T_C}{T}\right) \\
&T > T_D && S_d(T) = a_g \cdot S \cdot 2,5 \cdot \left(\frac{T_C \cdot T_D}{T^2}\right)
\end{aligned}
\qquad (5.1)
$$

For the same spectral shape described by Eqn. (5.1) the code recommends to use two different types of spectra:

- Type 1 (see Figure5.3a) for moderate to large magnitude earthquakes;
- Type 2 (see Figure5.3b) for low magnitude earthquakes with surface magnitude less than 5.5 at close distances.

The values to be ascribed to T_B, T_C, T_D and S for each ground type and type (shape) of spectrum to be used in a country may be found in its National Annex. However, the code provides recommended values for the spectral parameters.

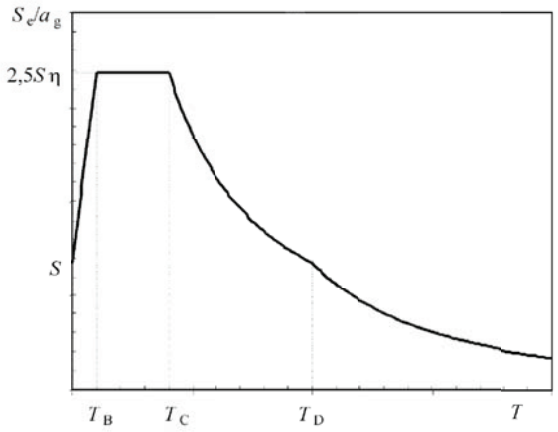

Figure 5.2 The shape of elastic acceleration response spectra in EC8 (source EN1998-1).

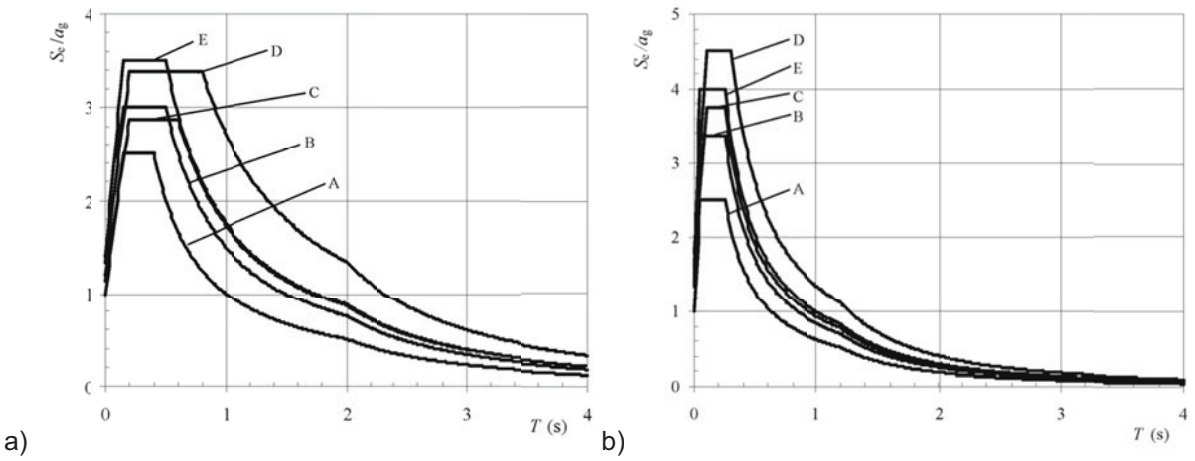

Figure5.3 Elastic response spectra recommended in EC8: Type 1 (a) and 2 (b) (source EN1998-1).

5.4 Design requirements for buildings

5.4.1 Design concept and ductility class

EN 1998 takes into account the capacity of structures to dissipate energy through inelastic deformations, so that the design seismic forces can be smaller than those related to a linear elastic response, but sophisticated non-linear structural analyses can also be avoided at the design stage. In fact, an elastic analysis based on a response spectrum reduced with respect to the elastic one, called the "design spectrum", can be performed. The reduction is accomplished by introducing the behaviour factor q (EN 1998-1 3.2.2.5(2)), which can be approximately intended as the ratio between the seismic forces that a single degree of freedom system equivalent to the real structure would experience if its response would be completely elastic (with 5% equivalent viscous damping) and the seismic forces that may be used in the design (EN 1998-1 3.2.2.5(3)). The values of the behaviour factor q are given for various materials and structural systems according to the relevant ductility classes within EN 1998. Indeed, as summarized in Figure 5.4, seismic resistant steel buildings may be designed in accordance with one of the following concepts (EN 1998-1 6.1.2(1)P):

- concept a): Low-dissipative structural behaviour;
- concept b): Dissipative structural behaviour.

In concept a) the action effects may be calculated on the basis of an elastic global analysis neglecting the non-linear behaviour. In this case, the behaviour factor assumed in the calculation must be less than 2. Structures designed in accordance with concept a) belong to the low dissipative structural class "DCL" (Ductility Class Low). Hence, the resistance of members and connections should be evaluated in accordance with EN 1993 without any additional requirement (EN 1998-1 6.1.2(4)). For non-base-isolated structures this simplified design is recommended only for low seismicity regions. Although the designation of low seismicity zone should be established by the competent National Authorities, a threshold value of design ground acceleration for the specific soil type is recommended as $\gamma_1 Sa_{gR}$ = 0,1g. It should be noted that in case of very low seismic zones (namely for the cases $\gamma_1 Sa_{gR}$ <0.05g) EC8 allows neglecting the seismic action in design of buildings.

In concept b) the capability of parts of the structure (dissipative zones) to undergo plastic deformations in case of an earthquake is taken into account. The behaviour factor q assumed in the calculation is larger than 2 and depends on the type of seismic resistant structural scheme. Structures designed in accordance with concept b) may belong to a medium structural ductility class "DCM" (Ductility Class Medium) or to a high ductility class "DCH" (Ductility Class High). These classes correspond to increased ability of the structure to dissipate energy through inelastic behaviour. Depending on the ductility class, specific design requirements are provided for both local and global structural aspects.

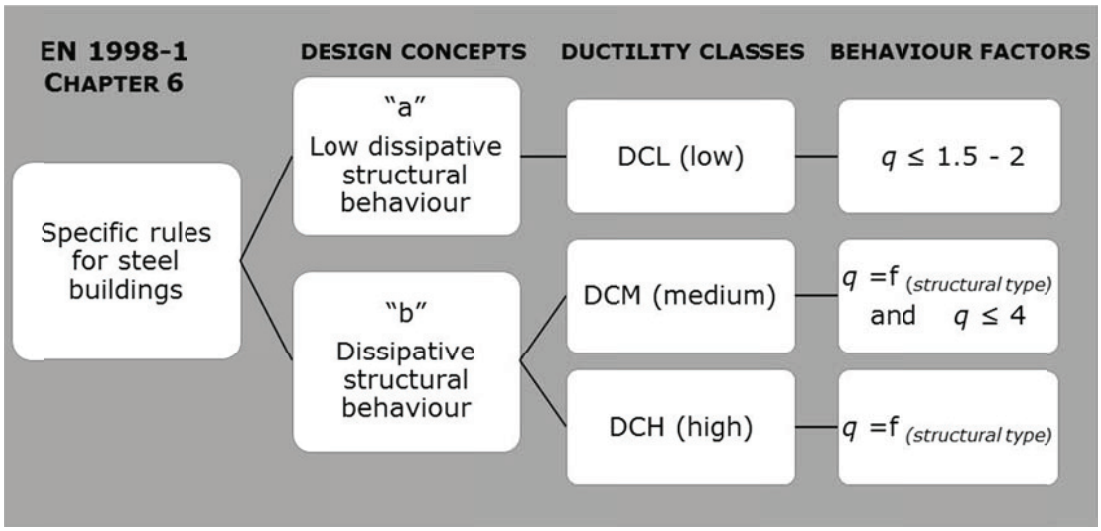

Figure 5.4 Design Concepts according to EN 1998–1.

Once fixed the behaviour factor q suitable for the structure to be calculated, the design response spectrum is obtained starting from the elastic spectrum (see Eqn. (5.1) using the following equations:

$$0 < T < T_B \qquad S_d(T) = a_g \cdot S \cdot \left(\frac{2}{3} + \frac{T}{T_B} \cdot \left(\frac{2,5}{q} - \frac{2}{3}\right)\right)$$

$$T_B < T < T_C \qquad S_d(T) = a_g \cdot S \cdot \frac{2,5}{q}$$

$$T_C < T < T_D \qquad S_d(T) \begin{cases} = a_g \cdot S \cdot \dfrac{2,5}{q} \cdot \left(\dfrac{T_C}{T}\right) \\ \geq \beta \cdot a_g \end{cases} \qquad (5.2)$$

$$T > T_D \qquad S_d(T) \begin{cases} = a_g \cdot S \cdot \dfrac{2,5}{q} \cdot \left(\dfrac{T_C \cdot T_D}{T^2}\right) \\ \geq \beta \cdot a_g \end{cases}$$

It should be noted that the parameter β is the lower bound factor for the horizontal design spectrum, whose appropriate value should be provided by the National Annex. However, EC8 recommends to assume β = 0,2.

For the sake of completeness, Figure 5.5 shows the comparison between elastic and design spectra, the latter obtained for two different *q* factors.

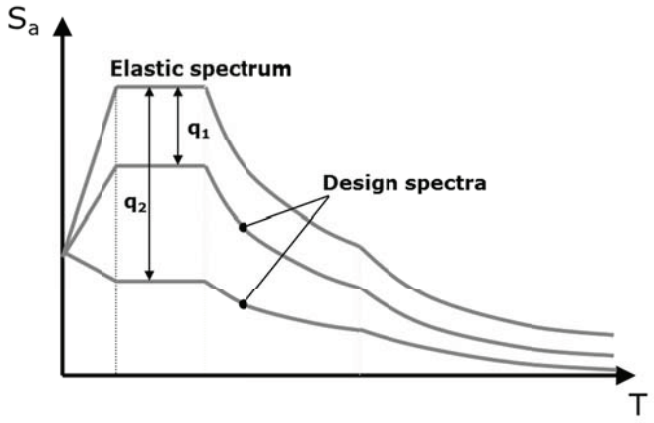

Figure 5.5 Elastic vs. design acceleration spectrum.

5.4.2 Analysis procedures and models

According to EC8 the following types of structural analysis can be performed to calculate and verify building structures:

- lateral force method (namely a linear static analysis with lateral distribution of forces);
- linear modal response spectrum analysis;
- nonlinear static pushover analysis;
- nonlinear dynamic response time-history analysis.

The lateral force method is characterized by a linear static analysis to be performed by applying a pre-defined lateral distribution of forces, which are proportional to the shape of the 1st translational vibration mode in the examined horizontal direction. In order to calculate the fundamental period T_1, the code provides an empirical equation depending on the structural typology (e.g. $T_1=0{,}085H^{3/4}$ for steel moment-resisting frames, $T_1=0{,}05H^{3/4}$ for braced buildings, being H the total building height expressed in *m*). This method can be used only for buildings regular both in plan and in elevation and in all cases where the effects of higher modes are negligible. This implies that for the most of practical applications it is not possible to perform linear static analyses. Therefore, in EC8 the linear modal response spectrum analysis is the typical method, which can be used for all structural typologies. For this type of analysis the modal contributions (i.e. internal forces, displacements, etc.) can be combined by rigorous application of either SRSS (Square Root of Sum of Squares) or CQC (Complete Quadratic Combination) rules. With this regard, the code requires to take into account a number of vibration modes that satisfy either of the following conditions:

1. the sum of the effective modal masses for the modes taken into account amounts to at least 90% of the total mass of the structure;
2. all modes with effective modal masses greater than 5% of the total mass are taken into account.

For what concerns nonlinear static analyses, according to EC8 two different lateral load distributions should be accounted for pushover analysis, as follows: i) a uniform lateral

load pattern; ii) the lateral forces pattern used in linear static analysis. The target displacement can be defined according to the N2 procedure as described in the Annex B.

In case of nonlinear response-history analysis at least 7 nonlinear time-history analyses should be performed using ground motions selected to be compatible with the elastic spectrum in accordance with EN 1998-1. The code states that the average of the response quantities from all of these analyses should be used as the design value of the action effect. Otherwise, the most unfavourable value of the response quantity among the analyses should be used.

The accuracy of numerical analysis strictly depends on the structural model. Therefore, according to EC8 the model of the building must represent the distribution of stiffness and mass so that all significant deformation shapes and inertia forces are properly accounted for under seismic actions.

With this regard, it is important to account for accidental torsional effects which conventionally take into account the possible uncertainties in the stiffness and mass distributions and/or a possible torsional component of the ground motion about a vertical axis. EC8 introduces accidental torsional effects by displacing the masses with respect to their nominal positions. This displacement is assumed to take place in any possible direction (in practice, along the two orthogonal directions of the horizontal seismic action components). All accidental eccentricities are considered at a time along the same horizontal direction. The accidental eccentricity of a horizontal seismic action component is specified as equal to 5% of the in-plan dimension of the storey measured perpendicular to this horizontal component.

The code allows a simplified modelling approach if the building is conforming to the criteria for regularity both in plan and in elevation. In such a case, when the lateral force method of analysis is used with a 3D model of the building structure, seismic effects on the generic lateral load-resisting system are multiplied by a factor δ (clause 4.3.3.2.4), in order to account for accidental torsional effects. This factor is given by:

$$\delta = 1 + 0,6\frac{x}{L_e} \tag{5.3}$$

where:

- x is the plan distance of the seismic resisting system under consideration from the centre of gravity of the building, measured perpendicularly to the direction of the seismic action considered;
- L_e is the distance between the two outermost lateral load resisting systems, measured perpendicularly to the direction of the seismic action considered.

However, when two separate 2D planar models are used, the effects of the accidental eccentricity can only be estimated through the simplified approach using the δ factor, but doubling the effect of the eccentricity. Indeed, in that case the second term in the amplification factor becomes $1,2x/L_e$, to account also for the otherwise unaccounted for effects of any static eccentricity between the storey centres of mass and stiffness.

Another important aspect to be taken into account is the influence of second order (P-Δ) effects on frame stability. Indeed, in case of large lateral deformation the vertical gravity loads can act on the deformed configuration of the structure so that to increase the overall deformation and force distribution in the structure thus leading to potential collapse in a sideway mode under seismic condition.

Generally, the majority of structural analysis software can automatically account for these effects in the analysis. However, it could be convenient to specify directly the entity of second order effects in order to control and optimise the structural design.

According to EN 1998-1, *P*-Δ effects are specified through a storey stability coefficient (θ) given as:

$$\theta = \frac{P_{tot} \cdot d_r}{V_{tot} \cdot h} \tag{5.4}$$

where:

- P_{tot} is the total vertical load, including the load tributary to gravity framing, at and above the storey considered in the seismic design situation;
- V_{tot} is seismic shear at the storey under consideration;
- h is the storey height;
- d_r is the design inter-storey drift, given by the product of elastic inter-storey drift from analysis and the behaviour factor q (i.e. $d_e \times q$).

Frame instability is assumed for $\theta \geq 0{,}3$. If $\theta \leq 0{,}1$, second-order effects could be neglected, whilst for $0{,}1 < \theta \leq 0{,}2$, *P*-Δ effects may be approximately taken into account in seismic action effects through the following multiplier:

$$\alpha = \frac{1}{(1-\theta)} \tag{5.5}$$

5.4.2.1 Combination of actions for seismic design situations

In case of buildings the seismic action should be combined with permanent and variable loads as follows:

$$\sum G_{k,i} \text{ "+" } \sum \psi_{2,i} \cdot Q_{k,i} \text{ "+" } A_{Ed} \tag{5.6}$$

where $G_{k,i}$ is the characteristic value of permanent action "*i*" (the self-weight and all other dead loads), A_{Ed} is the design seismic action (corresponding to the reference return period multiplied by the importance factor), $Q_{k,i}$ is the characteristic value of variable action "*i*" and $\psi_{2,i}$ is the combination coefficient for the quasi-permanent value of the variable action "*i*", which is a function of the destination of use of the building. Values for the combination coefficients $\psi_{2,i}$ are given in EN 1990:2002, Annex A1; Table 5.2 reports the list of $\psi_{2,i}$ for buildings.

Table 5.2 Values of the combination coefficients $\psi_{2,i}$.

Type of variable action	ψ_2
Category A : domestic, residential areas	0,3
Category B : office areas	0,3
Category C : congregation areas	0,6
Category D : shopping areas	0,6
Category E : storage areas	0,8
Category F : traffic area, vehicle weight ≤ 30 kN	0,6
Category G : traffic area, 30 kN < vehicle weight ≤ 160 kN	0,3
Category H : roofs	0
Snow loads on buildings (see EN 1991-1-3) Finland, Iceland, Norway, Sweden	0,2
Remainder of CEN Member States, for sites located at altitude *H* > 1000 m a.s.l.	0,2
Remainder of CEN Member States, for sites located at altitude *H* ≤ 1000 m a.s.l.	0
Wind loads on buildings (see EN 1991-1-4)	0
Temperature (non-fire) in buildings (see EN 1991-1-5)	0

5.4.2.2 Structural masses

In accordance with EN 1998-1 3.2.4 (2)P, the inertial effects in the seismic design situation have to be evaluated by taking into account the presence of the masses corresponding to the following combination of permanent and variable gravity loads:

$$\sum G_{k,i} \text{ "+" } \sum \psi_{E,i} \cdot Q_{k,i} \tag{5.7}$$

where $\psi_{E,i}$ is the combination coefficient for variable action "*i*", which takes into account the likelihood of the loads $Q_{k,i}$ to be not present over the entire structure during the earthquake, as well as a reduced participation in the motion of the structure due to a non-rigid connection with the structure. According to EN 1998-1 4.2.4(2)P, the combination coefficients $\psi_{E,i}$ should be computed from the following expression:

$$\psi_{E,i} = \varphi \cdot \psi_{2i} \tag{5.8}$$

Values to be ascribed to φ may be found in the National Annex. The recommended values for φ are listed in Table 5.3.

Table 5.3 Values of φ for calculating $\psi_{E,i}$

Type of variable action	Storey	φ
Categories A-C	Roof	1,0
	Storeys with correlated occupancies	0,8
	Independently occupied storeys	0,5
Categories D-F and Archives		1,0

5.4.3 Basic principles of conceptual design

EN 1998-1 requirements aim to mitigate seismic vulnerability within acceptable costs. The governing design concepts are hereafter summarized with a list of a few items (EN 1998-1 4.2.1(2)):

- structural simplicity: it consists in realizing clear and direct paths for the transmission of the seismic forces, thus allowing the modelling, analysis, detailing and construction of simple structures. It directly implies a simplified morphology of both the structural plan and elevation. In such a way structural behaviour uncertainties are limited;
- uniformity, symmetry and redundancy: uniformity is characterised by an even distribution of the structural elements both in-plan and along the height of the building, allowing short and direct transmission of the inertia forces and eliminating the occurrence of sensitive zones where concentration of stress or large ductility demands might prematurely cause collapse. Moreover, if the building configuration is symmetrical, a symmetrical layout of structural elements is envisaged. In addition, the use of distributed structural elements may increase redundancy and allow a redistribution of action effects and widespread energy dissipation across the entire structure;
- bi-directional resistance and stiffness: the building structure must be able to resist horizontal actions in any direction. To this purpose, the structural elements should be arranged in orthogonal in-plan structural patterns, ensuring similar resistance and stiffness characteristics in both the main directions;
- torsional resistance and stiffness: building structures should possess adequate torsional resistance and stiffness in order to limit torsional motions which tend to stress the structural systems in a non-uniform way;
- diaphragmatic behaviour at storey level: the floors (including the roof) should act as horizontal diaphragms that collect and transmit the inertia forces to the vertical structural systems and ensure that those systems behave together in resisting the horizontal seismic action. In order to guarantee this behaviour, floors should be provided with in-plan stiffness and resistance and with effective connection to the vertical structural systems;
- adequate foundation: the foundations have a key role, because they have to ensure that the whole building may be subjected to a uniform seismic excitation.

Satisfying the basic principles of conceptual design allows obtaining a regular building both in plan and in elevation, which is a fundamental requirement to achieve a high seismic performance and reliable structural model.

5.4.4 Damage limitation

According to EC8 the damage limitation requirement for buildings results in an upper limit on the interstorey drift ratio demand under the frequent (serviceability) seismic action (EN 1998-1 4.4.3.2). In general, member sizes will be controlled by the limit on interstorey drift ratio. For this reason, compliance with the damage limitation requirement should be established, before proceeding with dimensioning and detailing of members to satisfy the no-collapse requirement.

The interstorey drift ratio demand d_r for a generic storey is evaluated as the difference between the average lateral displacements d_s at the top and bottom of the storey under consideration. It should be determined under the frequent (serviceability) seismic action, which is defined by multiplying the entire elastic response spectrum of the design seismic action for 5% damping by the same factor ν that reflects the effect of the mean return periods of these two seismic actions.

In the code, damage limitation requirement is expressed by the following equation:

$$\nu d_r \leq \alpha \cdot h \tag{5.9}$$

where:

- α is the limit related to the typology of non-structural elements;
- d_r is the design interstorey drift;
- h is the storey height;
- ν is a displacement reduction factor depending on the importance class of the building, whose values are specified in the National Annex (as previously discussed in section 5.3).

The limits for α depend on the type of non-structural elements and they are set as follows:

- 0,5 %, if there are brittle non-structural elements attached to the structure so that they are forced to follow structural deformations (normally partitions);
- 0,75 %, if non-structural elements (partitions) attached to the structure as above are ductile;
- 1 %, if no non-structural elements are attached to the structure.

According to EN 1998-1 4.3.4, If the analysis for the design seismic action is linear-elastic based on the design response spectrum (i.e. the elastic spectrum with 5% damping divided by the behaviour factor q), then the values of the displacements d_s are those from that analysis multiplied by the behaviour factor q, as expressed by means of the following simplified expression:

$$d_s = q_d \cdot d_e \tag{5.10}$$

where:

- d_s is the displacement of the structural system induced by the design seismic action;
- q_d is the displacement behaviour factor, assumed equal to q;
- d_e is the displacement of the structural system, as determined by a linear elastic analysis under the design seismic forces.

If a non-linear analysis is performed, the interstorey drift ratio should be determined for a seismic action (acceleration time-history for time-history analysis, acceleration-displacement composite spectrum for pushover analysis) derived from the elastic spectrum (with 5% damping) of the design seismic action times ν.

5.5 Design criteria and detailing rules in steel buildings

5.5.1 Behaviour factors

The general design approach recommended by EC8 aims to control the inelastic structural behaviour by avoiding the formation of soft storey mechanisms and brittle failure modes. In order to achieve this purpose, the design rules are based on the capacity design of members and on detailing the dissipative zones parts with specific rules to improve their ductility and deformation capacity. This philosophy is specifically intended for buildings designed for ductility classes M and H. For these cases, the design forces calculated by means of linear elastic analysis (namely obtained from either lateral force method or modal response spectrum) can be obtained reducing the elastic spectrum by the behaviour factor q, which accounts for ductility and dissipative capacity of the structural system.

As clearly described in Figure 5.6, the behaviour factor q according to EN 1998-1 for regular structural systems is given as follows:

$$q = \frac{\alpha_u}{\alpha_1} \cdot q_o \tag{5.11}$$

where q_o is the reference value of the behaviour factor, while α_u/α_1 is the plastic redistribution parameter accounting for the system overstrength due to redundancy. The parameter α_1 is the multiplier of the horizontal seismic design action to reach the first plastic resistance in the structure and α_u is the multiplier of the horizontal seismic design action necessary to form a global mechanism. The ratio α_u / α_1 may be obtained from nonlinear static 'pushover' global analysis according to EC8, but is limited to 1,6. However, Eurocode 8 proposes some reference values for, as follows:

- 1 for inverted pendulum structures;
- 1,1 for one-storey frames;
- 1,2 for one-bay multistorey frames, eccentric bracing or dual systems with moment resisting frames and concentrically braced frames;
- 1,3 for multistorey multi-bay moment-resisting frames.

As reported in Table 5.4, EC8 also provides the upper limits for the behaviour factors q for the structural schemes depicted in Figure 5.7.

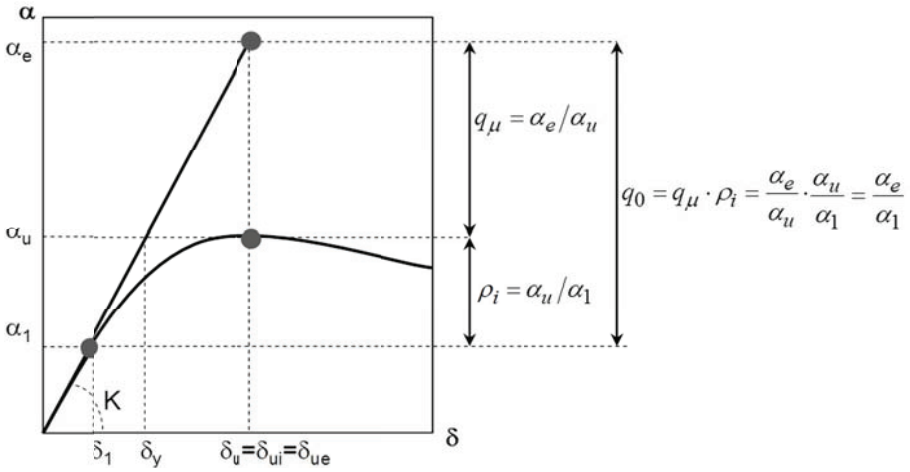

Figure 5.6 The behaviour factor *q* defined in EN 1998-1.

Table 5.4 Upper limit of reference values of behaviour factors for systems regular in elevation.

Structural type	Ductility Class	
	DCM	DCH
a) Moment resisting frame	4	$5(\alpha_u/\alpha_1)$
b) Frame with concentric bracings		
Diagonal bracings	4	4
V-bracings	2	2,5
c) Frame with eccentric bracings	4	$5(\alpha_u/\alpha_1)$
d) Inverted pendulum	2	$2(\alpha_u/\alpha_1)$
e) Structures with concrete cores or concrete walls	Are those defined for reinforced concrete structures	
f) Moment resisting frame with concentric bracings	4	$4(\alpha_u/\alpha_1)$
g) Moment resisting frames with infills		
Unconnected concrete or masonry infills, in contact with the frame	2	2
Connected reinforced concrete infills	Are those defined for composite steel – concrete buildings	
Infills isolated from moment frame (see moment frame)	4	$5(\alpha_u/\alpha_1)$

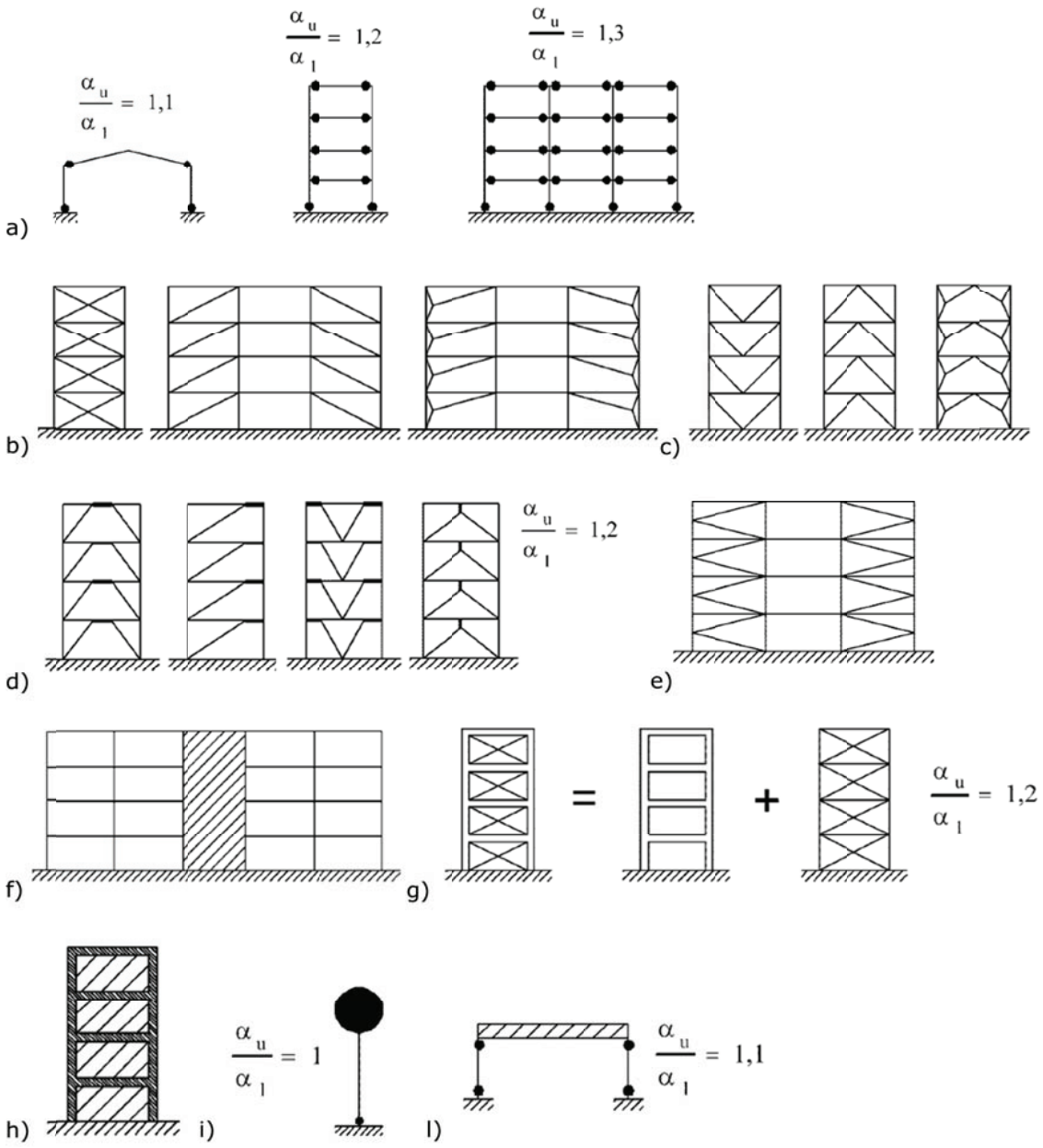

Figure 5.7 The structural schemes accounted for EC8: a) Moment resisting frames (dissipative zones in the beams and at the bottom of the columns); b) Frames with concentrically diagonal bracings (dissipative zones in tension diagonals only); c) Frame with V bracings (dissipative zones in both tension and compression diagonals); d) Frames with eccentric bracings (dissipative zones in bending or shear links); e) K-braced frames (not allowed); f) Structures with concrete cores or concrete walls; g) Moment resisting frame combined with concentric bracing (dissipative zone in moment frame and in tension diagonals); h) Moment resisting frames combined with infills; i) Inverted pendulum with dissipative zones at the column base; l) Inverted pendulum with dissipative zones in columns.

5.5.2 Design criteria and detailing rules for dissipative structural behaviour common to all structural types

The structures with dissipative zones should be designed and detailed such that yielding or local buckling or other phenomena due to hysteretic behaviour do not affect the overall stability of the structure.

To guarantee this condition, EC8 provides general design requirements that can be applied to all structural schemes. It is interesting to note that EC8 allows locating the dissipative zones in either members or connections. However, different criteria and requirements should be considered for each typology, as described hereinafter.

5.5.2.1 Ductility classes and rules for cross sections

As described above, three ductility classes (i.e. DCL, DCM and DCH) are provided for by EC8, depending on the accepted level of the plastic engagement into the dissipative parts. Indeed, in case of DCL poor plastic deformations are expected and the code allows performing global elastic analysis using q factor within 1,5–2,0 and verifying the strength of elements (both members and connections) according to EC3 without capacity design rules (recommended for low seismic areas, only). On the contrary, for DCM and DCH it is expected to have moderate and large plastic engagement in dissipative zones, respectively. Therefore, EC8 prescribes specific design rules both at global and local level in order to guarantee sufficient ductility in dissipative elements. In both cases, there are some rules common for all structural schemes and other specifically conceived for each typology. In addition, under these conditions, EC8 recommends to use q factor larger than 2. This assumption can be applied provided that the dissipative elements in compression or bending under seismic loading satisfy a set of cross-section requirements, namely by restricting the local slenderness ratios to limit local buckling phenomena under large deformation demand. To this aim EC8 adopts the EC3 classification for cross sections relating the restrictions to the value of q factor for each Ductility Class, as summarized in Table 5.5.

It is worth to note that several studies and researches carried out in the recent past (Mazzolani and Piluso, 1992 and 1996; Gioncu and Mazzolani, 1995; Gioncu, 2000, Plumier, 2000; Gioncu and Mazzolani, 2002, Elghazouli 2010, D'Aniello *et al*, 2012, 2013, Güneyisi *et a*l 2013, 2014) have highlighted some criticisms in the Eurocode classification mainly due to the small number of parameters considered to characterize the beam performance (Landolfo 2013). In fact, Eurocode relates rotation capacity to material and cross section factors only, neglecting very important behavioural issues, such as the flange-web interaction, the overall member slenderness, the moment gradient, the lateral restraints, the loading conditions (Landolfo 2013).

Table 5.5 Requirements on cross-sectional class of dissipative elements depending on Ductility Class and reference behaviour factor.

Ductility class	Reference value of behaviour factor q	Required cross-sectional class
DCM	$1,5 < q \leq 2,0$	class 1,2 or 3
	$2,0 < q \leq 4,0$	class 1 or 2
DCH	$q > 4,0$	class 1

5.5.2.2 Design rules for connections close to dissipative zones

EN 1998-1 6.5.5 provides a general rule for all types of non-dissipative connections belonging to the dissipative members of the structure, in order to ensure sufficient overstrength to avoid localization of plastic strains. In particular, the following connection overstrength criterion must be applied:

$$R_d \geq 1.1\gamma_{ov}R_{fy} \tag{5.12}$$

where R_d is the resistance of the connection, R_{fy} is the plastic resistance of the connected dissipative member based on the design yield stress of the material, γ_{ov} is the material overstrength factor.

5.5.2.3 Design rules and requirements for dissipative connections

EN 1998-1 6.6.4 allows using dissipative joints in case of MRFs. In particular, dissipative semi-rigid and/or partial strength connections are permitted, provided that all of the following requirements are verified:

- the connections have a rotation capacity consistent with the global deformations;
- members framing into the connections are stable at the ultimate limit state (ULS);
- the effect of connection deformation on global drift is taken into account using nonlinear static (pushover) global analysis or non-linear time history analysis;
- the rotation capacity of the dissipative connection θ_p is not less than 35 mrad for structures of ductility class DCH and 25 mrad for structures of ductility class DCM with $q > 2$;

The latter requirement can be verified by means of qualification tests to be carried out on joint sub-assemblages. In order to measure the joint ductility, EC8 defines the rotation θ_p as the chord rotation of the joint given by $\theta_p = \delta / 0{,}5L$, where δ is the beam deflection at midspan and L is the beam span.

The rotation capacity of the plastic hinge region θ_p should be ensured under cyclic loading without degradation of strength and stiffness greater than 20%. This requirement is valid independently of the intended location of the dissipative zones. As additional requirement to qualify the performance of the joint by means of testing, EC8 states that the column web panel shear deformation should not contribute for more than 30% of the plastic rotation capability θ_p.

5.5.3 Design criteria and detailing rules for Moment Resisting Frames

According to DCM and DCH concepts, in order to achieve a ductile global collapse mechanism, Moment Resisting Frames (MRFs) are designed to form plastic hinges in the beams or in the beam-to-column connections, but avoiding the plastification of columns with the exception of the base of the frame, at the top level of multi-storey buildings and for single storey buildings. This type of plastic mechanism is generally referred as "weak beam/strong column" behaviour. It is characterized by the most favourable performance, thus exploiting the beneficial dissipative capacity of steel beams. On the contrary the so-called "strong beam/weak column" behaviour, which typically characterizes non-seismic design, is characterized by premature storey collapse mechanisms, because of the poor and limited rotation capacity of columns.

Aside from the requirements regarding the cross-sectional classes (previously described in Sec. 5.5.2.1), EC8 requires additional condition for MRFs in order to avoid that compression and shear forces acting on beams could impair the full plastic moment resistance and the rotation capacity. To this aim, at clause 6.6.2(2) the code states that

the following inequalities should be verified at the location where the formation of hinges:

$$\frac{M_{Ed}}{M_{pl,Rd}} \leq 1 \tag{5.13}$$

$$\frac{N_{Ed}}{N_{pl,Rd}} \leq 0,15 \tag{5.14}$$

$$\frac{V_{Ed}}{V_{pl,Rd}} \leq 0,5 \tag{5.15}$$

being M_{Ed}, N_{Ed} and V_{Ed} the design forces, while $M_{pl,Rd}$, $N_{pl,Rd}$ and $V_{pl,Rd}$ are design resistances in accordance with EN 1993.

In general, owing to the presence of floor diaphragm axial forces in beams of MRFs are negligible. Instead, shear forces could be significant and should be limited to avoid flexural-shear interaction in plastic hinge zones. Hence, shear force demand at both beam ends should be calculated using capacity design principles as follows:

$$V_{Ed} = V_{Ed,G} + V_{Ed,M} \tag{5.16}$$

where $V_{Ed,G}$ is the shear force due to gravity forces in the seismic design situation and $V_{Ed,M}$ is the shear force corresponding to plastic hinges formed at the beam ends (namely $V_{Ed,M} = (M_{pl,A}+M_{pl,B})/L$, being $M_{pl,A}$ and $M_{pl,B}$ the beam plastic moments with opposite signs at the end sections A and B, while L is the beam length).

In order to obtain the "weak beam/strong column" behaviour, the forces acting on columns calculated by the elastic model have to be amplified by the magnification coefficient Ω, defined as:

$$\Omega = \min\left(\frac{M_{pl,Rd,i}}{M_{Ed,i}}\right) \tag{5.17}$$

where $M_{Ed,i}$ is the design value of the bending moment in beam *"i"* in the seismic design situation and $M_{pl,Rd,i}$ is the corresponding plastic moment. It is important to highlight that this ratio should be calculated for all beams in which dissipative zones are located.

Once Ω has been calculated, the columns should be verified against all resistance checks including those for element stability, according to the provisions of EC3 for the most unfavourable combination of bending moments M_{Ed}, the shear force V_{Ed} and axial forces N_{Ed} , based on the following (EN 1998-1 6.6.3(1)P):

$$M_{Ed} = M_{Ed,G} + 1,1 \cdot \gamma_{ov} \cdot \Omega \cdot M_{Ed,E} \tag{5.18}$$

$$V_{Ed} = V_{Ed,G} + 1,1 \cdot \gamma_{ov} \cdot \Omega \cdot V_{Ed,E} \tag{5.19}$$

$$N_{Ed} = N_{Ed,G} + 1,1 \cdot \gamma_{ov} \cdot \Omega \cdot N_{Ed,E} \tag{5.20}$$

where:

- $M_{Ed,G}$, $V_{Ed,G}$ and $N_{Ed,G}$, are the forces in the column due to the non-seismic actions included in the combination of actions for the seismic design situation;

- $M_{Ed,E}$, $V_{Ed,E}$ and $N_{Ed,E}$ are the forces in the column due to the design seismic action;
- γ_{ov} is the material overstrength factor.

In addition to the member checks based on the Ω criterion, EN 1998-1 4.4.2.3(4) requires that at every joint the following condition should be satisfied:

$$\frac{\sum M_{Rc}}{\sum M_{Rb}} \geq 1,3 \tag{5.21}$$

where:

- ΣM_{Rc} is the sum of the design values of the moments of resistance of the columns framing the joint;
- ΣM_{Rb} is the sum of the design values of the moments of resistance moments of the beams framing the joint.

5.5.4 Design criteria and detailing rules for Concentrically Braced Frames

Concentrically braced frames (CBFs) are characterized by a truss behaviour due to axial forces developed in the bracing members. According to EC8, the diagonal bracings in tension are the dissipative zones which have to yield, thus preserving the connected elements from damage. Therefore, the response of a CBF is basically influenced by the behaviour of its bracing elements. However, it should be noted that the role of bracing members differs with the CBF configurations, shown in Figure 5.8. Indeed, for X and Diagonal CBFs the energy dissipation capacity of braces in compression is neglected and the lateral forces are assigned to tension braces only. On the contrary, in frames with V and inverted V bracings both the tension and compression diagonals should be taken into account. This requirement is due to the geometrical configuration where the braces intersect the beams.

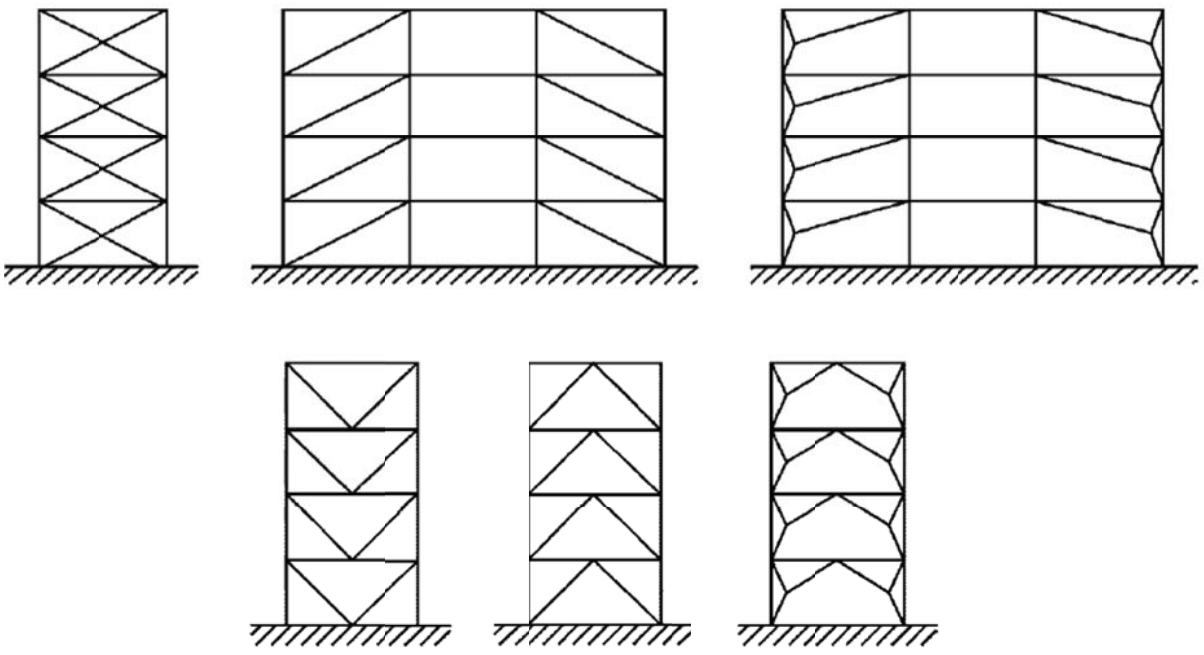

Figure 5.8 CBF configurations.

Depending on the ductility class and the behaviour factor *q* used in the design, tension bracings have to satisfy the requirements regarding the cross-sectional classes reported in Table 5.5. Moreover, the diagonal braces have to be designed and placed in such a way that, under seismic action reversals, the structure exhibits similar lateral load-deflection responses in opposite directions at each storey (EN 1998-1 6.7.1(2)P). This performance requirement is deemed to be satisfied if the following rule is met at every storey:

$$\frac{\left|A^{+} - A^{-}\right|}{A^{+} + A^{-}} \leq 0,05 \tag{5.22}$$

where A^+ and A^- are the areas of the vertical projections of the cross-sections of the tension diagonals (Figure 5.9) when the horizontal seismic actions have a positive or negative direction, respectively.

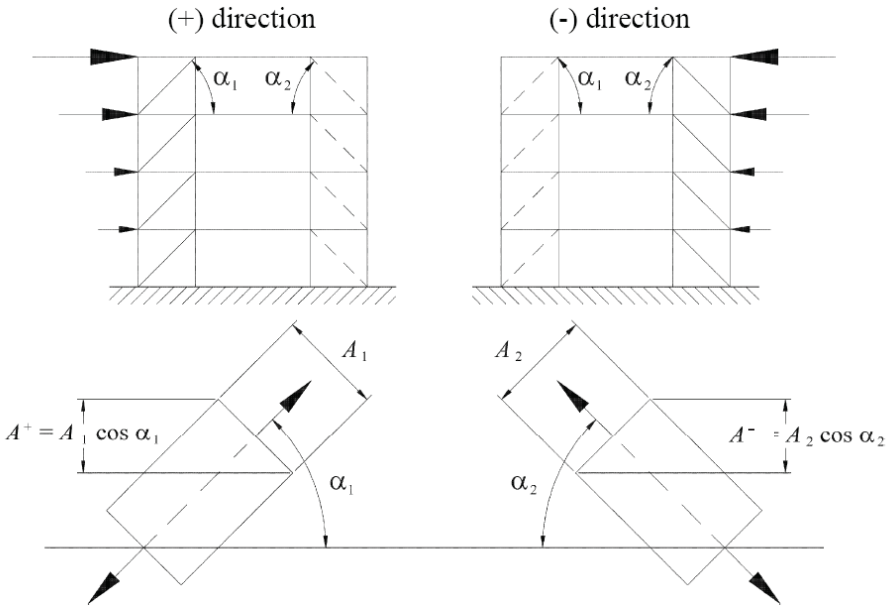

Figure 5.9 Example of application of requirement given by Eqn. (5.22).

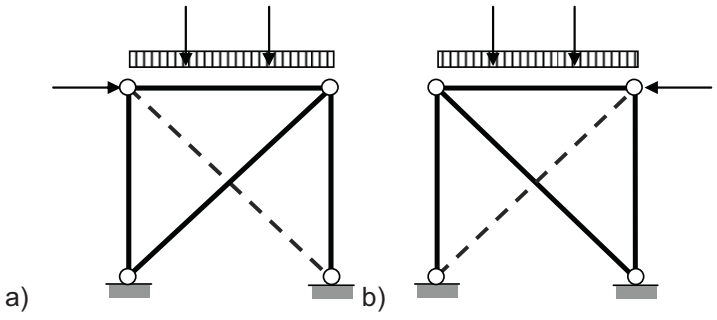

Figure 5.10 Calculation models of X-CBFs.

For X-CBFs, the diagonal braces have to be designed in such a way that the yield resistance $N_{pl,Rd}$ of their gross cross-section is such that $N_{pl,Rd} \geq N_{Ed}$, where N_{Ed} is calculated from the elastic model ideally composed by a single brace (i.e. the diagonal in tension). Generally speaking, in order to make tension alternatively developing in all the

braces at any storey, two models must be developed, one with the braces tilted in one direction and another with the braces tilted in the opposite direction, as shown in Figure 5.10 In addition, the brace slenderness must fall in the range $1,3 \le \bar{\lambda} \le 2,0$ (EN 1998-1 6.7.3(1)). The lower bound value is imposed in order to limit the maximum compression axial forces transmitted to column; the upper bound value is given in order to limit excessive vibrations and undesired buckling under service loads.

Differently from X-CBFs, in frame with inverted-V bracing compression diagonals should be designed for the compression resistance, such that $\chi N_{pl,Rd} \geq N_{Ed}$, where χ is the buckling reduction factor calculated according to EN 1993:1-1 6.3.1.2 (1), and N_{Ed} is the required strength. Differently from the case of X-CBFs, the code does not impose a lower bound limit for the non-dimensional slenderness $\bar{\lambda}$, while the upper bound limit ($\bar{\lambda} \le 2$) is retained.

For all types of bracing configurations, in order to guarantee the formation of a global mechanism, clause 6.7.4(1) of the EC8 imposes to verify the strength of beam-column members based on the Eqn.(5.23), as follows:

$$N_{pl,Rd}(M_{Ed}) \geq N_{Ed,G} + 1,1 \cdot \gamma_{ov} \cdot \Omega \cdot N_{Ed,E} \tag{5.23}$$

where:

- $N_{pl,Rd}(M_{Ed})$ is the design resistance to axial force of the beam or the column calculated in accordance with EN 1993:1-1, taking into account the interaction with the design value of bending moment, M_{Ed}, in the seismic design situation;
- $N_{Ed,G}$ is the axial force in the beam or in the column due to the non-seismic actions included in the combination of actions for the seismic design situation;
- $N_{Ed,E}$ is the axial force in the beam or in the column due to the design seismic action;
- γ_{ov} is the material overstrength factor;
- Ω is the minimum overstrength ratio $\Omega_i = N_{pl,Rd,i}/N_{Ed,i}$, which may vary within the range Ω to 1,25Ω. It is should be noted that, aiming to fit better the distribution of diagonal strengths $N_{pl,Rd,i}$ to the distribution of computed action effect $N_{Ed,i}$, this approach forces the use of different sections of diagonals over the height of the structure.

In addition, Eurocode 8 provides specific requirements only for the beams belonging to both V and inverted V CBFs. Indeed, for those types of structural schemes the seismic response is significantly influenced by the beam behaviour. Because, after the buckling of the compression brace, the resultant of the axial forces in the compression and in the tension braces has a vertical component acting on the connected beam and inducing a significant bending moment. In this situation the formation of a plastic hinge at mid-span of the beams must be avoided, because it would result in a drop of storey lateral resistance with consequent inelastic drift concentration at the storey with yielded beams. in order to prevent this undesirable behaviour of the frame, EC8 provisions require: i) the beams of the braced span must be able to carry all non-seismic actions without considering the intermediate support given by the diagonals; ii) the beams have to be designed to carry also the vertical component of the force transmitted by the tension and compression braces. This vertical component is calculated assuming that the tension brace transfers a force equal to its yield resistance ($N_{pl,Rd}$) and the compression brace transfers a force equal to a percentage of its original buckling strength ($N_{b,Rd}$) to take into account the strength degradation under cyclic loading. The reduced compression strength is estimated as equal to $\gamma_{pb} N_{pl,Rd}$ with a value of the factor γ_{pb} to be found in the National Annexes. The value recommended by EN 1998 is 0,30.

5.5.5 Design criteria and detailing rules for Eccentrically Braced Frames

In eccentrically braced frames (EBFs) at least one end of each brace is connected so as to isolate a segment of beam called "link", thus transmitting forces by shear and bending. Typical configurations for EBFs are depicted in Figure 5.11. The four EBF arrangements here presented are usually named as split-K-braced frame, D-braced frame, V-braced and finally inverted-Y-braced frame.

The links are the zones where the inelastic action is restricted differently from the case of CBFs where the braces are the dissipative members. This implies that the modelling approximations used for braces in CBFs should not be used for EBFs, because in such frames diagonal braces are part of non-dissipative zones and should be designed to be stable under seismic conditions.

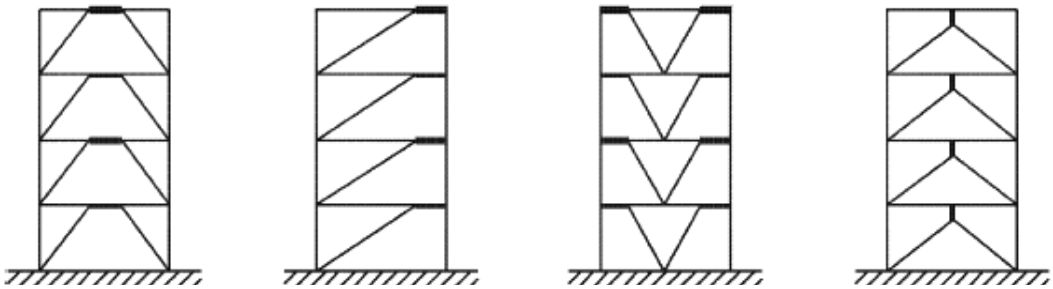

Figure 5.11 EBF configurations.

On the basis of the type of plastic mechanism, links are classified into three categories:

- short, which dissipate energy by yielding essentially in shear;
- intermediate, in which the plastic mechanism involves bending and shear;
- long, which dissipate energy by yielding essentially in bending.

The mechanical parameter influencing the plastic mechanism is the link length "*e*". It is related to the ratio between the plastic bending moment ($M_{p,link}$) over the plastic shear ($V_{p,link}$) of the link cross section, calculated according to EN 1998-1 6.8.2(3) as following:

$$M_{p,link} = f_y b t_f \left(d - t_f\right) \tag{5.24}$$

$$V_{p,link} = \left(f_y / \sqrt{3}\right) \cdot t_w \cdot \left(d - t_f\right) \tag{5.25}$$

where f_y is the value of steel yielding stress, d is the depth of the cross section, t_f is the flange thickness and t_w is the web thickness.

In the cases where equal moments could form simultaneously at both ends of the link (e.g. the split-K configuration) the link can be classified as follows:

Short links: $e \le e_s = 1,6 \dfrac{M_{p,link}}{V_{p,link}}$ (5.26)

Long links: $e \ge e_L = 3 \dfrac{M_{p,link}}{V_{p,link}}$ (5.27)

Intermediate links: $e_s < e < e_L$ (5.28)

However, these equations can be generalized to the design cases where only one plastic hinge would form at one end of the link (e.g. the case of inverted-Y configuration, where the link end connected to the beam develops the plastic flexural hinge, while the opposite end connected to the braces is in elastic field) as follows (EN 1998 6.8.2(9)):

Short links: $e \le e_s = 0,8 \cdot (1+\alpha) \dfrac{M_{p,link}}{V_{p,link}}$ (5.29)

Long links: $e \ge e_L = 1,5 \cdot (1+\alpha) \dfrac{M_{p,link}}{V_{p,link}}$ (5.30)

Intermediate links: $e_s < e < e_L$ (5.31)

where α is the ratio of the smaller bending moments $M_{Ed,A}$ at one end of the link in the seismic design situation, to the greater bending moment $M_{Ed,B}$ at the end where the plastic hinge would form, both moments being taken as absolute values.

It is interesting to note that the type of link plastic mechanism is directly related to the ductility capacity, namely plastic rotation, provided by the link in order to withstand the seismic ductility demand.

The link rotation is defined as rotation angle θ_p between the link and the element outside of the link. Figure 5.12 clarifies this definition and simple equations are given for estimating link rotation, which should be consistent with global deformation. As it can be observed, the shorter is the link length and the greater is the ductility demand.

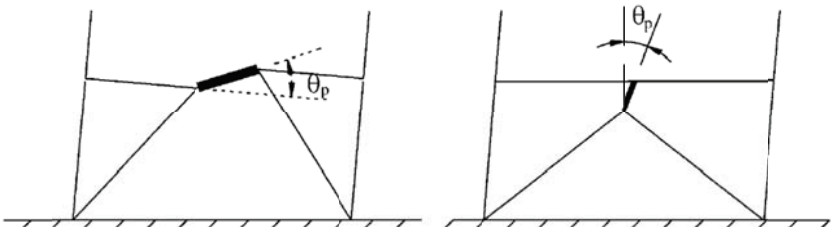

Figure 5.12 The link rotation angle θ_p.

EN 1998-1 6.8.2(10) states that the link rotation should not exceed the following values:

Short links:	$\theta_p \le \theta_{pR}$ =	0,08 radians	(5.32)
Long links:	$\theta_p \le \theta_{pR}$ =	0,02 radians	(5.33)
Intermediate links:	$\theta_p \le \theta_{pR}$ =	the value determined by linear interpolation between the above values	(5.34)

In order to guarantee the formation of a ductile collapse mechanism, the action effects on connections, beams and columns, calculated by the elastic model, have to be amplified according to the philosophy of capacity design implemented by EC8. This aim is

pursued using the magnification coefficient Ω, which is the minimum of the following values:

- the minimum value of $\Omega_i = 1{,}5V_{p,link,i}/V_{Ed,i}$ among all short links;
- the minimum value of $\Omega_i = 1{,}5M_{p,link,i}/M_{Ed,i}$ among all intermediate and long links.

where $V_{Ed,i}$ and $M_{Ed,i}$ are the design values of the shear force and of the bending moment in "*i*" link in the seismic design situation, while $V_{p,link,i}$ and $M_{p,link,i}$ are the corresponding shear and bending plastic design resistances as given by Eqn. (5.24) and (5.25).

Once Ω has been calculated, the design check of diagonal and column members of the frame is based on the following equation (see EN 1998-1 6.8.3(1)):

$$N_{pl,Rd}(M_{Ed},V_{Ed}) \geq N_{Ed,G} + 1{,}1 \cdot \gamma_{ov} \cdot \Omega \cdot N_{Ed,E} \tag{5.35}$$

where:

- $N_{pl,Rd}(M_{Ed},\ V_{Ed})$ is the design resistance to axial force the column or diagonal member calculated in accordance with EN 1993:1-1, taking into account the interaction with the design value of bending moment, M_{Ed}, and the shear force, V_{Ed}, in the seismic design situation;
- $N_{Ed,G}$ is the compression force in the column or diagonal member due to the non-seismic actions included in the combination of actions for the seismic design situation;
- $N_{Ed,E}$ is the compression force in the column or diagonal member due to the design seismic action;
- γ_{ov} is the material overstrength factor.

In any case the axial forces ($N_{Ed,E}$, $N_{Ed,G}$) induced by seismic and non-seismic actions are directly provided by the elastic numerical model.

5.6 Design worked example: multi-storey building with moment resisting frame

This section describes a design example for a six storey moment resisting frame according to EN1998-1:2005 and the main design criteria for multi-storey steel buildings in seismic areas. A preliminary description of the structural response and design criteria of typical MRFs is provided. Subsequently, the analysis of a specific case study structure and the verification of structural members are shown with some details.

5.6.1 Building description

The case study is a six storey office use building with a square plan, 18,00 m x 18,00 m. The storey height is equal to 3,50 m with exception of the first floor, which is 4,00 m high. The lateral force resisting system is placed at the perimeter of the plan of the buildings. The interior frames are assumed to be gravity frames and their lateral load resisting capacity is neglected. Two-dimensional frame models are used for the design, with appropriate selection of the tributary areas for gravity and seismic loads. A conceptual schematic with the typical building plan and the positioning of the lateral load resisting system are presented in Figure 5.13 (where the location of MRFs is indicated by the bold lines), and Figure 5.14.

The design of the structure is carried out using the provisions of EN 1993 and EN 1998-1. The material for all frame elements is S355 steel with an over-strength factor γ_{ov} = 1,25. The chosen member sections are standard metric sections which are commercially available. As required by DCH concept (see Table 5.5), it should be noted that all steel profiles are class 1 according to EN1993 cross section classification.

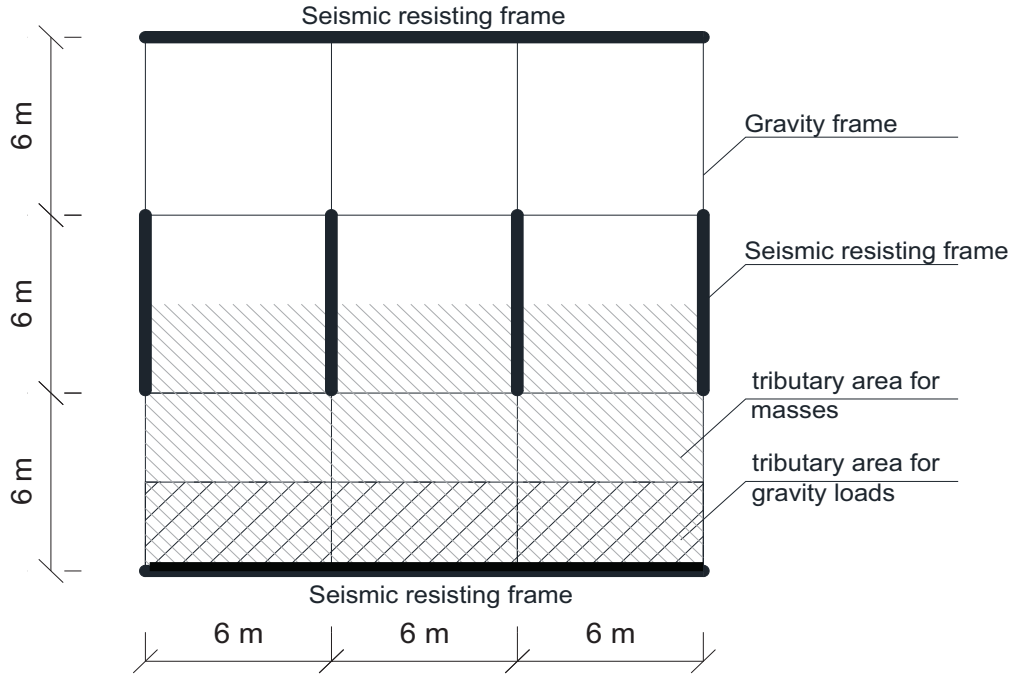

Figure 5.13 Plan and location of MRFs.

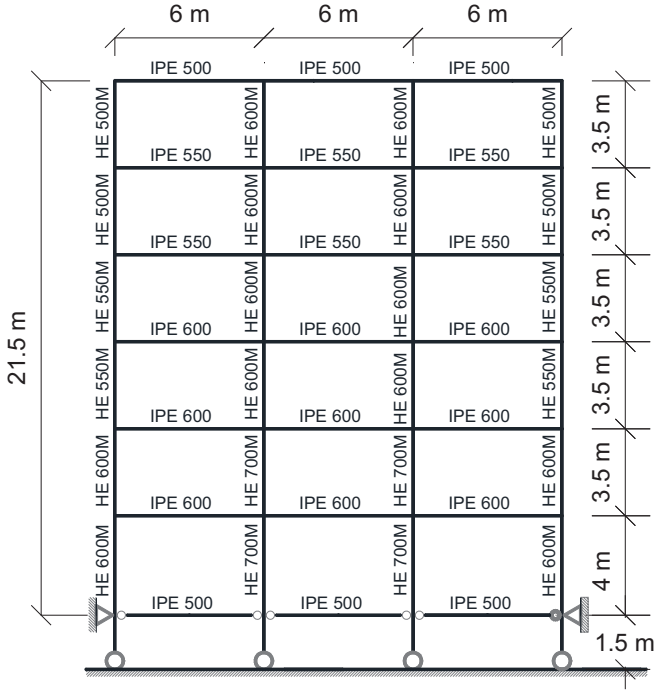

Figure 5.14 Configuration of the designed MRFs.

All floors are made of composite slabs with profiled steel sheetings that should be designed in order to resist the vertical loads and to behave as horizontal rigid diaphragms able to transmit the seismic actions to the seismic resistant frames. Slabs are supported by hot rolled "I-shaped" beams belonging to the MRFs placed along the two main plan directions of the building. Beams belonging to the first slab are simply pinned at both ends, because this level is assumed to be laterally restrained by the foundation (see Figure 5.14). The connection between slab and beams is provided by ductile headed shear studs that are welded directly through the metal deck to the beam flange. In order to avoid the composite action into the beam-to-column connections according to EN 1998-1 7.7.5, the slab is considered totally disconnected from the steel frame in a circular zone around a column of diameter $2b_{eff}$, with b_{eff} being the larger of the effective widths of the beams connected to that column. All beam-to-column connections are considered as rigid full strength. The column-to-foundation connections are pinned, being the translational fixity guaranteed by the foundation arrangement described in Figure 5.14.

5.6.2 Design actions

5.6.2.1 Characteristic values of unit loads

Table 5.6 summarizes the characteristic values of both persistent (G_k) and transient actions (Q_k). The value for the slab weight is inclusive of steel sheeting, infill concrete, finishing floor elements and partition walls. The vertical actions have been combined according to Eqn. (5.6).

Table 5.6 Characteristic values of vertical persistent and transient actions.

Location	Load (kN/m^2)	
	persistent	transient
Intermediate Storeys	5,8	3
Roof	5,0	3

5.6.2.2 Masses

Table 5.7 summarizes the masses used for this worked example, which have been combined according to Eqn. (5.7).

Table 5.7 Seismic Masses per Floor.

Location	Load (ton)
Intermediate Storeys	110,64
Roof	97,43

5.6.2.3 Seismic action

A reference peak ground acceleration equal to a_{gR} = 0,25 g (being g the gravity acceleration), a type C soil and a type 1 spectral shape have been assumed. An importance factor γ_1 equal to 1,0 has been considered in the design example, coherently with the building functions and associated importance. The spectral parameters in Eqns. (5.1) and (5.2) are S = 1,15, T_B = 0,20 s , T_C = 0,60 s and T_D = 2,00 s. In addition, the parameter β is the lower bound factor for the horizontal design spectrum, whose value should be found in National Annex. In this Handbook it was assumed β = 0,2, as recommended by the code (EN1998-1 3.2.2.5).

This worked example refers to DCH structures with multiple MRFs, whose behaviour factor was assigned according to Eqn. (5.11) as follows:

$$q = \frac{\alpha_u}{\alpha_1} \cdot q_o = 1,3 \cdot 5 = 6,5 \tag{5.36}$$

where q_o is the reference value of the behaviour factor for systems regular in elevation (see Table 5.4) while α_u/α_1 is the plastic redistribution parameter (see section 5.5.1).

Figure 5.15 shows both the elastic and the design spectra at ultimate limit state.

Regarding the Serviceability Limit State, drift levels at every storey are limited to 0,75% of the storey height (implying ductile non-structural elements connected to the frames) and it was attempted in the first instance to limit the inter-storey drift sensitivity coefficient θ (given by Eqn. (5.4)) to values smaller than 0,1, thus neglecting the P-Δ effects. However, the condition $\theta < 0,1$ leads to impractical design solutions (i.e. irrational increase of required steel sections), then in the example it is relaxed to $0,1 < \theta < 0,2$, with appropriate magnification of the seismic action effects by the factor $1/(1-\theta)$, as given by Eqn. (5.5).

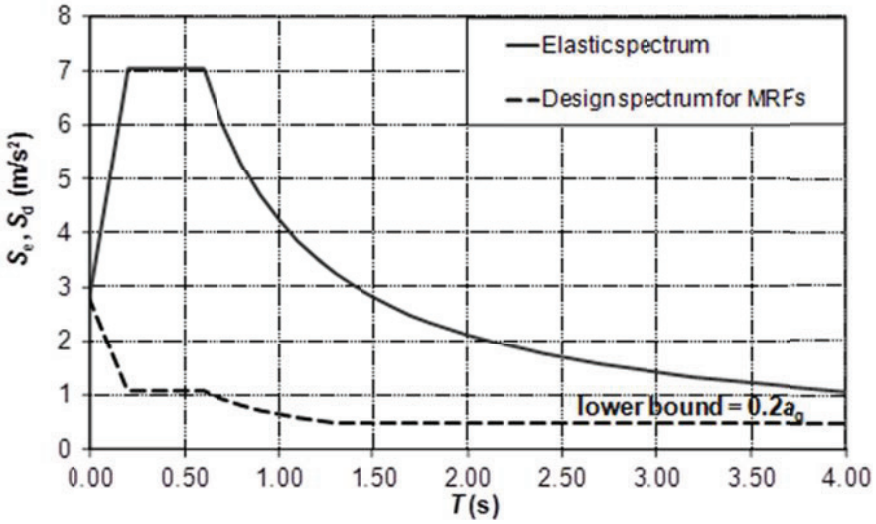

Figure 5.15 Elastic vs. design spectra for MRFs.

5.6.3 Calculation model and structural analysis

The model of the building must represent the distribution of stiffness and mass so that all significant deformation shapes and inertia forces are properly accounted for under seismic actions (EN 1998-1 4.3.1).

In this example a calculation 2D planar model has been used. This approach is allowed by the code (at clause 4.3.1(5)), since the examined building satisfies the conditions given by EN 1998-1 4.2.3.2 and 4.3.3.1(8), briefly described in Sec. 5.4.3 of this Chapter.

In the calculation model columns are considered continuous through each floor beam. All connections of the members belonging to the MRF have been considered full strength and full rigid and the flexibility of the panel zone has not been taken into account.

Masses have been considered as lumped into a selected master joint at each floor, because the floor diaphragms may be taken as rigid in their planes. This assumption implies that numerical model gives axial forces in beams equal to zero. Such a simplification can be considered acceptable for MRF structures.

Since the structure is characterized by full symmetry of in-plan distribution of stiffness and masses, in order to ensure a minimum of torsional strength and stiffness and to limit the consequences of unpredicted torsional response, EN 1998-1 introduces accidental torsional effects. The latter have to conventionally take into account the possible uncertainties in the stiffness and mass distributions and/or a possible torsional component of the ground motion about a vertical axis. As previously described in section 5.4.2, the effects of the accidental eccentricity can be estimated through the simplified approach using the δ factor to magnify the seismic forces calculated by the elastic model, which is the approach adopted in this example. Thus, the relevant δ factor for the examined case study is obtained as follows:

$$\delta = 1 + 1,2\frac{x}{L_e} = 1 + 1,2\frac{0,5L_e}{L_e} = 1,6 \tag{5.37}$$

The effects of actions included in the seismic design situation have been determined by means of a linear-elastic modal response spectrum analysis (EN 1998-1 4.3.3.1(2)), using the design spectrum depicted in Figure 5.15. According to EN 1998-1 4.3.3.3.1(3) it is required to take into account a number of vibration modes that satisfy either of the following conditions:

- the sum of the effective modal masses for the modes taken into account amounts to at least 90% of the total mass of the structure;
- all modes with effective modal masses greater than 5% of the total mass are taken into account.

In the present example, the first and second modes have been considered because they satisfy the first criterion. The fundamental modes of vibration, the relevant natural periods T_i and participating mass ratios M_i are shown in Figure 5.16. Since the first and second vibration modes in both X and Y direction may be considered as independent (being $T_2 \leq 0,9T_1$, EN 1998-1, 4.3.3.3.2) the SRSS (Square Root of the Sum of the Squares) method is used to combine the modal maxima.

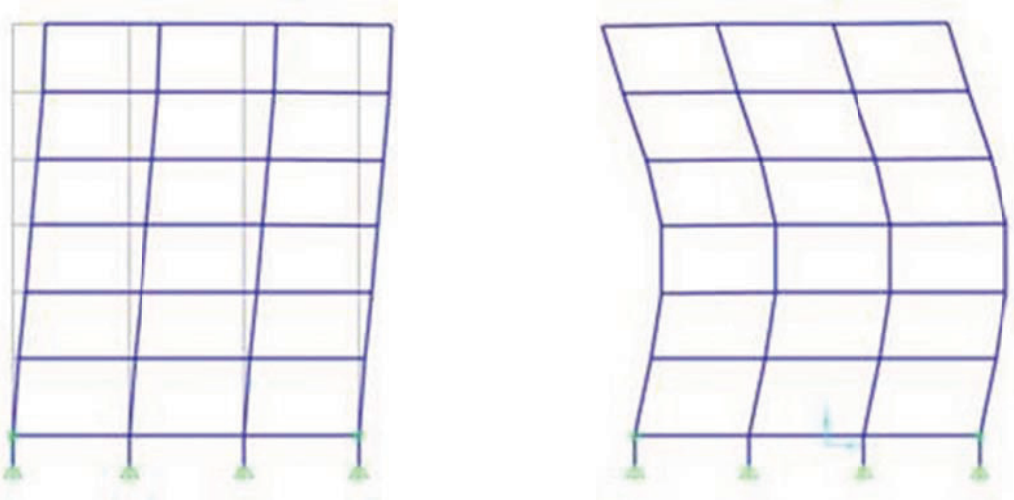

T_1 = 1,02s; M_1= 0,823 T_2 = 0,332s; M_2=0,115

Figure 5.16 Fundamental dynamic properties of the calculation model.

For clarity sake, the diagrams of internal forces (i.e. bending moments, shear and axial forces) for the vertical loads under seismic condition and those for the design response spectrum analysis are reported in Figure 5.17.

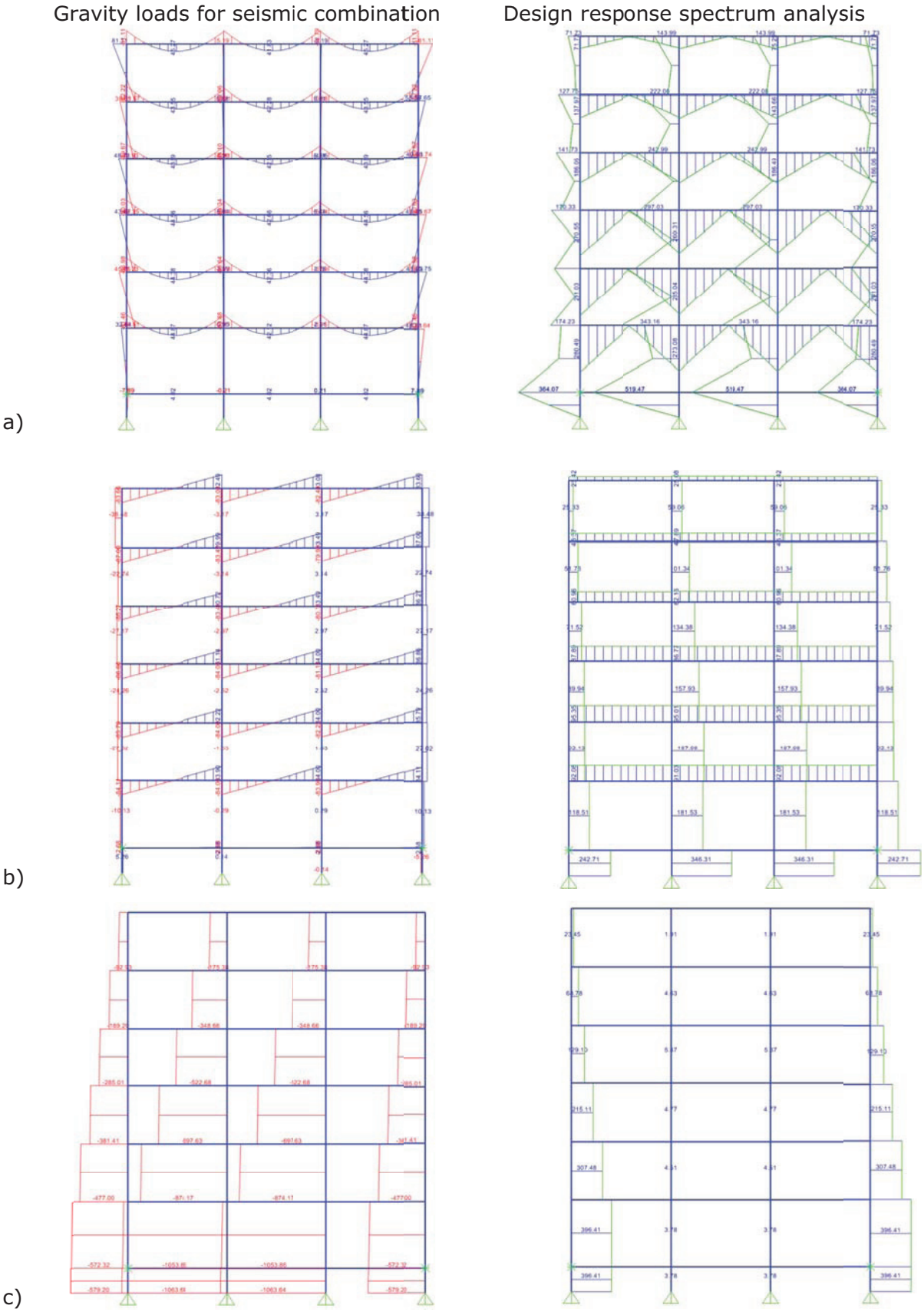

Figure 5.17 Calculated internal forces for MRFs: a) bending moments; b) shear forces); c) axial forces.

5.6.4 Frame stability and second order effects

P-Δ effects were specified through the inter-storey drift sensitivity coefficient θ given by Eqn. (5.4), and summarized in Table 5.8. As it can be observed the coefficient θ ranges within 0,1÷0,2. Hence, to take into account second order effects the seismic effects were magnified through the maximum multiplier α (indicated in bold in the Table 5.8), which are calculated at each storey having $\theta > 0,1$ according to Eqn. (5.5).

Table 5.8 Stability coefficients per floor in MRFs.

Storey	P_{tot} (kN)	V_{tot} (kN)	h (mm)	d_r (mm)	$\theta = \frac{P_{tot} \cdot d_r}{V_{tot} \cdot h}$ (-)	$\alpha = \frac{1}{(1-\theta)}$ (-)
VI	955,35	105,48	3500	24	0,07	1,07
V	2040,32	191,36	3500	34	0,11	1,12
IV	3125,29	257,39	3500	43	0,16	1,19
III	4210,27	309,83	3500	46	0,19	1,23
II	5295,24	350,14	3500	47	**0,20**	**1,25**
I	6380,21	375,06	4000	42	0,18	1,21

5.6.5 Design and verification of beams

All beams have been assumed as restrained against lateral-torsional buckling. Apart from the ultimate limit state verification under vertical loads, which is dealt with in the relevant Chapter about EN 1993:1-1, the bending and shear strengths are checked under the seismic load combination.

All beams are compliant to the requirements given by Eqn. (5.13),(5.14) and (5.15). With reference to the beam end sections, Table 5.9 reports the verification of bending strength and the relevant the overstrength factors Ω_i for beams belonging to external and internal bays (see Figure 5.13). Indeed, thanks to the symmetry, the seismic effects on the remaining bays are simply mirrored.

As it can be noted the minimum overstrength ratio Ω_{min} is equal to 2,76 (highlighted in bold in Table 5.9). Analysing the values reported in Table 5.9 it can be observed high values of beam overstrength. It is important to highlight that the use of oversize sections derived from the need to provide sufficient stiffness for drift control.

Table 5.10 summarizes the shear strength verifications for the same beams, where the shear force due to seismic action $V_{Ed,E}$ has been calculated according to Eqn. (5.16). As it can be observed the requirement expressed by Eqn. (5.15) is satisfied for all beams.

Table 5.9 Flexural checks for beams of MRFs.

	Storey	Left end				Right end				Ω_{min}
		$M_{Ed,G}$ (kNm)	$M_{Ed,E}$ (kNm)	M_{Ed} (kNm)	Ω_i	$M_{Ed,G}$ (kNm)	$M_{Ed,E}$ (kNm)	M_{Ed} (kNm)	Ω_i	
External span	VI	81,11	71,73	171,02	4,55	77,59	68,77	163,79	4,76	**2,76**
	V	92,22	137,97	265,16	3,73	71,17	134,26	239,46	4,13	
	IV	89,67	186,06	322,89	3,06	73,03	179,69	298,27	3,32	
	III	90,03	270,54	429,15	2,91	72,86	256,77	394,71	3,16	
	II	86,98	291,04	451,79	**2,76**	76,27	281,07	428,59	2,91	
	I	81,46	279,92	432,33	2,88	80,82	272,00	421,77	2,96	
Internal span	VI	82,79	75,25	177,11	4,40	82,79	75,25	177,11	4,40	
	V	82,96	143,66	263,04	3,76	82,96	143,66	263,04	3,76	
	IV	83,10	186,50	316,87	3,12	83,10	186,50	316,87	3,12	
	III	83,34	260,32	409,65	3,04	83,34	260,32	409,65	3,04	
	II	83,64	285,04	440,93	2,83	83,64	285,04	440,93	2,83	
	I	83,88	273,09	426,19	2,93	83,88	273,09	426,19	2,93	

Table 5.10 Shear checks for beams of MRFs.

	Storey	Left end					Right end			
		$V_{pl,Rd}$ (kN)	$V_{Ed,G}$ (kN)	$V_{Ed,E}$ (kN)	V_{Ed} (kN)	$\frac{V_{Ed}}{V_{pl,Rd}}$	$V_{Ed,G}$ (kN)	$V_{Ed,E}$ (kN)	V_{Ed} (kN)	$\frac{V_{Ed}}{V_{pl,Rd}}$
External span	VI	1236,97	83,66	259,62	343,28	0,28	82,49	259,62	342,11	0,28
	V	1474,17	87,00	329,80	416,80	0,28	79,99	329,80	409,79	0,28
	IV	1474,17	86,27	329,80	416,07	0,28	80,27	329,80	410,07	0,28
	III	1717,56	86,86	415,59	502,45	0,29	81,14	415,59	496,73	0,29
	II	1717,56	85,79	415,59	501,38	0,29	82,22	415,59	497,81	0,29
	I	1717,56	84,11	415,59	499,70	0,29	83,90	415,59	499,49	0,29
Internal span	VI	1236,97	83,07	259,62	342,69	0,28	83,07	259,62	342,69	0,28
	V	1474,17	83,49	329,80	413,29	0,28	83,49	329,80	413,29	0,28
	IV	1474,17	83,49	329,80	413,29	0,28	83,49	329,80	413,29	0,28
	III	1717,56	84,00	415,59	499,59	0,29	84,00	415,59	499,59	0,29
	II	1717,56	84,00	415,59	499,59	0,29	84,00	415,59	499,59	0,29
	I	1717,56	84,00	415,59	499,59	0,29	84,00	415,59	499,59	0,29

For clarity sake, based on the values from Table 5.9 and Table 5.10, the seismic demands on left end of the beam in the external bay at the first storey are obtained as follows:

$$M_{Ed} = M_{Ed,G} + \alpha \cdot M_{Ed,E} = 81,46\ \text{kNm} + 1,25 \cdot 279,92\ \text{kNm} = 432,33\ \text{kNm} \tag{5.38}$$

$$V_{Ed} = V_{Ed,G} + V_{Ed,M} = V_{Ed,G} + \left(\frac{2M_{pl,Rd}}{L_b}\right) = 84,11\,\text{kN} + \left(\frac{2 \cdot 1246,76}{6}\right)\text{kN} = 499,70\,\text{kN} \quad (5.39)$$

where $M_{Ed,G}$ and $M_{Ed,E}$ are the bending moment given by numerical model for gravity (i.e. due to $G_k + 0,3Q_k$) and seismic loads, respectively; α is the stability coefficient, reported in Table 5.8; $V_{Ed,G}$ is the shear force given by numerical model for gravity loads in seismic conditions, while $V_{Ed,M}$ is the shear force due to the hierarchy criterion corresponding to plastic hinges formed at both beam ends (see Eqn. (5.16)).

5.6.6 Design and verification of columns

The columns were verified on the basis of criteria described in section5.5.3. The global hierarchy criterion was applied according to Eqn. (5.18),(5.19) and (5.20). To this end, accounting also for the second order effects, the seismic elastic forces obtained by the numerical model have to be amplified by $1,1\gamma_{ov}\Omega$.

Table 5.11 and Table 5.12 summarize the strength verifications for columns belonging to the external column (see Figure 5.14) of the MRF.

Stability verifications of column in bending and axial compression have to be carried out according to EN 1993:1-1 6.3.3(4). Since the rules for the calculation of connection strength are given by Eurocode 3, the reader is referred to the relevant Eurocode for calculation examples of stability checks.

Table 5.11 Flexural checks for columns of MRFs.

	Storey	$M_{Ed,G}$ (kNm)	$M_{Ed,E}$ (kNm)	M_{Ed} (kNm)	$N_{Ed,G}$ (kN)	$N_{Ed,E}$ (kN)	N_{Ed} (kN)	$M_{N,Rd}$ (kNm)	$\frac{M_{Ed}}{M_{N,Rd}}$
Top end of column	VI	81,11	71,73	422,27	83,66	23,44	195,15	2518,37	0,17
	V	38,65	127,74	646,23	179,94	68,80	507,17	2518,37	0,26
	IV	48,74	141,73	722,83	275,47	129,09	889,44	2816,22	0,26
	III	43,67	170,32	853,75	371,87	215,04	1394,65	2816,22	0,30
	II	45,75	152,53	771,21	467,20	307,47	1929,61	3114,06	0,25
	I	32,64	111,57	563,28	561,11	396,41	2446,52	3021,14	0,19
Bottom end of column	VI	53,57	25,49	129,34	92,93	23,44	204,42	2518,37	0,05
	V	40,93	62,06	225,42	189,20	68,80	516,43	2518,37	0,09
	IV	46,35	116,32	392,13	285,01	129,09	898,98	2816,22	0,14
	III	41,23	150,48	488,55	381,41	215,04	1404,19	2816,22	0,17
	II	48,81	174,22	566,72	477,00	307,47	1939,41	3114,06	0,18
	I	7,89	356,06	1066,34	572,32	396,41	2457,73	3017,91	0,35

Table 5.12 Shear checks for columns of MRFs.

Storey	$V_{Ed,G}$ (kNm)	$V_{Ed,E}$ (kNm)	V_{Ed} (kNm)	$V_{pl,Rd}$ (kN)	$\frac{V_{Ed}}{V_{pl,Rd}}$
VI	38,48	25,33	158,95	2654,22	0,06
V	22,74	51,74	268,85	2654,22	0,10
IV	27,17	71,52	367,36	2861,23	0,13
III	24,26	89,94	452,06	2861,23	0,16
II	27,02	92,13	465,20	3068,24	0,15
I	10,13	118,51	573,80	3068,24	0,19

More in detail, on the basis on the values from Table 5.11 and Table 5.12, the seismic demands on the top end of the column at first storey in the external column are computed as follows:

$$M_{Ed} = M_{Ed,G} + \alpha \cdot 1,1 \cdot \gamma_{ov} \cdot \Omega \cdot M_{Ed,E} = \\ = 32,64\text{k Nm} + \left(1,25 \cdot 1,1 \cdot 1,25 \cdot 2,76\right) \cdot 111,57\ \text{kNm} = 563,28\ \text{kN}m \tag{5.40}$$

$$N_{Ed} = N_{Ed,G} + \alpha \cdot 1,1 \cdot \gamma_{\text{ov}} \cdot \Omega \cdot N_{Ed,E} = \\ = 561,11\ \text{kN} + \left(1,25 \cdot 1,1 \cdot 1,25 \cdot 2,76\right) \cdot 396,41\ \text{kN} = 2446,52\ \text{kN} \tag{5.41}$$

$$V_{Ed} = V_{Ed,G} + \alpha \cdot 1,1 \cdot \gamma_{ov} \cdot \Omega \cdot V_{Ed,E} = \\ = 10,13\ \text{kN} + \left(1,25 \cdot 1,1 \cdot 1,25 \cdot 2,76\right) \cdot 118,51\ \text{kN} = 573,80\ \text{kN} \tag{5.42}$$

As it can be observed the seismic effects are magnified by $\alpha \cdot 1,1 \cdot \gamma_{ov} \cdot \Omega \cdot M_{Ed,E} = 1,25 \cdot 1,1 \cdot 1,25 \cdot 2,7 = 4,74$ that considerably increases the design forces.

Notwithstanding so large design forces, it is worth noting that the need to satisfy drift limits required to adopt constant column cross sections along the building height and this explains the so large factors reported in Table 5.11 and Table 5.12.

In addition to the member checks, EN 1998-1 4.4.2.3(4) also requires the local hierarchy criterion at every joint, early described by Eqn. (5.21) in section 5.5.3. Table 5.13 summarizes this check for external and inner joints. In addition, for clarity sake, this check is performed in detail for an internal joint located at the first floor of the examined MRF, as follows:

$$\sum M_{Rc} = 2 \cdot M_{Rc} = 2 \cdot 3741,7\ \text{kNm} = 7483,4\ \text{kNm} \\ \sum M_{Rb} = 2 \cdot M_{Rb} = 2 \cdot 1246,76\ \text{kNm} = 2493,52\ \text{kNm} \\ \frac{\sum M_{Rc}}{\sum M_{Rb}} = 3,0 > 1,3 \tag{5.43}$$

Table 5.13 Local hierarchy criterion for external and inner columns of MRFs.

	External joints			*Inner joints*			
storey	M_{Rc} **(kNm)**	M_{Rb} **(kN)**	$\frac{\sum M_{Rc}}{\sum M_{Rb}}$	M_{Rc} **(kNm)**	$M_{Rb,\ \text{left side}}$ **(kNm)**	$M_{Rb,\ \text{right side}}$ **(kNm)**	$\frac{\sum M_{Rc}}{\sum M_{Rb}}$
VI	2518,37	778,87	3,23	3114,06	778,87	778,87	2,00
V	2518,37	989,39	5,09	3114,06	989,39	989,39	3,15
IV	2816,22	989,39	5,39	3114,06	989,39	989,39	3,15
III	2816,22	1246,76	4,52	3114,06	1246,76	1246,76	2,50
II	3114,06	1246,76	4,76	3741,70	1246,76	1246,76	2,75
I	3114,06	1246,76	5,00	3741,70	1246,76	1246,76	3,00

5.6.7 Damage limitation check for MRFs

The damage limitation requirement is satisfied. Indeed, the interstorey drifts calculated according to Eqn. (5.9) are smaller than 0,75% the interstorey height h. The displacement reduction factor ν was assumed equal to the recommended value that is $\nu = 0,5$ (being the structure calculated in the numerical example belonging to class II). The displacements d_s induced by the seismic actions for this limit state are obtained by means Eqn. (5.10) in accordance to EN 1998-1 4.3.4.

Table 5.14 summarizes this check, showing the lateral storey displacements subjected to the seismic load combination. The maximum interstorey drift ratio is equal to 0,67%, occurring between the second and the third floor.

Table 5.14 Interstorey drift ratios at Damage Limitation State for MRFs.

Storey	h **(mm)**	d_e **(mm)**	$d_s = d_e \times q$ **(mm)**	d_r **(mm)**	$\nu \frac{d_r}{h}$ **(-)**
VI	3500	36,16	235,04	24	0,34%
V	3500	32,48	211,12	34	0,49%
IV	3500	27,2	176,80	43	0,61%
III	3500	20,64	134,16	46	0,65%
II	3500	13,6	88,40	47	0,67%
I	4000	6,4	41,60	42	0,52%

5.7 Design worked example: multi-storey building with concentric braced frame

This section describes a design example for a six storey concentric braced frame according to EN1998-1:2005. As the example on MRF previously described and discussed, a preliminary description of the structural response and design criteria of typical CBFs is provided. Subsequently, the analysis of a specific case study structure and the verification of structural members are shown with some details.

5.7.1 Building description

The building layout is the same adopted in the previous case and described in section 5.6.1. As for MRFs, the lateral force resisting system is placed at the perimeter of the plan of the buildings. The interior frames are assumed to be gravity frames and their lateral load resisting capacity is neglected. Two-dimensional frame models are used for the design, with appropriate selection of the tributary areas for gravity and seismic loads. A conceptual schematic with the typical building plan and the positioning of the lateral load resisting system are presented in Figure 5.18 (where the location of CBFs is indicated by the bold lines), and Figure 5.19.

The design of the structure is carried out using the provisions of EN 1993 and EN 1998-1. The material for all frame elements is S355 steel with an over-strength factor γ_{ov} = 1,25. The chosen member sections are standard metric sections which are commercially available. As required by DCH concept (see Table 5.5), it should be noted that all steel profiles are class 1 according to EN1993 cross section classification.

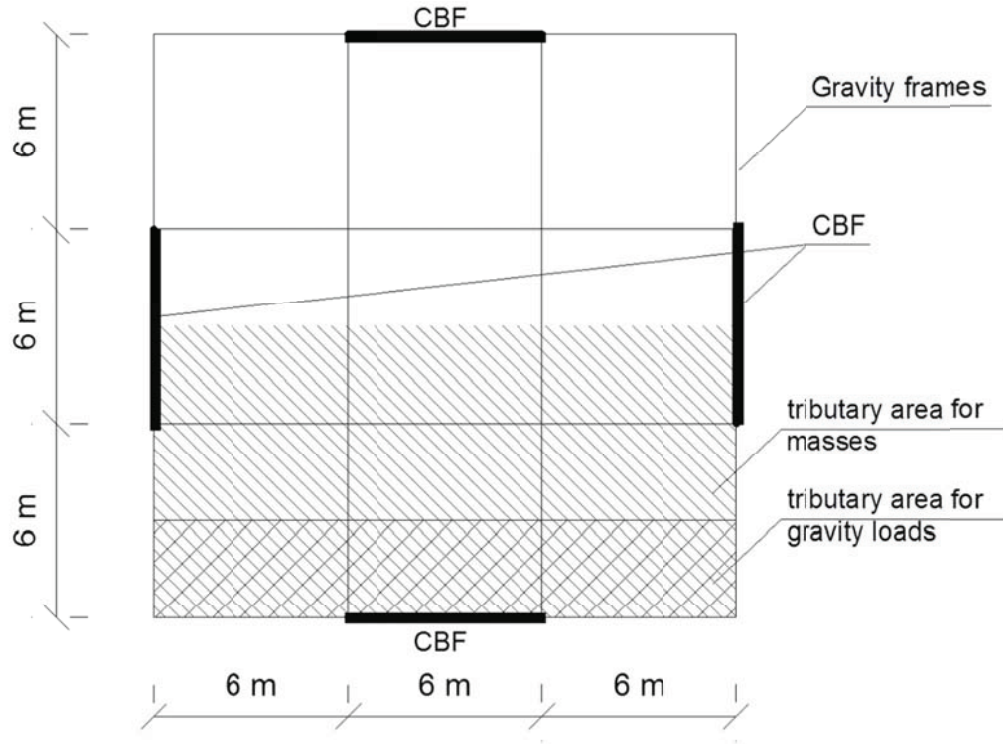

Figure 5.18 Plan and location of CBFs.

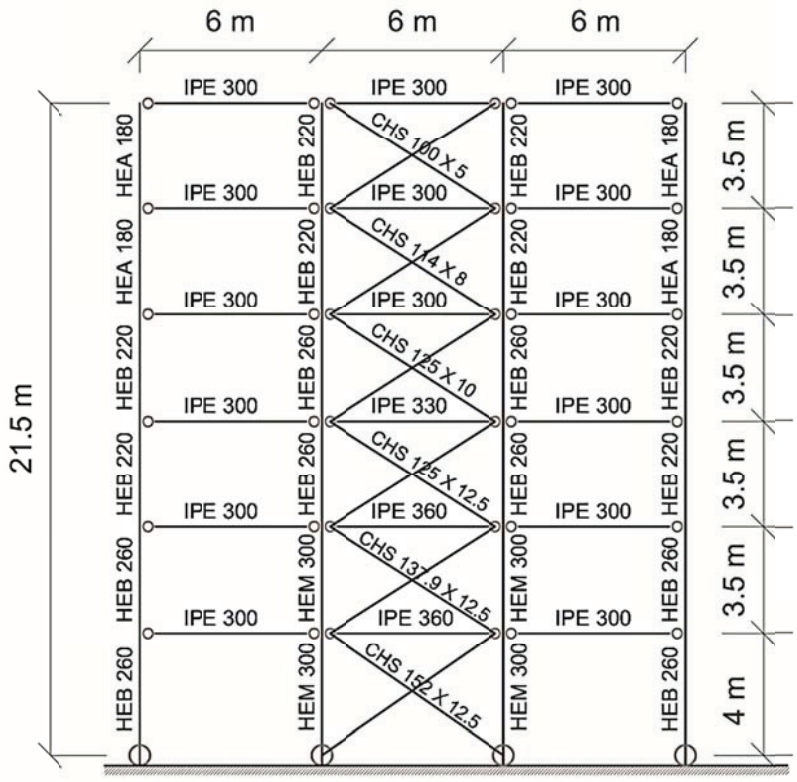

Figure 5.19 Configuration of the designed CBFs.

All floors are made of composite slabs with profiled steel sheetings that should be designed in order to resist the vertical loads and to behave as horizontal rigid diaphragms able to transmit the seismic actions to the seismic resistant frames. Slabs are supported by hot rolled "I-shaped" beams belonging to the CBFs placed along the two main plan directions of the building. The connection between slab and beams is provided by ductile headed shear studs that are welded directly through the metal deck to the beam flange. The beams are assumed as simply pinned at both ends (see Figure 5.19). The bracings are considered pinned at both ends, but rigidly connected together at mid-length. The column-to-foundation connections are pinned.

5.7.2 Design actions

5.7.2.1 Characteristic values of unit loads

The characteristic values of both persistent (G_k) and transient actions (Q_k) are the same considered for the example on MRFs, which are reported in Table 5.6 (see section 5.6.2.1). These vertical actions have been combined according to Eqn. (5.6).

5.7.2.2 Masses

Consistently with the gravity loads, the masses of CBFs are the same of the previous worked example (see Table 5.7). These masses have been combined according to Eqn. (5.7).

5.7.2.3 Seismic action

The elastic acceleration response spectrum used for this example is the same considered for MRF (see section 5.6.2.3). The behaviour factor q considered for this example is equal to 4, consistently with DCH concept (see Table 5.4).

Figure 5.20 shows both the elastic and the design spectra at ultimate limit state.

Regarding the Serviceability Limit State, drift levels at every storey are limited to 0,75% of the storey height (implying ductile non-structural elements connected to the frames).

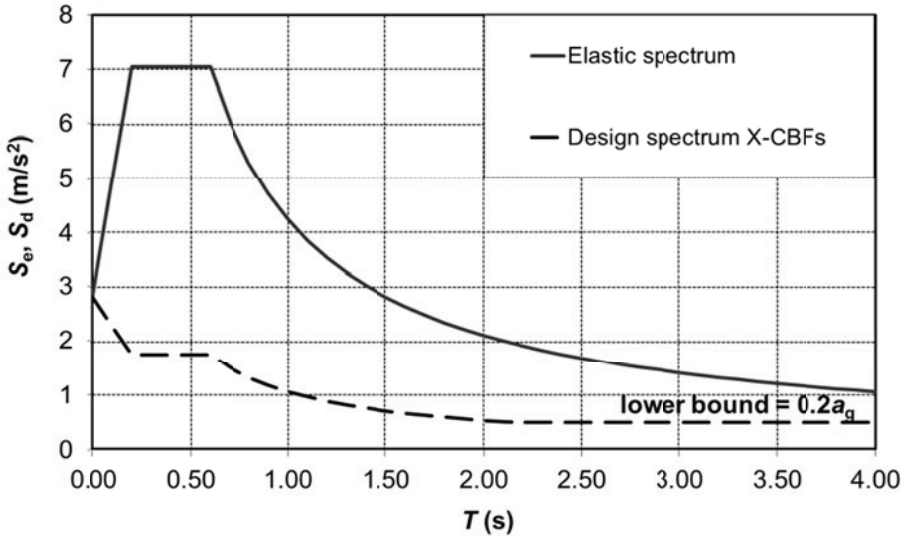

Figure 5.20 Elastic vs. design spectra for CBFs.

5.7.3 Calculation model and structural analysis

2D planar model has been used as in the previous example. However, differently from MRFs, in case of X-CBFs it should be necessary to do two different models for each planar frame, namely one with the braces tilted in one direction and another with the braces tilted in the opposite direction (see Figure 5.10), in order to make tension alternatively developing in all the braces at any storey. In the proposed example, the structure is perfectly symmetric. This implies that the internal forces due to seismic actions and calculated with the bracings tilted in one direction are mirrored as respect to the axis of symmetry in the model with the bracings tilted in the opposite direction, thus allowing using a single model to account for both directions of seismic action.

The general modelling assumptions are the following: i) only the bracing diagonal in tension is modelled; ii) the columns are considered continuous through each floor beam; iii) all connections of the beams and bracings are assumed pinned; iv) masses have been considered as lumped into a selected master joint at each floor, because the floor diaphragms may be taken as rigid in their planes. This assumption implies that numerical model gives axial forces in beams equal to zero. Therefore, axial forces in beams could be obtained by means of hand calculation on the basis of free body force distribution shown in Figure 5.21.

The torsional effects due to accidental eccentricity are accounted for through the δ factor given by Eqn. (5.37), which is used to magnify the seismic forces calculated by the elastic model.

The effects of actions included in the seismic design situation have been determined by means of lateral force method (EN 1998-1 4.3.3.2), using the design spectrum depicted in Figure 5.20. According to EN 1998-1 4.3.3.2.2, the design base shear force can be calculated as $F_b = S_d(T_1) \cdot m \cdot \lambda$, where $S_d(T_1)$ is the ordinate of the design spectrum at period T_1; T_1 is the fundamental period of vibration of the building; m is the total mass of the building above the foundation; λ is the correction factor, the value of which is equal to 0,85 if $T_1 < 2\ T_C$ (being TC the corner period of the spectrum, as shown in Figure 5.2) and the building has more than two storeys.

Since a linear static analysis has been carried out, the fundamental period of vibration period T_1 has been estimated by means of the following equation:

$$T_1 = C_t \cdot H^{3/4} \tag{5.44}$$

where:

- C_t is 0,05;
- H is the height of the building, expressed in meters, from the foundation or from the top of a rigid basement.

The distribution of the horizontal seismic forces has been calculated according to EN 1998-1 4.3.3.2.3(3), as following:

$$F_i = F_b \cdot \frac{z_i \cdot m_i}{\sum z_j \cdot m_j} \tag{5.45}$$

where z_i, z_j are the heights of the masses m_i and m_j above the level of application of the seismic action (foundation or top of a rigid basement).

The diagrams of internal forces (i.e. bending moments, shear and axial forces) for both gravity loads and seismic forces calculated for one model with the bracing tilted in a single direction are reported in Figure 5.22. The bending moment and shear forces due to seismic forces are obtained for columns only due to their flexural continuity. However, as it can be noted their values are negligible as respect to those calculated for gravity loads. This result is consistent with the modelling assumptions and the lattice structural scheme. In addition, as previously explained, the axial forces in the beams are equal to zero because of the internal diaphragm constraint.

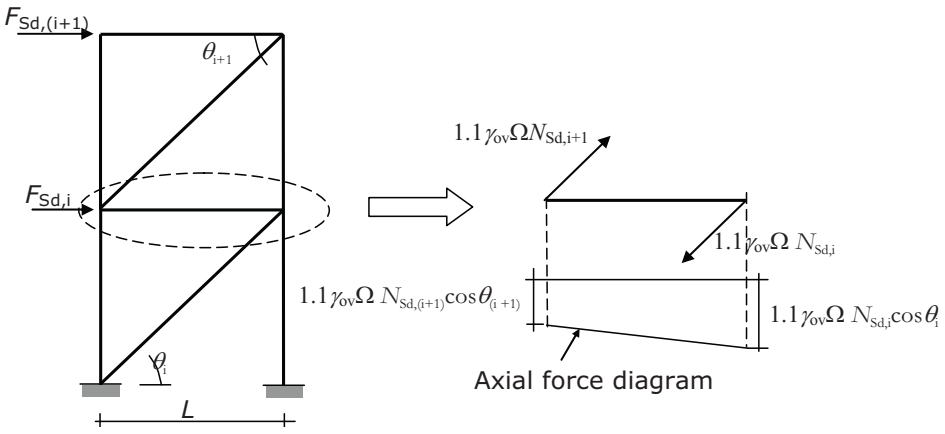

Figure 5.21 Calculation of axial force in the beam of the braced span.

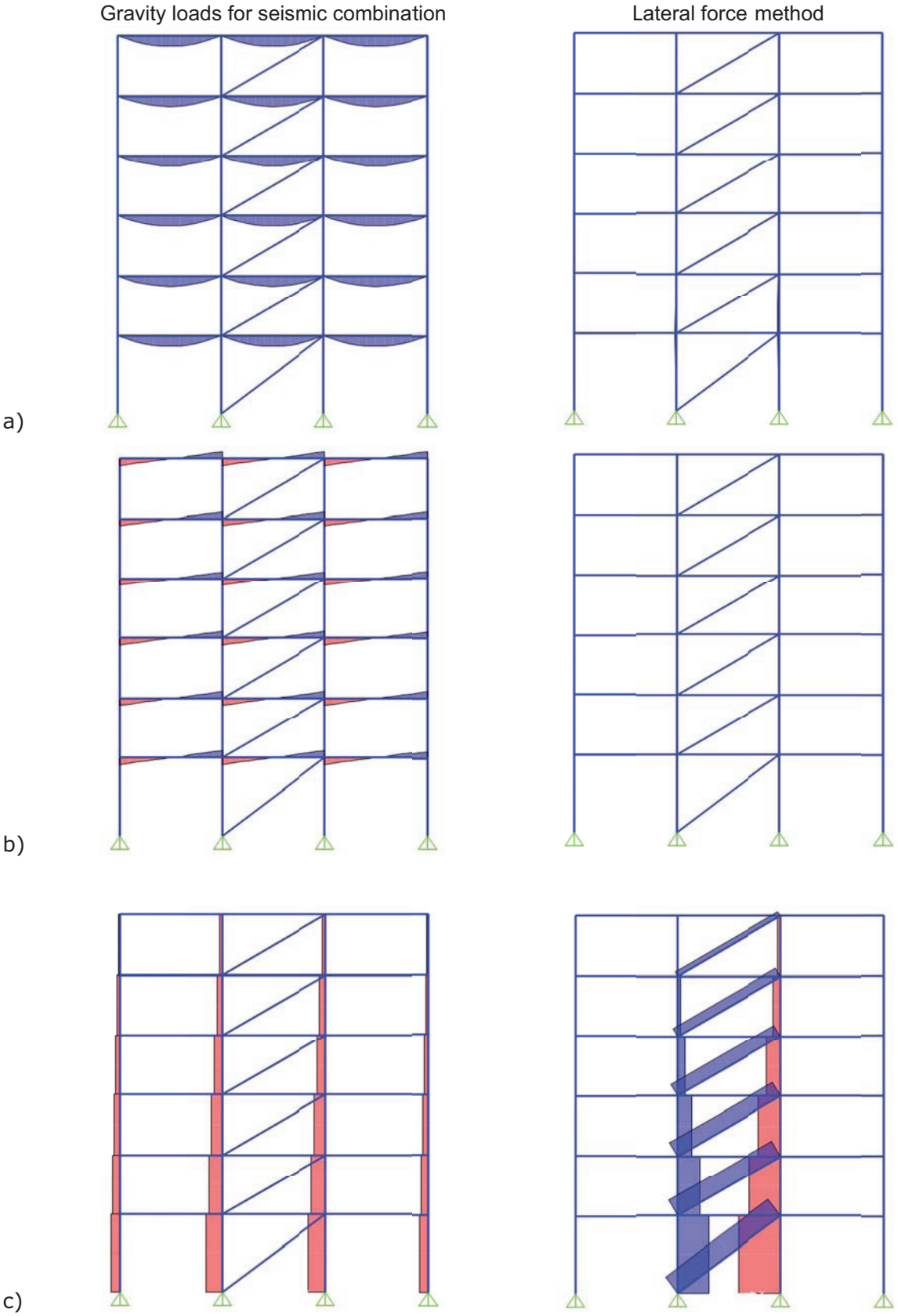

Figure 5.22 Calculated internal forces for CBFs: a) bending moments; b) shear forces); c) axial forces.

5.7.4 Frame stability and second order effects

P-Δ effects were specified through the inter-storey drift sensitivity coefficient θ given by Eqn. (5.4), and summarized in Table 5.15. As it can be observed the coefficient θ is smaller than 0,1. Hence, second order effects can be disregarded.

Table 5.15 Stability coefficients per floor in X-CBFs.

Storey	P_{tot} (kN)	V_{tot} (kN)	h (mm)	d_r (mm)	$\theta = \frac{P_{tot} \cdot d_r}{V_{tot} \cdot h}$ (-)	$\alpha = \frac{1}{(1-\theta)}$ (-)
VI	955,35	242,13	3500	1,76	0,002	1,002
V	2040,32	473,19	3500	1,6	0,002	1,002
IV	3125,29	659,32	3500	1,6	0,002	1,002
III	4210,27	800,53	3500	1,28	0,002	1,002
II	5295,24	896,80	3500	1,28	0,002	1,002
I	6380,21	948,15	4000	1,44	0,002	1,002

5.7.5 Design and verification of diagonal members for X-CBFs

Circular hollow sections and S 355 steel grade are used for bracings. The brace cross sections are class 1, as defined by EN 1993:1-1 5.6 ($d/t \leq 50\varepsilon^2$, where d is the cross section diameter, t the relevant thickness and ε is equal to $\sqrt{235/f_y}$). Table 5.16 summarizes the adopted cross sections and the calculated d/t ratios, showing that the latter are always smaller than the class 1 limiting value ($50\varepsilon^2$).

The circular hollow sections are suitable to satisfy both the slenderness limits ($1,3 < \bar{\lambda} \leq 2,0$) and the requirement of minimizing the variation among the diagonals of the overstrength ratio $\Omega_i = N_{pl,Rd}/N_{Ed}$, which may vary within the range Ω to 1,25Ω (as defined in section 5.5.4). In particular, the second requisite dominates the design choices. The selected brace cross sections, the relevant brace slenderness (λ and $\bar{\lambda}$), axial plastic strength ($N_{pl,Rd}$), axial force due to the seismic load combination (N_{Ed}), the overstrength factors Ω_i and their percentage variation along the building height $\left((\Omega_i - \Omega)/\Omega\right)$ are given in Table 5.17. The minimum overstrength ratio Ω is equal to 1,05 (highlighted in bold in Table 5.17). Hence, according to the capacity design criteria described in section 5.5.4, the seismic elastic forces obtained by the numerical model have to be amplified by $1,1\,\gamma_{ov}\Omega = 1,1x1,25x1,05 = 1,44$.

Table 5.16 X-braces cross section properties.

Storey	Brace cross section d x t (mm x mm)	d (mm)	t (mm)	d/t -	$.50\varepsilon^2$ -
VI	100x5	100	5	20,00	33,10
V	114x8	114	8	14,25	33,10
IV	125x10	125	10	12,50	33,10
III	125x12,5	125	12,5	10,00	33,10
II	139,7x12,5	139,7	12,5	11,18	33,10
I	152x12,5	152	12,5	12,16	33,10

Table 5.17 X-braces design checks.

Storey	Brace cross section d x t	λ	$\bar{\lambda}$	$N_{pl,Rd}$	N_{Ed}	Ω_i	$\left((\Omega_i - \dot{\Omega})/\Omega\right)$
	(mm x mm)	-	-	(kN)	(kN)	-	-
VI	100x5	146,03	1,91	529,75	448,50	1,18	0,12
V	114x8	130,69	1,71	945,75	876,50	1,08	0,03
IV	125x10	120,35	1,58	1282,56	1221,28	**1,05**	0,00
III	125x12,5	122,73	1,61	1568,34	1482,84	1,06	0,01
II	139,7x12,5	108,69	1,42	1773,27	1661,17	1,07	0,02
I	152x12,5	102,97	1,35	1944,74	1823,26	1,07	0,02

5.7.6 Design and verification of beams

All beams have been assumed as restrained against lateral-torsional buckling. Apart from the ultimate limit state verification under vertical loads, which is dealt with in the relevant Chapter about EN 1993:1-1, the axial, bending and shear strengths are checked under the seismic load combination in order to satisfy the requirement given by Eqn. (5.23). With reference to the end section of the beam directly connected to the brace in tension, Table 5.18 reports the beam axial strength checks performed according to EN 1993:1-1 6.2.4 under the seismic load combination calculated as shown in Figure 5.21.

In addition, Table 5.19 reports the beam combined bending-axial strength checks according to EN 1993:1-1 6.2.9, performed at the beam mid-span, where the largest bending moment is acting. In particular, $M_{N,Rd}$ is the plastic moment resistance reduced due to the beam axial force N_{Ed}.

Table 5.18 Axial strength checks at the beam end section of X-CBFs.

Storey	Beam section	N_{Rd}	$N_{Ed,G}$	$N_{Ed,E}$	$N_{Ed} = N_{Ed,G} + 1,1\gamma_{ov}\Omega N_{Ed,E}$	N_{Rd}/N_{Ed}
	-	(kN)	(kN)	(kN)	(kN)	-
VI	IPE 300	1910,26	0	387,86	448,05	4,26
V	IPE 300	1910,26	0	755,00	872,17	2,53
IV	IPE 300	1910,26	0	1052,14	1215,42	1,82
III	IPE 300	1910,26	0	1277,72	1476,00	1,50
II	IPE 300	1910,26	0	1422,07	1642,76	1,34
I	IPE 360	2580,85	0	1594,27	1841,69	1,62

Table 5.19 Combined bending-axial strength checks at mid-length of beams in X-CBFs.

Storey	Beam section	$N_{Ed,G}$	$N_{Ed,E}$	$N_{Ed} = N_{Ed,G}+1,1\gamma_{ov}\Omega N_{Ed,E}$	$M_{Ed,G}$	$M_{Ed,E}$	$M_{Ed} = M_{Ed,G}+1,1\gamma_{ov}\Omega M_{Ed,E}$	$M_{N,Rd}/M_{Ed}$
	-	(kN)	(kN)	(kN)	(kNm)	(kNm)	(kNm)	-
VI	IPE 300	0	193,93	224,02	106,20	0	106,20	2,10
V	IPE 300	0	571,43	660,11	120,60	0	120,60	1,52
IV	IPE 300	0	903,57	1043,79	120,60	0	120,60	1,05
III	IPE 300	0	1164,93	1345,71	120,60	0	120,60	1,49
II	IPE 300	0	1349,89	1559,38	120,60	0	120,60	1,49
I	IPE 360	0	1482,05	1712,05	120,60	0	120,60	1,27

Table 5.20 summarizes the shear strength verifications for the same beams, where it can be noted that the shear force due to seismic action $V_{Ed,E}$ is equal to zero due to the truss behaviour of the braced structure. As it can be observed this check is fully satisfied for all beams.

Table 5.20 Shear checks for beams of X-CBFs.

Storey	$V_{pl,Rd}$ (kN)	$V_{Ed,G}$ (kN)	$V_{Ed,E}$ (kN)	V_{Ed} (kN)	$\frac{V_{Ed}}{V_{pl,Rd}}$
VI	526,33	34,54	0	34,54	15,24
V	526,33	47,50	0	47,50	11,08
IV	526,33	47,50	0	47,50	11,08
III	631,53	47,50	0	47,50	13,29
II	720,19	47,50	0	47,50	15,16
I	720,19	47,50	0	47,50	15,16

5.7.7 Design and verification of columns of X-CBFs

The columns were verified on the basis of criteria described in section 5.5.4. The global hierarchy criterion was applied according to Eqn. (5.23). To this end, the seismic elastic forces obtained by the numerical model have to be amplified by $1,1\gamma_{ov}\Omega=1,44$.

As shown in Figure 5.22 the bending and shear forces due to both gravity and seismic actions are negligible. Therefore, the strength check is shown for axial forces only.

Table 5.21 summarizes the strength verifications for columns at right of the braced bay (see Figure 5.22), which have been carried out according to EN 1993:1-1 6.3.3(4).

Table 5.21 Axial checks for columns of X-CBFs.

Storey	Column section	$N_{Ed,G}$ (kN)	$N_{Ed,E}$ (kN)	N_{Ed} (kN)	$N_{pl,Rd}$ (kN)	$N_{b,Rd}$ (kN)	$\frac{N_{b,rd}}{N_{Ed}}$
VI	HE 220 B	160,80	226,67	413,87	3230,50	2098,85	5,07
V	HE 220 B	321,45	666,74	1065,83	3230,50	2098,85	1,97
IV	HE 260 B	482,42	1280,11	1911,61	4203,20	3055,13	1,60
III	HE 260 B	642,81	2025,23	2903,89	4203,20	3055,13	1,05
II	HE 300 M	804,84	2854,42	3991,67	10760,05	8622,55	2,16
I	HE 300 M	964,06	4004,94	5435,40	10760,05	8097,03	1,49

5.7.8 Damage limitation check for X-CBFs

The damage limitation requirement is satisfied. Indeed, the interstorey drifts (calculated according to Eqn. (5.9) are smaller than 0,75% the interstorey height h. The displacement reduction factor ν was assumed equal to the recommended value that is $\nu = 0{,}5$ (being the structure calculated in the numerical example belonging to class II). The displacements d_s induced by the seismic actions for this limit state are obtained by means Eqn. (5.10) in accordance to EN 1998-1 4.3.4.

Table 5.22 summarizes this check, showing the lateral storey displacements subjected to the seismic load combination. The maximum interstorey drift ratio is equal to 0,1%, occurring between the fifth and the sixth floor. As it can be noted by comparing the results in Table 5.22 with those reported in Table 5.14, CBFs are significantly stiffer than MRFs.

Table 5.22 Interstorey drift ratios at Damage Limitation State for X-CBFs.

Storey	h (mm)	d_e (mm)	$d_s = d_e \times q$ (mm)	d_r (mm)	$\nu \frac{d_r}{h}$ (-)
VI	3500	8,96	35,84	7,04	0.1%
V	3500	7,2	28,8	6,4	0.09%
IV	3500	5,6	22,4	6,4	0.09%
III	3500	4	16	5,12	0.07%
II	3500	2,72	10,88	5,12	0.07%
I	4000	1,44	5,76	5,76	0.07%

References

D'Aniello, M., Güneyisi, E.M., Landolfo, R., and Mermerdaş, K. 2013. Analytical prediction of available rotation capacity of cold-formed rectangular and square hollow section beams. Thin-Walled Structures. 10.1016/j.tws.2013.09.015.

D'Aniello, M., Landolfo, R., Piluso, V., Rizzano, G. 2012. Ultimate Behaviour of Steel Beams under Non-Uniform Bending. Journal of Constructional Steel Research 78: 144–158.

Elghazouli, A.Y. 2010. Assessment of European seismic design procedures for steel framed structures, Bulletin of Earthquake Engineering, 8:65-89.

EN 1990: 2002. Eurocode: Basis of structural design. CEN.

EN 1993-1-1: 2005. Eurocode 3: Design of Steel Structures – Part 1-1: general rules and rules for buildings. CEN.

EN 1998-1: 2005. Eurocode 8: Design of structures for earthquake resistance. Part 1: General rules, seismic actions and rules for buildings. CEN.

Gioncu, V. 2000. Framed structures, Ductility and seismic response: General Report, Journal of Constructional Steel Research, 55: 125–154.

Gioncu, V., Mazzolani, F.M. 1995. Alternative methods for assessing local ductility, In: Mazzolani FM, Gioncu V, editors. Behaviour of steel structures in seismic areas, STESSA'94. London: E&FN Spon, p. 182–90.

Gioncu, V., Mazzolani, F.M. 2002. Ductility of seismic resistant steel structures, London, Spon Press.

Güneyisi, E.M., D'Aniello, M., Landolfo, R., Mermerdaş, K. 2013. A novel formulation of the flexural overstrength factor for steel beams. Journal of Constructional Steel Research 90: 60-71.

Güneyisi, E.M., D'Aniello, M., Landolfo, R., Mermerdaş, K. 2014. Prediction of the flexural overstrength factor for steel beams using artificial neural network. Steel and Composite Structures, An International Journal, 17(3): 215-236.

Landolfo, R. 2013. Assessment of EC8 provisions for seismic design of steel structures. Technical Committee 13—Seismic Design, No 131/2013. ECCS—European Convention for Constructional Steelwork.

Mazzolani, F.M., Piluso, V. 1992. Member behavioural classes of steel beams and beam-columns, In: Proc. of First State of the Art Workshop, COSTI, Strasbourg. p. 517–29.

Mazzolani, F.M., Piluso, V. 1996. Theory and Design of Seismic Resistant Steel Frames, E & FN Spon, an imprint of Chapman & Hall, London.

Plumier, A. 2000. General report on local ductility, Journal of Constructional Steel Research, No. 55: 91–107.

CHAPTER 6

RESISTANCE OF MEMBERS AND CONNECTIONS TO FIRE

Paulo Vila Real

University of Aveiro, Portugal

6 Resistance of members and connections to fire

6.1 Introduction

This chapter deals with the basic principles of fire design of steel members and connections as they are defined in Part 1-2 of Eurocode 1 (actions on structures exposed to fire) and in Part 1-2 of Eurocode 3 (structural fire design). The focus will be on the fire resistance of individual members.

According the Eurocode 1 there are several ways to define the temperature to be considered for fire design, from nominal temperature-time curves to the natural fire models. An example of a nominal temperature-time curve is the standard fire curve ISO 834 defined by Eqn. (6.1) and represented in Figure 6.1.

$$\theta_g = 20 + 345\log_{10}(8t + 1) \tag{6.1}$$

where θ_g is the gas temperature in ºC and t is the time in minutes.

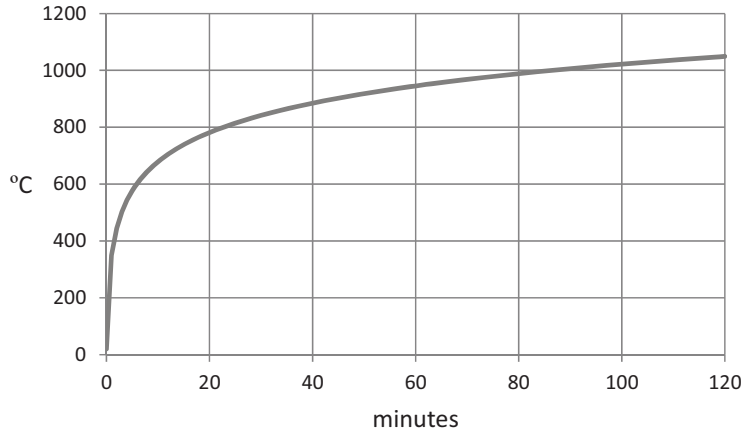

Figure 6.1 Standard fire curve

For the standard fire exposure, members shall comply with criteria R, E and I as follows (see Figure 6.2):

- separating only: integrity (criterion E) and, when requested, insulation (criterion I);
- load bearing only: mechanical resistance (criterion R);
- separating and load bearing: criteria R, E and, when requested, I.

Criterion R is assumed to be satisfied if the load bearing function is maintained during the required time of fire exposure. This criterion is defined in the national regulations for fire safety of buildings as a function of the type of building, the occupancy and its height, among other risk factors and should be identified by the letter R followed by a number representing the required fire resistance period, $t_{fi,requ}$. For example, R60 means that this criterion is assumed to be satisfied where the load bearing function is maintained for 60 minutes of standard fire exposure ($t_{fi,requ}$ = 60 minutes in this case).

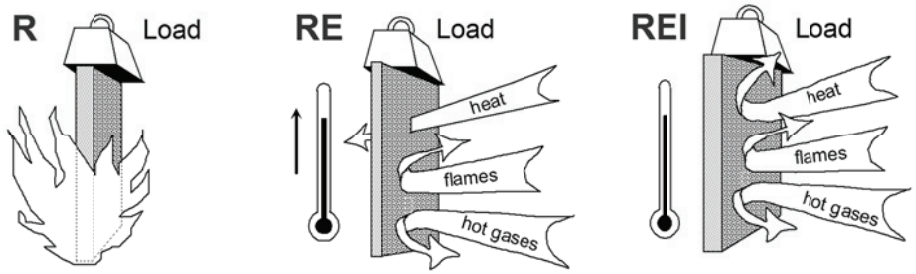

Figure 6.2 Fire resistance criteria

Eurocode 3 states that *for verifying standard fire resistance requirements, a member analysis is sufficient.* However, a member analysis can also be made for structures subject to other types of fires, such as natural fires. For the case of parametric fire exposure (a simple model to represent natural fires) it is stated that *the load-bearing function is ensured if collapse is prevented during the complete duration of the fire including the decay phase or during a required period of time*.

According to EN 1991-1-2, the mechanical analysis shall be performed for the same duration as used in the temperature analysis and the verification of fire resistance shall be made in one of the following three domains:

1. In the time domain (see 1 in Figure 6.3)

$$t_{fi,d} \geq t_{fi,requ} \tag{6.2}$$

2. In the strength domain (see 2 in Figure 6.3)

$$E_{fi,d,t} \leq R_{fi,d,t} \quad \text{at time} \quad t_{fi,requ} \tag{6.3}$$

3. In the temperature domain (see 3 Figure 6.3)

$$\theta_d \leq \theta_{cr,d} \quad \text{at time} \quad t_{fi,requ} \tag{6.4}$$

where:

$t_{fi,d}$ is the design value of the fire resistance, i.e., the failure time;

$t_{fi,requ}$ is the required fire resistance time;

$E_{fi,d,t}$ is the design value of the relevant effects of actions in the fire situation at time t, which is normally considered constant during the fire, $E_{fi,d}$;

$R_{fi,d,t}$ is the design value of the resistance of the member in the fire situation at time t;

θ_d is the design value of steel temperature;

$\theta_{cr,d}$ is the design value of the critical temperature, i.e., the collapse temperature of the structural steel member.

In Figure 6.3 (Franssen and Vila Real, 2010) these three possible domains are represented for the case of a steel member subjected to a nominal fire. This figure shows the temperature of the structural steel member, θ_d, assuming a uniform temperature throughout the cross section, the design value of the effect of actions in the fire situation, $E_{fi,d}$, which is considered as constant, the progressive loss of strength, $R_{fi,d,t}$ and the critical temperature of the member, $\theta_{cr,d}$.

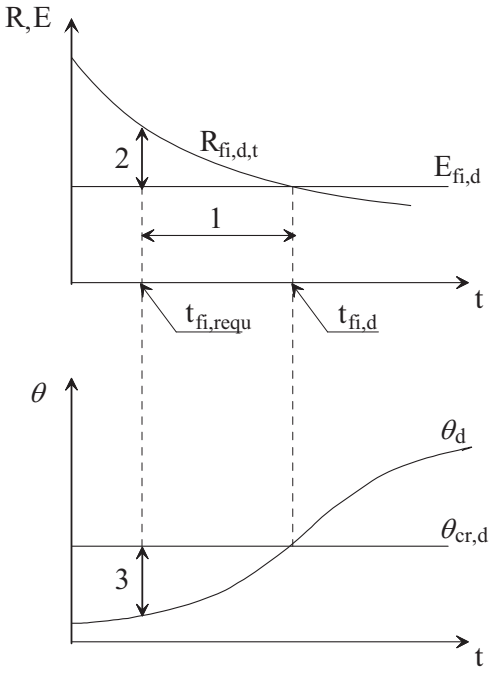

Figure 6.3 Time (1), load (2), and temperature (3) domains for a nominal fire

Three different assessment models can be used to determine the fire resistance of a structure or a single element. Each of these models is described below and increase in complexity:

- *Tabulated data* obtained from tests in standard furnaces, empirical methods or numerical calculations. Tabulated data are widely used for concrete and composite steel and concrete structures in Eurocodes 2 and 4, respectively. However, no tabulated data are presented in Eurocode 3;
- *Simple calculation models* making use of simple analytical formulae for isolated members. This approach is presented in Section 6.4.3;
- *Advanced calculation models*, which can be used in the following ways:
  a) global structural analysis. When a global structural analysis for the fire situation is carried out, the relevant failure mode, the temperature-dependent material properties and member stiffness, the effects of thermal expansions and deformations (indirect fire actions) shall be taken into account;
  b) analysis of part of the structure, for example a portal frame or any other substructure. The boundary conditions at supports and at the ends of members may be assumed to remain unchanged throughout the fire exposure;

c) member analysis, for example beams or columns, where only the effects of thermal deformations resulting from thermal gradients across the cross section need to be considered. The effects of axial or in-plane thermal expansions may be neglected. The boundary conditions at supports and at the ends of member may be assumed to remain unchanged throughout the fire exposure.

Tabulated data and simple calculation models normally apply only to member analyses. Figure 6.4 shows a member that has been extracted from a 2D frame to be checked for fire resistance using member analysis.

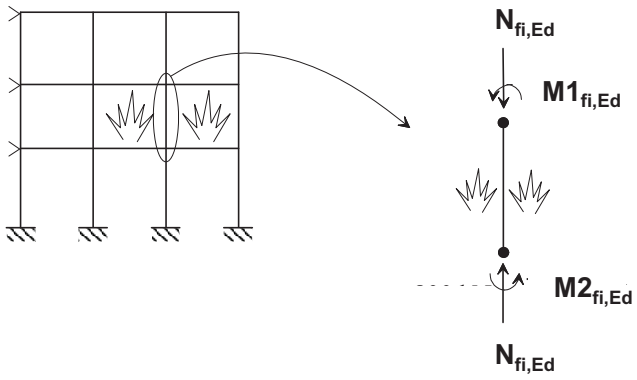

c) Figure 6.4 A member extracted from the 2D frame

6.2 Thermal and mechanical actions

6.2.1 Thermal actions

Thermal actions are defined in Part 1-2 of Eurocode 1 in terms of a net heat flux to the surface of the member, $\dot{h}_{net,d}$ (W/m^2). On the fire exposed surfaces the net heat flux $\dot{h}_{net,d}$ should be determined by considering heat transfer by convection ($\dot{h}_{net,c}$) and radiation ($\dot{h}_{net,r}$) as:

$$\dot{h}_{net,d} = \dot{h}_{net,c} + \dot{h}_{net,r} \quad \left(\mathrm{W/m^2}\right) \tag{6.5}$$

where:

$$\dot{h}_{net,c} = \alpha_c \left(\theta_g - \theta_m\right) \quad \left(\mathrm{W/m^2}\right) \tag{6.6}$$

and

$$\dot{h}_{net,r} = \Phi \cdot \varepsilon_m \cdot \varepsilon_f \cdot \sigma \cdot [(\theta_r + 273)^4 - (\theta_m + 273)^4] \quad \left(\mathrm{W/m^2}\right) \tag{6.7}$$

α_c is the coefficient of heat transfer by convection defined in EN 1991-1-2 (W/m^{2}K);

θ_g is the gas temperature in the vicinity of the fire exposed member (°C);

θ_g is the surface temperature of the member (°C);

σ is the Stephan Boltzmann constant (= 5,67 x 10^{-8} (W/m^2K^4));

Φ is the configuration factor, which should be taken as Φ = 1,0;

ε_m is the surface emissivity of the member, which should take the value 0,7 for carbon steel and 0,4 for stainless steel (EN 1993-1-2);

ε_f is the emissivity of the fire, taken in general as $\varepsilon_m = 1,0$;

θ_r is the effective radiation temperature of the fire environment (°C), in general $\theta_r = \theta_g$.

The use of the nominal temperature-time curves or, as an alternative, the use of the natural fire models to define θ_g, is a choice of the designer in accordance with the authorities and may be specified in the national annex of EN 1991-1-2.

6.2.2 Mechanical actions

According to EN 1991-1-2, for obtaining the relevant effects of actions $E_{fi,d,t}$ during fire exposure, the mechanical actions shall be combined in accordance with EN 1990 "Basis of structural design" for accidental design situations as given in Eqn. (6.8).

$$\sum_{j\geq 1} G_{k,j} + \left(\psi_{1,1} \text{ or } \psi_{2,1}\right) Q_{k,1} + \sum_{i>1} \psi_{2,i} \cdot Q_{k,i} + A_d \tag{6.8}$$

The representative value of the variable action Q_1 may be considered as the quasi-permanent value $\psi_{2,1}$ Q_1, or as an alternative the frequent value $\psi_{1,1}$ Q_1. The use of one or another may be specified in the national annex. EN 1991-1-2 recommends the use of $\psi_{2,1}$ Q_1, but some countries have adopted $\psi_{1,1}$ Q_1 to avoid the absence of horizontal forces due to the wind ($\psi_{2,1}$ = 0, when the wind is the leading action, according to Annex A1 of the EN 1990), leading to the danger situation of having unprotected bracing systems as shown in Figure 6.5, where *G* is the permanent load, *Q* is the live load and *W* is the wind. Recommended values of ψ factors for buildings can be found in the Annex A1 of EN 1990. In Eqn. (6.8) A_d should represent the design value of the indirect thermal action due to fire, like for example, the ones due to restraining thermal elongation.

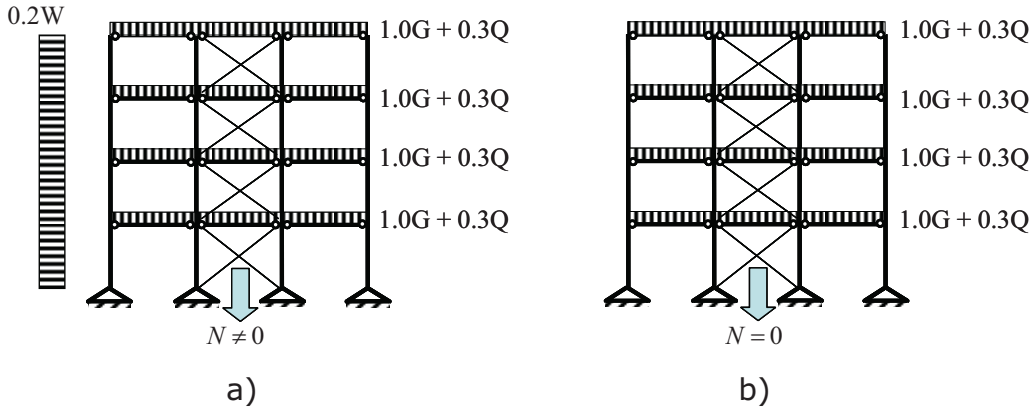

Figure 6.5 Load combinations for fire design. a) When $\psi_{1,1}$ Q_1 is adopted; b) When $\psi_{2,1}$ Q_1 is adopted

It worth be mentioned that for a member analysis, when verifying standard fire resistance requirements, A_d = 0 may be considered. In fact according to EN 1993-1-2, only the effects of thermal deformations resulting from thermal gradients across the cross-section need to be considered. The effects of axial or in-plain thermal expansions may be neglected.

Very often the designer that checks for the fire resistance of a structure is not the same that have made the design at normal temperature. To avoid the need of calculating the structure for the accidental load combinations in fire situation, EN 1993-1-2 allows to obtain the effect of actions in the fire situation $E_{d,fi}$ for each load combination, multiplying the effect obtained from a structural analysis for normal temperature design by a reduction factor η_{fi} as follow:

$$E_{d,fi} = \eta_{fi} E_d \tag{6.9}$$

where:

E_d is the design value of the corresponding force or moment for normal temperature design, for a fundamental combination of actions (see EN 1990);

η_{fi} is the reduction factor for the design load level for the fire situation.

The reduction factor η_{fi} for load combination, Eqn. (6.10), in EN 1990 should be taken as:

$$\eta_{fi} = \frac{G_k + \psi_{fi} Q_{k,1}}{\gamma_G G_k + \gamma_{Q,1} Q_{k,1}} \tag{6.10}$$

According to EN 1993-1-2, as a simplification the recommended value of η_{fi} = 0,65 may be used, except for imposed load according to load category *E* as given in EN 1991-1-1 (areas susceptible to accumulation of goods, including access areas) where the recommended value is 0,7.

6.3 Thermal and mechanical properties of steel

6.3.1 Thermal properties of steel

To evaluate the thermal response of steel members, the thermal properties should be known. The main properties that are needed are defined in Part 1-2 of Eurocode 3. In this section only the graphical representation of thermal conductivity and specific heat are shown, respectively in Figure 6.6.

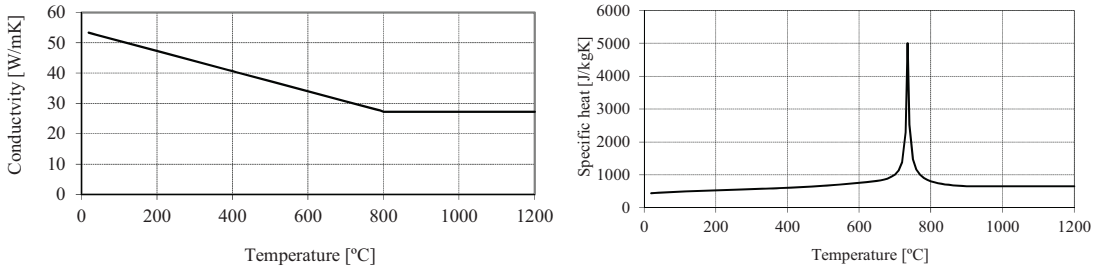

Figure 6.6 Conductivity and specific heat of steel

6.3.2 Mechanical properties of steel

The design values for the mechanical (strength and deformation) properties in the fire situation $X_{d,fi}$ are defined in Eurocode 3, as follows:

$$X_{d,fi} = k_\theta X_k / \gamma_{M,fi} \tag{6.11}$$

where:

X_k is the characteristic value of a strength or deformation property (generally f_{yk} or E_k) for normal temperature design to EN 1993-1-1;

k_θ is the reduction factor for a strength or deformation property ($X_{k,\theta} / X_k$), dependent on the material temperature;

$\gamma_{M,fi}$ is the partial safety factor for the relevant material property, for the fire situation, taken as $\gamma_{M,fi}$ = 1,0 (see Table 6.1), or other value defined in the National Annex.

Table 6.1 Partial factors γ_{Mi} for the resistance

Type of verification	Normal temperature	Fire situation
Resistance of cross-sections	γ_{M0} = 1,0	$\gamma_{M,fi}$ = 1,0
Resistance of members to instability	γ_{M1} = 1,0	$\gamma_{M,fi}$ = 1,0
Resistance of cross-sections in tension to fracture	γ_{M2} = 1,25	γ_{Mfi} = 1,0
resistance of joints	γ_{M2} = 1,25	$\gamma_{M,fi}$ = 1,0

In an accidental limit state such as fire, higher strains are acceptable. For this reason Eurocode 3 recommends a yield strength corresponding to 2% total strain rather than the conventional 0,2% proof strain (see Figure 6.7). However, for members with Class 4 cross sections, EN 1993-1-2 recommends, in its Annex E, a design yield strength based on the 0,2% proof strain.

The stress-strain relationship at elevated temperature shown in Figure 6.7 is characterised by the following three parameters:

- the limit of proportionality, $f_{p,\theta}$:
- the effective yield strength, $f_{y,\theta}$
- the Young's modulus, $E_{a,\theta}$

At elevated temperature, the shape of the stress-strain diagram is modified compared to the shape at room temperature. Instead of a linear-perfectly plastic behaviour as for normal temperature, the model recommended by EN 1993-1-2 at elevated temperature is an elastic-elliptic-perfectly plastic model, followed by a linear descending branch introduced at large strains when the steel is used as material in advanced calculation models to avoid numerical problems. Detailed aspects from this behaviour can be seen in Figure 6.7.

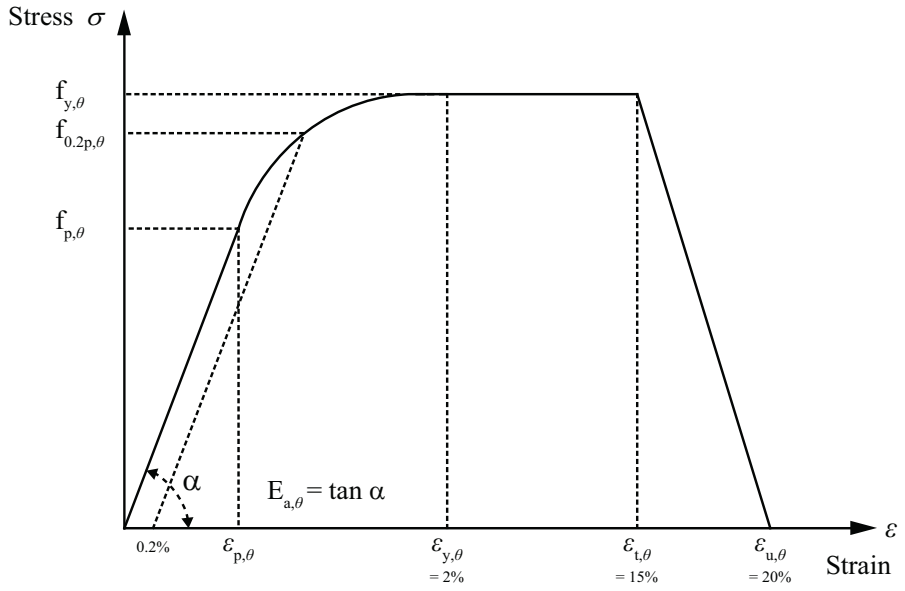

Figure 6.7 Stress-strain relationship for carbon steel at elevated temperatures

Strength and stiffness of steel decrease when the temperature increases. Beyond 400°C strength start to decrease and from 100ºC, steel begins to lose stiffness. For S355 structural steel, Figure 6.8 shows the stress-strain relationships at elevated temperatures.

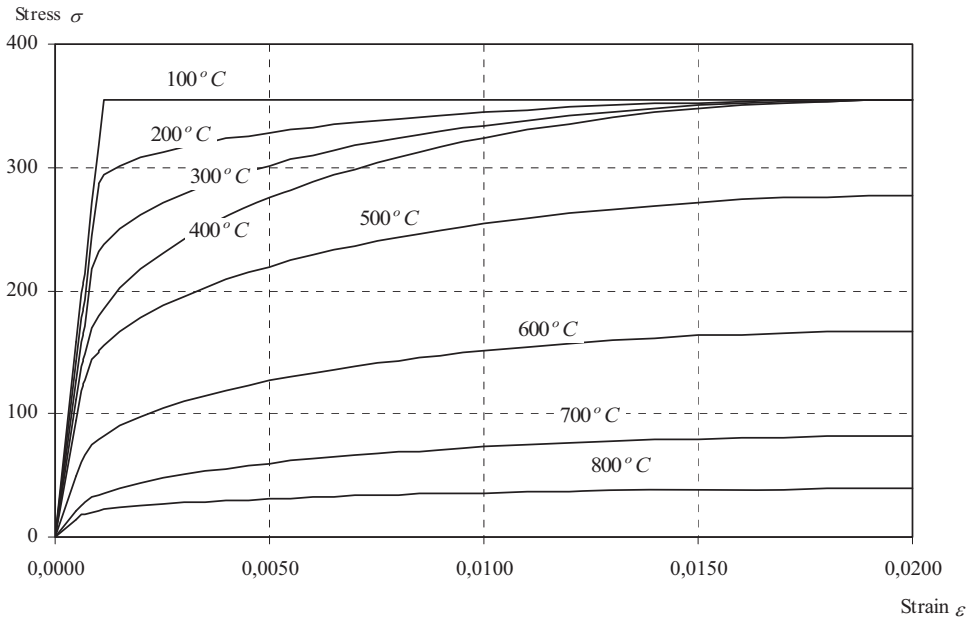

Figure 6.8 Stress-strain relationship for carbon steel S355 at elevated temperatures

More details on the stress-strain relationship for steel grades S235, S275, S355 and S460 are given in Annex C of the ECCS Design Manual, Franssen and Vila Real, 2010.

Following Eqn. (6.11) the yield strength at temperature θ, i.e., $f_{y,\theta}$, is a function of the yield strength, f_y, at 20 ºC, given by:

$$f_{y,\theta} = k_{y,\theta} f_y \tag{6.12}$$

The Young's modulus at temperature θ, i.e., $E_{a,\theta}$, is a function of the Young's modulus, E_a, at 20 ºC, given by:

$$E_{a,\theta} = k_{E,\theta} E_a \tag{6.13}$$

In the same way the proportional limit at elevated temperature is given by:

$$f_{p,\theta} = k_{p,\theta} f_y \tag{6.14}$$

As mention before, according to Annex E of EN 1993-1-2 for members with Class 4 cross-section under fire conditions, the design yield strength of steel should be taken as the 0,2% proof strain and thus for this class of cross-section the yield strength at temperature θ, i.e., $f_{y,\theta}$, is a function of the yield strength, f_y, at 20 ºC given by:

$$f_{y,\theta} = f_{0,2p,\theta} = k_{0,2p,\theta} f_y \tag{6.15}$$

Table 6.2 presents the reduction factors for the stress-strain relationship of carbon steel at elevated temperatures. In this table the reduction factor (relative to f_y) for the design strength of hot-rolled and welded thin-walled sections (Class 4), given in Annex E of EN 1993-1-2, is also presented. This table shows that carbon steel begins to lose strength above 400ºC. For example, at 700 ºC it has 23 % of its strength at normal temperature and at 800ºC it retains only 11% of that strength, and its strength reduces to 6% at 900ºC. Concerning the Young's modulus it begins to decrease earlier at 100ºC.

The reduction of the effective yield strength given by Table 6.2, which was obtained experimentally, can be approximated by the following equation:

$$k_{y,\theta} = \left\{ 0,9674 \left(e^{\frac{\theta_a - 482}{39,19}} + 1 \right) \right\}^{-1/3,833} \leq 1 \tag{6.16}$$

When inverted, this equation yields an equation that gives the temperature of the steel function of the reduction of the effective yield strength, i. e., $\theta_a = f\left(k_{y,\theta}\right)$, see Eqn. (6.34) in Section 6.5.3. This equation is used by the Eurocode to obtain the critical temperature.

The unit mass of steel ρ_a may be considered to be independent of the steel temperature.

Table 6.2 Reduction factors for carbon steel for the design at elevated temperatures

Steel Temperature θ_a	Reduction factors at temperature θ_a relative to the value of f_y or E_a at 20°C			
	Reduction factor (relative to f_y) for effective yield strength $k_{y,\theta}=f_{y,\theta}/f_y$	Reduction factor (relative to f_y) for proportional limit $k_{p,\theta}=f_{p,\theta}/f_y$	Reduction factor (relative to E_a) for the slope of the linear elastic range $k_{E,\theta}=E_{a,\theta}/E_a$	Reduction factor (relative to f_y) for the design strength of hot rolled and welded thin walled sections (Class 4) $k_{0,2p,\theta}=f_{0,2p,\theta}/f_y$
20 ºC	1,000	1,000	1,000	1,000
100 ºC	1,000	1,000	1,000	1,000
200 ºC	1,000	0,807	0,900	0,890
300 ºC	1,000	0,613	0,800	0,780
400 ºC	1,000	0,420	0,700	0,650
500 ºC	0,780	0,360	0,600	0,530
600 ºC	0,470	0,180	0,310	0,300
700 ºC	0,230	0,075	0,130	0,130
800 ºC	0,110	0,050	0,090	0,070
900 ºC	0,060	0,0375	0,0675	0,050
1000 ºC	0,040	0,0250	0,0450	0,030
1100 ºC	0,020	0,0125	0,0225	0,020
1200 ºC	0,000	0,0000	0,0000	0,000

NOTE: For intermediate values of the steel temperature, linear interpolation may be used.

6.4 Temperature in steel members

6.4.1 Unprotected steel members

For an equivalent uniform temperature distribution in the cross-section, the increase of temperature $\Delta\theta_{a,t}$ in an unprotected steel member during a time interval Δt is given by (EN 1993-1-2):

$$\Delta\theta_{a,t} = k_{sh}\frac{A_m/V}{c_a\rho_a}\dot{h}_{net,d}\Delta t \qquad (ºC) \tag{6.17}$$

where:

k_{sh} is the correction factor for the shadow effect;

A_m / V is the section factor for unprotected steel members, (≥ 10) (m^{-1});

A_m is the surface area of the member per unit length, (m^2/m);

V is the volume of the member per unit length, (m^3/m);

c_a is the specific heat of steel, (J/kgK);

$\dot{h}_{net,d}$ is the design value of the net heat flux per unit area according to Eqn. (6.5);

ρ_a is the unit mass of steel, 7850 (kg/m^3);

Δt is the time interval (s) (≤ 5 s).

Detailed definition of some of the previous symbols can be found in Franssen and Vila Real (2010).

Eqn. (6.17) is an incremental equation but it is non-linear due to the temperature dependence of the specific heat and the net heat flux. An iterative procedure should be implemented to obtain the steel temperature development or a very small time interval. Solving this equation, tables giving the temperature function of the time or nomograms can be built like the one shown in Figure 6.9, taken from Franssen and Vila Real (2010).

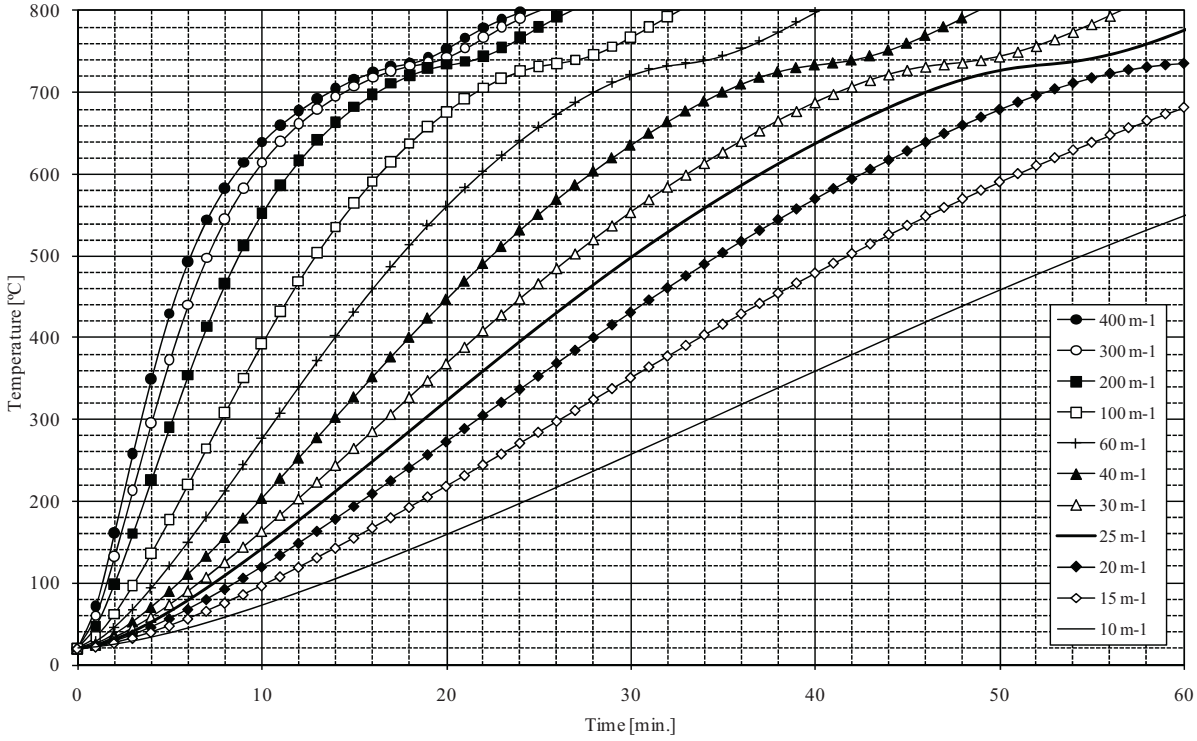

Figure 6.9 Nomogram for unprotected steel members subjected to the ISO 834 fire curve, for different values of $k_{sh}\, A_m/V$ (m^{-1})

6.4.2 Protected steel members

It is common practice to use thermal insulation to protect the steel to fulfil the required fire resistance. There are many forms of passive fire protection systems available to

control the rate of temperature rise in steel members exposed to fire. The insulation materials can be applied as contour encasement or hollow encasement. Basically there are three types of insulating materials: sprays, boards or intumescent paint.

EN 1993-1-2 provides a simple design method to evaluate the temperature development of steel members insulated with fire protection materials. Assuming uniform temperature distribution, the temperature increase $\Delta\theta_{a,t}$ of an insulated steel member during a time interval Δt, is given by:

$$\Delta\theta_{a,t} = \frac{\lambda_p A_p / V}{d_p c_a \rho_a} \frac{\left(\theta_{g,t} - \theta_{a,t}\right)}{\left(1 + \phi / 3\right)} \Delta t - \left(e^{\phi/10} - 1\right) \Delta\theta_{g,t} \qquad (^{o}C) \tag{6.18}$$

and

$$\Delta\theta_{a,t} \geq 0 \text{ if } \Delta\theta_{g,t} > 0$$

where the amount of heat stored in the protection is:

$$\phi = \frac{c_p d_p \rho_p}{c_a \rho_a} \cdot \frac{A_p}{V} \tag{6.19}$$

and

A_p / V is the section factor for protected steel members (m^{-1});

A_p is the appropriate area of fire protection material per unit length of the member (m^2/m);

V is the volume of the member per unit length, (m^3/m);

λ_p is the thermal conductivity of the fire protection system, (W/mK). Table 6.3 gives the thermal conductivity for a range of practical fire protection systems;

d_p is the thickness of the fire protection material (m);

c_p is the specific heat of the fire protection material, (J/kgK). Table 6.3 gives the specified heat for a range of fire protection systems;

ρ_p is the unit mass of the protection. Table 6.3 gives the unit mass for a range of fire protection materials (kg/m^3);

c_a is the temperature dependent specific heat of steel given in EN 1993-1-2, (J/kgK);

$\theta_{a,t}$ is the steel temperature at time t (°C);

$\theta_{g,t}$ is the ambient gas temperature at time t (°C);

$\Delta\theta_{g,t}$ is the increase of the gas temperature during the time interval Δt (K);

ρ_a is the unit mass of steel, 7850 (kg/m^3);

Δt is the time interval (s) ($\leq$30 s).

An incremental procedure has to be performed to obtain with Eqn. (6.18) the development of the temperature in the steel section as a function of time. EN 1993-1-2 recommends that the time step interval Δt should not be taken as more than 30 seconds, a value that will ensure convergence.

Any negative increment of the temperature $\Delta\theta_{a,t}$, given by Eqn.(6.18), corresponding to an increase of the gas temperature, $\Delta\theta_{a,t} > 0$, must be considered as zero.

Table 6.3 Properties of fire protection materials (ECCS, 1995)

Material	Unit mass, ρ_p [kg / m^3]	Moisture content, p %	Thermal conductivity, λ_p [W / (mK)]	Specific heat, c_p [J/(kgK)]
Sprays				
- mineral fibre	300	1	0,12	1200
- vermiculite cement	350	15	0,12	1200
- perlite	350	15	0,12	1200
High density sprays				
- vermiculite (or perlite) and cement	550	15	0,12	1100
- vermiculite (or perlite) and gypsum	650	15	0,12	1100
Boards				
- vermiculite (or perlite) and cement	800	15	0,20	1200
- fibre-silicate or Fibre-calcium -silicate	600	3	0,15	1200
- fibre-cement	800	5	0,15	1200
- gypsum boards	800	20	0,20	1700
Compressed fibre boards				
- fibre silicate, mineral-wool, stone-wool	150	2	0,20	1200
Concrete	2300	4	1,60	1000
Light weight concrete	1600	5	0,80	840
Concrete bricks	2200	8	1,00	1200
Brick with holes	1000	-	0,40	1200
Solid bricks	2000	-	1,20	1200

Eqn. (6.18) is non-linear and an iterative procedure is required to obtain the temperature development of the steel members. Nomograms, as the one shown in Figure 6.10 can be built to obtain the temperature function of time for different section factors. These nomograms can be built for light weight insulation materials for which Eqn. (6.18) can be simplified by taking $\phi = 0$. The method given in ECCS (1983) suggests that the heat capacity of the protection material can be ignored if it is less than half that of steel section, such that:

$$d_p A_p c_p \rho_p < \frac{c_a \rho_a V}{2} \tag{6.20}$$

In this expression, ρ_a = 7850 (kg/m^3) and a value c_a = 600 (J/kgK), for the specific heat of the steel can be used to check if the material is a light weight material or not. Eqn. (6.21) can be rewritten as:

$$\phi = \frac{c_p d_p \rho_p}{c_a \rho_a} \cdot \frac{A_p}{V} < 0,5 \tag{6.21}$$

If the specific heat of the protection material, c_p, is neglected, the amount of heat stored at the protection can be taken as $\phi = 0$ and Eqn. (6.18) becomes:

$$\Delta\theta_{a,t} = \frac{\lambda_p}{d_p} \frac{A_p}{V} \frac{1}{c_a \rho_a} \left(\theta_{g,t} - \theta_{a,t}\right) \Delta t \qquad (^{o}C) \tag{6.22}$$

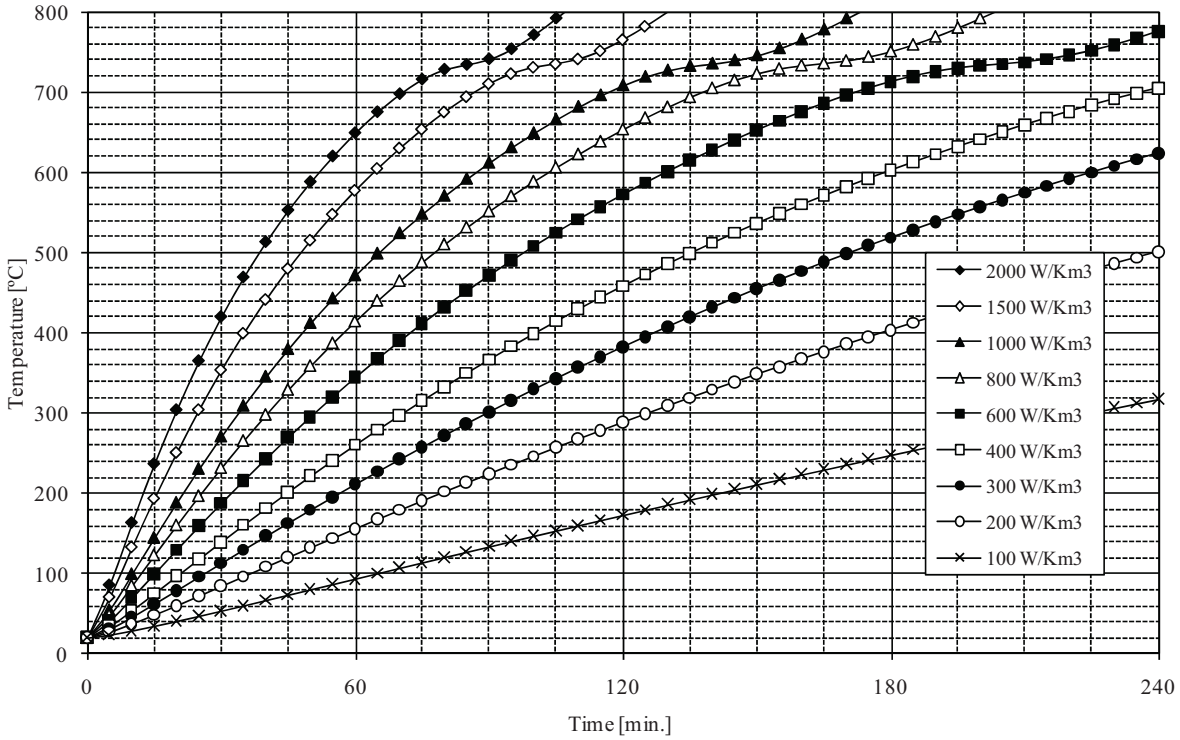

Figure 6.10 Nomogram for protected steel members subjected to the ISO 834 fire curve, for different values of $(A_p/V)(\lambda_p/d_p)$ (W/Km^3)

The advantage of using Eqn. (6.22) is that it is possible to build tables of two entries or nomograms like the one presented in Figure 6.10. One of the entries is the time and the other is the modified massivity factor:

$$\frac{A_p}{V} \cdot \frac{\lambda_p}{d_p} \qquad (\text{W/km}^3) \tag{6.23}$$

This nomogram provides conservative results, because the amount of heat stored in the protection has been neglected. The use of the nomogram avoids the need for solving the Eqn. (6.18). As the nomogram was built assuming $\phi = 0$, it is only valid for light weight insulation material. It can be used for heavy materials provided the modified massivity factor is corrected, using the following expression, according to ECCS (1983):

$$\frac{A_p}{V} \cdot \frac{\lambda_p}{d_p} \cdot \left(\frac{1}{1+\phi/2} \right) \tag{6.24}$$

6.4.3 Worked examples

Example 1 – Temperatures in a protected and unprotected profile

Consider a HEB 340 profile heated on four sides by the standard fire curve ISO 834.

a) What is the temperature of the profile after 30 minutes of fire exposure if it is unprotected?

b) What is the required thickness of gypsum board encasement so that the profile can be classified as R90 if the critical temperature is 598,5ºC?

Solution:

a) Temperature of the unprotected profile after 30 minutes

The section factor for the unprotected HEB 340 heated on the four sides is:

$A_m / V = 105,9 \ \text{m}^{-1}$

The HEB 340 has the following geometric characteristics:

$b = 300 \ \text{mm}$

$h = 340 \ \text{mm}$

$A = 17090 \ \text{mm}^2$

The box value of the section factor $[A_m / V]_b$ is

$$[A_m / V]_b = \frac{2 \times (b+h)}{A} = \frac{2 \times (0,3+0,34)}{170,9 \times 10^{-4}} = 74,9 \ \text{m}^{-1}$$

The shadow factor, k_{sh} is given by

$$k_{sh} = 0,9[A_m / V]_b / [A_m / V] = 0,9 \cdot 74,9 / 105,9 = 0,6365$$

Taking into account the shadow effect, the modified section factor has the value

$$k_{sh}[A_m / V] = 0,6365 \cdot 105,9 = 67,4 \ \text{m}^{-1}$$

This value could has been obtained without evaluating k_{sh}, as:

$$k_{sh}[A_m / V] = 0,9[A_m / V]_b = 0,9 \cdot 74,9 = 67,4 \ \text{m}^{-1}$$

With this value of the modified section factor and after 30 minutes of fire exposure the nomogram of Figure 6.9 gives the temperature of

$t_{fi,d} = 730 \ ^{o}\text{C}$

b) Thickness of gypsum board encasement

The following thermal properties of the gypsum boards are defined in Table 6.3:

$\lambda_p = 0,20$ W/(mk)

$c_p = 1700$ J/(kgK)

$\rho_p = 800$ kg/m^3

The massivity factor for the HEB 340 with hollow encasement, heated on four sides is:

$A_p / V = 74,9$ m^{-1}

From the nomogram of Figure 6.10, for a temperature of 598,5 ºC, at 90 minutes of standard fire exposure, the required modified section factor is:

$$\frac{A_p}{V} \cdot \frac{\lambda_p}{d_p} \leq 955 \text{ W/(m}^3\text{K)}$$

$$d_p \geq \frac{A_p / V}{955} \lambda_p = \frac{74,9}{955} \cdot 0,20 = 0,016\,\text{m} = 16\,\text{mm}$$

Knowing the thickness of the boards, it is possible to evaluate the amount of heat stored in the protection and check if it is a heavy or light fire protection material, according to Eqn. (6.21):

$$\phi = \frac{c_p d_p \rho_p}{c_a \rho_a} \cdot \frac{A_p}{V} = \frac{1700 \cdot 0,016 \cdot 800}{600 \cdot 7850} \cdot 74,9 = 0,346 < 0,5$$

Although this material is considered as a light material (ϕ < 0,5) a correction of the thickness of the boards will be made taking into account the amount of heat stored in the protection, ϕ, using Eqn. (6.24)

$$\frac{A_p}{V} \cdot \frac{\lambda_p}{d_p} \cdot \frac{1}{1 + \phi / 2} \leq 955 \text{ W/(m}^3\text{K)}$$

The following iterative procedure is needed to evaluate the corrected thickness:

d_p **(m)**	$\phi = \frac{c_p d_p \rho_p}{c_a \rho_a} \cdot \frac{A_p}{V}$	$d_p \geq \frac{A_p}{V} \cdot \frac{\lambda_p}{955} \cdot \left(\frac{1}{1 + \phi/2} \right)$
0,016	0,346	0,0134
0,0134	0,290	0,0137
0,0137	0,296	0,0137

With this procedure a thickness of $13,7 \approx 14$ mm is obtained, instead of the initial thickness of 16 mm. The gain was not big because the fire protection material is light, but nevertheless an economy of 12,5% was obtained.

The chart of Figure 6.11 a) shows the temperature development of the unprotected HEB 340 and the development of the temperature of the protected profile is shown in Figure 6.11 b). The S shape of the curve in the temperature range between 700 ºC and

800 ºC of the unprotected profile is due to the peak value on the heat capacity of steel shown in Figure 6.6.

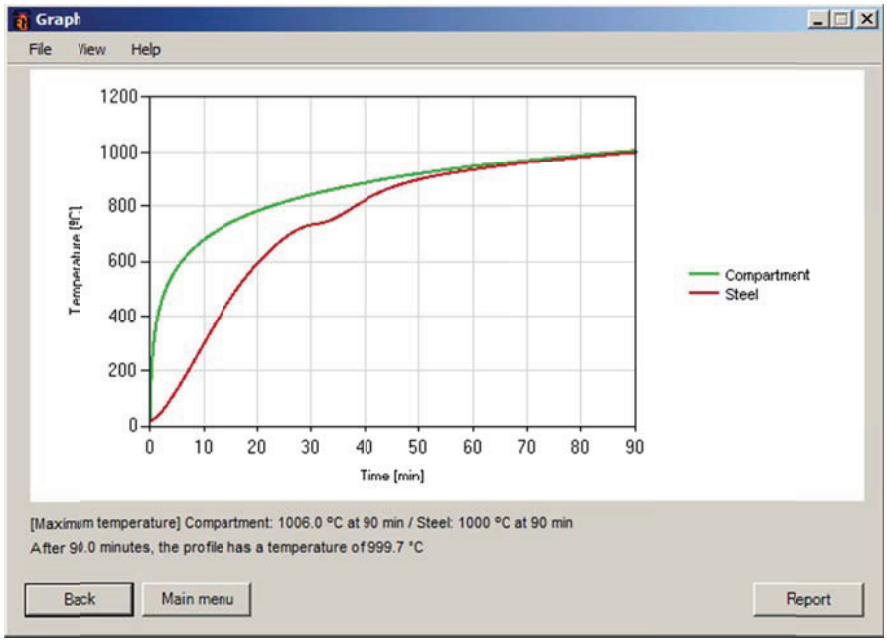

a)

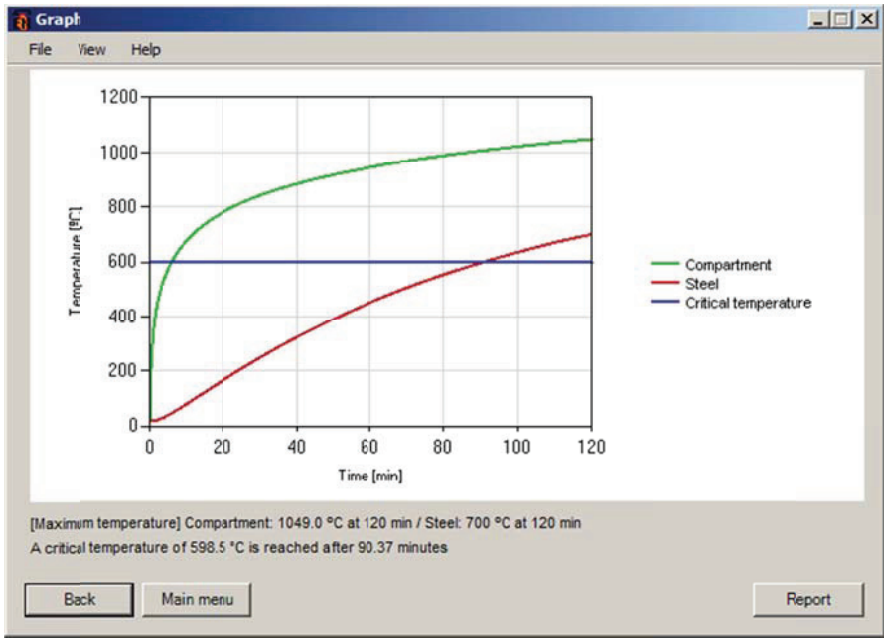

b)

Figure 6.11 Temperature development of a HEB 340 heated on four sides by the standard fire curve ISO 834. a) Unprotected; b) protected with gypsum boards

6.5 Fire resistance of structural members

Structural design at normal temperature requires the structure to support the design ultimate loads (the ultimate limit state) and the deformation and vibrations to be limited under serviceability conditions (the serviceability limit state). At room temperature most of the design effort of the structure focuses on limiting excessive deformations. Design for the fire situation is mainly concerned with preventing collapse before the specified fire resistance period. Large deformations are accepted during a fire and normally they do not need to be calculated in the fire design. EN 1993-1-2 does not give any simplified method for evaluating the deformation of the structural members.

The load-bearing function of a steel member is assumed to be lost at time *t* for a given fire, when:

$$E_{fi,d} = R_{fi,d,t} \tag{6.25}$$

where:

$E_{fi,d}$ is the design value of the relevant effects of actions in the fire situation;

$R_{fi,d,t}$ is the design value of the resistance of the member in the fire situation at time t.

The design resistance of a member in the fire situation at time *t*, $R_{fi,d,t}$, can be $M_{fi,t,Rd}$ (design bending moment resistance in the fire situation), $N_{fi,t,Rd}$ (design axial resistance in the fire situation) or any other force (separately or in combination) and the corresponding values of $M_{fi,Ed}$ (design bending moment in the fire situation), $N_{fi,Ed}$ (design axial force in the fire situation), etc. represent $E_{fi,d}$.

The design resistance $R_{fi,d,t}$ at time *t* shall be determined, (assuming a uniform temperature throughout the cross section) by modifying the design resistance for normal temperature design according to EN 1993-1-1, to take into account the mechanical properties of steel at elevated temperatures. The differences in the equations for cold design and fire design are mainly due to the fact that the shape of the stress-strain diagram at room temperature conditions is different from the shape of the diagram at elevated temperature. This is shown schematically in Figure 6.12

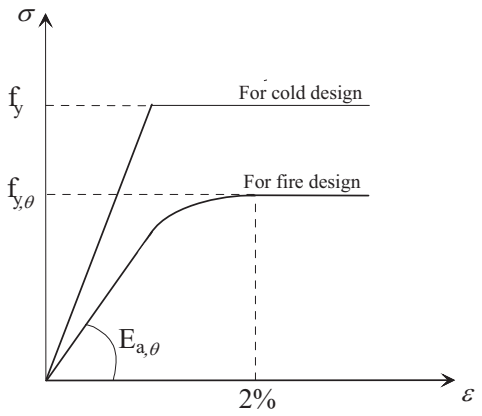

Figure 6.12 Stress-strain relationship with the yield strength to be used with Class 1, 2 and 3 cross-sections

Some adaptation to the design equations established for room temperature conditions is needed when they are used at elevated temperature. The main differences happen for the cases where the resistance is not directly proportional to the yield strength but also depends on the Young modulus, as it is the case when buckling is a potential mode of collapse, like for example lateral-torsional buckling of beams and flexural buckling of columns.

If a non-uniform temperature distribution is used, the design resistance for normal temperature design to EN 1993-1-1 should be modified on the basis of this temperature distribution. As an alternative to Eqn. (6.25), verification may be carried out in the temperature domain by using a uniform temperature distribution, or in the time domain, see Section 6.1.

In this Section only some particular concepts needed for the evaluation of the fire resistance of structural members, will be present. The reader should refer to the EN 1993-1-2 to get the formulae for fire design of structural members for each load case.

6.5.1 Classification of cross-sections

The parameter ε needed for the definition of the limits for the cross-sectional classification at 20ºC is defined as (see Franssen and Vila Real, 2010):

$$\varepsilon = \sqrt{\frac{235}{f_y}}\sqrt{\frac{E}{210000}} \quad \text{with } f_y \text{ and } E \text{ in MPa} \tag{6.26}$$

EN 1993-1-2 states that for the purpose of simplified rules the cross-sections may be classified as for normal temperature design with a reduced value for ε as given in Eqn. (6.27):

$$\varepsilon = 0,85\sqrt{\frac{235}{f_y}} \quad \text{with } f_y \text{ and } E \text{ in MPa} \tag{6.27}$$

where:

f_y is the yield strength at 20°C

The justification for the factor 0,85 used in Eqn. (6.27) is given in Franssen and Vila Real, 2010. Detailed examples at room temperature can also be found in Silva et al. 2010.

6.5.2 Members with Class 4 cross-section

Class 4 cross sections may be replaced by an effective Class 3 cross section. This new section is taken as the gross cross-section minus those parts where local buckling may occur (see non-effective zones in Figure 6.13). The effective Class 3 section can then be design using elastic cross-sectional resistance limited by yield strength in the extreme fibres. However, under fire conditions, because the original section is Class 4, the yield strength must be taken as the proof strength at 0,2% plastic strain given by Eqn. (6.15).

The effective area A_{eff} should be determined assuming that the cross section is subject only to stresses due to uniform axial compression (see Figure 6.13 a)) and the effective section modulus W_{eff} should be determined assuming that the cross section is subject

only to bending stresses (see Figure 6.13 b)). For biaxial bending effective section moduli should be determined about both main axes separately.

The effective areas of flat compression elements should be obtained from EN 1993-1-5, *Sec.4, Table 4.1* for internal elements and EN 1993-1-5, *Sec.4, Table 4.2* for outstand elements. The effective area of the compression zone of a plate with a gross cross-sectional area A_c should be obtained from:

$$A_{c,eff} = \rho A_c \tag{6.28}$$

where ρ is the reduction factor for plate buckling. Under fire conditions, the effective cross sectional area should be determined in accordance with EN 1993-1-3 and EN 1993-1-5, based on the material properties at 20°C.

When no verification is being conducted, it can be assumed that the fire resistance is maintained as long as the temperature in the section does not exceed a temperature of 350°C. This value is a nationally determined parameter and a different value may be given in the National Annex.

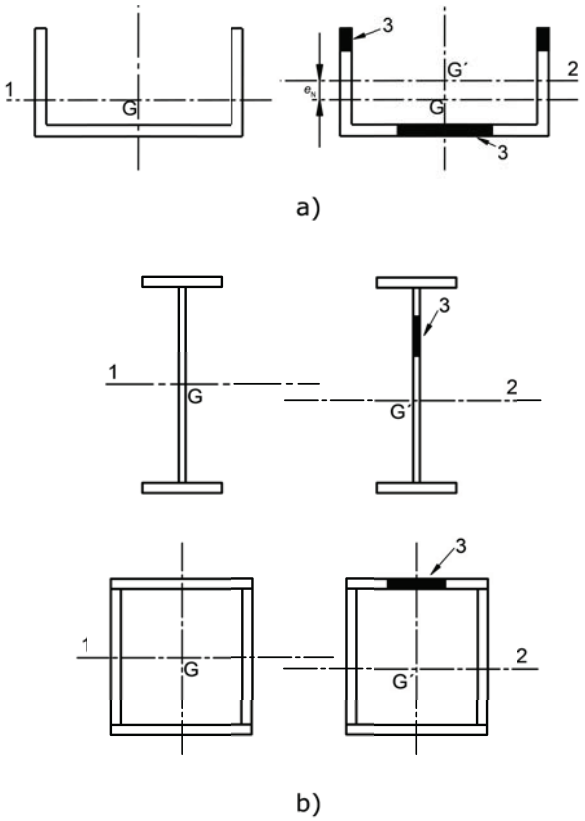

G - centroid of the gross cross section; G´ - centroid of the effective cross section

1 - centroidal axis of the gross cross section;

2 - centroidal axis of the effective cross section

3 - non effective zone

Figure 6.13 Class 4 cross section. a) For axial force; b) For bending moment (EN 1993-1-5)

6.5.3 Concept of critical temperature

It was shown in Section 6.1 that, in the temperature domain, the temperature of the structural member at the required time of fire resistance should not be bigger than the critical temperature. The concept of critical temperature or collapse temperature of a structural element with a uniform temperature distribution is presented in this section.

Collapse occurs when the design value of the relevant effects of actions in the fire situation equals the design value of the resistance of the member in the fire situation at time *t*. Considering the simplest case of a tension member, collapse occurs when:

$$N_{fi,Ed} = N_{fi,\theta,Rd} \tag{6.29}$$

Substituting the design resistance $N_{fi,\theta,Rd}$ of a tension member with a uniform temperature θ_a, given by EN 1993-1-2*, Sec 4, Eqn. (4.3)*, comes

$$N_{fi,Ed} = Ak_{y,\theta}f_y / \gamma_{M,fi} \tag{6.30}$$

which means that, collapse occurs when the yield strength equals the following expression:

$$f_{y,\theta} = k_{y,\theta}f_y = \frac{N_{fi,Ed}}{A / \gamma_{M,fi}} \tag{6.31}$$

or when the reduction factor for the effective yield strength takes the value

$$k_{y,\theta} = \frac{N_{fi,Ed}}{Af_y / \gamma_{M,fi}} \tag{6.32}$$

This equation can be written in the following general form:

$$k_{y,\theta} = \frac{E_{fi,d}}{R_{fi,d,0}} \tag{6.33}$$

where:

$E_{fi,d}$ is the design effect of the actions in case of fire;

$R_{fi,d,0}$ is the value of $R_{fi,d,t}$ for time t = 0, i.e., for 20 ºC, using Eqn. (6.12) with $k_{y,20^oC}$ = 1.

When the value of $k_{y,\theta}$ has been determined from Eqn. (6.33), the critical temperature can be obtained by interpolation from Table 6.2 or by inverting Eqn. (6.16), which leads to the following expression:

$$\theta_{a,cr} = 39,19\ln\left[\frac{1}{0,9674k_{y,\theta}^{3,833}} - 1\right] + 482 \tag{6.34}$$

Eurocode 3 adopts this equation, but, instead of the reduction factor, the degree of utilization μ_0 is used:

$$\theta_{a,cr} = 39,19 \ln\left[\frac{1}{0,9674\mu_0^{3,833}} - 1\right] + 482 \tag{6.35}$$

where, μ_0 must not be taken less than 0,013. For members with Class 1, Class 2 or Class 3 cross-sections and for tension members, Eurocode 3 defines the degree of utilisation μ_0 at time $t = 0$, i.e., for a temperature of 20ºC, as:

$$\mu_0 = \frac{E_{fi,d}}{R_{fi,d,0}} \tag{6.36}$$

This procedure can only be used for the cases where the load bearing capacity in a fire situation is directly proportional to the effective yield strength, which is the case for tension members and beams where lateral-torsional buckling is not a potential failure mode. For the cases where instability plays a role in the evaluation of $R_{fi,d,t}$ it is not possible to apply Eqn. (6.35) directly. This is the case for flexural buckling of columns, lateral-torsional buckling of beams and members under combined bending and compression. Determination of the critical temperature, in such cases, can be made only by an iterative procedure, as will be shown in Section 6.5.4. Alternatively an incremental procedure by successive verification in the load domain (see Eqn. (6.3)) may be used. This last procedure is convenient for computer implementation whereas the iterative procedure is more suitable for hand calculations.

Eqn. (6.36) cannot be used for all types of load. If it is applied, for instance, to a member in compression it leads to:

$$\mu_0 = \frac{E_{fi,d}}{R_{fi,d,0}} = \frac{N_{fi,Ed}}{N_{b,fi,0,Rd}} = \frac{N_{fi,Ed}}{\chi_{20ºC} A f_y / \gamma_{M,fi}} \tag{6.37}$$

This expression is wrong because the reduction factor for flexural buckling, χ, should in fact not be evaluated at 20 ºC but at the collapse temperature, as shown below.

Using Eqn. (6.25) the collapse of an axially loaded column is given by

$$N_{fi,Ed} = N_{b,fi,t,Rd} \tag{6.38}$$

Substituting EN 1993-1-2*, Sec 4, Eqn. (4.5)* in Eqn. (6.38), gives

$$N_{fi,Ed} = \chi_{fi} A k_{y,\theta} f_y / \gamma_{M,fi} \tag{6.39}$$

and

$$k_{y,\theta} = \frac{N_{fi,Ed}}{\chi_{fi} A f_y / \gamma_{M,fi}} \tag{6.40}$$

which shows that $k_{y,\theta}$ at collapse, is different from the degree of utilisation, μ_0, at time $t = 0$, as it is defined in Eqn. (6.37).

The reduction factor for flexural buckling should be evaluated at the collapse temperature and an iterative procedure is needed, starting with a temperature of 20ºC. Examples are given in Section 6.5.4.

6.5.4 Worked examples

Example 2 - Column

Consider the inner column E-3 at the base level of the building represented in Figure 1.27 of Chapter 1. The column has a length of 4,335 m and is composed by a section HEB 340 in steel S355. Consider that the axial compression load at normal temperature is N_{Ed} = 3326,0 kN. The column is heated on all four sides and is part of an office building with a required fire resistance time to the standard fire of t_{requ} = 90 minutes (R90).

a) Evaluate de critical temperature of the column;

b) Verify the fire resistance of the column:

b1) in the temperature domain;

b2) in the resistance domain;

b3) in the time domain.

c) Evaluate the thickness of gypsum boards needed to protect the column to fulfil the required fire resistance.

Solution:

i) Internal forces in fire situation

Considering that the load at normal temperature was obtained for a fundamental load combination and suppose that the designer does not know the accidental load combination for fire design, the load under fire condition can be obtained from Eqn. (6.9), using η_{fi} = 0,65:

$$N_{fi,Ed} = \eta_{fi} N_{Ed} = 0,65 \times 3326 = 2161,9 \text{ kN}$$

ii) Buckling lengths in fire situation

Assuming that the supports are fixed and that the frame is braced, the buckling length in fire situation is:

$$l_{y,fi} = l_{z,fi} = 0,5L = 0,5 \times 4335 = 2167,5 \text{ mm}$$

iii) Geometrical characteristics and material properties of the profile

The geometric characteristics of the section HEB 340 are: A = 170,9 cm^2, b = 300 mm, h = 340 mm, t_f = 21,5 mm, t_w = 12 mm, r = 27 mm, I_y = 36660 cm^4, I_z = 9690 cm^4. The mechanical properties of the steel are: f_y = 355 MPa and E = 210 GPa.

iv) Cross-sectional classification

$c = b/2 - t_w/2 - r$ = 117 mm (flange)

$c = h - 2t_f - 2r$ = 243 mm (web)

As the steel grade is S355, $\varepsilon = 0,85\sqrt{235 / f_y} = 0,692$

The class of the flange in compression is

c/t_f = 117/21,5 = 5,44 < 9ε = 6,23 $\Rightarrow$ Class 1

The class of the web in compression is

d/t_w = 243/12 = 20,25 < 33ε = 22,8 $\Rightarrow$ Class 1

Thus, the cross section of the HEB 340 under compression, in fire situation, is Class 1.

a) Evaluation of the critical temperature

As the buckling length in both directions is the same and in fire design there is only one buckling curve, it is only necessary to consider buckling about z-z.

The Euler critical load takes the value:

$$N_{cr} = \frac{\pi^2 EI}{l_{fi}^{\ 2}} = 42748867 \text{ N}$$

The non-dimensional slenderness at elevated temperature is given by

$$\bar{\lambda}_\theta = \bar{\lambda} \cdot \sqrt{\frac{k_{y,\theta}}{k_{E,\theta}}}$$

This is temperature dependent and an iterative procedure is needed to calculate the critical temperature. Starting with a temperature of 20 ºC at which $k_{y,\theta} = k_{E,\theta} = 1,0$:

$$\bar{\lambda}_\theta = \bar{\lambda}\sqrt{\frac{k_{y,\theta}}{k_{E,\theta}}} = \bar{\lambda} = \sqrt{\frac{Af_y}{N_{cr}}} = \sqrt{\frac{17090 \cdot 355}{42748867}} = 0,377$$

The imperfection factor takes the value:

$$\alpha = 0,65\sqrt{235 / f_y} = 0,65\sqrt{235 / 355} = 0,529$$

and

$$\phi = \frac{1}{2}(1 + 0,529 \cdot 0,377 + 0,377^2) = 0,673$$

Therefore the reduction factor for flexural buckling is:

$$\chi_{fi} = \frac{1}{0,673 + \sqrt{0,673^2 - 0,377^2}} = 0,813$$

The design value of the buckling resistance $N_{b,fi,t,Rd}$ at time t = 0:

$$N_{b,fi,0,Rd} = \chi_{fi} Af_y / \gamma_{M,fi} = 4932 \text{ kN}$$

and the degree of utilisation takes the value:

$$\mu_0 = \frac{N_{fi,Ed}}{N_{b,fi,0,Rd}} = \frac{2161,9}{4932} = 0,438$$

For this degree of utilisation the critical temperature, given by Eqn. (6.35), takes the value:

$$\theta_{a,cr} = 39,19 \ln\left[\frac{1}{0,9674\mu_0^{3,833}} - 1\right] + 482 = 605,7^{o}\,\mathrm{C}$$

Using this temperature, the non-dimensional slenderness $\bar{\lambda}_\theta$ can be corrected, which leads to another critical temperature. The iterative procedure should continue until convergence is reached, for a critical temperature of $\theta_{a,cr}$ = 598,5ºC as illustrated in the next table:

θ **(ºC)**	$\sqrt{\frac{k_{y,\theta}}{k_{E,\theta}}}$	$\bar{\lambda}_\theta = \bar{\lambda} \cdot \sqrt{\frac{k_{y,\theta}}{k_{E,\theta}}}$	χ_{fi}	$N_{fi,0,Rd} = \chi_{fi} A f_y$ **(kN)**	$\mu_0 = \frac{N_{fi,Ed}}{N_{fi,0,Rd}}$	$\theta_{a,cr}$ **(ºC)**
20	1,000	0,377	0,813	4932	0,438	605,7
605,7	1,208	0,455	0,777	4713	0,459	598,5
598,5	1,208	0,455	0,777	4713	0,459	598,5

If interpolation on the Table 6.2 has been used instead of using Eqn. (6.35) a critical temperature $\theta_{a,cr}$ = 603,6ºC would be obtained.

b) Verification of the fire resistance of the column

b1) Verification in the temperature domain

It is necessary to evaluate the temperature of the unprotected HEB 340 profile after 90 minutes of standard fire exposure (ISO 834) on four sides.

As seen in Example 1 of Section 6.4.3 the modified section factor of the unprotected HEB 340 heated on the four sides is:

$$k_{sh}[A_m / V] = 67,4 \ \mathrm{m}^{-1}$$

Using the nomogram of Figure 6.9 it can be concluded that the temperature after 90 minutes of standard fire exposure is bigger than the critical temperature of 598,5 ºC, i.e.,

$$\theta_d > \theta_{a,cr}$$

The column doesn't fulfil the required fire resistance R90 and fire protection is needed.

It should be mentioned that the nomogram of Figure 6.9 was built for periods of time less or equal to 60 minutes. It is unlikely that a required fire resistance bigger than 60 minutes could be fulfilled without using fire protection. If Eqn. (6.17) was used, using the program Elefir-EN (Vila Real and Franssen, 2014), a temperature of 999,7 ºC would be obtained as shown in Figure 6.11 a).

b2) Verification in the resistance domain

After 90 minutes of standard fire exposure, the temperature is θ_d = 999,7ºC. Interpolating for this temperature in Table 6.2 leads to a value of the reduction factors for the yield strength and the Young Modulus of:

$$k_{y,\theta} = 0,032$$

$k_{E,\theta} = 0,045$

The non-dimensional slenderness at 999,7ºC is given by

$$\bar{\lambda}_\theta = \bar{\lambda}\sqrt{\frac{k_{y,\theta}}{k_{E,\theta}}} = 0,377 \cdot \sqrt{\frac{0,032}{0,045}} = 0,318$$

The imperfection factor takes the value:

$\alpha = 0,65\sqrt{235 / f_y} = 0,65\sqrt{235 / 355} = 0,529$

and

$$\phi = \frac{1}{2}(1 + 0,529 \cdot 0,318 + 0,318^2) = 0,635$$

Therefore the reduction factor for flexural buckling is:

$$\chi_{fi} = \frac{1}{0,635 + \sqrt{0,635^2 - 0,318^2}} = 0,844$$

The design value of the buckling resistance $N_{b,fi,Rd}$ at time t = 90 minutes, is:

$N_{b,fi,Rd} = \chi_{fi} A k_{y,\theta} f_y / \gamma_{M,fi} = 0,844 \cdot 17090 \cdot 0,032 \cdot 355 \times 10^{-3} / 1,0 = 163,9\,\text{kN}$

which is less than the applied load in fire situation, $N_{fi,Ed} = 2161,9$ kN, i. e.,

$N_{fi,Rd} < N_{fi,Ed}$

The column doesn't fulfil the fire resistance criterion R90.

b3) Verification in the time domain

As seen before the modified section factor is:

$k_{sh}[A_m / V] = 67,4$ m^{-1}

Using the nomogram of Figure 6.9 the time need to reach the critical temperature of 598,5ºC is around 20 minutes (in this case it is not necessary to have a very precise value) which is far from the 90 minutes of required fire resistance. If the program Elefir-EN (Vila Real and Franssen, 2014) was used a time of 20,3 minutes would be obtained. The column doesn't fulfil the fire resistance of 90 minutes, i. e.,

$t_{fi,d} < t_{fi,requ}$

The procedures for verifying the fire resistance of the column were shown in all three domains. To achieve the required fire resistance of R90 the member must be protected.

c) Evaluation of the thickness of gypsum boards needed to protect the column to have a fire resistance of R90.

Example 1 of Section 6.4.3 has evaluated a thickness of d_p = 14 m

Example 3 - Restrained and unrestrained beam

Consider the same beam studied at Example 4 of Chapter 1. The lateral span with 6 m length that will be treated in this example is composed by an IPE 400 in steel S355. The shear and bending diagrams obtained at normal temperature are depicted in Figure 1.31. The beam supports a concrete slab but does not act compositely with the slab.

a) Considering that the beam is laterally restrained, verify if it is necessary to protect the beam for a fire resistance of R90. If fire resistance is needed, use spray based on vermiculite and cement.

b) Consider that the beam is only laterally braced at the end support sections and that lateral-torsional buckling can occur, evaluate the critical temperature of the beam.

Solution

i) Internal forces in fire situation

The shear and bending diagrams to be used for safety check under fire conditions are obtained, according to Eqn. (6.9), multiplying by η_{fi} = 0,65 the shear and bending diagram at normal temperature. The resulting diagrams are shown in Figure 6.14.

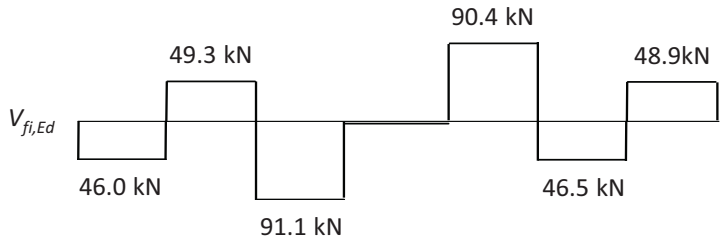

a)

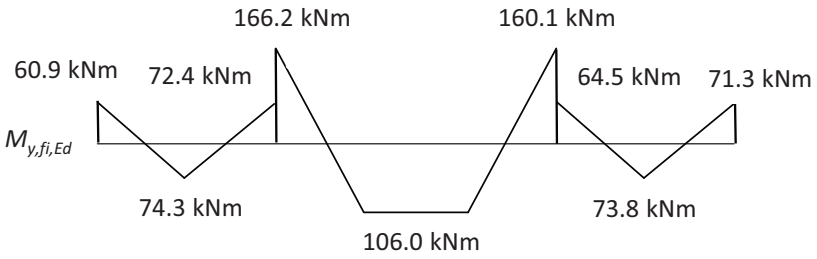

b)

Figure 6.14 a) Shear diagram under fire conditions; b) Bending diagram under fire conditions

iii) Geometrical characteristics and material properties of the profile

The geometric characteristics of the section IPE 400 are: A = 84,46 cm^2, b = 180 mm, h = 400 mm, t_f = 13,5 mm, t_w = 8,6 mm, r = 21 mm, $W_{pl,y}$ = 1307 cm^3. The mechanical properties of the steel are: f_y = 355 MPa and E = 210 GPa.

iv) Cross-sectional classification

c = b/2 - t_w/2 - r = 64,7 mm (flange)

$c = h - 2t_f - 2r$ = 331 mm (web)

As the steel grade is S355, $\varepsilon = 0,85\sqrt{235 / f_y} = 0,692$

The class of the flange in compression is

c/t_f = 64,5/13,5 = 4,79 < 9ε = 6,23 $\Rightarrow$ Class 1

The class of the web in compression is

d/t_w = 331/8,6 = 38,49 < 72ε = 49,8 $\Rightarrow$ Class 1

Thus, the cross-section of the IPE 400 under bending, in fire situation, is Class 1.

a) Laterally restrained beam

Critical temperature based on the design value of the bending moment resistance

The design value of the bending moment at mid span is:

$M_{fi,Ed}$= 74,3 kNm

The design value of the resistance moment at time $t = 0$, according to EN 1993-1-2, is

$M_{fi,0,Rd} = W_{pl,y} f_y \,/\, (k_1 k_2 \gamma_{M,fi})$

where:

$k_1 = 0,7$ for an unprotected beam exposed on three sides, with a concrete slab on the fourth side;

$k_2 = 1,0$ for sections not at the supports.

The plastic section modulus, $W_{pl,y}$, of the IPE 400 is:

$W_{pl,y}$ = 1307x10^3 mm^3

and

$$M_{fi,0,Rd} = \frac{w_{pl,y} f_y}{k_1 k_2 \gamma_{M,fi}} = \frac{1307000 \cdot 355}{0,7 \cdot 1,0 \cdot 1,0} \times 10^{-6} = 662,8 \text{ kNm}$$

The degree of utilisation takes the value:

$$\mu_0 = \frac{M_{fi,Ed}}{M_{fi,0,Rd}} = \frac{74,3}{662,8} = 0,112$$

and from Eqn. (6.35) the critical temperature is:

$\theta_{a,cr} = 812$ ºC

The critical temperature could have been evaluated in a different way: the collapse occurs when:

$$M_{fi,Rd} = M_{fi,Ed} \;\Rightarrow\; \frac{W_{pl,y} \cdot k_{y,\theta} f_y}{k_1 \cdot k_2 \gamma_{M,fi}} = M_{fi,Ed}$$

and

$$k_{y,\theta} = \frac{k_1 \cdot k_2 \cdot \gamma_{M,fi} \cdot M_{fi,Ed}}{W_{pl,y} \cdot f_y} = \frac{0,7 \cdot 1,0 \cdot 1,0 \cdot 74,3 \times 10^6}{1307 \times 10^3 \cdot 355} = 0,112$$

From Eqn. (6.34) the critical temperature is 812 ºC, as already evaluated. The critical temperature can also be obtained by interpolation in Table 6.2

Considering that the section factor for the IPE 400 heated in three sides is

$A_m / V = 152,3 \text{ m}^{-1}$

and that

$h = 400 \text{ mm}$

$b = 180 \text{ mm}$

$A = 84,46 \text{ cm}^2$

the box value of the section factor $[A_m / V]_b$, is

$$[A_m / V]_b = \frac{2h + b}{A} = \frac{2 \cdot 0,4 + 0,18}{84,46 \times 10^{-4}} = 116,0 \text{ m}^{-1}$$

The correction factor for the shadow effect is

$$k_{sh} = 0,9 \, [A_m / V]_b / [A_m / V] = 0,9 \cdot 116,0 / 152,3 = 0,6855$$

and the modified section factor thus takes the value

$$k_{sh}[A_m / V] = 0,6855 \cdot 152,3 = 104,4 \text{ m}^{-1}$$

The nomogram of Figure 6.9 gives a time of 33 min to reach the critical temperature, $\theta_{a,cr}$ = 812ºC. This is less than the required 90 min and therefore fire protection is needed to achieve the required fire resistance.

As the value of k_1 depends on whether or not the profile is protected, a new critical temperature must be obtained for the protected section. Considering k_1 = 0,85, the design value of the resistance moment at time t = 0, $M_{fi,0,Rd}$ is

$$M_{fi,0,Rd} = \frac{W_{pl,y} f_y}{k_1 k_2 \gamma_{M,fi}} = \frac{1307000 \cdot 355}{0,85 \cdot 1,0 \cdot 1,0} \times 10^{-6} = 545,9 \text{ kNm}$$

The degree of utilisation takes the value

$$\mu_0 = \frac{M_{fi,Ed}}{M_{fi,0,Rd}} = \frac{74,3}{545,9} = 0,136$$

and from Eqn. (6.35) the critical temperature is

$\theta_{a,cr} = 783$ ºC

Thickness of the spray vermiculite and cement

The thickness of a spray based on vermiculite and cement needed to prevent the steel temperature exceeding the critical temperature before the required time of 90 minutes is 8 mm (see the methodology for designing the thickness of the fire protection material in Example 1 of Section 6.4.3).

Critical temperature based on the design value of the shear force

The maximum shear force in the span is

$V_{fi,Ed} = 49,3 \text{ kN}$

The shear area is

$$A_v = A - 2bt_f + (t_w + 2r)t_f = 8446 - 2 \cdot 180 \cdot 13,5 + (8,6 + 2 \cdot 21)\,13,5 = 4269 \text{ mm}^2$$

The collapse based on the shear force, happens when:

$$V_{fi,Rd} = V_{fi,Ed} \Rightarrow \frac{A_v k_{y,\theta} f_y}{\sqrt{3}\,\gamma_{M,fi}} = V_{fi,Ed} \Rightarrow \frac{4269 \cdot k_{y,\theta} \cdot 355}{\sqrt{3} \cdot 1,0} \times 10^{-3} = 49,3$$

from where the value of the reduction factor $k_{y,\theta}$ can be taken as

$$k_{y,\theta} = 0,056$$

Interpolating in Table 6.2 for this value of $k_{y,\theta}$, the critical temperature based on the shear force is

$\theta_{a,cr}$ = 920,0ºC

Eqn. (6.34) would have given

$\theta_{a,cr}$ = 916,3ºC

The concept of degree of utilization μ_0 could also have been used

$$\mu_0 = \frac{V_{fi,Ed}}{V_{fi,0,Rd}} = \frac{V_{fi,Ed}}{A_v f_y / (\sqrt{3}\,\gamma_{M,fi})} = \frac{49300}{4269 \cdot 355 / (\sqrt{3} \cdot 1,0)} = 0,056$$

Eqn. (6.35) gives the same critical temperature of $\theta_{a,cr}$ = 916,3ºC.

This temperature is bigger than the critical temperature obtained based on the value of the bending moment. Thus, the critical temperature of the beam should be

$$\theta_{a,cr} = \min(783^{\circ}\mathrm{C};\ 916,3^{\circ}\mathrm{C}) = 783^{\circ}\mathrm{C}$$

Safety check of shear resistance

At the temperature of 783ºC, the reduction factor $k_{y,\theta}$ is equal to 0,136 and the resistance shear force takes the value

$$V_{fi,Rd} = \frac{A_v k_{y,\theta} f_y}{\sqrt{3}\,\gamma_{M,fi}} = \frac{4269 \cdot 0,136 \cdot 355}{\sqrt{3} \cdot 1,0} \times 10^{-3} = 119,0 \text{ kN}$$

As $V_{fi,Ed} < 0,5\ V_{fi,Rd}$ it is not necessary to take into account the effect of shear in the resistance moment and the critical temperature of 783ºC has been well defined.

b) Laterally unrestrained beam

The design lateral-torsional buckling resistance moment $M_{b,fi,t,Rd}$ at time t of a laterally unrestrained beam with a Class 1 or Class 2 cross-section, with a uniform temperature, is given by:

$$M_{b,fi,t,Rd} = \chi_{LT,fi} W_{pl,y} k_{y,\theta} f_y / \gamma_{M,fi}$$

At time $t = 0$, this resistance moment $M_{b,fi,0,Rd}$ should be determined from:

$$M_{b,fi,0,Rd} = \chi_{LT,fi} W_{pl,y} f_y / \gamma_{M,fi}$$

As the reduction factor for the lateral-torsional buckling moment, $\chi_{LT,fi}$, depends on the temperature, an iterative procedure must be used.

This reduction factor in fire situation is given by:

$$\chi_{LT,fi} = \frac{1}{\phi_{LT,\theta} + \sqrt{[\phi_{LT,\theta}]^2 - [\overline{\lambda}_{LT,\theta}]^2}}$$

with

$$\phi_{LT,\theta} = \frac{1}{2}\left[1 + \alpha\bar{\lambda}_{LT,\theta} + (\bar{\lambda}_{LT,\theta})^2\right]$$

where the imperfection factor is

$$\alpha = 0,65\sqrt{235 / f_y} = 0,529$$

and

$$\bar{\lambda}_{LT,\theta} = \bar{\lambda}_{LT}\sqrt{k_{y,\theta} / k_{E,\theta}}$$

The non-dimensional slenderness at normal temperature is given by:

$$\bar{\lambda}_{LT} = \sqrt{\frac{W_{pl,y} f_y}{M_{cr}}}$$

The elastic critical moment for lateral-torsional buckling, according the Example 4 of Chapter 1, takes the value:

$$M_{cr} = 164,7 \text{ kNm}$$

and

$$\bar{\lambda}_{LT} = \sqrt{\frac{W_{pl,y} f_y}{M_{cr}}} = 1,68$$

At time $t = 0$ the non-dimensional slenderness takes the value

$$\bar{\lambda}_{LT,20^oC} = \bar{\lambda}_{LT}\sqrt{\frac{k_{y,20^oC}}{k_{E,20^oC}}} = 1,68\sqrt{\frac{1,0}{1,0}} = 1,68$$

and

$$\phi_{LT,20^oC} = \frac{1}{2}(1 + 0,529 \cdot 1,68 + 1,68^2) = 2,36$$

and

$$\chi_{LT,fi} = \frac{1}{2,36 + \sqrt{2,36^2 - 1,68^2}} = 0,250$$

Resulting the design lateral-torsional buckling resistance moment $M_{b,fi,0,Rd}$ at time $t = 0$ in:

$$M_{b,fi,0,Rd} = 0,250 \cdot 1307000 \cdot 355 \times 10^{-6} = 116,0 \text{ kNm}$$

The degree of utilisation at time $t = 0$, is

$$\mu_0 = \frac{M_{fi,Ed}}{M_{b,fi,0,Rd}} = \frac{74,3}{116,0} = 0,641$$

and the critical temperature

$$\theta_{a,cr} = 39,19 \ln\left(\frac{1}{0,9674 \cdot 0,641^{3,833}} - 1\right) + 482 = 542,5\,^oC$$

Using this temperature, the non-dimensional slenderness $\bar{\lambda}_{LT,\theta}$ may be corrected. The procedure must be repeated until convergence is reached, as shown in the next table:

θ (ºC)	$\sqrt{\frac{k_{y,\theta}}{k_{E,\theta}}}$	$\bar{\lambda}_{LT,\theta} = \bar{\lambda}_{LT} \cdot \sqrt{\frac{k_{y,\theta}}{k_{E,\theta}}}$	$\chi_{LT,fi}$	$M_{b,fi,0,Rd} = \chi_{LT,fi} W_{pl,y} f_y$ (kNm)	$\mu_0 = \frac{M_{fi,Ed}}{M_{b,fi,0,Rd}}$	$\theta_{a,cr}$ (ºC)
20	1,00	1,680	0,250	116,0	0,641	542,5
542,5	1,159	1,947	0,197	91,4	0,813	492,0
492,0	1,156	1,942	0,198	91,9	0,808	493,5
493,5	1,154	1,939	0,198	91,9	0,808	493,5

Convergence was reached at a critical temperature of $\theta_{a,cr}$ = 493,5ºC, which is very close to the critical temperature, $\theta_{a,cr}$ = 494,9ºC obtained with the program Elefir-EN, Vila Real and Franssen, 2014.

Example 4 – Beam-column with Class 4 cross-section

Consider a 2,7 m high welded beam-column in steel grade S355, as shown in Figure 6.15. Assuming that the beam-column is subjected to a uniform bending moment diagram, which design value in fire situation is $M_{y,fi,Ed}$ = 20 kNm about major axis and to an axial compression force in fire situation of $N_{y,fi,Ed}$ = 20 kN and considering that lateral-torsional buckling is prevented, evaluate the critical temperature of the beam-column;

h = 460 mm (total depth of the section)

b = 150 mm

t_w = 4 mm

t_f = 5 mm

a = 5 mm (effective throat thickness of the fillet weld)

Area A = 3300 mm^2

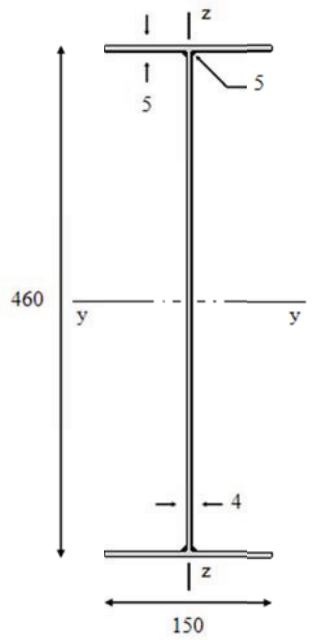

Figure 6.15 Dimensions of the built up cross section

Solution

To solve this worked example the following formulae will be used:

- For the fire resistance of the cross-section, Eqn. (6.44) from EN 1993-1-1 adapted to fire:

$$\frac{N_{fi,Ed}}{A_{eff}\ k_{0,2p,\theta}\ \frac{f_y}{\gamma_{M,fi}}} + \frac{M_{y,fi,Ed}}{W_{eff,y,\min}\ k_{0,2p,\theta}\ \frac{f_y}{\gamma_{M,fi}}} \le 1$$

- For the fire resistance of the beam-column, Eq. (4.21c) from EN 1993-1-2, adapted to profiles with class 4 cross-sections, i. e.,

$$\frac{N_{fi,Ed}}{\chi_{\min,fi}\ A_{eff}\ k_{0.2p,\theta}\ \frac{f_y}{\gamma_{M,fi}}} + \frac{k_y\ M_{y,fi,Ed}}{W_{eff,y}\ k_{0.2p,\theta}\ \frac{f_y}{\gamma_{M,fi}}} \le 1$$

$$\frac{N_{fi,Ed}}{\chi_{z,fi}\ A_{eff}\ k_{0,2p,\theta}\ \frac{f_y}{\gamma_{M,fi}}} + \frac{k_{LT}\ M_{y,fi,Ed}}{\chi_{LT,fi} W_{eff,y}\ k_{0,2p,\theta}\ \frac{f_y}{\gamma_{M,fi}}} \le 1$$

Note: In this example only the first equation will be checked.

Classification of the cross-section

For more details on the cross-sectional classification see Franssen and Vila Real, 2010.

Figure 6.16 shows the geometry of a fillet weld.

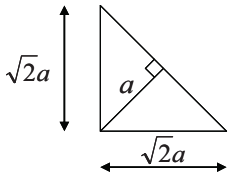

Figure 6.16 Effective throat thickness of the fillet weld

$c_f = b/2 - t_w/2 - \sqrt{2}\cdot 5 = 65,93$ mm (flange)

$c_w = h - 2t_f - 2\sqrt{2}\cdot 5 = 435,86$ mm (web)

As the steel grade is S355

$\varepsilon = 0,85\sqrt{235/f_y} = 0,692$

Classification of cross section

Combined bending about y-y (major axis) and compression:

The class of the flange in compression is:

$c/t_t = 65,93/5 = 13,16 > 14\varepsilon = 9,7 \Rightarrow$ Class 4

The class of the web in combined bending about y-y (major axis) and compression is:

Class 1 or 2:

$$\alpha = \frac{1}{2} + \frac{N_{Ed}}{2ct_w f_y} = \frac{1}{2} + \frac{20\times 10^3}{2\times 435,86\times 4\times 355} = 0,516$$

As $\alpha > 0,5$, and

$$c_w/t_w = 435,86/4 = 108,96 > \frac{496\varepsilon}{13\alpha - 1} = 60,13$$

The web is not Class 1 or 2

Class 3:

$$\psi = \frac{2N_{Ed}}{Af_y} - 1 = \frac{2 \times 20 \times 10^3}{3300 \times 355} - 1 = -0,966$$

$$c_w/t_w = 435,86/4 = 108,96 > 42\varepsilon / (0,67 + 0,33\psi) = 82,8 \Rightarrow \text{Class 4}$$

The cross section of the welded profile is Class 4 in combined bending about y-y (major axis) and compression.

Evaluation of the effective area and effective section modulus

Effective area

The effective area of the cross section in pure compression is obtained using EN 1993-1-5.

The normalised slenderness is given by

$$\bar{\lambda}_p = \sqrt{\frac{f_y}{\sigma_{cr}}} = \frac{\bar{b}/t}{28,4\varepsilon\sqrt{k_\sigma}}$$

For the flanges under compression:

$\bar{b} = c_f = 65,93$ mm

$t = t_f = 5$ mm

$\varepsilon = \sqrt{235/f_y} = 0,814$ (note: this factor is evaluated at normal temperature)

$k_\sigma = 0,43$

giving

$$\bar{\lambda}_p = \frac{65,93/5}{28,4 \times 0,814\sqrt{0,43}} = 0,87 > 0,748$$

and

$$\rho = \frac{\bar{\lambda}_p - 0,188}{\bar{\lambda}_p^2} = \frac{0,87 - 0,188}{0,87^2} = 0,901$$

and the effective with of the flange, b_{eff}, is (see Figure 6.17 with $\sigma_1 = \sigma_2$):

$b_{eff} = \rho\bar{b} = 0,901 \times 65,93 = 59,39$ mm

$b = 2b_{eff} + t_w + 2\sqrt{2} \times 5 = 2 \times 59,39 + 4 + 2\sqrt{2} \times 5 = 136,93$ mm

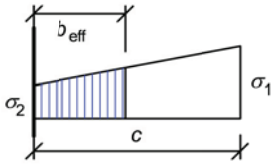

Figure 6.17 Effective[p] width b_{eff} of outstand compression elements

For the web under uniform compression ($\psi = 1,0$):

$\overline{b} = c_w = 435,86$ mm

$t = t_w = 4$

$\varepsilon = \sqrt{235/f_y} = 0,814$ (note: this factor is evaluated at normal temperature)

$k_\sigma = 4$

giving

$$\overline{\lambda}_p = \frac{435,86/4}{28,4 \times 0,814\sqrt{4}} = 2,358 > 0,5 + \sqrt{0,085 - 0,055\psi} = 0,673$$

and

$$\rho = \frac{\overline{\lambda}_p - 0,055(3+\psi)}{\overline{\lambda}_p^2} = \frac{2,358 - 0,055(3+1)}{2,358^2} = 0,385 \le 1,0$$

and the effective with of the web, b_{eff}, is (see Figure 6.18):

$b_{eff} = \rho \overline{b} = 0,385 \times 435,86 = 167,61$ mm

$b_{e1} = 0,5 b_{eff} = 0,5 \times 167,61 = 83,80$ mm

$b_{e2} = 0,5 b_{eff} = 0,5 \times 167,61 = 83,80$ mm

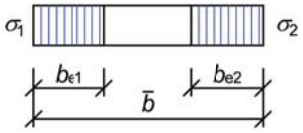

Figure 6.18 Effective[p] width $b_{eff} = b_{e1} + b_{e2}$ of internal compression elements

The effective area of the cross-section is shown in Figure 6.19, obtained with the program SteelClass, Couto et al., 2014.

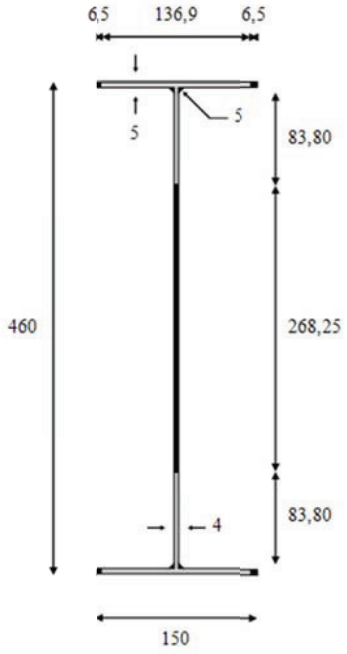

Figure 6.19 Effective cross-section when subjected to uniform compression

$$A_{eff} = A - (268,25 \times 4 + 4 \times 6,5 \times 5) = 2096,28 \text{ mm}^2$$

Effective section modulus y-y (major axis)

The effective section modulus of the cross section in bending about y-y (major axis) is obtained using clause 4.4(3) of EN 1993-1-5: "*For flange elements of I-sections and box girders the stress ratio ψ used in Table 4.1 and Table 4.2 should be based on the properties of the gross cross-sectional area, due allowance being made for shear lag in the flanges if relevant. For web elements the stress ratio ψ used in Table 4.1 should be obtained using a stress distribution based on the effective area of the compression flange and the gross area of the web*".

As the flange is under uniform compression, its effective area is the same as the one already obtained when the effective area of the cross-section under axial compression was evaluated, i. e.:

$$b_{eff} = \rho \bar{b} = 0,901 \times 65,93 = 59,39 \text{ mm}$$

$$b = 2b_{eff} + t_w + 2\sqrt{2} \times 5 = 2 \times 59,39 + 4 + 2\sqrt{2} \times 5 = 136,93 \text{ mm}$$

Evaluation of the new position of the centre of gravity, considering the effective area of the compression flange and the gross area of the web:

$$A' = A - \left[(150 - 136,93) \times 5\right] = 3234,646 \text{ mm}^2$$

$$z'_G = \frac{\left(A \times \frac{460}{2}\right) - \left[\left((150 - 136,93) \times 5\right) \times \left(460 - \frac{5}{2}\right)\right]}{A'} = 225,40 \text{ mm}$$

where z'_G is the distance from the centre of gravity to the bottom of lower flange.

Evaluation of the stress ratio ψ:

$$\psi = \frac{\sigma_2}{\sigma_1} = -\frac{b_t}{b_c}$$

where b_c and b_t are defined in Figure 6.20 and take the values:

$$b_t = z'_G - t_f - a\sqrt{2} = 225,40 - 5 - 5\sqrt{2} = 213,33 \text{ mm}$$

$$b_c = h - z'_G - t_f - a\sqrt{2} = 460 - 225,40 - 5 - 5\sqrt{2} = 222,53 \text{ mm}$$

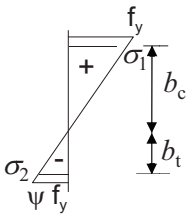

Figure 6.20 Compression and tension parts of the web

$$\psi = -\frac{b_t}{b_c} = -\frac{213,33}{222,53} = -0,9587$$

$$k_\sigma = 7,81 - 6,29\psi + 9,78\psi^2 = 22,83$$

The normalised slenderness is given by

$$\bar{\lambda}_p = \sqrt{\frac{f_y}{\sigma_{cr}}} = \frac{\bar{b}/t}{28,4\varepsilon\sqrt{k_\sigma}}$$

and

$$\bar{\lambda}_p = \frac{435,86/4}{28,4 \times 0,814\sqrt{22,83}} = 0,987 > 0,5 + \sqrt{0,085 - 0,055\psi} = 0,871$$

and

$$\rho = \frac{\bar{\lambda}_p - 0,055(3+\psi)}{\bar{\lambda}_p^2} = \frac{0,987 - 0,055(3 + (-0,9587))}{0,987^2} = 0,898 \le 1,0$$

and the effective width of the web, b_{eff}, is (see Figure 6.21):

$$b_{eff} = \rho b_c = \rho c_w / (1 - \psi) = 0,898 \times 435,86 / (1 - (-0,9587)) = 199,82 \text{ mm}$$

$$b_{e1} = 0,4 b_{eff} = 0,4 \times 199,82 = 79,93 \text{ mm}$$

$$b_{e2} = 0,6 b_{eff} = 0,6 \times 199,82 = 119,89 \text{ mm}$$

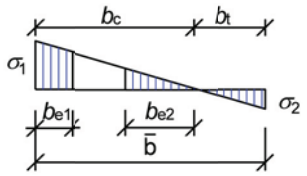

Figure 6.21 Effective width $b_{eff} = b_{e1} + b_{e2}$ of internal compression elements

The length of the non-effective area of the web is:

$$b = b_c - b_{e1} - b_{e2} = 222,53 - 79,93 - 119,89 = 22,71 \text{ mm}$$

The new position of the centre of gravity should be evaluated:

$$A'' = A - (150 - 136,93) \times 5 - 22,71 \times 4 = 3143,846 \text{ mm}^2$$

$$z''_G = \frac{\left(A \times \frac{460}{2}\right) - \left[(150 - 136,93) \times 5 \times \left(460 - \frac{5}{2}\right)\right]}{A''} - \frac{\left[22,71 \times 4 \times \left(460 - 5 - \sqrt{2} \times 5 - 79,93 - \frac{22,71}{2}\right)\right]}{A''}$$

$$= 221,6 \text{ mm}$$

The effective area of the cross section under bending about the major axis is depicted in Figure 6.22 obtained with the program SteelClass, Couto et al., 2014, where $209,5 = 221,6 - t_f - \sqrt{2}a$.

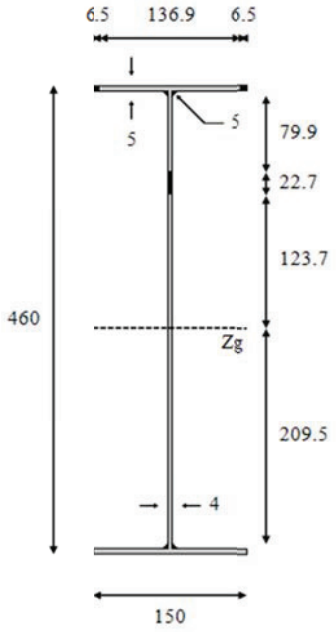

Figure 6.22 Effective width $b_{eff} = b_{e1} + b_{e2}$ of internal compression elements

The second moment of area of the effective cross section when subjected only to moment, takes the value:

$$I_{eff,y} = 102947672 \text{ mm}^4$$

and the effective section modulus is

$$W_{eff,y,\min} = \min\left(\frac{I_{eff,y}}{z''_G}; \frac{I_{eff.y}}{h - z''_G}\right) = 431848 \text{ mm}^3$$

Evaluation of the critical temperature

As the bending moment diagram along the member is uniform the cross sectional capacity is not more critical than the overall stability of the member. Although it is not necessary, in this case, to check the resistance of the cross section, this verification will be done here as an example.

Cross sectional verification

The collapse occurs, when:

$$\frac{N_{fi,Ed}}{A_{eff}\ k_{0,2p,\theta}\ \dfrac{f_y}{\gamma_{M,fi}}} + \frac{M_{y,fi,Ed}}{W_{eff,y,\min}\ k_{0,2p,\theta}\ \dfrac{f_y}{\gamma_{M,fi}}} = 1$$

from where it is possible to obtain the value of the reduction factor for the 0,2% proof strength of steel, $k_{0,2p,\theta}$ at collapse.

$$k_{0,2p,\theta} = \frac{N_{fi,Ed}}{A_{eff}\ \dfrac{f_y}{\gamma_{M,fi}}} + \frac{M_{y,fi,Ed}}{W_{eff,y,\min}\ \dfrac{f_y}{\gamma_{M,fi}}}$$

Substituting values in this equation, comes

$$k_{0,2p,\theta} = \frac{N_{fi,Ed}}{A_{eff}\ \dfrac{f_y}{\gamma_{M,fi}}} + \frac{M_{y,fi,Ed}}{W_{eff,y,\min}\ \dfrac{f_y}{\gamma_{M,fi}}} = \frac{20}{744,18} + \frac{20}{153,31} = 0,157$$

By interpolation on Table 6.2 of this chapter or in Table E.1 of EN 1993-1-2 for the proof strength at 0,2% plastic strain, the following critical temperature is obtained

$\theta_{a,cr}$ = 684 ºC

Buckling resistance of the beam-column

The buckling length is:

$l_{fi} = L = 2700\,\text{mmm}$

The non-dimensional slenderness at elevated temperature is given by:

$$\overline{\lambda}_\theta = \overline{\lambda} \cdot \sqrt{\frac{k_{0,2p,\theta}}{k_{E,\theta}}}$$

This non-dimensional slenderness depends on the temperature and an iterative procedure is needed to calculate the critical temperature. Starting with a temperature of 20ºC at which $k_{0,2p,\theta} = k_{E,\theta} = 1,0$:

$$\overline{\lambda}_{20ºC} = \overline{\lambda} = \sqrt{\frac{A_{eff} f_y}{N_{cr}}}$$

where the Euler critical load

about the major axis is: $N_{cr,y} = \dfrac{\pi^2 EI_y}{l_{fi}^2} = \dfrac{\pi^2 \times 210 \times 108012500}{2700^2} = 30709\,\text{kN}$

about the minor axis is: $N_{cr,z} = \dfrac{\pi^2 EI_z}{l_{fi}^2} = \dfrac{\pi^2 \times 210 \times 2814900}{2700^2} = 800$ kN

giving

about the major axis: $\bar{\lambda}_{y,20^oC} = \bar{\lambda}_y = \sqrt{\dfrac{A_{eff} f_y}{N_{cr,y}}} = 0,156$

about the minor axis: $\bar{\lambda}_{z,20^oC} = \bar{\lambda}_z = \sqrt{\dfrac{A_{eff} f_y}{N_{cr,z}}} = 0,964$

The reduction factor for the flexural buckling χ_{fi} is evaluated using:

$\alpha = 0,65 \cdot \sqrt{235/f_y} = 0,65 \cdot \sqrt{235/355} = 0,529$

The reduction factors for flexural buckling χ_{fi} at normal temperature are:

about the major axis:

$$\phi_{y,20^oC} = \frac{1}{2}\left[1 + \alpha \bar{\lambda}_{y,20^oC} + \bar{\lambda}^2_{y,20^oC}\right] = 0,553$$

and

$$\chi_{y,20^oC} = \frac{1}{\phi_{y,20^oC} + \sqrt{\phi^2_{y,20^oC} - \bar{\lambda}^2_{y,20^oC}}} = 0,922$$

about the minor axis:

$$\phi_{z,20^oC} = \frac{1}{2}\left[1 + \alpha \bar{\lambda}_{z,20^oC} + \bar{\lambda}^2_{z,20^oC}\right] = 1,220$$

and

$$\chi_{z,20^oC} = \frac{1}{\phi_{z,20^oC} + \sqrt{\phi^2_{z,20^oC} - \bar{\lambda}^2_{z,20^oC}}} = 0,508$$

The collapse occurs when the reduction factor for the 0,2% proof strength of steel, $k_{0,2p,\theta}$ takes the value:

$$k_{0,2p,\theta} = \frac{N_{fi,Ed}}{\chi_{\min,fi} A_{eff} f_y} + \frac{k_y M_{y,fi,Ed}}{W_{eff,y} f_y}$$

where:

$$k_y = 1 - \frac{\mu_y N_{fi,Ed}}{\chi_{y,fi} A_{eff} k_{0,2p,\theta} \dfrac{f_y}{\gamma_{M,fi}}} \le 3$$

with

$\mu_y = \left(2\beta_{M,y} - 5\right)\bar{\lambda}_{y,\theta} + 0,44\beta_{M,y} + 0,29 \le 0,8$ with $\bar{\lambda}_{y,20^oC} \le 1,1$

For a uniform bending diagram $\beta_{M,y}$ takes the value, with $\psi = 1$

$\beta_{M,y} = 1,8 - 1,7\psi = 1,8 - 1,7 \times 1,0 = 1,1$

and so

$$\mu_y = (2 \times 1,1 - 5) \times 0,156 + 0,44 \times 1,1 + 0,29 = 0,338$$

and

$$k_y = 1 - \frac{\mu_y N_{fi,Ed}}{\chi_{y,fi} A_{eff} k_{0,2p,\theta} \dfrac{f_y}{\gamma_{M,fi}}} = 0,990$$

From which the degree of utilization is:

$$k_{0,2p,\theta} = \frac{N_{fi,Ed}}{\chi_{\min,fi} A_{eff} f_y} + \frac{k_y M_{y,fi,Ed}}{W_{eff,y} f_y} = 0,182$$

By interpolation on Table 6.2 of this chapter or in Table E.1 of EN 1993-1-2 for the proof strength at 0,2% plastic strain, the following intermediate critical temperature is obtained

$\theta_{a,cr}$ = 669 ºC

The non-dimensional slendernesses at elevated temperature are a function of the temperature and the following iterative procedure is needed:

θ (ºC)	$\overline{\lambda}_{y,\theta}$	$\overline{\lambda}_{z,\theta}$	$\chi_{\min,fi}$	k_y	$k_{0,2p,\theta}$	$\theta_{a,cr}$ (ºC)
20	0,156	0,964	0,508	0,990	0,182	669
669	0,155	0,956	0,512	0,943	0,176	673
673	0,155	0,956	0,512	0,943	0,176	673

After two iterations a critical temperature of $\theta_{a,cr}$ = 673 ºC is obtained.

The critical temperature of the beam-column should be the minimum between the critical temperature of the cross-section and the critical temperature of the member:

$$\theta_{a,cr} = \min(684^{o}\,C;\ 673^{o}\,C) = 673^{o}\,C$$

6.6 Connections

This section deals with the fire design of bolted and welded joints. Tests and observations from real fires have shown that joints perform well in fires and in many cases may be left unprotected. For the case of bolted joints, Eurocode 3 states that net-section failure at fastener holes need not be considered, provided that there is a fastener in each hole. This is because the steel temperature in the joint is lower due to the presence of the additional joint material.

Eurocode 3 states that the fire resistance of bolted and welded joints may be assumed to be sufficient, provided that the following conditions are satisfied:

1. The thermal resistance $(d_f/\lambda_f)_c$ of the joint's fire protection is equal to or greater than the minimum value of the thermal resistance $(d_f/\lambda_f)_m$ of fire protection applied to any of the connected members, where:

d_f is the thickness of the fire protection material. For unprotected members, $d_f = 0$.

λ_f is the effective thermal conductivity of the fire protection material.

2. The degree of utilisation of the joint is equal to or less than the maximum degree of utilisation of any of the connected members. As a simplification, the utilisation of the joint and its connected members may be calculated at ambient temperature.
3. The resistance of the joint at ambient temperature is calculated in accordance with the recommendations given in EN 1993-1-8.

As an alternative to the above method, the fire resistance of a joint may be determined using the method given in Annex D of Part 1.2 of Eurocode 3. This method is presented and discussed in the following sections.

6.6.1 Temperature of joints in fire

When verifying the fire resistance of a joint, the temperature distribution of the joint components should be evaluated. These temperatures may be assessed using the local section factors *A*/*V* of the parts forming the joint. As a simplification, a uniform temperature distribution may be assumed within the joint. This temperature may be calculated using the maximum value of the *A*/*V* ratios of the connected steel members adjacent to the joint. For beam-to-column and beam-to-beam joints, where the beams are supporting a concrete floor, the temperature distribution, θ_h, of the joint may be determined from the temperature of the bottom flange of the connected beam at mid span using the method described below.

1. If the depth of the beam is less than or equal to 400 mm

$$\theta_h = 0,88\theta_0[1 - 0,3(h / D)] \tag{6.41}$$

where:

θ_h is the temperature at height *h* (mm) of the steel beam (Figure 6.23);

θ_0 is the bottom flange temperature of the steel beam remote from the connection, evaluated with Eqns. (6.17) or (6.18);

h is the height of the component being considered above the bottom of the beam in (mm) (Figure 6.23);

D is the depth of the beam in (mm).

2. If the depth of the beam is greater than 400 mm

- For $h \le D / 2$

$$\theta_h = 0,88\theta_0 \tag{6.42}$$

- For $h > D / 2$

$$\theta_h = 0.88\theta_0[1 + 0,2(1 - 2h / D)] \tag{6.43}$$

where the meaning of the symbols is the same as for Eqn. (6.41).

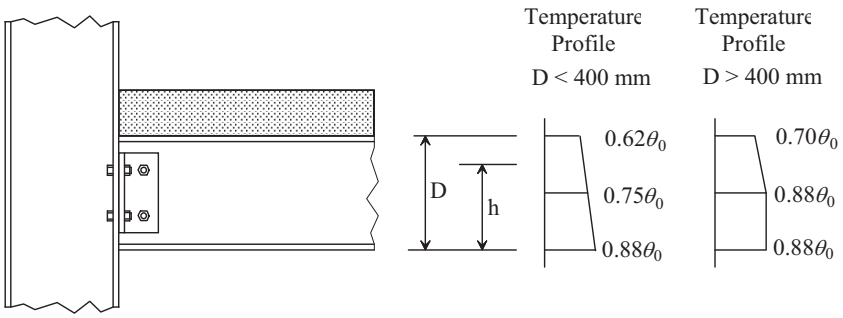

Figure 6.23 Thermal gradient within the depth of a composite joint (EN 1993-1-2)

6.6.2 Strength of bolts and welds at elevated temperature

Fire resistance of bolts and welds is based on the resistance at normal temperature according to EN 1993-1-8 multiplied by the reduction factors for bolts and welds at elevated temperatures given in Table 6.4.

Table 6.4 Strength reduction factors for bolts and welds

Temperature, θ_a (ºC)	Reduction factor for bolts, $k_{b,\theta}$ (Tension and shear)	Reduction factor for welds, $k_{w,\theta}$
20	1,000	1,000
100	0,968	1,000
150	0,952	1,000
200	0,935	1,000
300	0,903	1,000
400	0,775	0,876
500	0,550	0,627
600	0,220	0,378
700	0,100	0,130
800	0,067	0,074
900	0,033	0,018
1000	0,000	0,000

6.6.2.1 Design fire resistance of bolts in shear

Category A: Bearing Type

The design fire resistance of bolts loaded in shear should be determined from:

$$F_{v,t,Rd} = F_{v,Rd} k_{b,\theta} \frac{\gamma_{M2}}{\gamma_{M,fi}} \tag{6.44}$$

where:

$F_{v,Rd}$ is the design shear resistance of the bolt per shear plane calculated assuming that the shear plane passes through the threads of the bolt (Table 3.4 of EN 1993-1-8);

$k_{b,\theta}$ is the reduction factor determined for the appropriate bolt temperature from Table 6.4;

γ_{M2} is the partial safety factor at normal temperature;

$\gamma_{M,fi}$ is the partial safety factor for fire conditions

The design bearing resistance of bolts in fire should be determined from:

$$F_{b,t,Rd} = F_{b,Rd} k_{b,\theta} \frac{\gamma_{M2}}{\gamma_{M,fi}} \tag{6.45}$$

where:

$F_{b,Rd}$ is the design bearing resistance of bolts at normal temperature determined from Table 3.4 of EN 1993-1-8.

Category B (slip resistance at serviceability) and Category C (slip resistance at ultimate state)

Slip restraint connections should be considered as having slipped in fire and the resistance of a single bolt should be calculated as for bearing type bolts.

6.6.2.2 Design fire resistance of bolts in tension

Category D and E: non-preloaded and preloaded bolts

The design tension resistance of a single bolt in fire should be determined from:

$$F_{ten,t,Rd} = F_{t,Rd} k_{b,\theta} \frac{\gamma_{M2}}{\gamma_{M,fi}} \tag{6.46}$$

where:

$F_{t,Rd}$ is the tension resistance at normal temperature, determined from Table 3.4 of EN 1993-1-8.

6.6.2.3 Design fire resistance of welds

Butt Welds

According to the Eurocode 3 the design strength of a full penetration butt weld, for temperatures up to 700 ºC, should be taken as equal to the strength of the weaker connected part using the appropriate reduction factors for structural steel given in Table 6.2. For temperatures above 700 ºC the reduction factors for fillet welds given in Table 6.4 can also be used for butt welds.

Fillet Welds

The design resistance per unit length of a fillet weld in fire should be determined from:

$$F_{w,t,Rd} = F_{w,Rd} k_{w,\theta} \frac{\gamma_{M2}}{\gamma_{M,fi}} \tag{6.47}$$

where:

$F_{w,Rd}$ is the design weld resistance per unit length at normal temperature determined from Clause 4.5.3. EN 1993-1-8;

$k_{w,\theta}$ is the strength reduction factors for welds determined from Table 6.4.

6.6.3 Worked examples

Example 5 – Bolted joint

Consider the S355 bolted tension joint shown in Figure 6.24. Assuming that the design value of the tension force in fire situation is $N_{fi,Ed}$ = 195 kN, that the bolts are Grade 4.6, M20 and that the shear plane passes through the unthreaded portion of the bolt.

a) What is the critical temperature of the joint and connected members?

b) Verify if the unprotected joint can be classified as R30.

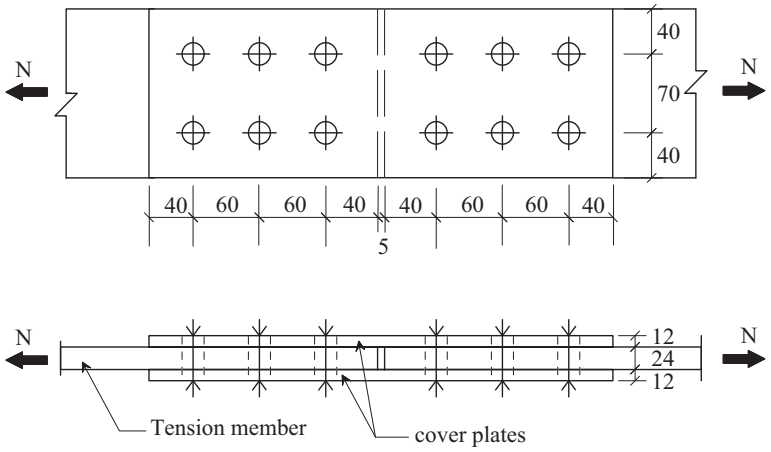

Figure 6.24 Bolted tension joint

Solution

a) Critical temperature of the joint and connected members

Critical temperature of the members

As net-section failure at fastener holes need not be considered (provided that there is a fastener in each hole), the gross cross-section design resistance $N_{fi,t,Rd}$ of the tension member at time t is:

$$N_{fi,t,Rd} = Ak_{y,\theta}f_y \,/\, \gamma_{M,fi}$$

The area of the gross cross-section is

$$A = 24 \cdot 150 = 3600\,\text{mm}^2$$

The collapse of the tension member occurs when:

$$N_{fi,Ed} = N_{fi,t,Rd}$$

thus

$$N_{fi,Ed} = N_{fi,t,Rd} \quad \Rightarrow \quad N_{fi,Ed} = Ak_{y,\theta}f_y \,/\, \gamma_{M,fi}$$

from where the reduction factor for the yield strength can be taken as

$$k_{y,\theta} = \frac{N_{fi,Ed}}{Af_y \,/\, \gamma_{M,fi}} = \frac{195000}{3600 \cdot 355 / 1,0} = 0,153$$

By interpolation in Table 6.2, the critical temperature of the tension member is

$$\theta_{a,cr} = 764,2\,^{o}\text{C}$$

There is no need to evaluate the critical temperature of the cover plates in this example, because their thickness is equal to half of the thickness of the connected members and should resist to half of the applied tension force.

Critical temperature based on the shear resistance of the bolts

The design shear resistance of the bolt per shear plane calculated assuming that the shear plane passes through the threaded part of the bolt (see definition of $F_{v,Rd}$ in Eurocode 3 Part 1-8)

$$F_{v,Rd} = \frac{0,6f_{ub}A_s}{\gamma_{M2}}$$

The design value of the shear resistance of a bolt per shear plane under fire conditions, at time t, is given by

$$F_{v,t,Rd} = F_{v,Rd}k_{b,\theta}\frac{\gamma_{M2}}{\gamma_{M,fi}}$$

As there are 6 bolts with two shear planes the total resistance force of the bolts is

$$F_{v,t,Rd,TOTAL} = 12 \cdot F_{v,Rd}k_{b,\theta}\frac{\gamma_{M2}}{\gamma_{M,fi}}$$

The collapse occurs when

$$N_{fi,Ed} = F_{v,t,Rd,TOTAL} \quad \Rightarrow \quad N_{fi,Ed} = 12 \cdot F_{v,Rd} k_{b,\theta} \frac{\gamma_{M2}}{\gamma_{M,fi}}$$

from where the reduction factor for the bolts can be taken as

$$k_{b,\theta} = \frac{N_{fi,Ed}}{12 \cdot F_{v,Rd} \dfrac{\gamma_{M2}}{\gamma_{M,fi}}}$$

In the present case

$$F_{v,Rd} = \frac{0,6 f_{ub} A_s}{\gamma_{M2}} = \frac{0,6 \cdot 400 \cdot 245}{1,25} \times 10^{-3} = 47\,\text{kN}$$

and

$$k_{b,\theta} = \frac{N_{fi,Ed}}{12 \cdot F_{v,Rd} \dfrac{\gamma_{M2}}{\gamma_{M,fi}}} = \frac{195}{12 \cdot 47 \cdot \dfrac{1,25}{1,0}} = 0,277$$

By interpolation in Table 6.4, the following critical temperature is obtained

$$\theta_{a,cr} = 582,7\,^{o}\text{C}$$

Critical temperature based on the bearing resistance of the bolts

According to Part 1-8 of Eurocode 3 the bearing resistance at normal temperature is given by:

$$F_{b,Rd} = \frac{k_1 \alpha_b f_u d t}{\gamma_{M2}}$$

where:

- for end bolts in the direction of load transfer

$$\alpha_b = \min\left(\frac{e_1}{3d_0}; \frac{f_{ub}}{f_u}; 1,0 \right)$$

- for inner bolts in the direction of load transfer

$$\alpha_b = \min\left(\frac{p_1}{3d_0} - \frac{1}{4}; \frac{f_{ub}}{f_u}; 1,0 \right)$$

In the safe side it can be considered that all the bolts have the minimum bearing resistance:

$$\alpha_b = \min\left(\frac{e_1}{3d_0}; \frac{p_1}{3d_0} - \frac{1}{4}; \frac{f_{ub}}{f_u}; 1,0 \right)$$

There are only edge bolts in the direction perpendicular to the direction of load transfer, thus

$$k_1 = \min\left(2,8 \frac{e_2}{d_0} - 1,7; 1,4 \frac{p_2}{d_0} - 1,7; 2,5 \right)$$

for all the bolts of the connection.

In this case

$e_1 = 40\,\text{mm}$; $p_1 = 60\,\text{mm}$; $t = 24\,\text{mm}$

$e_2 = 40\,\text{mm}$; $p_2 = 70\,\text{mm}$;

$d = 20\,\text{mm}$; $d_0 = 22\,\text{mm}$;

$f_{ub} = 400\,\text{N/mm}^2$; $f_u = 510\,\text{N/mm}^2$

leading to

$$\alpha_b = \min\left(\frac{40}{3\cdot 22}; \frac{60}{3\cdot 22}-\frac{1}{4}; \frac{400}{510}; 1,0\right) = \min\left(0,61;\ 0,66;\ 0,78;\ 1,0\right) = 0,61$$

and

$$k_1 = \min\left(2,8\frac{40}{22}-1,7;\ 1,4\frac{70}{22}-1,7;\ 2,5\right) = \min\left(3,39;\ 2,75;\ 2,5\right) = 2,5$$

The design value of the bearing resistance of a bolt under fire condition, at time *t*, is given by

$$F_{b,t,Rd} = F_{b,Rd} k_{b,\theta} \frac{\gamma_{M2}}{\gamma_{M,fi}}$$

As there are six bolts to resist to the applied tension force at each side

$$F_{b,t,Rd,TOTAL} = 6 \cdot F_{b,Rd} k_{b,\theta} \frac{\gamma_{M2}}{\gamma_{M,fi}}$$

The collapse occurs when

$$N_{fi,Ed} = F_{b,t,Rd,TOTAL} \quad \Rightarrow \quad N_{fi,Ed} = 6 \cdot F_{b,Rd} k_{b,\theta} \frac{\gamma_{M2}}{\gamma_{M,fi}}$$

The reduction factor for the bolts can be taken as

$$k_{b,\theta} = \frac{N_{fi,Ed}}{6 \cdot F_{b,Rd} \dfrac{\gamma_{M2}}{\gamma_{M,fi}}}$$

The bearing resistance is given by

$$F_{b,Rd} = \frac{k_1 \alpha_b f_u dt}{\gamma_{M2}} = \frac{2,5 \cdot 0,61 \cdot 510 \cdot 20 \cdot 24}{1,25} = 299 \times 10^3\,\text{N} = 299\,\text{kN}$$

and

$$k_{b,\theta} = \frac{N_{fi,Ed}}{6 \cdot F_{b,Rd} \dfrac{\gamma_{M2}}{\gamma_{M,fi}}} = \frac{195}{6 \cdot 299 \cdot \dfrac{1,25}{1,0}} = 0,087$$

Interpolating for this reduction factor in Table 6.4, the following critical temperature is obtained

$\theta_{a,cr} = 739,5\,^{o}\text{C}$

The critical temperature of the joint is

$\theta_{a,cr} = \min(764,2^{o}\text{C};\ 582,7^{o}\text{C};\ 739,5^{o}\text{C}) = 582,7^{o}\text{C}$

b) Check if the joint can be classified as R30

The section factors of the tension member and the joint are respectively:

$$\left[\frac{A_m}{V}\right]_{member} = \frac{2(0,024+0,15)}{0,024\cdot 0,15} = 96,7\,\mathrm{m}^{-1}$$

and

$$\left[\frac{A_m}{V}\right]_{joint} = \frac{2(0,048+0,15)}{0,048\cdot 0,15} = 55\,\mathrm{m}^{-1}$$

After 30 minutes of standard fire exposure the member has the following temperature obtained from the nomogram of Figure 6.9, using $k_{sh} = 1,0$

$$\theta_{a,member} = 763\,^{o}\mathrm{C}$$

which is lower than the critical temperature of the member (764,2ºC), and thus the member resists to 30 minutes of standard fire exposure.

After the same period of time the joint has the following temperature

$$\theta_{a,joint} = 700\,^{o}\mathrm{C}$$

which is higher than the critical temperature of the joint, and the joint cannot be classified as R30.

Example 6 – Welded joint

Consider a welded tension joint in S355 steel, as shown in Figure 6.25. Assuming that the design value of the tension force in the fire situation is $N_{fi,Ed}$ = 195 kN, what should be the throat thickness of the fillet welds *a*, so that the unprotected joint has a fire resistance of R30?

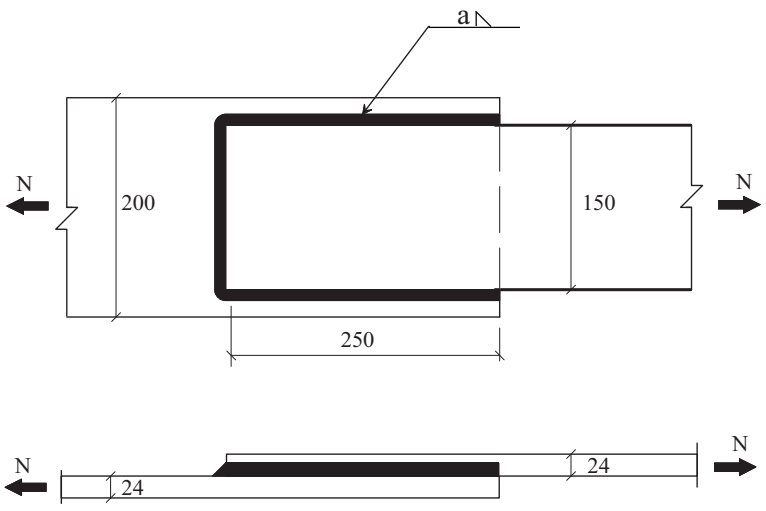

Figure 6.25 Welded tension joint

Solution

Verification of the fire resistance of the gross cross section

The gross cross section of the connected members is 150x24 mm^2. This is the same as the previous example, where it was found that the temperature after 30 minutes of standard fire exposure is:

$\theta_{a,member} = 763\,^{o}\mathrm{C}$

For a temperature of 763ºC, the reduction factor for the effective yield strength from Table 6.2, takes the value

$k_{y,\theta} = 0,1544$

As net-section failure at fastener holes need not be considered (provided that there is a fastener in each hole) the gross cross-section design resistance $N_{fi,\theta,Rd}$ of the tension member with a uniform temperature θ_a = 763ºC is:

$$N_{fi,\theta,Rd} = Ak_{y,\theta}f_y / \gamma_{M,fi} = 24 \cdot 150 \cdot 0,1544 \cdot 355 / 1,0 = 197 \times 10^3\,\mathrm{N} = 197\,\mathrm{kN}$$

This force is higher than the applied tension load in fire situation $N_{fi,Ed}$ = 195 kN.

Throat thickness of the fillet welds

The section factor, A_m/V, of the joint can be determined by considering a cross-section perpendicular to the main direction of the joint.

$$\frac{A_m}{V} = \frac{2 \cdot (0,2 + 0,048)}{0,2 \cdot 0,024 + 0,15 \cdot 0,024} = 59\,\mathrm{m}^{-1}$$

Assuming k_{sh} = 1,0, the temperature of the joint can be determined from the nomogram of Figure 6.9, giving

$\theta = 717\ ^{o}\mathrm{C}$

According to the simplified method for design resistance of fillet weld, presented in EN 1993-1-8, the design resistance of the fillet weld may be assumed to be adequate if, at every point along its length, the resultant of all the forces per unit length transmitted by the weld satisfy the following criterion:

$F_{w,Ed} \leq F_{w,Rd}$

where:

$$F_{w,Rd} = \frac{f_u / \sqrt{3}}{\beta_w \gamma_{M2}} a$$

$f_u = 510$ N/mm^2, for the steel grade S355

$\beta_w = 0,9$, for the steel grade S355

a is the effective throat thickness of the fillet weld

$\gamma_{M2} = 1,25$

leading to

$$F_{w,Rd} = \frac{f_u / \sqrt{3}}{\beta_w \gamma_{M2}} a = \frac{510 / \sqrt{3}}{0,9 \cdot 1,25} \cdot a = 261,7 \cdot a \text{ N/mm}$$

The design resistance per unit length of the fillet weld in fire, should be determined from Eqn. (6.47):

$$F_{w,t,Rd} = F_{w,Rd} k_{w,\theta} \frac{\gamma_{M2}}{\gamma_{M,fi}}$$

The reduction factor for welds for a temperature of 717ºC can be determined from Table 6.4 interpolating between 700ºC and 800 ºC:

$$k_{w,\theta} = 0,12$$

leading to

$$F_{w,t,Rd} = 261,7 \cdot a \cdot 0,12 \cdot \frac{1,25}{1,0} = a \cdot 39,255 \text{ N/mm}$$

Multiplying this value by the total length of the fillet weld (l = 650 mm) the design value of the fire resistance of the fillet weld is

$$F_{w,t,Rd,TOTAL} = a \cdot 39,255 \cdot 650 = a \cdot 25515,8 \text{ N} = a \cdot 25,5 \text{ kN}$$

It has to be

$$F_{w,t,Rd,TOTAL} \geq N_{fi,Ed} \quad \Rightarrow \quad a \cdot 25,52 \text{ kN} \geq 195$$

and

$$a \geq 7,64 \text{ mm}$$

A thickness of 8 mm would be enough to ensure a fire resistance of R30.

References

Couto, C., Vila Real, P., Lopes, N., Amaral, C. 2014. SteelClass – a software for Cross-sectional Classification, University of Aveiro.

ECCS, 1983. European Recommendations for the Fire Safety of Steel Structures. European Convention for Constructional Steelwork. ECCS, Elsevier.

ECCS TC3, 1995. Fire Resistance of Steel Structures. Fire Safety of Steel Structures. European Convention for Constructional Steelwork. ECCS Technical Note No. 89, Brussels, Belgium.

EN 1990-1:2002. Eurocode - Basis of structural design. CEN.

EN 1991-1-1:2002. Eurocode 1: Actions on structures - Part 1-1: General actions - Densities, self-weight, imposed loads for buildings. CEN.

EN 1991-1-2:2002. Eurocode 1: Actions on structures - Part 1-2: General actions - Actions on structures exposed to fire. CEN.

EN 1993-1-1:2005. Eurocode 3: Design of Steel Structures. Part 1.1: General rules and rules for buildings. CEN.

EN 1993-1-2:2005. Eurocode 3: Design of steel structures - Part 1-2: General rules - Structural fire design. CEN.

EN 1993-1-5:2006. Eurocode 3: Design of Steel Structures. Part 1.5: Plated structural elements. CEN.

EN 1993-1-8:2005. Eurocode 3: Design of steel structures - Part 1-8: Design of joints. CEN.

Franssen, J.-M., Vila Real, P. 2010. Fire Design of Steel Structures, ECCS Eurocode Design Manuals. Brussels: Ernst & Sohn a Wiley Company, 1st Edition.

Silva, L. S., R. Simões, H. Gervásio. 2010. Design of Steel Structures, ECCS Eurocode Design Manuals. Brussels: Ernt & Sohn A Wiley Company, 1st Edition.

Vila Real, P., Franssen, J. M. 2014. Elefir-EN V1.5.5, Software for fire design of steel structural members according the Eurocode 3. http://elefiren.web.ua.pt.

CHAPTER 7

SUSTAINABILITY ASPECTS OF STEEL BUILDINGS AND COMPONENTS

Milan VELJKOVIC[1] and Helena GERVÁSIO[2]

[1]University of Lulea, Sweden

[2]University of Coimbra, Portugal

7 Sustainability aspects of steel buildings and components

7.1 Introduction to life cycle thinking

Life Cycle Analysis (LCA) is an objective process to evaluate the environmental burdens associated with a product process or activity and to evaluate and implement opportunities to affect environmental improvements. It enables to identify and quantify material usage, energy requirements, solid wastes, and atmospheric and waterborne emissions throughout the product life cycle (i.e. from raw material acquisition to end-of-life, as illustrated in Figure 7.1).

Life cycle approaches are recommended by the Integrated Product Policy (IPP, 2003) for the assessment of potential impacts of products.

Potential environmental impacts occur throughout all life cycle stages of a building or other construction The main advantage of Life Cycle Thinking is that it avoids the shifting of burdens from one life cycle stage to another, from one geographic area to another and from one environmental medium (for example air quality) to another (for example water or land) (UNEP, 2004).

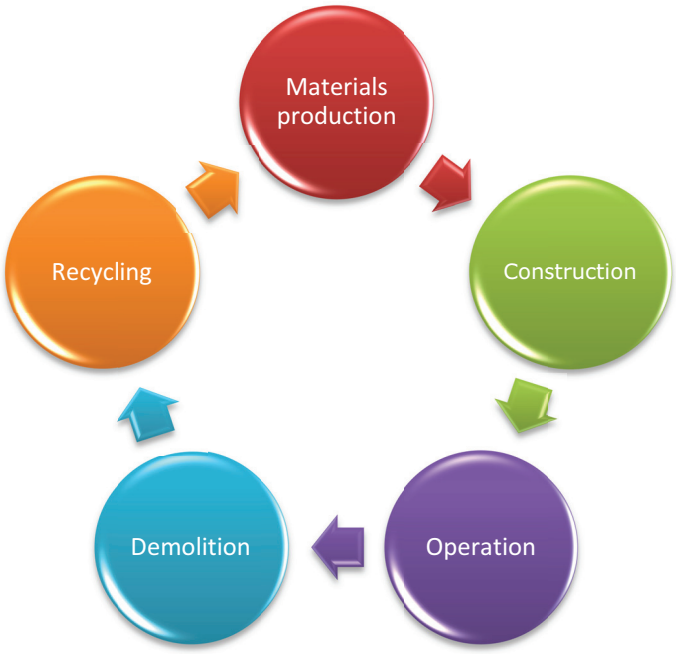

Figure 7.1 Life cycle perspective

Moreover, life cycle approaches enable better choices for the longer term. It implies that everyone in the whole chain of a product's life cycle, from cradle to grave, has a responsibility and a role to play, taking into account all the relevant impacts on the environment (UNEP, 2004).

By the quantification of all the emissions into air, water and land that take place in every life cycle phase, a life cycle approach enables to identify the most critical processes over

the product or system life, thus enhancing the potential for environmental improvement in the whole chain of the product.

This chapter focusses on LCA of steel products and steel buildings. In the first part the normative framework for LCA, according to international standards, is introduced followed by the discussion of specific aspects in the life cycle assessment of steel structures. Finally, worked examples are provided in the end of the chapter, which enable a better understanding of the methodology.

7.2 Life Cycle Analysis of construction works

7.2.1 General methodologies and tools

Construction is responsible for a major proportion of environmental impacts in the industrial sector. During the last years there has been an increasing interest in the environmental assessment of the built environment.

Currently there are two major classes of assessment tools for the built environment (Reijnders and Roekel, 1999):

(i) qualitative tools based on scores and criteria;

(ii) tools using a quantitative analysis of inputs and outputs based on life cycle approach.

Within the first group of tools there are systems such as LEED (in the US), BREAM (in the UK), GBTool (International Initiative for a Sustainable Built Environment (iiSBE)), etc. These methods, also known as rating systems, are usually based on auditing of buildings and on the assignment of scores to pre-defined parameters. Although mainly qualitative some parameters may also be quantitative and even use Life Cycle Analysis (LCA), mainly in the quantification of material credits. Usually these systems are used to obtain green building certifications and eco-labels. However, this kind of tools is outside the scope of this document, thus in the following the focus will be on the second group of tools, which are based on life cycle approaches.

LCA can be directly applied to the building sector. However, due to its characteristics there are additional problems in the application of standard life cycle to buildings and other constructions. The main causes may be listed as (IEA, 2001):

(i) the life expectancy of buildings is long and unknown and therefore subjected to a high level of uncertainties;

(ii) buildings are site dependent and many of the impacts are local;

(iii) building products are usually made of composite materials which implies more data to be collected and associated manufacturing processes;

(iv) the energy consumption in the use phase of a building is very much dependent on the behaviour of the users and of the services;

(v) a building is highly multi-functional, which makes it difficult to choose an appropriate functional unit;

(vi) buildings are closely integrated with other elements in the building environment, particularly urban infrastructure like roads, pipes, green spaces and treatment facilities, and it can be highly misleading to conduct LCA on a building in isolation.

In relation to life cycle assessment of buildings and its components, a distinction is made between LCA tools developed with aim of evaluating building materials and components

In relation to life cycle assessment of buildings and its components, a distinction is made between LCA tools developed with aim of evaluating building materials and components (e.g. BEES (Lippiatt, 2002) and life cycle approaches for evaluating the building as a whole (e.g. Athena (Trusty, 1997), Envest (Howard et al. 1999), EcoQuantum (Kortman et al., 1998)). The latter are usually more complex as the overall building performance depends on the interactions between individual components and sub-systems as well as interactions with the occupants and the natural environment. The selection of an appropriate tool depends on the specific environmental objectives of the project.

The precision and the relevance of LCA tools as a design aid were analyzed in a project developed in the frame of the European thematic network PRESCO (Practical Recommendations for Sustainable Construction) (Kellenberger, 2005). In this project, several LCA tools were compared based on case studies, with the global aim of the harmonization of LCA based assessment tools for buildings. Other comparative analysis regarding tools for environmental assessment of the built environment may be found in Jönsson (2000) and Forsberg & von Malmborg (2004).

As already referred, this document focuses on LCA and, in particular, its application to steel structures. In the following sub-sections, the normative framework for LCA is introduced. First, the international standards ISO 14040 (2006) and ISO 14044 (2006), establishing the general framework for LCA, are presented followed by the new European standards for the sustainability of construction works. It is noted that while the former have a general application, the European standards focuses on the assessment of buildings and other construction works.

7.2.2 Normative framework for LCA

7.2.2.1 Introduction

The International Standards ISO 14040 (2006) and 14044 (2006) specify the general framework, principles and requirements for conducting and reporting life cycle assessment studies. Regarding these standards, life cycle assessment shall include definition of goal and scope, inventory analysis, impact assessment, and interpretation of results. As represented in Figure 7.2, the various phases are interrelated and sometimes an iterative procedure is necessary in order to fulfil the aim and goal of the study. The different stages are detailed in the following sub-sections

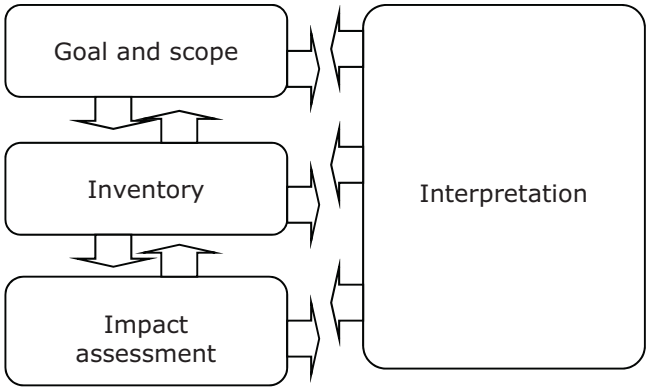

Figure 7.2 Normative framework for LCA (ISO 14044:2006)

7.2.2.2 Definition of goal and scope

The goal of an LCA study shall clearly state the intended application, the reasons for carrying out the study and the intended audience, i.e. to whom the results of the study are intended to be communicated.

In the scope of an LCA Study the main issues to be considered and clearly described are the functional unit and the system boundaries.

Function and functional unit

The scope of an LCA study shall clearly specify the functions of the system being studied. A functional unit is a measure of the performance of the functional outputs of the product system.

The primary purpose of a functional unit is to provide a reference to which the inputs and outputs are related. This reference is necessary to ensure comparability of LCA results. Comparability of results is particularly critical when different systems are being assessed to ensure that such comparisons are made on a common basis.

System boundaries

The system boundaries determine which unit process shall be included within the LCA. For a generic material, a LCA covers all stages from raw material production to end-of-life, as illustrated in Figure 7.3.

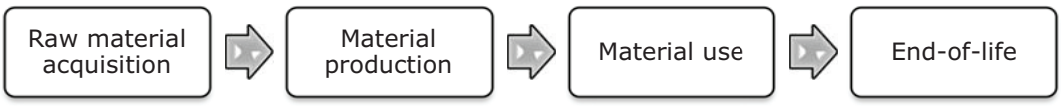

Figure 7.3 Processes included in a LCA of a generic material

When the LCA covers only the initial stages of material production the LCA is called a cradle-to-gate analysis. If the complete cycle is addressed (from raw material production to end-of-life) than the analysis is called a cradle-to-grave analysis. When recycling processes are considered in the end-of-life and the secondary materials avoid the production of new materials than the analysis is often called a cradle-to-cradle analysis.

Several factors determine the system boundaries, including the intended application of the study, the assumptions made, cut-off criteria, data and cost constraints, and the intended audience.

The selection of inputs and outputs, the level of aggregation within a data category, and the modelling of the system should be modelled in such a manner that inputs and outputs at its boundaries are elementary flows.

Data quality

In order to fulfil the goal and the scope of the analysis, the following requirements are indicated in ISO 14044:

- time-related coverage: age of data and the minimum length of time over which data should be collected;
- geographical coverage: geographical area from which data for unit processes should be collected to;
- technology coverage: specific technology or technology mix;

- precision: measure of the variability of the data values for each data expressed (e.g. variance);
- completeness: percentage of flow that is measured or estimated;
- representativeness: qualitative assessment of the degree to which the data set reflects the true;
- consistency: qualitative assessment of whether the study methodology is applied uniformly to the various;
- reproducibility: qualitative assessment of the extent to which information about the methodology and data;
- values would allow an independent practitioner to reproduce the results reported in the study;
- uncertainty of the information (e.g. data, models and assumptions).

7.2.2.3 Life cycle inventory analysis

Inventory analysis involves data collection and calculation procedures to quantify relevant inputs and outputs of a product system. These inputs and outputs may include the use of resources and releases to air, water and land associated with the system.

The qualitative and quantitative data for inclusion in the inventory shall be collected for each unit process that is included within the system boundaries.

Data collection can be a resource - intensive process. Practical constraints on data collection should be considered in the scope and documented in the study report.

7.2.2.4 Life cycle impact assessment

General calculation method

The impact assessment phase of LCA is aimed at evaluating the significance of potential environmental impacts using the results of the life cycle inventory analysis. In general, this process involves associating inventory data with specific environmental impacts, and is made of two parts:

(i) mandatory elements, such as classification and characterization;

(ii) optional elements, such as normalization, ranking, grouping and weighting.

The classification implies a previous selection of appropriate impact categories, according to the goal of the study, and the assignment of LCI results to the chosen impact categories. Characterization factors are then used representing the relative contribution of a LCI result to the impact category indicator result. According to this method impact categories are linear functions, i.e. characterization factors are independent of the magnitude of the environmental intervention, as given by Eqn. (7.1):

$$impact_{cat} = \sum_i m_i \times charact\_factor_{cat,i} \tag{7.1}$$

where m_i is the mass of the inventory flow i and $charact\_factor_{cat,\,i}$ is the characterization factor of inventory flow i for the impact category.

In relation to the optional steps in LCA, normalization is usually needed to show to what extend an impact category has a significant contribution to the overall environmental impact. In the weighting step the normalized result of each impact category is assigned a

numerical factor according to its relative importance. Weighting is based on value-choices rather than natural sciences, thus the ISO standard 14044 distinguishes between internal and external applications, and if results are intended to be compared and presented to the public, then weighting should not be used.

Grouping is another optional step of life cycle assessment in which impact categories are aggregated into one or more sets. In this case, according to ISO 14044, two possible procedures can be used: sorting of the category indicators on a nominal basis and ranking of the category indicators on an ordinal scale.

This document focuses on the mandatory steps of LCA; therefore, the optional elements referred above are not further addressed in this text.

Calculation of potential environmental impacts

The aim of LCA is to assess the potential environmental impacts associated with identified inputs and releases. In the following paragraphs a brief introduction to the most common environmental categories in LCA is provided in the following paragraphs.

i) Global warming potential (GWP)

The "Greenhouse effect" is due to the Infrared (IR) active gases, which are naturally present in the Earth's atmosphere (e.g. H_2O, CO_2 and O_3), that absorb the terrestrial (infrared) energy (or radiation) leaving the Earth and reflect some of this heat back to earth, contributing to warm the surface and the lower atmosphere.

The concentration of these gases, also known as Green House Gases (GHG), has been increasing since the industrial period, and is enhancing the natural Earth's greenhouse effect, causing a temperature rise at the Earth's surface and giving rise to concern over potential resultant climate changes.

Not all GHG are alike. While CO_2 is the most ubiquitous GHG, there are a number of other gases which contribute to climate change in the same way as CO2. The effect of different GHG is reported using Global Warming Potential (GWP).

GWP is a relative measure of the amount of CO_2 which would need to be released to have the same radiative forcing effect as a release of 1 kg of the GHG over a particular time period. GWP is therefore a way of quantifying the potential impact on global warming of a particular gas.

GWPs were calculated by the Intergovernmental Panel on Climate Change (IPCC, 2007) for three time horizons of 20, 100 and 500 years and they are indicated in Table 7.1 for three of the most important greenhouse gases and for the three time horizons.

Table 7.1 GWPs for given time horizons (in kg CO_2 eq./kg) (IPCC, 2007)

	20 years	100 years	500 years
Carbon Dioxide (CO_2)	1	1	1
Methane (CH_4)	62	25	7
Nitrous oxide (N_2O)	275	298	156

Hence, according to Eqn. (7.2), the determination of the indicator "Global Warming" is given by,

$$Global\ Warming = \sum_i GWP_i \times m_i \tag{7.2}$$

where, m_i is the mass of substance *i* released (in kg). This indicator is expressed in *kg of CO_2 equivalents*.

ii) Ozone Depletion Potential (ODP)

Ozone-depleting gases cause damage to stratospheric ozone or the "ozone layer" by releasing free radical molecules which breakdown ozone (O_3).

Damage to the ozone layer reduces its ability to prevent ultraviolet (UV) light entering the earth's atmosphere, increasing the amount of carcinogenic UVB light hitting the earth's surface. This in turn results in health problems in humans such as skin cancer or cataracts and sun related damage to animals and crops.

The major ozone depleting gases are CFCs, HCFCs and halons.

Growing concern in the 1980s led to world-wide efforts to curb the destruction of the ozone layer, culminating in the Montreal protocol which banned many of the most potent ozone depleting gases.

Ozone depletion potential is expressed as the global loss of ozone due to a substance compared to the global loss of ozone due to the reference substance CFC-11. This gives ODP a reference unit of kg chlorofluorocarbon-11 (CFC-11) equivalent. The characterization model has been developed by the World Meteorological Organization (WMO) and defines the ozone depletion potential of different gases. Hence, OPDs, assuming a steady-state, are indicated in Table 7.2 for selected substances (Guinée et al., 2002).

Table 7.2 *OPDs* for some substances (in kg CFC-11 eq./kg) (Guinée et al., 2002)

	Steady-state (t ≈ ∞)
CFC-11	1
CFC-10	1,2
Halon 1211	6,0
Halon 1301	12,0

Hence, according to Eqn. (7.3), the determination of the indicator "Global Warming" is given by,

$$Ozone\ \ Depletion = \sum_i ODP_i \times m_i \tag{7.3}$$

where, m_i is the mass of substance *i* released (in kg). This indicator is expressed in *kg of CFC-11 equivalents*.

iii) Acidification Potential (AP)

Acidification is the process where air pollution (mainly ammonia (NH_3), sulphur dioxide (SO_2) and nitrogen oxides (NO_x)) is converted into acid substances. Acidifying compounds emitted into the atmosphere are transported by wind and deposit as acidic particles or acid rain or snow. When this rain falls, often a considerable distance from the original source of the gas, it causes ecosystem damage of varying degrees, depending upon the nature of the landscape ecosystems.

Acidification potential is measured using the ability of a substance to release H+ ions, which is the cause of acidification, or it can be measured relative to an equivalent release of SO_2.

The characterisation factors adopted in this work are based in the model RAINS-LCA, which takes fate, background depositions and effects into account (Guinée et al., 2002). Thus, the average European characterisation factors for acidification are represented in Table 7.3.

Table 7.3 *Acidification potentials* (in kg SO_2 eq./kg) (Guinée et al., 2002)

	Ammonia (NH_3)	**Nitrogen Oxide (NO_x)**	**Sulphur Dioxide (SO_2)**
APi	1,60	0,50	1,20

Thus, the determination of the indicator acidification is given by Eqn. (7.4),

$$Acidification = \sum_i AP_i \times m_i \tag{7.4}$$

where, m_i is the mass of substance *i* released (in kg). This indicator is expressed in *kg of SO_2 equivalents.*

iv) Eutrophication Potential (EP)

Nutrients, such as nitrates and phosphates, are usually added to the soil through fertilization to stimulate the growth of plants and agricultural products. These nutrients are essential for life, but when they end up in sensitive natural water or land areas, this unintended fertilization may result in overproduction of plants or algae, which, in turn, can smother other organisms when they die and begin to decay. Therefore, Eutrophication or nutrient enrichment can be classified as the over-enrichment of water courses. Its occurrence can lead to damage of ecosystems, increasing mortality of aquatic fauna and flora and to loss of species dependent on low-nutrient environments. This leads to an overall reduction in the biodiversity of these environments and has knock-on effects on non-aquatic animals and humans who rely on these ecosystems.

Eutrophication is measured using the reference unit of kg nitrogen or phosphate equivalents. As such it is a measure of the extent to which a substance in the water causes the proliferation of algae, with nitrogen or phosphate as the reference substance. The major contributors to eutrophication are nitrogen compounds, such as nitrates, ammonia, nitric acid and phosphoric compounds including phosphates and phosphoric acid.

Taking phosphate as the reference substance, the characterization factors for selected substances are indicated in Table 7.4 (Guinée et al., 2002).

Table 7.4 Eutrophication potentials (in kg PO_4^{3-} eq./kg) (Guinée et al., 2002)

	Ammonia (NH_3)	**Nitrogen Oxide (NO_x)**	**Nitrate (N)**	**Phosphate (P)**
Epi	0,35	0,13	0,10	1,00

Hence, the eutrophication indicator is given by Eqn. (7.5),

$$Eutrophication = \sum_i EP_i \times m_i \tag{7.5}$$

where, m_i (kg) is the mass of substance *i* released to the air, water or soil. This indicator is expressed in *kg of* PO_4^{3-} *equivalents*.

v) Photochemical Ozone Creation Potential (POCP)

In atmospheres containing nitrogen oxides (NOx), a common pollutant and volatile organic compounds (VOCs), ozone and other air pollutants can be created in the presence of sunlight. Although ozone is critical in the high atmosphere to protect against ultraviolet (UV) radiation, low level ozone is implicated in impacts as diverse as crop damage and increased incidence of asthma and other respiratory complaints.

The most common manifestation of the effects of high levels of POCP-contributing gases is in the summer smog seen over large cities such as Los Angeles or Beijing. The principal source of NOx emissions is fuel combustion while VOCs are commonly emitted from solvents, which are heavily used in paints and coatings.

The POCP impact category is a measure of the relative ability of a substance to produce ozone in the presence of NOx and sunlight. POCP is expressed using the reference substance ethylene. Characterization factors for POCP have been developed using the United Nations Economic Commission for Europe (UNECE) trajectory model.

POCPs were calculated for two scenarios (Guinée et al., 2002):

- a scenario with a relatively high background concentration of NOx;
- a scenario with a relatively low background concentration of NOx.

These two characterization factors are indicated in Table 7.5 for some selected substances.

Table 7.5 *POCPs* for different concentration of NO_x and for some substances (in kg C_2H_4 eq./kg) (Guinée et al., 2002)

	High-NO_x POCPs	**Low-NO_x POCPs**
Acetaldehyde (CH_3CHO)	0,641	0,200
Butane (C_4H_{10})	0,352	0,500
Carbon monoxide (CO)	0,027	0,040
Ethyne (C_2H_2)	0,085	0,400
Methane (CH_4)	0,006	0,007
Nitrogen oxide (NO_x)	0,028	no data
Propene (C_3H_6)	1,123	0,600
Sulphur oxide (SO_x)	0,048	no data
Toluene ($C_6H_5CH_3$)	0,637	0,500

Thus, the determination of the indicator Photo-oxidant formation is given by Eqn. (7.6),

$$Photo-oxidant \quad formation = \sum_i POCP_i \times m_i \tag{7.6}$$

where, m_i is the mass of substance *i* released (in kg). This indicator is expressed in *kg of ethylene (C_2H_4) equivalents*.

vi) Abiotic Depletion Potential (ADP)

Abiotic depletion indicators aim to capture the decreasing availability of non-renewable resources as a result of their extraction and underlying scarcity. Two types of indicators are herein considered:

- Abiotic Depletion Elements, addressing the extraction of scarce elements (and their ores);
- Abiotic Depletion Energy/Fossil Fuels, addressing the use of fossil fuels as fuel or feedstock.

The Abiotic Depletion Potential for elements ($ADP_{elements}$) is determined for each extraction of elements based on the remaining reserves and rate of extraction. The ADP is based on the equation Production/Ultimate Reserve which is compared to the reference case, Antimony (Sb) (Guinée et al., 2002). Different measures use the economic or ultimate reserve within the earth's crust.

Therefore, the Abiotic Depletion Potential (Elements) of resource *i* (ADP_i) is given by the ratio between the quantity of resource extracted and the recoverable reserves of that resource, expressed in kg of the reference resource, Antimony, and the characterization factors for some selected resources are indicated in Table 7.6.

Table 7.6 Abiotic depletion potentials for some elements (in Sb eq./kg) (Guinée et al., 2002)

Resource	ADP element
Aluminium	1,09E-09
Cadmium	1,57E-01
Copper	1,37E-03
Iron	5,24E-08
Lead	6,34E-03

Thus, the determination of the indicator Abiotic Depletion (Elements) is given by Eqn. (7.7),

$$Abiotic\ \ Depletion = \sum_i ADP_i \times m_i \tag{7.7}$$

where, m_i is the quantity of resource *i* extracted (in kg). This indicator is expressed *in kg of antimony* (the reference resource).

Fossil Fuels were originally measured in the same way, but since 2010 they have been calculated slightly differently. In this case, an absolute measure is considered, based on the energy content of the fossil fuel (Guinée et al., 2002). This does not take into account the relative scarcity of different fossil fuels as fossil fuels are largely transferable resources, but in reality these only vary by 17% between coal (the most common) and gas (the most scarce). The indicator Abiotic Depletion Fossil is expressed in MJ.

7.2.2.5 Life cycle interpretation

Interpretation is the last step of LCA, in which the findings from the inventory analysis and the impact assessment are combined together. The main aim of this stage is to formulate the conclusions that can be drawn from the results of the LCA. In addition, the

results of previous stages of LCA and the choices made during the entire process should be analyzed, namely the assumptions, the models, the parameters and data used in the LCA should be consistent with the Goal and Scope of the study.

7.2.2.6 Illustrative example

In order to illustrate the different steps of life cycle assessment described in the previous paragraphs, a small example is herein provided.

1st step) Inventory analysis

For the production of 1 kg of a generic insulation material, the following emissions (see Table 7.7) were collected in the inventory stage.

Table 7.7 Emissions collected from the production of 1 kg of an insulation material

Emissions	Value (in kg)
carbon monoxide (CO)	0,12
carbon dioxide (CO_2)	0,60
ammonia (NH_3)	0,01
methane (CH_4)	0,05
nitrogen oxides (NO_x)	1,02
phosphorus (P)	0,35
sulfur dioxide (SO_2)	0,10

2nd step) Impact assessment

For the impact assessment stage the following environmental categories are selected:

(i) global warming potential (GWP);

(ii) acidification potential (AP);

(iii) eutrophication potential (EP).

The characterization factors of each emission for each environmental category are provided in Table 7.8.

Table 7.8 Characterization factors for selected environmental categories

	GWP (kg CO_2 eq.)	AP (kg SO_2 eq.)	EP (kg PO_4^{3-} eq.)
carbon monoxide (CO)	1,53	-	-
carbon dioxide (CO_2)	1,00	-	-
ammonia (NH_3)	-	1,60	0,35
methane (CH_4)	23,00	-	-
nitrogen oxides (NO_x)	-	0,50	0,13
phosphorus (P)	-	-	3,06
sulfur dioxide (SO_2)	-	1,20	-

Hence, the results of each environmental category are obtained from the product of each contributing emission by its respective characterization factor (e.g., for GWP: 0,12 x 1,53 + 0,60 x 1,00 + 0,05 x 23 = 1,93 kg CO_2 eq.) leading to the results indicated in Table 7.9.

Table 7.9 Final results of the selected environmental Indicators

GWP (kg CO_2 eq.)	AP (kg SO_2 eq.)	EP (kg PO_4^{3-} eq.)
1,93	0,65	1,21

7.2.3 European standards for LCA of construction works

7.2.3.1 Sustainability of construction works

The European Committee for Standardization (CEN) was mandated in 2005 for the development of harmonized, horizontal (i.e. applicable to all products and building types) approach for the measurement of embodied and operational environmental impacts of construction products and whole buildings, taking into account a lifecycle perspective.

CEN-TC 350 develops standards, technical reports and technical specifications to provide methodologies and indicators for the sustainability assessment of buildings. The work developed in TC350 is organized in different levels (framework, building and product levels), as illustrated in Table 7.10. In addition, standards are developed to cover environmental, economic and social aspects.

Table 7.10 Working program of CEN TC350

	General framework for sustainability assessment of buildings		
Framework level	Framework of environmental performance	Framework of social performance	Framework of economic performance
Building level	Assessment of environmental performance	Assessment of social performance	Assessment of economic performance
Product level	Environmental product declarations		

This chapter focusses on the environmental assessment. Therefore, only the standards developed for the environmental assessment are hereafter referred: EN 15804 (2012) and EN 15978 (2011), respectively for the assessment at the product level and at the building level.

7.2.3.2 Product level

EN 15804 (2012) provides core category rules enabling the production of Environmental Product Declarations (EPDs) for any construction product and construction service. EPDs are type III environmental declarations according to ISO 14025 (2006) that provide quantified environmental data of products, based on life cycle analysis and other relevant information.

A brief overview of the methodology provided in the standard is given in the following paragraphs focusing on the following key aspects: functional unit, life cycle stages and

environmental indicators. For a complete overview of the methodology the reading of the standard is advised.

Functional unit and declared unit

A functional unit is a measure of the performance of the functional outputs of the product system. It provides a reference by which all input and output data are normalized. When the precise function of the product at the building level is not known then a declared unit is used instead. Examples of a declared unit in EPDs are for instance: 1 kg of steel in sections, 1 cubic metre of concrete, etc.

However, any comparative assertions shall be based on the functional unit.

Life cycle stages

The system boundaries establish the scope of the life cycle analysis, i.e., determines the processes that are taken into account in the analysis. In this standard the life cycle is represented by a modular concept as illustrated in Table 7.11.

Table 7.11 Modules of a building life cycle (EN 15804, 2012)

Product Stage			**Constru. stage**		**Use stage**							**End-of-life stage**				
Raw material supply	Transport	Manufacturing	Transport	Construction process	Use	Maintenance	Repair	Replacement	Refurbishment	Operational energy use	Operational water use	Demolition	Transport	Waste processing	Disposal	Reuse/Recycling potential
A1	A2	A3	A4	A5	B1	B2	B3	B4	B5	B6	B7	C1	C2	C3	C4	D

The production stage includes modules A1 to A3, the construction stage includes modules A4 and A5, the use stage includes modules B1 to B7, the end-of-life stage modules includes C1 to C4, and module D includes the benefits and loads beyond the system boundary. In the following paragraphs a brief description of each stage and corresponding information modules is provided.

i) Product stage

The product stage includes the information modules A1 to A3. The system boundary with nature is set to include those processes that provide the material and energy inputs into the system and the following manufacturing, and transport processes up to the factory gate as well as the processing of any waste arising from those processes. This stage includes:

- ✓ A1 - Extraction and processing of raw materials; reuse of products or materials from a previous product system; processing of secondary materials used as input for manufacturing the product;
- ✓ A2 - Transportation up to the factory gate and internal transport;

- ✓ A3 - Production of ancillary materials, manufacturing of products and by-products; and manufacturing of packaging.

ii) Construction stage

The construction process stage includes the information modules for:

- ✓ A4 - Transportation from the production gate to the construction site;
- ✓ A5 - Installation of the product into the building including manufacture and transportation of ancillary materials and any energy or water required for installation or operation of the construction site. It also includes on-site operations to the product.

iii) Use stage

The use stage includes two types of information modules. Modules related to the building fabric (modules B1-B5) and modules related to the operation of building (modules B6-B7):

- ✓ B1 - Use of the installed product in terms of any emissions to the environment arising from components of the building and construction works during their normal (i.e. anticipated) use;
- ✓ B2 - Maintenance covers the combination of all planned technical and associated administrative actions during the service life to maintain the product installed in a building in a state in which it can perform its required functional and technical performance, as well as preserve the aesthetic qualities of the product;
- ✓ B3 - Repair covers a combination of all technical and associated administrative actions during the service life associated with corrective, responsive or reactive treatment of a construction product or its parts installed in the building to return it to an acceptable condition in which it can perform its required functional and technical performance;
- ✓ B4 - Replacement covers the combination of all technical and associated administrative actions during the service life associated with the return of a construction product to a condition in which it can perform its required functional or technical performance, by replacement of a whole construction element;
- ✓ B5 - Refurbishment covers the combination of all technical and associated administrative actions during the service life of a product associated with the return of a building to a condition in which it can perform its required functions;
- ✓ B6 - Energy use to operate building integrated technical systems, together with its associated environmental aspects and impacts including processing and transportation of any waste arising on site from the use of energy;
- ✓ B7 - Operational water use by building integrated technical systems, together with its associated environmental aspects and impacts considering the life cycle of water including production and transportation and waste water treatment.

iii) End-of-life stage

The end-of-life stage of the construction product includes all outputs that have reached the "end-of-waste" state, resulting from dismantling, deconstruction or demolition of the building. The end-of-life stage includes the optional Information modules:

- ✓ C1 - Deconstruction, including dismantling or demolition, of the product from the building, including initial on-site sorting of the materials;
- ✓ C2 - Transportation of the discarded product as part of the waste processing, e.g. to a recycling site and transportation of waste e.g. to final disposal;
- ✓ C3 - Waste processing e.g. collection of waste fractions from the deconstruction and waste processing of material flows intended for reuse, recycling and energy recovery.
- ✓ C4 - Waste disposal including physical pre-treatment and management of the disposal site.

iv) Benefits and loads beyond the product system boundary

Information module D includes all the net benefits or loads resulting from reusable products, recyclable materials and/or useful energy carriers leaving a product system e.g. as secondary materials or fuels.

Types of life cycle analyses

Depending on the information modules included in the system boundary, different types of life cycles analyses are considered.

When only information modules A1 to A3 are taken into account the LCA is called "cradle to gate".

On the other side, a "cradle to gate with options" is a LCA that takes into account information modules A1 to A3 plus optional modules such as end-of-life information modules (C1 to C4) and/or information module D.

Finally, a "cradle to grave" analysis is a LCA taking into account all information modules A1 to C4. In this case, module D may also be taken into account.

Life Cycle Impact Assessment

For the stage of life cycle impact assessment, two types of environmental categories are considered according to EN 15804: environmental indicators describing environmental impacts and environmental indicators describing input and output flows. Both types of indicators are indicated in the following paragraphs.

i) Indicators describing environmental impact

Six indicators are provided for the description of the impacts on the natural environmental, which are indicated in Table 7.12.

Table 7.12 Indicators describing environmental impacts (EN 15804, 2012)

Indicator	Unit
Global warming potential (GWP)	kg CO_2 equiv
Depletion potential of the stratospheric ozone layer (ODP)	kg CFC 11 equiv
Acidification potential of land and water (AP)	kg SO^{2-} equiv
Eutrophication potential (EP)	kg $(PO_4)^{3-}$ equiv
Formation potential of tropospheric ozone photochemical oxidants (POCP)	kg Ethene equiv
Abiotic Resource Depletion Potential for elements (ADP_elements)	kg Sb equiv
Abiotic Resource Depletion Potential of fossil fuels (ADP_fossil)	MJ

These indicators were already presented in the previous section of this document.

ii) Indicators describing input and output flows

Additional indicators are deemed for describing inputs and output flows. Therefore, indicators describing the resource use are indicated in Table 7.13. These indicators describe the use of renewable and non-renewable primary energy and water resources and they are calculated directly from input flows of the LCI.

Table 7.13 Indicators describing resource use (EN 15804, 2012)

Indicator	Unit
Use of renewable primary energy excluding energy resources used as raw material	MJ, net calorific value
Use of renewable primary energy resources used as raw material	MJ, net calorific value
Use of non-renewable primary energy excluding primary energy resources used as raw material	MJ, net calorific value
Use of non-renewable primary energy resources used as raw material	MJ, net calorific value
Use of secondary material	kg
Use of renewable secondary fuels	MJ
Use of non-renewable secondary fuels	MJ
Use of net fresh water	m^3

Also directly based on the input flows of the LCI are the indicators describing waste categories and output flows. The former are indicated in Table 7.14 and the latter in Table 7.15. Moreover, for the quantification of these indicators, scenarios are established for the appropriate processes and stages.

Table 7.14 Indicators describing waste categories (EN15804, 2012)

Indicator	Unit
Hazardous waste disposed	kg
Non-hazardous waste disposed	kg
Radioactive waste disposed	kg

Table 7.15 Indicators describing the output flows leaving the system (EN15804, 2012)

Indicator	Unit
Components for re-use	kg
Materials for recycling	kg
Materials for energy recovery (not being waste incineration)	kg
Exported energy	MJ for each energy carrier

7.2.3.3 Building level

EN 15978 (2011) provides calculation rules for the assessment of the environmental performance of new and existing buildings based on a life cycle approach. It is intended to support the decision-making process and documentation of the assessment of the environmental performance of a building.

The methodology provided in this standard follows the category rules defined in EN 15804. In the following paragraphs only a few aspects differing from EN 15804 are referred. For a complete overview of the methodology the reading of the standard is recommended.

Functional equivalent

The functional equivalent is defined as the "quantified functional requirements and/or technical requirements for a building or an assembled system (part of works) for use as a basis for comparison". Hence, comparison between buildings or systems will only be acceptable if the functions provided are the same. At least the following aspects shall be included in the functional equivalent of a building:

(i) building typology (e.g. residential, office, etc.);

(ii) pattern of use;

(iii) relevant technical and functional requirements; and

(iv) required service life.

Life cycle stages and impact assessment

According to this standard, the environmental assessment "includes all upstream and downstream processes needed to establish and maintain the function(s) of the building".

The information linked to the products integrated in the building is required to assess the environmental performance at the building level. This information should be consistent, and therefore, the same information modules of EN 15804 are taken into account in EN 15978.

Likewise, the life cycle impact assessment at the building level is based on the indicators from Table 7.12 to Table 7.15.

7.3 Sustainability and LCA of steel structures

7.3.1 Production of steel

Generally there are two different routes for steel manufacture (Worldsteel, 2011): the primary production and the secondary production.

The primary production generally refers to the manufacture of iron (hot metal) from iron ore in a blast furnace (BF), which is subsequently processed in the basic oxygen furnace (BOF) to make steel.

The secondary process or recycling route is typically the electric arc furnace (EAF) process, which converts scrap into new steel by remelting old steel.

However, as illustrated in Figure 7.4, primary steel production is not exclusive to the BF/BOF route and similarly secondary steel production is not exclusive to the EAF. Hence, both the EAF and BF/BOF processes produce primary and secondary steel.

The subsequent steelmaking processes do not depend on the production route, i.e. they are common to both routes.

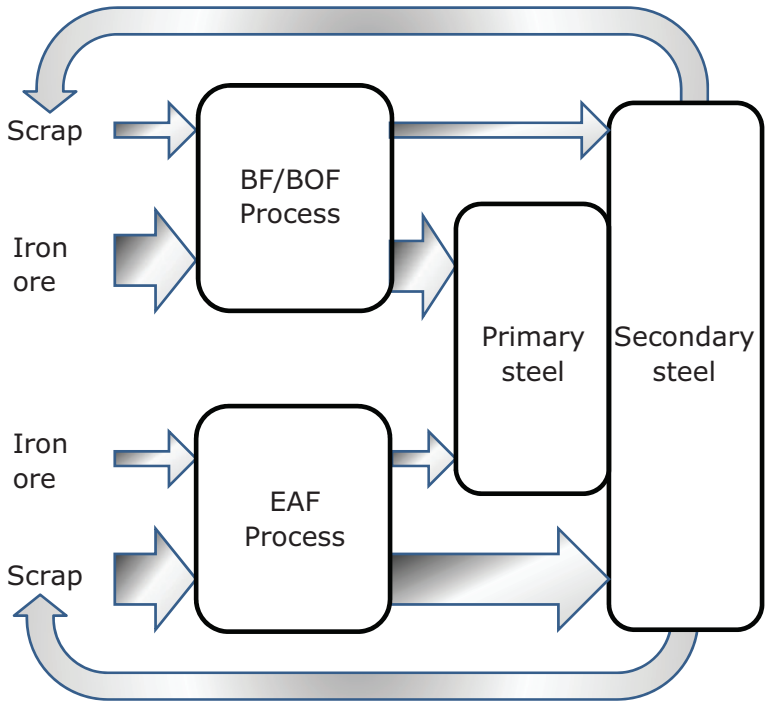

Figure 7.4 Primary/secondary steel production (based in (Worldsteel, 2011))

Therefore, in both processes scrap is an input and an output of the steel making process, and the methodology to address scrap allocation in LCA is described in the next sub-section.

7.3.2 Allocation of recycling materials and Module D

7.3.2.1 Introduction

Steel is 100% recyclable and scrap can be converted to the same quality of steel depending upon the metallurgy and recycling route (Worldsteel, 2011). Therefore, in the end-of-life of a steel structure, the structure is most probably dismantled and steel is sent for recycling or reusing (partially or completely). According to data from the Steel Recycling Institute (2009), in North America, the recycling rate of structural steel is about 97,5%. Graphs represented in Figure 7.5, show the trend of the recycling rates of structural steel and reinforcement steel in the construction sector, respectively.

The reuse and recycling of steel is a multi-functionality issue, requiring the use of an allocation process, as described in the following text.

7.3.2.2 Allocating processes

Most industrial processes are multifunctional, i.e., their output entails more than one product and the inputs for the production of products often include intermediate or discarded products. An allocation problem occurs when an appropriate decision is needed in order to allocate the input/output flows to the functional unit provided by the product system under study.

Allocation is defined in ISO 14040 (2006) as "partitioning the input or output flows of a process or a product system between the product system under study and one or more other product system". Thus, an allocation process addresses the partition of flows between unit processes or product systems.

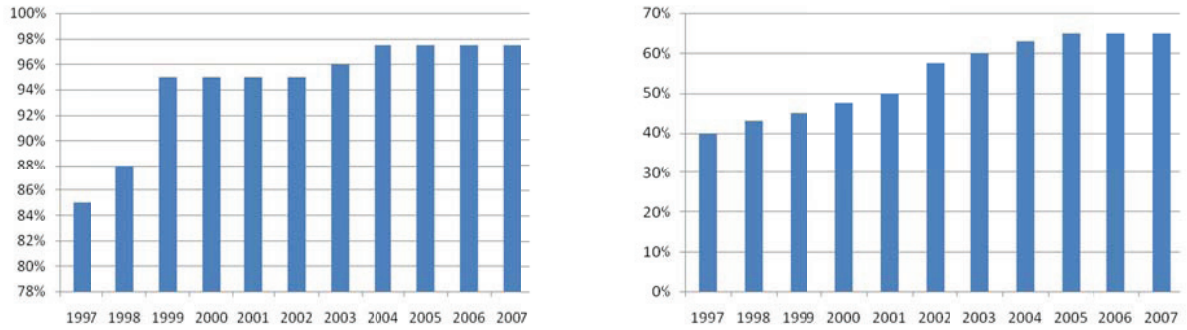

(a) (b)

Figure 7.5 Recycling rates of (a) structural steel and (b) reinforcement steel (Steel Recycling Institute, 2009)

According to ISO 14044 (2006), allocation should be avoided either by dividing the unit process to be allocated into two or more sub-processes and collecting the input and output data related to these sub-processes or by expanding the product system to include the additional functions related to the by-products (system expansion).

System expansion includes the avoided burden approach, which eliminates surplus-functions from the multifunctional process by subtracting equivalent mono-functional processes to obtain a mono-functional process.

When neither subdivision of processes nor system expansion are feasible for the scope and goal of the study, then allocation is unavoidable. In this case, two alternatives are recommended by ISO 14044 (2006): (i) the partition of inputs and outputs of the system is based on physical (or chemical or biological) causal relationships; or (ii) the allocation is based on other relationships (e.g. economic value of the products).

The consideration of reuse and recycling of materials is a multi-functionality issue, implying the use of allocation processes. The allocation principles and procedures mentioned above also apply to recycling and reuse situations, although in this case, the changes in the inherent properties of materials shall be taken into consideration when choosing the allocation procedure to be used (ISO 14044, 2006).

In this case, three main situations may occur (Werner, 2005):

i) material's inherent properties are not changed over the considered product system and the material is to be reused in the same application;

ii) material's inherent properties are changed over the considered product system and the material is to be reused in the same application;

iii) material's inherent properties are changed over the considered product system and the material is to be used in other applications.

In the first case, there is a closed-loop situation in which the substitution of primary material is assumed to be complete and therefore, no environmental burdens from primary material production or final disposal are allocated to the product system. The second case corresponds to an open-loop approach assuming a closed-loop situation. In this case, the changed material properties are considered irrelevant and recycling is addressed as a closed-loop situation. Finally, in the last case, there is an open-loop situation where the substitution of primary material is assumed to be partial. In this case, environmental burdens due to primary material production or final disposal have to be partially allocated to the system under study.

According to ISO 14044 (2006), in the case of a closed-loop situation allocation is avoided since the use of secondary material replaces the use of raw materials.

7.3.2.3 Avoiding scrap allocation

During the life cycle of steel, scrap arises from the manufacture phase, the final processing phase and the end-of-life phase (see Figure 7.6). Thus, an allocation procedure has to be taken into account for scrap outputs from the whole life system. Furthermore, as already described, steel is processed via different production routes, and the allocation of scrap inputs to steelmaking is another issue to be considered.

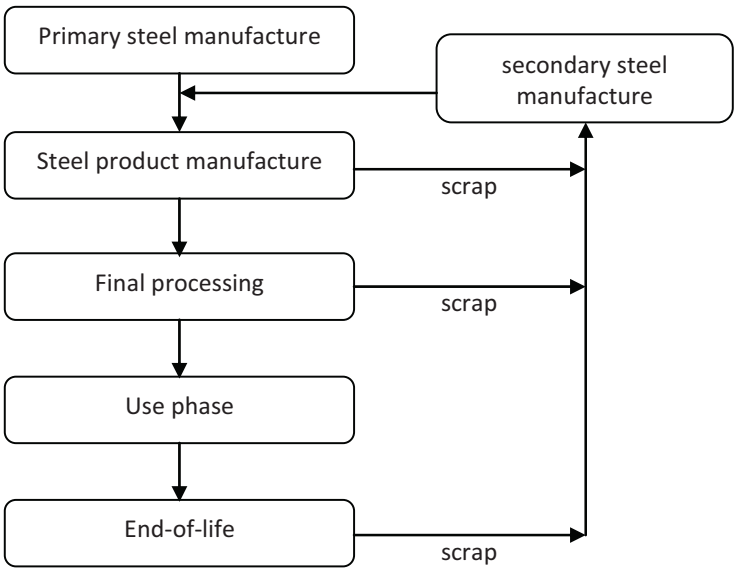

Figure 7.6 System boundary of LCI including end-of-life data on scrap (Worldsteel, 2011)

Finally, steel can be recycled or reused many times and an appropriate allocation method is needed to address multiple recycling and reuse of steel components.

Therefore, the adopted methodology to address the allocation problem of steel is the closed material loop recycling approach developed by the World Steel Association (Worldsteel, 2011). This methodology was developed in order to generate LCI data of steel products, accounting for end-of-life recycling. The adoption of a closed-loop approach is justified by the fact that scrap is re-melted to produce new steel with little or no change in its inherent properties. In this case, following the guidance of ISO standard 14044, the need for allocation is avoided since the use of secondary material replaces the use of raw (primary) materials.

As already explained, steel may be produced by the Blast Furnace (BF) route and by the Electric Arc Furnace (EAF). The main difference between the two routes is the input of scrap in the steelmaking process.

Thus, considering the two main routes for steel processing, and assuming the LCI data for steel production via the BF route (assuming 100% raw material) given by X_{pr} and the LCI data for steel production via the EAF route (assuming 100% secondary steel) given by X_{re}, then the LCI data associated with scrap is given by Eqn. (7.8) (Worldsteel, 2011):

$$LCI_{scrap} = Y\left(X_{pr} - X_{re}\right) \tag{7.8}$$

where, Y is the metallic yield, representing the efficiency of the secondary process in converting scarp into steel. According to the World Steel association (Worldsteel, 2011), about 1,05 kg of scrap is required to produce 1 kg of secondary steel.

Considering the BF route, assuming 100% input of raw material and a recovery rate (fraction of steel recovered as scrap over the life cycle of a steel product) of RR, then, at the end of the life-cycle, the net scrap produced is given by RR. Therefore, the LCI for 1 kg of steel, including the end of life, is given by the LCI for primary manufacture with a credit for the scrap produced, as given by Eqn. (7.9):

$$LCI = X_{pr} - RR\left[Y\left(X_{pr} - X_{re}\right)\right] \tag{7.9}$$

On the other end, assuming that 1 kg of secondary steel is used to produce new steel via the EAF route, and at the end of life RR kg of steel is recovered for recycling, then, the net scrap consumed is given by (1/Y – RR). In this case, the LCI for 1 kg of steel, including the end of life, is given by the LCI for secondary manufacture with a debit for the scrap consumed, as expressed by Eqn. (7.10):

$$LCI = X_{re} + \left(1/Y - RR\right)\left[Y\left(X_{pr} - X_{re}\right)\right] \tag{7.10}$$

Rearranging Eqn. (7.10) it leads to Eqn. (7.9), indicating that the LCI of the system does not depend upon the source of the material. It depends on the recycling ratio of steel at the end of life and the process yield associated with the recycling process. Hence, Eqn. (7.9) allows allocating steel scrap independently of the production route of steel.

The previous expressions were derived assuming 100% primary production and 100% secondary production. In reality, steel products produced via the primary route may also include some scrap consumption and products from the EAF may also include a small percentage of raw materials. In this case, the debit or credit given by Eqn. (7.8) may be re-written as expressed by Eqn. (7.11):

$$LCI_{scrap} = (RR - S) \times Y\left(X_{pr} - X_{re}\right) \tag{7.11}$$

where, *(RR - S)* represents the net scrap at the end-of-life. Considering the LCI data of a finished steel product given by *X'*, then the LCI for the product, including the end-of-life recycling, is given by Eqn. (7.12),

$$LCI = X' - \left[\left(RR - S\right) \times Y\left(X_{pr} - X_{re}\right)\right] \tag{7.12}$$

According to the European standards, EN 15804 and EN 15978, the credits or debits given by Eqn. (7.11) are allocated to Module D.

The closed loop recycling approach described in the previous paragraphs is the approach adopted in the tool described in the following sub-section. Hence, Eqn. (7.12) is adopted in the LCA methodology, to produce LCI data for steel products, including recycling at the end-of-life.

The importance of taking into account Module D in the LCA is illustrated in Worked Example 1.

7.3.3 Data and tools for LCA of steel structures

7.3.3.1 EPDs of steel products

One of the main barriers for the realization of a LCA is often the lack of data. Currently there are different databases available (e.g. Ecoinvent (Frischknecht and Rebitzer, 2005), PE Database (GaBi, 2012), etc.), which are usually included in commercial software for LCA. These databases provide generic data of products and services but are often limited, in particular in relation to construction materials.

Therefore, EPDs are a good source of data for LCA. EPDs are usually available, for free, from any registration program for type III environmental declarations. These registration systems verify and register EPDs and keep a library of EPDs and PCRs in accordance with the corresponding standards.

The use of EPDs as input data to perform LCA is illustrated in Worked Example 3.

7.3.3.2 Simplified methodologies for LCA

The construction sector is increasingly subjected to sustainability pressures: environmental product declarations, low energy building, etc. However, stakeholders are not always properly trained to be able to analyse the environmental performances of construction products.

Thermal performances of new buildings have been framed by regulations for a few years, compelling architects to have a good control and knowledge of the use phase of buildings. On the opposite, embodied energy and carbon footprint of materials are less known, but progressively integrated in calls for tenders. Few actors of the sector have the expertise to address both aspects.

Currently there are different tools for LCA and energy calculation of buildings. The tools differ in terms of scope and complexion, but usually required some level of expertise in the field.

In order to enable a simplified assessment of buildings in early stages of design, when usually data available is scarce, two simplified approaches were developed in the aim of the European research project SB_Steel (2014):

(i) A methodology for simplified life cycle approach based on macro-components (Gervásio et al., 2014);

(ii) A methodology for the calculation of the energy needs of a building for space cooling and space heating, which includes the energy need for domestic hot water production (Santos et al., 2014).

Both approaches are based on the principles of the European standards EN 15978 and EN 15804. The former includes the information modules indicated in Table 7.9, except Modules A5, B1, B6 and B7. The latter focusses exclusively in information Module B6.

Both approaches were implemented into software tools in the aim of the European dissemination project LVS^3: *Large Valorisation on Sustainability of Steel Structures*. The methodology based on macro-components was implemented into an application called **Buildings LCA** for mobile phones and tablets, which may be freely downloaded from the AppStore (version for iPhones and iPads) or Google Play (android version). The methodology enabling the calculation of the energy needs of a building was implemented into **AMECO**, a tool developed by ArcelorMittal.

The calculation of the operational energy of buildings, although is an important issue, will not be further addressed in this chapter. The tool used in the worked examples provided in the next section is **Buildings LCA**. Hence, in the following paragraphs a brief description of the tool is provided.

7.3.3.3 LCA based on the macro-components approach

Introduction

The building fabric, external and internal, plays a major role in the behaviour of the building in terms of the energy consumption and environmental burdens. This led the way for the creation of pre-assembled solutions for the main components of the building, i.e., the macro-components. Therefore, macro-components are pre-defined assemblages of different materials that fully compose the same component of a building (Gervásio et al., 2014).

For each building component different solutions were pre-assembled and the model used for the life cycle analysis of building, based on macro-components, is detailed in the following paragraphs.

i) Goal and scope

The goal of the tool is to quantify the environmental impacts of a simple building or building components, using predefined macro-components. Therefore, the approach enables the assessment to be made at two different levels: (a) the product and/or component level; and (b) the building level.

Three different types of LCA may be performed: a cradle to gate, a cradle to gate plus Module D and a cradle to grave (including Module D).

ii) Life Cycle Inventory

Most environmental datasets are provided from the database of GaBi software (2012), except for steel data. Steel datasets are provided by World Steel Association (Worldsteel, 2011) in collaboration with PE International.

iii) Life Cycle Impact Assessment

The environmental categories selected to describe the environmental impacts correspond to the environmental categories recommended in the European standards (EN 15804 and EN 15978) and they are indicated in Table 7.12.

The modular concept of the aforementioned standards was adopted in the approach. Therefore, the output of the life cycle environmental analysis is provided per information module or by the aggregate value of each stage.

The life cycle environmental analysis of each macro-component was performed by GaBi software (2012).

Classification of macro-components

Macro-components were defined for different building components according to the UniFormat classification scheme (2010). The following categories are considered: (A) Substructure, (B) Shell and (C) Interiors. Each main category is further sub-divided. The detailed classification scheme is represented in Table 7.16

Table 7.16 Building component classification scheme (UniFormat, 2010)

(A) Substructure	(A40) Slabs-on-grade	(A4010) Standard slabs-on-grade	
(B) Shell	(B10) Superstructure	(B1010) Floor construction	(B1010.10) Floor structural frame
			(B1010.20) Floor decks, slabs and toppings
		(B1020) Roof construction	(B1020.10) Roof structural frame
			(B1020.20) Roof decks, slabs and sheathing
	(B20) Exterior vertical enclosures	(B2010) Exterior walls	(B2010.10) Ext. wall veneer
			(B2010.20) Ext. wall construction
		(B2020) Exterior windows	
		(B2050) Exterior doors	
	(B30) Exterior horizontal enclosures	(B3010) Roofing	
		(B3060) Horizontal openings	
(C) Interiors	(C10) Interior construction	(C1010) Interior partitions	
	(C20) Interior finishes	(C2010) Wall finishes	
		(C2030) Flooring	
		(C2050) Ceiling finishes	

Within each building component the corresponding macro-components have the same function and have similar properties. The functional unit of each macro-component is 1 m^2 of a building component with similar characteristics, to fulfil a service life of 50 years.

Illustrative example of a macro-components assemblage

In some cases, in order to fulfil the function of a building component, different macro-components have to be considered simultaneously. An illustrative example is herein provided for an interior slab of a residential building.

Hence, for an interior slab of a building the following macro-components are selected:

(i) a macro-component for flooring (C2030);

(ii) a macro-component for a floor structural system (B1010.10);

(iii) a macro-component for ceiling finishes (C2050).

The selected assemblage of macro-components is illustrated in Table 7.17.

1st step) Functional unit and estimated service life of materials

The functional unit of the building component is an interior slab (per m^2) of a residential building, with a required service life of 50 years. The selected macro-components have to fulfil the same functional unit of the building component. Therefore, the estimated service life of the different materials has to be taken into account.

All materials indicated in Table 7.17 are considered to have a service life of 50 years, except ceramic tiles and painting, with a service life of 25 years and 10 years, respectively.

2nd step) Scenarios and assumptions

In order to fulfil the environmental information in all modules, scenarios and assumptions are needed.

Table 7.17 Macro-components assemblage for an interior slab

Macro-components assemblage	Macro-components	Material	Thickness (mm)/ Density (kg/m^2)
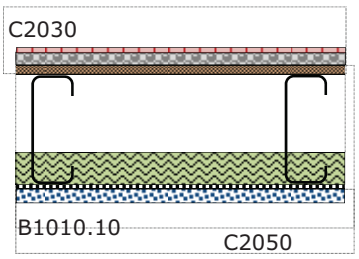	C2030 Flooring	Ceramic tiles	31 kg/m^2
		Concrete screed	13 mm
	B1010.10 Floor structural system	OSB	18 mm
		Air cavity	160 mm
		Rock wool	40 mm
		Light weight steel	14 kg/m^2
		Gypsum board	15 mm
	C2050 Ceiling finishes	Painting	0,125 kg/m^2

The functional unit is related to a time-span of 50 years. This means that each material in the macro-component needs to fulfil this requirement. Hence, materials with an expected service life lower than 50 years need to be maintained or even replaced during this period. Therefore, different scenarios are assumed for each material in order to comply with the time span of the analysis. Likewise, in the end-of-life stage, each material has a different destination according to its inherent characteristics. Thus, for each material an end-of-life scenario is considered taking into account the properties of each material.

All the aforementioned scenarios are set in accordance with the rules provided in EN 15804 and EN 15978.

i) Scenarios for the transportation of materials (Modules A4 and C2)

The transportation distances between the production plants to the construction site (module A4) and the distances between the demolition site and the respective recycling/disposal places (module C2) are assumed, by default, to be 20 km and the transportation is made by truck with a payload of 22 tonnes. However, the designer is able to specify other distances, enabling sensitivity analysis to be made in relation to the transportation of different materials.

ii) Scenarios for the use stage (Modules B1:B7)

Scenarios are pre-defined for the different materials in order to fulfil the required time span of 50 years. Therefore, in relation to the above macro-components assembly, the following scenarios are set:

- substitution of ceramic tiles every 25 years;
- painting of ceiling every 10 years.

iii) Scenarios for the end of life stage (Modules C1:C4) and recycling (Module D)

Different end-of-life scenarios are specified for the materials according to their inherent characteristics, as indicated in Table 7.18. Thus, OSB is considered to be incinerated (80%) in a biomass power plant and credits are given to energy recovery. Steel is recycled, assuming a recycling rate of 90%, and credits are obtained due to the net scrap in the end of the life-cycle process. Likewise, rock wool is considered to be recycled (80%). However, due to the lack of data of the recycling process, no credits are obtained apart from the reduction of waste sent to landfill.

Table 7.18 EOL options for materials

Material	Disposal/Recycling scenario	Credits
Ceramic tiles	Landfill (100%)	-
Concrete screed	Landfill (100%)	-
Gypsum plasterboard	Landfill (100%)	-
Rock wool	Recycling (80%) + Landfill (20%)	-
OSB	Incineration (80%) + Landfill (20%)	Credit due to energy recovery
Light-weight steel	Recycling (90%) + Landfill (10%)	Credit due to net scrap

All the remaining materials were considered to be sent to a landfill of inert materials.

3rd step) LCA of the macro-component

The results of the macro-component assemblies illustrated in Table 7.17, are represented in Table 7.19, per m^2.

Table 7.19: Life cycle environmental analysis of macro-components (per m^2)

Impact category	A1-A3	A4	B4	C2	C4	D	TOTAL
ADP elem. [kg Sb-Eq.]	1,86E-03	6,59E-09	1,83E-03	5,76E-09	5,93E-07	-1,96E-04	3,49E-03
ADP fossil [MJ]	1,31E+03	2,45E+00	8,12E+02	2,14E+00	2,31E+01	-3,35E+02	1,82E+03
AP [kg SO_2 Eq.]	2,47E-01	7,91E-04	9,14E-02	6,85E-04	1,01E-02	-4,45E-02	3,05E-01
EP [kg PO_4^{3-}Eq.]	2,61E-02	1,82E-04	1,40E-02	1,57E-04	1,54E-03	-1,01E-03	4,09E-02
GWP [kg CO_2 Eq.]	8,38E+01	1,77E-01	6,48E+01	1,54E-01	6,80E+00	-1,45E+01	1,41E+02
ODP [kg R11 Eq.]	2,80E-06	3,09E-12	2,04E-06	2,70E-12	1,27E-09	1,76E-07	5,01E-06
POCP [kg Ethene Eq.]	3,41E-02	-2,58E-04	1,43E-02	-2,23E-04	2,62E-03	-1,07E-02	3,98E-02

All macro-components in the database of the tool were computed in a similar way. As already referred, these macro-components enable to perform the life cycle analysis at the product level or at the building level, as exemplified in the following worked examples.

7.4 Life cycle analysis of steel products

7.4.1 Worked examples

7.4.1.1 Example 1: LCA of a steel beam

The aim of this example is to perform a LCA of a steel beam, in which the importance of informative module D is highlighted. Hence, the initial scope of the analysis is a cradle-to-gate analysis (Modules A1 to A3), i.e., it includes all the stages related to the production of the steel beam, until the gate of the factory. The selected beam is indicated in Figure 7.7.

The beam has three spans and a total length of 21 m and is located in alignment E, between axis 1 and 4, in the 2nd floor of the building, as illustrated in Figure 7.8. The beam is made of a hot-rolled **IPE 600 section**, in steel S355.

The LCA is performed by the use of the tool **Buildings LCA**[1] and the detailed steps of the analysis are described in the following paragraphs.

1st Step) Selection of steel section

The selection of the steel section is made in the left column of the application, as indicated in Figure 7.9.

[1] The version of Buildings LCA used in the exercises is for iPad and/or android tablet

Figure 7.7 LCA of a steel beam

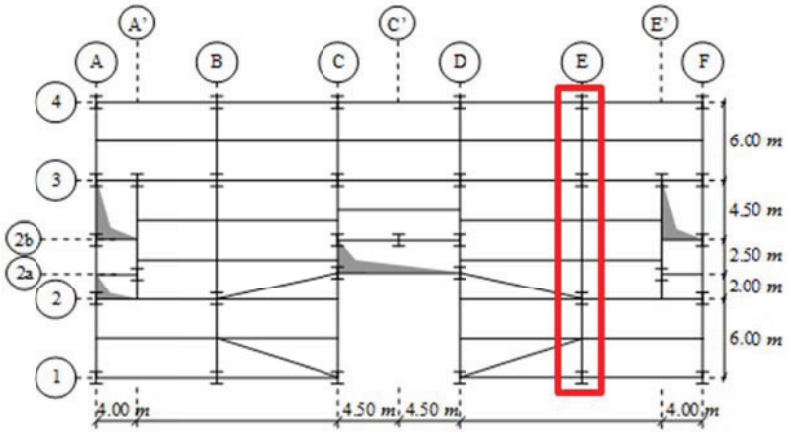

Figure 7.8 Location of the steel beam in plan

2nd Step) Input of data

The input parameters are introduced in the right column of the application (see Figure 7.9). Apart from the length of the beam (21 m), it is necessary to introduce the lifespan of the analysis and to define the scope of the analysis.

The lifespan of the analysis is herein considered to be 50 years. However, it is noted that in this case this information is irrelevant since the maintenance of the beam is not included in the scope of the analysis. As already referred, the scope of the analysis is a cradle-to-gate.

It is possible to define a coating system for the steel element; however, this option was not considered in this example.

3rd Step) Calculation and analysis of results

The calculation is performed once the Calculate bottom, in the upper right corner (see Figure 7.9), is selected.

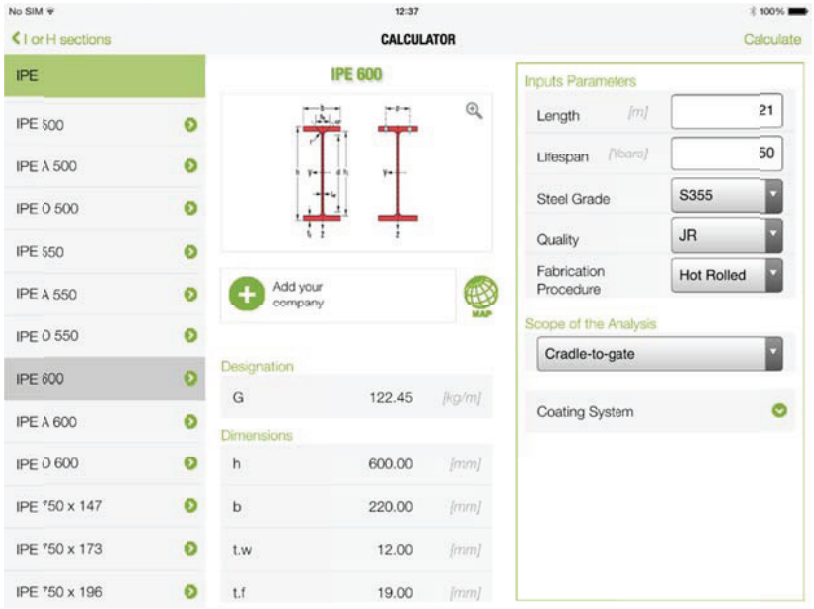

Figure 7.9 Input data for the beam

The results of the analysis are presented in Figure 7.10. Two types of indicators are provided: indicators describing the environmental impacts and indicators describing primary energy demand.

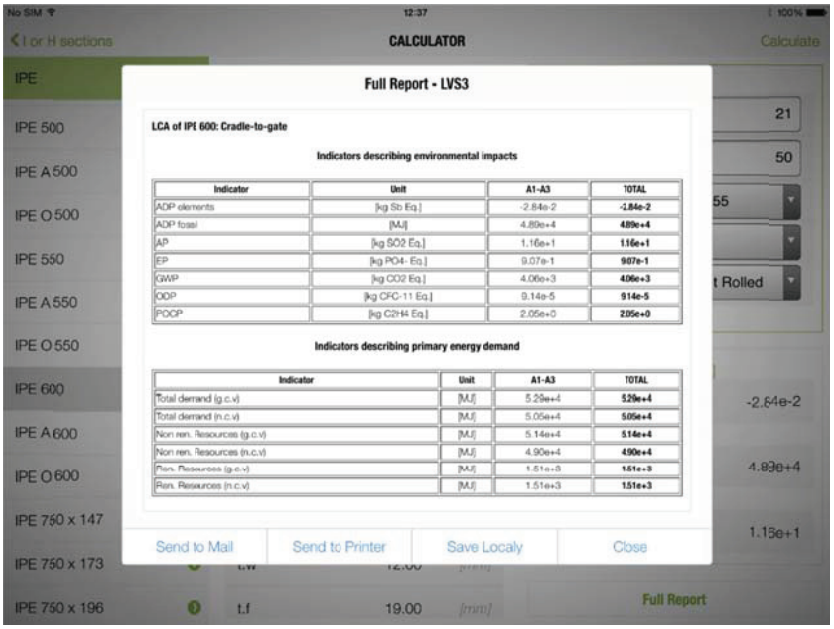

Figure 7.10 LCA calculation of the steel beam

Since the scope of the analysis was a cradle-to-gate, only the results from modules A1 to A3 are provided.

The detailed output report of the analysis may be printed directly from the application or sent by email to the user.

4th Step) LCA, including Module D

A new LCA is performed for the same beam taking into account the recycling at the end-of-life stage, i.e. Module D.

In this case additional data is needed: the recycling rate at the end-of-life stage. In the example a recycling rate of 99% was considered, as indicated in Figure 7.11.

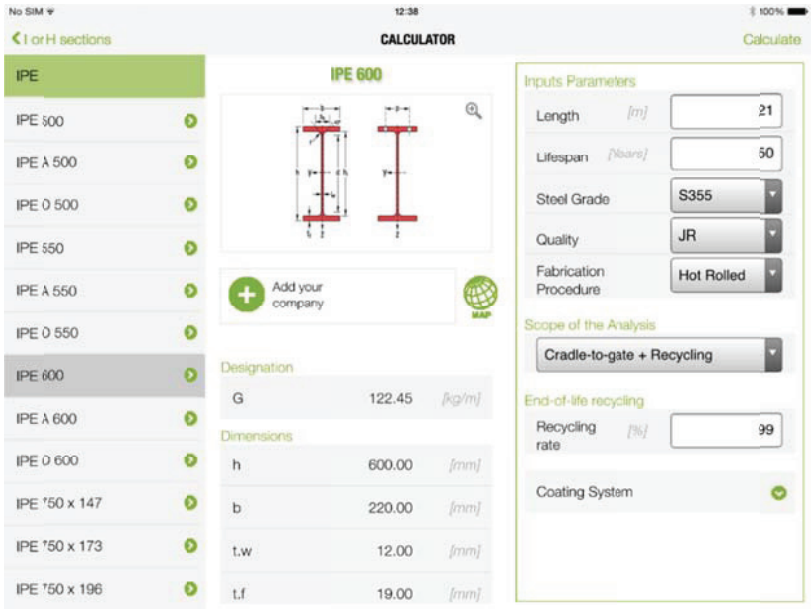

Figure 7.11 New input data

5th Step) Re-calculation and analysis of results

After re-calculation, the results of the LCA, including Module D, are illustrated in Figure 7.12. Thus, in this case the results of the analysis are given for Modules A1-A3 and D.

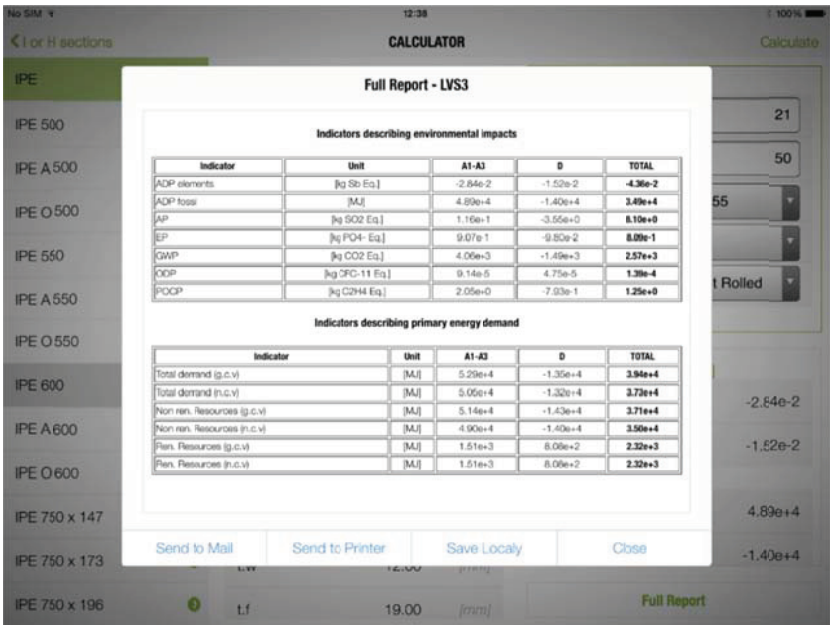

Figure 7.12 New calculation

Two indicators were selected to illustrate the relevance of Module D: global warming potential and primary energy demand. The graph of Figure 7.13, shows the reduction enabled by adding informative module D to the scope of the analysis: about -37% and -26% for global warming and primary energy demand, respectively.

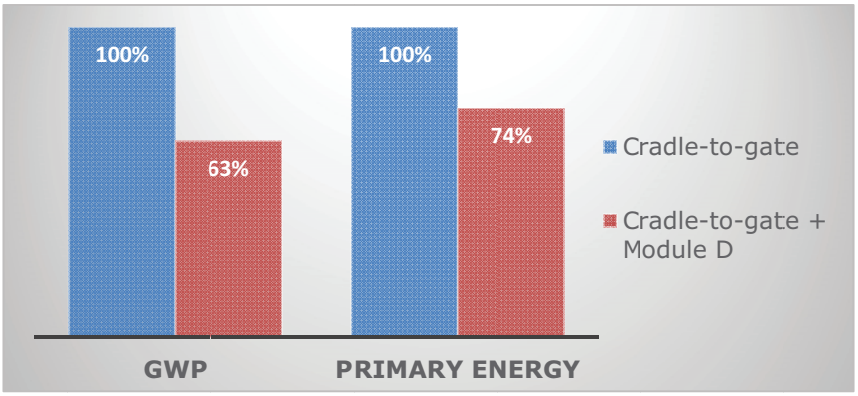

Figure 7.13 Comparative analysis – influence of Module D

7.4.1.2 Example 2: LCA of a steel column

The aim of the example is to perform the LCA of a steel column. In this case, the scope of the analysis is a cradle-to-grave analysis (Modules A to C) plus recycling (Module D), i.e., it includes all the stages related to the production of the steel column plus the end-of-life recycling. Moreover, it is assumed that the column is coated with a solvent-based paint and that the coating is partially replaced every 10 years. The total lifespan of the building is assumed to be 50 years. The selected column is indicated in Figure 7.14.

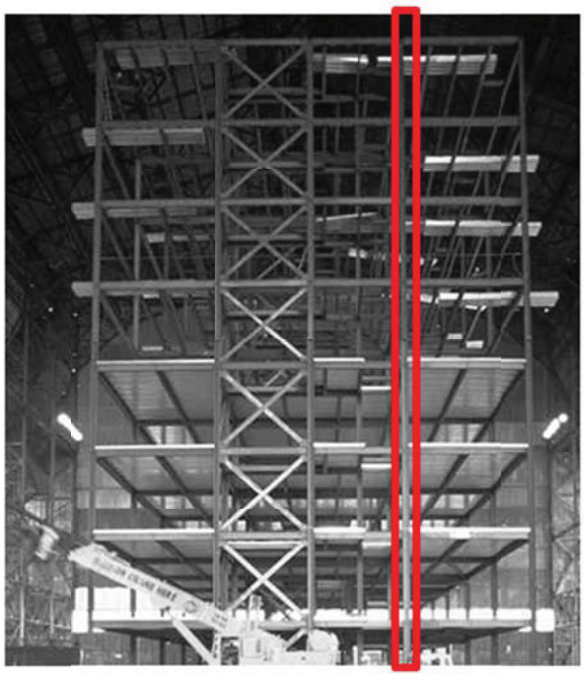

Figure 7.14 LCA of a steel column

The column has a total length of 30 m and it is made of a **HEB 320 section**, in steel S355.

The LCA is performed by the use of the tool **Buildings LCA** and the detailed steps of the analysis are described in the following paragraphs.

1st Step) Selection of steel section

The selection of the steel section is made in the left column of the application, as indicated in Figure 7.15.

2nd Step) Input of data

The input parameters are introduced in the right column of the application (see Figure 7.15). In this case, a length of 30 m is introduced for the column and a lifespan of 50 years is considered for the analysis. The scope of the analysis is a cradle-to-grave plus recycling. A recycling rate of 99% is assumed for the steel column.

It is considered that the column is coated with a solvent-based paint and the maintenance of the coating system, over the lifespan of the analysis, is made according to the following scenario: the coating is partially replaced (80%) every 10 years. No transportation is considered between the stages.

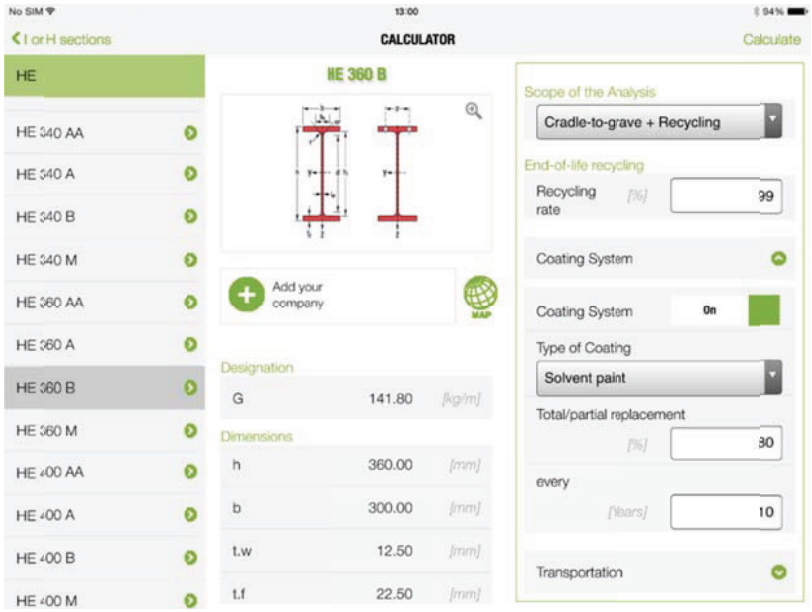

Figure 7.15 Input data for the column

3rd Step) Calculation and analysis of results

The results of the analysis are presented in Figure 7.16 for the indicators describing the environmental impacts and indicators describing primary energy demand.

The results are provided per module and by the total. Since no transportation was considered, Modules A4 and C2 have zero values.

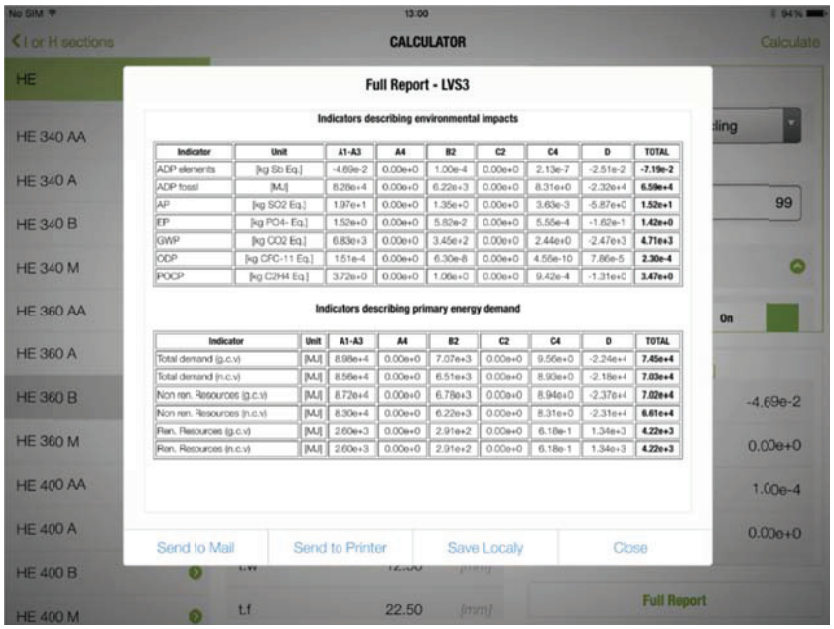

Figure 7.16 LCA calculation of the steel column

7.4.1.3 Example 3: Comparative LCA of columns

The aim of this example is to perform the LCA of the steel column presented in Exercise 3, taking into account alternative designs. The scope of the analysis is a cradle-to-grave analysis (Modules A to C) plus recycling (Module D). No coating and transportation between stages are considered in the analysis.

Only the column between the 1st and 2nd floors will be considered, as indicated in Figure 7.17. Thus, the column has a length of 4,335 m.

The functional unit is this example is: a restrained column, 4,335 m long, with a load bearing capacity of an axial force of 1704 kN and a bending moment of 24,8 kNm (around the strong axis for the profile column). All alternative designs for the column must **fulfill the same functional unit**.

In addition, the aim of this example is to show the use of Environmental Product Declarations (EPDs) as input data for LCA. In this case, the LCA is performed by the use of data provided from current EPDs of steel products provided by the Norwegian EPD foundation (available from www.EPD-norge.no).

The detailed steps of the analysis are described in the following paragraphs.

1st Step) Design of the column

For the design of the column five different sections are considered: a hot-rolled HEB, a hot finished and a cold formed circular hollow section, and a hot finished and a cold formed square hollow section. Taking into account the functional unit, the design of the column for the five solutions, is indicated in Table 7.20.

Figure 7.17 Comparative LCA of a steel column

Table 7.20 Alternative design of the column

Cross-section	Fabrication procedure	Weight (kg/m)	EPD
HEB 280	Hot-rolled	103,12	EDP no. 00239E (2014)
SHS 260X12	Hot-finished	92,23	EDP no. 00241E (2014)
SHS 260X12	Cold-formed	92,23	EDP no. 00240E (2014)
CHS 323.9X12	Hot-finished	92,30	EDP no. 00241E (2014)
CHS 323.9X12	Cold-formed	92,30	EDP no. 00240E (2014)

2nd Step) Gathering of data

In this example, EPDs are collected for the steel products indicated in Table 7.20 and they are indicated in the same table. It is noted that data provided in the EDPs is related to a declared unit of "per kg building steel structure with an expected service life of 100 years". Therefore, to compile the results of the analysis, data provided from EPDs is multiplied by the total amount of steel in each design solution. The respective results are presented in Figure 7.18 for selected environmental indicators.

3rd Step) Analysis of the results

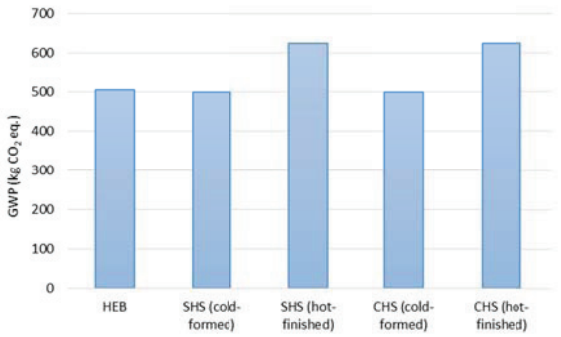

(a)

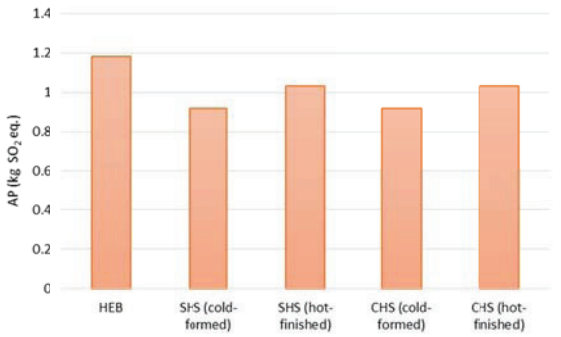

(b)

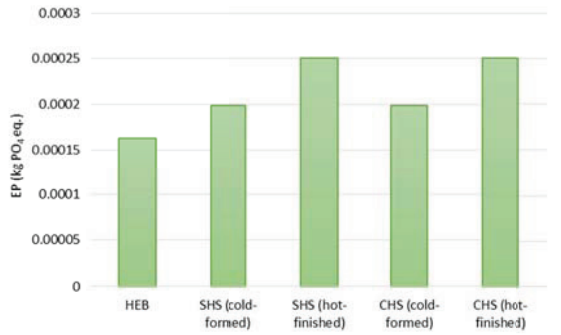

(c)

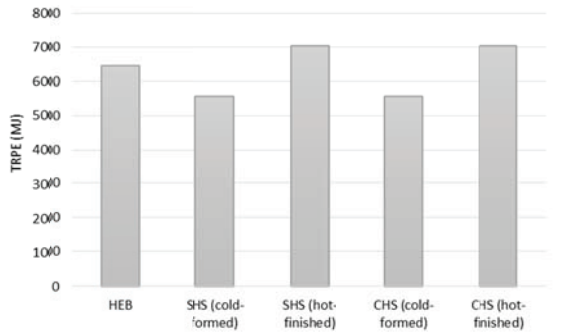

(d)

Figure 7.18 Results of the comparative analysis (a) Global warming potential (in kg CO_2 eq.), (b) Acidification potential (in SO_2 eq.), (c) Eutrophication potential (in PO_4^{3-} eq.) and (d) Total use of non-renewable primary energy resources (in MJ)

7.5 Life cycle analysis of steel buildings

7.5.1 Worked examples

7.5.1.1 Example 4: LCA of a steel building

The aim of this example is to perform the LCA of the steel building referred over this publication. The load-bearing structure is made of a hot-rolled steel structure, as illustrated in Figure 7.19. The total lifespan of the building is assumed to be 50 years.

The example is divided in two parts: (i) in the first part the LCA of the load bearing structure is performed and (ii) in the second part, the LCA is performed for the remaining building components (slabs, walls, etc).

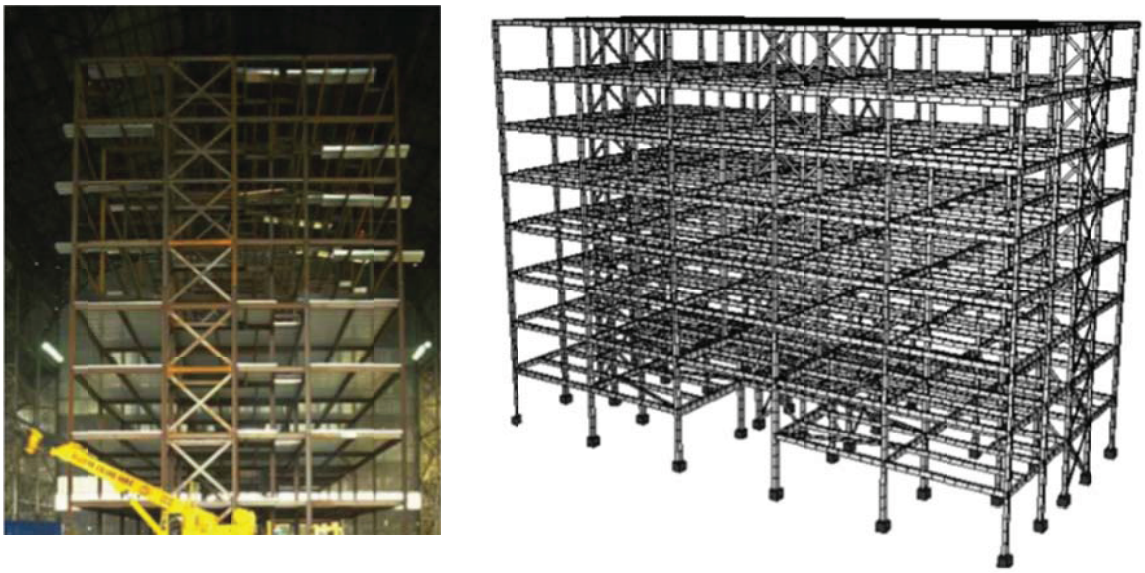

(a) (b)

Figure 7.19 (a) Elevation view of the steel building and (b) structural wire frame

The scope of the analysis is a cradle-to-grave analysis (Modules A to C) plus recycling (Module D). In addition, the following assumptions were considered for the analysis:

- ✓ type of coating for the steel structure - water based paint, with a partial replacement of 50% every 20 years;
- ✓ transportation Module A4 - 100% of steel transported by truck over 200 km;
- ✓ transportation Module C2 - 100% of steel transported by truck over 100 km;
- ✓ the recycling rate of steel (RR) is assumed to be 99% for all steel elements.

The bill of materials for the steel structure is indicated in Table 7.21, leading to a full tonnage of about 405 tonnes of steel.

Table 7.21 Bill of materials for the steel structure

Beams	Length (m)	Columns	Length (m)
IPE 400	2239	HEB 340	93
IPE 600	160	HEB 320	438
IPE 360	1916	HEB 260	567
HEA 700	32		

The LCA is performed by the use of the tool **Buildings LCA,** which enables the LCA to be performed at two levels: product level and building level. The detailed steps of the analysis are described in the following paragraphs.

Part 1: LCA of steel structure

1st Step) Selection of steel sections

The selection of the steel section is made in the left column of the application, as indicated in the previous exercises. The analysis is made individually for each steel section indicated in Table 7.21.

2nd Step) Input of data

Likewise, the input parameters are introduced in the right column of the application, as described for the previous exercises. In this case, the length of each steel element varies according to Table 7.21.

In all cases a lifespan of 50 years is considered for the analysis. The scope of the analysis is a cradle-to-grave plus recycling. A recycling rate of 99% is assumed for all steel elements. Moreover, the scenarios for the coating system and transportation described in the previous paragraphs are taken into account for all steel elements.

3rd Step) Calculation and analysis of results

The results of the analysis obtained for each steel section were summed up and they are indicated in Table 7.22 and Table 7.23 for the indicators describing the environmental impacts, and Table 7.24 for the indicators describing primary energy demand.

Table 7.22 Indicators describing environmental impacts

Indicator	**ADP elements** [kg Sb Eq.]	**ADP fossil** [MJ]	**AP** [kg SO2 Eq.]	**EP** [kg PO_4^{3-} Eq.]
A1-A3	-4,47E+00	7,95E+06	1,87E+03	1,46E+02
A4	1,53E-04	5,69E+04	1,82E+01	4,18E+00
B2	8,31E-03	2,53E+05	3,59E+01	3,12E+00
C2	7,58E-05	2,81E+04	9,02E+00	2,07E+00
C4	2,03E-05	7,91E+02	3,45E-01	5,29E-02
D	-2,39E+00	-2,20E+06	-5,58E+02	-1,54E+01
TOTAL	-6,84E+00	6,08E+06	1,37E+03	1,40E+02

Table 7.23 Indicators describing environmental impacts (cont.)

Indicator	GWP [kg CO2 Eq.]	ODP [kg CFC-11 Eq.]	POCP [kg C2H4 Eq.]
A1-A3	6,55E+05	1,44E-02	3,51E+02
A4	4,10E+03	7,17E-08	-5,92E+00
B2	1,52E+04	3,52E-06	2,80E+01
C2	2,03E+03	3,55E-08	-2,93E+00
C4	2,32E+02	4,33E-08	8,97E-02
D	-2,35E+05	7,47E-03	-1,25E+02
TOTAL	4,41E+05	2,19E-02	2,45E+02

Table 7.24 Indicators describing primary energy demand

Indicator	Total demand (g.c.v) [MJ]	Total demand (n.c.v) [MJ]	Non ren. Resourc. (g.c.v) [MJ]	Non ren. Resourc. (n.c.v) [MJ]	Ren. Resourc. (g.c.v) [MJ]	Ren. Resourc. (n.c.v) [MJ]
A1-A3	8,63E+06	8,21E+06	8,37E+06	7,96E+06	2,54E+05	2,54E+05
A4	6,32E+04	5,91E+04	6,10E+04	5,69E+04	2,23E+03	2,23E+03
B2	2,92E+05	2,68E+05	2,75E+05	2,53E+05	1,59E+04	1,59E+04
C2	3,13E+04	2,92E+04	3,02E+04	2,81E+04	1,10E+03	1,10E+03
C4	9,11E+02	8,50E+02	8,51E+02	7,91E+02	5,87E+01	5,87E+01
D	-2,13E+06	-2,07E+06	-2,26E+06	-2,20E+06	1,27E+05	1,27E+05
TOTAL	6,88E+06	6,50E+06	6,48E+06	6,10E+06	4,00E+05	4,00E+05

Part 2: LCA of building components

4th Step) Selection of macro-components for the building

The selection of the building macro-components is made in the left column of the application, as indicated in Figure 7.20.

Macro-components may be selected for the façades, partitions, internal floors and roof. In this case, the selected macro-components are indicated in Table 7.25. The details about the calculation of macro-components, including assumptions and scenarios considered, are provided in Annex A. The selection of the macro-component for the internal floors is illustrated in Figure 7.21.

Table 7.25 Selected macro-components for the building

	Macro-component reference	Material layers	Thickness [mm] Density [kg/m^2]
Roof			
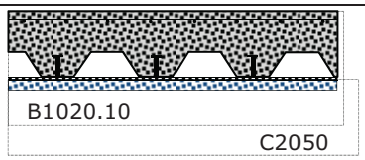	B1020.10 Roof structural frame	Composite steel-concrete deck	200 mm
		Gypsum board	15 mm
	C2050 Ceiling finishes	Painting	0,125 kg/m^2
Interior floor			
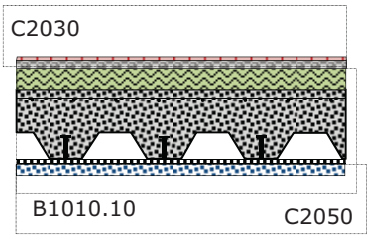	C2030 Flooring	Ceramic tiles	31 kg/m^2
		Concrete screed	13 mm
	B1010.10 Floor structural frame	Polyethylene foam	10 mm
		Composite steel-concrete deck	200 mm
		Gypsum board	15 mm
	C2050 Ceiling finishes	Painting	0,125 kg/m^2
Façade			
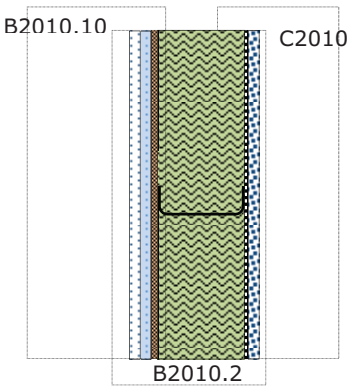	B2010.10 Exterior wall veneer	ETICS	13,8 kg/m^2
	B2010.20 Exterior wall construction	OSB	13 mm
		Rock wool	120 mm
		Light weight steel	15 kg/m^2
		Gypsum board	15 mm
	C2010 Interior wall finishes	Painting	0,125 kg/m^2
Partitions			
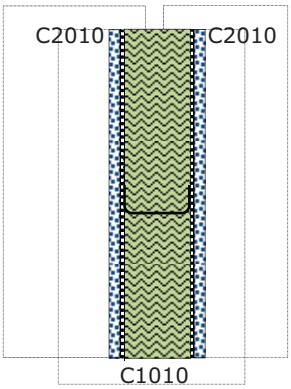	C2010 Interior wall finishes	Painting	0,125 kg/m^2
	C1010 Interior partitions	Gypsum board	15 mm
		Rock wool	60 mm
		Light weight steel	10 kg/m^2
		Gypsum board	15 mm
	C2010 Interior wall finishes	Painting	0,125 kg/m^2

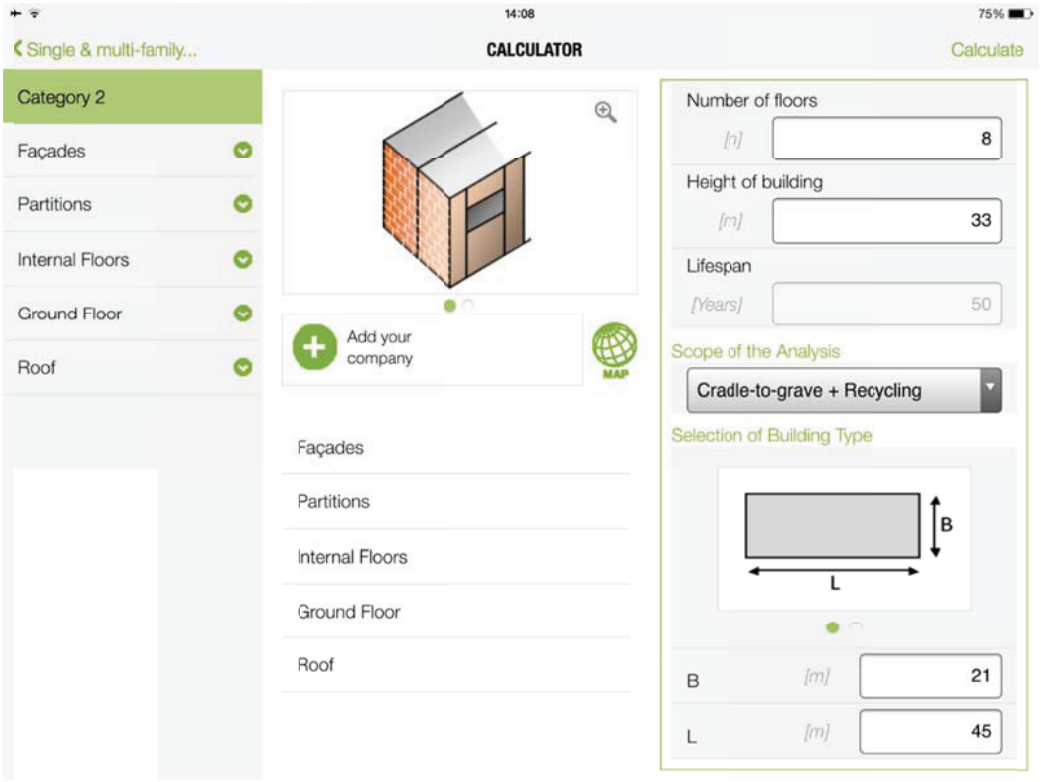

Figure 7.20 Selection of macro-components and input data

Figure 7.21 Selection of the macro-component for internal floors

5th Step) Input of data for the building

The remaining input parameters are introduced in the right column of the application (see Figure 7.20). The building has 8 floors and a total height of 33 m. The area of the building, in the horizontal plane, is rectangular with a wide of 21 m and a length of 45 m.

The scope of the analysis is a cradle-to-grave plus recycling. In this case, no further data is needed, since all the assumptions needed for the calculation of each macro-component are pre-defined and stored in the database of the application (see details in Annex A).

6th Step) Calculation and analysis of results

The results for the building (except load-bearing structure) are presented in Table 7.26 and Table 7.27 for the indicators describing the environmental impacts and Table 7.28 for the indicators describing primary energy demand.

Table 7.26 Indicators describing environmental impacts

Indicator	ADP elements [kg Sb Eq.]	ADP fossil [MJ]	AP [kg SO2 Eq.]	EP [kg PO_4^{3-} Eq.]
A1-A3	6,51E+00	1,23E+07	3,31E+03	3,45E+02
A4	1,94E-04	7,20E+04	2,33E+01	5,37E+00
B2	6,02E+00	2,46E+06	2,47E+02	2,75E+01
C2	1,69E-04	6,31E+04	2,01E+01	4,61E+00
C4	1,32E-02	5,11E+05	2,23E+02	3,42E+01
D	-2,20E+00	-2,78E+06	-6,10E+02	-1,73E+01
TOTAL	1,03E+01	1,26E+07	3,21E+03	4,00E+02

Table 7.27 Indicators describing environmental impacts (cont.)

Indicator	GWP [kg CO2 Eq.]	ODP [kg CFC-11 Eq.]	POCP [kg C2H4 Eq.]
A1-A3	1,22E+06	1,24E-02	4,50E+02
A4	5,19E+03	9,08E-08	-7,60E+00
B2	1,73E+05	6,75E-03	4,62E+01
C2	4,52E+03	7,92E-08	-6,54E+00
C4	1,57E+05	2,81E-05	5,78E+01
D	-2,31E+05	5,53E-03	-1,29E+02
TOTAL	1,33E+06	2,47E-02	4,12E+02

Table 7.28 Indicators describing primary energy demand

Indicator	Total demand (g.c.v) [MJ]	Total demand (n.c.v) [MJ]	Non ren. Resourc. (g.c.v) [MJ]	Non ren. Resourc. (n.c.v) [MJ]	Ren. Resourc. (g.c.v) [MJ]	Ren. Resourc. (n.c.v) [MJ]
A1-A3	1,46E+07	1,38E+07	1,33E+07	1,25E+07	1,30E+06	1,30E+06
A4	8,01E+04	7,47E+04	7,74E+04	7,20E+04	2,82E+03	2,82E+03
B2	2,94E+06	2,69E+06	2,88E+06	2,63E+06	6,49E+04	6,49E+04
C2	6,98E+04	6,53E+04	6,76E+04	6,31E+04	2,47E+03	2,47E+03
C4	5,88E+05	5,51E+05	5,51E+05	5,11E+05	3,81E+04	3,81E+04
D	-2,81E+06	-2,69E+06	-2,92E+06	-2,81E+06	1,12E+05	1,12E+05
TOTAL	1,55E+07	1,45E+07	1,40E+07	1,30E+07	1,52E+06	1,52E+06

The detailed results of the analysis, including the LCA for each building component, is provided in Annex B.

Part 3: LCA of steel building

7th Step) Calculation and analysis of results

The complete LCA of the building, i.e. load-bearing structure (calculated in Part 1) plus building components (calculated in Part 2) is given by the sum of Table 7.22, Table 7.23, Table 7.26 and Table 7.27, for the indicators describing the environmental impacts, and the sum of Table 7.24 and Table 7.28, for the indicators describing primary energy demand.

The results are presented in Table 7.29 and Table 7.30 for the indicators describing the environmental impacts.

Table 7.29 Indicators describing environmental impacts

Indicator	ADP elements [kg Sb Eq.]	ADP fossil [MJ]	AP [kg SO_2 Eq.]	EP [kg PO_4^{3-} Eq.]
A1-A3	2,04E+00	2,03E+07	5,18E+03	4,91E+02
A4	3,47E-04	1,29E+05	4,15E+01	9,55E+00
B2	6,03E+00	2,71E+06	2,83E+02	3,06E+01
C2	2,45E-04	9,12E+04	2,91E+01	6,68E+00
C4	1,32E-02	5,12E+05	2,23E+02	3,43E+01
D	-4,59E+00	-4,98E+06	-1,17E+03	-3,27E+01
TOTAL	3,46E+00	1,87E+07	4,58E+03	5,40E+02

Table 7.30 Indicators describing environmental impacts (cont.)

Indicator	GWP [kg CO2 Eq.]	ODP [kg CFC-11 Eq.]	POCP [kg C2H4 Eq.]
A1-A3	1,88E+06	2,68E-02	8,01E+02
A4	9,29E+03	1,63E-07	-1,35E+01
B2	1,88E+05	6,75E-03	7,42E+01
C2	6,55E+03	1,15E-07	-9,47E+00
C4	1,57E+05	2,81E-05	5,79E+01
D	-4,66E+05	1,30E-02	-2,54E+02
TOTAL	1,77E+06	4,66E-02	6,57E+02

The results, by information module, are summarized in Figure 7.22 for selected indicators. It is observed that the most importance stage in the LCA of the building is the product stage (informative modules A1 to A3), followed by the recycling of the building components (Module D).

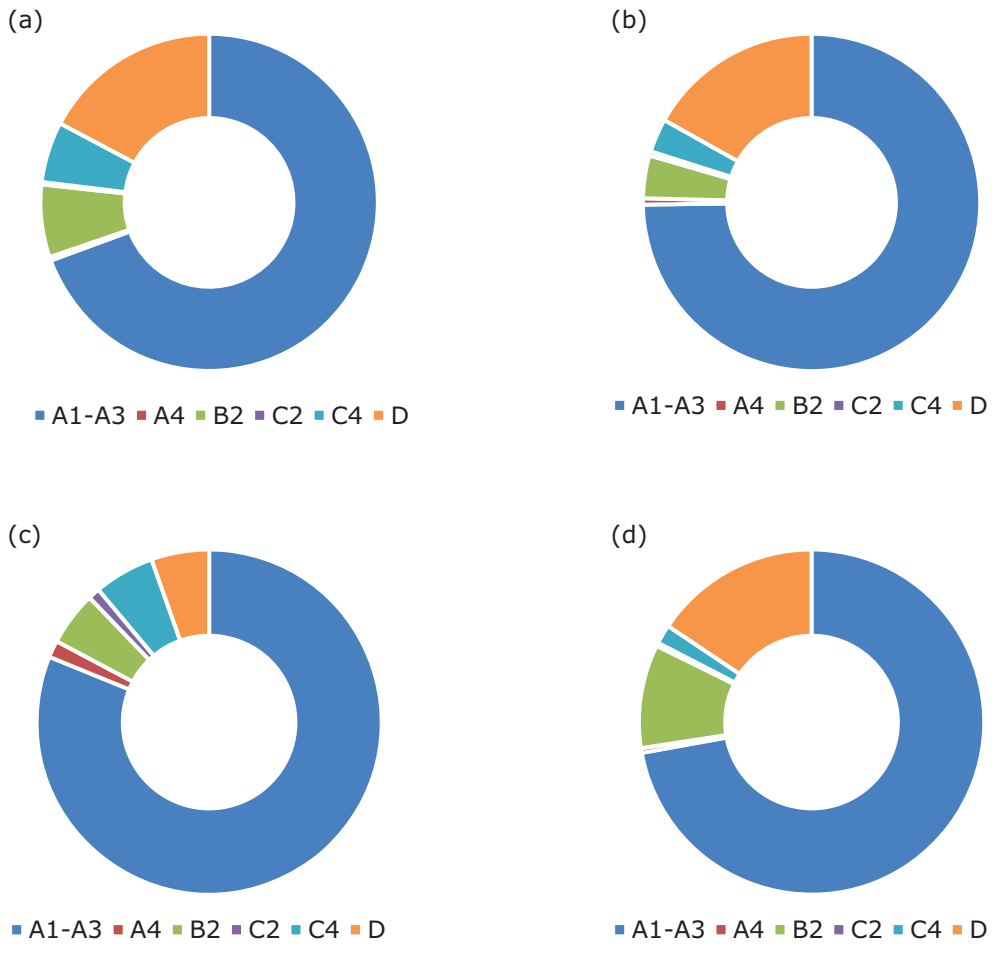

Figure 7.22 LCA of the building (a) Global warming potential, (b) Acidification potential, (c) Eutrophication Potential and (d) Total primary energy demand

References

EN 15804. 2012. Sustainability of Construction Works — Environmental product declarations – Core rules for the product category of construction products. European Committee for Standardization, Brussels, Belgium.

EN 15978. 2011. Sustainability of Construction Works — Assessment of environmental performance of buildings — Calculation method. European Committee for Standardization, Brussels, Belgium.EPD no 00239E. 2014. I, H, U, L, T and wide flats hot-rolled sections. Skanska Norge S.A. (available from www.epd-norge.no).

EPD no 00240E. 2014. Cold formed structural hollow sections (CFSHS). Skanska Norge S.A. (available from www.epd-norge.no).

EPD no 00241E. 2014. Hot finished structural hollow sections (HFSHS). Skanska Norge S.A. (available from www.epd-norge.no).

Forsberg, A., von Malmborg F. 2004. Tools for environmental assessment of the built environment. In: Building and Environment, 39, pp. 223-228.

Frischknecht, R., and Rebitzer, G. 2005. The ecoinvent database system: a comprehensive web-based database. Journal of Cleaner Production, Volume 13, Issues 13-14, pp. 1337–1343.

GaBi. 2012. Software-System and Databases for Life Cycle Engineering. Version 5.56. PE International AG, Leinfelden-Echterdingen, Germany.

Gervásio, H., Martins, R., Santos, P., Simões da Silva, L. 2014. A macro-component approach for the assessment of building sustainability in early stages of design", Building and Environment 73, pp. 256-270, DOI information: 10.1016/j.buildenv.2013.12.015.

Guinée, J., Gorrée, M., Heijungs, R., Huppes, G., Kleijn, R., Koning, A. de, Oers, L. van, Wegener Sleeswijk, A., Suh, S., Udo de Haes, H., Bruijn, H. de, Duin, R. van, Huijbregts, M. 2002. Handbook on life cycle assessment. Operational guide to the ISO standards. Kluwer Academic Publishers, ISBN 1-4020-0228-9, 692 pp.

Howard N., Edwards, S., and Anderson, J. 1999. Methodology for environmental profiles of construction materials, components and buildings. BRE Report BR 370. Watford. (http://www.bre.co.uk/service.jsp?id=52) .

IEA. 2001. LCA methods for buildings. Annex 31 – Energy-related environmental impact of buildings. International Energy Agency.

IPCC. 2007. Fourth Assessment Report – Climate Change 2007. IPCC, Geneva, Switzerland.

IPP. 2003. Integrated Product Policy - Building on Environmental Life-Cycle Thinking. COM(2003) 302 final. Communication from the commission to the council and the European Parliament, Brussels.

ISO 14025. 2006. Environmental labels and declarations - Type III environmental declarations - Principles and procedures.

ISO 14040. 2006. Environmental management – life cycle assessment – Principles and framework. International Organization for Standardization. Geneva, Switzerland.

ISO 14044. 2006. Environmental management – life cycle assessment – Requirements and guidelines. International Organization for Standardization, Geneva, Switzerland.

Jönsson, Å. 2000. Tools and methods for environmental assessment of building products - methodological analysis of six selected approaches. In: Building and Environment, 35, pp. 223-238.

Kellenberger, D. 2005. Comparison and benchmarking of LCA-based building related environmental assessment and design tools. EMPA Dubendorf, Technology and Society Laboratory, LCA group.

Kortman, J., van Ejwik, H., Mark, J., Anink, D., Knapen, M. 1998. Presentation of tests by architects of the LCA-based computer tool EcoQuantum domestic. Proceedings of Green Building Challenge 1998. Vancouver. Canada (http://www.ivambv.uva.nl/uk/producten/product7.htm).

LCI, 2001. World Steel Life Cycle Inventory. Methodology report 1999/2000. International Iron and Steel Institute. Committee on Environmental Affairs, Brussels.

Lippiatt, B. 2002. Building for environmental and economical sustainability. Technical manual and user guide (BEES 3.0). National Institute of Standards and Technology (NIST). Report NISTIR 6916. (http://www.bfrl.nist.gov/oae/software/bees.html).

Reijnders L., Roekel A. 1999. Comprehensiveness and adequacy of tools for the environmental improvement of buildings. Journal of Cleaner Production, 7, pp. 221-225.

Santos, P., Martins, R., Gervásio, H., Simões da Silva, L. 2014. "Assessment of building operational energy at early stages of design – A monthly quasi-steady-state approach", Energy & Buildings 79C, pp. 58-73, DOI information: 10.1016/j.enbuild.2014.02.084.

SB_Steel. 2014. Sustainable Building Project in Steel. Draft final report. RFSR-CT-2010-00027. Research Programme of the Research Fund for Coal and Steel.

Steel Recycling Institute. 2009. http://www.recycle-steel.org/construction.html (last accessed in 31/08/2009)

Trusty WB, Associates. 1997. Research guidelines. ATHENATM Sustainable Materials Institute. Merrickville. Canada. (http://www.athenasmi.ca/about/lcaModel.html)

UNEP, 2004. Why take a life cycle approach? United Nations Publication. ISBN 92-807-24500-9.

Uniformat, 2010. UniFormat™: A Uniform Classification of Construction Systems and Assemblies (2010). The Constructions Specification Institute (CSI), Alexandria, VA, and Construction Specifications Canada (CSC), Toronto, Ontario. ISBN 978-0-9845357-1-2.

Werner, F. 2005. Ambiguities in decision-oriented life cycle inventories – The role of mental models and values. Doi - 10.1007/1-4020-3254-4.

Worldsteel. 2011. Life cycle assessment methodology report. World Steel Association, Brussels.

CHAPTER 7

SUSTAINABILITY ASPECTS OF STEEL BUILDINGS AND COMPONENTS

ANNEX A – DETAILED DATA OF MACRO-COMPONENTS

Milan VELJKOVIC[1] and Helena GERVÁSIO[2]

[1]University of Lulea, Sweden

[2]University of Coimbra, Portugal

B1010.10 Floor structural frame				
B1010.10.2a	**Materials**	**Thickness/ density**	**End-of-life scenario**	**RR (%)**
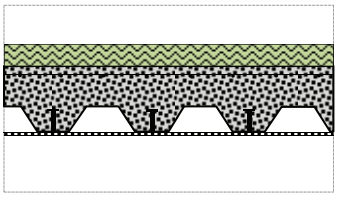	PE (mm)	20	Incineration	80
	Concrete (kg/m^2)	410	Recycling	70
	Rebar (kg/m^2)	8,24	Recycling	70
	Steel sheet (kg/m^2)	11,10	Recycling	70
	Gypsum board (mm)	15	Recycling	80
	Steel structure (kg/m^2)	40	Recycling	90

B1010.10.2a - LCA

	A1-A3	A4	C2	C4	D
ADP elements [kg Sb-Equiv.]	-4,61E-04	2,08E-08	1,81E-08	1,26E-06	-3,32E-04
ADP fossil [MJ]	1,56E+03	7,71E+00	6,74E+00	4,90E+01	-3,44E+02
AP [kg SO2-Equiv.]	3,93E-01	2,49E-03	2,16E-03	2,14E-02	-9,22E-02
EP [kg Phosphate-Equiv.]	3,65E-02	5,73E-04	4,96E-04	3,28E-03	-2,77E-03
GWP [kg CO2-Equiv.]	1,51E+02	5,56E-01	4,86E-01	1,58E+01	-3,67E+01
ODP [kg R11-Equiv.]	1,88E-06	9,73E-12	8,51E-12	2,68E-09	1,04E-06
POCP [kg Ethene-Equiv.]	6,27E-02	-8,13E-04	-7,01E-04	5,54E-03	-1,90E-02

Functional equivalent:

1 m^2 of a structural slab of a building, designed for a service life of 50 years.

Additional information:

List of datasets used in Modules A1-A3

Process	Data source	Geographical coverage	Date
Concrete	PE International	Germany	2011
Reinforcement rebars	Worldsteel	World	2007
Steel sheet	Worldsteel	World	2007
Structural steel	Worldsteel	World	2007
Gypsum board	PE International	Europe	2008
PE	PE International	Germany	2011

List of datasets used in Modules A4 and C2 (assuming distances of 20 km)

Process	Data source	Geographical coverage	Date
Transportation by truck	PE International	World	2011

List of datasets used in Module C4-D

Process	Data source	Geographical coverage	Date
Incineration PE	PE International	Europe	2011
Landfill of inert materials	PE International	Germany	2011
Recycling steel	Worldsteel	World	2007

B2010.20 Exterior wall construction				
B2010.20.1a	**Materials**	**Thickness/ density**	**End-of-life scenario**	**RR (%)**
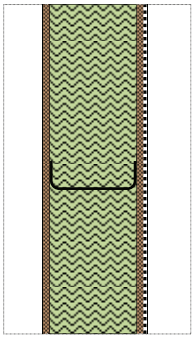	OSB (mm)	13	Incineration	80
	Rock wool (mm)	120	Recycling	80
	Gypsum board (mm)	15	Landfill	
	Light Weight Steel (kg/m^2)	15	Recycling	90

B1010.20.1a

	A1-A3	A4	C2	C4	D
ADP elements [kg Sb-Equiv.]	3,06E-05	2,19E-09	1,92E-09	4,32E-08	-2,10E-04
ADP fossil [MJ]	7,09E+02	8,14E-01	7,12E-01	1,68E+00	-3,05E+02
AP [kg SO2-Equiv.]	2,65E-01	2,63E-04	2,28E-04	7,35E-04	-4,81E-02
EP [kg Phosphate-Equiv.]	2,41E-02	6,05E-05	5,23E-05	1,13E-04	-1,17E-03
GWP [kg CO2-Equiv.]	6,50E+01	5,86E-02	5,13E-02	4,94E-01	-1,73E+01
ODP [kg R11-Equiv.]	6,43E-07	1,03E-12	8,98E-13	9,24E-11	3,41E-07
POCP [kg Ethene-Equiv.]	3,27E-02	-8,58E-05	-7,40E-05	1,91E-04	-1,13E-02

Functional equivalent:

1 m^2 of an exterior wall of a building, designed for a service life of 50 years.

Additional information:

List of datasets used in Modules A1-A3

Process	Data source	Geographical coverage	Date
OSB	PE International	Germany	2008
Gypsum board	PE International	Europe	2008
Light-weight steel (LWS)	Worldsteel	World	2007
Rock wool	PE International	Europe	2011

List of datasets used in Modules A4 and C2 (assuming distances of 20 km)

Process	Data source	Geographical coverage	Date
Transportation by truck	PE International	World	2011

List of datasets used in Module C4-D

Process	Data source	Geographical coverage	Date
Incineration OSB	PE International	Germany	2008
Landfill of inert materials	PE International	Germany	2011
Recycling steel	Worldsteel	World	2007

CHAPTER 7

SUSTAINABILITY ASPECTS OF STEEL BUILDINGS AND COMPONENTS

ANNEX B – DETAILED OUTPUT OF MACRO-COMPONENTS

Milan VELJKOVIC[1] and Helena GERVÁSIO[2]

[1]University of Lulea, Sweden

[2]University of Coimbra, Portugal

LCA REPORT FOR STEEL BUILDINGS

SUMMARY

Building Type: Single & multi-family building - Category 1

Building shape: Rectangular

No. floors: 8

Area per floor: 945 m^2

Scope: Cradle-to-grave + Recycling

Lifespan: 50 years

Environmental Impacts

Global warming potential (GWP): 1,33e^{+6} kg CO2 eq and 175,69 kg CO_2 eq/m^2

Primary Energy Demand

Total Primary Energy Demand: 1,55e^{+7} MJ and 2049,29 MJ/m^2

DETAILED RESULTS

Building Data

Building Type: Single & multi-family building - Category 1

Building shape: Rectangular

No. floors: 8

Area per floor: 945 m2

Declared unit and normative framework

Scope: Cradle-to-grave + Recycling

Declared Unit: A residential building with a lifespan of 50 years

Standards: ISO 14040:2006 + ISO 14044:2006 + EN 15804:2012 + EN 15978:2011

LCA Input Data

Table B.1 Building façade

Macro-components	Materials	Thickness (mm)	Density (kg/m^2)	End-of-life scenario	RR (%)
B2010.10	Painting	-	0,125	Landfill	-
	Cement mortar	15	-	Landfill	-
	OSB	13	-	Incineration	80
	Rock wool	120	-	Recycling	80
B2010.20	Gypsum plasterboard	15	-	Recycling	80
	Light weight steel (LWS)	-	15	Recycling	90
C2010	Painting	-	0,125	Landfill	-

Table B.2 Interior wall

Macro-components	Materials	Thickness (mm)	Density (kg/m^2)	End-of-life scenario	RR (%)
C1010	Gypsum plasterboard	15	-	Recycling	80
	Rock wool	60	-	Recycling	80
	Gypsum plasterboard	15	-	Recycling	80
	Light weight steel (LWS)	-	10	Recycling	90
C2010	Painting	-	0,125	Landfill	-

Table B.3 Roof floor

Macro-components	Materials	Thickness (mm)	Density (kg/m^2)	End-of-life scenario	RR (%)
B2010.10	Concrete	-	410	Recycling	70
	Steel rebar	-	8,24	Recycling	70
	PE	20	-	Incineration	80
	Gypsum plasterboard	15	-	Recycling	80
	Steel sheet	-	11,10	Recycling	70
C2050	Painting	-	0,125	Landfill	-

Table B.4 Internal floor

Macro-components	Materials	Thickness (mm)	Density (kg/m^2)	End-of-life scenario	RR (%)
B1010.10	Concrete	-	410	Recycling	70
	Steel rebar	-	8.24	Recycling	70
	PE	10	-	Incineration	80
	Gypsum pasterboard	15	-	Recycling	80
	Steel sheet	-	11.10	Recycling	70
C2030	Ceramic tiles	-	31	Landfill	-
	Concrete screed	13	-	Landfill	-
C2050	Painting	-	0.125	Landfill	-

LCA Results

LCA of Façades

Table B.5 Indicators describing environmental impacts

Indicator	Unit	A1-A3	A4	B2	C2	C4	D	TOTAL
ADP elements	[kg Sb Eq.]	1.73e-1	1.58e-5	3.79e-3	1.38e-5	9.12e-4	-9.17e-1	-7.39e-1
ADP fossil	[MJ]	3.23e+6	5.88e+3	6.25e+4	5.14e+3	3.56e+4	-1.33e+6	2.00e+6
AP	[kg SO2 Eq.]	1.19e+3	1.90e+0	1.22e+1	1.64e+0	1.55e+1	-2.10e+2	1.01e+3
EP	[kg PO_4^{3-} Eq.]	1.10e+2	4.37e-1	8.53e-1	3.78e-1	2.38e+0	-5.09e+0	1.09e+2
GWP	[kg CO2 Eq.]	3.00e+5	4.23e+2	2.89e+3	3.70e+2	1.04e+4	-7.49e+4	2.39e+5
ODP	[kg CFC-11 Eq.]	2.80e-3	7.41e-9	7.32e-7	6.48e-9	1.95e-6	1.49e-3	4.29e-3
POCP	[kg C2H4 Eq.]	1.54e+2	-6.19e-1	9.67e+0	-5.34e-1	4.04e+0	-4.94e+1	1.17e+2

Table B.6 Indicators describing primary energy demand

Indicator	Unit	A1-A3	A4	B2	C2	C4	D	TOTAL
Total demand (g.c.v)	[MJ]	4.24e+6	6.53e+3	7.07e+4	5.71e+3	4.10e+4	-1.40e+6	2.97e+6
Total demand (n.c.v)	[MJ]	4.06e+6	6.11e+3	6.55e+4	5.33e+3	3.83e+4	-1.32e+6	2.85e+6
Non ren. Resources (g.c.v)	[MJ]	3.42e+6	6.30e+3	6.75e+4	5.51e+3	3.80e+4	-1.44e+6	2.10e+6
Non ren. Resources (n.c.v)	[MJ]	3.24e+6	5.88e+3	6.25e+4	5.14e+3	3.56e+4	-1.37e+6	1.98e+6
Ren. Resources (g.c.v)	[MJ]	8.18e+5	2.30e+2	3.10e+3	2.01e+2	2.65e+3	4.25e+4	8.67e+5
Ren. Resources (n.c.v)	[MJ]	8.18e+5	2.30e+2	3.10e+3	2.01e+2	2.65e+3	4.25e+4	8.67e+5

LCA of Partitions

Table B.7 Indicators describing environmental impacts

Indicator	Unit	A1-A3	A4	B2	C2	C4	D	TOTAL
ADP elements	[kg Sb Eq.]	3.89e-2	2.92e-6	1.52e-3	2.55e-6	6.06e-5	-2.44e-1	-2.03e-1
ADP fossil	[MJ]	7.06e+5	1.09e+3	2.50e+4	9.50e+2	2.37e+3	-2.25e+5	5.10e+5
AP	[kg SO2 Eq.]	2.62e+2	3.51e-1	4.88e+0	3.04e-1	1.03e+0	-5.70e+1	2.12e+2
EP	[kg PO_4^{3-} Eq.]	2.17e+1	8.09e-2	3.41e-1	6.98e-2	1.58e-1	-1.57e+0	2.07e+1
GWP	[kg CO2 Eq.]	6.40e+4	7.83e+1	1.16e+3	6.83e+1	6.95e+2	-2.39e+4	4.22e+4
ODP	[kg CFC-11 Eq.]	3.22e-4	1.37e-9	2.93e-7	1.20e-9	1.30e-7	7.63e-4	1.09e-3
POCP	[kg C2H4 Eq.]	3.51e+1	-1.14e-1	3.87e+0	-9.88e-2	2.68e-1	-1.27e+1	2.62e+1

Table B.8 Indicators describing primary energy demand

Indicator	Unit	A1-A3	A4	B2	C2	C4	D	TOTAL
Total demand (g.c.v)	[MJ]	7.67e+5	1.21e+3	2.83e+4	1.05e+3	2.72e+3	-2.18e+5	5.82e+5
Total demand (n.c.v)	[MJ]	7.30e+5	1.13e+3	2.62e+4	9.85e+2	2.54e+3	-2.11e+5	5.50e+5
Non ren. Resources (g.c.v)	[MJ]	7.43e+5	1.17e+3	2.70e+4	1.02e+3	2.44e+3	-2.30e+5	5.44e+5
Non ren. Resources (n.c.v)	[MJ]	7.08e+5	1.09e+3	2.50e+4	9.50e+2	2.37e+3	-2.25e+5	5.12e+5
Ren. Resources (g.c.v)	[MJ]	2.25e+4	4.26e+1	1.24e+3	3.72e+1	1.76e+2	1.30e+4	3.70e+4
Ren. Resources (n.c.v)	[MJ]	2.25e+4	4.26e+1	1.24e+3	3.72e+1	1.76e+2	1.30e+4	3.70e+4

LCA of Internal Floors

Table B.9 Indicators describing environmental impacts

Indicator	Unit	A1-A3	A4	B2	C2	C4	D	TOTAL
ADP elements	[kg Sb Eq.]	6.25e+0	1.42e-4	6.02e+0	1.24e-4	1.00e-2	-8.26e-1	1.14e+1
ADP fossil	[MJ]	7.10e+6	5.27e+4	2.36e+6	4.62e+4	3.89e+5	-9.55e+5	9.00e+6
AP	[kg SO2 Eq.]	1.52e+3	1.70e+1	2.28e+2	1.47e+1	1.70e+2	-2.67e+2	1.68e+3
EP	[kg PO_4^{3-} Eq.]	1.77e+2	3.93e+0	2.61e+1	3.38e+0	2.61e+1	-8.17e+0	2.28e+2
GWP	[kg CO2 Eq.]	7.14e+5	3.80e+3	1.68e+5	3.31e+3	1.19e+5	-1.03e+5	9.05e+5
ODP	[kg CFC-11 Eq.]	8.76e-3	6.65e-8	6.75e-3	5.80e-8	2.14e-5	2.60e-3	1.81e-2
POCP	[kg C2H4 Eq.]	2.12e+2	-5.57e+0	3.07e+1	-4.78e+0	4.41e+1	-5.25e+1	2.24e+2

Table B.10 Indicators describing primary energy demand

Indicator	Unit	A1-A3	A4	B2	C2	C4	D	TOTAL
Total demand (g.c.v)	[MJ]	8.19e+6	5.86e+4	2.83e+6	5.11e+4	4.48e+5	-9.31e+5	1.06e+7
Total demand (n.c.v)	[MJ]	7.66e+6	5.47e+4	2.59e+6	4.78e+4	4.20e+5	-9.05e+5	9.87e+6
Non ren. Resources (g.c.v)	[MJ]	7.81e+6	5.67e+4	2.77e+6	4.95e+4	4.20e+5	-9.76e+5	1.01e+7
Non ren. Resources (n.c.v)	[MJ]	7.29e+6	5.27e+4	2.53e+6	4.62e+4	3.89e+5	-9.47e+5	9.37e+6
Ren. Resources (g.c.v)	[MJ]	3.74e+5	2.06e+3	6.00e+4	1.81e+3	2.90e+4	4.50e+4	5.12e+5
Ren. Resources (n.c.v)	[MJ]	3.74e+5	2.06e+3	6.00e+4	1.81e+3	2.90e+4	4.50e+4	5.12e+5

LCA of Roof

Table B.11 Indicators describing environmental impacts

Indicator	Unit	A1-A3	A4	B2	C2	C4	D	TOTAL
ADP elements	[kg Sb Eq.]	5.28e-2	3.32e-5	7.58e-4	2.90e-5	2.16e-3	-2.18e-1	-1.62e-1
ADP fossil	[MJ]	1.25e+6	1.23e+4	1.25e+4	1.08e+4	8.38e+4	-2.67e+5	1.11e+6
AP	[kg SO2 Eq.]	3.37e+2	3.98e+0	2.44e+0	3.45e+0	3.66e+1	-7.63e+1	3.07e+2
EP	[kg PO_4^{3-} Eq.]	3.65e+1	9.20e-1	1.71e-1	7.89e-1	5.62e+0	-2.50e+0	4.15e+1
GWP	[kg CO2 Eq.]	1.41e+5	8.89e+2	5.78e+2	7.74e+2	2.71e+4	-2.85e+4	1.42e+5
ODP	[kg CFC-11 Eq.]	5.31e-4	1.56e-8	1.46e-7	1.36e-8	4.60e-6	6.84e-4	1.22e-3
POCP	[kg C2H4 Eq.]	4.95e+1	-1.30e+0	1.93e+0	-1.12e+0	9.47e+0	-1.42e+1	4.43e+1

Table B.12 Indicators describing primary energy demand

Indicator	Unit	A1-A3	A4	B2	C2	C4	D	TOTAL
Total demand (g.c.v)	[MJ]	1.42e+6	1.37e+4	1.41e+4	1.20e+4	9.64e+4	-2.62e+5	1.29e+6
Total demand (n.c.v)	[MJ]	1.34e+6	1.28e+4	1.31e+4	1.12e+4	9.04e+4	-2.54e+5	1.21e+6
Non ren. Resources (g.c.v)	[MJ]	1.33e+6	1.33e+4	1.35e+4	1.16e+4	9.04e+4	-2.74e+5	1.19e+6
Non ren. Resources (n.c.v)	[MJ]	1.26e+6	1.23e+4	1.25e+4	1.08e+4	8.38e+4	-2.65e+5	1.11e+6
Ren. Resources (g.c.v)	[MJ]	8.20e+4	4.83e+2	6.20e+2	4.22e+2	6.24e+3	1.18e+4	1.02e+5
Ren. Resources (n.c.v)	[MJ]	8.20e+4	4.83e+2	6.20e+2	4.22e+2	6.24e+3	1.18e+4	1.02e+5

LCA of Residential Building: Modules A1-A3 to D

Table B.13 Indicators describing environmental impacts

Indicator	Unit	A1-A3	A4	B2	C2	C4	D	TOTAL
ADP elements	[kg Sb Eq.]	6.51e+0	1.94e-4	6.02e+0	1.69e-4	1.32e-2	-2.20e+0	1.03e+1
ADP fossil	[MJ]	1.23e+7	7.20e+4	2.46e+6	6.31e+4	5.11e+5	-2.78e+6	1.26e+7
AP	[kg SO2 Eq.]	3.31e+3	2.33e+1	2.47e+2	2.01e+1	2.23e+2	-6.10e+2	3.21e+3
EP	[kg PO_4^{3-} Eq.]	3.45e+2	5.37e+0	2.75e+1	4.61e+0	3.42e+1	-1.73e+1	4.00e+2
GWP	[kg CO2 Eq.]	1.22e+6	5.19e+3	1.73e+5	4.52e+3	1.57e+5	-2.31e+5	1.33e+6
ODP	[kg CFC-11 Eq.]	1.24e-2	9.08e-8	6.75e-3	7.92e-8	2.81e-5	5.53e-3	2.47e-2
POCP	[kg C2H4 Eq.]	4.50e+2	-7.60e+0	4.62e+1	-6.54e+0	5.78e+1	-1.29e+2	4.12e+2

Table B.14 Indicators describing primary energy demand

Indicator	Unit	A1-A3	A4	B2	C2	C4	D	TOTAL
Total demand (g.c.v)	[MJ]	1.46e+7	8.01e+4	2.94e+6	6.98e+4	5.88e+5	-2.81e+6	1.55e+7
Total demand (n.c.v)	[MJ]	1.38e+7	7.47e+4	2.69e+6	6.53e+4	5.51e+5	-2.69e+6	1.45e+7
Non ren. Resources (g.c.v)	[MJ]	1.33e+7	7.74e+4	2.88e+6	6.76e+4	5.51e+5	-2.92e+6	1.40e+7
Non ren. Resources (n.c.v)	[MJ]	1.25e+7	7.20e+4	2.63e+6	6.31e+4	5.11e+5	-2.81e+6	1.30e+7
Ren. Resources (g.c.v)	[MJ]	1.30e+6	2.82e+3	6.49e+4	2.47e+3	3.81e+4	1.12e+5	1.52e+6
Ren. Resources (n.c.v)	[MJ]	1.30e+6	2.82e+3	6.49e+4	2.47e+3	3.81e+4	1.12e+5	1.52e+6

European Commission
EUR 27346 EN – Joint Research Centre – Institute for the Protection and Security of the Citizen

Title: Eurocodes: Background & Applications. Design of Steel Buildings

Authors: M. Veljkovic, L. Simões da Silva, R. Simões, F. Wald, J.-P. Jaspart, K. Weynand, D. Dubină,
R. Landolfo, P. Vila Real, H. Gervásio

Editors: M. Veljkovic, M. L. Sousa, S. Dimova, B. Nikolova, M. Poljanšek, A. Pinto

Luxembourg: Publications Office of the European Union

2015 – 466 pp. – 21.0 x 29.7 cm

EUR – Scientific and Technical Research series – ISSN 1831-9424 (online)

ISBN 978-92-79-49573-1 (PDF)

doi:10.2788/605700

LB-NA-27346-EN-N

JRC Mission

As the Commission's in-house science service, the Joint Research Centre's mission is to provide EU policies with independent, evidence-based scientific and technical support throughout the whole policy cycle.

Working in close cooperation with policy Directorates-General, the JRC addresses key societal challenges while stimulating innovation through developing new methods, tools and standards, and sharing its know-how with the Member States, the scientific community and international partners.

Serving society
Stimulating innovation
Supporting legislation

doi:10.2788/605700

ISBN 978-92-79-49573-1

Publications Office